CATHERINE PARADIS-BLEAU

GÉNOMIQUE FONCTIONNELLE DES PROTÉINES DE DIVISION CELLULAIRE ET DU PEPTIDOGLYCANE: DÉVELOPPEMENT DE NOUVEAUX AGENTS ANTIBACTÉRIENS

Thèse présentée
à la Faculté des études supérieures de l'Université Laval
dans le cadre du programme de doctorat en microbiologie-immunologie
pour l'obtention du grade de Philosophiae doctor (Ph. D.)

DÉPARTEMENT DE BIOLOGIE MÉDICALE
FACULTÉ DE MÉDECINE
UNIVERSITÉ LAVAL
QUÉBEC

AVRIL, 2007

Résumé

Cette thèse de doctorat présente la problématique de résistance aux antibiotiques parmi les pathogènes bactériens en émergence et en réémergence à travers le monde. En effet, le développement et la propagation des mécanismes de résistance compromet l'efficacité des traitements antibactériens disponibles et met en danger la vie des patients infectés. Cette thèse se concentre sur l'identification de nouvelles cibles antibactériennes et sur le développement de nouvelles classes d'agents antibactériens en utilisant le pathogène opportuniste *Pseudomonas aeruginosa* en tan que modèle d'étude. Le premier chapitre aborde l'exploitation des protéines de division cellulaire FtsZ et FtsA en tant que cibles antibactériennes. Suite à une revue de la littérature détaillée, deux articles scientifiques décrivent la synthèse et la sélection d'inhibiteurs contre FtsZ et FtsA. Ces inhibiteurs représentent des candidats prometteurs en vue du développement d'une nouvelle classe d'agents antibactériens. Le deuxième chapitre du corps de la thèse porte sur l'utilisation des amides ligases MurC, MurD, MurE et MurF essentielles à la biosynthèse de la paroi bactérienne en tant que cibles antibactériennes. Suite à une revue de la littérature sur la biologie de ces enzymes, trois articles scientifiques relatent la sélection d'inhibiteurs peptidiques par présentation phagique contre les enzymes MurD, MurE et MurF. Le mode d'action innovateur de ces inhibiteurs permet d'envisager le développement de nouveaux agents antibactériens par peptidomimétisme. Le dernier chapitre expose le pouvoir antibactérien des endolysines de bactériophages. Une revue de la littérature résume le mode d'action et la biologie des endolysines en tant qu'agents antibactériens efficaces ciblant l'intégrité de la paroi bactérienne. Par la suite, un article décrit la capacité de l'endolysine du phage ϕKZ à hydrolyser la paroi bactérienne des bactéries à Gram-négatif et à outrepasser les membranes bactériennes. Ainsi, cette enzyme possède un potentiel antibactérien fort intéressant. En conclusion, cette thèse fournit plusieurs pistes attrayantes afin de développer de nouvelles stratégies antibactériennes pour contrer la problématique de résistance aux antibiotiques.

Abstract

This thesis first presents the critical outcome of antibiotic resistance among emerging and re-emerging bacterial pathogens worldwide. The incessant increase and spread of antibiotic resistance mechanisms compromise the efficiency of available antibacterial therapies and increase the impact of bacterial infections on human mortality and morbidity. This thesis focuses efforts to identify new antibacterial targets in order to develop novel classes of antibacterial agents using the opportunistic pathogen *Pseudomonas aeruginosa* as a research model. The first chapter of this thesis reports the exploitation of the cell division proteins FtsZ and FtsA as antibacterial targets. A detailed scientific review is presented along with two articles reporting the synthesis and selection of inhibitors against FtsZ and FtsA. These inhibitors represent potent candidates to develop new classes of antibacterial agents targeting the bacterial cell division process. The second chapter describes the use of the essential bacterial cell wall biosynthesis enzymes MurC, MurD, MurE and MurF as antibacterial targets. A scientific review first summarises the biology of these amide ligase enzymes and three scientific articles report the selection of peptide inhibitors against MurD, MurE and MurF by phage display. The novel mode of action of these inhibitors against the unexploited Mur enzymes can be the basis for future development of antibacterial agents targeting the cell wall biosynthesis pathway by peptidomimetism. The last chapter exposes the antibacterial potential of the phage-encoded endolysin enzymes. A review describes the mode of action and the biology of endolysins as efficient antibacterial agents targeting the integrity of the bacterial cell wall layer. Finally, an article presents the peptidoglycan hydrolytic activity of the *P. aeruginosa* phage ϕKZ gp144 lytic transglycosylase. This endolysin is able to pass through the bacterial membranes and thus represents a strong candidate for developing new antibacterial therapies against Gram-negative bacteria. In conclusion, this thesis provides various attractive ways to develop new antibacterial strategies and face the problem of antibiotic resistance.

Avant-Propos

Cette thèse de doctorat représente le fruit d'efforts soutenus pendant trois ans et demi. Ainsi, de longues journées au laboratoire et de maintes heures de rédaction prennent maintenant toute leur signification à travers les lignes de ce document. Cette thèse possède une signification très importante à mes yeux et elle conclue mon expérience en tant qu'étudiante graduée. J'espère sincèrement que les travaux de recherche effectués au cours de mon doctorat déboucheront un jour sur de nouvelles approches antibactériennes. Ainsi, les résultats présentés par cette thèse apporteront peut-être une lueur d'espoir aux patients atteints d'infections bactériennes persistantes. Je serais extrêmement heureuse de voir surgir sur le marché pharmaceutique des agents antibactériens inhibant la division cellulaire bactérienne ou ciblant les amides ligases essentielles à la biosynthèse de la paroi bactérienne. J'espère également que les endolysines de bactériophages et peut-être même les bactériophages eux-mêmes seront éventuellement utilisés en médecine humaine et animale. Les bactériophages détiennent un pouvoir antibactérien extrêmement efficace provenant de milliards d'années d'évolution. Ainsi, il serait vraiment désolant d'oublier cette ressource naturelle pour se concentrer uniquement sur la recherche et le développement d'agents antibactériens réalisés par l'être humain. La disponibilité naturelle des bactériophages pourrait permettre l'accessibilité des traitements antibactériens aux pays les plus pauvres et les plus touchés par les infections bactériennes. J'entretiens l'espoir que le capitalisme et la soif de brevets ne briment pas éternellement le développement de thérapies antibactériennes à base de bactériophages.

J'aimerais remercier les personnes qui m'ont généreusement accordé leur soutien scientifique et moral au cours de mes études doctorales. Je voudrais tout d'abord souligner l'aide précieuse du Dr Roger C. Levesque qui m'a fait confiance et qui a cru en moi en me permettant d'atteindre mes objectifs scientifiques. Le Dr Levesque m'a supportée tout au long de mes études graduées en me permettant de cheminer vers une autonomie scientifique. Il m'a également ouvert la voie afin que j'évolue en tant que chercheure indépendante. Les années passées au sein du laboratoire du Dr Roger Levesque ont été extrêmement intéressantes et enrichissantes tant au point de vue scientifique que personnel.

Je tiens également à remercier le Dr François Sanschagrin qui m'a fourni un support constant au laboratoire. Il m'a enseigné les rudiments de nombreuses techniques et approches scientifiques essentielles à la réalisation de mes études graduées.

Je tiens à remercier sincèrement les membres de ma famille qui m'encouragent et me supportent depuis toujours. Je remercie mes parents Hélène Paradis et Gilles Bleau qui m'ont guidée et appuyée tout au long de mes études. Je voudrais également remercier mon frère Simon Paradis-Bleau qui est toujours présent et disponible pour moi. Il s'est beaucoup intéressé à mon projet de recherche et m'a supportée. Je remercie aussi Céline Bergeon et Michel-Jaques Trottier pour leur appui et leurs encouragements. Je tiens à remercier spécialement mes amis Iréna Kukavica-Ibrulj, Sabrina Simard, Mélanie Plante, Marjorie Perron, Mathieu Barabé, Audrey Vigneault et Mélissa Rapin qui ont vécu avec moi les hauts et les bas des dernières années. Je voudrais aussi souligner l'importance de tous les membres de l'équipe du Dr Levesque qui m'ont aidée et encouragée. Je tiens également à remercier Isabelle Cloutier, la Dre Michèle Auger, le Dr Stéphane Gagné, Mélanie Beaumont, Lise Lemieux, le Dr Alain Garnier, le Dr Jérôme Laroche, Lydia Boudreault, le Dr Adrian Lloyd et le Dr Timothy D. H. Bugg pour leurs précieuses collaborations.

«Imagination is more important then knowledge»
Albert Einstein

Table des matières

Liste des figures

Section I - Mise en situation du projet de recherche

1 Problématique

1.1 La recrudescence des infections bactériennes

La problématique des infections bactériennes a subi un revers sans précédant suite à la découverte des antibiotiques et la mise au point de vaccins efficaces. De plus, l'évolution conjointe des espèces bactériennes pathogènes et de l'être humain a entraîné une diminution de susceptibilité de l'hôte grâce à la sélection naturelle. Enfin, la conscientisation de la population a réduit la transmission des infections bactériennes via une amélioration substantielle des conditions d'hygiène, des habitudes alimentaires et des soins de santé. L'ensemble de ces facteurs a considérablement diminué l'impact des infections bactériennes sur la santé humaine et l'espérance de vie de l'être humain a augmenté de 47 à 76 ans de 1900 à 1997 dans les pays développés (Cohen 2000).

Suite à la diminution importante de l'incidence et de la gravité des maladies infectieuses, la recherche sur la prévention et le traitement de ces infections a été dévalorisée. Convaincues de détenir un arsenal suffisant pour éliminer efficacement toutes les infections, les compagnies pharmaceutiques ont réduit leurs activités de recherche et de développement d'antibiotiques. Malheureusement, les générations suivantes ont sous-estimé le pouvoir évolutif des bactéries et ont véhiculé une attitude de négligence et de confiance aveugle envers les antibiotiques (Fauci 2001). Ainsi, une combinaison de changements sociaux et technologiques a contribué à la recrudescence des infections bactériennes. Le vieillissement de la population, la malnutrition ou l'obésité ainsi que l'augmentation de l'incidence des maladies non infectieuses comme le cancer et les maladies auto-immunes augmentent de façon importante la susceptibilité de l'être humain aux infections bactériennes. Les avancées technologiques et médicales déjouent le processus de sélection naturelle en permettant aux maladies infectieuses et génétiques de se propager dans une population d'hôtes de plus en plus vulnérable (Cohen 2000). Ainsi, les infections acquises en milieu hospitalier (infections nosocomiales) causées par des pathogènes bactériens opportunistes sont plus fréquentes que jamais et elles représentent une problématique très préoccupante en santé publique (Kaplan, Sepkowitz et al. 2001). De

plus, les changements démographiques tels que l'augmentation de la densité de la population humaine, les déplacements à grande vitesse et l'immigration favorisent la transmission des microorganismes pathogènes. Finalement, les changements environnementaux tel que le réchauffement de la planète font peser la balance en faveur des infections bactériennes au détriment de la santé humaine (Cohen 2000).

En conséquence, nous assistons présentement à l'émergence et la réémergence des infections bactériennes sur l'ensemble de la planète (Fauci 2001; Cohen 2000). De nouveaux pathogènes bactériens tel que *Escherichia coli* H7 ont récemment fait leur apparition (Brown and Wright 2005). De plus, certains pathogènes bactériens anciennement contrôlés tel que *Mycobacterium tuberculosis* réemergent dangereusement à travers les populations humaines les plus susceptibles (Bloom and Murray 1992; Levy and Marshall 2004). Ainsi, les maladies infectieuses représentent aujourd'hui la seconde cause de décès et la première cause de perte d'années de vie productives à travers le monde (Fauci 2001). De plus, les infections bactériennes représentent 70 % des cas de mortalité d'origine infectieuse (Walsh 2003). Finalement, les conséquences des infections bactériennes sur la santé humaine et animale, l'économie, la stabilité politique et le bioterrorisme méritent sérieusement d'attirer l'attention des chercheurs académiques, des compagnies pharmaceutiques et des gouvernements (Cohen 2000).

1.2 La problématique de résistance aux antibiotiques

L'origine des mécanismes de résistance aux antibiotiques provient des microorganismes environnementaux dont les espèces du genre *Streptomyces*. Les espèces bactériennes productrices d'antibiotiques ainsi que les populations microbiennes environnantes combattent l'action de ces agents antibactériens depuis plusieurs millions d'années. Un important facteur de sélection naturelle a donc favorisé le développement de multiples et ingénieuses stratégies de résistance. Afin d'échapper à l'action létale des antibiotiques, les bactéries utilisent principalement des mécanismes de résistance de nature génétique provenant d'un changement chromosomique ou extra chromosomique (McDermott, Walker et al. 2003; Hamilton-Miller 2004). Les modifications chromosomiques découlent de mutations stables qui confèrent rarement un désavantage évolutif. L'ADN polymérase

bactérienne introduit une mutation sur 10^7 paires de base et les foyers infectieux comprennent environ 10^9 bactéries alors il n'est pas surprenant de voir surgir des clones résistants (Walsh 2003). L'acquisition de matériel génétique sous forme de plasmide, de transposon, d'intégron, d'ADN libre ou de bactériophage compte pour environ 80 % des cas de résistance. Ainsi, les transferts de matériel génétique verticaux et horizontaux comme la conjugaison, la transformation et la transduction ont permis la propagation des mécanismes de résistance aux cellules filles puis aux diverses espèces bactériennes. Les cas de multirésistance se multiplient car les plasmides et les intégrons transportent souvent plusieurs gènes de résistance et peuvent en acquérir davantage par recombinaison homologue, transposition ou intégration (Normark and Normark 2002; Levy and Marshall 2004).

Les bactéries exploitent trois stratégies distinctes afin de se défendre contre l'action des antibiotiques (figure 1). Elles peuvent modifier ou détruire l'agent antibactérien à l'aide d'un gène de résistance extra chromosomique. Ce mécanisme agit principalement contre les antibiotiques naturels comme la pénicilline qui se retrouvent dans l'environnement depuis des millions d'années (Walsh 2003). Un second mécanisme consiste à prévenir l'accumulation de concentrations thérapeutiques d'antibiotiques dans le cytoplasme bactérien. Certaines espèces bactériennes restreignent l'entrée des agents antibactériens en modifiant leur perméabilité membranaire alors que d'autres espèces utilisent des pompes à efflux afin d'expulser activement les antibiotiques à l'extérieur de la cellule. Les pompes transmembranaires peuvent être acquises via un plasmide ou un transposon mais elles font souvent partie intégrante de la physiologie bactérienne. Finalement, les bactéries peuvent modifier ou remplacer la cible thérapeutique affectée par l'antibiotique. Suite à une mutation chromosomique, la cible antibactérienne peut être altérée et devenir insensible à l'action de l'antibiotique tout en conservant son activité biologique (Walsh 2003; Tenover 2006). Certaines espèces bactériennes comme *Streptococcus pneumoniae* peuvent également remplacer leur cible thérapeutique sensible par une cible insensible provenant d'un autre microorganisme (Normark and Normark 2002).

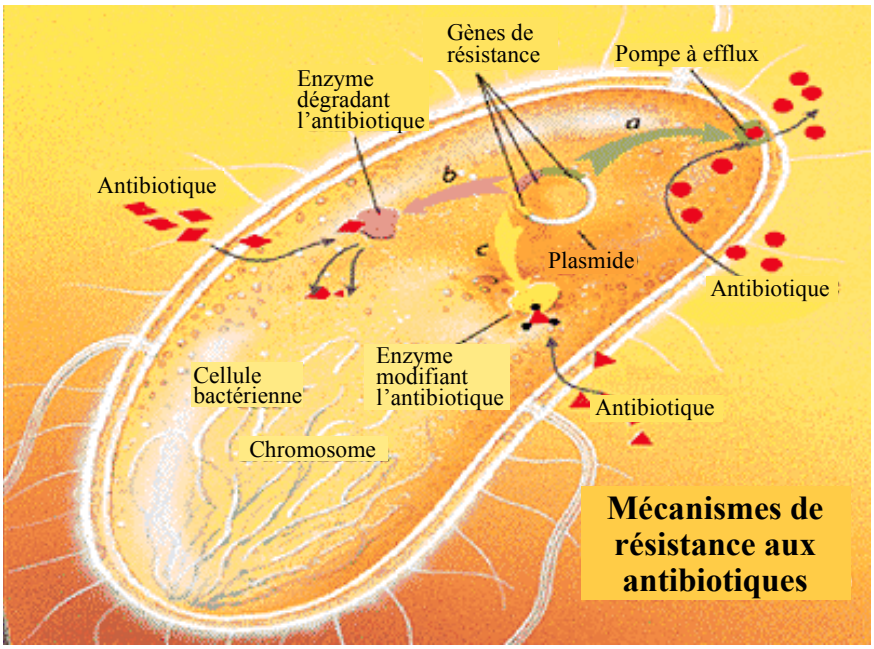

Figure 1. Schématisation des principaux mécanismes de résistance aux antibiotiques retrouvés chez les bactéries (figure adaptée de http://www.medscape.com - 2007).

.

L'utilisation abusive et maladroite des antibiotiques en médecine humaine et en alimentation animale a surexposé les espèces bactériennes pathogènes aux agents antibactériens pendant les six dernières décennies. En conséquence, une forte pression évolutive a sélectionné de nouvelles mutations spontanées et a favorisé la propagation des mécanismes de résistance parmi les pathogènes bactériens. Ce processus a entraîné une augmentation drastique et une propagation accélérée des mécanismes de résistance aux antibiotiques en quelques années (Normark and Normark 2002). La dissémination des grands clones épidémiques tel que les souches de *Staphylococcus aureus* résistantes à la méthycilline (SARM) et les entérocoques résistants à la vancomycine (ERV) en sont de bons exemples. De plus, des cas de *S. aureus* résistants à la vancomycine (SARV) ont récemment émergé (Rice 2006). Le cas des pathogènes bactériens opportunistes tel que *Pseudomonas aeruginosa* est également très inquiétant (Meyer 2005). Ces microorganismes possèdent un niveau de résistance élevé car ils subsistent généralement dans la flore normale du corps humain et sont fréquemment exposés aux antibiotiques. En fait, la problématique de résistance aux antibiotiques touche maintenant tous les agents antibactériens disponibles et toutes les espèces bactériennes pathogènes. La situation

actuelle compromet l'efficacité des traitements antibactériens et met en danger la vie des patients. De plus, le phénomène de résistance prolonge et aggrave les épisodes d'épidémie à travers le monde et cela contribue à la propagation des pathogènes bactériens multirésistants (Levy and Marshall 2004; Harbarth and Samore 2005; Tenover 2006). Finalement, la problématique de résistance fait grimper le prix des antibiotiques et cela diminue l'accès aux médicaments des populations les plus pauvres et souvent les plus affectées par les infections bactériennes (Prentice 2000). Ainsi, la résistance aux antibiotiques parmi les pathogènes bactériens en émergence et en réémergence représente désormais l'une des problématiques les plus préoccupantes en santé publique et il s'avère crucial d'y apporter des solutions concrètes (Cohen 2000; Fauci 2001; Normark and Normark 2002; Levy and Marshall 2004).

2 Objectifs de recherche

Les facteurs favorisant la recrudescence des infections bactériennes et la résistance aux antibiotiques ne vont que s'amplifier dans les prochaines années. Ainsi, il s'avère primordial de mettre en place des programmes internationaux afin de surveiller l'émergence et la réémergence des maladies infectieuses, de raffiner les différents systèmes de santé publique, de développer des stratégies d'intervention afin de diminuer la susceptibilité des populations et de prôner une utilisation adéquate des antibiotiques afin de diminuer la sélection des mécanismes de résistance (Cohen 2000). De plus, un effort soutenu devrait être investi pour mettre au point des tests de diagnostique rapides et efficaces afin d'établir les profils de résistance des pathogènes bactériens. Il est également important de lutter contre la propagation des souches bactériennes multirésistantes en détectant de façon précoce les personnes porteuses, en les isolant convenablement, en instaurant des protocoles de vaccination puis en améliorant les conditions d'hygiène. Cependant, les meilleurs programmes de surveillance et de prévention ne suffiront pas à contrebalancer l'évolution de la résistance aux antibiotiques. Ainsi, il s'avère essentiel de développer de nouvelles stratégies antibactériennes afin de protéger la santé humaine contre

les pathogènes bactériens résistants (Fauci 2001; McDermott, Walker et al. 2003; Hamilton-Miller 2004).

2.1 Développement de nouvelles classes d'agents antibactériens

Tel que mentionné, la recrudescence des infections bactériennes et l'occurrence d'une résistance accrue contre les antibiotiques disponibles engendrent un besoin urgent de nouvelles classes structurales et fonctionnelles d'agents antibactériens (Fauci 2001; Projan 2002; Tenover 2006). Ce développement thérapeutique peut être réalisé en criblant des microorganismes, en modifiant les agents antibactériens connus, en bloquant les mécanismes de résistance bactériens, en exploitant la chimie combinatoire puis en étudiant de nouvelles cibles antibactériennes (Cunha 2001). Par contre, les méthodes traditionnelles comme le criblage d'antibiotiques naturels vont inévitablement mener à l'identification de molécules appartenant aux classes de composés chimiques déjà exploitées. Le même résultat sera obtenu en synthétisant des analogues d'antibiotiques utilisés en médecine humaine. Malheureusement, ces «nouveaux» agents antibactériens vont rapidement sélectionner des mécanismes de résistance bactériens adaptés (Desnottes 1996; Chan, Macarron et al. 2002). Ainsi, les pathogènes bactériens n'auront qu'à modifier leurs mécanismes de résistance afin de combattre efficacement l'action de ces agents antibactériens ressemblant aux antibiotiques précédents. En ce qui concerne le blocage des mécanismes de résistance, cette stratégie apparaît extrêmement difficile à réaliser à l'aide de moyens conventionnels (Hamilton-Miller 2004). La communauté scientifique a été encouragée par la découverte d'inhibiteurs contre les principales enzymes bactériennes responsables de la résistance aux antibiotiques de type β-lactame. Plusieurs groupes de recherche tentent à présent de développer des molécules qui déstabilisent la membrane externe des bactéries à Gram-négatif et qui bloquent les pompes à efflux (Breithaupt 1999).

Heureusement, l'avenue de nouvelles méthodes de chimie combinatoire procure un grand enthousiasme en recherche thérapeutique. Ainsi, la synthèse de banques de molécules organiques et la synthèse d'inhibiteurs sur mesure dominent présentement la recherche pharmaceutique. La chimie combinatoire a comme avantage de permettre la synthèse de molécules innovatrices au point de vue structural et fonctionnel sans aucun homologue naturel. Cela réduit considérablement la probabilité de retrouver des gènes de résistance

environnementaux contre de telles molécules (Walsh 2003). De plus, la chimie combinatoire permet de produire rapidement toutes les combinaisons possibles d'un jeu de molécules. Cette diversité moléculaire révolutionnaire favorise la découverte de nouveaux agents antibactériens. Finalement, les méthodes classiques de chimie organique peuvent maximiser les propriétés pharmacologiques des agents antibactériens comme leur efficacité, leur stabilité et leur biodisponibilité (Hughes 2003).

Les récentes avancées technologiques en biologie moléculaire, en chimie, en génomique, en protéomique et en bioinformatique permettent maintenant une conception rationnelle d'antibiotiques. De plus, la modélisation moléculaire et les études structurales réalisées grâce aux techniques de cristallographie et de résonance magnétique nucléaire permettent d'analyser la conformation des protéines bactériennes. Il est donc possible de développer des stratégies de synthèse organique afin de cibler adéquatement et spécifiquement les structures moléculaires définies (Hughes 2003). La validité de cette stratégie repose entièrement sur le choix de la cible thérapeutique. Ce choix revêt une importance capitale car la problématique de résistance aux antibiotiques est engendrée par le répertoire limité de cibles antibactériennes. En fait, moins de 30 protéines bactériennes sont présentement ciblées en thérapie et aucune nouvelle classe d'antibiotiques s'attaquant à une cible bactérienne inédite n'a été commercialisée depuis 30 ans (Acar 1998; Brown and Wright 2005). Ainsi, il s'avère crucial d'identifier des cibles thérapeutiques inédites afin de développer de nouvelles structures antibactériennes et de nouveaux modes d'action moléculaire échappant aux mécanismes de résistance (Haselbeck, Wall et al. 2002; Brown and Wright 2005).

2.2 L'identification de nouvelles cibles antibactériennes

Les antibiotiques présentement utilisés en médecine humaine possèdent quatre cibles bactériennes principales tel qu'illustré à la figure 2. La vancomycine et les antibiotiques à noyau β-lactame ciblent la biosynthèse de la paroi bactérienne. Les aminoglycosides, la tétracycline, le chloramphénicol et les macrolides bloquent quant à eux la synthèse protéique. La synthèse d'acides nucléiques est inhibée par la rifampicine et les quinolones.

Finalement, la voie métabolique de l'acide folique est ciblée par les sulfamides et le triméthoprime (Franklin and Snow 1989; Axelsen 2002; Walsh 2003).

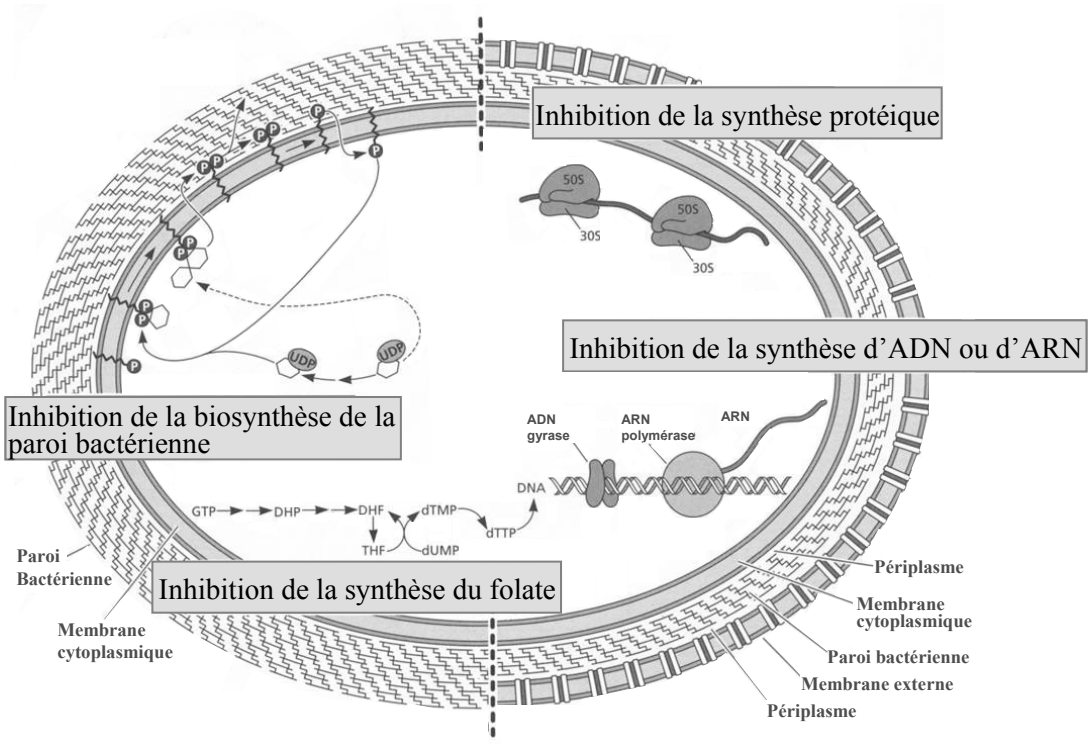

Figure 2. Représentation schématique des quatre grandes classes de cibles antibactériennes (figure adaptée de Walsh 2003).

Les protéines bactériennes doivent répondre à plusieurs critères afin d'être considérées comme des cibles thérapeutiques intéressantes. Ainsi, la cible antibactérienne parfaite doit être à l'origine d'une fonction biologique essentielle pour la viabilité bactérienne. L'inhibition de cette cible entraîne donc un phénotype létal et cela favorise le développement d'agents antibactériens bactéricides efficaces contre les infections bactériennes sévères et chroniques (Miesel, Greene et al. 2003). La cible idéale doit être génétiquement et structuralement conservée parmi les pathogènes bactériens. Malheureusement, le manque de tests de diagnostique rapides et précis force souvent les médecins à traiter les infections bactériennes sans connaître la nature de l'agent bactérien étiologique. Ainsi, les cibles thérapeutiques doivent être hautement conservées dans l'évolution bactérienne afin de combler le besoin d'agents antibactériens à large spectre (Projan 2002; Miesel, Greene et al. 2003; Brown and Wright 2005). Finalement, la cible

idéale doit être exprimée en quantité suffisante lors de l'infection et elle doit être absente des organismes eucaryotes (Haselbeck, Wall et al. 2002).

La cible antibactérienne typique est une enzyme responsable d'une étape biochimique essentielle et limitante. La structure tridimensionnelle et le mécanisme enzymatique doivent préférentiellement être élucidés afin de permettre la mise au point d'essais de criblage spécifique et les études d'inhibition de type structure–fonction (Projan 2002; Miesel, Greene et al. 2003; Brown and Wright 2005). Afin de s'assurer de l'absence de gènes de résistance environnementaux, les cibles thérapeutiques ne doivent pas être déjà exploitées par des approches antibactériennes en santé humaine ou animale. Dans le but de minimiser le développement de nouveaux mécanismes de résistance, l'idéal est de cibler un groupe d'enzymes semblables qui effectuent des étapes biochimiques différentes. Un tel groupe de cibles thérapeutiques peut être inhibé de façon efficace par un seul agent antibactérien. Les bactéries ne pourront donc pas échapper au mode d'action de cet agent antibactérien en modifiant une seule protéine cible. En fait, une série extrêmement improbable de mutations spontanées devrait se produire afin d'occasionner une résistance efficace (Projan 2002; Miesel, Greene et al. 2003). L'avenue de nouveaux mécanismes de résistance peut également être diminuée en ciblant des enzymes dont le site actif comprend des acides aminés invariables. Ainsi, les mutations spontanées risquant de modifier la cible antibactérienne et de conférer une résistance seront probablement létales pour la bactérie ou causeront un désavantage évolutif majeur (Miesel, Greene et al. 2003).

L'identification des protéines essentielles à la survie et à la virulence bactérienne est grandement facilitée par le séquençage des génomes bactériens combiné aux récentes avancées technologiques en génomique, en protéomique et en bioinformatique (Breithaupt 1999). Ainsi, plusieurs nouvelles cibles bactériennes ont été sélectionnées telles que la signalisation intracellulaire et intercellulaire, les facteurs de virulence, la synthèse du lipolysaccharide (LPS), la division cellulaire, les mécanismes d'acquisition du fer, la glycosylation puis la biosynthèse des acides gras (Breithaupt 1999; Projan 2002; Salyers and Whitt 2002).

3. Hypothèses du projet de recherche

Cette thèse de doctorat s'intéresse particulièrement à la division cellulaire et à la paroi bactérienne en tant que sources de nouvelles cibles thérapeutiques. Ainsi, la machinerie de division cellulaire bactérienne, les enzymes essentielles à la biosynthèse de la paroi bactérienne et l'intégrité de cette paroi sont étudiées et exploitées en tant que cibles. Le projet de recherche à la base de cette thèse présume que les protéines de division cellulaire FtsZ et FtsA, les enzymes MurD, MurE et MurF essentielles à la biosynthèse de la paroi et le peptidoglycane constituant la paroi bactérienne représentent des cibles thérapeutiques prometteuses. Une des hypothèses de ce projet de recherche soutient que des inhibiteurs de l'activité enzymatique de FtsZ, FtsA, MurD, MurE et MurF bloqueront spécifiquement la division cellulaire et la biosynthèse de la paroi bactérienne en engendrant un phénotype létal. Ainsi, ces inhibiteurs constitueront une base intéressante pour le développement de nouvelles classes d'agents antibactériens. Ce projet soutient également que les endolysines de bactériophages représentent des agents antibactériens efficaces ciblant l'intégrité de la paroi bactérienne. Par conséquent, ces endolysines peuvent être exploitées afin de développer une nouvelle approche antibactérienne.

Afin d'assurer la fluidité et la continuité de cette thèse de doctorat, la revue de littérature scientifique portant sur la division cellulaire, la paroi bactérienne et les endolysines de bactériophages fait partie intégrante du corps de la thèse. Il en est de même pour la validation du choix des cibles antibactériennes à l'étude. Ainsi, la première section de cette thèse fait office d'introduction puis la seconde section décrit le processus de division cellulaire bactérien et rapporte l'identification d'inhibiteurs contre les protéines de division cellulaire FtsZ et FtsA. La troisième section du corps de cette thèse aborde la biosynthèse de la paroi bactérienne et décrit l'identification d'inhibiteurs de l'activité des enzymes MurD, MurE et MurF. La quatrième section expose une revue de littérature sur les endolysines de bactériophages et relate l'étude de l'endolysine du bactériophage ϕKZ. Finalement, la cinquième section présente la conclusion de cette thèse et aborde les perspectives futures du projet de recherche.

4 Résumé des stratégies et méthodologies employées

4.1 Utilisation du pathogène opportuniste *P. aeruginosa* en tant que modèle d'étude

Tout au long de ce projet de recherche, le pathogène opportuniste ubiquitaire *P. aeruginosa* est utilisé en tant que modèle d'étude. Cette espèce bactérienne se présente sous la forme d'un bâtonnet mobile à Gram-négatif exprimant un pigment vert nommé pyocyanine tel qu'illustré par la figure 3 (Salyers and Whitt 2002). Ce pathogène regorge de mécanismes de résistance et il engendre de multiples infections intraitables et mortelles. En fait, *P. aeruginosa* profite des failles immunitaires des personnes immunodéprimées comme les grands brûlés, les personnes âgées, les nouveau-nés ainsi que les patients atteints de fibrose kystique. Ce pathogène cause alors une variété d'infections nosocomiales chroniques comme des infections urinaires, oculaires, pulmonaires ou des infections de plaies profondes entraînant un choc septique. *P. aeruginosa* représente ainsi l'une des principales causes d'infections opportunistes chez l'être humain (Stover, Pham et al. 2000). De plus, *P. aeruginosa* est la principale cause de décès chez les patients atteints de fibrose kystique (Davies 2002; Salyers and Whitt 2002). Cette maladie autosomale récessive affecte un nouveau-né sur 2000 chez les Caucasiens et cela en fait la maladie héréditaire létale la plus prévalente. La fibrose kystique est causée par une mutation du gène CFTR (Cystic Fibrosis Transmembrane Conductance Regulator) qui abolit sa fonction biologique de canal à chlore (May, Shinabarger et al. 1991; Goldberg and Pier 2000). Les patients présentent alors un transport anormal d'électrolytes et une sécrétion aberrante de mucus. La maladie se traduit principalement par une affliction pulmonaire chronique avec une toux persistante et une détresse respiratoire (May, Shinabarger et al. 1991). La mutation de la protéine CFTR et les défauts moléculaires subséquents favorisent la colonisation pulmonaire par *P. aeruginosa* (Davies 2002). En plus de résister à la majorité des antibiotiques disponibles, *P. aeruginosa* produit des immuno-évasines pour échapper au système immunitaire, il se protège sous une capsule d'alginate et il produit un biofilm. Ainsi, l'infection pulmonaire chronique causée

par *P. aeruginosa* perdure malheureusement jusqu'au décès du patient (Davies 2002, May, Shinabarger et al. 1991).

Figure 3. Photographie de *P. aeruginosa* prise en microscopie confocale (image provenant du site internet de renommée internationale http://www.pseudomonas.com).

Depuis les quelques dernières années, la fréquence et la sévérité des infections opportunistes causées par *P. aeruginosa* ont augmenté de façon inquiétante. De plus, plusieurs souches multirésistantes de *P. aeruginosa* ne sont maintenant sensibles qu'aux antibiotiques de type polymixine qui engendrent des effets secondaires néfastes chez l'être humain (Meyer 2005). Cependant, même un tel traitement ne réussit pas à enrayer les infections chroniques causées par *P. aeruginosa* qui demeure l'un des microorganismes les plus difficiles à traiter (Pierce, 2005; Salyers and Whitt 2002). En fait, ce pathogène détient plusieurs gènes de résistance intrinsèques, il dispose de quelques 72 pompes à efflux distinctes et il possède une faible perméabilité membranaire (Hancock and Brinkman 2002; Walsh 2003). Ainsi, l'importance médicale de ce pathogène combinée à l'absence de traitement efficace en fait un modèle d'étude idéal dans le cadre de ce projet de recherche. De plus, le génome de *P. aeruginosa* est entièrement séquencé et annoté; ce qui facilite grandement l'étude de nouvelles cibles antibactériennes en vue du développement de nouveaux agents antibactériens (Stover, Pham et al. 2000).

4.2 Méthodologies

Dans un premier temps, le projet vise à caractériser les protéines de division cellulaire FtsZ et FtsA et les enzymes MurD, MurE et MurF de *P. aeruginosa* en tant que nouvelles cibles antibactériennes. Les gènes respectifs ont donc été clonés dans des vecteurs d'expression à partir d'ADN génomique de *P. aeruginosa*, les protéines ont été exprimées dans des cellules recombinantes de *E. coli* puis les protéines ont été purifiées en quantité appréciable. L'activité biologique de ces cinq cibles antibactériennes a ensuite été confirmée et caractérisée. Afin d'évaluer le potentiel inhibiteur de futurs candidats antibactériens sur l'activité enzymatique essentielle de ces protéines, des essais de criblage spécifiques ont été mis au point pour FtsZ, FtsA, MurD, MurE et MurF. Par la suite, deux approches différentes ont été exploitées afin d'identifier des inhibiteurs possédant des structures et des modes d'action inusités contre ces cinq protéines. Dans le cas de FtsZ, une ingénieuse stratégie de synthèse organique en parallèle sur support solide a été employée. Cette approche est clairement expliquée et détaillée dans un article scientifique récemment accepté dans la revue «Bioorganic & Medicinal Chemistry» présent dans le premier chapitre du corps de cette thèse. Afin de sélectionner des inhibiteurs spécifiques de FtsA, MurD, MurE et MurF, une approche de présentation phagique a été utilisée.

La présentation phagique consiste en un criblage moléculaire de banques de peptides commerciales renfermant 10^9 combinaisons peptidiques distinctes fusionnées à la protéine mineure pIII du bactériophage M13. Les banques contiennent 1000 copies de chacune des combinaisons peptidiques qui se présentent sous la forme de 12 mers, de 7 mers ou de C7C (7 acides aminés flanqués de 2 cystéines). Cinq copies de la protéine pIII se retrouvent à la surface de la capside du bactériophage M13 et elles assurent l'adsorption du phage au pili sexuel de *E. coli* (Hoess 2001). Les bactériophages M13 présentent ainsi les fusions peptidiques à leur surface tel qu'illustré par la figure 4. L'avantage majeur de la présentation phagique réside dans l'étonnante diversité moléculaire qui permet d'identifier rapidement et efficacement de petits ligands peptidiques spécifiques interagissant avec une cible d'intérêt pharmacologique (Christensen, Gottlin et al. 2001; Peczuh and Hamilton 2000; Sidhu 2000). Le principe de la présentation phagique repose sur les rondes de biocriblage où une banque de bactériophages M13 est exposée à la protéine d'intérêt fixée

au fond des puits d'une microplaque (figure 4). Par la suite, les lavages éliminent les bactériophages codant pour des fusions peptidiques non spécifiques puis l'élution permet de récolter les phages adsorbés à la protéine cible. Finalement, les bactériophages sélectionnés subissent une amplification afin de constituer le matériel de départ nécessaire pour amorcer une seconde ronde de biocriblage (Kay, Kasanov et al. 2001).

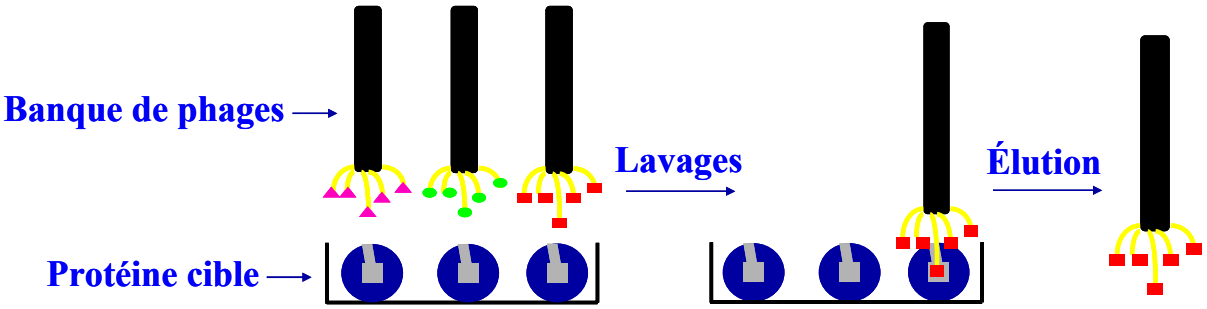

Figure 4. Représentation schématique d'une ronde typique de biocriblage par présentation phagique.

La spécificité et l'efficacité du criblage moléculaire par présentation phagique sont maximisées en effectuant trois rondes successives de biocriblage. Afin d'assurer une sélection de fusions peptidiques spécifiques pour la protéine d'intérêt, la rigueur des lavages est augmentée puis le temps de contact entre les bactériophages et la protéine cible est diminué au cours de ces rondes (Kay, Kasanov et al. 2001). La figure 5 illustre le principe des trois rondes de biocriblage où les bactériophages adhérés spécifiquement à la protéine d'intérêt sont élués avec de la glycine à pH acide qui altère les interactions entre les bactériophages et la protéine cible. Les bactériophages peuvent également être élués de façon compétitive à l'aide des substrats de l'enzyme d'intérêt ou à l'aide d'une autre protéine avec laquelle la protéine cible interagit. Suite à l'élution des phages spécifiques de la dernière ronde de biocriblage, l'ADN de 10 à 20 bactériophages est séquencé à l'aide d'amorces commerciales. Finalement, les analyses bioinformatiques subséquentes identifient les peptides sélectionnés par l'approche de présentation phagique.

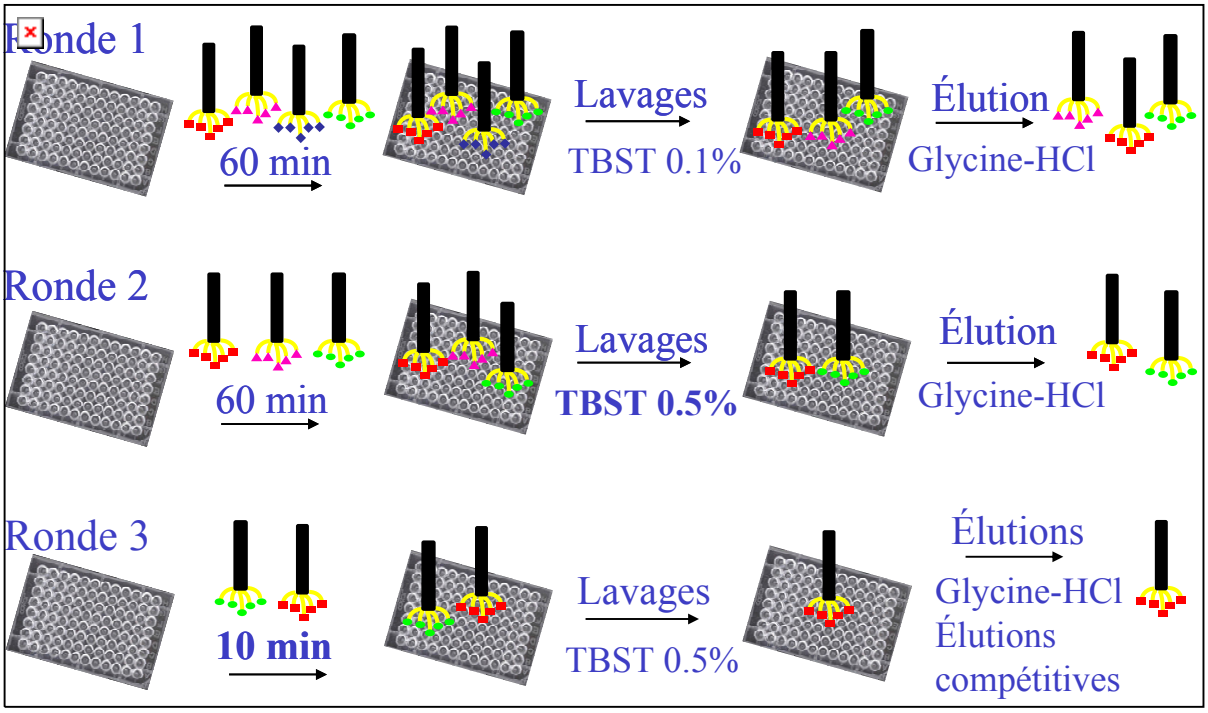

Figure 5. Schéma expérimental représentant les trois rondes de biocriblage effectuées lors d'un criblage par présentation phagique.

Suite à la sélection de peptides spécifiques pour les protéines FtsA, MurD, MurE et MurF et à la synthèse organique d'analogues du substrat de l'enzyme FtsZ, le pouvoir inhibiteur de ces molécules a été évalué. Ainsi, leur activité inhibitrice a été caractérisée sur l'activité enzymatique des protéines cibles et leur CI_{50} (Concentration Inhibitrice de 50 % de l'activité de l'enzyme) a été déterminée en exploitant les divers essais de criblage mis au point pour les enzymes à l'étude. Dans le cas des petites molécules organiques synthétisées contre FtsZ, leur potentiel antibactérien a été évalué sur des espèces bactériennes à Gram-négatif et à Gram-positif à l'aide d'un essai biologique sur gélose. Le mode d'action des peptides inhibiteurs sélectionnés contre les amides ligases MurE et MurF a également été élucidé à l'aide d'analyses biochimiques et enzymologiques. Les figures 6 et 7 résument la méthodologie employée afin de caractériser les cibles antibactériennes FtsZ, FtsA, MurD, MurE et MurF et d'identifier de nouveaux inhibiteurs prometteurs en vue du développement de nouvelles classes d'agents antibactériens ciblant la division cellulaire et la biosynthèse de la paroi bactérienne.

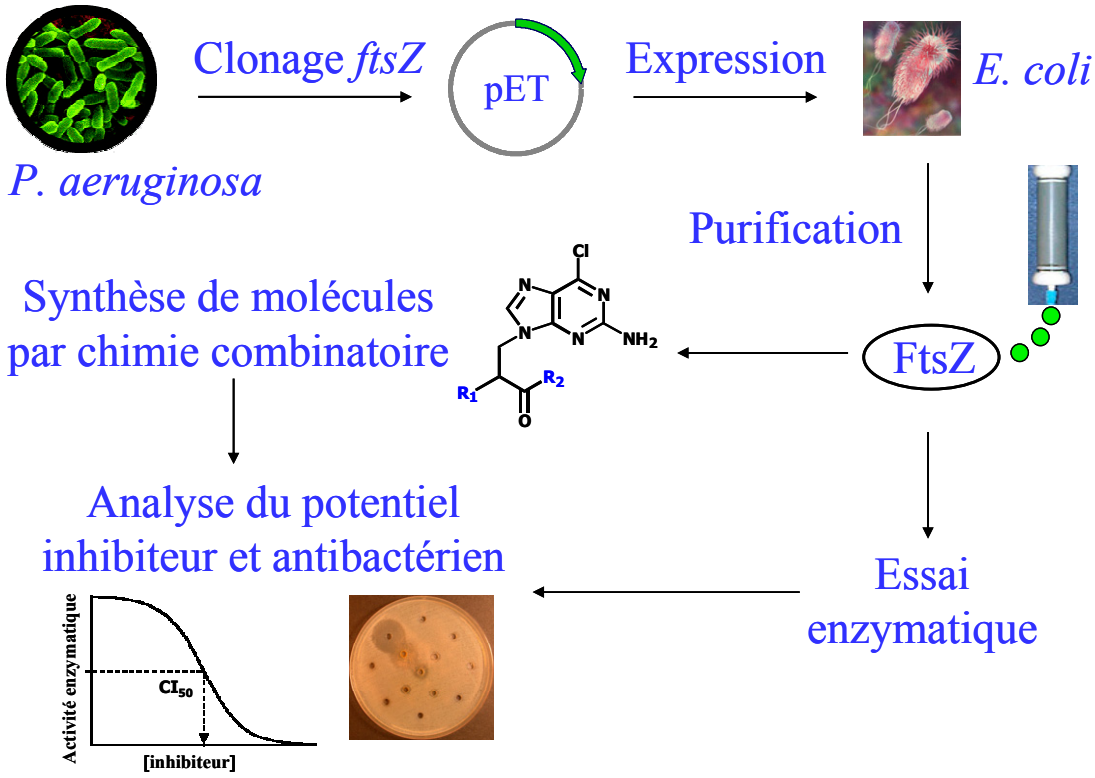

Figure 6. Schéma expérimental résumant la méthodologie employée afin d'étudier la cible antibactérienne FtsZ et de synthétiser des molécules inhibitrices par chimie combinatoire en vue du développement de nouveaux agents antibactériens ciblant la division cellulaire bactérienne.

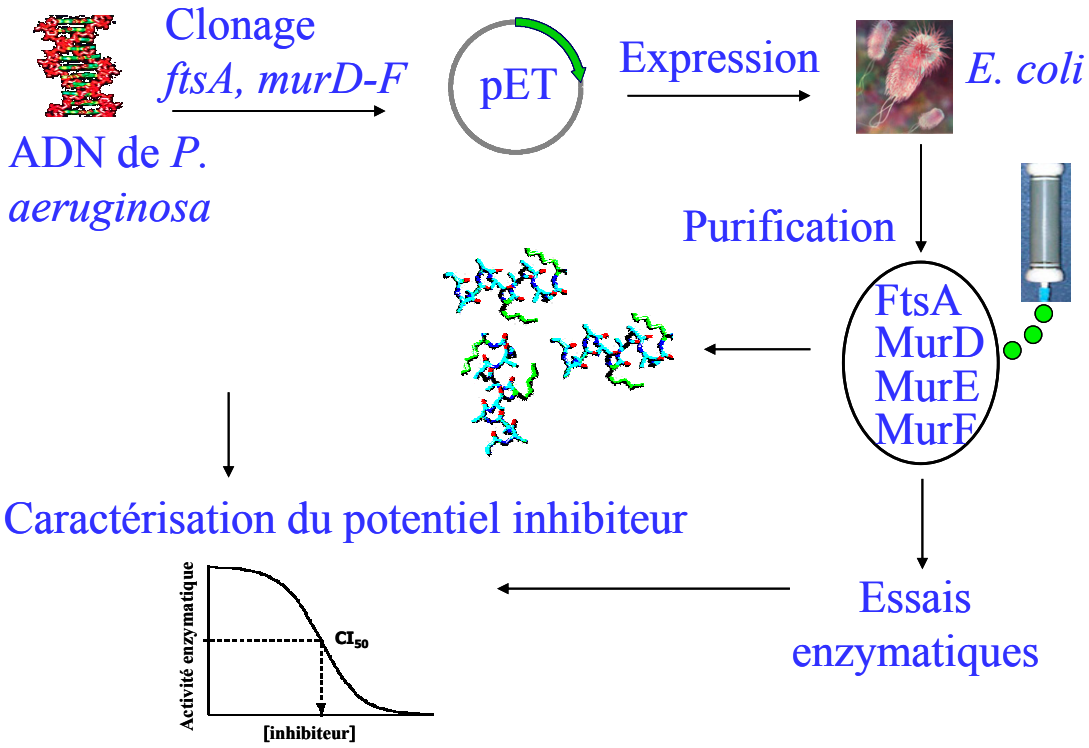

Figure 7. Schéma expérimental résumant la méthodologie employée afin d'étudier les cibles antibactériennes FtsA, MurD, MurE et MurF et de sélectionner des peptides inhibiteurs par présentation phagique.

Un dernier volet du projet de recherche exploite le potentiel antibactérien des endolysines de bactériophages. Ces enzymes dégradent la paroi bactérienne et représentent une source évoluée d'enzymes lytiques. Ainsi, le troisième chapitre du corps de cette thèse décrit la caractérisation de l'endolysine du bactériophage ϕKZ de *P. aeruginosa* en tant que nouvel agent antibactérien. Le gène codant pour l'endolysine a tout d'abord été cloné à partir de l'ADN génomique du phage ϕKZ. La protéine a ensuite été exprimée et purifiée à partir des cellules recombinantes de *E. coli*. L'activité muralytique et le pouvoir antibactérien de l'endolysine ont ensuite été caractérisés. Afin d'identifier le site de clivage enzymatique du peptidoglycane par l'endolysine, des analyses en spectrométrie de masse ont été effectuées. Cette technologie permet de séparer et de purifier les produits de dégradation du peptidoglycane par HPLC en phase inverse puis de déterminer de façon précise leur masse moléculaire (Glauner, 1988). Les données sont ensuite analysées afin de reconstituer le casse-tête en déterminant la structure des produits de dégradation. Plusieurs analyses ont

été réalisées afin d'étudier le mode de translocation de l'endolysine ainsi que son interaction avec les membranes. Ces expériences sont expliquées en détail dans un article scientifique présent dans le troisième chapitre du corps de cette thèse. Entre autres, des analyses de dichroïsme circulaire ont été effectuées afin d'observer le changement de structure secondaire de l'endolysine en présence de vésicules lipidiques synthétiques. Deux types de lipides ont été employés; le dimyristoylphosphatidylglycérol qui imite les membranes bactériennes anioniques et le dimyristoylphosphatidylcholine qui imite les membranes eucaryotes neutres. À l'aide de ces lipides, des vésicules synthétiques ont été préparées de façon à enfermer des molécules de calcéine fluorescente. Ainsi, un essai a été mis au point afin d'analyser l'interaction de l'endolysine avec les membranes en mesurant la relâche de calcéine fluorescente. La figure 8 illustre la méthodologie employée afin de caractériser cette endolysine en tant que nouvel agent antibactérien ciblant l'intégrité de la paroi bactérienne constituée de peptidoglycane.

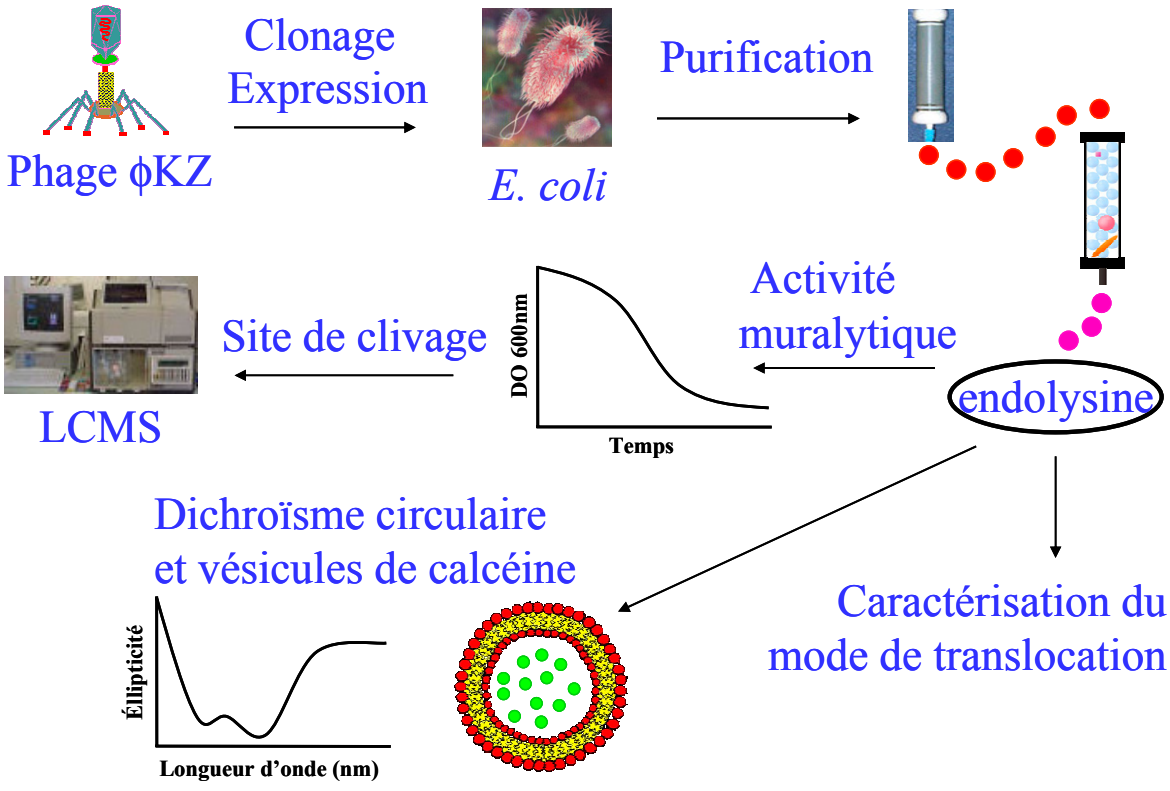

Figure 8. Schéma expérimental résumant la méthodologie utilisée afin d'étudier l'endolysine du bactériophage ϕKZ en tant que candidat prometteur pour le développement d'une nouvelle stratégie antibactérienne ciblant l'intégrité de la paroi bactérienne.

Section II - Les protéines de division cellulaire FtsZ et FtsA en tant que cibles antibactériennes et identification d'inhibiteurs par synthèse organique en parallèle et présentation phagique

Ce premier chapitre amorce le corps de ma thèse en regroupant trois articles scientifiques rédigés en anglais à des fins de publication au sein de revues scientifiques anglophones. Un premier manuscrit fait office d'introduction en résumant l'étendue de la littérature scientifique sur la division cellulaire bactérienne et les nombreuses protéines impliquées. L'article se concentre sur les protéines FtsZ et FtsA en tant que cibles antibactériennes. Par la suite, un article scientifique récemment accepté dans la revue «Bioorganic & Medicinal Chemistry» relate la synthèse de petites molécules organiques en tant qu'inhibiteurs de l'activité GTPase de FtsZ. Ces inhibiteurs démontrent un potentiel antibactérien fort intéressant en vue du développement d'une nouvelle classe d'agents antibactériens. Finalement, un article publié dans la revue «Protein Engineering Design and Selection» en mars 2005 décrit la sélection de peptides inhibiteurs de l'activité ATPase de FtsA. Ces peptides identifiés par la technique de présentation phagique représentent les premiers et les seuls inhibiteurs de FtsA caractérisés à ce jour.

Chapitre I - The bacterial cell division proteins as novel targets for antibacterial agents of the future

Résumé

Les protéines de division cellulaire en tant que nouvelles cibles thérapeutiques pour les agents antimicrobiens de l'avenir

Les mécanismes de résistance aux antibiotiques ne cessent de se développer et de se propager parmi les pathogènes bactériens en émergence et en réémergence à travers le monde. Ainsi, l'identification et la caractérisation de nouvelles cibles antibactériennes attrayantes constituent une priorité afin de développer de nouvelles classes d'agents antibactériens possédant des structures et des modes d'action inusités. La division cellulaire bactérienne représente un processus biologique essentiel et complexe mettant en scène de nombreuses protéines. Ces dernières possèdent un potentiel fort intéressant en tant que nouvelles cibles antibactériennes. Au cours de cet article de revue, un intérêt soutenu est accordé aux récentes avancées scientifiques afin de comprendre le processus de division cellulaire bactérien. Les principales caractéristiques de toutes les protéines de division cellulaire reportées à ce jour sont également résumées. Une attention particulière est consacrée à la biologie des protéines FtsZ et FtsA en tant que cibles antibactériennes spécifiques ainsi qu'aux études scientifiques ayant pour objectif d'identifier des inhibiteurs contre ces protéines de division cellulaire. Finalement, cet article de revue propose différentes avenues afin de mener à bien le développement et l'optimisation de traitements antibactériens efficaces ciblant la division cellulaire bactérienne.

Contribution des auteurs

En tant que première auteure de cet article de revue scientifique, j'ai réalisé une revue de littérature approfondie et détaillée sur la division cellulaire bactérienne et les différentes protéines impliquées. J'ai porté une attention particulière aux protéines FtsZ et FtsA en tant que cibles antibactériennes spécifiques. J'ai également relaté toutes les études scientifiques ayant pour objectif d'identifier et/ou de caractériser des inhibiteurs de la division cellulaire bactérienne. Suite à la revue de littérature, j'ai rédigé intégralement le manuscrit et j'ai préparé la figure du divisome ainsi que la tableau regroupant les principales caractéristiques de toutes les protéines de division cellulaire reportées à ce jour. Finalement, j'ai émis mon opinion sur les différentes avenues possibles afin de mener à bien le développement de nouvelles classes d'agents antibactériens ciblant la division cellulaire bactérienne. Le Dr Roger C. Levesque m'a guidée dans la conception du plan de l'article et m'a donnée de précieux conseils au sujet de la rédaction d'un article de revue scientifique. Il a également révisé le manuscrit pour en augmenter la fluidité et la qualité de la langue anglaise. Cet article sera soumis sous peu à la revue scientifique «FEMS Microbiology Reviews».

The bacterial cell division proteins as novel targets for antibacterial agents of the future

Catherine Paradis-Bleau & Roger C. Levesque

Département de Biologie Médicale, Faculté de Médecine, Université Laval, Québec, Québec, Canada, G1K 7P4

Keywords: bacterial cell division; cell division proteins, FtsZ, FtsA, antibacterial targets, antibacterial drug development

Address correspondence to: Roger C. Levesque, Département de Biologie Médicale, Pavillon Charles-Eugène Marchand, Université Laval, Québec, Québec, Canada, G1K 7P4, Tel: (1) 418 656-3070; Fax: (1) 418 656-7176; E-Mail: rclevesq@rsvs.ulaval.ca

Abstract

Antibiotic resistance has become one of the most critical global public health problems of the decade, resistance mechanisms increasing in diversity among emerging and re-emerging bacterial pathogens and spreading worldwide. Identification and characterization of new targets thus represent a high priority task to develop structurally and functionally novel classes of antibacterial agents. The bacterial cell division apparatus involves many proteins which represent excellent and unexploited antibacterial targets. In this review, we focus on recent advances in the field of bacterial cell division and we describe the principal features of all known cell division proteins. We emphasize FtsZ and FtsA as the best specific targets for antibacterial agents and we review all inhibitors active against them. We finally propose future directions for development and optimization of potent antibacterial therapies targeting the bacterial cell division process.

Introduction

The alarming worldwide emergence and re-emergence of bacterial pathogens combined with the increase and spread of antibiotic resistance has become one of the most serious public health problems over the past decade (Cohen 2000; Fauci 2001; Normark and Normark 2002; Levy and Marshall 2004). During the 20th century, the impact of bacterial infections on human mortality and morbidity was vastly decreased thanks to antibiotics, vaccines and reductions in host susceptibility and disease transmission due to improved hygiene, sanitation and nutrition (Cohen 2000). We are now witnessing an emergence of new bacterial pathogens such as *Escherichia coli* H7 and the re-emergence of formerly controlled infections such as tuberculosis (Brown and Wright 2005). This recrudescence is a consequence of the astonishing evolutionary potential of bacteria, combined with recent societal and technological changes that have increased the vulnerability of populations and the transmission of infectious agents while microbiological research has declined (Cohen 2000; Fauci 2001). Infectious diseases represent today the second leading cause of death and the leading cause of disability-adjusted life years worldwide (Fauci 2001; Walsh 2003).

The occurrence of bacterial resistance to all clinically useful antibiotics has seriously amplified the problem of the emergence and re-emergence of bacterial pathogens

(Cohen 2000). Antibiotics have existed for millions of years and microbes have developed ingenious strategies using chromosomal mutations and mobile genetic elements in evolutionary response to this selective pressure (McDermott, Walker et al. 2003; Hamilton-Miller 2004). Transfer by conjugation, transformation and transduction of genetic elements such as plasmids, transposons, integrons, bacteriophages and naked DNA have propagated resistance mechanisms among bacteria via homologous recombination, transposition and integration (Normark and Normark 2002; Levy and Marshall 2004). Mechanisms of bacterial resistance include modification or replacement of the target of the antibacterial agent, expulsion of the agent outside the cell via efflux pumps or restriction of the agent via permeability changes and enzymatic inactivation or structural alteration of the antibacterial compound (Walsh 2003; Tenover 2006). After six decades of widespread antibiotic misuse, resistance has become a global public health threat, involving all major bacterial pathogens, many of which now often express multiple resistance mechanisms. At the beginning of the 21st century, bacterial pathogens are becoming increasingly resistant in an aging, increasingly dense and sometimes immuno-suppressed host population (Levy and Marshall 2004; Harbarth and Samore 2005; Tenover 2006).

Among Gram-positive pathogens, methicillin-resistant *Staphylococcus aureus* (MRSA) and vancomycin-resistant enterococci (VRE) are of particular concern. MRSA causes 60% of the staphylococcal infections in American intensive care units and vancomycin-resistant *S. aureus* (VRSA) have also emerged (Rice 2006). Furthermore, the human immunodeficiency virus has enhanced re-emergence of multiresistant *Mycobacterium tuberculosis,* which remains the leading cause of death from a single infectious disease (Bloom and Murray 1992; Levy and Marshall 2004). Among Gram-negative pathogens, infections by *Pseudomonas aeruginosa* and *Acinetobacter spp*. have increased in frequency and severity and the worst-case scenario of infections treatable only by toxic polymyxins is now a reality (Meyer 2005). *P. aeruginosa* causes a wide variety of chronic nosocomial infections and represents the major cause of death in cystic fibrosis patients (Davies 2002).

To summarize, bacterial diseases in general and antibiotic-resistant bacterial infections specifically are increasing in both developing and developed countries, complicating treatment and increasing human morbidity (Fauci 2001; Projan 2002; Tenover

2006). To some extent, resistance can be contained by better use of antibiotics, surveillance programs, improved public health systems and research on bacterial pathogenicity and host predisposition to infection. However, development of novel approaches to treatment of bacterial infections will be crucial to the protection of human health against emerging resistant pathogens (Fauci 2001; McDermott, Walker et al. 2003; Hamilton-Miller 2004). New therapies may be developed by whole-cell screening of compound libraries, modifying existing antibacterial agents, attempting to block resistance mechanisms or by identifying new targets for antibacterial agents (Cunha 2001). However, attempting to select potent antibacterial agents from libraries will invariably yield compounds related to previously identified chemical classes and will rapidly trigger resistance, as does making new analogues from existing drugs (Desnottes 1996; Chan, Macarron et al. 2002). Lowering existing levels of resistance by conventional means appears to be extremely difficult if not impossible (Hamilton-Miller 2004). As the resistance problem is largely due to the limited repertoire of targets for antibacterial agents (fewer than 30 proteins) and as antimicrobial agent discovery is driven by the breadth and quality of potential targets, the answers lie in unexploited targets (Haselbeck, Wall et al. 2002; Brown and Wright 2005).

The perfect target for antibacterial agents would be functionally essential for bacterial viability and its inhibition would result in a lethal phenotype. It would also be highly conserved among bacterial pathogens and have no eukaryotic counterpart, be easily accessible for genetic manipulations and sufficiently expressed during host infection (Haselbeck, Wall et al. 2002). Targets required for viability are preferred because the compounds directed at them would be bactericidal and hence more efficient for treating serious infections (Miesel, Greene et al. 2003). The requirement for genetic and structural conservation of the target across all clinically relevant pathogens is based on the medical need for broad-spectrum antibiotics, since physicians often treat infections without prior identification of the infectious agents, due to the lack of rapid and precise diagnostic methods (Projan 2002; Miesel, Greene et al. 2003; Brown and Wright 2005). The ideal target typically would be an enzyme that performs a rate-limiting biochemical step with a fully elucidated mechanism amenable to high throughput screening supported by inhibitory investigations such as structure–activity relationships (Projan 2002; Miesel, Greene et al. 2003; Brown and Wright 2005). To minimize the emergence of resistance, families of

related but non-identical targets that can be inhibited by a single compound are to be preferred, (Projan 2002; Miesel, Greene et al. 2003) as are targets with invariant active-site amino acid residues, in the hope that resistance mutations would cause physiological fitness defects (Miesel, Greene et al. 2003). In this review, we provide an overview of the potential of the bacterial cell division process as a source of new targets for the next generation of antimicrobial agents.

Bacterial cell division proteins as a source of new targets for antibacterial agents

The bacterial cell division apparatus represents an excellent pool of new targets for antibacterial agents. The proteins involved in cell division are essential for bacterial growth and survival and their inhibition is not physiologically sustainable. The vast majority of these proteins are widely conserved among pathogenic bacterial species and absent in eukaryotic cells (Margolin 2000; Vicente, Rico et al. 2006). Furthermore, they are extremely sensitive to inhibition because the division process depends on recruitment of specific proteins with critical ratios in an absolutely essential cascade that forms the divisome (Projan 2002; Errington, Daniel et al. 2003; Margolin 2005). No existing antibacterial agent specifically targets either these proteins or the protein–protein interactions involved in the bacterial cell division process, suggesting that bacterial pathogens are not likely to have developed resistance mechanisms against agents that would do so. Cell division proteins thus represent very promising candidate antibacterial targets.

The divisome-forming pathway

Recent technological advances in the fields of cytology, genomics, structural biology, microscopy, biochemistry, bioinformatics and proteomics have led to deeper understanding of bacterial cell division. However, this physiological event represents one of the most complex bacterial processes and is subject to strict spatial, temporal and quantitative regulation that remains poorly understood. Overall, bacteria divide by binary fission, in which medial constriction of the mother cell yields two identical daughter cells. Bacterial

cells grow until they reach a critical size (usually 2 × unit mass, or volume) at which point chromosomal DNA replication is initiated at *oriC* via the DnaA initiator protein. The newly replicated chromosomes are then unlinked and segregation of the homologous genomes through the mother cell poles begins, with the help of the Muk proteins. Fission occurs when the distance between chromosomal centres exceeds half the cell length (Donachie 1993). The main cell division protein, FtsZ, polymerizes to form a ring around the inner surface of the cell membrane. Cytokinesis is then coordinated by a group of septation-specific proteins that localize and assemble at mid-cell at a specific time in the cell cycle to form the divisome. Recruitment of cell division proteins at mid cell is believed to be driven primarily by a complex protein–protein interaction network (Goehring and Beckwith 2005). This mid cell apparatus overlaps the bacterial inner membrane and the cell wall layer of the nascent daughter cells. Proteins of the divisome act in synergy to form the mid cell septum and physically separate the progenitor daughter cells (Den Blaauwen, Buddelmeijer et al. 1999). The coordinated biochemical and physical actions of the divisome-containing proteins, combined with osmotic pressure and surface tension, produce an invagination site continually driven by the divisome (Nanninga 1998). The constriction of the cytoplasmic ring tethered to the membrane pulls the inner membrane inward with the help of the divisome-containing proteins and the cell wall grows inward as a covalently bonded layer following the contracting ring. A specific and localized enhancement of cell wall biosynthesis forms a complete double cross-wall across the cell centre, completing the septum and forming the new cell poles of the daughter cells. Even as the peptidoglycan layer grows inward, cell wall hydrolases are at work splitting the septal cell wall to separate the daughter cells. Finally, the peptidoglycan layer is connected to the outer membrane of Gram-negative cells by a variety of bridging proteins such as Lpp (Braun's lipoprotein). Thus, the outer membrane is expected to follow the separating cell wall layers inward passively as new bridging proteins are incorporated in the wake of the peptidoglycan synthases (Donachie 1993; Weiss 2004). The cell wall biosynthesis pathway will be discussed in greater detail later in this article. The known functions of bacterial cell division proteins are described below. In spite of significant efforts, the functions of some cell division proteins still remain shrouded in mystery (Goehring and Beckwith 2005).

In the 1960s, a large collection of thermo-sensitive mutations affecting the growth and replication of *E. coli* allowed identification of the *fts* (filamentation thermo-sensitive) genes encoding essential cell division proteins. Mutants defective in these genes are specifically defective in cell division and display a characteristic filamentous phenotype at a non-permissive temperature, as a result of continuous growth without division (Van De Putte, Van et al. 1964; Hirota, Ryter et al. 1968; Goehring and Beckwith 2005). The vast majority of the cell division proteins are thus designated by the prefix Fts, derived from the unsustainable phenotype observed when the thermo-sensitive proteins are inactivated. This was extended to other cell division proteins, even if they were identified by methods other than production of thermo-labile filamentous mutants. Furthermore, Fts proteins such as FtsH, FtsJ, and FtsY, turned out to be involved in general processes that have pleiotropic effects on cell division (Vicente, Rico et al. 2006). The conserved *dcw* cluster located at 2 min on the genetic map of *E. coli* contains 16 genes essential for the cell division and cell wall biosynthesis pathways (Dai and Lutkenhaus 1992). Genes of this cluster are widely conserved and carefully regulated to ensure the proper cell division process (for a review see Dewar and Dorazi 2000).

As the order of cell division protein recruitment to the division site is thought to reflect their implication during cell division, let us begin by summarizing the known functions of these proteins, based on order of assembly in the divisome. In this hierarchy, a given protein requires the presence of all upstream proteins in order to localize at mid cell and is in turn required for the localization of all downstream proteins. A dependency of each cell division protein on most of the other proteins has been reported and no observable initiation of cell division takes place until all the cell division proteins are localized (Buddelmeijer and Beckwith 2002). Assembly of the divisome at the nascent division site is both highly regulated and highly dynamic, while the recruitment hierarchy reflects dependence relationships and does not necessarily reflect a temporal order (Goehring and Beckwith 2005). A linear view of the sequence of recruitment is confounded by the complexity of the cell division protein-protein interaction network. The recruitment cascade may be derived from a set of strong interactions that dominate under physiological conditions, while weaker interactions collectively strengthen the divisome but are detected individually only in experimental set-ups in which the proteins are overproduced (Vicente,

Rico et al. 2006). It is thus suggested that a cooperative association among the divisome proteins drives the cell division assembly, forming a dynamic multi-protein structure at the septum site, as is the case in *Bacillus subtilis,* in which all division proteins are completely interdependent for recruitment and assembly at the division site (Errington, Daniel et al. 2003; Karimova, Dautin et al. 2005). Overall, the order of assembly of proteins at mid cell for forming the divisome is as follows: FtsZ, [FtsA, ZipA, ZapA, YlmF], (FtsE, FtsX), FtsK, FtsQ, (FtsB, FtsL), FtsW, FtsI, FtsN, AmiC, EnvC, where the proteins within brackets are independent of each other but dependent on FtsZ and those within parentheses assemble interdependently and simultaneously at the division site (adapted from Vicente, Rico et al. 2006). Finally, the cell division process occurs in two steps, in which the Z-ring assembles with FtsA, ZipA and ZapA over a period of about 20 min until the later-recruited proteins downstream from FtsK localize in the ring for constriction. The Z-ring complex may be involved in the switch from cylindrical to polar cell wall biosynthesis, whereas the much later localizing cell division proteins may be responsible for the modification of the cylindrical envelope shape into that of two new poles (Aarsman, Piette et al. 2005).

FtsZ and FtsA

The most important protein of the bacterial cell division apparatus is unquestionably the cytoplasmic GTPase enzyme FtsZ. This protein is at the top of the hierarchical recruitment into the divisome and its polymerization into the Z-ring just underneath the cytoplasmic membrane allows the physical separation of the daughter cells (Lutkenhaus and Addinall 1997). Localization of FtsZ at mid-cell initiates the cell division process following bacterial genome replication and is subject to a strong temporal and spatial regulation. FtsZ accumulates at the cell division site between the replicated nucleoids during the segregation process and polymerizes to form an equatorial division ring. After physical septation of the mother cell, the Z-ring depolymerizes and new rings form at the mid cell of daughter cells (Margolin 1999). This major protein will be discussed in detail as a prospective specific target for antibacterial agents later in this review. The second most important component of the cell division apparatus is the ATPase enzyme FtsA. This protein interacts with FtsZ localizing at mid cell, stabilizes the Z-ring and is essential for the recruitment of all other downstream proteins forming the divisome. This key protein will also be discussed in depth

as a specific target for antibacterial agents in this review. The cell division process would not be possible without the remaining proteins required to form an efficient divisome apparatus. Before exploring the advantages of FtsZ and FtsA as specific targets for antibacterial agents, we will summarize the principal known characteristics and functions of the other proteins involved in the cell division apparatus, with focus on identifying new targets in this pathway.

ZipA

Z-interacting protein A (ZipA) is essential for the cell division process in Gram-negative bacteria. ZipA is recruited to the division site by FtsZ and is important for the subsequent recruitment of divisome proteins downstream (Hale and de Boer 1999; Hale and de Boer 2002; Pichoff and Lutkenhaus 2002). ZipA shows structural and functional similarity to microtubule-associated proteins and is able to stabilize the Z-ring by enhancing bundling of the FtsZ proto-filaments (RayChaudhuri 1999; Hale, Rhee et al. 2000). Furthermore, ZipA tethers the Z-ring to the inner side of the cytoplasmic membrane via an N-terminal membrane anchor connected to the C-terminal FtsZ-binding domain by a long flexible linker (Ohashi, Hale et al. 2002). The ZipA protein has also been found to homodimerize (Di Lallo, Fagioli et al. 2003). It has been shown that ZipA is required both for recruitment of the ^{D}MinC/DicB complex to the Z-ring and DicB-induced inhibition of cell division, which secures proper localization of the Z-ring at mid cell (Johnson, Lackner et al. 2004). The Min system will be discussed further in this review.

ZapA

The widely conserved ZapA protein (also named YgfE in *B. subtilis*) interacts with FtsZ to enhance the polymerization of the Z-ring. This small ZapA protein induces FtsZ proto-filaments to associate into large bundles, thereby stabilizing and tuning Z-ring polymerization. ZapA appears to be dispensable for division under normal growth conditions yet essential at low FtsZ concentrations or in the absence of the modulators EzrA or DivIVA, whose usual presence inhibits Z-ring assembly (Gueiros-Filho and Losick 2002). Resolution of the crystal structure of ZapA from *P. aeruginosa* reveals two dimers associating via an extensive C-terminal coiled-coil protrusion to form an elongated anti-

parallel tetramer. The ZapA dimer is thought to engage FtsZ molecules on a stoichiometric basis over the whole Z-ring to form stabilizing molecular bridges between FtsZ proto-filaments (Low, Moncrieffe et al. 2004). ZapA has been found to interact strongly with both FtsZ and FtsA in a two-hybrid system (Di Lallo, Fagioli et al. 2003).

YlmF

Recently, two independent research groups have identified a new cell division protein. The YlmF protein was first discovered by Hamoen *et al* and renamed SepF (Hamoen, Meile et al. 2006). This protein is conserved in Gram-positive bacteria and encoded by the *ylm* locus of *B. subtilis,* located next to the *dcw* cluster. Localization of SepF at the division site is Z-ring dependent and plays a non-essential role in septum development. It becomes essential in the absence of EzrA, a negative regulator of FtsZ. SepF interacts with itself and with FtsZ and is thought to participate in the constriction process and/or the synthesis of the septum cell wall. It is thus postulated that SepF acts as a late division protein, even though it is an early recruit to the Z-ring (Hamoen, Meile et al. 2006). The non-essential YlmF protein identified by Ishikawa *et al*. has also been found to localize at the division site in an FtsZ-dependent manner and to interact with both FtsZ and itself, becoming essential in the absence of FtsA (Ishikawa, Kawai et al. 2006).

FtsEX

FtsE and FtsX are widely conserved among bacteria and display homology with the ABC transporter super-family of proteins. FtsE is the ATP-binding cassette (ABC) component while FtsX is the membrane component. FtsEX seems to be unrelated to import and both components are involved in the cell division process. FtsE and FtsX are recruited to the septal ring by FtsZ, FtsA and ZipA. In turn, FtsEX is involved in the recruitment of downstream cell division proteins. FtsEX is non-essential for cell division at high salt concentration. In the absence of salt, cells depleted of FtsEX stop dividing before any change in growth rate is apparent. It has been proposed that ionic conditions affect the folding, assembly, and/or function of one or more of the downstream division proteins and that there is a synergistic effect when combined with the loss of FtsEX. The septal ring would thus fail to assemble or function properly if both salt and FtsEX were lacking.

Addition of salt can rescue the ring slightly in the absence of FtsEX. As for many downstream division proteins, the exact roles of FtsEX remain to be determined (Schmidt, Peterson et al. 2004).

FtsK

The next protein involved at the division site is the large multifunctional membrane-bound FtsK, which coordinates the cell division process and has a major role in the segregation of the replicated chromosomes (Liu, Draper et al. 1998). The *ftsK* gene represents an exception among the genes involved in bacterial cell division since it does not belong to the *dcw* cluster but rather lies at 20 minutes on the *E. coli* genetic map. Transcription of *ftsK* is partially controlled by an SOS-inducible promoter and the increase of *ftsK* expression as part of the SOS system increases the resistance to DNA damage via the RecA-dependent DNA protection and repair system (Wang and Lutkenhaus 1998; Diez, Gustavsson et al. 2000; Dorazi and Dewar 2000). FtsK is also involved in the XerCD-mediated site-specific recombination process at the *dif* site, which is required to resolve chromosome dimers formed during the replication process into monomers for proper segregation (Recchia, Aroyo et al. 1999). The ATPase domain of FtsK tightly regulates the Xer recombinases and mediates a switch in the catalytic state of XerCD such that XerD initiates duplex recombination (Aussel, Barre et al. 2002). FtsK also interacts with the ParC subunit of topoisomerase IV, recruits it close to the septum and stimulates its chromosome decatenation activity (Espeli, Lee et al. 2003). FtsK thus has a major role in resolving linkages between the newly replicated chromosomes as part of the topoisomerase IV and XerCD recombinase process to allow an efficient genome partitioning. The N-terminal transmembrane domain of FtsK is essential for septum formation and for the recruitment of the downstream proteins FtsQ, FtsL and FtsI. FtsK has been shown to interact directly with FtsQ, FtsI and FtsZ and to heterodimerize with FtsL (Chen and Beckwith 2001; Di Lallo, Fagioli et al. 2003; Karimova, Dautin et al. 2005). The intermediate linker domain of FtsK also has a role in cell division, while the C-terminal domain is required for ATP-dependent chromosome dimer resolution by XerCD *dif* site-specific recombination and DNA translocation (Bigot, Corre et al. 2004). FtsK is thus an efficient ATP-dependent translocase that moves towards distant *dif* sites and applies force to work against a heavy

load. FtsK is rendered stationary by its insertion into the septum and must move a considerable section of the chromosome burdened with large transcription and translation complexes. At the time of cell division, some DNA may remain in the septal region and FtsK appears to act as a pump to clear this region of DNA across the closing septum in order to allow correct segregation of the daughter chromosomes. Bacterial cells can divide with the singular N-terminal portion of FtsK but the resulting chromosomal segregation defects may cause guillotination of the chromosomes (Liu, Draper et al. 1998; Hendricks, Szerlong et al. 2000). FtsK displays structural homology with the archeal HerA protein, similarly mediating DNA pumping into the progeny cells during archeal cell division and repairing double-stranded breaks (Pease, Levy et al. 2005). These observations indicate that FtsK plays a central role in chromosome segregation both by activating recombination and decatenation and by pumping chromosomal DNA across the septum (Iyer, Makarova et al. 2004).

FtsQ

The FtsQ protein, named DivIB in *B. subtilis*, is thought to be the next protein recruited for forming the divisome. This bitopic membrane protein is specifically required for septum formation (Carson, Barondess et al. 1991; Harry, Partridge et al. 1994) and is essential for the recruitment of downstream cell division proteins such as FtsL and FtsW (Chen, Minev et al. 2002; Mercer and Weiss 2002). Several clues suggest that FtsQ may be involved in peptidoglycan synthesis. It is found only in bacteria with a cell wall, shares limited sequence identity in *E. coli* with the Mpl enzyme involved in peptidoglycan recycling, and its concentration is higher in bacteria with thicker cell walls (such as *B. subtilis*). In *Caulobacter crescentus* FtsQ has conserved motifs found in peptidoglycan binding proteins and it has a topology that would allow its essential periplasmic domain to interact with the cell wall synthesis apparatus (Carson, Barondess et al. 1991; Chen, Minev et al. 2002; Martin, Trimble et al. 2004). Moreover, FtsQ has been shown to interact with FtsI, the cell wall biosynthesis enzyme specifically involved in the division process (Goehring and Beckwith 2005). FtsQ also interacts with FtsA, FtsK, FtsL, FtsB, FtsW and FtsN (Di Lallo, Fagioli et al. 2003; Goehring and Beckwith 2005; Karimova, Dautin et al. 2005; Vicente and Rico 2006). Indeed, FtsQ is the cell division protein that establishes the highest number

of interactions with the other proteins of the divisome. It has a polypeptide transport-associated (POTRA) domain, which is functionally associated with protein interactions or chaperone function, suggesting that it might be a connector protein that nucleates or regulates the assembly of the other membrane proteins (Sanchez-Pulido, Devos et al. 2003; Vicente, Rico et al. 2006).

FtsL

The next essential cell division protein, FtsL, is a small bitopic inner membrane protein with a poorly conserved primary sequence. Several bacterial genomes contain short open reading frames at the same position in the *dcw* cluster and have similar predicted secondary structures, suggesting that FtsL is indeed conserved (Vicente, Rico et al. 2006). FtsL localizes at the septum where it forms a ring analogous to the cytoplasmic Z-ring (Guzman, Barondess et al. 1992). It has an unusual periplasmic repeated heptad motif reminiscent of leucine zipper structures, which may indicate a structural role (Ghigo, Weiss et al. 1999). This domain has been shown to be important for localization of FtsL at the division plane, for proper cell division and for the formation of sodium dodecyl sulfate-resistant multimers. This is consistent with the predicted propensity of the FtsL periplasmic domain to adopt a helical coiled-coiled multimerization structure conserved in all Gram-negative and Gram-positive FtsL homologues (Ghigo and Beckwith 2000). FtsL has been found to heterodimerize with FtsK, to interact with FtsQ, FtsW and FtsB and to recruit FtsB and FtsW (Sievers and Errington 2000; Buddelmeijer, Judson et al. 2002; Mercer and Weiss 2002; Di Lallo, Fagioli et al. 2003; Karimova, Dautin et al. 2005). Finally, a recent study highlights a possible direct or indirect role of FtsL in promoting Z-ring disassembly and constriction (Kawai and Ogasawara 2006).

FtsB

FtsB (originally called YgbQ and also called DivIC in *B. subtilis*) is a membrane cell division protein presenting a periplasmic leucine zipper-like motif similar to FtsL. FtsB is required for the proper recruitment of FtsL indicating that FtsL and FtsB may form heterodimers and co-dependently localize at the division site (Buddelmeijer, Judson et al. 2002). FtsL and FtsB are thermodynamically unstable proteins that are likely to be

unfolded and degraded unless stabilized by interactions with other components of the divisome, such as FtsQ (Robson, Michie et al. 2002; Sanchez-Pulido, Devos et al. 2003). Indeed, it has been shown that FtsQ, FtsL and FtsB are interdependent for their stabilities and localization. These proteins form a well-conserved trimeric complex in which FtsQ associates with a heterodimer of FtsL and FtsB. It is proposed that assembly of this essential complex is regulated during the cell cycle through controlled formation of the FtsB/FtsL heterodimer (Noirclerc-Savoye, Le Gouellec et al. 2005; Buddelmeijer and Beckwith 2004).

FtsW

The next actor involved in the division site is the large membrane protein FtsW, which contains up to 10 membrane-spanning segments (Gerard, Vernet et al. 2002). FtsW is present in virtually all bacteria that have a peptidoglycan cell wall and recruit FtsI to the division site. It is also proposed that FtsW facilitates the septal peptidoglycan synthesis of FtsI (Boyle, Khattar et al. 1997; Mercer and Weiss 2002). It is a member of the SEDS (shape, elongation, division and sporulation) family of proteins and hence related to cell wall synthesis class B PBP (penicillin-binding protein) enzymes (Henriques, Glaser et al. 1998). FtsW is similar to the RodA protein of *E. coli* and to the SpoVE protein of *B. subtilis* and is thought to collaborate with the cognate FtsI enzyme (Ikeda, Sato et al. 1989). In Gram-negative bacteria, *ftsW* is always physically linked to *murG,* which is responsible for the synthesis of the lipid-linked peptidoglycan precursor and it has been proposed that FtsW and RodA might be involved in the translocation of this precursor through the cytoplasmic membrane (Gerard, Vernet et al. 2002). FtsW has been shown to interact directly with FtsQ, FtsL FtsI and FtsN (Di Lallo, Fagioli et al. 2003). Furthermore, FtsW from *M. tuberculosis* interacts with FtsZ via a prominent C-terminal extension of FtsW that is absent in other bacteria. In mycobacteria, the interaction between FtsW and FtsZ allows the formation of productive FtsZ rings. Since the mycobacterial genome lacks any identifiable analogues of ZipA and FtsA, the role of FtsW could be to tether FtsZ to the membrane and link septum formation to peptidoglycan synthesis (Datta, Dasgupta et al. 2002; Rajagopalan, Maloney et al. 2005).

FtsI

The bitopic membrane protein FtsI achieves the synthesis of the septation cell wall. FtsI is a penicillin binding protein (PBP) of high molecular mass named PBP3 in *E. coli* and PBP 2B in *B. subtilis*. The massive insertion of peptidoglycan triplets at the site of septation by FtsI forms the cell wall septum and widely contributes to the physical in-growth and separation of daughter cells. Since FtsI is integrated into the internal membrane, synthesis of the cell wall septum follows inward when the membrane invaginates (Weiss 2004). The constriction of the outer cell membrane is also coupled to the highly localized synthesis of septal cell wall (Bernhardt and de Boer 2003). The final stages of peptidoglycan synthesis involve flipping the lipid-linked precursor from the cytoplasm to the periplasm and its incorporation into the cell wall via transglycosylation and transpeptidation reactions (El Zoeiby, Sanschagrin et al. 2003). The FtsI enzyme efficiently catalyzes transpeptidation reactions but lacks glycan polymerization activity (Adam, Fraipont et al. 1997). Indeed, FtsI is a transpeptidase that catalyzes cross-linking of the cell wall exclusively at the developing septum and other cell wall biosynthesis enzymes must be present to generate the newly formed polar cap cell wall (Bernhardt and de Boer 2003). Furthermore, FtsI performs a precise transpeptidase reaction specific to the septum and this catalytic activity depends on division status and on a preference for tripeptide side-chain substrates (Goehring and Beckwith 2005). It has been hypothesized that the catalytic activity of FtsI is stimulated by interactions with other division proteins such as FtsW (Eberhardt, Kuerschner et al. 2003). FtsI is required for the proper recruitment of FtsQ and FtsL in *B. subtilis* and of FtsN in *E. coli* (Daniel, Harry et al. 2000; Wissel and Weiss 2004). Finally, FtsI is thought to homodimerize and to interact directly with FtsA, FtsK, FtsQ, FtsW and FtsN (Di Lallo, Fagioli et al. 2003; Karimova, Dautin et al. 2005).

FtsN

FtsN is an essential cell division protein recruited to the divisome of Gram-negative bacteria (Margolin 2000). FtsN has a simple bitopic topology and localizes to the septum in a ring pattern similar to that observed for FtsZ (Addinall, Cao et al. 1997). The C-terminal region of FtsN has a weak sequence similarity to the non-catalytic domain of certain cell-wall-degrading enzymes such as CwlC from *B. subtilis*. FtsN exhibits an amidase-like fold

at its C-terminus, which has been shown to bind peptidoglycan, but no cell-wall-degrading activity has been detected. FtsN may thus either stabilize the septal region or have a function in peptidoglycan remodelling (Ursinus, van den Ent et al. 2004). Finally, FtsN is thought to homodimerize, to be required for the proper localization of AmiC and to interact with FtsA, FtsQ, FtsW and FtsI (Bernhardt and de Boer 2003; Di Lallo, Fagioli et al. 2003; Karimova, Dautin et al. 2005).

AmiC

The periplasmic N-acetylmuramoyl-L-alanine amidase AmiC of *E. coli* localizes at the division site at the beginning of the constriction process. This non-essential bacterial cell division enzyme hydrolyzes cell wall cross-links by cleaving the peptide moiety from N-acetylmuramic acid while helping to split the septal cell wall to complete the cell division process. AmiC is translocated to the periplasm via the Tat protein export pathway as a folded protein and is then recruited at mid-cell via FtsN. This may explain why a blockage of the Tat system has been associated with a disturbed cell septation phenotype and pleiotropic defects of the outer membrane (Stanley, Findlay et al. 2001). This chain-forming phenotype is observed when AmiC is defective, since the constriction of the outer cell membrane is coupled to the septal cell wall. In-growth and separation of the bacterial cell wall are expected to require extensive synthesis, remodelling and degradation of peptidoglycan (Goehring and Beckwith 2005). It is thus proposed that other cell wall degrading enzymes must be present at the septal ring to cleave the septal cell wall and properly separate the daughter cells (Bernhardt and de Boer 2003). For example, the Atl autolysin enzyme of *S. aureus* is analogous to AmiC, localizes at the division site and seems to be involved in the bacterial cell division process (Baba and Schneewind 1998; Weiss 2004).

EnvC and EnvA

EnvC (YibP) is part of the septal ring apparatus and is proposed to represent a lysostaphin-like metallo-endopeptidase with peptide cross-link hydrolytic activity. In contrast to AmiC, it is predicted that EnvC is translocated to the periplasm by the general secretory (Sec) pathway. EnvC has been shown to possess a cell-wall-degrading activity and is thought to

play a modest role in septal cell wall cleavage to allow outer membrane constriction and daughter cell separation (Bernhardt and de Boer 2004). The EnvA protein was originally thought to be involved in the cell division process through *N*-acetylmuramyl-L-alanine amidase activity (Wolf-Watz and Normark 1976). It turns out to be the UDP-3-*O*-acyl-GlcNAc deacetylase involved in the second enzymatic step in lipid A biosynthesis and is not involved directly in bacterial cell division (Young, Silver et al. 1995). Some years later, Heidrich *et al* showed that the amidases AmiA, AmiB and AmiC are involved in splitting of the cell wall septum during cell division, confirming that highly stressed cell wall trimeric and tetrameric cross-bridges are concentrated at the cell division plane and have to be hydrolyzed for proper cell division. It is suggested that the role of EnvA in cell division could be associated with other changes in the cell wall and not necessarily directly related to amidase activity (Heidrich, Templin et al. 2001). EnvA may display multiple functions or its function in the biosynthesis of lipid A may be involved in the cell division process by helping to link the other membrane to the in-growing cell wall layer.

Other proteins required for the bacterial cell division process

In addition to the proteins described above, others are also required for cell division but are not specific for this process. The major membrane phospholipid phosphatidylethanolamine is essential for proper Z-ring formation and for the constriction process. A lack of phospholipid phosphatidylethanolamine may affect the interaction of FtsZ with membrane nucleation sites and alter Z-ring structure to delay or prevent its constriction (Mileykovskaya, Sun et al. 1998).

The chaperones GroEL and HscA are also involved in proper Z-ring formation (Uehara, Matsuzawa et al. 2001; Ogino, Wachi et al. 2004). Localization of GroEL is strictly dependent on FtsZ and GroEL temperature-sensitive mutants form elongated cells having asymmetrically localized Z-rings or none at all at the restrictive temperature. It thus seems likely that GroEL is required for recruitment of cell division proteins to the Z-ring or the maintenance of the assembled divisome. It is also possible that GroEL works simply to stabilize the Z-ring or to allow the efficient polymerization of FtsZ (Ogino, Wachi et al. 2004).

The S-adenosylmethionine synthetase protein (SAM) is required for a large number of reactions in the cell as methyl donor and has been shown to be essential for the cell division process and for proper recruitment of FtsQ, FtsW, FtsI or FtsN to the divisome. The requirement for SAM suggests that some methylation reaction may be needed in the complete assembly of the septal ring (Wang, Arends et al. 2005). The potential bacterial cell division gene *mraW* is universally conserved in bacterial genomes and is associated with other division genes. The essential *mraW* gene encodes a cytoplasmic *S*-adenosyl-methionine-dependent methyltransferase of unknown function. This protein may collaborate with SAM in the cell division process (Carrion, Gomez et al. 1999; Wang, Arends et al. 2005).

Many cell division proteins have been identified over the past few years and various other proteins will certainly be discovered to shed additional light on the cell division mechanism. Several studies implicate non-division PBPs in the bacterial cell division process and demonstrate that their activity is essential for both lateral and septal cell wall biosynthesis. In *B. subtilis*, all class A PBPs, many class B PBPs and low-molecular-weight PBPs are localized at the division site and PBP1 has been found to be required for proper septum formation (Scheffers and Errington 2004; Scheffers, Jones et al. 2004). In *E. coli*, the bifunctional transpeptidase-transglycosylases PBP1A, PBP1B and the monofunctional transpeptidase PBP2 are believed involved in the cell division process (Holtje and Heidrich 2001; Den Blaauwen, Aarsman et al. 2003). It has also been suggested that septal cell wall synthesis could be performed by the conserved monofunctional glycosyltransferase encoded by the *mgt* gene. This enzyme is able to use the lipid-II precursor as substrate, yielding weakly cross-linked cell wall products available to be cross-linked by the transpeptidase FtsI (Di Berardino, Dijkstra et al. 1996; Aarsman, Piette et al. 2005). Furthermore, many cell-wall-degrading enzymes are believed required to complete daughter cell separation efficiently. The amidases are thought to be predominant and the endopeptidase and lytic transglycosylase enzymes must also play a role in hydrolyzing the cell wall septum (Heidrich, Templin et al. 2001; Holtje and Heidrich 2001).

The need to identify specific antibacterial agents targeting the cell division process

The β-lactam drugs pipericillin, cephalexin and aztreonam preferentially inhibit FtsI activity while specifically blocking cell division without significantly inhibiting the activity of other PBPs that synthesize the lateral cell wall. These drugs are currently the only known antibacterial agents that directly target the cell division apparatus (Pogliano, Pogliano et al. 1997; Margolin 2000). Inactivation of FtsI by antibiotics induces SOS exposure, altering the lethal effects of these drugs (Miller, Thomsen et al. 2004). This induction enhances the survival of bacteria exposed to β-lactams and may affect the transfer of genetic material while increasing dissemination of antibiotic resistance among microbial populations (Beaber, Hochhut et al. 2004; Miller, Thomsen et al. 2004). Other specific antibacterial targets must thus be identified and exploited in order to develop new classes of antibacterial agents that inactivate the bacterial cell division process and cause cell death. All the mentioned proteins involved in the bacterial cell division process present interesting advantages as specific drug targets. All display multiple functions and protein-protein interactions essential for proper division of daughter cells. We selected FtsZ and FtsA as the best specific targets among the pool of cell division proteins.

FtsZ as a specific target

FtsZ represents an excellent target for new antibacterial agents for several reasons. It is the most important protein of the bacterial cell division process and the first known to localize at the division site, where it performs the process-initiating step. FtsZ polymerizes into a circumferential ring-like structure (the Z-ring) abutting the inner membrane to allow the physical separation of the daughter cells (Bi and Lutkenhaus 1991; Addinall, Bi et al. 1996; Lutkenhaus and Addinall 1997). Indeed, inactivation of FtsZ is lethal for bacteria and leads to the formation of long filaments with neither constriction nor colony-forming ability (Begg and Donachie 1985; Dai and Lutkenhaus 1991). FtsZ is also the most conserved protein of the cell division apparatus and almost all pathogenic bacteria contain a single copy of the *ftsz* gene (Margolin 1999; van den Ent, Amos et al. 2001). Furthermore, FtsZ is at the top of the hierarchic recruitment, acting as a framework for the divisome. FtsZ is thus exclusively essential for the recruitment of all other cell division proteins, none of which

are seen at mid cell in its absence (Buddelmeijer and Beckwith 2002). The polymerization of FtsZ is coupled with its essential GTPase activity and this quantifiable enzymatic activity can be exploited to screen and analyze inhibitory molecules (de Boer, Crossley et al. 1992). The FtsZ substrate is commercially available and various enzymatic assays have already been devised. FtsZ GTPase activity can be quantified via hydrolysis of radioactive GTP, (de Boer, Crossley et al. 1992; Paradis-Bleau, Sanschagrin et al. 2004) by measuring the release of inorganic phosphate or by assessing protein polymerization (Bramhill and Thompson 1994; Mukherjee, Cao et al. 1998; Yan, Sossong et al. 2001; Wang, Galgoci et al. 2003) and by a spectrophotometric assay following the real time GTPase reaction (Paradis-Bleau, Beaumont et al. 2007). The 40 kDa cytoplasmic FtsZ protein can be highly purified in substantial quantity and the crystal structures of FtsZ from many bacterial species are available as support for driving and optimizing drug development. FtsZ also displays many protein-protein interactions via its C-terminal region and these essential interactions are extremely susceptible to inhibition (see Table I). Finally, it has been confirmed that inhibition of FtsZ leads to cell lysis. Three or four hours of FtsZ depletion result in cells that are not viable and cannot be rescued. Consequently, antimicrobial compounds developed against FtsZ should be bactericidal and not merely bacteriostatic (Pinho and Errington 2003). Since FtsZ has been extensively reviewed, we will focus on the principal characteristics of FtsZ as an excellent target for antibacterial agents.

FtsZ conservation and evolution

At the heart of the cell division process, FtsZ was the first cell division protein to be identified and is by far the most highly conserved protein of the divisome (Bi and Lutkenhaus 1991; Margolin 2000). FtsZ can be divided into two major segments: a large N-terminal segment of approximately 320 residues that is highly conserved and a C-terminal segment that is of quite variable length and less well conserved. Indeed, FtsZ proteins vary from just over 320 amino acids to over 500 amino acids due largely to differences at the C-terminus (Wang, Huang et al. 1997). FtsZ is conserved in nearly all bacteria and throughout the euryarchaeal phylum with few exceptions. Species within the *Crenarchaeota* phylum lack FtsZ and no other cell division proteins have yet been identified in these organisms. Groups of bacteria such as the planctomycetes and *Chlamydia*, also lack FtsZ homologues

(Margolin and Bernander 2004). The absence of FtsZ among these species can be partially explained by the facts that the obligate intracellular *Chlamydiaceae* may use host mechanisms for division (Vaughan, Wickstead et al. 2004). *Prosthecobacter dejongii*, a member of the verrucomicrobial group, lacks FtsZ but contains genes that encode a tubulin-like structure, although substantially different from eukaryotic tubulin (Margolin 2005). Many of the wall-less mollicutes contain FtsZ, such as *Spiroplasma kunkelii,* which has a FtsZ remarkably similar to FtsZ proteins from other eubacteria (Zhao, Hammond et al. 2004). Somehow, the free-living mycoplasma *Ureaplasma urealyticum* can divide even without an FtsZ equivalent. The mechanism by which cell division occurs in the absence of *ftsZ* is not known for any species (Margolin 2005).

FtsZ homologues have also been found in a number of eukaryotes and there is good evidence that these are required for division of either chloroplasts or primitive mitochondria, (Gilson, Yu et al. 2003; Vaughan, Wickstead et al. 2004) internal organelles that multiply by division as do bacteria but whose proliferation is regulated by the host nucleus (Kiefel, Gilson et al. 2004). With respect to their endosymbiotic origins, phylogenetic analyses show that chloroplast and mitochondrial FtsZ proteins are most closely related to FtsZ from cyanobacteria and α-proteobacteria, respectively (Vaughan, Wickstead et al. 2004; Margolin 2005). These FtsZ homologues were likely transferred to the eukaryotic host nuclear genome as part of the symbiotic process and the nuclear-encoded FtsZ homologues were imported into chloroplasts and mitochondria of primitive organisms such as protists to ensure proper division of these organelles (Osteryoung and Nunnari 2003; Kuroiwa, Nishida et al. 2006). FtsZ eukaryotic homologues have been found in organelles of green plants, red, green, brown, and golden algae and the non-chloroplast-containing mycetozoan organism *Dictyostellium discoideum*. Chloroplasts use proteins derived from the ancestral prokaryotic cell division apparatus, including the FtsZ protein, forming a ring that is presumably required for marking the division site and/or constricting the inner membrane (Amos, van den Ent et al. 2004). However, FtsZ is absent from most mitochondria, including those of fungi and animals, in which it appears that dynamin-related proteins have taken over the role of FtsZ (Vaughan, Wickstead et al. 2004; Margolin 2005). Mitochondria have lost FtsZ and largely evolved a division apparatus that

lacks bacterial cell division components (Osteryoung and Nunnari 2003; Kiefel, Gilson et al. 2004; Kuroiwa, Nishida et al. 2006).

Despite low amino acid sequence similarity between FtsZ and tubulin, the tridimensional structures of both proteins share extensive homology (Lowe and Amos 1998). FtsZ is thought to be the phylogenetic ancestor of tubulin, the building block of the eukaryotic cytoskeleton microtubules. Tubulin may thus arise from a duplication of the *ftsZ* gene followed by a series of diverging mutations (Margolin 1999). However, the weak sequence homology between FtsZ and tubulin may support the argument that both proteins are the result of convergence rather than true homology (van den Ent, Amos et al. 2001).

FtsZ GTP binding and GTPase activities

The resemblance between FtsZ and tubulin extends to the enzymatic activity of both proteins (van den Ent, Amos et al. 2001). Like tubulin, FtsZ specifically binds and hydrolyzes GTP. FtsZ contains the GTP binding sequence motif GGGTGTG, which is very similar to the tubulin signature motif GGGTGSG (de Boer, Crossley et al. 1992). A mutation altering this sequence results in loss of function *in vivo* and a loss of GTPase activity *in vitro* (Wang, Huang et al. 1997). The GTPase reaction of FtsZ can be dissociated into a GTP-dependent activation stage dependent on FtsZ concentration and a hydrolysis stage in which GTP is hydrolyzed to GDP. The GTP binding and hydrolysis activities of FtsZ have been shown to be essential for its role in bacterial cell division (de Boer, Crossley et al. 1992). FtsZ usually hydrolyzes five to eight molecules of GTP to GDP and inorganic phosphate (P_i) per minute *in vitro* (Stricker, Maddox et al. 2002; Romberg and Mitchison 2004). There is a marked difference in the GTP binding of FtsZ and tubulin. FtsZ binds GTP or GDP with a K_d in the μM range and does not require Mg^{2+} for binding but does for hydrolysis (de Boer, Crossley et al. 1992; Mukherjee, Dai et al. 1993). In contrast, tubulin binds GTP with a K_d in the nM range with Mg^{2+} required for this high-affinity binding while GDP is bound with a 100-fold lower affinity that does not require Mg^{2+} (Farr and Sternlicht 1992). The GTPase activity of FtsZ from seven organisms has been measured *in vitro* and is up to 100-fold higher than that of tubulin (Addinall and Holland 2002). Although FtsZ and tubulin share the same typical GTP-binding sequence and are GTPases, neither contains the sequence motifs that characterize the GTPase

superfamily (Lutkenhaus and Addinall 1997). Indeed, FtsZ and tubulin form a distinct family of GTPase enzymes (Nogales, Downing et al. 1998). The FtsZ active site is formed when two FtsZ monomers associate. The GTPase activity of FtsZ is activated by the catalytic residue present in the cation-coordinating T7 loop of one monomer inserted into the GTP-binding site of an adjacent monomer (Mukherjee, Saez et al. 2001; Scheffers, de Wit et al. 2002). GTP thus binds to a pocket at the top of an FtsZ subunit that comes into contact with the bottom of another subunit, of which the T7 loop is responsible for triggering hydrolysis. The polymerization of FtsZ, at least the dimerization, is thus essential for the GTPase activity (Scheffers, de Wit et al. 2002). The eukaryotic tubulin displays the same T7-dependent mechanism of GTPase activation (Erickson 1998; Lowe, van den Ent et al. 2004). In the case of tubulin heterodimers, the T7 loop of α-tubulin was thought to enhance hydrolysis of the GTP substrate bound to β-tubulin in another dimer, but it turns out that the T7 loop of β-tubulin simply traps the GTP that is bound to its own α-tubulin partner (Amos, van den Ent et al. 2004).

Polymerization of FtsZ and formation of the Z-ring

FtsZ polymerizes in a GTP-dependent fashion to form the contractile ring at mid cell (Bi and Lutkenhaus 1991). *In vivo*, formation of the Z-ring has been observed to be initiated by a single nucleation event and then to expand bidirectionally around the bacterial cell (Addinall, Bi et al. 1996). However, the FtsZ polymerization process is still unclear, since the nature of the Z-ring has limited the vast majority of the studies to *in vitro* observations.

Efficient formation of the Z-ring requires a series of successive steps in which FtsZ monomers polymerize into proto-filaments that subsequently assemble into a ring (Hamoen, Meile et al. 2006). GTP binding first induces the self-assembly of FtsZ into a head-to-tail linear polymer with potent active sites (Mukherjee and Lutkenhaus 1994; Scheffers, de Wit et al. 2002; Oliva, Cordell et al. 2004). The lateral associations between FtsZ polymers then allow the formation of bundles or sheets predicted to be extremely important *in vivo* (Marrington, Small et al. 2004). This bundling is induced by the interaction of FtsZ with the cell division proteins ZipA and ZapA (Hale, Rhee et al. 2000; Gueiros-Filho and Losick 2002). FtsZ polymer bundling is also enhanced by calcium or elevated levels of magnesium while increasing polymer length and rigidity and reducing

GTPase activity (Mukherjee and Lutkenhaus 1999; Lu, Reedy et al. 2000; Marrington, Small et al. 2004). There is interesting evidence suggesting that calcium flux may coordinate FtsZ assembly through a calcium-sensitive protein (Ferguson and Shaw 2004). In any event, it has been shown that divalent calcium ion binds directly to FtsZ and alters the bound conformation of GTP, displacing the phosphates from the active site and reducing GTPase activity. Furthermore, the specific conformational change and the flip of the guanine moiety in FtsZ-bound GTP into the macrochelate conformation move it to a more surface-exposed position, where it forms a new interface for bundling (Marrington, Small et al. 2004). The residue R174 seems to be involved in membrane interaction and bundling of *E. coli* FtsZ. However, the loop containing R174 is not conserved in the known sequences of FtsZ (Koppelman, Aarsman et al. 2004). Koppelman *et al* also described a mutant form of FtsZ that fails to support division and can assemble into proto-filaments but cannot form Ca^{2+}-induced bundles. This strongly suggests that a higher order FtsZ structure is involved in cell division. Overall, *in vitro* biochemical and microscopic studies indicate that the Z-ring is most likely composed of linear proto-filaments bundled together by lateral interactions (Carballido-Lopez and Errington 2003; Huecas and Andreu 2003).

The actual mechanism of FtsZ assembly into proto-filaments and bundles remains the subject of controversy. The vast majority of studies support the claim that the polymerization of FtsZ into proto-filaments is cooperative and implies a defined critical concentration for assembly, as for most biological polymers (Mukherjee and Lutkenhaus 1998; Mukherjee and Lutkenhaus 1999; Caplan and Erickson 2003; Huecas and Andreu 2003; Chen, Bjornson et al. 2005; Margolin 2005). This cooperative mechanism may include a monomer activation step where FtsZ undergoes nucleotide exchange from GDP to GTP followed by the formation of a weak dimer nucleus and elongation (Chen, Bjornson et al. 2005). However, the apparent cooperativity observed during FtsZ assembly is not compatible with the existence of linear single stranded filaments one subunit thick (Erickson and Stoffler 1996; Romberg, Simon et al. 2001; Chen, Bjornson et al. 2005). The appearance of single proto-filaments in electron micrographs of assembled FtsZ in the absence of bundling factors and the presence of only one binding face for a new monomer to attach into an existing proto-filament suggests an isodesmic assembly mechanism (Rivas, Lopez et al. 2000; Romberg, Simon et al. 2001; Margolin 2005). Recently, a model

of isodesmic polymerization followed by a cyclization process has been proposed to explain the cooperative behaviour earlier attributed only to the formation of double-stranded filaments (Anderson, Gueiros-Filho et al. 2004; Gonzalez, Velez et al. 2005; Mingorance, Tadros et al. 2005). In this model, FtsZ initially assembles isodesmically as a curved proto-filament and the proto-filament ends contact each other after they have reached a certain length. This cyclization process would induce the formation of additional lateral bonds while resulting in cooperativity. Indeed, proto-filament rings hundreds of nanometres in diameter have been observed (Gonzalez, Velez et al. 2005). The Z-ring could be a single cyclized proto-filament if the cyclization process is partially suppressed *in vivo*. This single cyclized proto-filament may extend into a short spiral of cyclizing proto-filaments following longitudinal pulling. Such spiral FtsZ structures are often observed *in vivo*. However, the 125–200 subunit circles would require 30 to 40 sec to assemble at the diffusion-limited assembly rate of 4.6 per sec and are therefore not compatible with the kinetics of initial assembly nor with the turnover at steady state *in vitro* and *in vivo* (Anderson, Gueiros-Filho et al. 2004; Chen, Bjornson et al. 2005; Chen and Erickson 2005; Margolin 2005). As it stands, there is currently no explanation for the cooperative assembly of a single-stranded proto-filament (Margolin 2005).

Role of the GTP binding and GTPase activities of FtsZ in the polymerization process

It is clear that FtsZ polymerizes in a GTP-dependent manner and that the GTPase activity of FtsZ regulates the assembly process (Bi and Lutkenhaus 1991; de Boer, Crossley et al. 1992; Mukherjee, Dai et al. 1993; Mukherjee and Lutkenhaus 1994; Mukherjee and Lutkenhaus 1999; Scheffers, den Blaauwen et al. 2000; Romberg, Simon et al. 2001). However, the precise role of the GTP binding and GTPase activities of FtsZ in the polymerization process is still unclear. It has been proposed that GTP hydrolysis occurs rapidly in FtsZ polymers and that this activity may be required for efficient polymerization (Mukherjee and Lutkenhaus 1998; Scheffers, den Blaauwen et al. 2000; Lu, Stricker et al. 2001; Scheffers and Driessen 2002). In this case, FtsZ subunits in the Z-ring would contain mostly GDP (Scheffers, den Blaauwen et al. 2000; Scheffers and Driessen 2002). Although GTP binding favours FtsZ polymer formation, the hydrolysis of GTP to GDP promotes polymer shortening and bending. Polymers assembled with GDP are dependent on

bundling-promoting agents, display more curvature and are substantially weaker than polymers assembled with GTP (Lu, Reedy et al. 2000; Rivas, Lopez et al. 2000; Huecas and Andreu 2003). Moreover, FtsZ polymers are greatly consolidated by addition of a non-hydrolysable analogue of GTP and destabilized by addition of GDP (Scheffers, den Blaauwen et al. 2000; Errington, Daniel et al. 2003). Finally, stable FtsZ polymers can be formed in the absence of the Mg^{2+} cofactor required for GTPase activity (Mukherjee and Lutkenhaus 1999). These observations clearly indicate that GTPase activity is not required for FtsZ polymerization. FtsZ from *M. tuberculosis* seems to behave as an exception as it requires an Mg^{2+}-dependent GTPase activity for proper assembly (Leung, Lucile White et al. 2004). Unlike other eubacterial FtsZ proteins, the *M. tuberculosis* form shows weak GTP hydrolysis activities associated with very stable polymers (White, Ross et al. 2000). It has been shown that optimal GTP-dependent polymerization and hydrolysis activities are essential for mycobacterial cell division *in vivo* (Rajagopalan, Atkinson et al. 2005).

Recently, it has been shown that curved, highly flexible and circular single-stranded FtsZ filaments can be formed with GTP or GDP (Mingorance, Tadros et al. 2005). FtsZ might thus form various GDP-containing polymers that may not be functionally active in the Z-ring (Huecas and Andreu 2003). The vast majority of the most recent studies indicate that FtsZ polymerizes with the concomitant binding of GTP and that the hydrolysis to GDP leads to rapid disassembly (Lutkenhaus and Addinall 1997; Mukherjee and Lutkenhaus 1998; Romberg, Simon et al. 2001; Stricker, Maddox et al. 2002; Errington, Daniel et al. 2003). Evidence thus supports the assertion that FtsZ monomers in the Z-ring are predominantly bound to GTP (Romberg and Levin 2003; Romberg and Mitchison 2004). A Z-ring composed of FtsZ-GTP would be stable and the release of energy would presumably occur in small quanta. This is not well suited for generating large forces, in contrast to a hypothetical FtsZ-GDP meta-stable polymer (Romberg and Levin 2003; Weiss 2004). The nucleotide-binding site of FtsZ seems to be accessible to the cytoplasm, which is rich in GTP and should therefore rapidly restore GTP binding (Oliva, Cordell et al. 2004). GTP hydrolysis would thus be the rate-limiting step for FtsZ assembly and FtsZ proto-filaments would probably consist mostly of resistant FtsZ–GTP (Oliva, Cordell et al. 2004; Romberg and Mitchison 2004). In fact, once the pool of GTP is exhausted, FtsZ proto-filaments disassemble (Mukherjee and Lutkenhaus 1998; Margolin 2005). Overall, the GTP binding

activity of FtsZ is required for proper polymerization and GTPase activity enhances depolymerization. Furthermore, FtsZ GTPase activity constitutes the basis of Z-ring assembly dynamics.

Z-ring dynamics

Although the Z-ring appears to be a static structure, FtsZ polymers are extremely dynamic both *in vitro* and *in vivo* and undergo exchange with a cytoplasmic pool of FtsZ with rapid turnover (Stricker, Maddox et al. 2002). Indeed, the Z-ring must allow a rapid and continuous disassembly and reassembly of proto-filaments at steady state in order to react to cell division defects and redeploy the Z-ring quickly (Romberg and Levin 2003; Chen and Erickson 2005). The FtsZ concentration present inside a cell is approximately one order of magnitude greater than the critical concentration required for assembly. Under these conditions, about 30% of the FtsZ molecules polymerize into the Z-ring during cell division and the rest remains in a cytoplasmic pool (Lu, Stricker et al. 1998; Stricker, Maddox et al. 2002). Interestingly, the polymerization process is rapid, since the Z-ring can be formed in a few seconds (Stricker, Maddox et al. 2002). Recent studies have calculated a half-life of about 7-8 sec for the Z-ring (Romberg and Levin 2003; Anderson, Gueiros-Filho et al. 2004; Chen and Erickson 2005). This turnover rate implies that each FtsZ molecule cycles in and out of the Z-ring approximately five times per minute. This rate is strikingly similar to the rate of GTP hydrolysis of about five to eight GTP molecules per FtsZ per minute (Stricker, Maddox et al. 2002; Romberg and Mitchison 2004; Weiss 2004). Various studies propose that remodelling of the Z-ring and assembly dynamics are indeed regulated by GTP hydrolysis (Mukherjee and Lutkenhaus 1999; Stricker, Maddox et al. 2002; Huecas and Andreu 2003; Romberg and Levin 2003; Anderson, Gueiros-Filho et al. 2004; Huecas and Andreu 2004; Romberg and Mitchison 2004; Goehring and Beckwith 2005). Consequently, factors that influence the GTP hydrolysis rate have a direct effect on the dynamic behaviour of FtsZ polymers (Mukherjee and Lutkenhaus 1998; Mukherjee and Lutkenhaus 1999). Furthermore, the turnover of FtsZ polymers decreases as GTPase activity is reduced (Anderson, Gueiros-Filho et al. 2004). The dynamic behaviour is slower without effective GTP hydrolysis and GTP consumption is accompanied by a continuous restructuring of the filaments (Mingorance, Tadros et al. 2005). It is thus proposed that

GTPase activity is the rate-limiting step of Z-ring turnover. When GTP-bound FtsZ assembles into straight polymers, active sites are formed and FtsZ can hydrolyze GTP at a rate of 5-8/min. FtsZ polymers exchange nucleotide much more rapidly than they hydrolyze it. Consequently, 80% of the FtsZ polymer subunits are bound to GTP at steady state. A step following the rapid release of the P_i product is also partially rate-limiting for the Z-ring turnover and explains that a small fraction of FtsZ subunits are bound to GDP (Romberg and Mitchison 2004). The bundling of polymers *in vivo* may explain why turnover of subunits in the Z-ring occurs at a rate somewhat slower than that seen *in vitro* without a bundling-promoting agent (Romberg and Mitchison 2004) such as Ca^{2+}, which reduces the dynamic behaviour of FtsZ assembly (Mukherjee and Lutkenhaus 1999).

Z-ring dynamics cannot be explained by mechanisms such as tubulin-like dynamic instability or tread-milling, since FtsZ polymers are composed mostly of GTP-bound monomers (Romberg and Levin 2003; Romberg and Mitchison 2004). It has been proposed that fragmentation and re-annealing may contribute significantly to the dynamics of FtsZ filament assembly (Anderson, Gueiros-Filho et al. 2004; Mingorance, Tadros et al. 2005). Since FtsZ filaments are single-stranded and consist largely of GTP-bound subunits, FtsZ proto-filaments must represent linear polymers of interacting monomers all having the potential to dissociate from neighbouring monomers. For single-stranded filaments, the balance between GTP hydrolysis and rapid nucleotide exchange along the filament could produce transient and labile monomer interactions that could make inner monomer dissociation as energetically feasible as dissociation of end monomers (Huecas and Andreu 2003; Mingorance, Tadros et al. 2005). It has been stated that since excess GDP causes proto-filament disassembly with a half time of 5 sec, GDP cannot exchange with intact proto-filaments. Chen *et al* propose instead that subunits are released following GTP hydrolysis. The subunits then exchange GDP for GTP and reassemble into new proto-filaments, all on a time scale of 7 sec. This statement contradicts the conclusion of Oliva *et al* to the effect that a gap in the FtsZ filament interface might allow nucleotide exchange (Oliva, Cordell et al. 2004). However, the model of Chen *et al* suggesting that FtsZ subunits need to disassemble to exchange the GDP product for the GTP substrate and initiate a new round of assembly seems plausible (Chen and Erickson 2005).

Comparison between the Z-ring and the microtubules

FtsZ filaments show contact points very similar to those in tubulin microtubules (Oliva, Cordell et al. 2004). However, whereas tubulin assembles into microtubules comprising 13 proto-filaments arranged around a hollow core, FtsZ proto-filaments do not assemble into microtubule-like cylindrical polymers (Lowe, van den Ent et al. 2004) but instead associate laterally to form bundles or sheets (Margolin 2005; Nogales and Wang 2006). FtsZ and tubulin form equivalent longitudinal contacts in their proto-filaments (Oliva, Cordell et al. 2004). The lateral contacts between tubulin proto-filaments are made by polypeptide loops that are missing from FtsZ (Nogales, Downing et al. 1998). GTP hydrolysis and subsequent nucleotide exchange from FtsZ filaments also differ from that of microtubules (Scheffers, de Wit et al. 2002; Oliva, Cordell et al. 2004). FtsZ proto-filaments consist of mostly resistant subunits (FtsZ–GTP) whereas microtubule proto-filaments consist mostly of GDP–tubulin subunits with a GTP cap. Microtubules are thus susceptible to rapid de-polymerization and energy release once the cap is hydrolyzed (Oliva, Cordell et al. 2004; Romberg and Mitchison 2004; Margolin 2005). The de-polymerization rate-limiting steps are GTP hydrolysis activity for FstZ and nucleotide exchange for tubulin (Oliva, Cordell et al. 2004). Moreover, FtsZ polymers are formed of identical subunits while tubulin contains two different subunits and only the β-tubulin can undergo GTP hydrolysis due to the lack of the catalytic residue on the T7 loop of the α-tubulin neighbouring subunit. The α/β-tubulin pair constitutes the “asymmetric unit” of the microtubules whereas FtsZ polymers do not present such an asymmetry and each subunit can perform GTPase activity (Leung, Lucile White et al. 2004). Both tubulin and FtsZ polymers show similar subunit spacing, become unstable after GTP hydrolysis and exhibit dynamic behaviour. *In vivo*, the Z-ring is even more dynamic than microtubules (Erickson and Stoffler 1996; Mukherjee and Lutkenhaus 1998; Stricker, Maddox et al. 2002). GTP hydrolysis kinetics differ significantly between FtsZ and tubulin, estimated at more than two orders of magnitude faster in rapidly growing microtubules than observed for FtsZ (Vandecandelaere, Brune et al. 1999; Romberg and Mitchison 2004). GTP hydrolysis arises on the order of a minute after incorporation of FtsZ into proto-filaments whereas hydrolysis by tubulin occurs in seconds or less (Romberg, Simon et al. 2001).

Z-ring constriction

Unfortunately, *in vivo* Z-ring ultra-structure is not known, nor is any mechanism of membrane constriction (Carballido-Lopez and Errington 2003). The exact nature of the constriction force also remains uncertain. Such a force could arise from a rearrangement of the Z-ring, or the division ring may contract passively and the force could come from a divisome protein such as FtsA or from septal cell wall biosynthesis (Errington, Daniel et al. 2003). However, invagination of the cytoplasmic membrane has been observed to continue in *E. coli* and *B. subtilis* even after septal cell wall synthesis has been blocked (Daniel, Harry et al. 2000; Heidrich, Ursinus et al. 2002; Weiss 2004). Moreover, FtsZ is the only conserved protein of the cell division apparatus in organisms lacking a cell wall, suggesting that it may provide the major force for the constriction (Donachie 2001). The force may be derived either from a shift in polymer curvature due to GTP hydrolysis or via a purse string model driven by de-polymerization of the Z-ring (Lu, Reedy et al. 2000; Romberg and Levin 2003). Non-equilibrium polymerization and de-polymerization reactions of actin filaments and tubulin microtubules are thought to generate force for movement in various kinds of cell motility (Theriot 2000). The precise role of the energy released by the GTPase activity of FtsZ is not clear and it might provide the contractile force to enhance the disassembly of FtsZ polymers (Huecas and Andreu 2004). The Z-ring consists primarily of FtsZ-GTP subunits and has a limited capacity to generate force, while turnover does not appear to be coupled to the constriction process (Weiss 2004). Turnover must thus be altered to enhance the release of monomer units and limit the reassembly of FtsZ monomers from the cytoplasmic pool. An unknown signal must therefore trigger ring contraction and probably disassembly as well. This might involve stimulation of GTP hydrolysis, which would increase the number of GDP-bound subunits and consequently cause the formation of curved proto-filaments (Margolin 2005). The coupling of GTP hydrolysis and polymer turnover in FtsZ bundles could be used to regulate the constriction force in several ways. The energy from hydrolysis can be used to destabilize a previously stable structure to produce mechanical work. Inhibition of GDP release by such bundling may allow polymers to use the energy from hydrolysis to curve and produce force during ring constriction. Alternatively, lateral interactions may stiffen FtsZ filaments, limiting both curvature and disassembly; the coordinated dissolution of such bundles might then allow

concerted de-polymerization during septation (Romberg and Mitchison 2004). The rapid net loss of FtsZ monomers from the tethered Z-ring could then exert a pinching force on the membrane (Margolin 2005). FtsZ polymers could also slide over each other with the help of a motor protein to reduce the circumference of the ring and provide constriction (Errington, Daniel et al. 2003).

Tridimensional structure of FtsZ

The crystal structure of *Methanococcus jannaschii* FtsZ is compact and globular (Lowe 1998). FtsZ contains four domains: a short N-terminal segment, a highly conserved core region, a variable spacer and a C-terminal conserved peptide. This domain structure applies to most FtsZ proteins but the N-terminus and variable spacer domains are highly variable in length, weakly conserved and their precise functions are unknown (Weiss 2004; Margolin 2005). Residues 38 to 227 of the core region form the Rossmann fold-like GTP-binding domain conserved in FtsZ and tubulin proteins with the characteristic six-stranded parallel β-sheet managing the GTP substrate with the core helix H7 (Erickson 1998; Lowe and Amos 1998; Nogales, Downing et al. 1998). FtsZ and tubulin share a similar GTP-binding sequence located in the T4 loop between β-sheet S4 and helix H4 (Nogales, Downing et al. 1998). Furthermore, FtsZ and tubulin display the same enzymatic mechanism requiring an interaction of a key residue for catalysis in the conserved T7 loop on the opposite side of the GTP-binding site (located between helix H7 and H8) and the GTP substrate bound in the neighbouring monomer subunit (Scheffers, de Wit et al. 2002). The substrate binds on one side of the sheet of FtsZ and makes contact with six loops: loop T1 is part of a strand-turn-helix motif and binds one side of the GDP phosphates; loop T2 interacts with the β (and probably γ) phosphate; loop T3 is farther away from the phosphates but may contact the γ-phosphate; loop T4 contains the tubulin signature motif and is the second half of the glycine-rich pocket formed by T1 and T4, which binds the phosphates on two sides; loop T5 has been called the sugar-binding loop because it contains Glu165, which binds to the hydroxyls of the ribose moiety and loop T6 contains a conserved Asn 192 residue that forms part of the guanine-binding pocket. Most of the guanine contacts are in H7, including Asp212 and Phe208, which stacks to the aromatic system of the base (Lowe 1998; Lowe and Amos 1998). The conserved core region of FtsZ is thus responsible for the GTP

binding and hydrolysis activities and is specifically required for FtsZ self-interactions (Wang, Huang et al. 1997; Margolin 2005). Recently, this core region has been shown to consist of two independently folding N-terminal and C-terminal segments: the Nt core and Ct core, respectively. The Nt core contains the GTP-binding site and binds the bottom portion of the adjacent monomer in the proto-filament, whereas the Ct core binds the top portion of the adjacent monomer in the proto-filament (Oliva, Cordell et al. 2004; Margolin 2005). Finally, the conserved C-terminal peptide is exposed on the surface of the FtsZ filaments and is available to interact with other cell division proteins recruited by FtsZ and might function mainly to anchor the Z-ring to the membrane using these proteins (Wang, Huang et al. 1997; Ma and Margolin 1999; Margolin 2005).

It has been shown that the GTP-bound form of FtsZ has a more compact conformation than the GDP-bound form. This conformational change is though to be due to the interaction between the γ-phosphate of GTP and the loop T3. In the stimulated GTP-bound state, loop T3 is pulled by the γ-phosphate into a more compact conformation than with GDP. Such a structural change may bend the GDP filament upon hydrolysis by pushing against helix H8 of the next monomer, providing a mechanism by which FtsZ could generate the constriction force (Diaz, Kralicek et al. 2001). This finding has been corroborated by Leung *et al,* who showed that the presence of a γ-phosphate in the FtsZ active site modulates the conformation of loop T3 and is directly coupled to an α-to-β secondary structure conformational switch by steric overlap. This study links the GTP binding and hydrolysis activity of FtsZ to the lateral assembly and Z-ring constriction (Leung, Lucile White et al. 2004). However, the X-ray crystal structure of FtsZ in a variety of nucleotide and polymerization states has been obtained and the conformation of FtsZ does not appear to be affected (Oliva, Cordell et al. 2004). In fact, these structures cannot even account for the conformational changes in the T3 loop (Nogales and Wang 2006). As it stands, there is presently no convincing structural explanation to link FtsZ GTP binding and hydrolysis activity to Z-ring assembly and constriction.

Comparison of FtsZ and tubulin tridimensional structures

Comparison of the atomic structures of FtsZ and tubulin reveals a very close mechanistic relationship that distinguishes them from GTPase proteins of known families (Nogales,

Downing et al. 1998). FtsZ and tubulin in fact appear to form a structurally distinct family of GTPase enzymes and their determinants for the specificity of GTP binding are quite different from those of the GTPase super-family (Bourne, Sanders et al. 1991; Nogales, Downing et al. 1998). Even though the tridimensional structures of FtsZ and tubulin are quite similar, the proteins display many dissimilarities. Tubulin has two additional large C-terminal helices that lie on the outer microtubule surface and are thought to be the main interaction site for motor proteins and other proteins able to bind microtubules. FtsZ lacks these long C-terminal α-helices, displays shorter loops between secondary structures and possesses an N-terminal extension absent in tubulin (Lowe and Amos 1998). Furthermore, the corresponding loop T5 in tubulin shows very limited homology with FtsZ and has a different conformation (Nogales, Downing et al. 1998). Finally, the nucleotide-binding pocket of FtsZ is significantly more open than that of tubulin (Nogales and Wang 2006).

Extended functions of FtsZ

In addition to its key role at the heart of the mid cell division, FtsZ has various other functions. It has been shown that this protein is required for proper sporulation of *B. subtilis*. Sporulation occurs following an asymmetric division allowing the formation of a polar septum and yielding a small resistant forespore and a mother cell. The forespore is then engulfed by the mother cell in a phagocyte-like process that results in the forespore becoming pinched off as a free protoplast within the mother cell (Kemp, Driks et al. 2002). FtsZ is important in this process, not only as a main cell division protein but also as a regulator. FtsZ is required for formation of the sporulation septum and for N-terminal proteolytic processing of the inactive pro-σ^3 to the active transcription factor σ^3 that initiates the sporulation process (Beall and Lutkenhaus 1991). During sporulation, the Z-ring switches from a medial to a bipolar pattern of localization via a spiral-like intermediate and forms a ring near each pole of the cell (Ben-Yehuda and Losick 2002).

FtsZ also plays a role in mechanisms of bacterial resistance to β-lactam antibiotics. In response to β-lactam antibiotics targeting essential PBP enzymes, bacteria often produce β-lactamases. These enzymes specifically hydrolyze the β-lactam nucleus of such antibiotics. It is generally agreed that β-lactam antibiotics do not enter the bacterial cytoplasm and are thus unlikely to be direct inducers of β-lactamases. It has been shown

that FtsZ is involved in the process of β-lactamase induction in response to the antibiotic cefoxitin. This induction requires normal FtsZ enzyme activity (Ottolenghi and Ayala 1991), an observation confirmed over the past decade and now fully explained. An FtsZ defect blocks the initiation of cell division, inhibiting septal cell wall synthesis and causing an accumulation of the cytoplasmic cell wall precursor UDP-MurNAc-pentapeptide. This precursor in turn acts as a co-repressor of β-lactamase expression and prevents the induction (Uehara and Park 2002). It has also been shown that the expression of the *ftsA-ftsZ* promoter ftsA1p by the RcsB effector is greatly increased in mucoid mutants of *Salmonella typhimurium* resistant to mecillinam, a β-lactam antibiotic that specifically inhibits PBP 2, which is the PBP involved in maintenance of bacillar cell shape in enterobacteria (Spratt 1975). Costa *et al* demonstrated that the mecillinam resistance of these mucoid mutants is due to over-expression of the *ftsZ* and/or *ftsA* gene(s) (Costa and Anton 2001).

In *C. crescentus*, the extended coil of the actin homologue MreB, which contributes to the rod shape, contracts towards the mid cell in an FtsZ-dependent manner upon initiation of division (Figge, Divakaruni et al. 2004; Margolin 2005). In contrast to the static levels of FtsZ normally observed throughout the cell division cycle, the protein is not present in swarmer cells of *C. crescentus*. In fact, it accumulates only in stalked cells, where it is thought to facilitate proper morphogenesis (Rueda, Vicente et al. 2003; Martin, Trimble et al. 2004).

The association of FtsZ with the cell wall biosynthesis pathway seems to be important for cell division and maintenance of bacterial shape. The switch from the elongating mode to the septal mode of cell wall biosynthesis relies on FtsZ (de Pedro, Quintela et al. 1997). In FtsZ-depleted cells, the cell wall synthetic apparatus becomes dispersed and new cell wall material is made in patches dispersed over the entire cell surface, which may increase in volume by up to eightfold before lysing (Pinho and Errington 2003). FtsZ significantly influences gross cell shape in addition to its classic function of determining the site and progression of septation, with morphological variation stemming from interaction between the FtsZ-dependent division pathway and the peptidoglycan modification pathway. It has been shown that FtsZ works in conjunction with PBP, specifically PBP 5, to generate bacterial cell shape in *E. coli* (Varma and Young

2004). Under certain circumstances, improper FtsZ function can destroy the structural integrity of the cell. Finally, FtsZ has been observed to move rapidly in helical patterns around the cytoplasm (Thanedar and Margolin 2004) and may also function as part of a bacterial cytoskeleton-like apparatus.

A recently identified novel group of FtsZ-related plasmid-encoded proteins has been found to be required for the replication of virulence plasmids in *B. anthracis* and possibly in related organisms. The replication initiator protein of plasmid pXO1 has been identified as RepX and shares limited homology with FtsZ. The pXO1 plasmid encodes the major virulence factor of *B. anthracis* known as the anthrax toxin. Plasmid pXO1 also codes for genes involved in spore germination and in regulation of the expression of anthrax toxin and other virulence factors as well as genes resembling those involved in the horizontal transfer of plasmids. The GTP binding motif of FtsZ is totally conserved in the RepX protein and the GTP binding and/or GTPase activity of RepX is critical for its function as a replication protein (Tinsley and Khan 2006).

The extended functions of FtsZ indicate that an antibacterial therapy targeted against FtsZ may not only inhibit the essential bacterial cell division process. In addition, such a therapy will probably block sporulation, reduce bacterial resistance to β-lactam antibiotics, impair bacterial morphogenesis and cell wall biosynthesis and may affect the replication of virulence plasmids.

Spatial and temporal regulation of FtsZ: the *min* system and the nucleoid occlusion process

Proper function of the cell division process depends on accurately balanced FtsZ polymerization at mid cell. In response to a yet unidentified cell cycle signal, the Z-ring assembles at the exact centre of the bacterial cell after chromosome replication and during the segregation process when the replication origins are near the poles. The strong spatial and temporal regulation of FtsZ allows the division of the mother cell into two identical daughter cells with an intact and integral genome. This regulation is achieved mainly by control of FtsZ assembly dynamics via specific inhibitors. Since FtsZ has the potential to assemble at any point along the cell and its concentration is much higher than the critical concentration for polymerization, FtsZ regulators are essential for maintaining the pool of

unassembled FtsZ and preventing aberrant Z-ring formation (Yu and Margolin 1999; Stricker, Maddox et al. 2002; Haeusser, Schwartz et al. 2004). Furthermore, polymerization is very sensitive to variations in FtsZ concentrations and a complex network of negative and positive regulatory proteins is needed to ensure the spatial and quantitative regulation of the dynamic Z-ring (Kawai and Ogasawara 2006).

Correct localization of the Z-ring at mid cell depends on the MinCDE system and on nucleoid occlusion, overlapping regulation systems that allow Z-ring assembly at mid cell only when nucleoids are segregated (Vicente, Rico et al. 2006). The *min* system was identified 15 years ago from a series of mutations causing the formation of *E. coli* mini-cells (de Boer, Crossley et al. 1989). It allows spatial regulation of Z-ring assembly while restricting Z-ring polymerization exclusively to mid cell.

The MinC protein acts as a specific inhibitor of FtsZ and works in conjunction with MinD to block FtsZ polymerization and to destabilize improper Z-rings without altering the GTPase activity of FtsZ (Hu, Mukherjee et al. 1999). MinC is not likely to change the stability of proto-filaments or their nucleotide exchange rates, although it is thought to reduce the length or bundling of FtsZ polymers without completely inhibiting FtsZ self-association (Romberg and Levin 2003). Some observations suggest that MinCD acts after Z-ring formation and prevents the recruitment of FtsA to the Z-ring while inhibiting the constriction process (Justice, Garcia-Lara et al. 2000). However, this conclusion is not supported under alternative fixation conditions and Pichorff *et al* have found that the MinCD complex prevents Z-ring assembly via direct interaction with FtsZ (Pichoff and Lutkenhaus 2001). The inhibitory activity of MinC requires interaction with the MinD ATPase, the ATP-bound form of which specifically activates MinC by concentrating it at the inner membrane and enhancing its affinity for an unidentified septal component (Hu, Mukherjee et al. 1999; Suefuji, Valluzzi et al. 2002; Johnson, Lackner et al. 2002). The MinCD inhibitory complex occupies a zone extending from one pole to another in an oscillatory cycle dependent on MinE and involving oligomerization of MinD to restrict Z-ring formation to the division site (Zhou, Schulze et al. 2005; Suefuji, Valluzzi et al. 2002; Rothfield, Taghbalout et al. 2005). The polar inhibitory complex is thus prevented from reaching mid cell by an annular MinE structure that caps the medial edge of the inhibitory zone (Pichoff and Lutkenhaus 2001; Rothfield, Taghbalout et al. 2005). The time-averaged

concentration of the division inhibitor is therefore maintained at a high level near the poles and at a low level near mid cell (Rothfield, Taghbalout et al. 2005). MinE interacts with MinD at the division site to displace MinC, thus nullifying the inhibitory character of the complex. MinE also stimulates the ATPase activity of MinD and ADP-bound MinD detaches from the membrane (Hu, Saez et al. 2003; Lackner, Raskin et al. 2003). The MinE ring itself is not released and remains associated with the medial edge of the shrinking polar zone until disassembly is completed (Rothfield, Taghbalout et al. 2005). Cytoplasmic MinD–ADP is converted to MinD–ATP via nucleotide exchange and MinD-ATP moves to the other cell pole (because of the transient presence of MinE at the original site) and tethers itself to the inner membrane to form a new inhibitory complex with MurC (Suefuji, Valluzzi et al. 2002; Huang, Meir et al. 2003). The oscillation cycle is thus repeated and leaves mid cell as the only available location for formation of the Z-ring (Rothfield, Taghbalout et al. 2005).

MinE is absent from many bacteria, such as *B. subtilis* (Addinall and Holland 2002), in which the protein DivIVA attracts the bipartite cell MinCD inhibitory complex away from the cell centre and towards the cell pole (Edwards and Errington 1997; Perry and Edwards 2004). MinC and MinD are present in many Gram-positive and Gram-negative species, with MinD showing the highest degree of sequence conservation. MinE and its apparent functional homologue DivIVA, respectively in Gram-negative and Gram-positive bacteria, are also widely distributed (Rothfield, Taghbalout et al. 2005). Finally, the DicB protein, encoded by the cryptic prophage Kim (Qin) on the *E. coli* chromosome, can target the MinC inhibitor directly at the Z-ring in a ZipA-dependent and MinE-independent fashion without directing MinC to the membrane (Johnson, Lackner et al. 2004).

The nucleoid occlusion process prevents FtsZ assembly at nucleoid-containing areas. This process allows spatial and temporal regulation of bacterial cell division and prevents guillotination of the daughter cell genomes. The nucleoid occlusion model was proposed about 15 years ago but the molecular basis for this regulation process remained elusive until the past two years (Woldringh, Mulder et al. 1991). The *B. subtilis* YyaA protein was the first molecular effector of nucleoid occlusion to be identified and has consequently been renamed Noc (Wu and Errington 2004). This non-specific DNA-binding protein localizes almost uniformly over the nucleoid and prevents the division apparatus

from assembling in the vicinity of the nucleoid. Noc is thought to inhibit FtsZ accumulation or polymerization near the nucleoid. It is less abundant in the medial part of the longer nucleoids corresponding to the unreplicated terminus region. This might allow assembly of the Z-ring ahead of the complete termination of replication. Noc may also affect the spatial organization and allow topological restriction of the Z-ring rather than conferring general inhibition of polymerization. Many bacteria do not contain a recognizable homologue of Noc, and Wu *et al* conclude that there is some evidence for a weak *noc*-independent system that biases division to internucleoid spaces (Wu and Errington 2004). The SlmA protein was later identified as the first nucleoid occlusion factor in *E. coli* (Bernhardt and de Boer 2005). This DNA-associated protein directly prevents Z-ring assembly on portions of the membrane surrounding the nucleoid. Indeed, SlmA mediates nucleoid occlusion through direct interaction with FtsZ. It is intriguing that SlmA promotes the bundling of FtsZ filaments *in vitro*. Since FtsZ has not been observed on nucleoids, it is suggested that SlmA may actively cause the de-polymerization of FtsZ *in vivo*. SlmA may require partner molecules to inhibit FtsZ *in vivo,* such as specific DNA sequences. It is also proposed that SlmA may compete with membrane-associated FtsZ-binding proteins such as FtsA and ZipA to prevent them from developing a Z-ring (Bernhardt and de Boer 2005). SlmA and Noc belong to completely different families of DNA-binding proteins and lack obvious primary sequence similarity. However, $SlmA^{-}$ and Noc^{-} mutants share similar genetic and cytological properties. The higher concentration of both proteins at the pole-proximal regions may allow initiation of Z-ring assembly prior to completion of nucleoid segregation. It is therefore likely that the apparent preference of the septal ring for nucleoid-free regions not only results from interference with Z-ring assembly by nucleoid-associated factors but also from the ability of the septal ring to clear away underlying DNA (Bernhardt and de Boer 2005). Since FtsZ structures do not form over nucleoids in cells that contain the Min proteins but lack Noc or SlmA, this formation would appear to be prevented by MinC, which normally blocks Z-ring formation along the entire length of the cell, except for the region near mid cell. The nucleoid occlusion system therefore seems to be a fail-safe mechanism, especially important in cells lacking the Min system or when the nucleoid replication or segregation is defective. Finally, the state of the nucleoid is thought

to have a role in allowing nucleoid occlusion to function and additional system components undoubtedly remain to be discovered (Rothfield, Taghbalout et al. 2005).

In rod-shaped cells, the generation of identical daughter cells requires that the septum be orientated parallel to the plane of the preceding division event. Although the number of division planes that could generate two identical daughter cells from spherical cells is infinite, division-plane selection is clearly not random. The selection of the correct orientation of the division plane depends on knowledge of the division plane used in the previous division cycle and the basis of such topological memory is unknown (Rothfield, Taghbalout et al. 2005). It is likely that the complex problem of identifying the plane of division is determined in part by Min oscillation, which tends to follow the cell long axis (Margolin 2005). Finally, study of the localization of the IcsA protein involved in the assembly of the actin tail has revealed that polar positional information is present at mid cell independent of known cell division factors. The structure recognized at the cell pole by IcsA, and perhaps by other polar localized proteins, is present in some form in the cytoplasm or at the cytoplasmic side of the inner membrane and at or near the cell division site. Furthermore, recognition of this polar positional information by IcsA inhibits cell division. This effect may arise from a blockage of the proper localization or function of FtsZ (Janakiraman and Goldberg 2004). Overall, the above observations highlight the fact that the FtsZ regulation picture is still incomplete.

The SOS system

In response to DNA damage or DNA replication defects, bacterial cells induce the SOS system to repair DNA and delay cell division. Numerous damage-inducible genes are activated by the lexA promoter (via the protein RecA) to repair DNA (Little and Mount 1982). As part of the SOS response in *E. coli*, the protein SulA (previously named SfiA) is expressed. This protein induces a transient delay in the cell division process until the damage is resolved. It interacts directly with FtsZ, inhibiting Z-ring formation to prevent guillotination of the genome and propagation of damaged DNA (Bi and Lutkenhaus 1993), specifically inhibiting the formation of the GTPase active site and the polymerizing activity of FtsZ (Cordell, Robinson et al. 2003). The crystal structure of SulA has been resolved in complex with FtsZ from *P. aeruginosa* and has revealed that SulA binds the T7 loop

surface of the FtsZ monomer (Cordell, Robinson et al. 2003). The crystallization clues thus explain why FtsZ GTPase activity and polymer turnover are required for SulA inhibition (Higashitani, Higashitani et al. 1995). The efficient inhibition of FtsZ by SulA works because the Z-ring is remarkably dynamic (Stricker, Maddox et al. 2002). FtsZ monomers constantly come in and out of the polymer and SulA binds to them with high affinity (Lowe, van den Ent et al. 2004). The SulA inhibitor is found only in proteobacteria closely related to *E. coli* and no SulA homologue has been identified in *B. subtilis*. In contrast, the protein YneA acts as a functional homologue of SulA and delays the cell division process during the SOS response in *B. subtilis*. YneA affects Z-ring formation but no direct interaction between YneA and FtsZ has been detected. YneA might thus suppress Z-ring assembly indirectly by acting on downstream divisome proteins that stabilize the Z-ring, such as FtsA, or on FtsZ regulators such as EzrA and ZapA. YneA might also affect the location of Z-ring formation. Aside from *B. subtilis*, only the genomes of *Listeria innocua* and *Listeria monocytogenes* have conserved YneA (Kawai, Moriya et al. 2003). A recent report suggests that YneA interferes with assembly of the late division complex by suppressing the recruitment of FtsL and/or FtsB to the divisome (Kawai and Ogasawara 2006).

EzrA

The membrane protein EzrA is a non-essential division protein modulating the frequency and position of Z-ring assembly in Gram-positive bacteria with low GC content. EzrA has been found to prevent Z-ring formation at inappropriate sites and to increase the critical concentration of FtsZ required for ring formation (Levin, Kurtser et al. 1999). It is widely distributed throughout the cell membrane to prevent Z-ring formation at aberrant locations on the cell membrane. EzrA interacts directly with FtsZ and accumulates at mid cell in an FtsZ-dependent mode (Levin, Kurtser et al. 1999; Haeusser, Schwartz et al. 2004). However, EzrA is unable to disassemble preformed polymers and does not significantly alter GTPase activity (Haeusser, Schwartz et al. 2004). At mid cell, EzrA competes with the effects of positive regulators of FtsZ assembly such as ZapA and FtsA and the balance shifts in favour of FtsZ assembly, leading to medial Z-ring formation. EzrA may inhibit the formation of stabilizing lateral interactions between FtsZ proto-filaments or prevent the

addition of new FtsZ subunits to the ring. Overall, EzrA ensures that the Z-ring is dynamic enough to respond to the signals governing the cell division process (Haeusser, Schwartz et al. 2004; Kawai and Ogasawara 2006). EzrA inactivation stabilizes the Z-ring while lengthening the time between Z-ring formation and constriction, which results in cell elongation. Reduction of the FtsZ monomer pool due to aberrant Z-ring formation at cell poles is a possible cause of delays in Z-ring formation and maturation in an *ezrA* mutant. EzrA not only inhibits aberrant Z-ring formation on the cell membrane but incorporated into the Z-ring also participates in mid cell division, possibly by maintaining ring dynamics and ensuring proper timing of Z-ring constriction (Kawai and Ogasawara 2006).

Other endogenous inhibitors of FtsZ

A plasmid-encoded protein that arrests cell division in *E. coli* has been identified as the product of a short open reading frame of the prophage Rac expressed only under conditions of prophage induction. This *orfE* encodes a killing function and has thus been renamed *kil*. The division inhibition by Kil can be specifically relieved by over-expression of FtsZ and inhibition increases in conditions of high levels of the cyclic AMP receptor protein-cAMP complex. Kil also distorts the rod shape of the cells at high levels of expression (Conter, Bouche et al. 1996).

The protein ClpX has been identified as an inhibitor of FtsZ assembly in *B. subtilis*. ClpX is an ATP-binding protein and its proteolysis and chaperone-like activities require ATP hydrolysis. ClpX is the substrate recognition subunit of the protease ClpXP and it has been shown that ClpX but not ClpP inhibits Z-ring formation *in vivo*. *In vitro*, ClpX inhibits FtsZ polymerization in a ClpP-independent manner through a mechanism that does not require ATP hydrolysis. Since ClpX does not affect the GTPase activity of FtsZ, it may help to maintain the cytoplasmic pool of unassembled FtsZ required for the dynamic nature of the Z-ring. Since ClpX is conserved throughout bacteria and has been shown to interact directly with FtsZ (in *E. coli*), it may represent a general regulator of cell division in a wide variety of bacteria (Weart, Nakano et al. 2005).

The integral membrane protein CrgA from *Streptomyces coelicolor* localizes to apical syncytial cells of aerial hyphae and inhibits the formation of a productive Z-ring as well as promoting proteolytic turnover of FtsZ. CrgA is important for coordinating growth

and cell division in sporogenic hyphae of *S. coelicolor* and is extensively conserved among actinomycete genomes. Given the absence of known prokaryotic cell division inhibitors in these bacteria CrgA may have an important conserved function influencing Z-ring formation (Del Sol, Mullins et al. 2006).

Numerous studies report the filamentation of intracellular Gram-negative pathogens including *S. typhimurium* growing in murine fibroblast cells (Martinez-Moya, de Pedro et al. 1998), MelJuSo cells (a human melanoma cell line), other skin-related cells (Martinez-Lorenzo, Meresse et al. 2001), γ-IFN-treated macrophages (Rosenberger and Finlay 2002), bone marrow-derived macrophages (Rosenberger, Gallo et al. 2004) and contractile vacuoles of amoebae (Gaze, Burroughs et al. 2003) as well as filamentation of *Salmonella enterica* in macrophages (Vazquez-Torres, Xu et al. 2000) and uropathogenic *E. coli* in superficial bladder epithelial cells (Mulvey, Schilling et al. 2001). These observations may imply that eukaryotic cells have developed specific inhibitor(s) of the bacterial cell division process. However, a filamentation phenotype is not always indicative of a cell division defect. Filamentous cells of *S. typhimurium* have been shown to have distinct FtsZ bands at presumptive mid cell locations and a defect in the histidine biosynthetic pathway has been correlated with the observed filamentation phenotype (Henry, Garcia-Del Portillo et al. 2005). A recent study suggests that the filamentation phenotype of *M. tuberculosis* during intracellular growth in macrophages arises from a cell division delay attributable to compromised function of FtsZ. Only a small fraction of filamentous *M. tuberculosis* cells had mid-cell Z-rings and the majority of these contained non-ring, spiral-like FtsZ structures along their entire length. The intraphagosomal milieu must thus alter the expression of *M. tuberculosis* genes affecting Z-ring formation and hence cell division (Chauhan, Madiraju et al. 2006).

Non-endogenous inhibitors

Until recently, the bacterial cell division protein FtsZ has not been a specific target of therapeutic inhibitors and no pharmacologically active inhibitors of division proteins are currently available. However, interest in identifying new FtsZ inhibitors has grown in recent years. Since FtsZ inhibitors have not been reviewed recently, we shall describe all new compounds identified as able to interfere with FtsZ. Such a description provides

valuable clues about the validity of FtsZ, GTPase activity, polymerization activity and FtsZ dynamics as specific targets for antibacterial agents.

The compound 3-Methoxybenzamide, known to inhibit ADP-ribosyltransferase, has also been found to inhibit cell division in *B. subtilis*. The primary target of this drug is the process involving FtsZ function during both vegetative growth and sporulation (Ohashi, Chijiiwa et al. 1999).

To investigate the structural relatedness of tubulin and FtsZ, various inhibitors of tubulin assembly have been analyzed for activity on FtsZ. The usual tubulin inhibitors, such as colchicine, colcemid, benomyl, and vinblastine, have no effect on Ca^{2+}-promoted GTP-dependent assembly of FtsZ. However, the hydrophobic probe 5,5'bis-8-anilino-1-naphthalenesulfonate (bis-ANS) inhibits FtsZ polymerization with an IC_{50} value in the low micromolar range. ANS (8-anilino-1-naphthalenesulfonate), a hydrophobic probe similar to bis-ANS, has no inhibitory effect on tubulin or FtsZ assembly. Divalent calcium ion, which promotes GTP-dependent FtsZ assembly, were found to stimulate binding of bis-ANS or ANS to FtsZ (Yu and Margolin 1998). This study showed that some tubulin inhibitors display strong specificity for tubulin while others may be modified to obtain new FtsZ inhibitors. Four years later, compounds originally designed as putative tubulin inhibitors were tested as anti-tubercular agents for inhibition of *M. tuberculosis* FtsZ. Initial screening of 2-alkoxycarbonylpyridines revealed several compounds inhibiting *M. tuberculosis* growth. Two of these, SRI-3072 and SRI-7614, inhibit FtsZ polymerization and GTPase activity. They are equipotent against susceptible and single-drug-resistant strains of *M. tuberculosis*. SRI-3072 also reduces *M. tuberculosis* growth in mouse bone marrow macrophages and the concentration effecting 90% and 99% reduction in mycobacterial growth after 7 days is 0.23 μM and 2.7 μM. SRI-3072 is specific for FtsZ and does not inhibit tubulin, whereas SRI-7614 inhibits polymerization of both FtsZ and tubulin. These types of compound could be developed into specific anti-tubercular drugs effective against the current multi-resistant strains of *M. tuberculosis* (White, Suling et al. 2002). An analogue of the most promising compound identified by White *et al* has been synthesized. This analogue, 2-carbamoylpteridine, is a potent inhibitor of FtsZ polymerization, suggesting that the full pteridine nucleus represents an acceptable substitution. However, it appears to be less effective than the original SRI-3072 compound against whole *M.*

tuberculosis. It also efficiently inhibits FtsZ polymerization and GTPase activity but unfortunately also inhibits tubulin polymerization (Reynolds, Srivastava et al. 2004). It has recently been shown that the SRI-3072 compound disrupts Z-ring assembly and inhibits cell division and growth of *M. tuberculosis* (Chauhan, Madiraju et al. 2006). Screening a library of taxane compounds known to affect tubulin assembly has identified a number of anti-tuberculosis compounds. Rational optimization of selected compounds has led to the discovery that C-seco-taxane-multi-drug-resistance reversal agents (C-seco-TRAs) are non-cytotoxic at the upper limit of solubility and detection (> 80μM), while maintaining MIC_{99} values of 1.25-2.5 μM against drug-resistant and drug-sensitive strains of *M. tuberculosis*. The specificity of these novel taxanes to microtubules compared to FtsZ appears to have been completely reversed through systematic rational drug design. Treatment of *M. tuberculosis* cells with the TRA 3aa and 10a compounds at the MIC cause cell elongation and filamentation, in phenotypic response to FtsZ inactivation. Preliminary results on TRA 10a indicate a dose-dependent stabilization of FtsZ against de-polymerization (Huang, Kirikae et al. 2006).

A large screening of microbial fermentation broths and plants has led to the identification of viriditoxin, a product from *Aspergillus* sp. MF6890. Viriditoxin blocks FtsZ polymerization with an IC_{50} of 8.2 μg/ml and a concomitant GTPase inhibition with an IC_{50} of 7.0 μg/ml. Viriditoxin exhibits broad-spectrum antibacterial activity via inhibition of FtsZ against clinically relevant Gram-positive pathogens, including methicillin-resistant *S. aureus* and vancomycin-resistant enterococci, without affecting the viability of eukaryotic cells (Wang, Galgoci et al. 2003).

Using a high throughput protein-based chemical screen to identify small molecules that target assembly-dependent GTPase activity of FtsZ, the Zantrin compounds have been identified. These compounds inhibit FtsZ GTPase with IC_{50} values ranged between 4 and 25 μM either by destabilizing FtsZ proto-filaments or by inducing filament hyperstability through increased lateral association. The two classes of Zantrins perturb Z-ring assembly in *E. coli* cells and cause lethality in a variety of bacteria in broth culture, indicating that FtsZ antagonists may serve as chemical leads for the development of new broad-spectrum antibacterial agents (Margalit, Romberg et al. 2004).

Using a well-focused phage display screening approach against the *P. aeruginosa* FtsZ enzyme, the C-7-C peptides FtsZp1 and FtsZp2 have been selected as specific inhibitors of FtsZ GTPase activity with IC_{50} values of 0.45 mM and 1.5 mM. The reducing agent dithiothreithol significantly reduces the inhibitory potential of the two C-7-C peptides, indicating that the disulphide bond formed by the two cysteine residues and the subsequent loop conformation are important for inhibition. Inhibitory peptides such as these may constitute the core of new peptidomimetic antibacterial agents (Paradis-Bleau, Sanschagrin et al. 2004).

Using a cell-based assay to isolate new inhibitors, Stokes *et al* have identified a compound targeting FtsZ. Compound PC58538 specifically inhibits FtsZ polymerization and GTPase activity, with an IC_{50} value of 362 μM and a K_i of 82 μM. Several analogues of this compound have been prepared, of which the most promising, PC170942, competitively inhibits FtsZ of *B. subtilis* and *E. coli* with IC_{50} values of 44 μM (K_i of 10 μM) and 1100 μM, respectively. These compounds are active against Gram-positive and Gram-negative bacteria and have the potential to provide novel antibiotics (Stokes, Sievers et al. 2005).

Using the first efficient route to hydroxybenzylated natural flavanone products, Urgaonkar *et al* have synthesized dichamanetin and 2"'-hydroxy-5"-benzylisouvarinol-B. These compounds are potent inhibitors of FtsZ GTPase activity, with IC_{50} values of about 10 μM and exhibit a high level of antibacterial activity against Gram-positive bacteria, showing MIC values comparable to those of clinically relevant antibiotics (Urgaonkar, La Pierre et al. 2005).

It has been found that sanguinarine, a benzophenanthridine alkaloid, strongly induces filamentation in both Gram-positive and Gram-negative bacteria and prevents bacterial cell division by disrupting Z-ring formation. In addition, sanguinarine strongly reduces the frequency of the occurrence of Z-ring in *B. subtilis* without affecting nucleoid segregation. It binds to FtsZ with a dissociation constant of 18-30 μM, inhibiting assembly, reducing proto-filament bundling *in vitro* and providing additional direct evidence of the critical role of FtsZ assembly and bundling in the bacterial cell division process (Beuria, Santra et al. 2005).

The GTP analogue 8-bromoguanosine-5'-triphosphate has been synthesized and acts as a competitive inhibitor of both FtsZ polymerization and GTPase activity, with a K_i of 31.8 μM for GTPase activity. This GTP analogue does not inhibit tubulin assembly, thus suggesting an exploitable structural difference between the GTP-binding pockets of FtsZ and tubulin (Lappchen, Hartog et al. 2005).

A library of GTP analogues with a guanine-like moiety linked to an alanine side chain has been synthesized using a parallel solid-state synthesis strategy. These analogues inhibit the GTPase activity of FtsZ with IC_{50} values between 450 μM and 2.6 mM and five of them inhibit *S. aureus* growth. Synthesis of new derivatives of the most active compound offers a promising avenue for the design of efficient and specific inhibitors of bacterial cell division (Paradis-Bleau, Beaumont et al. 2007).

Finally, the FtsZ–ZipA protein–protein interaction has been studied as a specific target for antibacterial agents. Phage display screening has been employed to identify a unique peptide related to the specific C-terminal sequence of FtsZ that interacts with ZipA. One peptide thus selected and modified displays a higher affinity for ZipA than the actual FtsZ interacting sequence. Assay parameters using the phage display peptide have been optimized and adapted for the high throughput screen. A screening of 250,000 compounds has identified 29 hits with inhibition of the FtsZ-ZipA protein-protein interaction equal to or greater than 30% at 50 μg/ml. The most potent inhibitor, pyridylpyrimidine, has a competitive K_i value of 12 μM. X-ray analysis of the pyridylpyrimidine/ZipA C-terminal FtsZ-binding domain co-structure has revealed that the inhibitor binds to the same hydrophobic pocket as the FtsZ interacting sequence (Kenny, Ding et al. 2003). In a recent study, previously identified indoles 1 and 2 and oxazole 3 (see Rosenmund 1979, Freed, Hertz et al. 1964 and Brown, Cavalla et al. 1968) have been shown to be weak inhibitors of FtsZ–ZipA protein–protein interaction, with IC_{50} values between 1170 and 2750 μM. These compounds have been optimized and new chimeric molecules incorporating structural features of both the indoles and the oxazole display enhanced activity. The improved compounds inhibit the ZipA–FtsZ interaction with IC_{50} between 192 and 1060 μM and interact with the FtsZ-binding site of ZipA. The activity of the new compounds against Gram-negative and Gram-positive bacteria is also improved (Sutherland, Alvarez et al. 2003). Jennings *et al* have identified a small molecule inhibitor of the ZipA–FtsZ

interaction among a set of structurally diverse lead-like compounds. The compound 1,2,3,4,12,12b-Hexahydro-indolo[2,3-a]quinolizin-7-one (1) occupies the hydrophobic cavity on the surface of ZipA, necessary for the binding of FtsZ. Small molecules based on this compound have been prepared by parallel synthesis, one of which (10b) displays (by X-ray analysis) an unexpected binding mode in complex with ZipA, facilitated by desolvation of loosely bound surface water. However, this compound does not show significantly improved activity: 46% inhibition at 1 mM compared to 39% for compound 1 (Jennings, Foreman et al. 2004). Following this study, the design and parallel synthesis of a combinatorial library of small molecules targeting the FtsZ binding area on ZipA and causing cell elongation was described. The most promising compound, 16.a.4, shows an IC_{50} value of 296 μM and a K_D value of 105 μM with promising activity against Gram-negative and Gram-positive bacteria (Jennings, Foreman et al. 2004). As a first prospective application of the shape-comparison Rapid Overlay of Chemical Structures (ROCS) program, a high throughput screening has identified a set of novel weak inhibitors of the ZipA-FtsZ protein-protein interaction. These platform compounds present opportunities for further optimization of biological affinity and drug development via synthesis and high throughput screening (Rush, Grant et al. 2005).

In order to design antibacterial agents that target FtsZ specifically, particular consideration must be given to the eukaryotic GTPase enzymes. *A priori,* it is improbable that FtsZ inhibitors affect eukaryotic GTPases other than tubulin, as FtsZ and tubulin form a distinct family of GTPase enzymes (Nogales, Downing et al. 1998). Furthermore, many of the described FtsZ inhibitors specifically target FtsZ without affecting tubulin. Finally, it would be a bonus for FtsZ inhibitors to target other bacterial GTPases, since these enzymes play major roles in the regulation of ribosome function and DNA segregation (Caldon and March 2003). This however, is unlikely and it is expected that FtsZ inhibitors will be very specific, given the characteristic structural features of FtsZ. We will now focus our attention on FtsA as a target for antibacterial agents within the cell division apparatus.

FtsA as a specific target

Among the bacterial division proteins, the 43 kDa cytoplasmic FtsA protein represents a promising target for specific antibacterial agents. It is the second most highly conserved protein of the divisome after FtsZ and almost all pathogenic bacteria contain a single copy of the *ftsA* gene (Margolin 1999; van den Ent, Amos et al. 2001). Although FtsA shares some structural homology with the eukaryotic protein actin, its overall structure is quite distinct and MreB, a protein required for maintaining cell shape, is a better candidate for a functional prokaryotic homologue of actin (van den Ent and Lowe 2000; Jones, Carballido-Lopez et al. 2001; van den Ent, Amos et al. 2001; Romberg and Levin 2003). Furthermore, FtsA is essential and constitutes a key component of the cell division apparatus. When FtsA is non-functional, bacteria still grow but cell division is blocked, leading to a lethal phenotype (Rothfield, Justice et al. 1999). FtsA localizes at mid cell in a solely FtsZ-dependent manner and its presence in the divisome is needed for recruitment of downstream proteins and Z-ring constriction (Begg, Nikolaichik et al. 1998; Pichoff and Lutkenhaus 2002; Vicente, Rico et al. 2006). It displays an essential and highly conserved interaction with FtsZ that relies on a precise ratio and represents a rate-limiting protein extremely sensible to alteration (Begg, Nikolaichik et al. 1998; Yu and Margolin 1999; Errington, Daniel et al. 2003). Its ATPase activity is essential and can be quantified and exploited to screen and characterize inhibitory molecules (Feucht, Lucet et al. 2001; Paradis-Bleau, Sanschagrin et al. 2005). As is the case for FtsZ, the substrate of FtsA is commercially available and an enzymatic assay has already been devised. The ATPase activity has been quantified by hydrolysis of radioactive ATP (Feucht, Lucet et al. 2001; Paradis-Bleau, Sanschagrin et al. 2005). Numerous reliable high-throughput ATPase assays can be set up rapidly under specific hydrolytic conditions. Such assays may measure the release of inorganic phosphate or involve secondary enzymes with spectrophotometric measurement. Finally, many studies describe the purification of FtsA in acceptable yields, although this has proven more difficult than for FtsZ since FtsA has an affinity for the bacterial inner membrane (Pichoff and Lutkenhaus 2005). FtsA often accumulates in inclusion bodies but efficient purification of biologically active protein can be achieved by a multi-step solubilization and renaturation process. The renaturation protocol must take

into account the presence of disulfide bonds and the Mg^{2+} cofactor and is coupled to a gel filtration step (Paradis-Bleau, Sanschagrin et al. 2005). For purposes of lead compound development, the crystal structure of FtsA will be of precious help (van den Ent and Lowe 2000). FtsA also displays many protein-protein interactions that could eventually become specific targets for antibacterial agents. Finally, no known antibacterial agent nor endogenous inhibitor targets FtsA and therefore no resistance mechanism has likely ever developed in bacteria. The role of FtsA enzyme during the cell division process remains to be fully characterized but should represent opportunities for developing antibacterial agents with novel modes of action. Much less is known about FtsA than about FtsZ and we will now describe its principal features in terms of targeting with inhibitors.

Conservation of FtsA

FtsA is the second most highly conserved protein of the divisome and consists of well-conserved ATP-binding site and secondary structural elements surrounded by regions that may include insertions of variable size (Rothfield, Justice et al. 1999; Lowe and van den Ent 2001; Fiskus, Padmalayam et al. 2003). FtsA is well conserved in almost all bacteria and is lacking only in mycobacteria, cyanobacteria, mycoplasmas, actinobacteria, chloroflexus and archaea (Margolin 2000), in which another protein must perform its essential function, and is also absent in eukaryotic organelles (Vaughan, Wickstead et al. 2004; Pichoff and Lutkenhaus 2005). FtsA was thought to be absent in the mollicutes, but the presence of an *ftsA* gene in the cell division cluster of a mollicute species has been characterized recently (Margolin 2000; Zhao, Hammond et al. 2004). FtsA is part of the compact genome of *Spiroplasma kunkelii*, a parasitic wall-less bacterium harbouring a gene set approaching the minimal complement necessary for multiplication and pathogenesis (Zhao, Hammond et al. 2004). As discussed below, FtsA directly and specifically interacts with FtsZ and this interaction has coevolved between bacterial species. In fact, interspecies FtsA-FtsZ interactions can occur as long as the sequence divergence between the homologues is not too large (Ma, Sun et al. 1997). The *ftsA* gene is usually present immediately upstream from *ftsZ* within the *dcw* gene cluster and the *ftsA-ftsZ* pair forms one of the more highly conserved gene tandems in bacteria (Margolin 2000; Pichoff and Lutkenhaus 2005).

ATP binding and ATP hydrolysis activities of FtsA

Analysis of the structural features of FtsA has identified a strong ATP-binding site and probable ATPase activity (Bork, Sander et al. 1992; van den Ent and Lowe 2000). The FtsA protein from *E. coli*, *Thermotoga maritima, B. subtilis P. aeruginosa* and *Streptococcus pneumoniae* has been reported to bind ATP (Sanchez, Valencia et al. 1994; van den Ent and Lowe 2000; Yim, Vandenbussche et al. 2000; Feucht, Lucet et al. 2001; Lara, Rico et al. 2005; Paradis-Bleau, Sanschagrin et al. 2005). The affinity for ATP is strong and preferential (Feucht, Lucet et al. 2001; Lara, Rico et al. 2005; Paradis-Bleau, Sanschagrin et al. 2005). Feucht *et al* demonstrated the ATPase activity of highly purified FtsA from *B. subtilis* and its requirement for Mg^{2+} as cofactor (Feucht, Lucet et al. 2001). This activity is believed to be required for cell division and may enhance Z-ring dynamics or provide additional energy to bring about membrane constriction (Feucht, Lucet et al. 2001). The essentiality of FtsA enzymatic activity is supported by two temperature-sensitive mutations which irreversibly inactivate *E. coli* FtsA at 42°C and cause extensive damage to the division machinery (Robinson, Begg et al. 1988). Structural studies indicate that both of these are probably structural mutants that indirectly affect nucleotide binding of FtsA (van den Ent and Lowe 2000). Highly purified FtsA from *P. aeruginosa* has been shown more recently to hydrolyze ATP to ADP, AMP and inorganic phosphate (Paradis-Bleau, Sanschagrin et al. 2005). There is also evidence that *E. coli* FtsA can be phosphorylated at a position corresponding to the autophosphorylation site of DnaK, but the conservation, essentiality and molecular consequences of such a phosphorylation remain unclear (Sanchez, Valencia et al. 1994; Errington, Daniel et al. 2003). The purified FtsA from *S. pneumoniae* is able to polymerize in an ATP-dependent and Mg^{2+}-dependent manner, but no detectable ATPase activity has been found (Lara, Rico et al. 2005). According to unpublished results from a study by J. Mingorance and M. Vicente, *E. coli* and *T. maritima* FtsA do not exhibit ATPase activity (Rico, Garcia-Ovalle et al. 2004; Lara, Rico et al. 2005). This may be due to unfolding of the extremely sensitive FtsA protein. Our team has observed that many conditions, including exposure to temperatures of -20°C or less, improper buffer or concentrations of DTT and Mg^{2+} during renaturation, lead to incorrect folding and total loss of ATPase activity. Extreme vigilance and patience are thus required to observe the ATPase activity of the highly fastidious FtsA protein (Paradis-

Bleau *et al*; unpublished observations). We hypothesize that all FtsA proteins have ATPase activity under proper *in vitro* conditions and probably *in vivo*.

The FtsA-FtsZ interaction

FtsA localizes to the division site at mid cell and this localization is strictly and solely dependent on FtsZ (Addinall and Lutkenhaus 1996; Ma, Ehrhardt et al. 1996; Ma, Sun et al. 1997; Wang, Huang et al. 1997; Begg, Nikolaichik et al. 1998; Hale and de Boer 1999; Yan, Pearce et al. 2000; Pichoff and Lutkenhaus 2002). Localization of FtsA seems to be independent from its ATP binding and hydrolysis activities (Ma, Ehrhardt et al. 1996). The C-terminus and the particularly conserved residue Trp 415 are essential for the presence of FtsA at mid cell (Yim, Vandenbussche et al. 2000). The pattern and timing of FtsA mid cell localization is quite similar to that for FtsZ, suggesting that both proteins localize at the division site simultaneously or that FtsA is recruited immediately after FtsZ (Ma, Ehrhardt et al. 1996; Den Blaauwen, Buddelmeijer et al. 1999; Rueda, Vicente et al. 2003; Jensen, Thompson et al. 2005). There is strong evidence that FtsA interacts directly with the C-terminus of FtsZ and that this interaction is essential for the cell division process (Sanchez, Valencia et al. 1994; Addinall and Lutkenhaus 1996; Ma, Ehrhardt et al. 1996; Ma, Sun et al. 1997; Wang, Huang et al. 1997; Din, Quardokus et al. 1998; Ma and Margolin 1999; Hale, Rhee et al. 2000; Yan, Pearce et al. 2000; Haney, Glasfeld et al. 2001; Di Lallo, Fagioli et al. 2003). FtsA interacts with the final 70 residues of FtsZ and binds specifically to the consensus sequence LDXPXFOR/K (O = hydrophobic residue; X = any residue) at the C-terminus. The FtsA-FtsZ protein-protein interaction is believed extremely conserved and the FtsZ consensus sequence is highly conserved. FtsZ of archeobacteria, which lack an FtsA homologue, are exceptions to this rule (Ma, Sun et al. 1997; Yan, Pearce et al. 2000; Haney, Glasfeld et al. 2001). The precise sequence required for FtsA-FtsZ interaction seems to be more dispersed on the FtsA protein. The residue Phe 376 has been identified but no clear sequence has been pointed out (Ma, Ehrhardt et al. 1996; Yan, Pearce et al. 2000). It has recently been shown that FtsA interacts with FtsZ prior to Z-ring assembly at mid cell in *B. subtilis*. This suggests that these proteins are always together in a complex, possibly as a subunit of an assembled ring structure, and localize as such at the division site (Jensen, Thompson et al. 2005).

The requirement for a precise ratio of FtsA and FtsZ was the first indication of potential FtsA-FtsZ interaction. Cell division is blocked by over-expression of either FtsA or FtsZ and this effect can be reversed by the coordinated over-expression of the other protein (Dai and Lutkenhaus 1992; Dewar, Begg et al. 1992; Begg, Nikolaichik et al. 1998; Yan, Pearce et al. 2000). Elevated FtsA level is lethal to bacteria and blocks cell division at a very early stage, similar to the blockage caused by inhibition of FtsZ (Wang and Gayda 1990; Dewar, Begg et al. 1992). Increases in FtsA are thus equivalent to FtsZ deficiency, although the same effect results from excess FtsZ (Dai and Lutkenhaus 1992). In *E. coli*, the proper FtsA:FtsZ ratio was thought to be 1:100 (Dai and Lutkenhaus 1992; Dewar, Begg et al. 1992; Wang and Gayda 1992). In *B. subtilis*, this ratio is 1:5 and it has been speculated that the higher amount of FtsA in the Gram-positive species may compensate for the absence of a ZipA homologue or that more ATP hydrolysis is required for cell division because of the much thicker cell wall or the higher internal osmotic pressure (Feucht, Lucet et al. 2001). However, the ratio has recently been reported to be 1:5 in *E. coli* as well (Rueda, Vicente et al. 2003). Since FtsA and FtsZ concentrations must stay the same throughout the cell cycle, strict transcriptional and translational regulation is required (Rueda, Vicente et al. 2003). In contrast to *ftsA*, the distal *ftsZ* gene is expressed from an additional promoter, which means that it is likely transcribed more frequently. In addition, the ribosome-binding sites of *ftsZ* and *ftsA* display different efficiencies and the translation of *ftsA* mRNA is very inefficient compared to *ftsZ* mRNA (Yi, Rockenbach et al. 1985; Mukherjee and Donachie 1990; Dai and Lutkenhaus 1992). More recently, it has been shown that RNase E is associated with the proper processing of the polycistronic *ftsQAZ* transcripts and that RNase E regulates the relative abundances of FtsZ and FtsA, cleaving the *ftsQAZ* transcripts at two sites between the contiguous *ftsA* and *ftsZ* genes (Cam, Rome et al. 1996). RNase E is required for efficient translation of the *ftsZ* mRNA and depletion of RNase E results in decreased FtsZ and increased FtsA. It has been shown that RNase E activity is required for maintenance of the proper FtsA:FtsZ ratio in *E. coli* (Tamura, Lee et al. 2006).

FtsA does not contain a membrane-spanning domain but is found in both the cytoplasm and membranes of bacterial cells (Chon and Gayda 1988; Pla, Dopazo et al. 1990; Sanchez, Valencia et al. 1994; Ma, Ehrhardt et al. 1996; Hale and de Boer 1997). It

has also been observed that the cytoplasmic form of FtsA is phosphorylated and can bind ATP while the membrane form is unphosphorylated and does not bind ATP (Sanchez, Valencia et al. 1994). Dai *et al* suggested that FtsA links the Z-ring to the membrane (Dai and Lutkenhaus 1992), a hypothesis later confirmed. FtsA indeed has an essential and conserved C-terminal amphipathic helix that directs FtsA to the inner membrane, allowing it to tether the Z-ring to the membrane via direct interaction. The interaction of FtsA with the membrane is essential for the bacterial cell division process and seems to regulate the FtsA-FtsZ interaction. It has been shown that FtsA must be directed to the membrane before it interacts with FtsZ and localizes with the Z-ring. Since the FtsZ–FtsA pair is so well conserved, it is believed that FtsA must tether the Z-ring to the membrane in most bacteria (Pichoff and Lutkenhaus 2005).

Overall, FtsA and FtsZ collaborate closely and specifically to make bacterial cell division an efficient process. It has been shown that the Z-ring can assemble at mid cell without FtsA but cannot constrict. FtsA seems to provide an essential stabilization of the Z-ring and it has been suggested that it restricts the GTPase activity of FtsZ while decreasing turnover dynamics and consolidating the ring (Romberg, Simon et al. 2001). FtsA levels affect ring stability and function, but the ability of FtsA to modulate FtsZ polymer stability *in vitro* has not yet been directly examined (Romberg and Levin 2003). Jensen *et al* have confirmed that FtsA is required for proper Z-ring formation in *B. subtilis* and suggest that it may be involved in the bundling of FtsZ proto-filaments (Jensen, Thompson et al. 2005). Since FtsA interacts with the C-terminus of FtsZ and this domain has been shown to interfere with FtsZ polymerization through an anti-bundling effect, the FtsA interaction may enhance Z-ring assembly (Dai and Lutkenhaus 1992; Wang, Huang et al. 1997; Yan, Pearce et al. 2000; Lowe, van den Ent et al. 2004). Being required for Z-ring stabilization, the ability of FtsA to dimerize (see below) suggests a possible secondary role in FtsZ proto-filament cross-linking (Feucht, Lucet et al. 2001; Pichoff and Lutkenhaus 2002). The FtsA-FtsA protein-protein interaction at the inner membrane may also enhance FtsZ bundling and stabilize the Z-ring (Pichoff and Lutkenhaus 2005). Further evidence that FtsA may promote FtsZ proto-filament bundling came from an FtsA mutation that bypasses the requirement for ZipA. This mutation enhances the Z-ring-stabilizing capacity of FtsA and confers resistance to excess MinC (Geissler, Elraheb et al. 2003). Over-expression of wild-

type FtsA has previously been shown to suppress MinC-mediated cell filamentation (Justice, Garcia-Lara et al. 2000). Nevertheless, FtsA is clearly required for Z-ring stabilization, perhaps through membrane association (Pichoff and Lutkenhaus 2005). This membrane association is needed in turn for proper Z-ring constriction and it is proposed that FtsA may also have a structural/mechanical role in Z-ring function (Vicente, Rico et al. 2006).

FtsA and divisome formation

FtsA is a key component in the sequential recruitment of all known essential cell division proteins to the Z-ring, with the exceptions of FtsZ and ZipA. It is thus required for directing FtsK and all downstream components to the Z-ring (Addinall, Cao et al. 1997; Wang, Huang et al. 1997; Wang and Lutkenhaus 1998; Chen, Weiss et al. 1999; Ghigo, Weiss et al. 1999; Rothfield, Justice et al. 1999; Weiss, Chen et al. 1999; Margolin 2000; Yim, Vandenbussche et al. 2000; Buddelmeijer and Beckwith 2002; Hale and de Boer 2002; Anderson, Gueiros-Filho et al. 2004; Vicente, Rico et al. 2006). The majority of the cell division proteins do not interact directly with FtsZ but rather depend upon FtsA (see Table I), without which cell division proteins are not recruited (Margolin 2000). Recruitment may be achieved through early interaction of FtsA with the Z-ring, ensuring the formation of a Z-ring capable of recruiting downstream proteins, and/or through direct FtsA protein-protein interactions (Jensen, Thompson et al. 2005). In addition to direct interaction of FtsA with FtsZ and with itself, FtsA is also capable of interacting with ZapA, FtsQ, FtsI and FtsN (Yim, Vandenbussche et al. 2000; Di Lallo, Fagioli et al. 2003; Corbin, Geissler et al. 2004; Goehring and Beckwith 2005; Karimova, Dautin et al. 2005; Vicente and Rico 2006). It has been shown that FtsA can recruit at least two late proteins, FtsI and FtsN, independently of the Z-ring, suggesting that these division proteins may not depend of Z-ring modification by FtsA. A possible explanation for the absence of recruitment of FtsK, FtsQ, and FtsW independently of FtsZ is that FtsA is not directly involved with downstream proteins other than FtsI and FtsN but instead enhances the recruiting ability of another septal component. Alternatively, FtsA may not normally recruit FtsI and FtsN to the Z-ring until it is activated by another later septation protein, such as FtsW (Corbin, Geissler et al. 2004). Experiments so far have not shown whether FtsA interactions with

FtsI and FtsN are direct or indirect and a model in which FtsA binds to and recruits downstream proteins is not sufficient to explain the observed localization dependency relationships (Goehring and Beckwith 2005; Vicente and Rico 2006). The FtsA-FtsI interaction is better characterized. The first clue that FtsA may interact directly with FtsI came from an *ftsA* mutant allele that alters the ampicillin-binding ability of FtsI (Tormo, Ayala et al. 1986). This was inconclusive, since the mutagen used (nitrosoguanidine) has induced secondary mutations in the bacterial strain employed (Eberhardt, Kuerschner et al. 2003). However, evidence has mounted that FtsA and FtsI interact directly (Di Lallo, Fagioli et al. 2003; Corbin, Geissler et al. 2004; Goehring and Beckwith 2005; Karimova, Dautin et al. 2005). FtsA may thus be involved in the modulation of FtsI transpeptidase activity and/or may help linking divisome formation with redirection of cell wall biosynthesis to form the septal cell wall (Tormo, Ayala et al. 1986; Dai and Lutkenhaus 1992; Margolin and Bernander 2004). FtsA is absent among archeobacteria lacking a cell wall layer (Nanninga 1998). It has recently been shown that FtsQ fused with the FtsZ-binding protein ZapA is recruited to the Z-ring independently of FtsA and FtsK. Since the FtsQ-ZapA fusion can coordinate the recruitment of downstream proteins other than FtsN, recruitment does not depend on FtsA-catalyzed Z-ring modification but rather on physical interaction between proteins (Goehring, Gueiros-Filho et al. 2005). Under these conditions, the function of FtsA can be bypassed only partially and the rings formed are not functional for division, probably because they lack FtsN and perhaps other activities of FtsA (Goehring, Gueiros-Filho et al. 2005; Vicente, Rico et al. 2006). The failure of FtsN recruitment in this system indicates that proper assembly of all components at the septum, particularly FtsA, might be essential for its localization (Margolin 2005). FtsA is required to recruit FtsQ at the division site and is able to recruit FtsI and FtsN independently of FtsZ (Chen, Weiss et al. 1999; Corbin, Geissler et al. 2004). Cell division proteins are thus related by a small but complex interaction network in which the most ubiquitous partners appear to be FtsQ and FtsA (Vicente, Rico et al. 2006).

FtsA as a motor protein

There is ample evidence that FtsA acts as a motor protein, providing the energy required for proper septation. It has two essential features in this respect: ATPase activity and the

ability to tether the Z-ring to the inner membrane (Feucht, Lucet et al. 2001; Paradis-Bleau, Sanschagrin et al. 2005; Pichoff and Lutkenhaus 2005). Furthermore, it should be borne in mind that the Z-ring can assemble but cannot constrict without FtsA (Begg, Nikolaichik et al. 1998; Pichoff and Lutkenhaus 2002; Geissler, Elraheb et al. 2003). FtsA could thus provide energy to drive Z-ring constriction and inner membrane invagination using its ATPase activity. The major distortion of the inner cell membrane conformation that must occur when septum ingrowth starts is conceivably an energetic barrier to be overcome (Errington, Daniel et al. 2003). It has been proposed that FtsA may draw closer to divisome subunits during septation and drive membrane invagination (Nanninga 1998; Feucht, Lucet et al. 2001; Errington, Daniel et al. 2003). For this to be the case, an unknown signal would have to regulate the ATPase motor force. Since phosphorylation often plays a regulatory role in biological systems and FtsA occurs in different phosphorylation states related to its ATP binding ability, the signal could be phosphorylation by an unknown enzyme. Finally, FtsA itself may form a constricting ring to allow inner membrane invagination, as discussed below.

The FtsA-FtsA interaction: formation of an A-ring?

The FtsA protein from *E. coli*, *B. subtilis* and *P. aeruginosa* forms native dimers and a small proportion of multimers has also been observed (Yim, Vandenbussche et al. 2000; Feucht, Lucet et al. 2001; Rico, Garcia-Ovalle et al. 2004; Paradis-Bleau, Sanschagrin et al. 2005). It has also been demonstrated that FtsA interacts with itself and that this interaction is essential for its biological function and hence for bacterial cell division (Sanchez, Valencia et al. 1994; Yan, Pearce et al. 2000; Yim, Vandenbussche et al. 2000). The C-terminus seems to be important for this self-interaction (Yim, Vandenbussche et al. 2000). Although FtsA does not form actin-like filaments, it localizes as a ring-like structure (Addinall and Lutkenhaus 1996; Yim, Vandenbussche et al. 2000; Feucht, Lucet et al. 2001) and thus may form a multiproteic higher-order structure and assemble as a mid cell ring (Addinall and Lutkenhaus 1996; van den Ent, Amos et al. 2001; Anderson, Gueiros-Filho et al. 2004). However, the predicted FtsA:FtsZ ratio of 1:100 in *E. coli* would not allow the formation of an FtsA ring (Wang and Gayda 1992; Addinall and Lutkenhaus 1996; Feucht, Lucet et al. 2001; Errington, Daniel et al. 2003). Based on more recent data

indicating a ratio of about 1:5 in both *E. coli* and *B. subtilis* (Feucht, Lucet et al. 2001; Rueda, Vicente et al. 2003), the number of FtsA molecules per cell could be sufficient to form a complete circumferential ring at the cell division site (Feucht, Lucet et al. 2001). A study by Carettoni *et al* has revealed that FtsA homodimerizes with the help of the subdomain 1C and a group of amino acids encompassing the ATP-binding site in subdomain 2B. It has been speculated that the nucleotide-binding status of FtsA could regulate head-to-tail interaction between FtsA monomers by settling subdomain 1C in an orientation favourable for intermolecular docking, thus allowing the assembly of FtsA units into polymers (Carettoni, Gomez-Puertas et al. 2003). Based on a study by Rico *et al*, FtsA homodimerization involves the subdomain 1C and the C-terminus end and essentially agrees with the model of Carettoni *et al*. In this model, there would be a free subdomain 2B and a free subdomain 1C at each end of the FtsA polymer that might be available for interaction with other division proteins (Rico, Garcia-Ovalle et al. 2004). *S. pneumoniae* has an FtsA:FtsZ ratio of 1:1.5 and thus contains more FtsA molecules than *B. subtilis* or *E. coli* (Feucht, Lucet et al. 2001; Rueda, Vicente et al. 2003; Lara, Rico et al. 2005). Purified FtsA from *S. pneumoniae* has recently been shown to polymerize in long and stable helix-like polymers dependent on ATP and Mg^{2+}. The higher affinity for ATP than for ADP and the lower stability of ADP-bound polymers suggest that FtsA may hydrolyse ATP in a cycle that regulates polymer dynamics, but this would likely require the assistance of other proteins *in vivo* (Lara, Rico et al. 2005). Finally, Pichoff *et al* propose that FtsA interaction with the inner membrane regulates self-interaction and that removal of the membrane-targeting motif allows the protein to undergo unregulated polymerization in the cytoplasm. The membrane interaction would thus direct FtsA self-interaction, with further interaction with FtsZ resulting in cooperative linkage of FtsZ polymers to form the Z-ring (Pichoff and Lutkenhaus 2005).

Overlapping roles of FtsA

Although FtsA and ZipA share nothing in terms of sequence or even architecture, they share some overlapping functions, since both proteins stabilize the Z-ring and recruit essential downstream division proteins (Hale and de Boer 1999; RayChaudhuri 1999; Pichoff and Lutkenhaus 2002; Geissler, Elraheb et al. 2003; Lowe, van den Ent et al. 2004).

Both depend on FtsZ to localize at the division site and bind FtsZ to a conserved sequence near the C-terminus, although they probably do not compete for the same binding sites (Wang, Huang et al. 1997; Hale and de Boer 1999; Ma and Margolin 1999; Yan, Pearce et al. 2000; Haney, Glasfeld et al. 2001; Pichoff and Lutkenhaus 2002; Errington, Daniel et al. 2003). It has also been shown that the Z-ring assembles at mid cell in the absence of FtsA or ZipA. However, the Z-ring is unable to form and preformed Z-ring destabilizes in the absence of both proteins. ZipA and FtsA are both required for recruitment of additional division proteins and for septal constriction but either is capable of supporting Z-ring formation and stabilization. Although both proteins tether the Z-ring to the membrane, it is quite possible that Z-ring-FtsA and Z-ring-ZipA have structural differences (Pichoff and Lutkenhaus 2002; Errington, Daniel et al. 2003). ZipA is anchored to the inner membrane through a single N-terminal transmembrane helix followed by a charged domain while FtsA is anchored via a C-terminal amphipathic helix (Ohashi, Hale et al. 2002; Pichoff and Lutkenhaus 2005).

Many studies highlight that FtsA has a much more important role than ZipA. FtsA is more highly conserved than ZipA, which appears to be present only in a subset of Gram-negative bacteria (Hale and de Boer 1997; RayChaudhuri 1999; Margolin 2000). FtsA has many more known interactions than ZipA with other bacterial cell division proteins (see Table I). The role of ZipA may be to enhance protein recruitment indirectly by modulating Z-ring dynamics, stabilizing ring components or altering ring conformational structure (Goehring and Beckwith 2005; Margolin 2005; Vicente, Rico et al. 2006). The most important clue is that an FtsA point mutation at the tip of domain 2B that changes the conserved Asn 286 to a Trp residue can completely bypass the requirement for ZipA, indicating that it is dispensable for the recruitment of downstream proteins (Geissler, Elraheb et al. 2003). Although ZipA is required to recruit a number of later septation proteins, its dispensability indicates that it does not directly recruit the later proteins but instead enhances the ability of another septal component to recruit them (Hale and de Boer 2002; Corbin, Geissler et al. 2004). The mutant form of FtsA is able to fulfill all tasks attributable to ZipA while stabilizing the FtsZ assembly, tethering the Z-ring to the membrane and recruiting all the downstream proteins required for an efficient divisome. This may explain why many bacteria can divide without an obvious ZipA homologue. In

addition, FtsA probably serves as the principal membrane anchor for the Z-ring (Geissler, Elraheb et al. 2003; Pichoff and Lutkenhaus 2005). It has been suggested that the point mutation change alters the ability of FtsA monomers to self-interact and/or to interact with FtsZ (Yim, Vandenbussche et al. 2000; Geissler, Elraheb et al. 2003). Bacterial species lacking ZipA may contain an FtsA with properties similar to the mutant FtsA protein (Geissler, Elraheb et al. 2003). These species may also have significantly higher intracellular concentrations of FtsA to compensate for the requirement for ZipA. However, it has been shown that *E. coli* and *B. subtilis,* the latter lacking a ZipA homologue, both contain the same relative amount of FtsA (Rueda, Vicente et al. 2003).

The FtsN cell division protein has been identified as a multi-copy suppressor of a thermo-sensitive mutation in *ftsA* and over-expression of FtsN has been shown to provide partial suppression of thermosensitive mutations in *ftsA, ftsK*, *ftsQ* and *ftsI* (Dai, Xu et al. 1993; Draper, McLennan et al. 1998). However, FtsN does not suppress an *ftsA*-null allele, suggesting that residual FtsA activity is necessary (Dai, Xu et al. 1993; Buddelmeijer and Beckwith 2002). FtsN may have an FtsZ stabilizing effect or modulate the ability of the cell envelope to invaginate and these functions may partially overlap with FtsA (Draper, McLennan et al. 1998; Margolin 2000). FtsA seems also to share some functions with the recently identified YlmF cell division protein (Ishikawa, Kawai et al. 2006). This protein is characterized by Z-ring-dependent division site localization and interacts with itself and with FtsZ, as does ZipA (Ohashi, Hale et al. 2002; Di Lallo, Fagioli et al. 2003; Hamoen, Meile et al. 2006; Ishikawa, Kawai et al. 2006). In contrast to ZipA, YlmF plays a non-essential role in septum development and is present in firmicutes (Gram-positive bacteria with a low GC content), symbiobacteria, fusobacteria, actinobacteria (Gram-positive bacteria with a high GC content), and cyanobacteria (Hale and de Boer 1997; Hamoen, Meile et al. 2006; Ishikawa, Kawai et al. 2006). YlmF becomes essential for the cell division process in the absence of EzrA or FtsA, whose functions are strikingly different (Hamoen, Meile et al. 2006; Ishikawa, Kawai et al. 2006). YlmF in excess has been shown to compensate for FtsA for both cell division protein recruitment and Z-ring constriction. Furthermore, expression of either protein is essential for *B. subtilis* cell division and growth. This suggests that some structure in the Z-ring promoted by FtsA and/or YlmF may recruit downstream cell division proteins in *B. subtilis* (Ishikawa, Kawai et al. 2006). YlmF

is present in some bacteria having no FtsA homologue and is thought to have an overlapping function with FtsA in stimulating Z-ring formation by cross-linking FtsZ proto-filaments. It has also been suggested that YlmF would play a critical role for cell division in FtsA-lacking bacteria, as FtsA does in YlmF-lacking bacteria, and that both FtsA and YlmF would work additively with FtsZ in bacteria that possess both proteins. However, FtsA contributes more strongly to cell division than does YlmF (Ishikawa, Kawai et al. 2006).

Even with overlapping functions, FtsA remains an essential protein and has a key role in the progression of the bacterial cell division process. This is confirmed by many studies reporting the inability of bacterial cells to divide when FtsA is inactivated, such as by temperature-sensitive mutation. Under these conditions, the apparently normal Z-ring is formed but constriction is blocked and the cells form long multinucleated non-septated filaments (Walker, Kovarik et al. 1975; Osley and Newton 1977; Fletcher, Irwin et al. 1978; Donachie, Begg et al. 1979; Lutkenhaus and Donachie 1979; Tormo and Vicente 1984; Begg and Donachie 1985; Descoteaux and Drapeau 1987; Robinson, Begg et al. 1988; Wang and Gayda 1990; Cook and Rothfield 1994; Addinall, Bi et al. 1996; Ohta, Ninfa et al. 1997; Hale and de Boer 1999). The FtsA protein has also been shown to be essential for bacterial survival, since *ftsA*-null is not viable in *E. coli* (Lutkenhaus and Donachie 1979), *C. crescentus* (Sackett, Kelly et al. 1998) or *S. pneumoniae* (Lara, Rico et al. 2005). In *B. subtilis*, deletion of *ftsA* can be viable, but the cells are severely impaired in division and growth, extremely filamentous, present distorted Z-rings and have reduced viability as well as reduced sporulation efficiency (Beall and Lutkenhaus 1992; Jensen, Thompson et al. 2005). Deletion of *ftsA* was in fact the first situation identified in which the loss of a single septation protein led to such a drastic reduction in the level of apparently normal Z-rings. The role of FtsA in Z-ring formation is thus critical and even more important in Gram-positive bacteria lacking a ZipA homologue (Jensen, Thompson et al. 2005). Finally, the limited viability of *ftsA*-null *B. subtilis* must rely on an important difference in the hierarchical assembly of the divisome. In *B. subtilis*, all division proteins are completely interdependent for recruitment and assembly at the division site (Errington, Daniel et al. 2003; Karimova, Dautin et al. 2005). The low level of normal Z-ring in *ftsA*-null *B. subtilis* is apparently sufficient to recruit the membrane-bound division proteins and

the role of FtsA appears to be indirect, though ensuring that FtsZ forms a proper ring (Jensen, Thompson et al. 2005).

Extended functions of FtsA

There is evidence indicating that FtsA influences the formation and maintenance of bacterial shape. Mutation at the C-terminus of FtsA transforms wild-type rod-shaped cells into curved C-shaped cells with aggregates of striated cylindrical structures crossing the cytoplasm. Aggregates of up to five cylinders are arrayed diagonally to the long axis of the curved cells and the ends of these aggregates appear to be at or near the cell membrane. FtsA thus acts directly on cell morphology phenotype (Gayda, Henk et al. 1992). It is also proposed that FtsA may redirect cell wall biosynthesis to form the septal cell wall required for proper division via an interaction with FtsI (Tormo, Ayala et al. 1986; Dai and Lutkenhaus 1992; Margolin and Bernander 2004). Since *S. pneumoniae* contains much more FtsA than does *B. subtilis* or *E. coli,* it has been postulated that large amounts of FtsA may be required for the continual septal synthesis required to maintain the quasi-spherical cell shape of cocci (Lara, Rico et al. 2005).

It is more obvious that FtsA has an important role in sporulation. The first clue came from the *B. subtilis ftsA*-null strain, which is characterized by reduced sporulation efficiency (Beall and Lutkenhaus 1992). Consistent with a crucial role in sporulation, FtsA has previously been called SpoIIN in *B. subtilis* and a thermo-sensitive mutation in this protein impairs vegetative cell division as well as sporulation. This mutant form of FtsA has been shown to be defective in Spo0A-controlled transcription required for switching the localization of FtsZ from a medial to a bipolar division site at the onset of sporulation (Karmazyn-Campelli, Fluss et al. 1992; Louie, Lee et al. 1992; Levin and Losick 1996). In sporulating cells of *B. subtilis*, FtsZ is recruited to potential division sites at both poles but asymmetric division occurs at only one pole. In contrast, FtsA is recruited to only one cell pole, suggesting that it may play an important role in the generation of asymmetry (Feucht, Lucet et al. 2001). An FtsA mutant that exhibits little or no detectable defect in medial division but forms aberrant polar septa during sporulation has also been identified. The mutation targets a residue conserved in FtsA among endospore-forming bacteria and other closely related species. Maturation of the sporulation septum is impaired in sporulating

cells of this mutant, resulting in a defect in the engulfment of the spore by the mother cell. The mutant is also defective in polar septum formation dependent activation of σF. Conserved residues of FtsA may be involved in a sporulation-specific protein interaction that facilitates sporulation septum maturation and the activation of σF (Kemp, Driks et al. 2002).

Finally, like FtsZ, FtsA seems to be involved in antibiotic resistance. Expression of the *ftsA-ftsZ* promoter submitted to RcsB is greatly increased in mecillinam-resistant mucoid mutants of *S. typhimurium*. The resistance of mucoid mutants to mecillinam would be due to over-expression of *ftsZ* and/or *ftsA* genes due to the increased activity of the RcsB effector (Costa and Anton 2001). FtsA is also needed to obtain full expression of *Citrobacter freundii ampC* β-lactamase. In the absence of FtsA, an accumulation of the corepressor UDP-MurNAc-pentapeptide represses β-lactamase expression (Uehara and Park 2002). The implication of FtsA in bacterial morphogenesis, sporulation and bacterial resistance mechanisms suggests that an antibacterial therapy against FtsA may affect these processes in addition to inhibiting cell division.

Tridimensional structure of FtsA and homology with eukaryotic actin

The crystal structure of FtsA from *T. maritima* has been resolved in the apo and ATP-bound forms (van den Ent and Lowe 2000). FtsA is a scattered and elongated protein consisting of two domains with the nucleotide-binding site in the interdomain cleft of the common core. This characteristic binding site is also found in the actin family of proteins. Each domain can be divided into two subdomains. The two larger subdomains, 1A and 2A, are similar and consist of a five-stranded β-sheet surrounded by three α-helices. The two other subdomains are smaller, more variable among the actin family and composed of different combinations of strands and helices. Subdomain 1C is composed of a three-stranded antiparallel β-sheet adjacent to an α-helix and has the same topology as the antiparallel β-sheet that comprises strands 2–5 and helix 1 of subdomain 1A, but with the chain traced in the opposite direction. The connection of subdomain 1C to the rest of the protein is flexible and movement of the second domain narrows the width of a cleft located between subdomains 1A and 1C. The angle of rotation of subdomain 1C is 13.5°, with

residue Glu 89 acting as the mechanical hinge. At the end of the insertion, strand 7 goes into helix 3 of subdomain 1A, which aligns perfectly with helix 5 of actin. Helix 3 is connected to strand 8 and, via helix 4, reaches subdomain 2A. This subdomain is again divided into two parts with regard to the primary sequence, but this time the insertion of subdomain 2B is in exactly the same position as in actin: inserted after helix 5 and three antiparallel β-strands of subdomain 2A. Helices 6 and 7 of subdomain 2B are both involved in co-coordinating the nucleotide. Subdomain 2B is completed with two additional short antiparallel β-strands and the N-terminal part of helix 8. Helix 8 contributes to the structure of both subdomains 2A and 2B. A partially disordered loop connects helix 8 to strand 14, the latter being part of the five-stranded β-sheet of subdomain 2A. Strand 15 is connected by a long loop to the C-terminal helix, which belongs to subdomain 1A. The last 27 residues of FtsA are disordered and have not been resolved. The position of this C-terminal tail is most likely oriented on the same direction and in close proximity to subdomain 1C (van den Ent and Lowe 2000).

The nucleotide-binding pocket of FtsA is located in a cleft formed at the interface between subdomains 1A, 2A and 2B. The adenosine is positioned in a hydrophobic pocket composed of residues that belong to a short 3_{10}-helix of subdomain 2A and part of a helix in subdomain 2B. The pocket is closed at the back by two residues of subdomain 2B, which form hydrogen bonds. The other side of the pocket is open to the outside. The phosphate moiety of the nucleotide is bound by two loops. Each loop connects the first and second strands of subdomain 1A and 2A, respectively. The first loop binds the β-phosphate and makes hydrogen bonds with both the α- and the β-phosphates. The second loop makes hydrogen bonds with the γ- and α-phosphates. A magnesium ion is located in a hydrophilic pocket formed by the β- and γ-phosphates and by Asp14, Lys21, Ser190 and Asn212. A water molecule 3.5 Å from the γ-phosphate is a putative attacking nucleophile, positioned by hydrogen bonds with the main-chain nitrogen of Gly219 and the main-chain oxygen of Phe217 (van den Ent and Lowe 2000). The active site of FtsA contains 25 amino acids, of which seven are in common with actin. Despite the very limited overall sequence similarity between actin and FtsA, the order of their secondary structure elements is very similar with the exception of the second subdomain. In actin, this subdomain is inserted after the third β-strand, whereas the third β-strand in FtsA is followed by a helix and the fourth β-strand of

subdomain 1A, before the second subdomain is inserted. The fold and the topology of subdomain 1C in FtsA are unusual for the actin family and suggest that subdomain 1C has an important functional role specific to FtsA. Other differences of minor impact exist between the structures of FtsA and actin and likely reflect specific functional differences, for example, the very long loop connecting subdomain 2A to the C-terminal helix of FtsA. Since this loop is in close proximity to subdomain 1C, it may be involved in an FtsA-specific function. Since striking similarity has been found in proteins with entirely different functions, it has previously been postulated that these domains are the result of divergent evolution from a common ancestor (Bork, Sander et al. 1992; van den Ent and Lowe 2000).

In general however, FtsA is typical of the actin superfamily, possessing two domains with a common core and an interdomain cleft harbouring the nucleotide-binding site. FtsA is thus part of the functionally diverse actin/hexokinase/HSP70 superfamily of proteins (Bork, Sander et al. 1992). Although the most significant homology of FtsA is shared with actin (van den Ent and Lowe 2000), FtsA is not considered a true functional prokaryotic homologue of actin. MreB, a protein required for maintaining bacterial cell shape and polymerizing into helical actin-like proto-filaments that extend from one cell pole to the other, is much more like actin (Jones, Carballido-Lopez et al. 2001; van den Ent, Amos et al. 2001; Romberg and Levin 2003). The structure and biochemical activity of MreB are also much closer than FtsA to actin and provide strong support for the existence of true actin homologues in bacteria (van den Ent and Lowe 2000; van den Ent, Amos et al. 2001; Anderson, Gueiros-Filho et al. 2004; Moller-Jensen and Lowe 2005). FtsA is thus believed to have diverged from a putative actin ancestor following a gene duplication and fusion process to develop a unique structural feature (van den Ent, Amos et al. 2001; Anderson, Gueiros-Filho et al. 2004).

Functionality of the C-terminal tail and of the subdomains 1C and 2B of FtsA

Crystal structure has revealed a conserved 10–13 residue motif at the C-terminal tail in all FtsA proteins. This motif may facilitate recruitment and directing of downstream proteins to the divisome (Lowe and van den Ent 2001). The tail seems to have an important biological function, since deletion of 28 residues at the C-terminus produces a curved filament phenotype in growing cells (Gayda, Henk et al. 1992). Thin sections of these cells

reveal that an intracellular structure connects two points of the cell envelope, forcing curved growth. The helix probability is high for the last 13 residues of the C-terminal motif, which is separated from the core domain by a hydrophilic linker that is variable in size and makes the motif accessible to other proteins (Lowe and van den Ent 2001). The C-terminal end is involved in the interaction between FtsA molecules in *E. coli* (Rico, Garcia-Ovalle et al. 2004). It has been shown previously by yeast two-hybrid analysis that an FtsA protein lacking the last five residues does not interact with itself. Furthermore, this truncated FtsA protein localizes at the division site but has no activity in septation (Yim, Vandenbussche et al. 2000). The C-terminal tail of FtsA has also been shown to perform the essential function of tethering FtsA and therefore FtsZ to the inner membrane. The conserved motif at the extreme C-terminus of FtsA is not present in the crystal structure, indicating that it is not organized, although computer predictions indicate that this motif is an amphiphatic helix (Pichoff and Lutkenhaus 2005).

Subdomain 1C of FtsA is located on the side of the first domain opposite from its position in actin. This unexpected position has not been recognized in the prediction of a tridimensional model of FtsA based on a multiple sequence alignment of the actin family of proteins (Sanchez, Valencia et al. 1994). The insertion of this subdomain is an important difference between FtsA and the actin family of proteins. Its movement partially encloses a groove, which could bind the C-terminus of FtsZ. However, there is no clear homology between subdomain 1C and any known structure (van den Ent and Lowe 2000). Subdomain 1C has thus fueled numerous studies. Its distinctive structure has led to the definition of a novel and distinct evolutionarily mobile domain with a simple fold utilized as a common theme in a variety of biological functions. This fold contains a core of three strands forming a curved sheet and a single helix in a strand–helix–strand–strand (SHS2) configuration and appears to mediate heteromeric protein–protein interactions by means of strand 1 and the loop between strands 2 and 3 (Anantharaman and Aravind 2004). FtsA has been shown to recruit FtsI and FtsN independently of the Z-ring via subdomain 1C (Corbin, Geissler et al. 2004). Artificially directing this subdomain to the Z-ring partially suppresses a thermosensitive *ftsA* mutation, suggesting that FtsA may be the major protein connecting the Z-ring and the downstream proteins, and that subdomain 1C is a completely independent functional domain with an important role in interacting with septation protein

subassembly (Corbin, Geissler et al. 2004; Vicente, Rico et al. 2006). Subdomain 1C is not required for the localization of FtsA to the Z-ring and seems not to be involved in the FtsA-FtsZ interaction. One key role of FtsA and of subdomain 1C in particular is to interact either directly or indirectly with an FtsI-FtsN subassembly (Corbin, Geissler et al. 2004). Phage-display screening against FtsA has selected a degenerate consensus sequence having striking similarity with residues 126–133 of subdomain 1C. These residues are probably involved in homodimerization of FtsA and have been shown to be essential for the proper function of FtsA and related to a group of amino acids encompassing the ATP-binding site on the domain 2B facing monomer as well as a set of residues immediately downstream from amino acids 126–133. Since the connection of subdomain 1C with the rest of the protein is flexible, it has been tempting to speculate that the nucleotide-binding status of FtsA could regulate its homodimerization by settling subdomain 1C in a favorable orientation for intermolecular docking (Carettoni, Gomez-Puertas et al. 2003). A study by Rico *et al* also confirms the homodimerization model involving subdomain 1C. FtsA protein lacking subdomain 1C has been found to localize correctly but does not interact with other FtsA and fails to recruit FtsQ and FtsN into the division ring, resulting in an incomplete divisome that does not support division. Subdomain 1C is essential for FtsA–FtsA self-interaction and the recruitment of downstream division proteins but would not be directly involved in the FtsA–FtsZ interaction. The model of Carettoni *et al*. postulates interaction between FtsA molecules involving domains 1C and 2B, while within domain 2B, β-strands S12 and S13 are proposed to interact with residues 126–133 of domain 1C. However, Rico *et al* have found that this last interaction would not be essential for dimerization. Even in the absence of β-strands S12 and S13, there is still a large enough contact surface between domains 1C and 2B to maintain interaction, although the complex formed would not be fully functional (Rico, Garcia-Ovalle et al. 2004).

The tips of strands S12–S13 of domain 2B have been shown to affect Z-ring localization and dynamics. In the absence of these strands, the distribution of active division rings becomes altered and misplaced, yielding short cells with no DNA and other aberrant cells. Since a point mutation in β-strand S13 bypasses the need for ZipA and seems to counteract the inhibition of Z-ring formation by MinC, the putative enhanced FtsZ stabilizing activity of FtsA lacking the S12–13 strands may allow Z-ring formation at

abnormal locations, even near the poles (Geissler, Elraheb et al. 2003; Rico, Garcia-Ovalle et al. 2004). Subdomain 2B must interact with FtsZ and the absence of S12–S13 strands may increase ring stability, which is then able to overcome the actions of the Min and nucleoid occlusion systems at least partially. These observations support a regulatory role for FtsA (Rico, Garcia-Ovalle et al. 2004; Vicente, Rico et al. 2006).

Inhibitors of FtsA

In contrast to FtsZ, very few inhibitors have been identified against FtsA and only one study has been published with the aim of identifying FtsA inhibitors. A well-focused phage display screening using competitive elutions with ATP, a non-hydrolysable analogue of ATP, and the FtsZ protein has identified many peptide sequences that presumably interact with FtsA (Paradis-Bleau, Sanschagrin et al. 2005). Consensus peptide sequences, as well as peptide sequences having the highest affinity for the target protein and which therefore represent potential specific inhibitors, have been sequenced. Five of the six peptides synthesized specifically inhibit the ATPase activity of FtsA. The most promising of these has an IC_{50} value of 700 μM and their discovery represents the first step towards the future development of potent inhibitors via peptidomimetism (Paradis-Bleau, Sanschagrin et al. 2005).

This study also reports the selection of a perfect 12-mer consensus peptide by a specific elution step with FtsZ. The corresponding peptide does not inhibit the ATPase activity of FtsA and the sequence displays a KPSPR motif homologous with the FtsA interaction site of FtsZ. It has been proposed that this peptide may be an inhibitor of the essential FtsA–FtsZ interaction, which represents a more sensitive and specific target than the ATPase activity of FtsA alone (Yan, Pearce et al. 2000; Haney, Glasfeld et al. 2001; Paradis-Bleau, Sanschagrin et al. 2005). Furthermore, destabilization of the FtsA–FtsZ or FtsA–FtsA protein-protein interaction severely affects the bacterial cell division process (Ma and Margolin 1999; Yim, Vandenbussche et al. 2000; Rico, Garcia-Ovalle et al. 2004). Since the FtsA and ZipA interaction sites overlap on the FtsZ protein, it would be interesting to evaluate the inhibitory potential of FtsZ-ZipA inhibitors for FtsZ-FtsA interaction.

Concluding remarks and future perspectives

The complex bacterial cell division process involves many proteins which possess most of the characteristics of ideal antibacterial targets. Theses proteins are thus interesting in the prospect of developing new antibacterial therapies in order to face critical increase and spread of antibiotic resistance mechanisms and to control emerging bacterial pathogens. We have focused on FtsZ and FtsA as the most promising antibacterial targets but mostly all cell division proteins represent attractive targets to design novel classes of antibacterial agents with innovative structures and new modes of action. The multifunctional FtsK protein is the most promising antibacterial target after FtsZ and FtsA. This protein is required for both septum formation and cell division protein recruitment in addition to coordinating cell division with segregation of the replicated chromosomes. Antibacterial strategies targeting FtsK would thus be highly efficient, affecting both cell division and integrity of bacterial DNA. The essential FtsW and FtsI proteins also represent good candidates for development of new antibacterial agents. FtsW facilitates the septal peptidoglycan synthesis of FtsI, which allows proper division and formation of the new cell poles of daughter cells. Antibacterial strategies targeting FtsW and FtsI would therefore strongly inhibit the cell division process. The few current β-lactam drugs which preferentially inhibit FtsI unfortunately induce the SOS system of DNA repair (Miller, Thomsen et al. 2004). To circumvent this problem, these β-lactams could be use in combination with inhibitors of FtsK. The cell division proteins ZipA, FtsQ, FtsN, AmiC and EnvC are present only in limited sets of bacterial species and could be used as targets to develop narrow- spectrum antibacterial agents.

FtsZ represents the most appealing antibacterial target of the cell division apparatus, as it is the most important and conserved protein. Many FtsZ inhibitors have been described and these molecules have to be pharmacologically optimized in order to develop effective and safe antibacterial therapies. The biggest problem is how to get the inhibitors to cross the bacterial membranes and avoid actions of efflux pumps in order to accumulate and remain at a concentration high enough in the cytoplasm and for long enough to inhibit the targeted FtsZ proteins. To meet this challenge and thwart bacterial resistance, inhibitory molecules may be conjugated to a stable bacterial transport moiety that promotes uptake via

active transport mechanisms required for bacterial virulence. Chemical parameters can also be explored as an avenue to obtaining passive diffusion of small inhibitory compounds through bacterial membranes without disturbing host cell membranes (Silver 2003; Silver 2006). In the case of Gram-negative pathogens, the selective permeation barrier of the LPS-containing outer membrane can be perturbed by specific polycationic permeabilizers such as polymyxin B, cationic peptides and aminoglycosides (Nikaido 2003). Such permeabilizers could be used synergistically with FtsZ inhibitors or the inhibitors could be transformed or complexed to mimic the permeabilization effect of polycationic compounds. Finally, filamentous phages can be used as specific and efficient targeted drug carriers and FtsZ inhibitors could be linked to these by means of chemical conjugation through a labile linker subject to controlled release in the bacterial cytoplasm (Yacoby, Shamis et al. 2006). Some of the described FtsZ inhibitors efficiently cross the bacterial membranes and their structures can be used as templates for further optimization. Finally, designing inhibitors which interact with invariant sites of FtsZ should help to reduce the likelihoop of resistance development (Miesel, Greene et al. 2003).

In contrast to FtsZ, few FtsA inhibitors have been discovered. The peptides active against FtsA have to be pharmacologically optimized to enhance their inhibitory potential and antimicrobial activity and new inhibitors will have to be identified via a rational design to develop novel classes of antibacterial agents targeting FtsA. The design of specific ATPase inhibitors is a promising approach. The structural diversity among the ATPase enzymes can be exploited to develop selective, specific and potent inhibitors, based on the structural properties of the nucleotide-binding site and complete active site, the conformation of the bound nucleotide and the adenosine–protein interactions (Chene 2002). As a proof of principle, FtsA presents a more complex nucleotide-binding site then most common P-loop ATPases which contain the classical mononucleotide-binding motif. Furthermore, FtsA binds the nucleotide in a different orientation in comparison to the vast majority of ATPases. The ATPase inhibitors of FtsA must be able to cross the bacterial membranes and to efficiently compete with the high ATP concentration present in the cell. Since phosphate-containing molecules are characterized by lower bioavailability and poor stability, the challenge will be to synthesize ATP mimics that lack phosphate groups. To compensate for the loss in binding energy, phosphate-free molecules must bind more

tightly to the adenosine-binding region by filling non-occupied hydrophobic pockets. However, FtsA does not contain an empty cavity at the ATP-binding site and the design of non-competitive inhibitors might be more advantageous. ATPase inhibitors must also be highly selective, because of the similarity of the nucleotide-binding sites on FtsA, actin and Hsp70 proteins. Exploration of structural and sequence diversity among these ATPase would likely permit the design of selective and safe compounds (Chene 2002).

For a strong effect against bacterial growth and survival, a typical enzyme inhibitor must be very strong, as the vast majority of the proteins can fulfill their biological function at only 5% residual activity. However, FtsZ and FtsA escape this rule as 50 % inhibition of either changes the effective FtsA:FtsZ ratio and efficiently blocks the essential bacterial cell division process (Haney, Glasfeld et al. 2001). Indeed, it should be borne in mind that the cell division protein-protein interaction network represents an excellent and unexploited source of targets for antibacterial agents.

References

Aarsman, M. E., A. Piette, et al. (2005). "Maturation of the *Escherichia coli* divisome occurs in two steps." Mol Microbiol **55**(6): 1631-45.

Adam, M., C. Fraipont, et al. (1997). "The bimodular G57-V577 polypeptide chain of the class B penicillin-binding protein 3 of *Escherichia coli* catalyzes peptide bond formation from thiolesters and does not catalyze glycan chain polymerization from the lipid II intermediate." J Bacteriol **179**(19): 6005-9.

Addinall, S. G., E. Bi, et al. (1996). "FtsZ ring formation in *fts* mutants." J Bacteriol **178**(13): 3877-84.

Addinall, S. G., C. Cao, et al. (1997). "FtsN, a late recruit to the septum in *Escherichia coli*." Mol Microbiol **25**(2): 303-9.

Addinall, S. G. and B. Holland (2002). "The tubulin ancestor, FtsZ, draughtsman, designer and driving force for bacterial cytokinesis." J Mol Biol **318**(2): 219-36.

Addinall, S. G. and J. Lutkenhaus (1996). "FtsA is localized to the septum in an FtsZ-dependent manner." J Bacteriol **178**(24): 7167-72.

Amos, L. A., F. van den Ent, et al. (2004). "Structural/functional homology between the bacterial and eukaryotic cytoskeletons." Curr Opin Cell Biol **16**(1): 24-31.

Anantharaman, V. and L. Aravind (2004). "The SHS2 module is a common structural theme in functionally diverse protein groups, like Rpb7p, FtsA, GyrI, and MTH1598/TM1083 superfamilies." Proteins **56**(4): 795-807.

Anderson, D. E., F. J. Gueiros-Filho, et al. (2004). "Assembly dynamics of FtsZ rings in *Bacillus subtilis* and *Escherichia coli* and effects of FtsZ-regulating proteins." J Bacteriol **186**(17): 5775-81.

Aussel, L., F. X. Barre, et al. (2002). "FtsK is a DNA motor protein that activates chromosome dimer resolution by switching the catalytic state of the XerC and XerD recombinases." Cell **108**(2): 195-205.

Baba, T. and O. Schneewind (1998). "Targeting of muralytic enzymes to the cell division site of Gram-positive bacteria: repeat domains direct autolysin to the equatorial surface ring of *Staphylococcus aureus*." Embo J **17**(16): 4639-46.

Beaber, J. W., B. Hochhut, et al. (2004). "SOS response promotes horizontal dissemination of antibiotic resistance genes." Nature **427**(6969): 72-4.

Beall, B. and J. Lutkenhaus (1991). "FtsZ in *Bacillus subtilis* is required for vegetative septation and for asymmetric septation during sporulation." Genes Dev **5**(3): 447-55.

Beall, B. and J. Lutkenhaus (1992). "Impaired cell division and sporulation of a *Bacillus subtilis* strain with the *ftsA* gene deleted." J Bacteriol **174**(7): 2398-403.

Begg, K., Y. Nikolaichik, et al. (1998). "Roles of FtsA and FtsZ in activation of division sites." J Bacteriol **180**(4): 881-4.

Begg, K. J. and W. D. Donachie (1985). "Cell shape and division in *Escherichia coli*: experiments with shape and division mutants." J Bacteriol **163**(2): 615-22.

Ben-Yehuda, S. and R. Losick (2002). "Asymmetric cell division in *B. subtilis* involves a spiral-like intermediate of the cytokinetic protein FtsZ." Cell **109**(2): 257-66.

Bernhardt, T. G. and P. A. de Boer (2003). "The *Escherichia coli* amidase AmiC is a periplasmic septal ring component exported via the twin-arginine transport pathway." Mol Microbiol **48**(5): 1171-82.

Bernhardt, T. G. and P. A. de Boer (2004). "Screening for synthetic lethal mutants in *Escherichia coli* and identification of EnvC (YibP) as a periplasmic septal ring factor with murein hydrolase activity." Mol Microbiol **52**(5): 1255-69.

Bernhardt, T. G. and P. A. de Boer (2005). "SlmA, a nucleoid-associated, FtsZ binding protein required for blocking septal ring assembly over chromosomes in *E. coli*." Mol Cell **18**(5): 555-64.

Beuria, T. K., M. K. Santra, et al. (2005). "Sanguinarine blocks cytokinesis in bacteria by inhibiting FtsZ assembly and bundling." Biochemistry **44**(50): 16584-93.

Bi, E. and J. Lutkenhaus (1993). "Cell division inhibitors SulA and MinCD prevent formation of the FtsZ ring." J Bacteriol **175**(4): 1118-25.

Bi, E. F. and J. Lutkenhaus (1991). "FtsZ ring structure associated with division in *Escherichia coli*." Nature **354**(6349): 161-4.

Bigot, S., J. Corre, et al. (2004). "FtsK activities in Xer recombination, DNA mobilization and cell division involve overlapping and separate domains of the protein." Mol Microbiol **54**(4): 876-86.

Bloom, B. R. and C. J. Murray (1992). "Tuberculosis: commentary on a reemergent killer." Science **257**(5073): 1055-64.

Bork, P., C. Sander, et al. (1992). "An ATPase domain common to prokaryotic cell cycle proteins, sugar kinases, actin, and hsp70 heat shock proteins." Proc Natl Acad Sci U S A **89**(16): 7290-4.

Bourne, H. R., D. A. Sanders, et al. (1991). "The GTPase superfamily: conserved structure and molecular mechanism." Nature **349**(6305): 117-27.

Boyle, D. S., M. M. Khattar, et al. (1997). "*ftsW* is an essential cell-division gene in *Escherichia coli*." Mol Microbiol **24**(6): 1263-73.

Bramhill, D. and C. M. Thompson (1994). "GTP-dependent polymerization of *Escherichia coli* FtsZ protein to form tubules." Proc Natl Acad Sci U S A **91**(13): 5813-7.

Brown, E. D. and G. D. Wright (2005). "New targets and screening approaches in antimicrobial drug discovery." Chem Rev **105**(2): 759-74.

Brown, K., J. F. Cavalla, et al. (1968). "Diaryloxazole and diarylthiazolealkanoic acids: two novel series of non-steroidal anti-inflammatory agents." Nature **219**(150): 164.

Buddelmeijer, N. and J. Beckwith (2002). "Assembly of cell division proteins at the *E. coli* cell center." Curr Opin Microbiol **5**(6): 553-7.

Buddelmeijer, N. and J. Beckwith (2004). "A complex of the *Escherichia coli* cell division proteins FtsL, FtsB and FtsQ forms independently of its localization to the septal region." Mol Microbiol **52**(5): 1315-27.

Buddelmeijer, N., N. Judson, et al. (2002). "YgbQ, a cell division protein in *Escherichia coli* and *Vibrio cholerae*, localizes in codependent fashion with FtsL to the division site." Proc Natl Acad Sci U S A **99**(9): 6316-21.

Caldon, C. E. and P. E. March (2003). "Function of the universally conserved bacterial GTPases." Curr Opin Microbiol **6**(2): 135-9.

Cam, K., G. Rome, et al. (1996). "RNase E processing of essential cell division genes mRNA in *Escherichia coli*." Nucleic Acids Res **24**(15): 3065-70.

Caplan, M. R. and H. P. Erickson (2003). "Apparent cooperative assembly of the bacterial cell division protein FtsZ demonstrated by isothermal titration calorimetry." J Biol Chem **278**(16): 13784-8.

Carballido-Lopez, R. and J. Errington (2003). "A dynamic bacterial cytoskeleton." Trends Cell Biol **13**(11): 577-83.

Carettoni, D., P. Gomez-Puertas, et al. (2003). "Phage-display and correlated mutations identify an essential region of subdomain 1C involved in homodimerization of *Escherichia coli* FtsA." Proteins **50**(2): 192-206.

Carrion, M., M. J. Gomez, et al. (1999). "*mraW*, an essential gene at the *dcw* cluster of *Escherichia coli* codes for a cytoplasmic protein with methyltransferase activity." Biochimie **81**(8-9): 879-88.

Carson, M. J., J. Barondess, et al. (1991). "The FtsQ protein of *Escherichia coli*: membrane topology, abundance, and cell division phenotypes due to overproduction and insertion mutations." J Bacteriol **173**(7): 2187-95.

Chan, P. F., R. Macarron, et al. (2002). "Novel antibacterials: a genomics approach to drug discovery." Curr Drug Targets Infect Disord **2**(4): 291-308.

Chauhan, A., M. V. Madiraju, et al. (2006). "*Mycobacterium tuberculosis* cells growing in macrophages are filamentous and deficient in FtsZ rings." J Bacteriol **188**(5): 1856-65.

Chen, J. C. and J. Beckwith (2001). "FtsQ, FtsL and FtsI require FtsK, but not FtsN, for co-localization with FtsZ during *Escherichia coli* cell division." Mol Microbiol **42**(2): 395-413.

Chen, J. C., M. Minev, et al. (2002). "Analysis of ftsQ mutant alleles in *Escherichia coli*: complementation, septal localization, and recruitment of downstream cell division proteins." J Bacteriol **184**(3): 695-705.

Chen, J. C., D. S. Weiss, et al. (1999). "Septal localization of FtsQ, an essential cell division protein in *Escherichia coli*." J Bacteriol **181**(2): 521-30.

Chen, Y., K. Bjornson, et al. (2005). "A rapid fluorescence assay for FtsZ assembly indicates cooperative assembly with a dimer nucleus." Biophys J **88**(1): 505-14.

Chen, Y. and H. P. Erickson (2005). "Rapid in vitro assembly dynamics and subunit turnover of FtsZ demonstrated by fluorescence resonance energy transfer." J Biol Chem **280**(23): 22549-54.

Chene, P. (2002). "ATPases as drug targets: learning from their structure." Nat Rev Drug Discov **1**(9): 665-73.

Chon, Y. and R. Gayda (1988). "Studies with FtsA-LacZ protein fusions reveal FtsA located inner-outer membrane junctions." Biochem Biophys Res Commun **152**(3): 1023-30.

Cohen, M. L. (2000). "Changing patterns of infectious disease." Nature **406**(6797): 762-7.

Conter, A., J. P. Bouche, et al. (1996). "Identification of a new inhibitor of essential division gene *ftsZ* as the *kil* gene of defective prophage Rac." J Bacteriol **178**(17): 5100-4.

Cook, W. R. and L. I. Rothfield (1994). "Development of the cell-division site in FtsA-filaments." Mol Microbiol **14**(3): 497-503.

Corbin, B. D., B. Geissler, et al. (2004). "Z-ring-independent interaction between a subdomain of FtsA and late septation proteins as revealed by a polar recruitment assay." J Bacteriol **186**(22): 7736-44.

Cordell, S. C., E. J. Robinson, et al. (2003). "Crystal structure of the SOS cell division inhibitor SulA and in complex with FtsZ." Proc Natl Acad Sci U S A **100**(13): 7889-94.

Costa, C. S. and D. N. Anton (2001). "Role of the ftsA1p promoter in the resistance of mucoid mutants of *Salmonella enterica* to mecillinam: characterization of a new type of mucoid mutant." FEMS Microbiol Lett **200**(2): 201-5.

Cunha, B. A. (2001). "Effective antibiotic-resistance control strategies." Lancet **357**(9265): 1307-8.

Dai, K. and J. Lutkenhaus (1991). "*ftsZ* is an essential cell division gene in *Escherichia coli*." J Bacteriol **173**(11): 3500-6.

Dai, K. and J. Lutkenhaus (1992). "The proper ratio of FtsZ to FtsA is required for cell division to occur in *Escherichia coli*." J Bacteriol **174**(19): 6145-51.

Dai, K., Y. Xu, et al. (1993). "Cloning and characterization of *ftsN*, an essential cell division gene in *Escherichia coli* isolated as a multicopy suppressor of *ftsA12*(Ts)." J Bacteriol **175**(12): 3790-7.

Daniel, R. A., E. J. Harry, et al. (2000). "Role of penicillin-binding protein PBP 2B in assembly and functioning of the division machinery of *Bacillus subtilis*." Mol Microbiol **35**(2): 299-311.

Datta, P., A. Dasgupta, et al. (2002). "Interaction between FtsZ and FtsW of *Mycobacterium tuberculosis*." J Biol Chem **277**(28): 24983-7.

Davies, J. C. (2002). "*Pseudomonas aeruginosa* in cystic fibrosis: pathogenesis and persistence." Paediatr Respir Rev **3**(2): 128-34.

de Boer, P., R. Crossley, et al. (1992). "The essential bacterial cell-division protein FtsZ is a GTPase." Nature **359**(6392): 254-6.

de Boer, P. A., R. E. Crossley, et al. (1989). "A division inhibitor and a topological specificity factor coded for by the minicell locus determine proper placement of the division septum in *E. coli*." Cell **56**(4): 641-9.

de Pedro, M. A., J. C. Quintela, et al. (1997). "Murein segregation in *Escherichia coli*." J Bacteriol **179**(9): 2823-34.

Del Sol, R., J. G. Mullins, et al. (2006). "Influence of CrgA on assembly of the cell division protein FtsZ during development of *Streptomyces coelicolor*." J Bacteriol **188**(4): 1540-50.

Den Blaauwen, T., M. E. Aarsman, et al. (2003). "Penicillin-binding protein PBP2 of *Escherichia coli* localizes preferentially in the lateral wall and at mid-cell in comparison with the old cell pole." Mol Microbiol **47**(2): 539-47.

Den Blaauwen, T., N. Buddelmeijer, et al. (1999). "Timing of FtsZ assembly in *Escherichia coli*." J Bacteriol **181**(17): 5167-75.

Descoteaux, A. and G. R. Drapeau (1987). "Regulation of cell division in *Escherichia coli* K-12: probable interactions among proteins FtsQ, FtsA, and FtsZ." J Bacteriol **169**(5): 1938-42.

Desnottes, J. F. (1996). "New targets and strategies for the development of antibacterial agents." Trends Biotechnol **14**(4): 134-40.

Dewar, S. J., K. J. Begg, et al. (1992). "Inhibition of cell division initiation by an imbalance in the ratio of FtsA to FtsZ." J Bacteriol **174**(19): 6314-6.

Dewar, S. J. and R. Dorazi (2000). "Control of division gene expression in *Escherichia coli*." FEMS Microbiol Lett **187**(1): 1-7.

Di Berardino, M., A. Dijkstra, et al. (1996). "The monofunctional glycosyltransferase of *Escherichia coli* is a member of a new class of peptidoglycan-synthesising enzymes." FEBS Lett **392**(2): 184-8.

Di Lallo, G., M. Fagioli, et al. (2003). "Use of a two-hybrid assay to study the assembly of a complex multicomponent protein machinery: bacterial septosome differentiation." Microbiology **149**: 3353-9.

Diaz, J. F., A. Kralicek, et al. (2001). "Activation of cell division protein FtsZ. Control of switch loop T3 conformation by the nucleotide gamma-phosphate." J Biol Chem **276**(20): 17307-15.

Diez, A., N. Gustavsson, et al. (2000). "The universal stress protein A of *Escherichia coli* is required for resistance to DNA damaging agents and is regulated by a RecA/FtsK-dependent regulatory pathway." Mol Microbiol **36**(6): 1494-503.

Din, N., E. M. Quardokus, et al. (1998). "Dominant C-terminal deletions of FtsZ that affect its ability to localize in *Caulobacter* and its interaction with FtsA." Mol Microbiol **27**(5): 1051-63.

Donachie, W. D. (1993). "The cell cycle of *Escherichia coli*." Annu Rev Microbiol **47**: 199-230.

Donachie, W. D. (2001). "Co-ordinate regulation of the *Escherichia coli* cell cycle or the cloud of unknowing." Mol Microbiol **40**(4): 779-85.

Donachie, W. D., K. J. Begg, et al. (1979). "Role of the *ftsA* gene product in control of *Escherichia coli* cell division." J Bacteriol **140**(2): 388-94.

Dorazi, R. and S. J. Dewar (2000). "The SOS promoter dinH is essential for *ftsK* transcription during cell division." Microbiology **146**: 2891-9.

Draper, G. C., N. McLennan, et al. (1998). "Only the N-terminal domain of FtsK functions in cell division." J Bacteriol **180**(17): 4621-7.

Eberhardt, C., L. Kuerschner, et al. (2003). "Probing the catalytic activity of a cell division-specific transpeptidase *in vivo* with beta-lactams." J Bacteriol **185**(13): 3726-34.

Edwards, D. H. and J. Errington (1997). "The *Bacillus subtilis* DivIVA protein targets to the division septum and controls the site specificity of cell division." Mol Microbiol **24**(5): 905-15.

El Zoeiby, A., F. Sanschagrin, et al. (2003). "Structure and function of the Mur enzymes: development of novel inhibitors." Mol Microbiol **47**(1): 1-12.

Erickson, H. P. (1998). "Atomic structures of tubulin and FtsZ." Trends Cell Biol **8**(4): 133-7.

Erickson, H. P. and D. Stoffler (1996). "Protofilaments and rings, two conformations of the tubulin family conserved from bacterial FtsZ to alpha/beta and gamma tubulin." J Cell Biol **135**(1): 5-8.

Errington, J., R. A. Daniel, et al. (2003). "Cytokinesis in bacteria." Microbiol Mol Biol Rev **67**(1): 52-65.

Espeli, O., C. Lee, et al. (2003). "A physical and functional interaction between *Escherichia coli* FtsK and topoisomerase IV." J Biol Chem **278**(45): 44639-44.

Farr, G. W. and H. Sternlicht (1992). "Site-directed mutagenesis of the GTP-binding domain of beta-tubulin." J Mol Biol **227**(1): 307-21.

Fauci, A. S. (2001). "Infectious diseases: considerations for the 21st century." Clin Infect Dis **32**(5): 675-85.

Ferguson, P. L. and G. S. Shaw (2004). "Human S100B protein interacts with the *Escherichia coli* division protein FtsZ in a calcium-sensitive manner." J Biol Chem **279**(18): 18806-13.

Feucht, A., I. Lucet, et al. (2001). "Cytological and biochemical characterization of the FtsA cell division protein of *Bacillus subtilis*." Mol Microbiol **40**(1): 115-25.

Figge, R. M., A. V. Divakaruni, et al. (2004). "MreB, the cell shape-determining bacterial actin homologue, co-ordinates cell wall morphogenesis in *Caulobacter crescentus*." Mol Microbiol **51**(5): 1321-32.

Fiskus, W., I. Padmalayam, et al. (2003). "Identification and characterization of the *ddlB*, *ftsQ* and *ftsA* genes upstream of *ftsZ* in *Bartonella bacilliformis* and *Bartonella henselae*." DNA Cell Biol **22**(11): 743-52.

Fletcher, G., C. A. Irwin, et al. (1978). "Identification of the *Escherichia coli* cell division gene *sep* and organization of the cell division-cell envelope genes in the *sep-mur-ftsA-envA* cluster as determined with specialized transducing lambda bacteriophages." J Bacteriol **133**(1): 91-100.

Freed, M. E., E. Hertz, et al. (1964). "Antidepressants. II. Derivatives of polynuclear indoles." J Med Chem **53**: 628-32.

Gayda, R. C., M. C. Henk, et al. (1992). "C-shaped cells caused by expression of an *ftsA* mutation in *Escherichia coli*." J Bacteriol **174**(16): 5362-70.

Gaze, W. H., N. Burroughs, et al. (2003). "Interactions between *Salmonella typhimurium* and *Acanthamoeba polyphaga*, and observation of a new mode of intracellular growth within contractile vacuoles." Microb Ecol **46**(3): 358-69.

Geissler, B., D. Elraheb, et al. (2003). "A gain-of-function mutation in *ftsA* bypasses the requirement for the essential cell division gene *zipA* in *Escherichia coli*." Proc Natl Acad Sci U S A **100**(7): 4197-202.

Gerard, P., T. Vernet, et al. (2002). "Membrane topology of the *Streptococcus pneumoniae* FtsW division protein." J Bacteriol **184**(7): 1925-31.

Ghigo, J. M. and J. Beckwith (2000). "Cell division in *Escherichia coli*: role of FtsL domains in septal localization, function, and oligomerization." J Bacteriol **182**(1): 116-29.

Ghigo, J. M., D. S. Weiss, et al. (1999). "Localization of FtsL to the *Escherichia coli* septal ring." Mol Microbiol **31**(2): 725-37.

Gilson, P. R., X. C. Yu, et al. (2003). "Two *Dictyostelium* orthologs of the prokaryotic cell division protein FtsZ localize to mitochondria and are required for the maintenance of normal mitochondrial morphology." Eukaryot Cell **2**(6): 1315-26.

Goehring, N. W. and J. Beckwith (2005). "Diverse paths to midcell: assembly of the bacterial cell division machinery." Curr Biol **15**(13): R514-26.

Goehring, N. W., F. Gueiros-Filho, et al. (2005). "Premature targeting of a cell division protein to midcell allows dissection of divisome assembly in *Escherichia coli*." Genes Dev **19**(1): 127-37.

Gonzalez, J. M., M. Velez, et al. (2005). "Cooperative behavior of *Escherichia coli* cell-division protein FtsZ assembly involves the preferential cyclization of long single-stranded fibrils." Proc Natl Acad Sci U S A **102**(6): 1895-900.

Gueiros-Filho, F. J. and R. Losick (2002). "A widely conserved bacterial cell division protein that promotes assembly of the tubulin-like protein FtsZ." Genes Dev **16**(19): 2544-56.

Guzman, L. M., J. J. Barondess, et al. (1992). "FtsL, an essential cytoplasmic membrane protein involved in cell division in *Escherichia coli*." J Bacteriol **174**(23): 7716-28.

Haeusser, D. P., R. L. Schwartz, et al. (2004). "EzrA prevents aberrant cell division by modulating assembly of the cytoskeletal protein FtsZ." Mol Microbiol **52**(3): 801-14.

Hale, C. A. and P. A. de Boer (1997). "Direct binding of FtsZ to ZipA, an essential component of the septal ring structure that mediates cell division in *E. coli*." Cell **88**(2): 175-85.

Hale, C. A. and P. A. de Boer (1999). "Recruitment of ZipA to the septal ring of *Escherichia coli* is dependent on FtsZ and independent of FtsA." J Bacteriol **181**(1): 167-76.

Hale, C. A. and P. A. de Boer (2002). "ZipA is required for recruitment of FtsK, FtsQ, FtsL, and FtsN to the septal ring in *Escherichia coli*." J Bacteriol **184**(9): 2552-6.

Hale, C. A., A. C. Rhee, et al. (2000). "ZipA-induced bundling of FtsZ polymers mediated by an interaction between C-terminal domains." J Bacteriol **182**(18): 5153-66.

Hamilton-Miller, J. M. (2004). "Antibiotic resistance from two perspectives: man and microbe." Int J Antimicrob Agents **23**(3): 209-12.

Hamoen, L. W., J. C. Meile, et al. (2006). "SepF, a novel FtsZ-interacting protein required for a late step in cell division." Mol Microbiol **59**(3): 989-99.

Haney, S. A., E. Glasfeld, et al. (2001). "Genetic analysis of the *Escherichia coli* FtsZ.ZipA interaction in the yeast two-hybrid system. Characterization of FtsZ residues essential for the interactions with ZipA and with FtsA." J Biol Chem **276**(15): 11980-7.

Harbarth, S. and M. H. Samore (2005). "Antimicrobial resistance determinants and future control." Emerg Infect Dis **11**(6): 794-801.

Harry, E. J., S. R. Partridge, et al. (1994). "Conservation of the 168 *divIB* gene in *Bacillus subtilis* W23 and *B. licheniformis*, and evidence for homology to *ftsQ* of *Escherichia coli*." Gene **147**(1): 85-9.

Haselbeck, R., D. Wall, et al. (2002). "Comprehensive essential gene identification as a platform for novel anti-infective drug discovery." Curr Pharm Des **8**(13): 1155-72.

Heidrich, C., M. F. Templin, et al. (2001). "Involvement of N-acetylmuramyl-L-alanine amidases in cell separation and antibiotic-induced autolysis of *Escherichia coli*." Mol Microbiol **41**(1): 167-78.

Heidrich, C., A. Ursinus, et al. (2002). "Effects of multiple deletions of murein hydrolases on viability, septum cleavage, and sensitivity to large toxic molecules in *Escherichia coli*." J Bacteriol **184**(22): 6093-9.

Hendricks, E. C., H. Szerlong, et al. (2000). "Cell division, guillotining of dimer chromosomes and SOS induction in resolution mutants (dif, xerC and xerD) of *Escherichia coli*." Mol Microbiol **36**(4): 973-81.

Henriques, A. O., P. Glaser, et al. (1998). "Control of cell shape and elongation by the *rodA* gene in *Bacillus subtilis*." Mol Microbiol **28**(2): 235-47.

Henry, T., F. Garcia-Del Portillo, et al. (2005). "Identification of *Salmonella* functions critical for bacterial cell division within eukaryotic cells." Mol Microbiol **56**(1): 252-67.

Higashitani, A., N. Higashitani, et al. (1995). "A cell division inhibitor SulA of *Escherichia coli* directly interacts with FtsZ through GTP hydrolysis." Biochem Biophys Res Commun **209**(1): 198-204.

Hirota, Y., A. Ryter, et al. (1968). "Thermosensitive mutants of *E. coli* affected in the processes of DNA synthesis and cellular division." Cold Spring Harb Symp Quant Biol **33**: 677-93.

Holtje, J. V. and C. Heidrich (2001). "Enzymology of elongation and constriction of the murein sacculus of *Escherichia coli*." Biochimie **83**(1): 103-8.

Hu, Z., A. Mukherjee, et al. (1999). "The MinC component of the division site selection system in *Escherichia coli* interacts with FtsZ to prevent polymerization." Proc Natl Acad Sci U S A **96**(26): 14819-24.

Hu, Z., C. Saez, et al. (2003). "Recruitment of MinC, an inhibitor of Z-ring formation, to the membrane in *Escherichia coli*: role of MinD and MinE." J Bacteriol **185**(1): 196-203.

Huang, K. C., Y. Meir, et al. (2003). "Dynamic structures in *Escherichia coli*: spontaneous formation of MinE rings and MinD polar zones." Proc Natl Acad Sci U S A **100**(22): 12724-8.

Huang, Q., F. Kirikae, et al. (2006). "Targeting FtsZ for antituberculosis drug discovery: noncytotoxic taxanes as novel antituberculosis agents." J Med Chem **49**(2): 463-6.

Huecas, S. and J. M. Andreu (2003). "Energetics of the cooperative assembly of cell division protein FtsZ and the nucleotide hydrolysis switch." J Biol Chem **278**(46): 46146-54.

Huecas, S. and J. M. Andreu (2004). "Polymerization of nucleotide-free, GDP- and GTP-bound cell division protein FtsZ: GDP makes the difference." FEBS Lett **569**(1-3): 43-8.

Ikeda, M., T. Sato, et al. (1989). "Structural similarity among *Escherichia coli* FtsW and RodA proteins and *Bacillus subtilis* SpoVE protein, which function in cell division, cell elongation, and spore formation, respectively." J Bacteriol **171**(11): 6375-8.

Ishikawa, S., Y. Kawai, et al. (2006). "A new FtsZ-interacting protein, YlmF, complements the activity of FtsA during progression of cell division in *Bacillus subtilis*." Mol Microbiol **60**(6): 1364-80.

Iyer, L. M., K. S. Makarova, et al. (2004). "Comparative genomics of the FtsK-HerA superfamily of pumping ATPases: implications for the origins of chromosome segregation, cell division and viral capsid packaging." Nucleic Acids Res **32**(17): 5260-79.

Janakiraman, A. and M. B. Goldberg (2004). "Evidence for polar positional information independent of cell division and nucleoid occlusion." Proc Natl Acad Sci U S A **101**(3): 835-40.

Jennings, L. D., K. W. Foreman, et al. (2004). "Combinatorial synthesis of substituted 3-(2-indolyl)piperidines and 2-phenyl indoles as inhibitors of ZipA-FtsZ interaction." Bioorg Med Chem **12**(19): 5115-31.

Jennings, L. D., K. W. Foreman, et al. (2004). "Design and synthesis of indolo[2,3-a]quinolizin-7-one inhibitors of the ZipA-FtsZ interaction." Bioorg Med Chem Lett **14**(6): 1427-31.

Jensen, S. O., L. S. Thompson, et al. (2005). "Cell division in *Bacillus subtilis*: FtsZ and FtsA association is Z-ring independent, and FtsA is required for efficient midcell Z-ring assembly." J Bacteriol **187**(18): 6536-44.

Johnson, J. E., L. L. Lackner, et al. (2002). "Targeting of (D)MinC/MinD and (D)MinC/DicB complexes to septal rings in *Escherichia coli* suggests a multistep mechanism for MinC-mediated destruction of nascent FtsZ rings." J Bacteriol **184**(11): 2951-62.

Johnson, J. E., L. L. Lackner, et al. (2004). "ZipA is required for targeting of DMinC/DicB, but not DMinC/MinD, complexes to septal ring assemblies in *Escherichia coli*." J Bacteriol **186**(8): 2418-29.

Jones, L. J., R. Carballido-Lopez, et al. (2001). "Control of cell shape in bacteria: helical, actin-like filaments in *Bacillus subtilis*." Cell **104**(6): 913-22.

Justice, S. S., J. Garcia-Lara, et al. (2000). "Cell division inhibitors SulA and MinC/MinD block septum formation at different steps in the assembly of the *Escherichia coli* division machinery." Mol Microbiol **37**(2): 410-23.

Karimova, G., N. Dautin, et al. (2005). "Interaction network among *Escherichia coli* membrane proteins involved in cell division as revealed by bacterial two-hybrid analysis." J Bacteriol **187**(7): 2233-43.

Karmazyn-Campelli, C., L. Fluss, et al. (1992). "The *spoIIN279*(ts) mutation affects the FtsA protein of *Bacillus subtilis*." Biochimie **74**(7-8): 689-94.

Kawai, Y., S. Moriya, et al. (2003). "Identification of a protein, YneA, responsible for cell division suppression during the SOS response in *Bacillus subtilis*." Mol Microbiol **47**(4): 1113-22.

Kawai, Y. and N. Ogasawara (2006). "*Bacillus subtilis* EzrA and FtsL synergistically regulate FtsZ ring dynamics during cell division." Microbiology **152**: 1129-41.

Kemp, J. T., A. Driks, et al. (2002). "FtsA mutants of *Bacillus subtilis* impaired in sporulation." J Bacteriol **184**(14): 3856-63.

Kenny, C. H., W. Ding, et al. (2003). "Development of a fluorescence polarization assay to screen for inhibitors of the FtsZ/ZipA interaction." Anal Biochem **323**(2): 224-33.

Kiefel, B. R., P. R. Gilson, et al. (2004). "Diverse eukaryotes have retained mitochondrial homologues of the bacterial division protein FtsZ." Protist **155**(1): 105-15.

Koppelman, C. M., M. E. Aarsman, et al. (2004). "R174 of *Escherichia coli* FtsZ is involved in membrane interaction and protofilament bundling, and is essential for cell division." Mol Microbiol **51**(3): 645-57.

Kuroiwa, T., K. Nishida, et al. (2006). "Structure, function and evolution of the mitochondrial division apparatus." Biochim Biophys Acta **1763**(5-6): 510-21.

Lackner, L. L., D. M. Raskin, et al. (2003). "ATP-dependent interactions between *Escherichia coli* Min proteins and the phospholipid membrane *in vitro*." J Bacteriol **185**(3): 735-49.

Lappchen, T., A. F. Hartog, et al. (2005). "GTP analogue inhibits polymerization and GTPase activity of the bacterial protein FtsZ without affecting its eukaryotic homologue tubulin." Biochemistry **44**(21): 7879-84.

Lara, B., A. I. Rico, et al. (2005). "Cell division in cocci: localization and properties of the *Streptococcus pneumoniae* FtsA protein." Mol Microbiol **55**(3): 699-711.

Leung, A. K., E. Lucile White, et al. (2004). "Structure of *Mycobacterium tuberculosis* FtsZ reveals unexpected, G protein-like conformational switches." J Mol Biol **342**(3): 953-70.

Levin, P. A., I. G. Kurtser, et al. (1999). "Identification and characterization of a negative regulator of FtsZ ring formation in *Bacillus subtilis*." Proc Natl Acad Sci U S A **96**(17): 9642-7.

Levin, P. A. and R. Losick (1996). "Transcription factor Spo0A switches the localization of the cell division protein FtsZ from a medial to a bipolar pattern in *Bacillus subtilis*." Genes Dev **10**(4): 478-88.

Levy, S. B. and B. Marshall (2004). "Antibacterial resistance worldwide: causes, challenges and responses." Nat Med **10**(12 Suppl): S122-9.

Little, J. W. and D. W. Mount (1982). "The SOS regulatory system of *Escherichia coli*." Cell **29**(1): 11-22.

Liu, G., G. C. Draper, et al. (1998). "FtsK is a bifunctional protein involved in cell division and chromosome localization in *Escherichia coli*." Mol Microbiol **29**(3): 893-903.

Louie, P., A. Lee, et al. (1992). "Roles of *rpoD*, *spoIIF*, *spoIIJ*, *spoIIN*, and *sin* in regulation of *Bacillus subtilis* stage II sporulation-specific transcription." J Bacteriol **174**(11): 3570-6.

Low, H. H., M. C. Moncrieffe, et al. (2004). "The crystal structure of ZapA and its modulation of FtsZ polymerisation." J Mol Biol **341**(3): 839-52.

Lowe, J. (1998). "Crystal structure determination of FtsZ from *Methanococcus jannaschii*." J Struct Biol **124**(2-3): 235-43.

Lowe, J. and L. A. Amos (1998). "Crystal structure of the bacterial cell-division protein FtsZ." Nature **391**(6663): 203-6.

Lowe, J. and F. van den Ent (2001). "Conserved sequence motif at the C-terminus of the bacterial cell-division protein FtsA." Biochimie **83**(1): 117-20.

Lowe, J., F. van den Ent, et al. (2004). "Molecules of the bacterial cytoskeleton." Annu Rev Biophys Biomol Struct **33**: 177-98.

Lu, C., M. Reedy, et al. (2000). "Straight and curved conformations of FtsZ are regulated by GTP hydrolysis." J Bacteriol **182**(1): 164-70.

Lu, C., J. Stricker, et al. (1998). "FtsZ from *Escherichia coli*, *Azotobacter vinelandii*, and *Thermotoga maritima*--quantitation, GTP hydrolysis, and assembly." Cell Motil Cytoskeleton **40**(1): 71-86.

Lu, C., J. Stricker, et al. (2001). "Site-specific mutations of FtsZ--effects on GTPase and *in vitro* assembly." BMC Microbiol **1**: 7.

Lutkenhaus, J. and S. G. Addinall (1997). "Bacterial cell division and the Z ring." Annu Rev Biochem **66**: 93-116.

Lutkenhaus, J. F. and W. D. Donachie (1979). "Identification of the *ftsA* gene product." J Bacteriol **137**(3): 1088-94.

Ma, X., D. W. Ehrhardt, et al. (1996). "Colocalization of cell division proteins FtsZ and FtsA to cytoskeletal structures in living *Escherichia coli* cells by using green fluorescent protein." Proc Natl Acad Sci U S A **93**(23): 12998-3003.

Ma, X. and W. Margolin (1999). "Genetic and functional analyses of the conserved C-terminal core domain of *Escherichia coli* FtsZ." J Bacteriol **181**(24): 7531-44.

Ma, X., Q. Sun, et al. (1997). "Interactions between heterologous FtsA and FtsZ proteins at the FtsZ ring." J Bacteriol **179**(21): 6788-97.

Margalit, D. N., L. Romberg, et al. (2004). "Targeting cell division: small-molecule inhibitors of FtsZ GTPase perturb cytokinetic ring assembly and induce bacterial lethality." Proc Natl Acad Sci U S A **101**(32): 11821-6.

Margolin, W. (1999). "The bacterial cell division machine." ASM News **65**(3): 137-143.

Margolin, W. (2000). "Themes and variations in prokaryotic cell division." FEMS Microbiol Rev **24**(4): 531-48.

Margolin, W. (2005). "FtsZ and the division of prokaryotic cells and organelles." Nat Rev Mol Cell Biol **6**(11): 862-71.

Margolin, W. and R. Bernander (2004). "How do prokaryotic cells cycle?" Curr Biol **14**(18): R768-70.

Marrington, R., E. Small, et al. (2004). "FtsZ fiber bundling is triggered by a conformational change in bound GTP." J Biol Chem **279**(47): 48821-9.

Martin, M. E., M. J. Trimble, et al. (2004). "Cell cycle-dependent abundance, stability and localization of FtsA and FtsQ in *Caulobacter crescentus*." Mol Microbiol **54**(1): 60-74.

Martinez-Lorenzo, M. J., S. Meresse, et al. (2001). "Unusual intracellular trafficking of *Salmonella typhimurium* in human melanoma cells." Cell Microbiol **3**(6): 407-16.

Martinez-Moya, M., M. A. de Pedro, et al. (1998). "Inhibition of *Salmonella* intracellular proliferation by non-phagocytic eucaryotic cells." Res Microbiol **149**(5): 309-18.

McDermott, P. F., R. D. Walker, et al. (2003). "Antimicrobials: modes of action and mechanisms of resistance." Int J Toxicol **22**(2): 135-43.

Mercer, K. L. and D. S. Weiss (2002). "The *Escherichia coli* cell division protein FtsW is required to recruit its cognate transpeptidase, FtsI (PBP3), to the division site." J Bacteriol **184**(4): 904-12.

Meyer, A. L. (2005). "Prospects and challenges of developing new agents for tough Gram-negatives." Curr Opin Pharmacol **5**(5): 490-4.

Miesel, L., J. Greene, et al. (2003). "Genetic strategies for antibacterial drug discovery." Nat Rev Genet **4**(6): 442-56.

Mileykovskaya, E., Q. Sun, et al. (1998). "Localization and function of early cell division proteins in filamentous *Escherichia coli* cells lacking phosphatidylethanolamine." J Bacteriol **180**(16): 4252-7.

Miller, C., L. E. Thomsen, et al. (2004). "SOS response induction by beta-lactams and bacterial defense against antibiotic lethality." Science **305**(5690): 1629-31.

Mingorance, J., M. Tadros, et al. (2005). "Visualization of single *Escherichia coli* FtsZ filament dynamics with atomic force microscopy." J Biol Chem **280**(21): 20909-14.

Moller-Jensen, J. and J. Lowe (2005). "Increasing complexity of the bacterial cytoskeleton." Curr Opin Cell Biol **17**(1): 75-81.

Mukherjee, A., C. Cao, et al. (1998). "Inhibition of FtsZ polymerization by SulA, an inhibitor of septation in *Escherichia coli*." Proc Natl Acad Sci U S A **95**(6): 2885-90.

Mukherjee, A., K. Dai, et al. (1993). "*Escherichia coli* cell division protein FtsZ is a guanine nucleotide binding protein." Proc Natl Acad Sci U S A **90**(3): 1053-7.

Mukherjee, A. and W. D. Donachie (1990). "Differential translation of cell division proteins." J Bacteriol **172**(10): 6106-11.

Mukherjee, A. and J. Lutkenhaus (1994). "Guanine nucleotide-dependent assembly of FtsZ into filaments." J Bacteriol **176**(9): 2754-8.

Mukherjee, A. and J. Lutkenhaus (1998). "Dynamic assembly of FtsZ regulated by GTP hydrolysis." Embo J **17**(2): 462-9.

Mukherjee, A. and J. Lutkenhaus (1999). "Analysis of FtsZ assembly by light scattering and determination of the role of divalent metal cations." J Bacteriol **181**(3): 823-32.

Mukherjee, A., C. Saez, et al. (2001). "Assembly of an FtsZ mutant deficient in GTPase activity has implications for FtsZ assembly and the role of the Z ring in cell division." J Bacteriol **183**(24): 7190-7.

Mulvey, M. A., J. D. Schilling, et al. (2001). "Establishment of a persistent *Escherichia coli* reservoir during the acute phase of a bladder infection." Infect Immun **69**(7): 4572-9.

Nanninga, N. (1998). "Morphogenesis of *Escherichia coli*." Microbiol Mol Biol Rev **62**(1): 110-29.

Nikaido, H. (2003). "Molecular basis of bacterial outer membrane permeability revisited." Microbiol Mol Biol Rev **67**(4): 593-656.

Nogales, E., K. H. Downing, et al. (1998). "Tubulin and FtsZ form a distinct family of GTPases." Nat Struct Biol **5**(6): 451-8.

Nogales, E. and H. W. Wang (2006). "Structural mechanisms underlying nucleotide-dependent self-assembly of tubulin and its relatives." Curr Opin Struct Biol **16**(2): 221-9.

Noirclerc-Savoye, M., A. Le Gouellec, et al. (2005). "*In vitro* reconstitution of a trimeric complex of DivIB, DivIC and FtsL, and their transient co-localization at the division site in *Streptococcus pneumoniae*." Mol Microbiol **55**(2): 413-24.

Normark, B. H. and S. Normark (2002). "Evolution and spread of antibiotic resistance." J Intern Med **252**(2): 91-106.

Ogino, H., M. Wachi, et al. (2004). "FtsZ-dependent localization of GroEL protein at possible division sites." Genes Cells **9**(9): 765-71.

Ohashi, T., C. A. Hale, et al. (2002). "Structural evidence that the P/Q domain of ZipA is an unstructured, flexible tether between the membrane and the C-terminal FtsZ-binding domain." J Bacteriol **184**(15): 4313-5.

Ohashi, Y., Y. Chijiiwa, et al. (1999). "The lethal effect of a benzamide derivative, 3-methoxybenzamide, can be suppressed by mutations within a cell division gene, *ftsZ*, in *Bacillus subtilis*." J Bacteriol **181**(4): 1348-51.

Ohta, N., A. J. Ninfa, et al. (1997). "Identification, characterization, and chromosomal organization of cell division cycle genes in *Caulobacter crescentus*." J Bacteriol **179**(7): 2169-80.

Oliva, M. A., S. C. Cordell, et al. (2004). "Structural insights into FtsZ protofilament formation." Nat Struct Mol Biol **11**(12): 1243-50.

Osley, M. A. and A. Newton (1977). "Mutational analysis of developmental control in *Caulobacter crescentus*." Proc Natl Acad Sci U S A **74**(1): 124-8.

Osteryoung, K. W. and J. Nunnari (2003). "The division of endosymbiotic organelles." Science **302**(5651): 1698-704.

Ottolenghi, A. C. and J. A. Ayala (1991). "Induction of a class I beta-lactamase from *Citrobacter freundii* in *Escherichia coli* requires active *ftsZ* but not *ftsA* or *ftsQ* products." Antimicrob Agents Chemother **35**(11): 2359-65.

Paradis-Bleau, C., F. Sanschagrin, et al. (2004). "Identification of *Pseudomonas aeruginosa* FtsZ peptide inhibitors as a tool for development of novel antimicrobials." J Antimicrob Chemother **54**(1): 278-80.

Paradis-Bleau, C., F. Sanschagrin, et al. (2005). "Peptide inhibitors of the essential cell division protein FtsA." Protein Eng Des Sel **18**(2): 85-91.

Paradis-Bleau, C., M. Beaumont, et al. (2007). "Parallel solid synthesis of inhibitors of the essential cell division FtsZ enzyme as a new potential class of antibacterials" Bioorg Med Chem

Pease, P. J., O. Levy, et al. (2005). "Sequence-directed DNA translocation by purified FtsK." Science **307**(5709): 586-90.

Perry, S. E. and D. H. Edwards (2004). "Identification of a polar targeting determinant for *Bacillus subtilis* DivIVA." Mol Microbiol **54**(5): 1237-49.

Pichoff, S. and J. Lutkenhaus (2001). "*Escherichia coli* division inhibitor MinCD blocks septation by preventing Z-ring formation." J Bacteriol **183**(22): 6630-5.

Pichoff, S. and J. Lutkenhaus (2002). "Unique and overlapping roles for ZipA and FtsA in septal ring assembly in *Escherichia coli*." Embo J **21**(4): 685-93.

Pichoff, S. and J. Lutkenhaus (2005). "Tethering the Z ring to the membrane through a conserved membrane targeting sequence in FtsA." Mol Microbiol **55**(6): 1722-34.

Pinho, M. G. and J. Errington (2003). "Dispersed mode of *Staphylococcus aureus* cell wall synthesis in the absence of the division machinery." Mol Microbiol **50**(3): 871-81.

Pla, J., A. Dopazo, et al. (1990). "The native form of FtsA, a septal protein of *Escherichia coli*, is located in the cytoplasmic membrane." J Bacteriol **172**(9): 5097-102.

Pogliano, J., K. Pogliano, et al. (1997). "Inactivation of FtsI inhibits constriction of the FtsZ cytokinetic ring and delays the assembly of FtsZ rings at potential division sites." Proc Natl Acad Sci U S A **94**(2): 559-64.

Projan, S. J. (2002). "New (and not so new) antibacterial targets - from where and when will the novel drugs come?" Curr Opin Pharmacol **2**(5): 513-22.

Rajagopalan, M., M. A. Atkinson, et al. (2005). "Mutations in the GTP-binding and synergy loop domains of *Mycobacterium tuberculosis ftsZ* compromise its function *in vitro* and *in vivo*." Biochem Biophys Res Commun **331**(4): 1171-7.

Rajagopalan, M., E. Maloney, et al. (2005). "Genetic evidence that mycobacterial FtsZ and FtsW proteins interact, and colocalize to the division site in *Mycobacterium smegmatis*." FEMS Microbiol Lett **250**(1): 9-17.

RayChaudhuri, D. (1999). "ZipA is a MAP-Tau homolog and is essential for structural integrity of the cytokinetic FtsZ ring during bacterial cell division." Embo J **18**(9): 2372-83.

Recchia, G. D., M. Aroyo, et al. (1999). "FtsK-dependent and -independent pathways of Xer site-specific recombination." Embo J **18**(20): 5724-34.

Reynolds, R. C., S. Srivastava, et al. (2004). "A new 2-carbamoyl pteridine that inhibits mycobacterial FtsZ." Bioorg Med Chem Lett **14**(12): 3161-4.

Rice, L. B. (2006). "Antimicrobial resistance in gram-positive bacteria." Am J Infect Control **34**(5 Suppl): S11-9.

Rico, A. I., M. Garcia-Ovalle, et al. (2004). "Role of two essential domains of *Escherichia coli* FtsA in localization and progression of the division ring." Mol Microbiol **53**(5): 1359-71.

Rivas, G., A. Lopez, et al. (2000). "Magnesium-induced linear self-association of the FtsZ bacterial cell division protein monomer. The primary steps for FtsZ assembly." J Biol Chem **275**(16): 11740-9.

Robinson, A. C., K. J. Begg, et al. (1988). "Mapping and characterization of mutants of the *Escherichia coli* cell division gene, *ftsA*." Mol Microbiol **2**(5): 581-8.

Robson, S. A., K. A. Michie, et al. (2002). "The *Bacillus subtilis* cell division proteins FtsL and DivIC are intrinsically unstable and do not interact with one another in the absence of other septasomal components." Mol Microbiol **44**(3): 663-74.

Romberg, L. and P. A. Levin (2003). "Assembly dynamics of the bacterial cell division protein FtsZ: poised at the edge of stability." Annu Rev Microbiol **57**: 125-54.

Romberg, L. and T. J. Mitchison (2004). "Rate-limiting guanosine 5'-triphosphate hydrolysis during nucleotide turnover by FtsZ, a prokaryotic tubulin homologue involved in bacterial cell division." Biochemistry **43**(1): 282-8.

Romberg, L., M. Simon, et al. (2001). "Polymerization of FtsZ, a bacterial homolog of tubulin. is assembly cooperative?" J Biol Chem **276**(15): 11743-53.

Rosenberger, C. M. and B. B. Finlay (2002). "Macrophages inhibit *Salmonella typhimurium* replication through MEK/ERK kinase and phagocyte NADPH oxidase activities." J Biol Chem **277**(21): 18753-62.

Rosenberger, C. M., R. L. Gallo, et al. (2004). "Interplay between antibacterial effectors: a macrophage antimicrobial peptide impairs intracellular *Salmonella* replication." Proc Natl Acad Sci U S A **101**(8): 2422-7.

Rosenmund, P., Trommer W, Dorn-Zachertz D und Ewerdwalbesloh U (1979). "Synthesen in der ß-Carbolinreihe, II; (±)-Yohimban und (±)-Epialloyohimban durch eine neue Indolsynthese." Liebigs Ann. Chem. 1643-1656.

Rothfield, L., S. Justice, et al. (1999). "Bacterial cell division." Annu Rev Genet **33**: 423-48.

Rothfield, L., A. Taghbalout, et al. (2005). "Spatial control of bacterial division-site placement." Nat Rev Microbiol **3**(12): 959-68.

Rueda, S., M. Vicente, et al. (2003). "Concentration and assembly of the division ring proteins FtsZ, FtsA, and ZipA during the *Escherichia coli* cell cycle." J Bacteriol **185**(11): 3344-51.

Rush, T. S., 3rd, J. A. Grant, et al. (2005). "A shape-based 3-D scaffold hopping method and its application to a bacterial protein-protein interaction." J Med Chem **48**(5): 1489-95.

Sackett, M. J., A. J. Kelly, et al. (1998). "Ordered expression of *ftsQA* and *ftsZ* during the *Caulobacter crescentus* cell cycle." Mol Microbiol **28**(3): 421-34.

Sanchez-Pulido, L., D. Devos, et al. (2003). "POTRA: a conserved domain in the FtsQ family and a class of beta-barrel outer membrane proteins." Trends Biochem Sci **28**(10): 523-6.

Sanchez, M., A. Valencia, et al. (1994). "Correlation between the structure and biochemical activities of FtsA, an essential cell division protein of the actin family." Embo J **13**(20): 4919-25.

Scheffers, D. J., J. G. de Wit, et al. (2002). "GTP hydrolysis of cell division protein FtsZ: evidence that the active site is formed by the association of monomers." Biochemistry **41**(2): 521-9.

Scheffers, D. J., T. den Blaauwen, et al. (2000). "Non-hydrolysable GTP-gamma-S stabilizes the FtsZ polymer in a GDP-bound state." Mol Microbiol **35**(5): 1211-9.

Scheffers, D. J. and A. J. Driessen (2002). "Immediate GTP hydrolysis upon FtsZ polymerization." Mol Microbiol **43**(6): 1517-21.

Scheffers, D. J. and J. Errington (2004). "PBP1 is a component of the *Bacillus subtilis* cell division machinery." J Bacteriol **186**(15): 5153-6.

Scheffers, D. J., L. J. Jones, et al. (2004). "Several distinct localization patterns for penicillin-binding proteins in *Bacillus subtilis*." Mol Microbiol **51**(3): 749-64.

Schmidt, K. L., N. D. Peterson, et al. (2004). "A predicted ABC transporter, FtsEX, is needed for cell division in *Escherichia coli*." J Bacteriol **186**(3): 785-93.

Sievers, J. and J. Errington (2000). "The *Bacillus subtilis* cell division protein FtsL localizes to sites of septation and interacts with DivIC." Mol Microbiol **36**(4): 846-55.

Silver, L. L. (2003). "Novel inhibitors of bacterial cell wall synthesis." Curr Opin Microbiol **6**(5): 431-8.

Silver, L. L. (2006). "Does the cell wall of bacteria remain a viable source of targets for novel antibiotics?" Biochem Pharmacol **71**: 996-1005.

Spratt, B. G. (1975). "Distinct penicillin binding proteins involved in the division, elongation, and shape of *Escherichia coli* K12." Proc Natl Acad Sci U S A **72**(8): 2999-3003.

Stanley, N. R., K. Findlay, et al. (2001). "*Escherichia coli* strains blocked in Tat-dependent protein export exhibit pleiotropic defects in the cell envelope." J Bacteriol **183**(1): 139-44.

Stokes, N. R., J. Sievers, et al. (2005). "Novel inhibitors of bacterial cytokinesis identified by a cell-based antibiotic screening assay." J Biol Chem **280**(48): 39709-15.

Stricker, J., P. Maddox, et al. (2002). "Rapid assembly dynamics of the *Escherichia coli* FtsZ-ring demonstrated by fluorescence recovery after photobleaching." Proc Natl Acad Sci U S A **99**(5): 3171-5.

Suefuji, K., R. Valluzzi, et al. (2002). "Dynamic assembly of MinD into filament bundles modulated by ATP, phospholipids, and MinE." Proc Natl Acad Sci U S A **99**(26): 16776-81.

Sutherland, A. G., J. Alvarez, et al. (2003). "Structure-based design of carboxybiphenylindole inhibitors of the ZipA-FtsZ interaction." Org Biomol Chem **1**(23): 4138-40.

Tamura, M., K. Lee, et al. (2006). "RNase E maintenance of proper FtsZ/FtsA ratio required for nonfilamentous growth of *Escherichia coli* cells but not for colony-forming ability." J Bacteriol **188**(14): 5145-52.

Tenover, F. C. (2006). "Mechanisms of antimicrobial resistance in bacteria." Am J Infect Control **34**(5 Suppl): S3-S10.

Thanedar, S. and W. Margolin (2004). "FtsZ exhibits rapid movement and oscillation waves in helix-like patterns in *Escherichia coli*." Curr Biol **14**(13): 1167-73.

Theriot, J. A. (2000). "The polymerization motor." Traffic **1**(1): 19-28.

Tinsley, E. and S. A. Khan (2006). "A novel FtsZ-like protein is involved in replication of the anthrax toxin-encoding pXO1 plasmid in *Bacillus anthracis*." J Bacteriol **188**(8): 2829-35.

Tormo, A., J. A. Ayala, et al. (1986). "Interaction of FtsA and PBP3 proteins in the *Escherichia coli* septum." J Bacteriol **166**(3): 985-92.

Tormo, A. and M. Vicente (1984). "The *ftsA* gene product participates in formation of the *Escherichia coli* septum structure." J Bacteriol **157**(3): 779-84.

Uehara, T., H. Matsuzawa, et al. (2001). "HscA is involved in the dynamics of FtsZ-ring formation in *Escherichia coli* K12." Genes Cells **6**(9): 803-14.

Uehara, T. and J. T. Park (2002). "Role of the murein precursor UDP-N-acetylmuramyl-L-Ala-gamma-D-Glu-meso-diaminopimelic acid-D-Ala-D-Ala in repression of beta-lactamase induction in cell division mutants." J Bacteriol **184**(15): 4233-9.

Urgaonkar, S., H. S. La Pierre, et al. (2005). "Synthesis of antimicrobial natural products targeting FtsZ: (+/-)-dichamanetin and (+/-)-2' "-hydroxy-5' '-benzylisouvarinol-B." Org Lett **7**(25): 5609-12.

Ursinus, A., F. van den Ent, et al. (2004). "Murein (peptidoglycan) binding property of the essential cell division protein FtsN from *Escherichia coli*." J Bacteriol **186**(20): 6728-37.

Van De Putte, P., D. Van, et al. (1964). "The selection of mutants of *Escherichia coli* with impaired cell division at elevated temperature." Mutat Res **106**: 121-8.

van den Ent, F., L. Amos, et al. (2001). "Bacterial ancestry of actin and tubulin." Curr Opin Microbiol **4**(6): 634-8.

van den Ent, F., L. A. Amos, et al. (2001). "Prokaryotic origin of the actin cytoskeleton." Nature **413**(6851): 39-44.

van den Ent, F. and J. Lowe (2000). "Crystal structure of the cell division protein FtsA from *Thermotoga maritima*." Embo J **19**(20): 5300-7.

Vandecandelaere, A., M. Brune, et al. (1999). "Phosphate release during microtubule assembly: what stabilizes growing microtubules?" Biochemistry **38**(25): 8179-88.

Varma, A. and K. D. Young (2004). "FtsZ collaborates with penicillin binding proteins to generate bacterial cell shape in *Escherichia coli*." J Bacteriol **186**(20): 6768-74.

Vaughan, S., B. Wickstead, et al. (2004). "Molecular evolution of FtsZ protein sequences encoded within the genomes of archaea, bacteria, and eukaryota." J Mol Evol **58**(1): 19-29.

Vazquez-Torres, A., Y. Xu, et al. (2000). "*Salmonella* pathogenicity island 2-dependent evasion of the phagocyte NADPH oxidase." Science **287**(5458): 1655-8.

Vicente, M. and A. I. Rico (2006). "The order of the ring: assembly of *Escherichia coli* cell division components." Mol Microbiol **61**(1): 5-8.

Vicente, M., A. I. Rico, et al. (2006). "Septum enlightenment: assembly of bacterial division proteins." J Bacteriol **188**(1): 19-27.

Walker, J. R., A. Kovarik, et al. (1975). "Regulation of bacterial cell division: temperature-sensitive mutants of *Escherichia coli* that are defective in septum formation." J Bacteriol **123**(2): 693-703.

Walsh, C. (2003). Antibiotics : actions, origins, resistance. Washington, D.C., ASM Press.

Wang, H. and R. C. Gayda (1992). "Quantitative determination of FtsA at different growth rates in *Escherichia coli* using monoclonal antibodies." Mol Microbiol **6**(17): 2517-24.

Wang, H. C. and R. C. Gayda (1990). "High-level expression of the FtsA protein inhibits cell septation in *Escherichia coli* K-12." J Bacteriol **172**(8): 4736-40.

Wang, J., A. Galgoci, et al. (2003). "Discovery of a small molecule that inhibits cell division by blocking FtsZ, a novel therapeutic target of antibiotics." J Biol Chem **278**(45): 44424-8.

Wang, L. and J. Lutkenhaus (1998). "FtsK is an essential cell division protein that is localized to the septum and induced as part of the SOS response." Mol Microbiol **29**(3): 731-40.

Wang, S., S. J. Arends, et al. (2005). "A deficiency in S-adenosylmethionine synthetase interrupts assembly of the septal ring in *Escherichia coli* K-12." Mol Microbiol **58**(3): 791-9.

Wang, X., J. Huang, et al. (1997). "Analysis of the interaction of FtsZ with itself, GTP, and FtsA." J Bacteriol **179**(17): 5551-9.

Weart, R. B., S. Nakano, et al. (2005). "The ClpX chaperone modulates assembly of the tubulin-like protein FtsZ." Mol Microbiol **57**(1): 238-49.

Weiss, D. S. (2004). "Bacterial cell division and the septal ring." Mol Microbiol **54**(3): 588-97.

Weiss, D. S., J. C. Chen, et al. (1999). "Localization of FtsI (PBP3) to the septal ring requires its membrane anchor, the Z ring, FtsA, FtsQ, and FtsL." J Bacteriol **181**(2): 508-20.

White, E. L., L. J. Ross, et al. (2000). "Slow polymerization of *Mycobacterium tuberculosis* FtsZ." J Bacteriol **182**(14): 4028-34.

White, E. L., W. J. Suling, et al. (2002). "2-Alkoxycarbonylaminopyridines: inhibitors of *Mycobacterium tuberculosis* FtsZ." J Antimicrob Chemother **50**(1): 111-4.

Wissel, M. C. and D. S. Weiss (2004). "Genetic analysis of the cell division protein FtsI (PBP3): amino acid substitutions that impair septal localization of FtsI and recruitment of FtsN." J Bacteriol **186**(2): 490-502.

Woldringh, C. L., E. Mulder, et al. (1991). "Toporegulation of bacterial division according to the nucleoid occlusion model." Res Microbiol **142**(2-3): 309-20.

Wolf-Watz, H. and S. Normark (1976). "Evidence for a role of N-acetylmuramyl-L-alanine amidase in septum separation in *Escherichia coli*." J Bacteriol **128**(2): 580-6.

Wu, L. J. and J. Errington (2004). "Coordination of cell division and chromosome segregation by a nucleoid occlusion protein in *Bacillus subtilis*." Cell **117**(7): 915-25.

Yacoby, I., M. Shamis, et al. (2006). "Targeting antibacterial agents by using drug-carrying filamentous bacteriophages." Antimicrob Agents Chemother **50**(6): 2087-97.

Yan, K., K. H. Pearce, et al. (2000). "A conserved residue at the extreme C-terminus of FtsZ is critical for the FtsA-FtsZ interaction in *Staphylococcus aureus*." Biochem Biophys Res Commun **270**(2): 387-92.

Yan, K., T. M. Sossong, et al. (2001). "Regions of FtsZ important for self-interaction in *Staphylococcus aureus*." Biochem Biophys Res Commun **284**(2): 515-8.

Yi, Q. M., S. Rockenbach, et al. (1985). "Structure and expression of the cell division genes *ftsQ*, *ftsA* and *ftsZ*." J Mol Biol **184**(3): 399-412.

Yim, L., G. Vandenbussche, et al. (2000). "Role of the carboxy terminus of *Escherichia coli* FtsA in self-interaction and cell division." J Bacteriol **182**(22): 6366-73.

Young, K., L. L. Silver, et al. (1995). "The *envA* permeability/cell division gene of *Escherichia coli* encodes the second enzyme of lipid A biosynthesis. UDP-3-O-(R-

3-hydroxymyristoyl)-N-acetylglucosamine deacetylase." J Biol Chem **270**(51): 30384-91.

Yu, X. C. and W. Margolin (1998). "Inhibition of assembly of bacterial cell division protein FtsZ by the hydrophobic dye 5,5'-bis-(8-anilino-1-naphthalenesulfonate)." J Biol Chem **273**(17): 10216-22.

Yu, X. C. and W. Margolin (1999). "FtsZ ring clusters in *min* and partition mutants: role of both the Min system and the nucleoid in regulating FtsZ ring localization." Mol Microbiol **32**(2): 315-26.

Zhao, Y., R. W. Hammond, et al. (2004). "Cell division gene cluster in *Spiroplasma kunkelii*: functional characterization of *ftsZ* and the first report of *ftsA* in mollicutes." DNA Cell Biol **23**(2): 127-34.

Zhou, H. and J. Lutkenhaus (2005). "MinC mutants deficient in MinD- and DicB-mediated cell division inhibition due to loss of interaction with MinD, DicB, or a septal component." J Bacteriol **187**(8): 2846-57.

Zhou, H., R. Schulze, et al. (2005). "Analysis of MinD mutations reveals residues required for MinE stimulation of the MinD ATPase and residues required for MinC interaction." J Bacteriol **187**(2): 629-38.

Table I. Principal features of all known cell division proteins.

Protein	Functions	Enzymatic activity	Proposed protein-protein interactions	Conservation	References
FtsZ	Formation of the Z-ring Recruitment of downstream proteins forming the divisome	GTPase	FtsZ, FtsA, ZipA, FtsK	Extensive	(de Boer, Crossley et al. 1992; Lutkenhaus and Addinall 1997; Margolin 2000; Di Lallo, Fagioli et al. 2003; Vicente and Rico 2006)
FtsA	Septum Formation Tethering FtsZ to the membrane Stabilization of the Z-ring Recruitment of downstream proteins forming the divisome	ATPase	FtsZ, FtsA, ZapA, FtsQ, FtsI, FtsN	Extensive	(Pichoff and Lutkenhaus 2002; Di Lallo, Fagioli et al. 2003; Goehring and Beckwith 2005; Karimova, Dautin et al. 2005; Vicente and Rico 2006)
ZipA	Septum Formation Tethering FtsZ to the membrane Stabilization of the Z-ring Recruitment of downstream proteins forming the divisome and of the ^{D}MinC/DicB complex Important for DicB-induced cell division inhibition	None	FtsZ, ZipA	In Gram-negatives only	(Hale and de Boer 2002; Ohashi, Hale et al. 2002; Pichoff and Lutkenhaus 2002; Di Lallo, Fagioli et al. 2003; Johnson, Lackner et al. 2004)
YlmF (SepF)	Septum Formation (non-essential)	None	FtsZ, SepF	In Gram-positives only	(Hamoen, Meile et al. 2006)
ZapA (YgfE, YshA)	Probing FtsZ polymerization Stabilization of the Z-ring (non-essential)	None	FtsZ, FtsA, ZapA	High	(Gueiros-Filho and Losick 2002; Di Lallo, Fagioli et al. 2003; Low, Moncrieffe et al. 2004)
FtsEX	Recruitment of downstream proteins (essential in salt-free media)	ATPase for FtsE	N. D.	High	(Schmidt, Peterson et al. 2004)

FtsK	Septum Formation Coordination of cell division with genome segregation Genome translocation Activation of genome dimer resolution Activation of topoisomerase IV Increasing resistance to DNA damage via the RecA-dependent protection and repair system Recruitment of downstream FtsQ, FtsL, FtsB and FtsI	ATPase	FtsZ, FtsQ,FtsL, FtsI ParC subunit of topoisomerase IV	High	(Diez, Gustavsson et al. 2000; Margolin 2000; Chen and Beckwith 2001; Aussel, Barre et al. 2002; Espeli, Lee et al. 2003; Di Lallo, Fagioli et al. 2003; Bigot, Corre et al. 2004; Buddelmeijer and Beckwith 2004; Karimova, Dautin et al. 2005; Pease, Levy et al. 2005)
FtsQ (DivIB)	Septum Formation Recruitment of downstream cell division proteins such as FtsL, FtsW, FtsB, FtsI and FtsN Unconfirmed role for FtsQ in peptidoglycan synthesis	None	FtsA, FtsK, FtsQ, FtsL, FtsB, FtsW, FtsI, FtsN	Moderate	(Carson, Barondess et al. 1991; Addinall, Cao et al. 1997; Margolin 2000; Buddelmeijer, Judson et al. 2002; Chen, Minev et al. 2002; Mercer and Weiss 2002; Di Lallo, Fagioli et al. 2003; Martin, Trimble et al. 2004; Buddelmeijer and Beckwith 2004;Goehring and Beckwith 2005; Noirclerc-Savoye, Le Gouellec et al. 2005; Karimova, Dautin et al. 2005; Vicente and Rico 2006)

FtsL	Septum Formation Recruitment of downstream cell division proteins, FtsB, FtsW and FtsI	None	FtsK, FtsQ, FtsL, FtsB, FtsW	High	(Ghigo and Beckwith 2000; Sievers and Errington 2000; Buddelmeijer, Judson et al. 2002; Mercer and Weiss 2002; Di Lallo, Fagioli et al. 2003; Buddelmeijer and Beckwith 2004; Goehring and Beckwith 2005; Noirclerc-Savoye, Le Gouellec et al. 2005;Vicente, Rico et al. 2006)
FtsB (YgbQ, DivIC)	Recruitment of FtsL, FtsW and FtsI	None	FtsQ, FtsL	High	(Buddelmeijer, Judson et al. 2002; Buddelmeijer and Beckwith 2004; Goehring and Beckwith 2005; Noirclerc-Savoye, Le Gouellec et al. 2005)
FtsW	Septum Formation Recruitment of FtsI	None	FtsQ, FtsL, FtsI, FtsN, *Mycobacterium FtsZ*	High	(Boyle, Khattar et al. 1997; Datta, Dasgupta et al. 2002; Mercer and Weiss 2002; Di Lallo, Fagioli et al. 2003)
FtsI (PBP3, PBP2B, PBP-2X)	Septum Formation Recruitment of FtsQ and FtsB in *B. subtilis* and of FtsN Synthesis of the cell wall septum	Transpepti dase	FtsA, FtsK, FtsQ, FtsW, FtsI, FtsN	High	(Adam, Fraipont et al. 1997; Daniel, Harry et al. 2000; Di Lallo, Fagioli et al. 2003; Wissel and Weiss 2004; Karimova, Dautin et al. 2005)
FtsN	Septum Formation Recruitment of AmiC	None	FtsA, FtsQ, FtsW, FtsI, FtsN	In Gram-negatives only	(Addinall, Cao et al. 1997; Margolin 2000; Bernhardt and de Boer 2003; Di Lallo, Fagioli et al. 2003; Karimova, Dautin et al. 2005)

AmiC	Cell wall hydrolysis (non-essential)	Amidase	N.D.	Potentially in Gram-neg.	(Bernhardt and de Boer 2003)
EnvC	Cell wall hydrolysis (non-essential)	Cell wall degrading	N.D.	Potentially in Gram-neg.	(Bernhardt and de Boer 2004)

Figure Legends

Figure 1. Schematic representation of the bacterial divisome showing all proteins known to be recruited at the division site for cell division under normal conditions (some of the proteins are present only in limited sets of bacterial species. See Table I). FtsZ and FtsA first localize at mid cell and FtsZ polymerizes into a Z-ring tethered to the cytoplasmic side of the inner membrane by FtsA, followed by FtsZ-dependent recruitment of proteins ZipA, ZapA and YlmF. The remaining cell division proteins are then directed to the divisome in a hierarchical recruitment process dependent mostly on FtsA and FtsQ. FtsE and FtsX then localize, followed by FtsK, followed by FtsQ, FtsB and FtsL, which localize as a trimeric complex. Finally, FtsW localizes at the division site, followed by FtsI, FtsN, AmiC and EnvC.

Figure 2. Tridimensional structure of FtsZ from *M. jannaschii* resolved at 2.8 Angström; α-helices are red, β-sheets are yellow and loops are green. The active site of FtsZ contains the GTP substrate and the magnesium cofactor. (Lowe and Amos 1998)

Figure 3. Tridimensional structure of FtsA from *T. maritima* resolved at 1.9 Angström; α-helices are red, β-sheets are yellow and loops are green. The active site of FtsA contains the ATP substrate in grey and the magnesium cofactor in mauve. (van den Ent and Lowe 2000)

Figure 1.

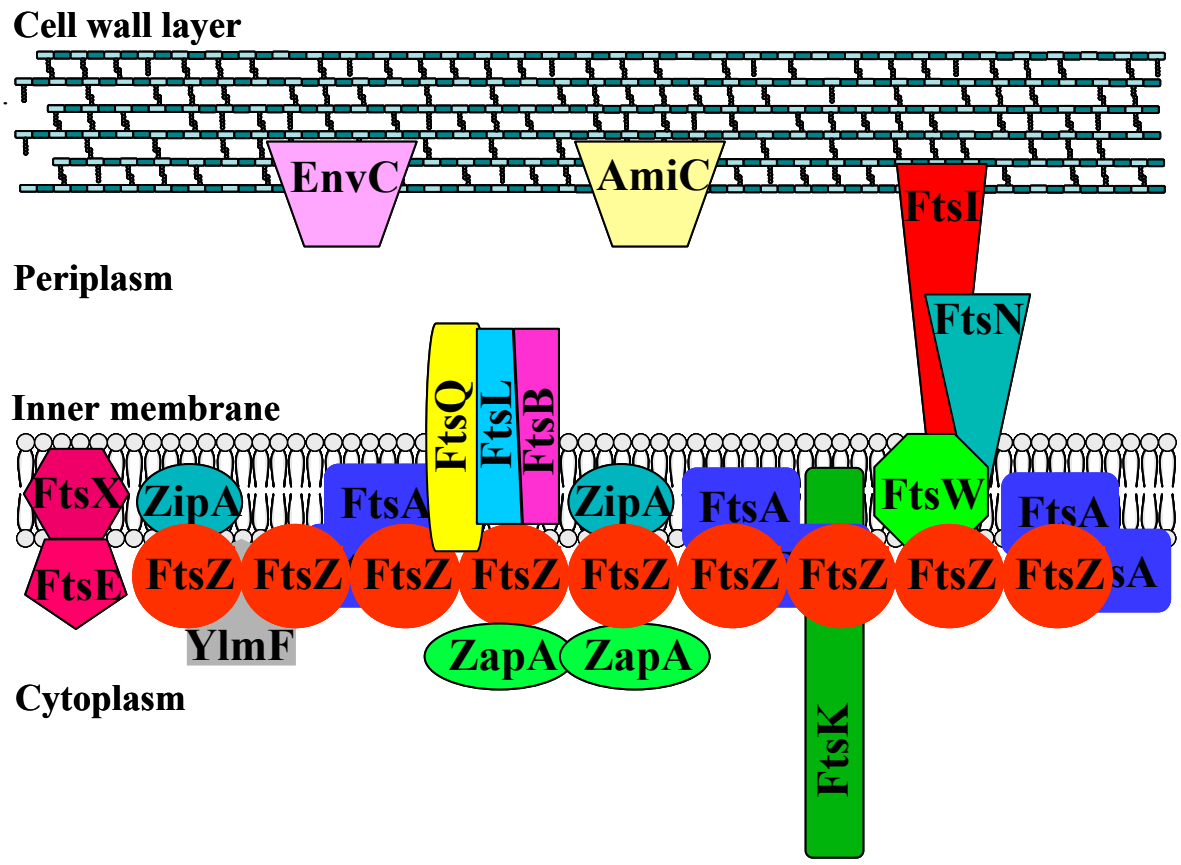
Cell wall layer
EnvC
AmiC
FtsI
Periplasm
FtsN
Inner membrane
FtsQ
FtsL
FtsB
FtsX
ZipA
FtsA
ZipA
FtsA
FtsW
FtsA
FtsE
FtsZ
FtsZ
FtsZ
FtsZ
FtsZ
FtsZ
FtsZ
FtsZ
FtsZ
sA
YlmF
ZapA
ZapA
FtsK
Cytoplasm

Figure 2.

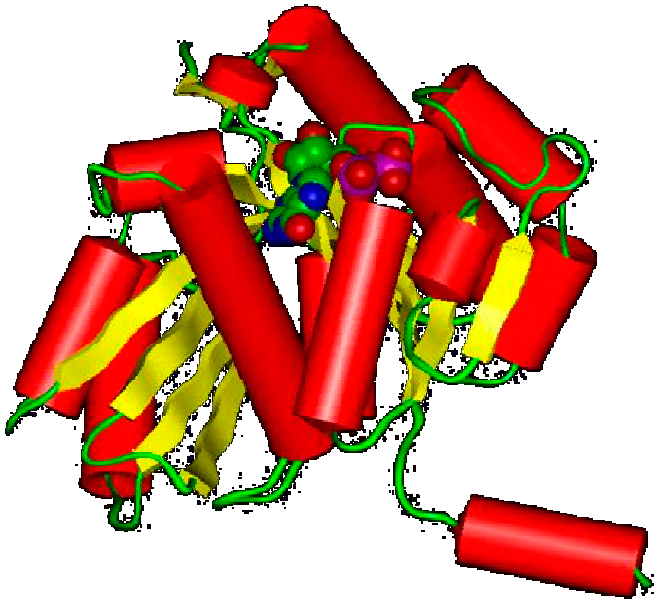

Figure 3.

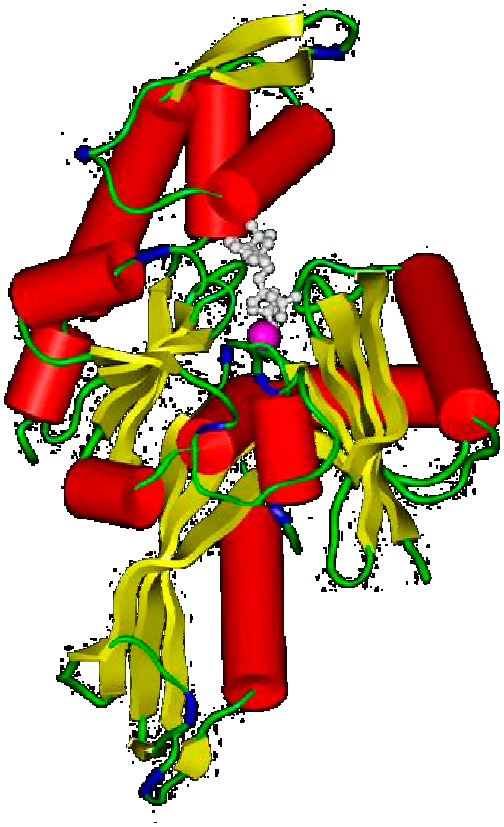

Chapitre 2 - Parallel solid synthesis of inhibitors of the essential cell division FtsZ enzyme as a new potential class of antibacterials

Résumé

Synthèse d'inhibiteurs de l'enzyme FtsZ essentielle à la division cellulaire bactérienne en tant que nouvelle classe potentielle d'agents antibactériens

La résistance aux antibiotiques représente l'une des problématiques les plus préoccupantes en santé publique car la diminution de l'efficacité des traitements antibactériens met en danger la vie des patients. Ainsi, le développement de nouvelles classes d'agents antibactériens possédant des structures et des modes d'action inusités est une priorité afin de protéger la santé humaine contre les pathogènes bactériens résistants aux antibiotiques connus. L'enzyme FtsZ constitue une cible antibactérienne de premier choix afin de développer des inhibiteurs efficaces contre la division cellulaire bactérienne. La protéine FtsZ a tout d'abord été purifiée par chromatographie d'affinité, son activité GTPase a été confirmée puis son affinité et sa spécificité pour le GTP ont été démontrées. Une banque d'analogues de GTP a ensuite été créée par une ingénieuse stratégie de synthèse organique en parallèle sur support solide. Un essai spectrophotométrique a été développé afin de cribler efficacement le potentiel inhibiteur des molécules synthétisées sur l'activité GTPase de FtsZ. Les petites molécules organiques synthétisées inhibent l'activité GTPase de FtsZ avec des valeurs de CI_{50} entre 450 μM et 2,6 mM. De plus, 5 composés inhibent la croissance de *S. aureus* et possèdent une activité antibactérienne prometteuse. Ainsi, cette étude présente la première étape du développement d'une nouvelle classe d'agents antibactériens ciblant une protéine essentielle à la division cellulaire bactérienne.

Contribution des auteurs

Cinq auteurs signent la réalisation de cet article scientifique récemment publié par la revue «Bioorganic & Medicinal Chemistry». Tout d'abord, la chimiste Mélanie Beaumont a mis au point la stratégie de synthèse organique en parallèle sur support solide sous la supervision du Dr Normand Voyer et du Dr Roger C. Levesque. Au cours de sa maîtrise, Mélanie a synthétisé, purifié et analysé les analogues du GTP à la base de cette étude. En tant que première auteure, j'ai exprimé l'enzyme FtsZ de *P. aeruginosa* dans les cellules recombinantes de *E. coli* puis j'ai purifié la protéine FtsZ par chromatographie d'affinité. J'ai vérifié l'activité enzymatique de l'enzyme FtsZ purifiée puis j'ai caractérisé l'affinité et la spécificité de FtsZ pour différents substrats nucléotidiques. Par la suite, j'ai mis au point un essai spectrophotométrique afin d'analyser le potentiel inhibiteur des molécules synthétisées sur l'activité GTPase de FtsZ. J'ai ainsi déterminé la CI_{50} pour chaque molécule inhibitrice. J'ai également vérifié le potentiel antibactérien des molécules inhibitrices sur *E. coli* et *S. aureus*. Finalement, j'ai analysé les résultats, j'ai rédigé le manuscrit et j'ai préparé les figures et tableaux. Cependant, la section du manuscrit sur la synthèse organique en parallèle a été tirée du mémoire de Mélanie Beaumont. J'ai donc sélectionné l'information pertinente pour l'article et j'ai traduit le texte en anglais avec la collaboration du Dr Normand Voyer. Les figures illustrant la stratégie de synthèse et la structure des molécules synthétisées ont été préparées en collaboration avec Mélanie Beaumont. En ce qui concerne le Dr François Sanschagrin, il m'a apportée un support technique et scientifique au cours de ce projet de recherche. Le Dr Roger C. Levesque est à l'origine de l'idée de départ et de la conceptualisation du projet de recherche à la base de cet article. Ce projet consiste à cibler les protéines bactériennes essentielles à la division cellulaire afin de développer une classe innovatrice d'agents antibactériens. Finalement, le Dr Levesque et le Dr Voyer ont judicieusement orienté le projet et ont révisé le manuscrit pour en augmenter la fluidité et la valeur scientifique.

Graphical abstract

GTP analogues were synthesized with a guanine-like moiety linked to an Ala side chain using combinatorial chemistry as FtsZ GTPase inhibitors. Lead compound **14** showed prominent inhibitory and antibacterial activities.

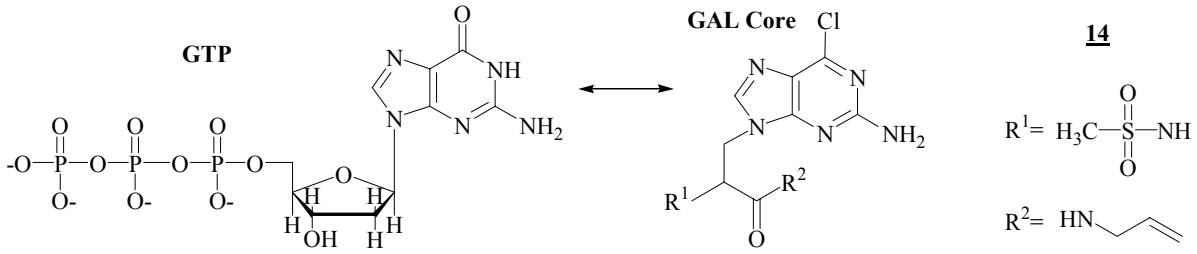

Parallel solid synthesis of inhibitors of the essential cell division FtsZ enzyme as a new potential class of antibacterials

Catherine Paradis-Bleau,[a] Mélanie Beaumont,[b] François Sanschagrin,[a] Normand Voyer[b] and Roger C. Levesque[a,*]

[a]*CREFSIP, Département de Biologie Médicale, Faculté de médecine, Université Laval, Sainte-Foy, Québec, G1K 7P4, Canada*

[b]*CREFSIP, Département de chimie, Faculté des sciences et génie, Université Laval, Sainte-Foy, Québec, G1K 7P4, Canada*

Keywords: Parallel synthesis; GTP analogues; *Pseudomonas aeruginosa;* FtsZ inhibitors, *Staphylococcus aureus*.

*Corresponding author. Mailing address: CREFSIP, Faculté de médecine, Pavillon Charles-Eugène-Marchand, Université Laval, Sainte-Foy, Québec, Canada, G1K 7P4. Tel.: 1-418-656-3070; fax: 1-418-656-7176; e-mail: rclevesq@rsvs.ulaval.ca

Abstract

As a model system for designing new inhibitors of bacterial cell division, we studied the essential and highly conserved FtsZ GTPase from *Pseudomonas aeruginosa*. A collection of GTP analogues were prepared using the solid-phase parallel synthesis approach. The synthesized GTP analogues inhibited the GTPase activity of FtsZ with IC_{50} values between 450 μM and 2.6 mM, and 5 compounds inhibited *Staphylococcus aureus* growth in a biological assay. The FtsZ spectrophotometric assay developed for screening of synthesized compounds is the first step in identification of antibacterials targeting the bacterial cell division essential proteins.

1. Introduction

The widespread misuse of antibiotics has applied an immense pressure selecting for bacteria resistant to all classes of antibiotics. The critical human health outcome of antibiotic resistance among bacterial pathogens worldwide necessitates the development of structurally new antibacterials against targets essential for growth, whose inhibition should give a lethal phenotype.[1] The bacterial cell division process encodes essential proteins forming the divisome representing some of the best antibacterial targets. These proteins are extremely sensitive to inhibition since the cell division depends on recruitment of specific proteins in an essential cascade for forming the divisome.[2,3] Among those proteins, we selected FtsZ as a specific target because this is the most important and conserved protein of the cell division machinery.[4] FtsZ is at the top of hierarchic recruitment in the divisome and its polymerization into the Z-ring allows the physical separation of daughter cells.[5] The polymerization of FtsZ depends upon GTP hydrolysis and this essential enzymatic activity can be exploited to screen inhibitory molecules.[6] The FtsZ strategy proposed here is supported by the absence of bacterial resistance against FtsZ inhibitors MinC and SulA which constitute active regulators of cell division.[7,8] We focused efforts on the FtsZ protein of *Pseudomonas aeruginosa*, one of the major opportunistic pathogens causing severe nosocomial infections.[9,10] We used FtsZ from *P. aeruginosa* because this bacterium is

extensively studied as a model system resistant to most antibiotics. FtsZ is highly conserved amongst bacteria and we also tested compounds for growth inhibition of *Staphylococcus aureus* because of the differences in permeability between both species and because of the MRSA problem.

To develop drugs with novel structures, we decided to synthesize a manageable number of molecules by combinatorial chemistry. This technology allows the quick generation of large numbers of structurally related compounds.[11] Combinatorial chemistry was first developed to synthesize peptides but we adapted recent advances to small organic compound synthesis.[12] This approach can be achieved either in solution or in solid-phase. We opted for the time-saving solid support strategy permitting to obtain higher yields where automated reactions can be accelerated by using excess reagents, simplified washing and purification steps.[12] We thus used the solid-phase chemistry method to synthesize GTP analogues and parallel synthesis was adopted to branch out rapidly the core structure to obtain sufficient amounts of unique small organic compounds in the library.

This work identifies a new potential class of antibacterial agents targeting the essential FtsZ cell division GTPase. We describe the synthesis of highly diversified GTP analogues having chosen unique structures as potential FtsZ inhibitors. The GTP binding and hydrolytic activities of the purified *P. aeruginosa* FtsZ protein were characterized. The inhibitory activity of each synthesized GTP analogue was then evaluated individually in vitro against the FtsZ GTPase activity and in vivo on whole bacterial cells. As part of our continued interest in the development of novel antimicrobials using essential targets, we present here the development of a simple, cost-effective, and rapid assay for screening FtsZ GTPase inhibitors.

2. Results

2.1 Purification of the P. aeruginosa FtsZ protein. The FtsZ protein was efficiently expressed in soluble form in the cytoplasmic fraction of *Escherichia coli* BL21 (λDE3) cells as depicted in Figure 1, lane 1. The nickel affinity chromatography permitted the purification of FtsZ with a yield of 20 mg/L. The purified FtsZ protein was visualized as a

single 42 kDa band on SDS–PAGE (Fig. 1, lane 2). N-terminal sequencing of the first 15 amino acid residues confirmed the identity of the purified protein as *P. aeruginosa* FtsZ (100% identity with the published sequence).

2.2 Characterization of the GTP binding and GTPase hydrolysis activity of purified FtsZ. An UV cross-link binding assay was performed to characterize the substrate specificity of FtsZ. The autoradiography showed that FtsZ binds preferentially GTP amongst the four radioactive nucleotides tested as substrates (Fig. 2A). The negative control included in the GTPase assay described in Section 4.3 gave no GTP hydrolysis (Fig. 2B). This assay showed that the purified FtsZ was biologically active when using 12 μM FtsZ which hydrolyzed 85% of the P^{32}-labeled GTP substrate into GDP after 1 h at 37 °C (Fig. 2B).

2.3 Strategy, design and synthesis of GTP analogues in the library. A combination of solid-phase combinatorial chemistry and parallel synthesis was used to synthesize highly diversified GTP analogues. The general strategy was optimized from published procedures to allow a S_N2 nucleophilic attack of 2-amino-6-chloropurine on the β-lactone **2**.[13,14] The β-lactone opening was done by a nucleophilic attack on the sp^3 carbon at the β position of the cycle and not on the sp^2 carbon. The hydroxyl function of the serine was thus substituted by the 2-amino-6-chloropurine by a nucleophilic attack of the N^9 atom of the purine. The central nucleus of molecules was a guanine moiety linked to an Ala called GAL core structure (Figure 3 and Figure 4). To obtain the desired library, an *N*-tert-butoxycarbonyl (Boc)-protected guanine modified amino acid (product **4** in Fig. 3) was required. The *N*-(Boc)-(2-amino-6-chloropuryl)-L-Ala (**4**) was synthesized by the formation of a β-lactone and its opening by 2-amino-6-chloropurine (**3**). The most critical step was the formation of the Ser β-lactone (product **2** in Fig. 3) from the (Boc)-L-Ser. This step was achieved by the Mitsunobu reaction with variable and modest yields between 25% and 40%. Different methods were attempted to improve yield of this critical step. The method described by Sliedregta gave similar yields but involved a trityl protecting group.[15] The use of dimethylazodicarboxylate or diisopropylazodicarboxylate instead of diethylazodicarboxylate (DEAD) gave lower yields and the method based upon the mixed

anhydrides was not successful (data not shown).[16] We thus optimized the Mitsunobu reaction and the yield was raised to 87.7% of a 99% pure product when working on a small scale. Analysis of the purified Ser β-lactone product by NMR spectroscopy confirmed the structure (see Section 4). We observed that the purification process must be done as rapidly as possible to avoid a re-opening of the β-lactone cycle. The guanine group was then added on the side chain of Ser β-lactone by a nucleophilic displacement reaction using 2-amino-6-chloropurine giving **4** (see Section 4).

The core structure **4** was utilized for parallel synthesis and the oxime resin was chosen as solid support. This resin displayed an oxime function linked on a polystyrene bead permitting the cleavage with different nucleophiles to obtain more functional diversity. The initial amino acid was linked on the resin by the formation of an ester bond between the carboxylic acid of the amino acid and the oxime resin. This bond was sufficiently stable under anhydrous acidic conditions to use a BOC protection strategy and to permit the N-terminal modification of the core structure. After transformations, the C-terminal was modified by cleavage of the bound ester with nucleophiles using relatively mild conditions. The target compounds illustrated in Figure 4 were synthesized via modification of both N- and C-terminals of the core structure. Six different chemical R^1 groups were used to modify the functionality of the N-terminal and three different R^2 nucleophiles were used to adapt the C-terminal (Fig. 4). We thus synthesized nine different low molecular weight molecules.

LC/MS and ^{1}H NMR analyses confirmed the expected structure of each compound (see Section 4). In mass spectrometry, molecular ion $(M+H)^+$ peak was observed for **12** and **14**, whereas the M^+ peak was observed for other compounds. All observed *m*/*z* data corresponded to the exact calculated mass of the compounds. The mass spectrometry results also confirmed that chloropurine was not hydrolyzed to a guanine function during acid treatment required for BOC deprotection. All spectroscopic data confirmed the chemical structures of compounds described in Figure 4.

2.4 Development of a screening assay for FtsZ inhibitors. We developed a rapid and reliable screening assay to evaluate the GTPase FtsZ inhibitory potential of synthesized molecules. A spectrophotometric coupled enzymatic assay was used which allowed

quantitative analysis of the FtsZ GTPase activity with high sensibility and rapidity. We decided to determine initial velocities for all GAL compounds and results for compounds **10**, **14**, and **15** are presented in Table 1. Quantitative analysis of the FtsZ GTPase enzymatic reaction was done by monitoring the oxidation of NADH as a decrease in absorbance at 340 nm described in Section 4.5 and in Figure 5.

2.5 Evaluation of GTP analogues as inhibitors of the GTPase activity of FtsZ. Synthesized compounds were analyzed for their capability to inhibit GTPase activity of FtsZ in vitro. The FtsZ conversion of GTP into GDP was used to assess the inhibitory properties of the synthesized compounds. All the GTP analogues inhibited the GTPase activity of FtsZ with significant IC_{50} values between 450 μM and 2.6 mM as given in Table 2. Each compound showed a linear response between an increase in concentration and a decrease of the GTPase activity. This correlation is well represented by compound **14** in Figure 6. The inhibition curves of all nine inhibitors displayed a sigmoidal dose–response trend having variable slopes as shown in Figure 6. GTP analogues included in control reactions did not affect the PK and LDH enzyme reaction rate (see Section 4.6 and in Fig. 5) used to measure the release of GDP by FtsZ. The nine GTP analogues thus specifically inhibited FtsZ.

2.6 Testing of synthesized compounds in a biological assay. The antibacterial activity of GTP analogues was evaluated with *E. coli* and *S. aureus* cells. Kanamycin used as a control showed an inhibition of growth with a diameter of 30 mm at 20 g/L for both species (Fig. 7). None of the GAL compounds inhibited *E. coli* growth. Among the nine synthesized compounds, **5** inhibited *S. aureus* growth (Fig. 7 and Table 2). Compounds **14** and **15** showed the most promising antibacterial activity with inhibition of growth having a diameter of 28 and 15 mm, respectively, at 20 g/L. Compounds **10**, **13**, and **17** presented a moderate antibacterial activity at 20 g/ L (Fig. 7 and Table 2).

3. Discussion

In the last few years, there has been growing interest in identifying new antibacterial targets using essential proteins implicated in cell growth and division.[17] Until recently, bacterial cell division proteins such as FtsZ had not been used as targets and no pharmacologically active inhibitors of division proteins identified. We targeted the most conserved and essential cell division protein FtsZ which polymerizes as a ring to allow septation of daughter cells via an essential GTPase activity.[4,6] The GTPase activity of FtsZ was confirmed.[7] It has previously been shown that FtsZ binds GTP.[18] Here, we demonstrated the strong binding affinity and specificity of FtsZ for the GTP substrate.

Since FtsZ specifically binds and hydrolyzes GTP via an essential activity, we developed active inhibitors mimicking the natural GTP substrate.[6,19] To optimize the specificity of inhibitors for FtsZ and restrict their interference in eukaryotic cells, we have synthesized a core structure composed of a guanine-like moiety linked to an Ala side chain. We argued that the guanyl group will form a bond in the FtsZ active site. Synthesized compounds will thus either compete with the natural substrate as competitive inhibitors or block the GTP binding to FtsZ by restricting access to the active site and act as irreversible inhibitors.

The core structure was quite tedious to obtain on a large scale. We optimized the method described by Pansare and we used the more reactive 2-amino-6-chloropurine instead of a guanine surpassing the yield of other methods.[20-22,15,16] Concerning the preparation of the β-lactone, the optimized Mitsunobu reaction allowed the synthesis of **2** in good yields only when working on a small scale; whereas it was previously reported as 72% in yield when starting from 5 g of (Boc)-L-Ser.[13,14] Several attempts for preparing the β-lactone and using 5 g of (Boc)-L-Ser as described previously gave poor yields which could be due to variations in the quality of (Boc)-L-Ser preparations used.

The diversity of compounds in our focus library was created by substituting the core structure at the N- and C-terminal positions. The oxime resin was used as the most convenient solid support for our parallel synthesis strategy in comparison to other support such as the Merrifield resin.[12,23,24] This strategy is most efficient in Boc, permits gentle cleavage with nucleophiles, and eventually permits incorporation of a C-terminal amino

group in a single step. A vast majority of the chemical groups in R^1 used to modify the N-terminal functionality were aromatics as many known antibiotics possess an aromatic group. We also minimized the bulk of the R^2 group so as to presumably facilitate the binding in the FtsZ GTP active site.

Various methods have already been used to evaluate the biological activity of FtsZ. The FtsZ GTPase activity was quantified via hydrolysis of radioactive GTP substrate.[6,25] The FtsZ activity was also quantified by measuring the release of inorganic phosphate or by assessing protein polymerization.[26-28] These methods required high amounts of FtsZ except for radioactive assays. The spectrophotometric assay permitted to follow in real time the GTPase reaction in comparison to other assays where only end-point data are obtained. Our assay is also less time-consuming, cost-effective, highly reproducible, and could be well adapted to a HTS screening in microtiter plates.

The GAL core structure of analogues was efficient in mimicking GTP and impairing the FtsZ activity. First, we determined their initial velocity (Table 1) and used these data to calculate IC_{50} values which were in the μM range (Table 2). The most active compounds were **10**, **14**, and **15**. The three best FtsZ inhibitors showed an antibacterial activity against *S. aureus*. Compound **14** is the most promising structure giving the best antibacterial activity and an IC_{50} value of 600 μM. As shown in Figure 4, the sole difference between compounds **14** and **15** is the presence of a double bond at the C-terminus of **14**. We will focus efforts to pursue characterization of **14** and its chemical structure will constitute the basic core structure for synthesis of more potent FtsZ inhibitors.[29-31]

FtsZ shares a highly conserved central core structure with tubulin.[32,33] However, FtsZ has a N-terminal extension absent in tubulin, while tubulin subunits display two long C-terminal α-helices absent in FtsZ.[34] Several tubulin inhibitors are presently used in cancer treatment, but are not very effective against FtsZ.[35,36]

To date, few FtsZ inhibitors have been identified.[25, 37-42] The Zantrin compounds perturb the FtsZ ring assembly causing lethality to a variety of bacteria in broth cultures, indicating that FtsZ antagonists may serve as chemical leads for the development of new broad-spectrum antibacterial agents.[43] The antibacterial activity of GAL compounds may be similar to Zantrins and could be attributable to inhibition of the Z-ring polymerization

dependent on the FtsZ GTPase activity.[43] The viriditoxin product from *Aspergillus* sp. MF6890 blocked FtsZ polymerization with an IC_{50} of 8.2 μg/mL and inhibited GTPase activity with an IC_{50} of 7.0 μg/mL.[41] The antibacterial action of viriditoxin via inhibition of FtsZ was confirmed by the observation of its effects on cell morphology, macromolecular synthesis, DNA-damage response, and increased minimum inhibitory concentration as a result of an increase in FtsZ expression. Viriditoxin exhibited broad-spectrum antibacterial activity against clinically relevant Gram-positive pathogens, including methicillin-resistant *S. aureus* and vancomycin-resistant enterococci, without affecting the viability of eukaryotic cells.[41] The sole GTP analogue identified as an FtsZ inhibitor did not have antibacterial activity.[44] The 8-bromoguanosine 5′-triphosphate acts as a competitive inhibitor of both FtsZ polymerization and GTPase activity with a K_i of 31.8 μM. The observation that this GTP analogue did not inhibit tubulin assembly suggested a structural difference of the GTP-binding pockets of FtsZ and tubulin.[44] Structures of the published FtsZ inhibitors could be exploited to enhance the inhibitory potential of compound **14**.[40,43]

To our knowledge, this is the first report describing GTP analogues having promising inhibitory properties of the GTPase activity of FtsZ and validated antimicrobial properties against whole bacterial cells. The synthesis of derivatives of these compounds is a promising avenue in investigating the structure–activity relationships for the design of efficient and specific inhibitors of bacterial cell division and we are currently working along these lines.

4. Experimental

4.1 Reagents, solvents and bacterial strains. Amino acids were purchased from Advanced ChemTech (Louisville, Kentucky, USA) and all other reagents were purchased from Sigma–Aldrich (Oakville, Ontario, Canada) unless otherwise indicated. The reagents and solvents were treated as follows: dichloromethane (DCM) was distilled; dimethylformamide (DMF) was degassed using nitrogen; water was deionized and filtered using a 0.45 μm membrane; tetrahydrofuran (THF) was distilled over Na and benzophenone; *n*-propylamine was distilled over KOH. Other reagents and solvents were

used directly; methanol ACS grade (EM Science, VWR International, Mont-Royal, Québec, Canada); acetonitrile spectroscopic quality (Laboratoire MAT, Beauport, Québec, Canada); diethyl ether ACS grade (BDH, VWR International); chloroform spectroscopic quality. The recombinant plasmid containing the *ftsZ* gene was propagated in *E. coli* NovaBlue, *endA1 hsdR17* r_{K12}^{-} m_{K12}^{+} *supE44 thi-1 recA1 gyrA96 relA1 lac* [F′ *proA*$^{+}$*B*$^{+}$ *lacI*^{q} *Z*Δ *M15*::Tn*10*] prior to protein synthesis in *E. coli* BL21, F^{-} *ompT hsdS*$_B$ r_B^{-} m_B^{-} *gal dcm* (λDE3) (Novagen, Madison, WI, USA).

4.2 Purification of biologically active FtsZ enzyme. Polymerase chain reaction (PCR) amplification was used to obtain DNA fragments encoding *P. aeruginosa* PAO1 *ftsZ* gene. The construction fused a His-tag at the C-terminus of the FtsZ protein. The *ftsZ* PCR product was cloned into the expression vector pET24b (Novagen) as described previously.[45] The recombinant plasmid pMON2020 containing the *ftsZ* gene was maintained in *E. coli* NovaBlue prior to protein expression in *E. coli* BL21.[45] Expression of the recombinant FtsZ protein was performed by adding 1 mM IPTG at an OD 600 nm of 0.8 during the exponential phase of growth. The *E. coli* BL21 culture was then incubated for 4 h at 37 °C under agitation. Cells were centrifuged and the bacterial pellet was treated with lysozyme and sonicated.[45] FtsZ was purified to homogeneity by affinity chromatography using a His-bind nickel resin (Novagen) with 150 mM imidazole during elution. Purified FtsZ was dialyzed in buffer (20 mM Tris–HCl, pH 7.6, 10 mM NaCl, and 1 mM EDTA) and conserved in 50% (v/v) glycerol at −80 °C.[46] Purified FtsZ was visualized on SDS–PAGE and the protein concentration was determined using the Bradford method (Bio-Rad, Mississauga, Ontario, Canada). N-terminal sequencing was done by the Edman degradation technique at the Biotechnology Research Institute (National Research of Council Canada, Montreal, Québec, Canada).[45]

4.3 Biochemical characterization of FtsZ. An UV cross-link specific nucleotide-binding assay was performed with purified FtsZ and with the radioactive nucleotides ATP, GTP, CTP, and TTP.[47] Briefly, 3 μg of purified FtsZ was mixed with each of the four P^{32}-labeled nucleotides (Perkin-Elmer, Woodbridge, Ontario, Canada). The samples were incubated for 30 min at 0 °C and irradiated for 10 min at 254 nm in a microtiter plate on top of a chilled

lead brick in iced water. The samples were purified prior to analysis by SDS–PAGE and visualized by autoradiography. The GTPase activity of purified FtsZ was confirmed using a thin-layer chromatography (TLC) assay with P^{32}-labeled GTP as substrate. The FtsZ GTPase assay was performed using 12 μM FtsZ in reaction buffer Z (50 mM Bis-Tris propane, pH 7.4, 10 mM $MgCl_2$ and 2.5 mM DTT) and 1 μL of GTP^{32} 10 μCi/μL (Perkin-Elmer) in a final volume of 20 μL.[25] The mixture was incubated for 1 h at 37 °C and 2 μL was deposited on a TLC along with a negative control (without enzyme). Hydrolysis of the radioactive substrate was measured by autoradiography using a Phosphorimager (Fuji, Stanford, California, USA).

4.4 Synthesis of the GTP analogue library using combinatorial chemistry.

4.4.1 Synthesis of the β-lactone 2 from (BOC)-L-Ser. The general strategy was from Pansare et al.[21] The method was optimized on a small scale and the reaction was repeated to accumulate the desired amount of (Boc)-L-Ser β-lactone **2**. In a typical experiment (1 g, 4.87 mmol) (Boc)-L-Ser (1 g, 4.87 mmol) was dissolved in 5 mL of anhydrous THF and the solution was introduced in an addition funnel on a 100 mL 3-necked flask. Triphenylphosphine (1.28 g, 4.87 mmol) was added to the reaction mix and the assembly was kept under inert atmosphere. Twenty-five microliters of anhydrous THF was added to dissolve triphenylphosphine and the solution was cooled down to −78 °C using a dry ice-acetone bath. When the temperature was stable, DEAD (0.77 mL, 4.87 mmol) was added dropwise over a period of 10 min at constant temperature. The (Boc)-L-Ser solution was then added dropwise over a period of 15 min. After an agitation period of 20 min at −78 °C, the temperature was slowly raised to room temperature. The mixture was stirred for 2.5 h and the solvent was evaporated to precipitate the triphenylphosphine oxide. A column chromatography was performed to purify the (Boc)-L-Ser-β-lactone product using silica gel as adsorbent and a hexane/AcOEt 65:35 at elution.

4.4.2 Ser β-lactone (2). HPLC: R_t = 10.9 min. ^{1}H NMR (300 MHz, DMSO-d_6) δ: 1.41 (s, 9H, *t*-butyl), 4.29 and 4.41 (7 lines, 2H, J_{AB} = 4.5 Hz, CH_2), 5.14 (m, 1H, CH_α), 7.81 (d,

1H, N*H*, 8.0 Hz). ^{13}C NMR (75 MHz, DMSO-d_6) δ: 28.1 (*C*H$_3$ *t*-butyl), 58.8 (*C*H$_2$), 65.8 (*C*H$_\alpha$), 79.3 (*C* *t*-butyl), 154.7 (*C*═O *t*-butyl), 170.6 (*C*═O). Yield: 87.7%; purity >99%.

4.4.3 Opening of the β-lactone 2 and formation of N-(BOC)-(2-amino-6-chloropuryl)-L-Ala (4). (Boc)-L-Ser-β-lactone (1.4 g, 7.5 mmol) and 2-amino-6-chloropurine (1.9 g, 11.2 mmol, 1.5 equiv) were dissolved in 20 mL of anhydrous DMF. Cesium carbonate (3.66 g, 11.2 mmol) was added and the solution was heated to reflux during 3 h. The solution was cooled and water was added to stop the reaction. The pH was adjusted to 5 and 6 extractions were done using 20 mL of ethyl acetate with moderate agitation. The organic phase was dried with anhydrous $MgSO_4$, filtered, evaporated, and kept under vacuum.

4.4.4 N-(BOC)-(2-amino-6-chloropuryl)-L-Ala (4). HPLC: R_t = 10.66 min. MS (MALDI-TOF): *m*/*z* 357.1 = (M+H)$^+$. ^{1}H NMR (300 MHz, DMSO-d_6) δ: 1.30 (s, 9H, *t*-butyl), 4.24 (m, 1H, C*H*$_\alpha$), 4.44 (m, 2H, C*H*$_2$), 6.97 (s, 2H, N*H*$_2$), 7.31, (d, 1H, *J* = 8 Hz N*H*), 7.95, (s, 1H, C*H*═N), 13.01 (m, 1H, COO*H*) ^{13}C NMR (75 MHz, DMSO-d_6) δ: 28.02 (*C*H$_3$ *t*-butyl), 43.49 (*C*H$_2$), 52.44 (*C*H$_\alpha$), 78.59 (*C* *t*-butyl), 123.29 (C1–*C*═N), 143.44 (*C*H═N), 149.32 (NH$_2$–*C*═N), 154.16 (*C*═C), 155.26 (C═*C*), 159.83 (*C*═O *t*-butyl), 171.24 (*C*OOH).Yield: 63.7%; purity >96%.

4.4.5 Preparation of the oxime resin. To obtain the desired oxime resin, polystyrene beads reticulated with divinylbenzene were treated with *p*-nitrobenzoyl chloride following the Friedel-Crafts conditions.[23,24] Once the acylation of the polystyrene was completed, hydroxylamine gave a reaction with the ketone to yield the oxime groups. After several washes, the oxime resin was composed of 1% divinylbenzene crosslinked polystyrene with randomly grafted *p*-nitrobenzoyloxime groups.

4.4.6 Coupling of the GAL core molecule 4 on oxime resin. Oxime resin (5 g) with a loading of 0.5 mmol/g was introduced into a solid-phase synthesis vessel with a sintered glass extremity and a Teflon cap. The resin was swollen with 100 mL DCM and washed twice with 100 mL of this solvent. *N*-(Boc)-(2-amino-6-chloropuryl)-L-Ala **4** (3.66 g, 11.2

mmol) was dissolved in 80 mL of a DCM/DMF 1:1 mixture and the solution was cooled to 0 °C. 1.26 mL of diisopropylcarbodiimide (DIC) (10.0 mmol; 4.0 equiv) was added and the suspension was shaken for 30 min. The resulting suspension was poured into the reaction vessel containing the oxime resin. The resulting mixture was shaken during 24 h, and its content was filtered by suction. The resin coupled with *N*-(Boc)-(2-amino-6-chloropuryl)-L-Ala was washed 3 times with 100 mL of DMF and 3 times with 100 mL of methanol. Washing steps were repeated and the resin was dried under vacuum.

4.4.7 Acetylation of non-substituted sites on the oxime resin. The non-substituted sites were blocked by acetylation as described in the literature.[48] Briefly, the resin was washed with DMF and an acetic anhydride/DMF 1:1 mixture was added to the vessel followed by DIEA. After 2 h of shaking, the content was filtered and the resin was washed with DMF, with methanol and then dried under vacuum. In this specific case, the concentration of resin to be loaded cannot be determined by the Kaser's quantitative colorimetric ninhydrin test because of the guanine moiety.[49] We pursued the synthesis assuming a substitution level of 0.4 mmol/g of dried resin.

4.4.8 Deprotection of the n-BOC group of GAL core molecule. Resin **5** was swollen with 100 mL DCM and washed twice with 100 mL of this solvent. Eighty microliters of a 2,2,2-trifluoroacetic/DCM 1:1 mixture was added and the mixture was shaken mechanically for 30 min. The vessel content was filtered by suction, washed with DMF and with methanol as mentioned above, and dried under vacuum.

4.4.9 Modification of the N-terminal of GAL core molecule (R1). The resin (500 mg, 0.20 mmol) was swollen with 10 mL DMF and washed twice with this solvent. An excess of 1 mmol (5 equiv) of the desired R^1 group was added to the resin solution with 5 mL DCM and shaken for 2 h. The R^1 group was obtained from carboxylic acids, acid chlorides, isocyanates or sulfonyl chlorides. In the case of the carboxylic acids, it was activated with DIC and hydroxybenzotriazole (HOBt). To do so, 1 mmol (5 equiv) of the carboxylic acid was dissolved in 8 mL of a DCM/DMF 1:1 mixture and the solution was cooled to 0 °C. One hundred and fifty-seven microliters of DIC (1 mmol; 5 equiv) was added and the

solution was shaken for 5 min. One hundred and thirty-five micrograms of HOBt–H_2O (1 mmol and 5 equiv) was added and the whole mixture was shaken for 30 min. The suspension was introduced into the vessel, 52 μL DIEA (0.3 mmol; 1.5 equiv) was added, and the content was shaken for 2 h. For each R^1 group, the ampoule content was filtered by suction, washed with DMF and methanol as described previously, and dried under vacuum. For N-terminal modifications with acid chlorides, isocyanates or sulfonyl chlorides, the deprotected resin was swollen and washed with DMF. The acid solution of the desired reagent (5 equiv) in DCM was added to the resin, followed by addition of 52 μL DIEA. After 2 h of shaking, the reaction mixtures were filtered, washed with a cycle of DMF and methanol, and then dried under vacuum to yield the appropriate N-modified compounds linked to the resin.

4.4.10 Cleavage and modification of the C-terminal (R2). The cleavages were performed using three nucleophiles: sodium hydroxide, *n*-propylamine or allylamine.[50] The sodium hydroxide cleavage was done by first swelling the resin with 20 mL THF and washing it twice with 20 mL of this solvent. Thirty microliters of a THF solution containing 10% of 0.1 N NaOH was introduced into the reaction vessel and the resulting mixture shaken for 4 h. The vessel content was filtered by suction and washed 3 times with 30 mL DCM and 30 mL of methanol. This step was repeated and the solvents and washings were combined and evaporated under vacuum. The dried crude product was dissolved in glacial acetic acid and lyophilized. The *n*-propylamine cleavage was done by treating the swollen resin in DCM with 20 μL (1 equiv) of *n*-propylamine and 30 mL DCM. The resulting mixture was shaken for 1 h.[50] The vessel content was then recovered and the resin treated as described for the sodium hydroxide cleavage. The allylamine cleavages were performed as with *n*-propylamine.

4.4.11 Synthesis of the specific compounds in library. Each molecule under investigation was synthesized in a parallel fashion using the general method described previously.

4.4.12. N-Phenylacetyl-(2-amino-6-chloropuryl)-l-Ala (9) HPLC: R_t = 9.5 min. MS (API-ES): m/z 373.2 = M^+. ^{1}H NMR (300 MHz, DMSO-d_6): 3.65 (s, 2H, CH_2), 4.37 (m, 1H,

CH_{α}), 4.63 (d, 1H, J = 4.0 Hz, CH_2 ala), 4.71 (d, 1H, J = 4.2 Hz, CH_2 ala), 7.06–7.31 (m, 5H, H_{arom}), 8.51 (s, 1H, N–CH═N). Yield: 61%; purity >95%.

4.4.13. N-Phenylcarbamoyl-(2-amino-6-chloropuryl)-l-Ala (10) HPLC: R_t = 5.4 min. MS (API-ES): m/z 374 = M^+. ^{1}H NMR (300 MHz, DMSO-d_6): 4.24 (m, 1H, CH_{α}), 4.51 (m, 2H, CH_2 ala), 6.61 (d, 1H, J = 5.25 Hz, NH_{α}), 6.72 (s, 1H, NH–C_6H_5), 7.16–7.49 (m, 5H, H_{arom}), 8.08 (s, 1H, N–CH═N).Yield: 84%; purity >95%.

4.4.14. N-Benzenesulfonyl-(2-amino-6-chloropuryl)-l-Ala (11) HPLC: R_t = 10.3 min. MS (API-ES): m/z 395 = M^+. ^{1}H NMR (300 MHz, DMSO-d_6): 4.33 (m, 1H, CH_{α}), 4.52 (m, H, CH_2), 6.86 (d, 1H, J = 10.6 Hz, NH), 7.24–7.98 (m, 5H, H_{arom}), 8.08 (s, 1H, N–CH═N). Yield 43%; purity >96%.

4.4.15. Allyl amide of N-(R)-(+)-α-methylbenzylcarbamoyl-(2-amino-6-chloropuryl)-l-Ala (12) HPLC: R_t = 13.7 min. MS (API-ES): m/z 443 = $(M+H)^+$. ^{1}H NMR (300 MHz, DMSO-d_6): 1.31 (m, 2H, CH_2═CH–CH_2), 1.24 (d, 3H, J = 7.3 Hz, CH–CH_3), 3.64 (m, 1H, CH–CH_3), 5.05 (m, 1H, CH_{α}), 5.28 (m, 2H, CH_2 ala), 5.82 (m, 2H, CH_2═CH–CH_2), 5.94 (m, 1H, CH_2═CH–CH_2), 7.30 (m, 5H, H_{arom}), 7.95 (s, 1H, N–CH═N). Yield 23%; purity >96%.

4.4.16. n-Propyl amide of N-(R)-(+)-α-methylbenzylcarbamoyl-(2-amino-6-chloropuryl)-l-Ala (13) HPLC: R_t = 15.1 min. MS (API-ES): m/z 443 = M^+. ^{1}H NMR (300 MHz, DMSO-d_6): 0.92 (t, 3H, J = 7.7 Hz, CH_3–CH_2–CH_2), 1.39 (m, 2H, CH_3–CH_2–CH_2), 2.05 (d, 3H, J = 7.5 Hz, CH_3–CH), 2.75 (m, 2H, CH_3–CH_2–CH_2), 2.98 (q, 1H, J = 6.1 Hz, CH_3–CH), 3.65 (m, 2H, CH_2 ala), 3.80 (m, 1H, CH_{α}), 7.34 (m, 5H, H_{arom}). Yield: 24%; purity >96%.

4.4.17. Allyl amide of N-methanesulfonyl-(2-amino-6-chloropuryl)-l-Ala (14) HPLC: R_t = 4.7 min. MS (API-ES): m/z 374 = $(M+H)^+$. ^{1}H NMR (300 MHz, DMSO-d_6): 128 (m, 2H, CH_2–CH═CH_2), 2.31 (s, 3H, CH_3), 3.70 (m, 2H, CH_2 ala), 5.02 (m, 1H, CH_{α}), 5.41 (d, 2H, CH_2═CH), 5.89 (m, 1H, CH_2═CH), 7.93 (s, 1H, N–CH═H). Yield: 34%; purity >96%.

4.4.18. n-Propyl amide of N-methanesulfonyl-(2-amino-6-chloropuryl)-l-Ala (15) HPLC: R_t = 13.7 min. MS (API-ES): *m*/*z* 374 = M^+. ^{1}H NMR (300 MHz, DMSO-d_6): 0.89 (t, 3H, *J* = 7.5 Hz, C*H*$_3$–CH$_2$–CH$_2$), 1.40 (m, 2H, CH$_3$–C*H*$_2$–CH$_2$), 1.58 (m, 2H, CH$_3$–CH$_2$-C*H*$_2$), 2.32 (s, 3H, CH$_3$–SO$_2$), 3.00 (m, 2H, CH–C*H*$_2$), 3.84 (m, 1H, C*H*$_\alpha$), 6.93 (m, 1H, N*H*$_\alpha$), 7.87 (s, 1H, N–C*H*═N). Yield: 38%; purity >95%.

4.4.19. Allyl amide of N-p-toluenesulfonyl-(2-amino-6-chloropuryl)-l-Ala (16) HPLC: R_t = 13.7 min. MS (API-ES): *m*/*z* 448 = M^+. ^{1}H NMR (300 MHz, DMSO-d_6): 1.28 (m, 2H, CH$_2$═CH–C*H*$_2$), 2.30 (s, 3H, C*H*$_3$–C$_6$H$_4$), 3.47 (d, 2H, *J* = 5.9 Hz, C*H*$_2$ ala), 5.03 (m, 1H, C*H*$_\alpha$), 5.34 (d, 2H, *J* = 11.3 Hz, C*H*$_2$═CH), 5.87 (m, 1H, C*H*$_2$═CH), 7.12 (d, 2H, *J* = 7.9 Hz, H$_{arom}$ *H*$_2$, H$_6$), 7.48 (d, 2H, *J* = 8.0 Hz, H$_{arom}$ *H*$_3$, *H*$_5$), 7.99 (s, 1H, N–C*H*═N). Yield: 23%; purity, 95%.

4.4.20. n-Propyl amide of N-p-toluenesulfonyl-(2-amino-6-chloropuryl)-l-Ala (17) HPLC: R_t = 14.0 min. MS (API-ES): *m*/*z* 450 = M^+. ^{1}H NMR (300 MHz, DMSO-d_6): 0.92 (t, 3H, *J* = 7.5 Hz, C*H*$_3$–CH$_2$–CH$_2$), 1.54 (m, 2H, CH$_3$–C*H*$_2$–CH$_2$), 2.30 (s, 3H, C*H*$_3$–C$_6$H$_4$), 2.75 (t, 2H, *J* = 7.5 Hz, CH$_3$–CH$_2$-C*H*$_2$), 3.00 (m, 2H, C*H*$_2$ ala), 7.12 (d, 2H, *J* = 7.8 Hz, H$_{arom}$ *H*$_2$, *H*$_6$), 7.48 (d, 2H, *J* = 7.9 Hz, H$_{arom}$ *H*$_3$, *H*$_5$), 7.68 (m, 3H, N–C*H*═N + N*H*$_{2(2\text{-amino-6-chloropuryl})}$). Yield: 25%; purity, >96%.

4.4.21 Analysis of synthesized molecules by mass spectrometry and NMR. Analysis of aliquots was first performed on a LC/MS system (Agilent Technologies, model HP 1100 LC-MSD) with an atmospheric pressure electrospray ionization (API-ES) and a quadrupole mass spectrometer detector (MSD).[48] Briefly, the separation was done using a C5 reversed-phase column 0.46 × 25 cm (Phenomenex, Torrance, CA, USA) at room temperature. The flow rate was 0.5 mL/min and the injection volume was 10 µL. A linear gradient from a 10:90 to 100:0 ACN–water (with 0.1% of TFA) was used over 45 min. Mass spectrometry detection was performed with the ESI set at Vcap = 4500 V, nebulizing gas pressure = 35 psi, drying gas flow rate = 13 L/min, drying gas temperature = 350 °C with the quadrupole scanning from 50 to 500 *m*/*z* every 1.03 s with a step size of 0.15 amu. The

^{1}H NMR experiments were done on a Bruker AC-F-300 MHz spectrometer using standard software. All measurements were made at 25 °C on a 5 mg sample dissolved in 0.6 mL DMSO-d_6. The residual proton resonance of DMSO was used as an internal reference at 2.5 ppm for ^{1}H NMR spectra.

4.5 Screening assay for FtsZ inhibitors. A spectrophotometric coupled enzymatic assay was developed to measure the FtsZ activity. The GTPase enzymatic reaction was quantified by monitoring the oxidation of NADH as a decrease in absorbance at 340 nm. FtsZ hydrolyzed GTP into GDP and inorganic phosphate. The GDP product is used as substrate with phosphoenol pyruvate (PEP) by the pyruvate kinase (PK) enzyme to give GTP and pyruvic acid as products. The pyruvic acid is then used as substrate with NADH + H^+ by the D(−)lactate dehydrogenase (LDH) enzyme giving lactate and NAD^+. The NADH + H^+ molecule could be detected at 340 nm but the final NAD^+ product gave no absorbance. The decrease in NADH + H^+ absorbance at 340 nm follows proportionally the FtsZ GTPase enzymatic activity (Fig. 5). This coupled enzymatic assay was optimized for specificity and for several parameters including reaction buffer, FtsZ, GTP, DTT, and DMSO. The assay contained 50 mM Bis–Tris Propane (pH 7.4), 3.5 μM of purified FtsZ, 5 mM GTP, 5 mM $MgCl_2$, 2.5 mM DTT, 2 mM of phosphoenolpyruvate, 1.4 U of PK enzyme (Roche Diagnostics, Québec, Canada, EC: 2.1.7.40, 200 U/mg), 380 μM NADH, 2.1 U of LDH enzyme from *Lactobacillus leichmannii* (Roche Diagnostics, EC: 1.1.1.28, 300 U/mg), and 25% DMSO (Laboratoire MAT). The reaction was performed in a 100 μL volume using a Submicro Cell (Varian, Mississauga, Ontario, Canada). The optical density was monitored at 340 nm for a period of 15 min at room temperature with a Cary spectrophotometer (Varian). The FtsZ enzyme kinetics were determined from the linear portion of the curve using the least-squares calculation as described.[51] A negative control was performed without the FtsZ enzyme and a positive control was done using 0.5 mM GDP and without FtsZ.

4.6 Inhibition assays of FtsZ and IC50 determination. Each synthesized compound was dissolved in 100% DMSO at 0.1 g/L, the pH was adjusted to 7, and the buffered solution was kept at −20 °C. Inhibition of the FtsZ GTPase activity was determined using various

concentrations of each GAL compound. The final DMSO concentration was adjusted to 25%. Reaction mixtures without FtsZ were incubated at 37 °C for 10 min and the FtsZ enzyme was added. The velocity of FtsZ GTPase activity was determined with each compound at various concentrations as described in Section 4.5. The percentage of GTPase residual activity was obtained by comparing the enzyme velocity from each compound concentration with the velocity obtained with the wild-type FtsZ reaction. The compound concentrations required to inhibit 50% of the FtsZ GTPase activity (IC_{50}) were obtained by plotting the percentage of residual GTPase activity.[25] As controls, concentrations of each compound leading to inhibition of GTPase activity were analyzed using the coupled enzymatic assay. The inhibition of enzymes in the coupled assay was evaluated by using 0.5 mM GDP without FtsZ. The velocities of the PK and LDH enzymes were determined for each compound and similar values were obtained as for the wild-type enzyme.

4.7 Agar diffusion assay. Cultures of *E. coli* ATCC 25922 and *S. aureus* ATCC 25923 were grown in 10 mL of Mueller Hinton broth (MHB, Becton Dickinson Microbiology Systems, Sparks, Maryland, USA) overnight at 37 °C. The bacterial cultures were diluted in MHB to obtain a McFarland standard turbidity of 0.5. Agar plates were prepared by pouring 100 mL of Mueller Hinton Agar (Becton–Dickinson Microbiology Systems) into 150 mm Petri dishes. Plates were dried for 30 min at 37 °C and wells were made in the agar with a sterile Pasteur pipette. Sterile cotton tip applicators were used to uniformly inoculate the surface of agar plates with the bacterial cultures. As control, 100 µL DMSO and 100 µL of a 20 g/L kanamycin solution were added to wells. Each GAL compound was diluted in DMSO to reach a 20 g/L concentration and 100 µL of each solution (2 mg) was added to wells. Plates were incubated at 37 °C overnight without being inverted.

Acknowledgments

This work was supported by a FQRNT team grant to Roger C. Levesque. Catherine Paradis-Bleau obtained a studentship from Le Fonds de la Recherche en Santé du Québec

and Mélanie Beaumont obtained a CREFSIP studentship. R. C. Levesque is a FRSQ scholar of exceptional merit.

References

1. Levy, S. B.; Marshall, B. Nat. Med. 2004, 10, S122.
2. Margolin, W. Nat. Rev. Mol. Cell. Biol. 2005, 6, 862.
3. Projan, S. J. Curr. Opin. Pharmacol. 2002, 2, 513.
4. van den Ent, F.; Amos, L.; Lowe, J. Curr. Opin. Microbiol. 2001, 4, 634.
5. Lutkenhaus, J.; Addinall, S. G. Annu. Rev. Biochem. 1997, 66, 93.
6. de Boer, P.; Crossley, R.; Rothfield, L. Nature 1992, 359, 254.
7. Errington, J.; Daniel, R. A.; Scheffers, D. J. Microbiol. Mol. Biol. Rev. 2003, 67, 52.
8. Cordell, S. C.; Robinson, E. J.; Lowe, J. Proc. Natl. Acad. Sci. U.S.A. 2003, 100, 7889.
9. Pierce, G. E. J. Ind. Microbiol. Biotechnol. 2005, 32, 309.
10. Hoiby, N. J. Cyst. Fibros. 2002, 1, 249.
11. Plunkett, M. J.; Ellman, J. A. Sci. Am. 1997, 276, 68.
12. Balkenhahl, F.; Bussche-Hu¨nnefeld, C.; Lansky, A.; Zechel, C. Angew. Chem., Int. Ed. Engl. 1996, 35, 2288.
13. Arnold, L. D.; Kalantar, T. H.; John, C. J. Am. Chem. Soc. 1985, 107, 7105.
14. Ciapetti, P.; Soccilini, F.; Taddei, M. Tetrahedron 1997, 53, 1167.
15. Sliedregta, K. M.; Schoutenb, A.; Kroonb, J.; Rob, M. J. Tetrahedron Lett. 1996, 37, 4237.
16. Bodanszky, M. Peptide Chemistry: A Practical Textbook; Springer Verlag: Berlin, New York, 1988, p 58.
17. Breithaupt, H. Nat. Biotechnol. 1999, 17, 1165.
18. Diaz, J. F.; Kralicek, A.; Mingorance, J.; Palacios, J. M.; Vicente, M., et al. J. Biol. Chem. 2001, 276, 17307.
19. Marrington, R.; Small, E.; Rodger, A.; Dafforn, T. R.; Addinall, S. G. J. Biol. Chem. 2004, 279, 48821.
20. Lewis, I. Tetrahedron Lett. 1993, 34, 5697.
21. Pansare, S. V.; Arnold, L. D.; Vederas, J. C. Org. Syn. 1993, 70, 10.
22. Pansare, S. V.; Huyer, G.; Arnold, L. D.; Vederas, J. C. Org. Syn. 1993, 70, 1.
23. DeGrado,W.F.; Kaiser, E. T. J. Org. Chem. 1980, 45, 1295.
24. DeGrado,W.F.; Kaiser, E. T. J. Org. Chem. 1982, 47, 3258.
25. Paradis-Bleau, C.; Sanschagrin, F.; Levesque, R. C. J. Antimicrob. Chemother. 2004, 54, 278.
26. Sossong, T. M., Jr.; Brigham-Burke, M. R.; Hensley, P.; Pearce, K. H., Jr. Biochemistry 1999, 38, 14843.
27. Bramhill, D.; Thompson, C. M. Proc. Natl. Acad. Sci. U.S.A. 1994, 91, 5813.
28. Mukherjee, A.; Cao, C.; Lutkenhaus, J. Proc. Natl. Acad. Sci. U.S.A. 1998, 95, 2885.
29. Thompson, L. A.; Ellman, J. A. Chem. Rev. 1996, 96, 555.
30. Hughes, D. Nat. Rev. Genet. 2003, 4, 432.

31. Nefzi, A.; Dooley, C.; Ostresh, J. M.; Houghten, R. A. Bioorg. Med. Chem. Lett. 1998, 8, 2273.
32. Nogales, E.; Downing, K. H.; Amos, L. A.; Lowe, J. Nat. Struct. Biol. 1998, 5, 451.
33. Carballido-Lopez, R.; Errington, J. Trends Cell. Biol. 2003, 13, 577.
34. Leung, A. K.; Lucile White, E.; Ross, L. J.; Reynolds, R. C.; DeVito, J. A., et al. J. Mol. Biol. 2004, 342, 953.
35. Yu, X. C.; Margolin, W.; Gonzalez-Garay, M. L.; Cabral, F. J. Cell. Sci. 1999, 112, 2301.
36. White, E. L.; Suling, W. J.; Ross, L. J.; Seitz, L. E.; Reynolds, R. C. J. Antimicrob. Chemother. 2002, 50, 111.
37. Stokes, N. R.; Sievers, J.; Barker, S.; Bennett, J. M.; Brown, D. R., et al. J. Biol. Chem. 2005, 280, 39709.
38. Jennings, L. D.; Foreman, K. W.; Rush, T. S., 3rd; Tsao, D. H.; Mosyak, L., et al. Bioorg. Med. Chem. 2004, 12, 5115.
39. Reynolds, R. C.; Srivastava, S.; Ross, L. J.; Suling, W. J.; White, E. L. Bioorg. Med. Chem. Lett. 2004, 14, 3161.
40. Urgaonkar, S.; La Pierre, H. S.; Meir, I.; Lund, H.; RayChaudhuri, D., et al. Org. Lett. 2005, 7, 5609.
41. Wang, J.; Galgoci, A.; Kodali, S.; Herath, K. B.; Jayasuriya, H., et al. J. Biol. Chem. 2003, 278, 44424.
42. RayChaudhuri, D.; Park, J. T. Nature 1992, 359, 251.
43. Margalit, D. N.; Romberg, L.; Mets, R. B.; Hebert, A. M.; Mitchison, T. J., et al. Proc. Natl. Acad. Sci. U.S.A. 2004, 101, 11821.
44. Lappchen, T.; Hartog, A. F.; Pinas, V. A.; Koomen, G. J.; den Blaauwen, T. Biochemistry 2005, 44, 7879.
45. Paradis-Bleau, C.; Sanschagrin, F.; Levesque, R. C. Protein Eng. Des. Sel. 2005, 18, 85.
46. Zhulanova, E.; Mikulik, K. Biochem. Biophys. Res. Commun. 1998, 249, 556.
47. Feucht, A.; Lucet, I.; Yudkin, M. D.; Errington, J. Mol. Microbiol. 2001, 40, 115.
48. Zoeiby, A. E.; Beaumont, M.; Dubuc, E.; Sanschagrin, F.; Voyer, N., et al. Bioorg. Med. Chem. 2003, 11, 1583.
49. Stewart, J. M.; Young, J. D. In Solid Phase Synthesis; Pierce Chemical Company: Rockford, Illinois, 1984, p 105.
50. Voyer, N.; Lavoie, A.; Pinette, M.; Bernier, J. Tetrahedron Lett. 1994, 35, 355.
51. Savoie, A.; Sanschagrin, F.; Palzkill, T.; Voyer, N.; Levesque, R. C. Protein Eng. 2000, 13, 267.

Table I. Initial velocities of three synthesized compounds used to calculate IC_{50} values.

Compound[a]	Concentration (mM)	V_0 ($\Delta DO_{340\ nm}$/min)
10	0	0.014
	0.3	0.010
	0.5	0.007
	0.7	0.004
	0.9	0.003
	1.3	0
14	0	0.014
	0.3	0.013
	0.5	0.012
	0.6	0.007
	0.7	0.004
	0.9	0
	1.3	0
15	0	0.014
	0.3	0.013
	0.5	0.011
	0.7	0.007
	0.8	0.006
	0.9	0.005
	1.1	0.004
	1.2	0

a, Initial velocities were determined with FtsZ for each of the nine compounds using a spectrophotometric coupled enzyme assay with NADH (Fig. 5). Details are given in section 4.5.

Table II. IC_{50} values and antibacterial activity for the nine FtsZ inhibitors synthesized.[a]

Compounds	MW (g/mol)	IC_{50} (mM)	Antibacterial[b] (mm)
9	356	2	No inhibition
10	357	0.45	10
11	378	1.2	No inhibition
12	424	1.8	No inhibition
13	426	1.8	11
14	355	0.6	28
15	357	0.7	15
16	431	1.7	No inhibition
17	433	2.6	11

[a] Molecular weights (MW) are indicated along with the IC_{50} value for each GTP analogue inhibiting the GTPase activity of FtsZ. The activity was measured by a coupled enzyme spectrophotometric assay.

[b] Antibacterial activity of the GAL compounds was evaluated by a biological assay using *S. aureus* cells and the measurement of the diameter of the zone of inhibition of growth.

Figure Legends

Figure 1. SDS-PAGE showing overexpression of the FtsZ protein in *E. coli* BL21 (λDE3) cells (Lane 1) and the near homogeneity of the purified FtsZ protein (Lane 2).

Figure 2. (A) UV cross-link specific nucleotide binding assay showing that FtsZ binds preferentially GTP. (B) Autoradiogram demonstrating FtsZ GTPase activity. **Lanes: 1,** control without enzyme; **2,** hydrolysis of GTP to GDP by FtsZ.

Figure 3. Solid-support combinatorial chemistry strategy and chemical reactions used to synthesize the library of GTP analogues.

Figure 4. (A) GAL core mimicking the natural GTP substrate of FtsZ; the relative positions of side chains R^1 and R^2 used for the parallel synthesis are indicated. (B) Chemical structure of individual GTP analogues found in the library with R^1 and R^2 groups used to modify the N- and C-terminal of the GAL core.

Figure 5. Spectrophotometric FtsZ enzymatic coupled assay. The GDP product of FtsZ is used as substrate with phosphoenol pyruvate (PEP) by the pyruvate kinase (PK) enzyme that gave GTP and pyruvic acid. The pyruvic acid is used as substrate with NADH + H^+ by the lactate dehydrogenase (LDH) enzyme giving lactate and NAD^+. The NADH + H^+ molecule can be detected at 340 nm but the final NAD^+ product gave no absorbance at 340 nm.

Figure 6. IC_{50} determination for the compound **14** inhibitor of the GTPase activity of FtsZ. The residual activity of FtsZ was measured as a function of the concentration of **14**. The positive control used with GDP showed a rapid decrease in absorbance at 340 nm indicating that the coupled enzymatic assay was efficient. The negative control performed without the FtsZ enzyme gave a stable absorbance at 340 nm in a time-dependent fashion.

This demonstrated that the drop of absorbance in the FtsZ assay was attributable to the FtsZ GTPase activity.

Figure 7. Agar diffusion assay showing inhibition of growth of *S. aureus* by GAL compounds.

Figure 1.

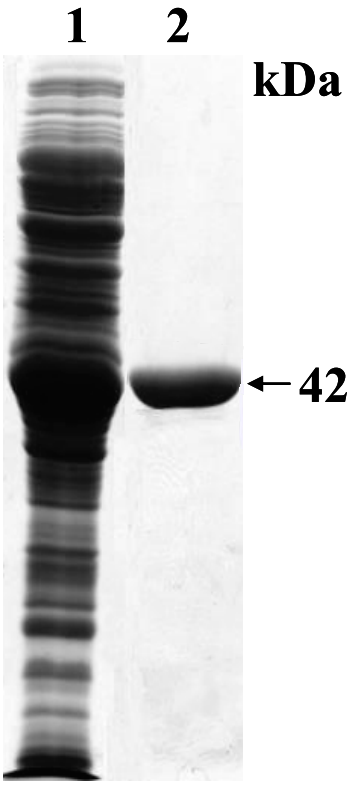

Figure 2.

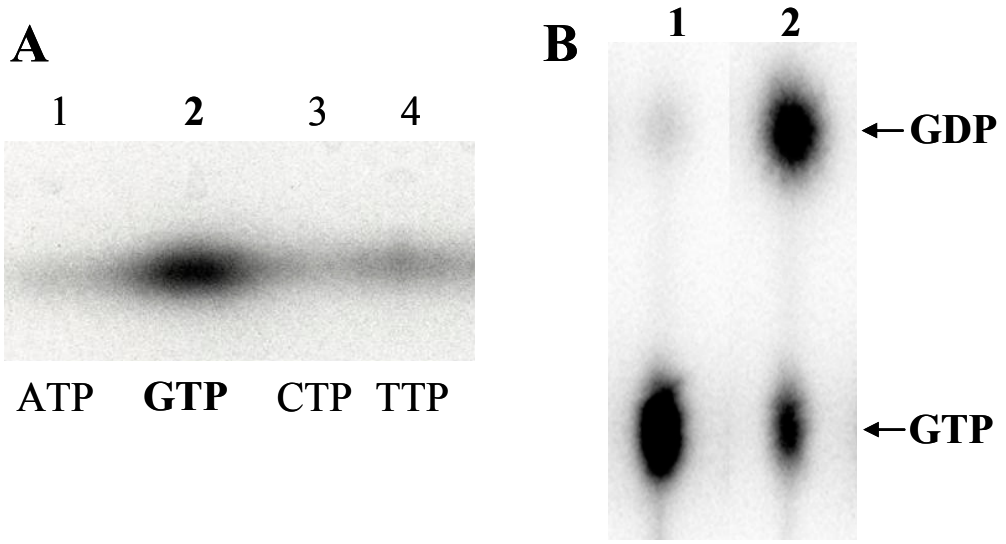

Figure 3.

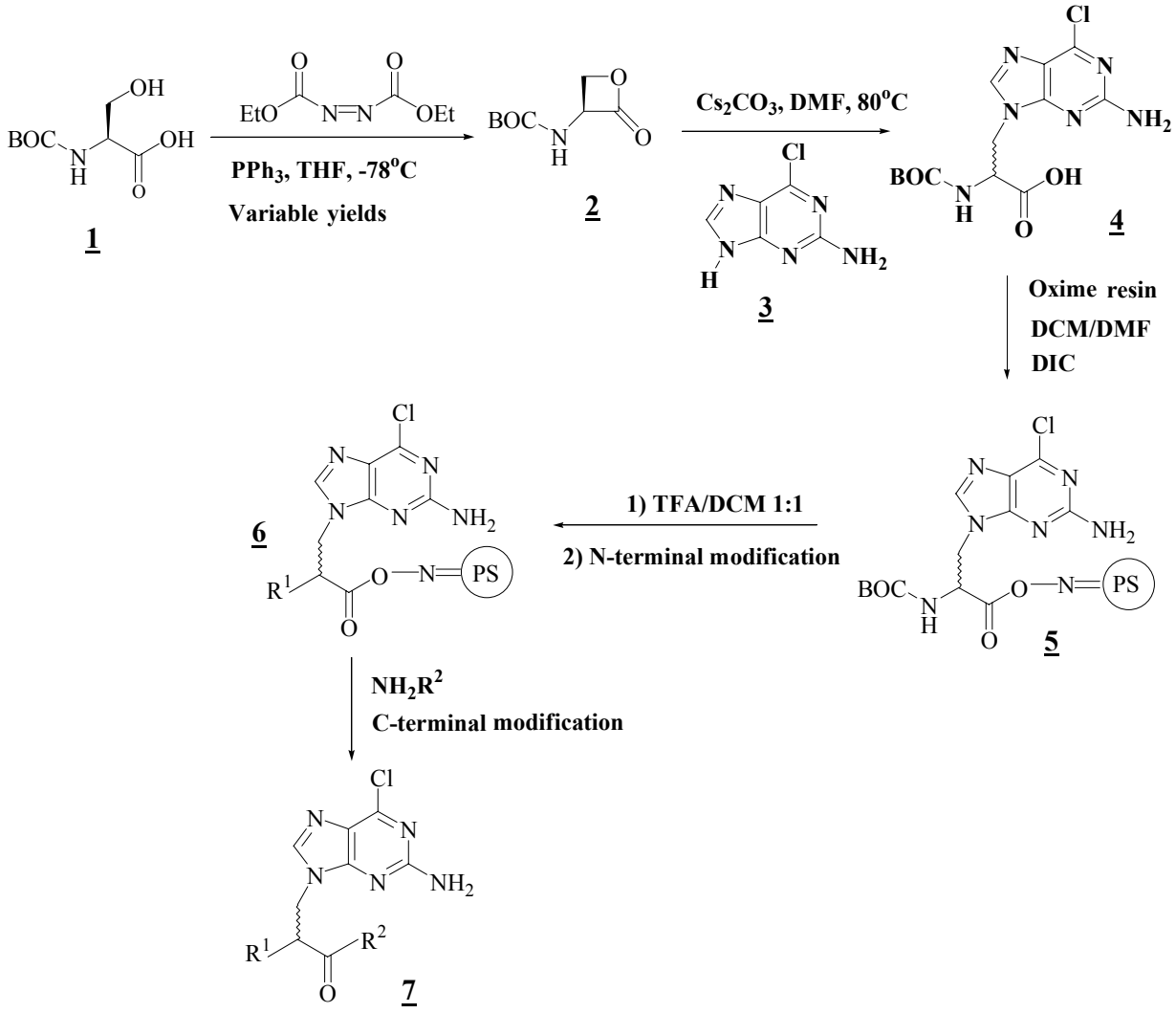
PPh3, THF, -78°C
Variable yields
Cs2CO3, DMF, 80°C
Oxime resin
DCM/DMF
DIC
1) TFA/DCM 1:1
2) N-terminal modification
NH2R2
C-terminal modification
1
2
3
4
5
6
7

Figure 4.

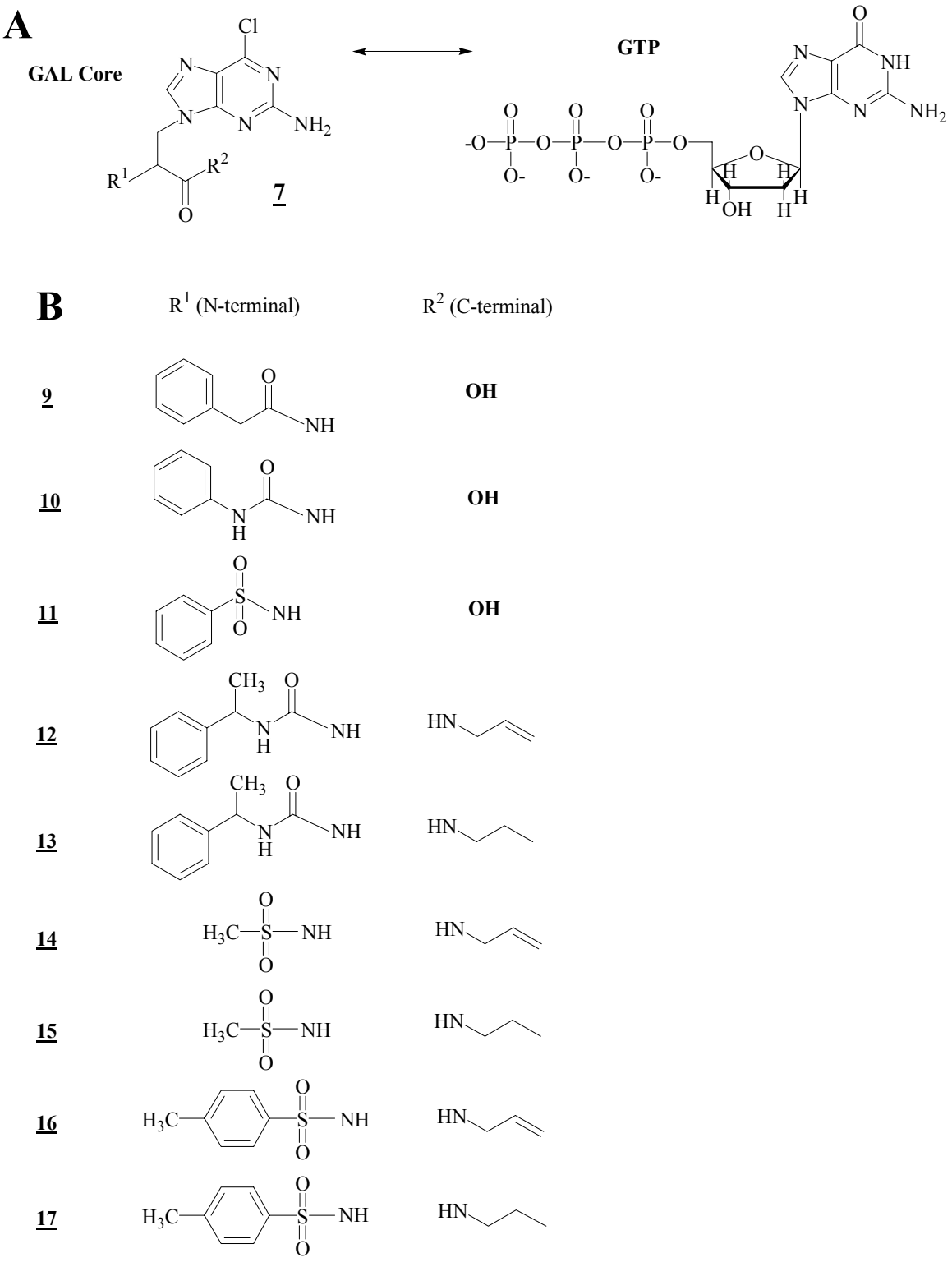
A
GAL Core
Cl
N
N
N
N
NH2
R1
R2
O
7
GTP
O
NH
N
N
NH2
-O
P
O-
H
OH
B
R1 (N-terminal)
R2 (C-terminal)
9
OH
10
OH
11
OH
12
CH3
HN
13
HN
14
H3C
HN
15
H3C
HN
16
H3C
HN
17
H3C
HN

Figure 5.

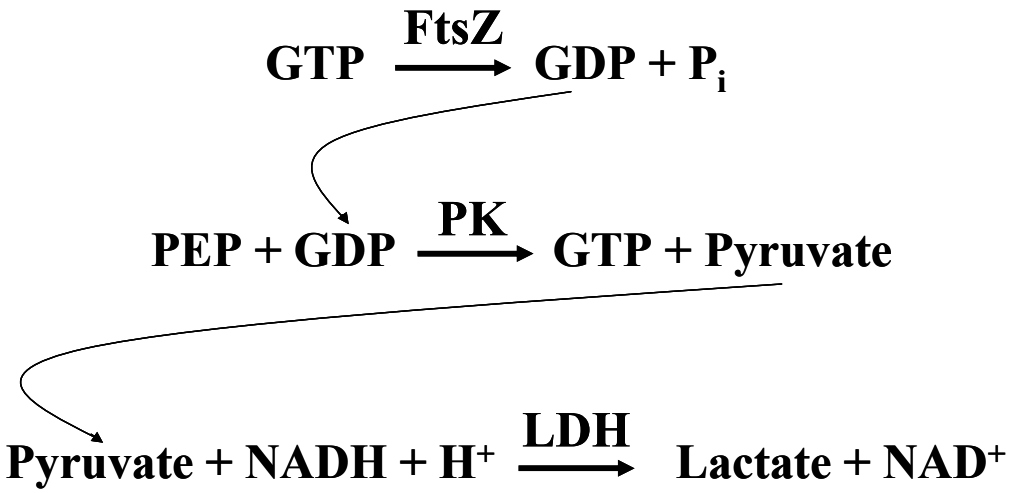
GTP
FtsZ
GDP + P_i
PEP + GDP
PK
GTP + Pyruvate
Pyruvate + NADH + H^+
LDH
Lactate + NAD^+

Figure 6.

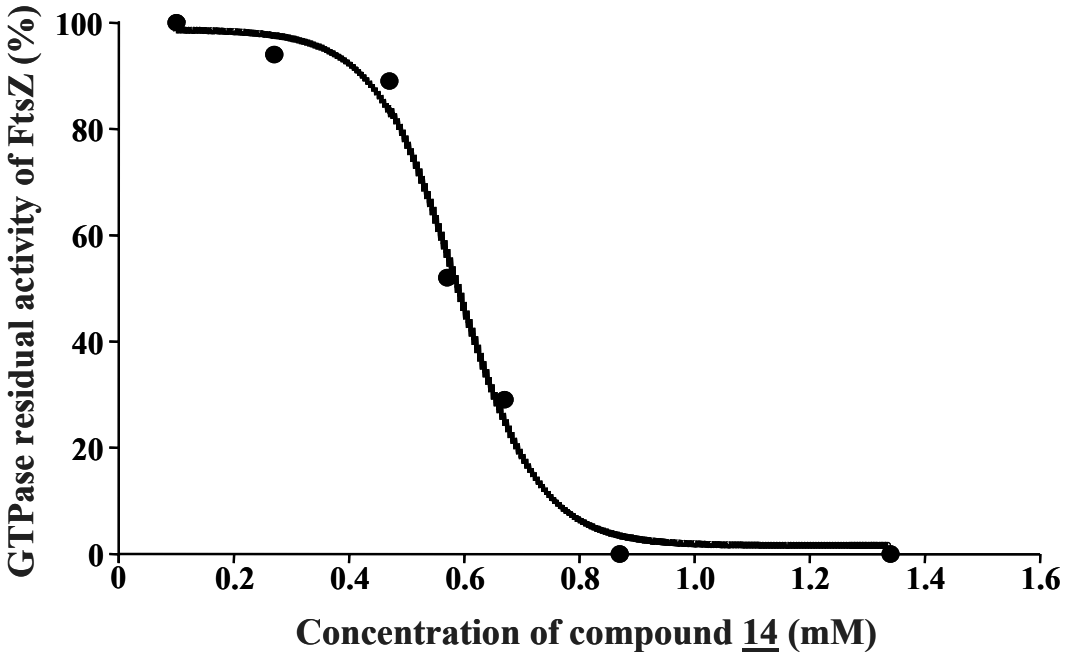
GTPase residual activity of FtsZ (%)
100
80
60
40
20
0
0
0.2
0.4
0.6
0.8
1.0
1.2
1.4
1.6
Concentration of compound 14 (mM)

Figure 7.

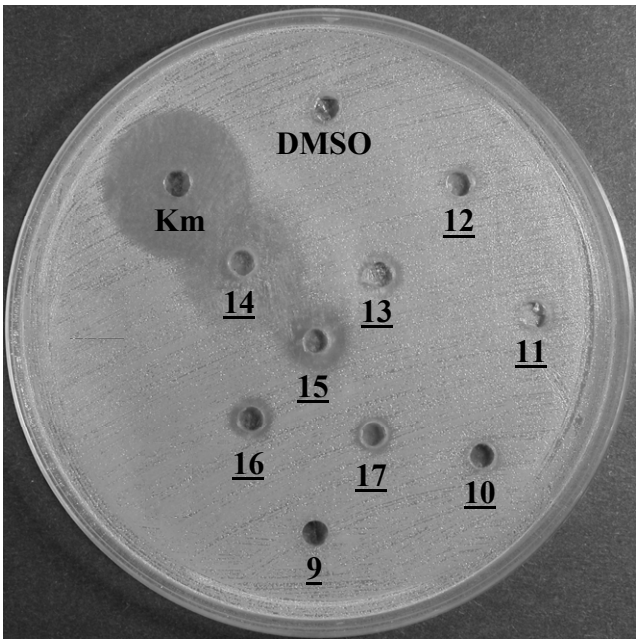

.

Chapitre 3 - Peptide Inhibitors of the Essential Cell Division Protein FtsA

Résumé

Sélection de peptides inhibiteurs de la protéine FtsA essentielle à la division cellulaire bactérienne

La problématique de résistance aux antibiotiques représente un fléau inquiétant qui touche toutes les espèces bactériennes d'importance médicale dont le pathogène opportuniste *P. aeruginosa*. Dans le but d'identifier de nouveaux agents antimicrobiens, nous utilisons la machinerie de division cellulaire bactérienne en tant que cible. La protéine de division cellulaire FtsA de *P. aeruginosa* a été sélectionnée comme l'une des meilleures cibles antibactériennes car elle est essentielle et hautement conservée. Le gène *ftsA* a tout d'abord été cloné et la protéine biologiquement active a été obtenue par renaturation des corps d'inclusion purifiés. Le séquençage en N-terminal a confirmé l'identité de FtsA et un essai de chromatographie sur couche mince a confirmé l'activité enzymatique de FtsA. Un essai de fixation à l'UV a également démontré que FtsA lie préférentiellement l'ATP parmi les 4 nucléotides. L'enzyme purifiée a été utilisée pour cribler des banques de peptides avec la technique de présentation phagique. La spécificité du criblage a été maximisée en effectuant 3 rondes de biocriblage et en optimisant le contact peptide-enzyme via les paramètres de temps et de lavage. Les phages possédant une affinité spécifique pour FtsA ont été élués avec de la glycine à pH acide, de l'ATP, un analogue non-hydrolysable de l'ATP et avec FtsZ. La spécificité de l'interaction entre les peptides sélectionnés et FtsA a été évaluée par ELISA. Les quatre peptides les plus affins et les deux consensus peptidiques sélectionnés contre FtsA ont été synthétisés et testés sur l'activité ATPase de FtsA. Cinq de ces six peptides inhibent spécifiquement l'activité ATPase de FtsA avec des valeurs de CI_{50} entre 0.7 mM et 35 mM. Le sixième peptide pourrait inhiber l'interaction entre FtsA et FtsZ étant donné qu'il a été sélectionné par une élution compétitive avec FtsZ. Ainsi, la technique de présentation phagique a permis la découverte de peptides inhibiteurs prometteurs et des études de peptidomimétisme devraient permettre le développement d'une nouvelle classe d'agents antibactériens.

Contribution des auteurs

Cet article scientifique publié dans la revue «Protein Engineering Design and Selection» en mars 2005 comporte trois auteurs. En tant que première auteure, j'ai réalisé l'ensemble des expériences décrites, j'ai analysé les résultats, j'ai préparé les figures et tableaux et puis j'ai entièrement rédigé le manuscrit. J'ai également participé à l'étude en proposant des alternatives afin de purifier la protéine FtsA biologiquement active à partir des corps d'inclusion. Finalement, j'ai aidé à orienter le projet en proposant de vérifier l'affinité des peptides obtenus par présentation phagique afin de guider le choix des peptides à synthétiser en tant qu'inhibiteurs potentiels de FtsA. Quant au Dr François Sanschagrin, il m'a guidée et supportée périodiquement au laboratoire. Le Dr Roger C. Levesque est à l'origine de l'idée de départ et de la conceptualisation du projet de recherche. Le Dr Levesque m'a fournit un environnement de travail propice à la réussite et il a judicieusement sélectionné la méthodologie de présentation phagique. Finalement, Dr Levesque a corrigé le manuscrit pour en augmenter la qualité de l'anglais ainsi que la valeur scientifique.

Peptide Inhibitors of the Essential Cell Division Protein FtsA

Catherine Paradis-Bleau, François Sanschagrin and Roger C. Levesque*

Département de Biologie Médicale, Université Laval, Sainte-Foy, Québec, G1K 7P4, Canada.

Running Title: FtsA Peptide Inhibitors

Keywords: FtsA/FtsZ/inhibitory peptides/phage display/*Pseudomonas aeruginosa*

*To whom correspondence should be addressed.

Centre de recherche sur la fonction, structure et ingénierie des protéines

Faculté de médecine, pavillon Charles-Eugène-Marchand, Université Laval

Sainte-Foy, Québec, Canada, G1K 7P4

Tel: (1) (418) 656-3070

Fax: (1) (418) 656-7176

E-mail: rclevesq@rsvs.ulaval.ca

Abstract

The revolutionary era of antibiotics has been overwhelmed by the evolutionary capacity of microorganisms such as *Pseudomonas aeruginosa* to develop resistance to all classes of antibiotics. In the perspective of identifying new antimicrobials using novel strategies, we targeted the essential and highly conserved FtsA protein from the bacterial cell division machinery of *P. aeruginosa*. In a series of experiments we cloned, overproduced and purified the FtsA and FtsZ proteins. Expression of FtsA into *Escherichia coli* cells led to its accumulation in inclusion bodies. We developed a protocol permitting the purification and refolding of enzymatically active FtsA hydrolysing ATP. The purified enzyme was used to screen for peptide inhibitors of ATPase activity using phage display. Selective biopanning assays were done and phages were eluted using ATP, a non-hydrolysable ATP analogue and the protein FtsZ known to interact with FtsA in the divisome during the process of bacterial cell division. We identified two consensus peptide sequences interacting with FtsA and a competitive ELISA was used to identify peptides having high affinity for the target protein. Five of the six peptides synthesized showed specific inhibition of ATPase activity of FtsA with IC_{50} values between 0.7 and 35 mM. Discovery of peptides inhibiting the essential cell division machinery in bacteria is the first step for the future development of antimicrobial agents via peptidomimetism.

Introduction

The alarming increase and spread of resistance among emerging and re-emerging bacterial pathogens to all clinically useful antibiotics is one of the most serious public health problems of the last decade (Cohen, 2000; Fauci, 2001; Normark and Normark, 2002). This critical situation necessitates the design of novel classes of antibacterial agents having new modes of action against essential and novel bacterial targets.

Recent developments in genomics, proteomics and bio-informatics coupled to bacterial genetics facilitates the identification of novel essential genes and their products as antibacterial targets (Breithaupt, 1999; Projan, 2002). The perfect bacterial target should be essential for bacterial survival, highly conserved in bacterial evolution but absent in the

animal kingdom, easily accessible for genetic manipulations and sufficiently expressed during the infection of the host. We selected the prokaryotic cell division machinery to identify attractive new targets because they encode essential proteins leading to a lethal phenotype when inhibited. These proteins are highly conserved in bacterial species but absent in eukaryotic cells. They are extremely sensitive to inhibition because the division process depends on recruitment of specific proteins in an absolutely essential cascade forming the divisome (Dai and Lutkenhaus, 1992; Projan, 2002; Errington *et al*., 2003). To our knowledge, the intrinsic cell division inhibitors MinC (Errington *et al*., 2003) and SulA (Cordell *et al*., 2003) which constitute active regulators of this physiological process do not select resistance. Among bacterial division proteins, we chose FtsA as a specific target. This highly conserved protein (van den Ent *et al*., 2001) presumably constitutes a key bacterial component because of its essential protein–protein interaction with FtsZ and its ATPase enzymatic activity (Errington *et al*., 2003) that can be exploited to screen and analyse inhibitory molecules.

The FtsZ protein is at the top of hierarchical recruitment in the divisome and its polymerization into the Z-ring allows the physical separation of daughter cells (Lutkenhaus and Addinall, 1997). The localization of FtsA follows the mid cell accumulation of FtsZ and is essential for protein recruitment in the divisome (Pichoff and Lutkenhaus, 2002) and for Z-ring constriction (Begg *et al*., 1998). The FtsZ–FtsA protein–protein interaction and the FtsZ:FtsA ratio are crucial for the progress of bacterial cell division (Dai and Lutkenhaus, 1992; Yan *et al*., 2000; Lowe *et al*., 2004). Accumulating evidence suggests that FtsA plays the role of a motor protein in providing energy for constriction by way of its ATPase activity (Nanninga, 1998; Feucht *et al*., 2001; Errington *et al*., 2003). Hence this cytoplasmic enzyme and its protein interactions remain to be fully characterized but can be an elegant tool with the aim of developing antibacterials with novel modes of action.

In order to identify specific inhibitors of FtsA, we used the phage-display technique, which represents a powerful tool for the selection of short peptide ligands having high binding affinities to proteins of interest among a large pool of random peptide permutations (Sidhu, 2000; Christensen *et al*., 2001). This approach has been useful for the detection of various enzyme inhibitors (Hyde-DeRuyscher *et al*., 2000), including the cell division

protein FtsZ (Paradis-Bleau *et al*., 2004) and MurC implicated in the biosynthesis of the bacterial cell wall (El Zoeiby *et al*., 2003).

In this paper, we describe the purification and biochemical characterization of FtsA and FtsZ cell division proteins of *Pseudomonas aeruginosa*. We systematically exploit the use of two different phage display libraries and demonstrate how the design of a strategic biopanning approach can lead to the identification of specific peptide inhibitors. Three rounds of phage display screening led to the identification of clear consensus peptide sequences and high affinity binding peptides presumably active against FtsA. Of six peptides synthesized, five showed a significant and specific inhibition of the ATPase activity of FtsA. In order to obtain promising lead compounds with appropriate pharmacological properties, inhibitory peptides can be chemically modified and their sequences will constitute the core for the synthesis of libraries of peptidomimetic molecules.

Materials and methods

Plasmid construction, bacterial strains, reagents and media

All reagents were purchased from Sigma Aldrich (Oakville, Ontario, Canada) unless indicated otherwise. Restriction endonucleases and T4 ligase were obtained from New England Biolabs (Mississauga, Ontario, Canada). Agarose gel electrophoresis and plasmid DNA preparations were performed according to published procedures (Sambrook *et al*., 1989). Recombinant plasmids containing *P. aeruginosa* PAO1 *ftsZ* and *ftsA* genes were maintained in *Escherichia coli* NovaBlue, *endA1 hsdR17*(r_{K12}^{-} m_{K12}^{+}) *supE44 thi-1 recA1 gyrA96 relA1 lac* [F' $proA^{+}B^{+}$ $lacI^{q}Z\Delta$ *M15*::Tn*10*] prior to protein synthesis in *E. coli* BL21, F^{-} *ompT hsdS*$_B$(r_B^{-} m_B^{-}) *gal dcm* (λDE3) (Novagen, Madison, WI).

Cloning of P.aeruginosa ftsA, ftsZ and DNA sequencing

Polymerase chain reaction (PCR) cloning was used to obtain DNA fragments encoding FtsA and FtsZ proteins and a His-tag at their C-terminus. The *ftsA* insert was amplified from genomic DNA of *P. aeruginosa* PAO1 (70 ng) with primers FtsA–*Nde*I 5'-GTA ATA CAT ATG GCA AGC GTG CAG A-3' and FtsA–*Hin*dIII 5'-TTG AAG CTT AAT TGC CCT GGA CCC-3' in frame with the His-tag changing the two last amino acids N–F for K–L. Amplification of the *ftsZ* insert was done with forward and reverse primers FtsZ–*Nde*I 5'-GGA GAG GGC ATA TGT TTG AAC TGG-3' and FtsZ–*Xho*I 5'-TTA CTT CAC TCG AGC TGA CGA CGC-3' changing the two last amino acids A–D for L–E. PCRs were done with primers at a concentration of 0.1 μM each, dNTPs (Amersham Biosciences, Baie d'Urfe, Québec, Canada) at 0.2 mM each and 2 mM $MgCl_2$. DNA amplification was done using 30 cycles with 2.5 U of Hot Start TAQ polymerase (Qiagen, Mississauga, Ontario, Canada) and annealing at 56.3°C for *ftsA* or with 2.5 U of the Expand High Fidelity TAQ polymerase (Roche Diagnostics, Laval, Québec, Canada) using annealing at 60°C for *ftsZ*. PCR products were digested with appropriate restriction enzymes and cloned into the corresponding sites of the expression vector pET30a for *ftsA* and pET24b (Novagen) for the *ftsZ* insert. The recombinant plasmids pMON2023 encoding *ftsA* and pMON2020 expressing *ftsZ* were electroporated into competent *E. coli* NovaBlue cells. For both plasmids, the insert was completely sequenced for both DNA strands using the universal T7 primers (Novagen).

Overexpression of FtsA

The pMON2023 plasmid was transformed into competent *E. coli* BL21 (λDE3) cells by $CaCl_2$ transformation for expression of FtsA. A bacterial culture of 1.9 l of LB broth (Difco Laboratories, Detroit, MI) supplied with 0.05 g/l of kanamycin was inoculated with an overnight culture of 100 ml of *E. coli* BL21 (λDE3) carrying pMON2023. Cells were incubated at 37°C with agitation at 260 r.p.m. until an optical density (O.D.) of 0.65 at 600 nm. Protein expression was carried out by adding 1 mM of IPTG and incubating for 6 h; cells were centrifuged and the pellets were immediately stored at –80°C.

Purification of inclusion bodies and refolding of FtsA

The bacterial pellet was resuspended in wash buffer from the Protein Refolding Kit (Novagen) as recommended by the manufacturer and treated with lysozyme at 100 μg/ml for 15 min at 30°C. Cells were lysed by sonication for 30 s/ml using a Virsonic Digital 475 ultrasonic cell disrupter (Virtis, Gardiner, NY) and a cocktail of protease inhibitors was immediately added as recommended by the manufacturer (Roche Diagnostics). Disrupted cells were centrifuged for 10 min at 5000 *g*; the pellets were resuspended in wash buffer (Novagen) and centrifuged for 10 min. The pellets were resuspended again, centrifuged for 10 min at 10 000 *g* and stored at –80°C. Solubilization of inclusion bodies was performed by gently resuspending the pellets in solubilization buffer (Novagen) with 0.3% *N*-laurylsarcosine and 0.1% dithiothreithol (DTT) to a final concentration of 5 mg/ml. The suspension was incubated for 30 min, centrifuged for 30 min at 25 000 *g* at room temperature and the supernatant was conserved at 4°C for a maximum of 2 months. Refolding of FtsA was carried by multistep dialysis of solubilized inclusion bodies, first in 75 volumes of dialysis buffer (20 mM Tris–HCl pH 8.5) with 0.1% (v/v) DTT for 4 h at 4°C and overnight at 4°C with fresh buffer. The suspension was then dialysed in 100 volumes of dialysis buffer with 10 mM $MgCl_2$ overnight at 4°C and 5 h at 4°C with fresh buffer. Refolded FtsA protein was visualized by SDS–PAGE with Coomassie Brilliant Blue staining, the concentration was measured by the Bradford method (BioRad, Mississauga, Ontario, Canada) and it was stored at 4°C.

Overexpression and purification of FtsZ

The recombinant plasmid pMON2020 was introduced into competent *E.coli* BL21 (λDE3) cells for expression of FtsZ. Protein expression was carried as described for FtsA except that the culture was induced at an O.D. of 0.8 and incubated for 4 h. Cells were centrifuged and the pellet was resuspended in 3.33 times their weight of sonication buffer (50 mM Tris–HCl pH 8.6 and 2 mM EDTA), treated with lysozyme and lysed by sonication as for FtsA. Cellular debris were removed by centrifugation at 17 000 *g* for 30 min. Recombinant FtsZ protein was purified to homogeneity by affinity chromatography using a His-bind nickel

resin (Novagen) with 150 mM imidazole during elution. Purified FtsZ was dialysed in conservation buffer (20 mM Tris–HCl pH 7.6, 10 mM NaCl and 1 mM EDTA) (Zhulanova and Mikulik, 1998) and conserved in 50% (v/v) glycerol at –80°C.

FtsA and FtsZ N-terminal sequencing

After separation by SDS–PAGE (Sambrook *et al*., 1989), 2 µg each of FtsA and FtsZ protein preparations were transferred on PVDF membrane using a transfer buffer without glycine [10 mM CAPS pH 11 and 10% (v/v) methanol]. The membrane was stained with Ponceau Red and FtsA and FtsZ protein bands were cut out and rinsed with water. N-terminal sequencing was done by the Edman degradation technique at the Biotechnology Research Institute (National Research of Council Canada, Montreal, Québec, Canada).

Biochemical characterization of FtsA and FtsZ

The ATPase and GTPase enzymatic activities of FtsA and FtsZ were confirmed using a thin-layer chromatographic (TLC) assay with ^{32}P-labelled nucleotides as substrates. The FtsA ATPase assay was done using 4 µM renatured FtsA in reaction buffer A (50 mM Tris–HCl pH 7.2, 50 mM potassium acetate, 10 mM $MgCl_2$ and 1 mM DTT) (Feucht *et al*., 2001) and 1 µl of 10 µCi/µl [^{32}P]ATP (PerkinElmer, Woodbridge, Ontario, Canada) in a final volume of 20 µl. The FtsZ GTPase assay was performed using 12 µM FtsZ in reaction buffer Z (Paradis-Bleau *et al*., 2004) and 1 µl of 10 µCi/µl [^{32}P]GTP (PerkinElmer) in a final volume of 20 µl. The mixtures were incubated for 2 and 1 h, respectively, at 37°C and 2 µl of each sample were deposited on a TLC plate along with negative controls (without enzyme). Hydrolysis of radioactive substrates was measured by autoradiography using a Phosphorimager (Fuji, Stanford, CA). A UV cross-link specific nucleotide-binding assay was performed with FtsA and FtsZ against the four radioactive nucleotides. Amounts of 3 µg of FtsA or FtsZ protein were mixed with each of the four ^{32}P-labelled nucleotides (PerkinElmer) and the UV cross-link assay was carried out as described (Feucht *et al*., 2001). Briefly, the samples were incubated for 30 min at 0°C and irradiated for 10 min at 254 nm in wells of a microtitre plate on top of a chilled lead brick in iced water. The protein

samples were then purified prior to analysis by SDS–PAGE and visualized by autoradiography.

Gel filtration of FtsA

To improve the purity of the inclusion body purified FtsA, an aliquot was analysed by gel filtration chromatography. A refolded FtsA sample was first concentrated five times with a stirred ultrafiltration cell using an ultrafiltration membrane with a cut-off of 10 kDa (Millipore, Bedford, MA, USA). A 200 µl volume of concentrated FtsA was injected onto an analytical Tricorn Superdex 75 column (Amersham Biosciences) equilibrated with buffer A and elution was performed with buffer A at a flow rate of 0.8 ml/min. Collected fractions were analysed by SDS–PAGE with SYPRO Orange staining (BioRad) and tested for ATPase activity as described. Molecular standards (LMW Gel Filtration Calibration Kit, Amersham Biosciences) were applied to the column under the same conditions to determine the molecular weight of eluted peaks.

Affinity selection of phage displayed peptides against FtsA

Phage display screening was carried out with the PH.D.-12 and PH.D.-C-7-C phage libraries (New England Biolabs) containing ~2.7 x 10^9 12 mers and ~3.7 x 10^9 C-7-C mers random peptide sequences. Specificity during the three rounds of biopanning was obtained by increasing the stringency of the washes and decreasing the time of contact between the peptides and the target protein as described (El Zoeiby *et al*., 2003), but using the following modifications. The second- and third-round phage inputs were calculated as 2 x 10^{11} phages for each library. Phages adsorbed on FtsA at the third round of biopanning were eluted by non-specific disruption of binding interactions using glycine and by a competitive elution using 100 µl of 1 mM ATP, with 100 µl of 1 mM 5'-adenylylimidodiphosphate (a non-hydrolysable analogue of ATP) and with 100 µl of 1 mM FtsZ.

Phage DNA preparation and sequencing

The M13 DNA purification and sequencing were done as described (El Zoeiby *et al*., 2003) except that 12 phages were sequenced for each of the two phage libraries eluted using four sets of elution conditions.

Affinity ELISA

This experiment was adapted from Carettoni *et al*. (2003). Briefly, 150 µl of FtsA (100 µg/ml) was adsorbed overnight at 4°C on Ni-NTA strips (Qiagen) along with BSA as a control. The strips were washed four times with TBS (50 mM Tris–HCl pH 7.5, 150 mM NaCl) and blocked with BSA for 1 h at room temperature. After a brief wash, 2×10^9 plaque-forming units (pfus) per well of each amplified phage samples were incubated in triplicate for 1 h in FtsA-coated wells. TBS was added in triplicate to BSA-coated wells to evaluate non-specific signal. The strips were washed six times with TBS 1% Triton, twice for 10 min and six times again. A 150 µl amount of biotin-labelled anti-fd rabbit polyclonal antibodies diluted 1:2500 in TBS 1% Triton was incubated for 1 h at room temperature. After four washes, 150 µl of 1 µg/ml HRP-labelled streptavidin (Roche Diagnostics) were added to the strips for 30 min at room temperature and the excess was removed with four washes. The strips were incubated for 20 min with 100 µl of ABTS (Roche Diagnostics) and the results were analysed at an O.D. of 405 nm. The results were an average from triplicates and the BSA non-specific signal was subtracted from all values. Specific affinity ratios for phages from the third round of biopanning were determined by dividing the value by the non-specific control phage value.

Selection and synthesis of peptides

Specific peptides were synthesized on an ABI 433A Peptide Synthesizer using FastMoc chemistry (El Zoeiby *et al*., 2003) from the consensus peptide sequences and high-affinity peptides were identified.

FtsA inhibitory enzymatic assay

The inhibitory capacities of the synthesized peptides were determined by preincubating FtsA in buffer A lacking DTT with various concentrations of peptide buffered solutions for 20 min at room temperature. ^{32}P-labelled ATP was then added and mixtures were immediately incubated for 2 h at 37°C. Each sample was separated by TLC along with positive and negative controls and the 50% inhibitory concentrations (IC_{50}s) of peptides were calculated (Paradis-Bleau *et al*., 2004). As controls, non-specific peptides were tested for inhibition of the ATPase activity of FtsA and a competitive assay was done with casein at 10 times the enzyme concentration. The non-specific peptides were a circular C-7-C mer that had previously been shown to inhibit L-1 ß-lactamase and a 12 mer known to bind to the herpes virus capsid (Sanschagrin and Levesque, 2005). The reducing DTT effect was analysed by evaluating the peptide inhibition with 10 mM DTT.

Results

Purification of P. aeruginosa FtsA and FtsZ

The expressed FtsA protein was detected solely in inclusion bodies and FtsZ was found in the soluble cytoplasmic fraction. The renaturation of purified inclusion bodies containing the 42.6 kDa FtsA at >99% homogeneity (Figure 1) gave a yield of 2.5 mg of FtsA from 1 l of *E. coli* cell culture. Gel filtration chromatography improved the purity of the inclusion body purified FtsA since elution gave a single significant peak with a molecular weight corresponding to FtsA dimer of 85.2 kDa and three trace peaks eluted after one column volume. SDS–PAGE analysis of the collected fractions showed that the principal peak contains a single protein of 42.6 kDa and that the three minor peaks contain no protein detected by the sensitive SYPRO Orange staining (data not shown). The nickel affinity chromatography permitted the purification of FtsZ with a yield of 20 mg/l. The N-terminal sequencing of the first 15 amino acid residues confirmed the nature of both proteins (100% identity with published sequences in both cases).

Characterization of FtsA and FtsZ ATPase and GTPase activities

As depicted in Figure 2A, analysis by autoradiography showed that 4 μM FtsA hydrolysed 85% of ATP, giving as substrates 8% ADP, 3.4% AMP and 73.6% inorganic phosphate, after 2 h at 37°C. The ATPase assay was also performed on fractions obtained from gel filtration by FPLC. A single significant peak obtained corresponding to the expected FtsA size on SDS–PAGE had ATPase activity (data not shown, but available upon request). The FtsZ enzyme used at 12 μM hydrolysed 85% of GTP to GDP after 1 h at 37°C. These data confirmed that both enzymes were active and that FtsA was properly refolded. To determine the nucleotide substrate specificity for each enzyme, a UV cross-link binding assay was performed and autoradiography confirmed that FtsA binds preferentially ATP (Figure 2B) and that FtsZ binds preferentially GTP among the four radioactive nucleotides tested as substrates.

Affinity selection of FtsA binding peptides

After the third round of biopanning and depending on the type of elution strategy utilized, the DNA sequencing of randomly selected phages identified a variety of peptide sequences (Figure 1 in the Supplementary data available at *PEDS* Online). The analysis of the frequency of phage recovery revealed a consensus peptide sequence for each library that both contained a P-S-P motif (Table I). The 12 mer consensus sequence was the only peptide sequence recovered when using FtsZ as a biopanning competitor against FtsA (Figure 1 in the Supplementary material). A FASTA search was carried out with each peptide reported in Figure 1 in the Supplementary material but no homologous proteins were identified in databases.

Affinity ELISA for binding specificity

The relative affinity of peptides expressed from phages selected randomly was evaluated by ELISA to identify the best binding peptide sequences. The relative affinity ratios defined as the value of specific binding phage divided by the value of non-specific binding phage

varied from 2.7 to 43.1 (Table I). For example, a 43.1 relative affinity ratio indicated that the specific phage had 43.1 times more affinity for the target FtsA protein compared with the binding of random peptides. We noted that the frequency of peptide recovery did not correlate with the values of affinity ratios (Table I). The average ratio of the 12 mer phage expressed peptides was 25 ± 14 and was significantly higher than the C-7-C mer mean ratio of 11 ± 6. An interesting fact is that the two best binding peptides with relative affinity ratios of 43.1 and 42.4 have the same G-P-H conserved motif at their N-termini and ended with a P. The second and third strongest binding peptides with ratio values of 42.4 and 32 contained a G-M motif at their centre and ended with an R-P motif (Table I). We noted also that the two C-7-C mer peptide sequences with the highest ratio values 16.0 and 23.3 have a W-A motif (Table I). We noted that the 12 mer and C-7-C mer lowest binding peptide sequences were identified when using the non-hydrolysable analogue 5'-adenylylimidodiphosphate in the biopanning. Indeed, elution at the biopanning step with glycine, ATP and FtsZ gave phage expressing peptides with similar affinity ratio values; although the best binding peptides came from the glycine and ATP (Table I, and Figure 1 in the Supplementary data).

Selection and synthesis of peptides

To establish the inhibitory capacity of selected peptides against the ATPase activity of FtsA, peptide sequences were chosen on the basis of their frequency of recovery and their relative affinity ratios. Indeed, the two consensus peptides were synthesized along with the two peptides having the highest relative affinity values from each phage library (Table I).

Inhibition of FtsA ATPase activity

Of the six peptides synthesized, five inhibited the ATPase activity of FtsA and had IC_{50} values between 0.7 and 35 mM (Table I). The C-7-C mer consensus peptide FtsAp1 gave an IC_{50} value of 22 mM but the 12 mer consensus peptide FtsAp2 did not inhibit the enzymatic activity of FtsA. The 12 mer peptide with the highest relative affinity ratios, FtsAp3 and FtsAp4, gave IC_{50} values of 0.7 (Figure 3) and 25 mM, respectively. The C-7-C

mer peptides FtsAp5 and FtsAp6 had IC_{50} values of 2.5 and 35 mM, respectively. Competitive rescue assays using BSA gave identical IC_{50} values (data not shown). The reducing agent DTT had no effect on the inhibitory capacity of FtsAp3, FtsAp4 and FtsAp5. The C-7-C mer FtsAp1 lost 20% of its inhibitory capacity when DTT was added to the reaction and the C-7-C mer peptide FtsAp6 was affected by DTT as its inhibitory potential was raised by a factor of 1.5. The IC_{50} value of FtsAp6 was 52 mM without DTT and 35 mM with DTT. Analysis of FtsA activity using random peptides at high concentrations showed that the reaction rate was not reduced by the peptides (data not shown), indicating that the ATPase activity of FtsA was not inhibited by non-specific C-7-C mer or 12 mer peptides.

Discussion

There has been growing interest in identifying new bacterial targets from essential mechanisms (Breithaupt, 1999) such as cell division (Wang *et al*., 2003; Jennings *et al*., 2004; Margalit *et al*., 2004; Paradis-Bleau *et al*., 2004). In this work, we selected specific peptide inhibitors of the highly conserved and essential cell division protein FtsA (Feucht *et al*., 2001).

The purification of biologically active FtsA was a challenge because this protein accumulates in inclusion bodies. We developed a multi-step solubilization and renaturation protocol coupled with gel filtration that may be useful for any insoluble protein when taking into account the presence of disulfide bonds and the cofactor or stabilizing molecule.

The ATPase activity of FtsA has been demonstrated (Feucht *et al*., 2001) but we are the first to show that FtsA hydrolyses ATP to ADP, AMP and inorganic phosphate (Figure 2A). To confirm that ATPase activity is not due to traces of a contaminating ATPase, the inclusion body containing FtsA was separated by gel filtration chromatography and ATPase activity was determined for eluted fractions. The unique FtsA peak obtained had ATPase activity.

Our results support the hypothetical role of FtsA as a motor protein in providing energy for the Z-ring constriction via ATP (Feucht *et al*., 2001) and that FtsZ utilizes GTP

(Diaz *et al*., 2001). We showed that FtsA binds preferentially ATP amongst the four nucleotides and confirmed the native dimer nature of FtsA (Feucht *et al*., 2001).

We noted that the non-specific disruption of phage interactions with glycine, the allosteric competition by FtsZ and the active site competition by ATP and non-hydrolysable analogue gave different peptide sequences binding FtsA. This confirmed the validity of using different elution conditions to obtain a variety of peptide sequences interacting with diverse sites on the target protein. We hypothesize that the FtsA nucleotide binding site is functionally related to the FtsZ interaction site(s) as the ATP binding and/or hydrolysis may lead to a conformational change that could affect the FtsZ interaction site(s) or vice versa. Indeed, ATP elution could yield phage encoded peptides binding to the nucleotide binding site and to the FtsZ interaction site(s).

We did not find peptide homologues in databases but we assumed that peptide sequences have conformational homology with cell division proteins interacting with FtsA as FtsA itself, FtsZ, PBP3, FtsQ or FtsN (Yim *et al*., 2000; Di Lallo *et al*., 2003). FtsA binds to the conserved consensus sequence LD**XPX**FOR/**K** (O, hydrophobic residue; X, any residue) at the C-terminus of FtsZ (Yan *et al*., 2000; Haney *et al*., 2001). We noted that the perfect 12 mer consensus sequence selected by the FtsZ elution contained a **KPS**P**R** motif and the C-7-C mer consensus sequence had a **APS**PS**K** motif sharing homology with the interaction site of FtsZ indicated in bold.

Anderluzzi's group recently reported a phage display using *E.coli* FtsA against the PH.D.-7 library and a single glycine elution (Carettoni *et al*., 2003). There is no redundancy between the two phage display screenings since different phage libraries were used. The inhibitory potential of some selected 7 mer peptides needs to be determined.

ELISA showed that the 12 mer peptides bind more tightly to the scattered and elongated structure of FtsA (van den Ent and Lowe, 2000) than the C-7-C mer peptides, requiring less space since C residues constrain the peptide in a disulfide loop. We noted that elution with non-hydrolysable ATP analogue gave peptides with the lowest binding affinities. Hence this artificial molecule presumably binds less tightly to FtsA. Conserved motifs identified in peptides having the highest affinity ratios must be important for binding to FtsA. We noted that the relative affinity values did not correlate with the frequency of phage recovery. Apart from the binding affinity, several factors such as phage infection and

replication efficiency, protein translocation and folding bias, pIII coat stability and retained phages will affect phage recovery (Carettoni *et al*., 2003). Furthermore, phages with very high binding properties cannot be recovered with the mild elution conditions used to preserved phage particle integrity (Hoess, 2001).

The inhibitory capacity of peptide against the FtsA ATPase activity was evaluated for consensus peptides and the two peptides having the highest relative affinity ratios for each phage library (Table I). Five synthesized peptides were able to inhibit ATPase activity of FtsA. DTT had no effect on the inhibitory capacity of 12 mer peptides; the three C-7-C mer inhibitory peptides reacted differently to the reducing agent. FtsAp1 partially lost its inhibitory capacity, indicating that the disulfide loop was important for inhibition of FtsA. In contrast, the loop conformation of FtsAp5 was not essential for inhibition since DTT did not change the IC_{50} value. FtsAp6 gave a higher inhibition value with DDT, suggesting that this peptide was more active in the linear monomeric form.

The perfect 12 mer consensus peptide eluted with FtsZ (Figure 1 in the Supplementary data) could bind into a FtsA allosteric site. The corresponding peptide FtsAp2 having the **KPS**P**R** motif homologous with the FtsA interaction site of FtsZ was the only one that did not inhibit ATPase activity. We assume that it could be an inhibitor of the essential FtsA–FtsZ interaction that represented a more sensitive and specific target than the ATPase activity of FtsA alone (Yan *et al*., 2000; Haney *et al*., 2001). The C-7-C mer FtsAp1 with a **APS**PS**K** motif had homology with the conserved C-terminal interaction site of FtsZ and showed inhibition of FtsA. FtsAp1 could inhibit ATPase activity of FtsA due to binding to an FtsZ interacting site. The FtsA allosteric site(s) binding FtsZ could regulate the enzymatic activity even if FtsA binds and hydrolyses ATP without FtsZ. It as already been hypothesized that FtsZ interaction may change the FtsA conformation and enhance ATP hydrolysis (van den Ent and Lowe, 2000). This may regulate the ATPase motor force required for the Z-ring constriction.

Peptide IC_{50} values did not correlate with the frequency of phage recovery, with the relative affinity ratio values or with the phage library (Table I). The inhibitory capacity depends primarily on localization of the peptide interaction with the target protein and secondarily on the affinity strength.

Characterizing the specificity and inhibition mechanism of five peptides identified will be essential as kinetic analysis did not reveal a general trend in peptide inhibitory mechanisms (Hyde-DeRuyscher *et al*., 2000). To obtain promising lead compounds, inhibitory peptides will undergo chemical modifications; this will constitute the core for the synthesis of peptidomimetic molecules (Nefzi *et al*., 1998; Bursavich and Rich, 2002). Inhibition of FtsA in Gram-negative bacteria needs to be studied since ZipA absent in Gram-positive bacteria share overlapping functions with FtsA (Pichoff and Lutkenhaus, 2002; Geissler *et al*., 2003; Lowe *et al*., 2004).

Acknowledgments

We express our gratitude to Le Service de Séquence de Peptides de l'Est du Québec and Le Service d'Analyse et de Synthèse d'Acides Nucléiques de l'Université Laval. This work was funded by the Canadian Bacterial Diseases Network via the Canadian Centers of Excellence, an FCAR infrastructure team grant to R.C. Levesque and a CRSNG studentship to Catherine Paradis-Bleau.

References

Begg,K., Nikolaichik,Y., Crossland,N. and Donachie,W.D. (1998) *J. Bacteriol.*, **180**, 881–884.

Breithaupt,H. (1999) *Nat. Biotechnol.*, **17**, 1165–1169.

Bursavich,M.G. and Rich,D.H. (2002) *J. Med. Chem.*, **45**, 541–558.

Carettoni,D., Gomez-Puertas,P., Yim,L., Mingorance,J., Massidda,O., Vicente,M., Valencia,A., Domenici,E. and Anderluzzi,D. (2003) *Proteins*, **50**, 192–206.

Christensen,D.J., Gottlin,E.B., Benson,R.E. and Hamilton,P.T. (2001) *Drug Discov. Today*, **6**, 721–727.

Cohen,M.L. (2000) *Nature*, **406**, 762–767.

Cordell,S.C., Robinson,E.J. and Lowe,J. (2003) *Proc. Natl Acad. Sci. USA*, **100**, 7889–7894.

Dai,K. and Lutkenhaus,J. (1992) *J. Bacteriol.*, **174**, 6145–6151.

Diaz,J.F., Kralicek,A., Mingorance,J., Palacios,J.M., Vicente,M. and Andreu,J.M. (2001) *J. Biol. Chem.*, **276**, 17307–17315.

Di Lallo,G., Fagioli,M., Barionovi,D., Ghelardini,P. and Paolozzi,L. (2003) *Microbiology*, **149**, 3353–3359.

El Zoeiby,A., Sanschagrin,F., Darveau,A., Brisson,J.R. and Levesque,R.C. (2003) *J. Antimicrob. Chemother.*, **51**, 531–543.

Errington,J., Daniel,R.A. and Scheffers,D.J. (2003) *Microbiol. Mol. Biol. Rev.*, **67**, 52–65.
Fauci,A.S. (2001) *Clin. Infect. Dis.*, **32**, 675–685.
Feucht,A., Lucet,I., Yudkin,M.D. and Errington,J. (2001) *Mol. Microbiol.*, **40**, 115–125.
Geissler,B., Elraheb,D. and Margolin,W. (2003) *Proc. Natl Acad. Sci. USA*, **100**, 4197–4202.
Haney,S.A., Glasfeld,E., Hale,C., Keeney,D., He,Z. and de Boer,P. (2001) *J. Biol. Chem.*, **276**, 11980–11987.
Hoess,R.H. (2001) *Chem. Rev.*, **101**, 3205–3218.
Hyde-DeRuyscher,R. *et al*. (2000) *Chem. Biol.*, **7**, 17–25.
Jennings,L.D. *et al*. (2004) *Bioorg. Med. Chem. Lett.*, **14**, 1427–1431.
Lowe,J., van den Ent,F. and Amos,L.A. (2004) *Annu. Rev. Biophys. Biomol. Struct.*, **33**, 177–198.
Lutkenhaus,J. and Addinall,S.G. (1997) *Annu. Rev. Biochem.*, **66**, 93–116.
Margalit,D.N., Romberg,L., Mets,R.B., Hebert,A.M., Mitchison,T.J., Kirschner,M.W. and RayChaudhuri,D. (2004) *Proc. Natl Acad. Sci. USA*, **101**, 11821–11826.
Nanninga,N. (1998) *Microbiol. Mol. Biol. Rev.*, **62**, 110–129.
Nefzi,A., Dooley,C., Ostresh,J.M. and Houghten,R.A. (1998) *Bioorg. Med. Chem. Lett.*, **8**, 2273–2278.
Normark,B.H. and Normark,S. (2002) *J. Intern. Med.*, **252**, 91–106.
Paradis-Bleau,C., Sanschagrin,F. and Levesque,R.C. (2004) *J. Antimicrob. Chemother.*, **54**, 278–280.
Pichoff,S. and Lutkenhaus,J. (2002) *EMBO J.*, **21**, 685–693.
Projan,S.J. (2002) *Curr. Opin. Pharmacol.*, **2**, 513–522.
Sambrook,J., Fritsch,E.F. and Maniatis,T. (1989) *Molecular Cloning. A Laboratory Manual*, 2nd ed. Cold Spring Harbor Laboratory Press, Cold Spring Harbor, NY.
Sanschagrin,F. and Levesque,R.C. (2005) *J. Antimicrob. Chemother.*, **55**, 252–255.
Sidhu,S.S. (2000) *Curr. Opin. Biotechnol.*, **11**, 610–616.
van den Ent,F. and Lowe,J. (2000) *EMBO J.*, **19**, 5300–5307.
van den Ent,F., Amos,L. and Lowe,J. (2001) *Curr. Opin. Microbiol.*, **4**, 634–638.
Wang,J. *et al*. (2003) *J. Biol. Chem.*, **278**, 44424–44428.
Yan,K., Pearce,K.H. and Payne,D.J. (2000) *Biochem. Biophys. Res. Commun.*, **270**, 387–392.
Yim,L., Vandenbussche,G., Mingorance,J., Rueda,S., Casanova,M., Ruysschaert,J.M. and Vicente,M. (2000) *J. Bacteriol.*, **182**, 6366–6373.
Zhulanova,E. and Mikulik,K. (1998) *Biochem. Biophys. Res. Commun.*, **249**, 556–561.

Legends to figures

Figure 1. SDS–PAGE showing the homogeneity purified protein FtsA expressed in *E.coli* BL21 (λDE3) cells.

Figure 2. (**A**) Autoradiogram of TLC demonstrating enzymatic activity of ATPase FtsA. Lanes: 1, negative control without enzyme; 2, hydrolysis of ATP to ADP, AMP and P_i. (**B**) UV cross-link specific nucleotide binding assay showing that FtsA binds preferentially ATP among the four radioactive nucleotides used as substrates.

Figure 3. IC_{50} determination for the FtsAp3 peptide inhibitor of FtsA ATPase activity.

Figure 1 (Supplementary data). Peptide sequences of the Ph.D.-12 and Ph.D.-C-7-C phage libraries obtained against FtsA after sequencing 92 eluted phages selected as described in Materials and methods. Acidic amino acids (D, E) are in green, polar amino acids (Q, N) are in light green, basic amino acids (K, R, H) are in blue, hydrophobic amino acids (I, L, M, V) are in rose, hydrophobic aromatic amino acids (F, Y, W) are in red, small amino acids (A, S, C, T) are in pink, G (tiny amino acid) is in orange and P (leading to turn formation) is in black (classified according to the Venn diagram for defining the relationships between amino acids).

Table I. Frequency of recovery, ELISA relative affinity ratio and IC_{50} values of selected peptide sequences for ATPase inhibition

12 mer sequence	Frequency of recovery	Ratio	IC_{50} (mM)	C-7-C mer sequence	Frequency of recovery	Ratio	IC_{50} (mM)
S V S V G M K P S P R P[a]	21	32.0	N.D.	C L A P S P S K C[b]	14	3.2	22
F T T S N H T S R H G S	2	26.7		C S S A T G K S C	3	12.9	
T P S L P P T M F R L T	3	17.8		C L G Q T K M R C	2	15.4	
G P H H Y W Y H L R L P[c]	1	43.1	0.7	C G H R P Y Q Y C	3	11.1	
Q S P V N H H Y H Y H I	1	7.7		C W A F P L H H C[d]	1	16.0	2.5
N M T T Y P M H N N T V	1	5.1		C T L N S H S N C	1	12.7	
S L L P H S N H A K H Y	1	31.4		C E I S A K R T C	1	9.4	
E F E Y F H P A T F R L	1	16.5		C H I L H A Q A C	1	2.7	
G P H L G M N Q R R R P[e]	1	42.4	25	C P R P P S L E C	1	4.9	
				C T G H W A S E C[f]	1	23.3	35

[a]12 mer consensus peptide FtsAp2

[b]C-7-C mer consensus peptide FtsAp1

[c]12 mer peptide that had the highest relative affinity ratio value FtsAp3

[d]C-7-C mer peptide that had the second highest relative affinity ratio value FtsAp5

[e]12 mer peptide that had the second highest relative affinity ratio value FtsAp4

[f]C-7-C mer peptide that had the highest relative affinity ratio value FtsAp6

Figure 1

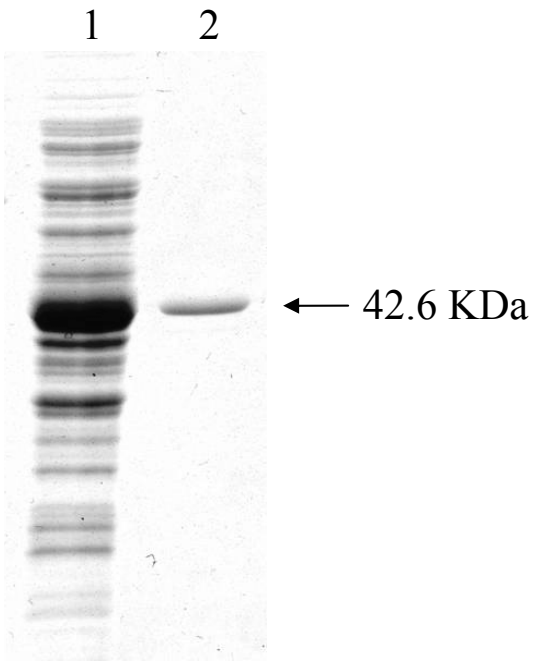

Figure 2

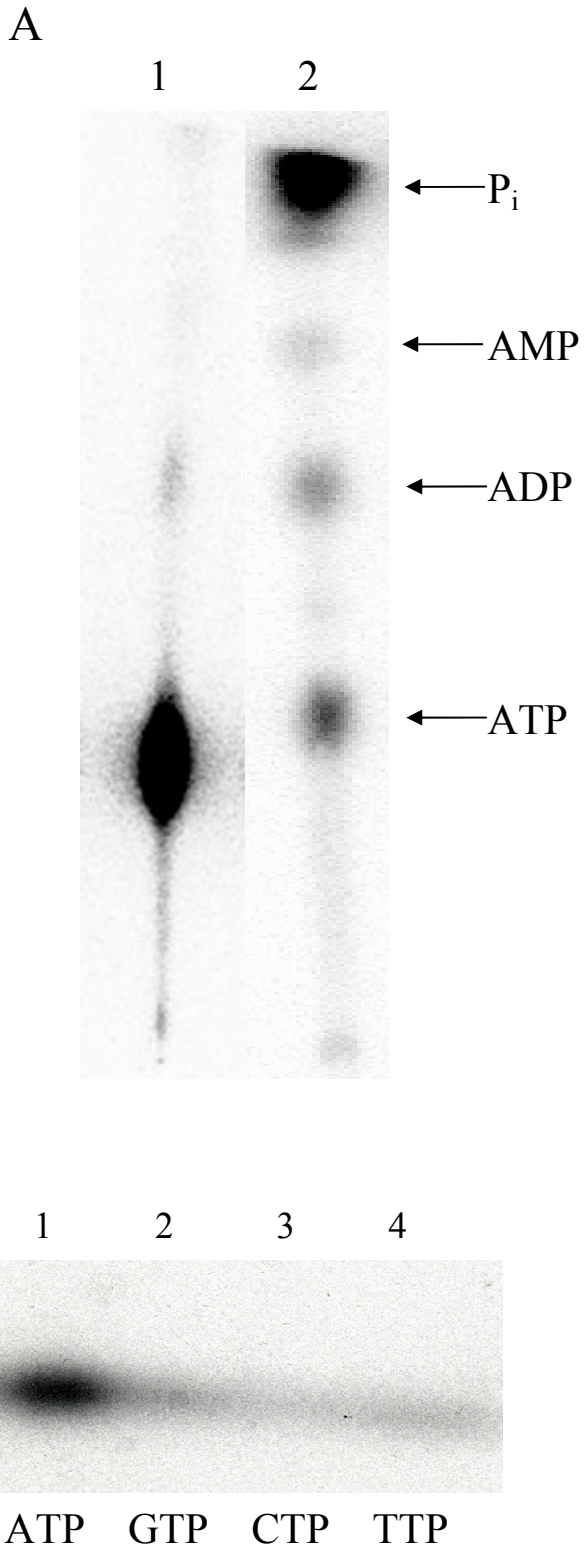

Figure 3

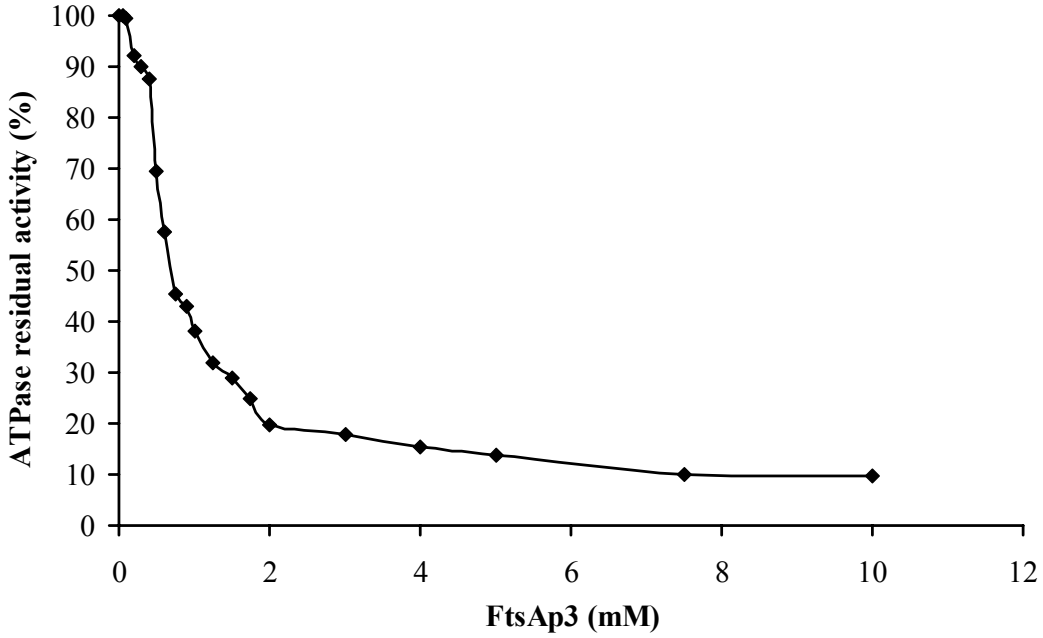
ATPase residual activity (%)
100
90
80
70
60
50
40
30
20
10
0
0
2
4
6
8
10
12
FtsAp3 (mM)

Figure 1 (Supplementary data)

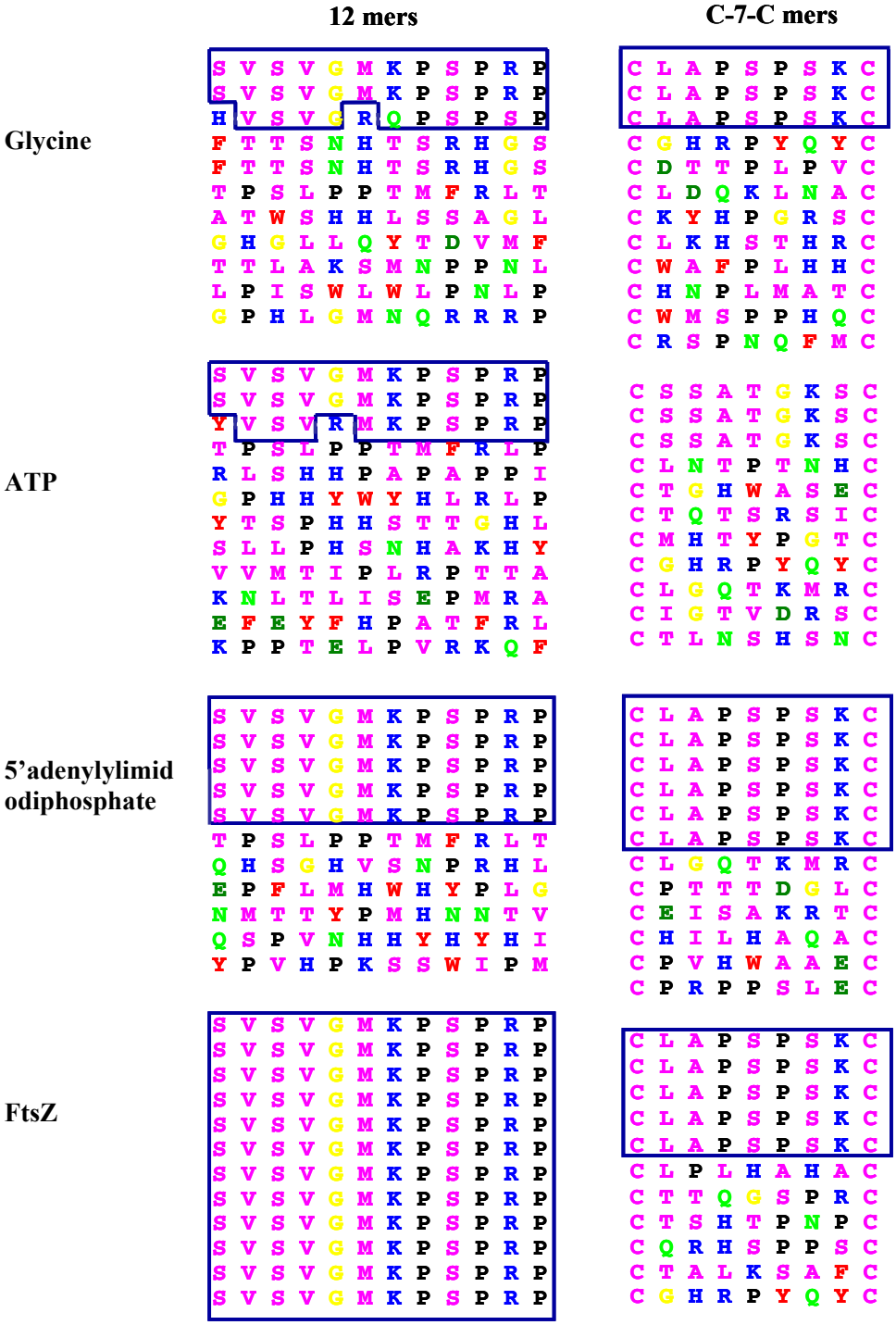

Section III - Les amides ligases MurC, MurD, MurE et MurF en tant que cibles antibactériennes: identification d'inhibiteurs peptidiques ciblant la biosynthèse de la paroi bactérienne

Ce deuxième chapitre du corps de ma thèse regroupe quatre articles scientifiques rédigés en anglais à des fins de publication au sein de revues scientifiques anglophones. Un premier manuscrit fait office d'introduction en décrivant la biologie des amides ligases MurC, MurD, MurE et MurF impliquées dans la biosynthèse de la paroi bactérienne. L'article se concentre sur le potentiel de ces protéines en tant que cibles antibactériennes prometteuses et inusitées. Par la suite, un article scientifique paru en mars 2006 dans la revue «Peptides» reporte la sélection de peptides inhibant l'activité ATPase de l'amide ligase MurD. Un de ces peptides fait preuve d'une activité inhibitrice impressionnante et représente un candidat fort intéressant en vue du développement d'une nouvelle classe d'agents antibactériens. Finalement, deux manuscrits relatent l'utilisation de la technique de présentation phagique afin de sélectionner des peptides inhibiteurs des amides ligases MurE et MurF. Ces manuscrits décrivent l'enzymologie des enzymes MurE et MurF ainsi que le mode d'action des peptides inhibiteurs de l'activité enzymatique de ces amides ligases.

Chapitre 4 - The biology of Mur ligases as a source of targets for new antibacterial agents

Résumé

La biologie des amides ligases MurC, MurD, MurE et MurF en tant que source de nouvelles cibles antibactériennes

L'augmentation et la propagation continuelle des mécanismes de résistance aux antibiotiques parmi les pathogènes bactériens en émergence et en réémergence à travers le monde engendrent un besoin urgent de nouvelles classes d'agents antibactériens à large spectre. La biosynthèse de la paroi bactérienne est sans aucun doute la source de cibles antibactériennes la plus reconnue et la plus validée. Parmi les enzymes impliquées dans cette biosynthèse, les amides ligases MurC, MurD, MurE et MurF possèdent un potentiel fort intéressant en tant que nouvelles cibles antibactériennes. En plus de présenter des caractéristiques attrayantes en tant que cibles spécifiques, la biologie des quatre amides ligases peut être exploitée en tant que cible unique. En fait, ces enzymes partagent le même mécanisme catalytique et possèdent une similarité au niveau de leur séquence primaire et de leur structure tridimensionnelle. La similitude et la conservation de ces amides ligases permettent d'envisager le développement de nouveaux inhibiteurs spécifiques ciblant ces quatre protéines essentielles à la biosynthèse de la paroi bactérienne. Ces inhibiteurs pourraient être optimisés afin de constituer une nouvelle classe d'agents antibactériens représentant une arme formidable contre les espèces bactériennes pathogènes. En ciblant plusieurs protéines essentielles, de tels agents antibactériens seraient très peu susceptibles au développement de mécanismes de résistance.

Contribution des auteurs

En tant que première auteure de cet article de revue scientifique, j'ai réalisé une revue approfondie et détaillée de la littérature scientifique sur la biosynthèse de la paroi bactérienne et sur les différentes enzymes impliquées. J'ai porté une attention particulière aux amides ligases MurC, MurD, MurE et MurF puis j'ai sélectionné les articles scientifiques les plus pertinents afin de rédiger une revue scientifique concise témoignant du potentiel de ces protéines en tant que cibles antibactériennes. Finalement, j'ai préparé les deux premières figures et j'ai rédigé intégralement le manuscrit en vue d'une soumission à la revue «Current Opinion in Microbiology». Le Dr François Sanschagrin a préparé la figure du manuscrit illustrant les structures tridimensionnelles des amides ligases MurC, MurD, MurE et MurF. Le Dr Roger C. Levesque m'a guidée dans la conception de l'article et m'a aidée à conserver un esprit de synthèse. Il a également corrigé le manuscrit afin d'en augmenter la qualité et la fluidité.

The biology of Mur ligases as a source of targets for new antibacterial agents

Catherine Paradis-Bleau, François Sanschagrin and Roger C. Levesque

Département de Biologie Médicale, Faculté de Médecine, Université Laval, Québec, Québec, Canada, G1K 7P4

Keywords: bacterial cell wall biosynthesis pathway, MurC, MurD, MurE, MurF

Address correspondence to: Roger C. Levesque, Département de Biologie Médicale, Pavillon Charles-Eugène Marchand, Université Laval, Québec, Québec, Canada, G1K 7P4, Tel: (1) 418 656-3070; Fax: (1) 418 656-7176; E-Mail: rclevesq@rsvs.ulaval.ca

Abstract

With antibiotic resistance mechanisms increasing in diversity among emerging and re-emerging bacterial pathogens and spreading worldwide, the development of novel classes of broad-spectrum antibacterial agents targeting hitherto unexploited targets in bacterial cells has become a high-priority task. The cell wall biosynthesis pathway is the most recognized and well-validated source of targets for antibacterial agents. Within this pathway are the Mur ligase enzymes (essential for the synthesis of the cell wall precursor monomer unit uridyl diphosphate-*N*-acetylmuramyl-pentapeptide), which are described in this article as highly suitable and currently unexploited targets for specific inhibitors. Each individual Mur ligase possesses features that constitute attractive physiological targets and the four share conserved amino acid regions as well as a common catalytic mechanism and structural features that can be exploited for the design of inhibitors that simultaneously target them all. A class of novel inhibitors of this type would provide a formidable weapon against pathogenic bacteria, with reduced likelihood of the emergence of resistant variants.

Introduction

The astonishing adaptive capabilities of bacteria, combined with modern human behavior and widespread antibiotic misuse, have resulted in alarming increases in resistance to all clinically useful antibiotics among emerging and re-emerging pathogens and the spread of resistant strains worldwide[1-3]. This situation has become one of the most critical global public health problems over the past decade, involving all major bacterial pathogens, complicating the treatment of infectious diseases and increasing human morbidity, mortality and health care costs[3,4]. The development of new, structurally novel broad-spectrum bactericidal compounds with novel modes of action against judiciously chosen physiological targets must be given top priority if humanity is to meet the challenge posed by emerging resistant pathogens[3,5].

The principal features of an ideal physiological target for bacterial inhibitors include functional essentiality for bacterial viability (i.e. inhibition leads unconditionally to effects that are lethal to the bacterial cell), high genetic and structural conservation among all

clinically relevant bacterial pathogens, no eukaryotic equivalent and a level of expression during host infection that ensures the effectiveness of the inhibition. The perfect target would be an enzyme performing a rate-limiting biochemical step with a fully elucidated mechanism amenable to high throughput screening and inhibitory investigations such as structure–activity relationships[5-7]. In order to minimize the emergence of resistance, new antibacterial approaches must target families of related but non-identical enzymes that have invariant active site residues and that can be inhibited by a single compound[6,7]. The Mur ligase enzymes, which catalyze essential steps in the bacterial cell wall biosynthesis pathway, fulfill all of these requirements and represent one of the best targets for antibacterial agents. In this review, the biology of these amide ligases is described in terms of their suitability as targets for a new generation of therapeutic antimicrobial agents.

The cell wall biosynthesis pathway and the functionality of the Mur ligases

The bacterial cell wall biosynthesis pathway can be divided into three distinct topological steps that are valid for all eubacteria. Cytoplasmic enzymes first synthesize the cell wall precursor uridyl diphosphate-*N*-acetylmuramyl-pentapeptide from uridyl diphosphate-*N*-acetylglucosamine (UDP-GlcNAc). Membrane-bound enzymes then catalyze the formation of the final lipid-containing precursor, after which the periplasmic enzymes incorporate this monomer unit into the growing cell wall layer. Cytoplasmic substrate UDP-GlcNAc is synthesized from D-fructose-6-phosphate by three enzymatic steps. D-fructose-6-phosphate is first converted into glucosamine-6-phosphate by amidotransferase GlmS and phosphoglucosamine mutase GlmM then catalyzes the formation of glucosamine-1-phosphate. Finally, the bifunctional GlmU enzyme performs the acetylation of glucosamine-1-phosphate into *N*-acetylglucosamine-1-phosphate and the uridylation to yield UDP-GlcNAc. This product is utilized for cell wall biosynthesis and for the synthesis of teichoic acids or lipopolysaccharides[8].

The first cell-wall-specific step of the pathway, namely UDP-*N*-acetylmuramyl-pentapeptide synthesis, is catalyzed by a series of cytoplasmic enzymes called MurA through MurF. MurA catalyzes the transfer of enolpyruvate from phosphoenolpyruvate to

position 3 of UDP-GlcNAc to yield UDP-GlcNAc-enolpyruvate. MurB then reduces the enolpyruvate moiety to D-lactoyl, utilizing one equivalent of NADPH and a solvent proton to form UDP-*N*-acetylmuramic acid (UDP-MurNAc)[7,8]. Next, the four ATP-dependent amide ligases (MurC, MurD, MurE and MurF) perform the stepwise addition of five amino acids using the newly synthesized carboxylate as the first acceptor site to form the peptide moiety of the cell wall precursor[7,9]. The pentapeptide is thus formed by the successive addition of, in most cases, L-Alanine (L-Ala), D-Glutamine (D-Glu), a di-amino acid (usually diaminopimelic acid (A2pm) or L-Lysine (L-Lys)) and a dipeptide D-Ala-X (X = typically D-Ala and less commonly D-lactate or D-serine) to the D-lactoyl group of UDP-MurNAc, by MurC, MurD, MurE, and MurF, respectively[9,10], yielding the cell wall cytoplasmic precursor UDP-MurNAc-pentapeptide, as depicted in Figure 1.

This precursor then becomes the substrate for the membrane step of the cell wall biosynthesis pathway. The translocase MraY transfers the phospho-MurNAc-pentapeptide moiety of UDP-MurNAc-pentapeptide to the membrane acceptor undecaprenyl phosphate to form MurNAc-(pentapeptide)-pyrophosphoryl undecaprenol or lipid I. Thereafter, the transferase MurG catalyzes the addition of GlcNAc to lipid I, yielding GlcNAc-MurNAc-(pentapeptide)-pyrophosphoryl undecaprenol or lipid II[8].

This final disaccharide pentapeptide precursor is then translocated by an unknown mechanism from the inner side of the cytoplasmic membrane to the outer side, where it becomes the substrate for the periplasmic step. The transglycosylation and transpeptidation actions of periplasmic penicillin-binding proteins (PBPs) incorporate the newly made monomer unit into the growing cell wall polymer. This polymerization reaction involves the formation of elongating linear disaccharide chains and peptide cross-bridges between the new glycan chains and the preexisting cell wall network[8]. The essential cell wall layer is thus composed of alternating units of UDP-GlcNAc and UDP-MurNAc cross-linked via short peptide chains. This network confers the bacterial cell shape, enables the cell to survive variations in osmotic pressure and provides the rigidity, flexibility and strength for cell integrity, growth and division[7,11,12]. Indeed, bacterial cells with defective cell walls eventually burst and die[11].

The potential of the Mur ligase enzymes as antibacterial targets

The cell wall biosynthesis pathway, which produces the essential and unusual cell wall structure exclusive to prokaryotes, represents one of the best known and most validated sources of targets for antibacterial therapy. Many clinically useful antibiotics interfere with this pathway[13]. The β-lactam, glycopeptide, bacitracin, D-cycloserine, fosfomycin, ramoplanin, tunicamycin and mureidomycin compounds inhibit different steps of cell wall biosynthesis, but no known antibacterial agent targets the amide ligase enzymes[13,14]. The ligases may thus be considered as unexploited targets, now attracting interest because of the antibiotic resistance "crisis" upon us[7,8].

Within the cell wall biosynthesis pathway, the Mur ligases represent one of the best specific targets for developing new, structurally novel antibacterial agents with novel modes of action. In fact, these enzymes present most of the characteristics sought in ideal antibacterial targets. They catalyze key reactions in bacterial cell wall biosynthesis and their functions are absolutely essential for bacterial growth, division and pathogenesis. Their inhibition leads to the lethal cell-lysis phenotype associated with impaired cell wall biosynthesis[15-17]. They are sufficiently expressed during host infection to constitute excellent targets and antibacterial agents developed against them will consequently be bactericidal and not merely bacteriostatic. Furthermore, each of the unique and highly specific Mur ligases is genetically and structurally conserved as a single gene copy in a wide variety of Gram-positive and Gram-negative pathogens, with no mammalian counterpart[9,18]. In fact, the active sites of MurC, MurD, MurE and MurF are conserved in almost all medically relevant bacteria and even among all members of the *Chlamydiaceae* family[9,18-22]. Potent inhibitors of these enzymes would thus be expected to act as broad-spectrum antibacterials[23,24]. Homologues of the amide ligase enzymes have been found in a number of chloroplast-containing organisms and there is good evidence that these eukaryotic Mur proteins are required for chloroplast division in mosses[25]. In contrast, mitochondria, which have lost the cell division and cell wall biosynthesis genes from their endosymbiotic origins, appear to have evolved a division apparatus that lacks bacterial components[26]. There is therefore no reason to believe *a priori* that antibiotic therapy using agents directed against Mur ligases would have adverse side effects on eukaryotic cells.

As no existing antibacterial agent or known endogenous inhibitor specifically targets Mur ligases, no resistance mechanism against such inhibitors is likely to have evolved in bacteria. Mur ligases can be obtained in large quantities at high purity and detailed catalytic mechanisms and structures of the four enzymes from many bacterial species are now available for driving and optimizing drug development[19,20,27-30]. Mur enzyme activity is coupled with an essential ATP hydrolysis, which can be quantified and exploited to screen and analyze inhibitory molecules. Although ATP and the Mur ligase amino acid substrates are commercially available, the nucleotide cell wall substrates are not. The use of such substrates can be bypassed by measuring Mur ligase activity as incorporation of a radioactive precursor into cell walls, but this method is time, cost and effort intensive. Enzymatic assays have therefore been devised, based on quantifying Mur ligase ATPase activity with synthesized nucleotide intermediates. The specific nucleotide substrate of each amide ligase can be prepared using purified cell wall biosynthesis enzymes and the commercially available substrate of MurA[31,32]. A recent study has described the generation of a mixture of UDP-MurNAc-Ala-Glu-Lys and UDP-Ala-Glu-A2pm using the nonessential Mpl cell-wall recycling enzyme[22]. Another alternative relies on an assay that can detect inhibitors of the entire cell wall cytoplasmic pathway by a ‘‘one pot’’ reaction where one enzyme provides substrate for the next. A permeabilized whole cell assay that monitors the incorporation of radioactive UDP-GlcNAc into the cell wall has been reported, as well as biochemical assays using the purified enzymes MurA through MurF[33].

Advantages of specifically targeting each Mur ligase with antibacterial agents

In addition to its key enzymatic role in the cell wall biosynthesis pathway, each amide ligase has significant advantages as a specific target for antibacterial agents. We shall therefore describe the characteristics and specific features of each Mur ligase enzyme.

MurC is specific for the substrate L-Ala, which it adds to the nucleotide precursor UDP-MurNAc, thus attaching the first amino acid residue of the cell wall peptide moiety and yielding the product UDP-MurNAc-Ala. Purified *E. coli* MurC is a protein of about 50

kDa, characterized by equilibrium between its monomeric and active dimeric forms. The L-Ala-adding activity of MurC seems to be dependent on its oligomerization state and this feature appears to be unique among the Mur ligases. Somehow, the two cysteine residues of the *E. coli* MurC protein are poorly conserved among bacteria and not critical for catalytic activity, although one of these is involved in enzyme stability and binding of ATP[34]. The MurC enzyme from the obligate intracellular pathogens among the genus *Chlamydia* is of particular interest, since unlike the vast majority of eubacteria, *Chlamydia* do not synthesize detectable cell wall, even though they have cell wall biosynthesis genes and are susceptible to cell wall-targeting antibiotics. The MurC enzyme of *Chlamydia* is synthesized as an unusual bi-functional protein called MurC-Ddl, with the MurC domain displaying ligase activity both *in vivo* and *in vitro*[35] and Ddl ligase activity of the type required for the synthesis of the D-Ala-D-Ala substrate of MurF. The Ddl activity of MurC-Ddl has been shown to depend on the N-terminal MurC portion but not on the MurC enzymatic activity[21]. These recent findings suggest that *Chlamydiaceae* can synthesize a cell-wall-like structure. Furthermore, potent inhibitors of MurC will presumably be of special interest for combating *Chlamydiaceae* infections, since they may be able to inhibit both the MurC and Ddl enzymatic functions through alteration of the MurC-Ddl protein conformation.

MurD catalyzes the formation of an amide bond between a D-Glu residue and UDP-MurNAc-Ala to form UDP-MurNAc-Ala-Glu. This protein of about 47 kDa displays extremely high specificity for its amino acid substrate and D-Glu is practically the only residue found at position 2 of the cell wall peptide moiety[8,36]. Furthermore, D-Glu residues occur exclusively in the cell wall and in capsular exo-polypeptides of a few species. D-Glu can be synthesized by a direct racemase-catalyzed conversion of L-Glu or by a transamination process catalyzed by a D-Ala aminotransferase using D-Ala and α-ketoglutarate. *Bacillus subtilis*, *Bacillus sphaericus* and staphylococci use both routes of synthesis, although the Glu racemase is typically the essential enzyme for providing D-Glu as a substrate for MurD[8]. The fact that MurD performs its function on an amino acid with the D configuration is especially interesting from the perspective of developing selective broad-spectrum antibacterial agents[24], as D residues constitute the most distinctive structural feature of the cell wall layer and are metabolized only in prokaryotes, which need

them presumably to provide resistance to degradation by external enzymes[37]. Indeed, MurD has been identified as one of the most promising new targets for the discovery of broad-spectrum antibacterial agents to face the emergence of multi-resistant *Mycobacterium tuberculosis*[30]. It has been suggested that the MurD reaction is the step at which cell wall synthesis is regulated, for example to maintain the relatively thin Gram-negative cell wall[24]. Finally, the surface-located enzyme glyceraldehyde phosphate dehydrogenase (GAPDH) is defined as a virulence factor in various bacterial pathogens and it has been suggested that MurD could bind cytoplasmic GAPDH to the cell wall[32]. Indeed, antibiotic therapy targeting MurD could alter the regulation of the cell wall biosynthesis pathway as well as the GAPDH virulence factor localization, in addition to inhibiting the highly specific MurD enzyme.

The third amino acid residue is added to the cell wall peptide moiety by a 52 kDa protein called MurE. MurE is the only member of the Mur ligases to display amino acid substrate specificity that varies from one bacterial species to another. Typically, Gram-negative bacteria and bacilli contain a meso-A2pm residue at the third position of the cell wall peptide moiety while Gram-positive bacteria contain an L-Lys residue [38]. The third residue plays a key role in maintaining bacterial cell wall integrity and cell shape. It is involved in cross-linkages between the peptide moiety of the glycan chains, joining the cell wall into a macromolecular network of high tensile strength and rigidity[38]. The subsequent transpeptidation reactions lead to the formation of essential bonds between the di-amino acid residue at the third position of a peptide moiety and a D-Ala or a di-amino acid residue of the next peptide side chain[39]. The di-amino acid is also involved in transpeptidation reactions required for proper bacterial cell division[38]. Furthermore, the high specificity of the transpeptidation step is particularly dependent on the di-amino acid used as an acceptor and the incorporation by MurE of a “wrong” amino acid results in cell lysis[8,38]. MurE must therefore select the “correct” substrate among closely related amino acids that coexist within the cell[40]. MurE enzymes from Gram-negative and Gram-positive bacteria have been shown to discriminate efficiently between di-amino acids via structural determinants to catalyze only the addition of either meso-A2pm or L-Lys to the nucleotide precursor UDP-MurNAc-Ala-Glu[8,38]. In most bacteria, meso-A2pm is synthesized by an L,L-A2pm epimerase but it can also be synthesized directly from L-tetrahydrodipicolinate by an A2pm

dehydrogenase enzyme. The L,L-A2pm decarboxylase then produces L-Lys from the meso-A2pm precursor in a biosynthetic pathway absent in mammals[37,41]. Finally, targeting MurE may lead to perturbation of the regulation of antibiotic resistance and competence mechanisms. MurE has recently been shown to influence methicillin resistance in *Staphylococcus aureus* by regulating the expression of two PBPs[42] and to influence DNA uptake in *Haemophilus influenzae* by causing induction of the normal competence pathway via a previously unsuspected signal[43].

The final amide ligase enzyme, the 46 kDa protein MurF, is less selective than the others, accepting a broader range of substrates[38]. Its function is to add the dipeptide D-Ala-D-Ala to UDP-MurNAc-tripeptide, yielding the cell wall precursor UDP-MurNAc-pentapeptide[7,23]. MurF is at a crucial junction in cell wall biosynthesis, mobilizing the cytoplasmic building block for the next steps of the pathway. MurF is an especially attractive target for selective broad-spectrum antibacterials as, like MurD, it exclusively utilizes D-amino acids as substrates[37]. The D-Ala-D-Ala dipeptide is specific to the cell wall and is formed by a pathway absent in mammals that involves alanine racemase and the Ddl enzyme[8,44]. D-Ala-D-Ala is also a central molecule in cell wall assembly and cross-linking, providing the cell wall with mechanical strength and flexibility. There is no active metabolism in the periplasm and the essential transpeptidation reaction between two glycan strands is energized by the hydrolysis of the D-Ala-D-Ala bond. The PBPs thus cleave the D-Ala-D-Ala of a donor pentapeptide precursor with concomitant release of the terminal D-Ala and formation of a cross-link between the carboxyl group of the D-Ala in position 4 and the amino group of an acceptor di-amino acid residue in another acceptor peptide moiety[39]. The D-Ala-D-Ala residues at the end of the peptide moiety are also important for the recognition of cell wall and the action of PBPs, β-lactams and glycopeptides[13,14,45]. Furthermore, the terminal D-Ala-D-Ala is required by the FtsI transpeptidase enzyme, which is responsible for the cell wall synthesis that occurs during division septum formation[46]. Indeed, aberrant septum formation and increases in cell diameter have been observed when MurF is defective. MurF also affects the level of β-lactam antibiotic resistance in methicillin-resistant *S. aureus* and the transcription of two PBPs[45]. Finally, MurF plays a key role in the mechanisms of bacterial resistance to glycopeptide antibiotics[8]. The functions of MurF thus exceed its primary task in peptidoglycan

biosynthesis, and targeting this enzyme could therefore lead to perturbation of cell division and thus thwart the development of antibiotic resistance for a long time.

When their unity is our strength: simultaneously targeting all the Mur ligases

The amide ligases MurC, MurD, MurE and MurF described above all share identical characteristics that can conceivably be exploited to design potent inhibitors targeting all four enzymes. Fifteen years ago, it was determined that 10 to 20% of the primary sequence is identical and the ATP-binding site is highly similar among these ligases[37]. Further comparison has revealed the presence of common invariants: seven amino acids and the ATP-binding consensus sequence GXXGKT/S[9]. Four regions of homology critical for proper functioning of the proteins were subsequently identified. Homologous region I includes the highly invariant nucleotide fold, region II is an extended domain in the middle of the proteins containing an invariant Glu and a highly conserved His lying between two acidic residues nested within a generally hydrophobic region, region III presents a short concentrated set of acidic residues conserved among most of the ligases in the form of a dyad and the region IV constitutes a hydrophobic patch[18]. The Mur ligases thus appear to be a well-defined class of functionally closely related proteins originating presumably in a common ancestor[9].

The only other enzymes found to share the same common conserved amino acids as observed for the Mur ligases are folylpoly-γ-L-glutamate ligase, CapB and cyanophycin synthetases[8,18]. Bouhss *et al* noted that folylpoly-γ-L-glutamate ligase presents the same conserved residues except for the most N-terminal invariant residue[9]. This enzyme catalyzes the addition of successive L-Glu residues either to folate monoglutamate in eukaryotes or to dihydropteroate in prokaryotes to produce folylpolyglutamates required for effective intracellular retention of folate[18,47]. Both prokaryotic and eukaryotic forms of the enzyme bear the signature Mur ligase regions I and II and elements of region IV identified by Eveland *et al*[18]. The four homologous regions have been identified in the CapB protein of *Bacillus anthracis,* implicated in the synthesis of capsular poly-γ-D-glutamate[18]. Finally, the C-terminal part of cyanophycin synthetase from *Synechocystis* sp. PCC 6803 involved

in the synthesis of the multi-L-Arg-poly-L-Asp polymer of cyanobacteria also shows sequence similarities with Mur ligases[48].

Over the past decade, there has been growing interest in elucidating the detailed catalytic mechanisms and structural features of the Mur ligases. The strong homology between the proteins associated with the catalytic functions supports the argument that these enzymes form a superfamily of three substrate amide ligases proceeding via a similar mechanism[18]. Indeed, MurC, MurD, MurE and MurF display similar levels of ligase activity with concomitant hydrolysis of ATP to ADP and inorganic phosphate (P_i). They thus use phosphate bond energy to drive the non-ribosomal addition of specific amino acids to the growing cell wall peptide moiety, beginning with UDP-MurNAc. This activity is dependent on the cofactor Mg^{2+} and sensitive to pH, with an optimum around 8. This formation of amide peptides of very particular types is not a frequently encountered biochemical reaction and involves acyl phosphate and tetrahedral intermediates[49]. The Mur ligases thus operate according to the mechanism depicted in Figure 2A, involving activation of the carboxyl group of UDP-MurNAc or the C-terminal carboxyl group of UDP-MurNAc-peptide via transfer of the γ-phosphate of ATP and formation of an acyl phosphate intermediate. The amino group of the condensing amino acid then displaces the phosphate by nucleophilic attack with the concomitant formation of a peptide bond and a tetrahedral intermediate, which breaks down into the lengthened peptide and P_i[23,28,36,49]. The four Mur ligases proceed via an ordered kinetic mechanism with a sequential substrate binding order beginning with ATP, followed by the nucleotide substrate and ending with the amino acid or dipeptide[9,23].

The tridimensional structure of the four Mur ligase proteins is now known. The structures of MurD, MurE and MurF were determined several years ago, while the crystal structure of MurC was solved more recently, thus completing the Mur ligase structural picture. The tridimensional features have confirmed that the homologous sequences conserved among the proteins are involved in the catalytic process[19,20,27,28,36,50]. Although each amide ligase displays high specificity for its respective substrate, the overall structure of MurC, MurD, MurE and MurF is very similar.

These four proteins share the same three-domain topology and active site architecture[28,29]. Each Mur ligase thus presents an N-terminal domain 1, a central domain 2

and a C-terminal domain 3, with an active structure assembling at the common domain interfaces when all three substrates are bound[28]. Domain 1 consists of a five-stranded parallel β-sheet surrounded by two α-helices in MurE, three helices in MurF and four α-helices in MurC and MurD. This fold binds the UDP moiety of the nucleotide substrate while the MurNAc-(peptide) portion extends into the cleft formed among the three domains. The N-terminal domain is reminiscent of the Rossmann dinucleotide-binding fold in MurC and MurD[20,27,28,51,52]. In order to accommodate the longer nucleotide substrate, MurD binds the UDP moiety in an orientation opposite that observed in MurC[28]. In contrast to MurC and MurD, MurE and MurF present a more usual N-terminal fold[20,27]. The mode of UDP recognition by MurE is similar to that observed for MurC, although MurE undergoes a more pronounced domain rotation to widen the interdomain cleft and accommodate the longer substrate[28]. In the case of MurF, the N-terminal domain binds the uracyl ring of UDP but does not present the typical nucleotide-binding fold, while part of the central domain extends out towards the N-terminal domain to bind the pyrophosphate of the nucleotide substrate[27].

The central domain represents a common fold seen in all Mur ligases, consisting of a central six-stranded parallel β-sheet for MurD, MurE and MurF whereas a seven-stranded, mostly parallel β-sheet is present in MurC. This β-sheet is surrounded by seven α-helices in MurD and MurE, by five helical segments in MurC and by eight α-helices in MurF. This domain is also flanked by a smaller antiparallel, three-stranded β-sheet. In all Mur ligases, the central domain contains a typical mononucleotide-binding fold and is responsible for the binding of ATP[20,27,28,36,50]. The Mur ligases present shortened versions of the classical P-loop, perhaps an evolutionary novelty, with a "deletion" of two residues between the invariant first Gly and the Gly-Lys. The P-loop normally has the consensus sequence GxxxxGKT/S with four variable residues between the two glycine residues, in contrast with the Mur ligase ATP-binding consensus sequence GXXGKT/S[9,47].

The third domain is conserved among the four Mur ligases and consists of a central six-stranded β-sheet with one antiparallel and five parallel β-strands, surrounded by five α-helices. This domain contains the Rossmann dinucleotide-binding fold and binds principally the amino acid substrates of the amide ligase enzymes[20,27,28,50,52]. This C-

terminal domain plays a dual role in both capping the ATP binding site and inserting a loop into the enzyme active site to position the appropriate amino acid substrate[28].

To form a potent active site for ligation to occur between the nucleotide and the amino acid substrates, the "open" substrate-free Mur ligase structures must undergo an important conformational change upon substrate binding in order to bring the C-terminal domain towards the N-terminal and central domains in close proximity for forming a functional enzyme-substrate complex. ATP binding is believed to initiate such a conformational change, but the Mur ligases assemble into an active "closed" tertiary structure only when the three substrates are bound. Indeed, the latter substrates must be brought together and correctly oriented for acyl-phosphate intermediate formation after the binding of ATP. Next, the ligase must orient the amino acid substrate for nucleophilic attack and stabilize the tetrahedral intermediate, thereby lowering the activation barrier and accelerating catalysis[20,27,28,36,51].

In summary, the critical amino acids, the catalytic mechanism and the tridimensional structure of the Mur ligase enzymes are widely conserved. These proteins differ from one another by the topology of their N-terminal UDP-binding domain. Such diversity, combined with more minor alterations in domain packing and tertiary structure allow the Mur ligases to bind a lengthening cell wall nucleotide substrate and a distinct amino acid ligand[28]. Finally, MurE has a special feature that distinguishes it from the other ligases, namely specific binding pockets for the γ- and α-carboxyl groups towards the ATP binding site for formation of the acyl phosphate intermediate. This ligase uses the γ- rather than the α-carboxyl group of D-Glu to form a peptide bond with the amino acid being added to the cell wall[36,53].

Development of a Mur ligase-targeted antibacterial therapy

Aided by knowledge of enzyme kinetics, catalytic mechanisms and structural features as well as the availability of screening assays, the rational design of novel classes of ingenious antibacterial agents targeting the Mur ligases becomes feasible in a practical sense. Since each of the Mur ligases is essential, such a multimodal inhibitor would be a formidable weapon against bacteria, with the added benefit of dramatic decreases in the likelihood of

resistance being acquired through a single point mutation[13,18,23,28,33]. Such a new class of antibacterials would also take advantage of the various substrate and feedback inhibitions as well as specific activation mechanisms reported to occur for most of the cell wall cytoplasmic enzymes. As the Mur ligase enzymes become inhibited, their respective substrates will accumulate in the bacterial cytoplasm and contribute to interference with the cell wall biosynthesis pathway. The interdependence of the Mur reactions is extensive: MurA is tightly inhibited by the UDP-MurNAc product of MurB (and substrate of MurC) through a feedback inhibition mechanism;[54] the activity of racemase MurI, essential for forming the D-Glu substrate of MurD, absolutely and specifically depends on the UDP-MurNAc-Ala activator (the product of MurC);[55] UDP-MurNAc-Ala at concentrations greater than normal significantly inhibits MurD through a substrate inhibition mechanism;[24] MurE is strongly inhibited by elevated concentrations of its UDP-MurNAc-dipeptide substrate[40]; the Ddl enzyme is very sensitive to D-Ala-D-Ala feedback inhibition,[16,56] and MurF is strongly inhibited by its nucleotide substrate UDP-MurNAc-tripeptide[23]. Moreover, changes in cell-wall precursor biosynthesis, such as variations of substrate pool levels and shortening of the peptide cross-bridges, have been correlated with variations in susceptibility/resistance behavior towards β-lactam antibiotics[8]. Finally, the likelihood of resistance would be much lower if a potent Mur ligase inhibitor were used as part of an antibacterial cocktail comprising fosfomycin inhibiting MurA and D-cycloserine interfering with the formation of D-Ala-D-Ala by targeting alanine racemase and the enzyme Ddl. Vancomycin can also be used on Gram-positive bacteria or teicoplanin derivatives on Gram-negative bacteria to obtain a synergistic effect[57]. This may allow decreases in D-cycloserine and glycopeptide doses and their associated toxic side effects.

It has been argued that the rapid discovery of new drugs is greatly facilitated when a family of related proteins is targeted by a similar chemical approach. ATPases represent very good candidates for such a family-based approach. Indeed, it is possible to target the nucleotide-binding site of all the ATPases among a specific family of proteins with a single chemical strategy[58]. The structural diversity among the ATPases can be exploited to design selective, specific and potent inhibitors, based on the structural properties of the nucleotide-binding site and complete active site, the conformation of the bound nucleotide and adenosine–protein interactions[59]. As a proof of principle, the Mur ligases present a P-loop

conformation that differs from the classical ATP-binding P-loop, forming a rather sharp turn between the β-strand and the α-helix[9,47].

Understanding of the common catalytic mechanism of the Mur ligases through kinetic and structural studies has led to the design of appropriately substituted transition state analogue inhibitors. Very few inhibitors have been described for the Mur ligases, but the most potent and best known are phosphinates or derivatives of phosphinic acid, consisting of a dipeptide analogue linked to uridine diphosphate by a hydrophobic spacer. The remarkable feature of this inhibition is that the amide ligase enzymes promote the transfer of the γ-phosphate of ATP onto the phosphinate anion to produce ADP and a phosphorylated inhibitor. The resulting phosphoryl phosphinate exhibits a transition-state inhibition moiety very closely mimicking the tetrahedral intermediate transition state of the nucleotide substrate that has been proven to form in the normal pathway of the reactions catalyzed by the Mur ligases (Fig. 2B). Thus, this tetrahedral intermediate-like phosphoryl phosphinate moiety is tightly bound by the enzymes[13]. Specific phosphinate inhibitors have been developed for each Mur ligase, but no antibacterial activity has been reported, probably due to inefficient transport of these molecules into the cytoplasm[33]. Using the conserved binding motifs and structural features of the Mur ligases, the design of new phosphinate analogues of the nucleotide substrates could result in specific inhibitors of the four Mur ligase enzymes.

Finally, such a novel class of ATPase or phosphinate inhibitors targeting the four Mur ligases will have to be evaluated for possible activity against folylpoly-*γ*-L-glutamate ligase, which performs an essential function in eukaryotic cells. Despite a low level of sequence identity, this enzyme presents conserved regions and structural similarity with the Mur ligases. Nevertheless, the folylpoly-*γ*-L-glutamate protein differs from Mur ligases by significant variation in the relative domain orientations, discrepancy between the P-loops as well as insertions and deletions in the structures[47]. Furthermore, there is no obvious structural analogy between the substrate of the folylpoly-*γ*-L-glutamate ligase (tetrahydrofolate) and the nucleotide substrates of the Mur enzymes[9]. In fact, domain 1 of the Mur ligases is absent from the folylpoly-*γ*-L-glutamate ligase. In contrast to the cell wall biosynthesis amide ligases, folylpoly-*γ*-L-glutamate accommodates a “growing” peptide chain[47]. These primary sequence, structural and catalytic differences can be

exploited in order to design Mur ligase inhibitors that do not interfere with folylpoly-γ-L-glutamate ligase.

Concluding remarks and future prospects

The Mur ligase cell wall biosynthesis enzymes constitute a group of closely related bacterial proteins with characteristics that make them highly suitable as targets for a new class of broad-spectrum antibacterial agents, which must be designed in order to face the impending crisis of rampant antibiotic resistance. However, successful antibiotic therapy with Mur inhibitors will not become reality until the conditions required for actual antibacterial activity have been determined and optimized. For a strong effect against bacterial growth and survival, it is likely that Mur ligases will have to be very strongly inhibited in the whole cell. Synergistic inhibitors of multiple steps in the Mur ligase pathway would require less complete inhibition of each step and would lead to lower rates of selection of resistant variants[33]. The biggest problem is how to get the inhibitor to cross the bacterial membranes and avoid the actions of efflux pumps to remain in the cell cytoplasm for long enough and at a concentration high enough to inhibit the targeted enzymes. To meet this challenge, inhibitory molecules may be conjugated to a stable bacterial transport moiety that promotes uptake via active transport mechanisms. To thwart bacterial resistance, inhibitors may exploit transport mechanisms required for bacterial virulence. Chemical parameters can also be explored as an avenue to obtaining passive diffusion of small inhibitory compounds through bacterial membranes without disturbing host cell membranes[14,33]. In the case of Gram-negative pathogens, the selective permeation barrier of the LPS-containing outer membrane can be perturbed by specific polycationic permeabilizers such as polymyxin B, cationic peptides and aminoglycosides in order to increase permeability[60]. Such permeabilizers could be used synergistically with Mur ligase inhibitors or the inhibitors could be transformed or complexed to mimic the permeabilization effect of polycationic compounds. Finally, filamentous phages can be used as specific and efficient targeted drug carriers and Mur inhibitors could be linked to these by means of chemical conjugation through a labile linker subject to controlled release in the bacterial cytoplasm[61].

For the purpose of targeting Mur ligases with ATPase inhibitors, the inhibitory molecules must be able to compete with the high ATP concentration present in the cell and must also be highly selective, because of the similarity of the ATP-binding site on ATPases and other ATP-binding proteins. Since phosphate-containing molecules are characterized by lower bioavailability and poor stability, the challenge will be to synthesize ATP mimics that lack phosphate groups[59]. In the case of phosphinate inhibitors, the diphosphate and phosphinate moieties would have to be modified, since they presumably prevent cell penetration. Exploration of combinatorial or modular chemistry could lead to compounds with an acceptable balance of specific inhibitory potential and good cell penetration[14].

References

1 Cohen, M.L. (2000) Changing patterns of infectious disease. *Nature* 406 (6797), 762-767

2 Fauci, A.S. (2001) Infectious diseases: considerations for the 21st century. *Clin Infect Dis* 32 (5), 675-685

3 Levy, S.B. and Marshall, B. (2004) Antibacterial resistance worldwide: causes, challenges and responses. *Nat Med* 10 (12 Suppl), S122-129

4 Tenover, F.C. (2006) Mechanisms of antimicrobial resistance in bacteria. *Am J Infect Control* 34 (5 Suppl), S3-S10

5 Brown, E.D. and Wright, G.D. (2005) New targets and screening approaches in antimicrobial drug discovery. *Chem Rev* 105 (2), 759-774

6 Miesel, L. et al. (2003) Genetic strategies for antibacterial drug discovery. *Nat Rev Genet* 4 (6), 442-456

7 Projan, S.J. (2002) New (and not so new) antibacterial targets - from where and when will the novel drugs come? *Curr Opin Pharmacol* 2 (5), 513-522

8 van Heijenoort, J. (2001) Recent advances in the formation of the bacterial peptidoglycan monomer unit. *Nat Prod Rep* 18 (5), 503-519

9 Bouhss, A. et al. (1997) Invariant amino acids in the Mur peptide synthetases of bacterial peptidoglycan synthesis and their modification by site-directed mutagenesis in the UDP-MurNAc:L-alanine ligase from *Escherichia coli*. *Biochemistry* 36 (39), 11556-11563

10 van Heijenoort, J. (1998) Assembly of the monomer unit of bacterial peptidoglycan. *Cell Mol Life Sci* 54 (4), 300-304

11 Young, K.D. (2003) Bacterial shape. *Mol Microbiol* 49 (3), 571-580

12 Goehring, N.W. and Beckwith, J. (2005) Diverse paths to midcell: assembly of the bacterial cell division machinery. *Curr Biol* 15 (13), R514-526

13 El Zoeiby, A. et al. (2003) Structure and function of the Mur enzymes: development of novel inhibitors. *Mol Microbiol* 47 (1), 1-12

14 Silver, L.L. (2003) Novel inhibitors of bacterial cell wall synthesis. *Curr Opin Microbiol* 6 (5), 431-438

15 Lugtenberg, E.J. et al. (1972) Murein synthesis and identification of cell wall precursors of temperature-sensitive lysis mutants of *Escherichia coli*. *J Bacteriol* 109 (1), 326-335

16 Lugtenberg, E.J. and van Schijndel-van Dam, A. (1972) Temperature-sensitive mutants of *Escherichia coli* K-12 with low activities of the L-alanine adding enzyme and the D-alanyl-D-alanine adding enzyme. *J Bacteriol* 110 (1), 35-40

17 Lugtenberg, E.J. and van Schijndel-van Dam, A. (1972) Temperature-sensitive mutants of *Escherichia coli* K-12 with low activity of the diaminopimelic acid adding enzyme. *J Bacteriol* 110 (1), 41-46

18 Eveland, S.S. et al. (1997) Conditionally lethal *Escherichia coli* murein mutants contain point defects that map to regions conserved among murein and folyl poly-gamma-glutamate ligases: identification of a ligase superfamily. *Biochemistry* 36 (20), 6223-6229

19 Bouhss, A. et al. (1999) Role of the ortholog and paralog amino acid invariants in the active site of the UDP-MurNAc-L-alanine:D-glutamate ligase (MurD). *Biochemistry* 38 (38), 12240-12247

20 Gordon, E. et al. (2001) Crystal structure of UDP-N-acetylmuramoyl-L-alanyl-D-glutamate: meso-diaminopimelate ligase from *Escherichia coli*. *J Biol Chem* 276 (14), 10999-11006

21 McCoy, A.J. and Maurelli, A.T. (2005) Characterization of *Chlamydia* MurC-Ddl, a fusion protein exhibiting D-alanyl-D-alanine ligase activity involved in peptidoglycan synthesis and D-cycloserine sensitivity. *Mol Microbiol* 57 (1), 41-52

22 Baum, E.Z. et al. (2006) Utility of muropeptide ligase for identification of inhibitors of the cell wall biosynthesis enzyme MurF. *Antimicrob Agents Chemother* 50 (1), 230-236

23 Anderson, M.S. et al. (1996) Kinetic mechanism of the *Escherichia coli* UDPMurNAc-tripeptide D-alanyl-D-alanine-adding enzyme: use of a glutathione S-transferase fusion. *Biochemistry* 35 (50), 16264-16269

24 Walsh, A.W. et al. (1999) Comparison of the D-glutamate-adding enzymes from selected gram-positive and gram-negative bacteria. *J Bacteriol* 181 (17), 5395-5401

25 Machida, M. et al. (2006) Genes for the peptidoglycan synthesis pathway are essential for chloroplast division in moss. *Proc Natl Acad Sci U S A* 103 (17), 6753-6758

26 Kuroiwa, T. et al. (2006) Structure, function and evolution of the mitochondrial division apparatus. *Biochim Biophys Acta* 1763 (5-6), 510-521

27 Yan, Y. et al. (2000) Crystal structure of *Escherichia coli* UDPMurNAc-tripeptide D-alanyl-D-alanine-adding enzyme (MurF) at 2.3 A resolution. *J Mol Biol* 304 (3), 435-445

28 Mol, C.D. et al. (2003) Crystal structures of active fully assembled substrate- and product-bound complexes of UDP-N-acetylmuramic acid:L-alanine ligase (MurC) from *Haemophilus influenzae*. *J Bacteriol* 185 (14), 4152-4162

29 Spraggon, G. et al. (2004) Crystal structure of an UDP-N-acetylmuramate-alanine ligase MurC (TM0231) from *Thermotoga maritima* at 2.3 A resolution. *Proteins* 55 (4), 1078-1081

30 Anishetty, S. et al. (2005) Potential drug targets in *Mycobacterium tuberculosis* through metabolic pathway analysis. *Comput Biol Chem* 29 (5), 368-378

31 El Zoeiby, A. et al. (2003) Identification of novel inhibitors of *Pseudomonas aeruginosa* MurC enzyme derived from phage-displayed peptide libraries. *J Antimicrob Chemother* 51 (3), 531-543

32 Paradis-Bleau, C. et al. (2006) Selection of peptide inhibitors against the *Pseudomonas aeruginosa* MurD cell wall enzyme. *Peptides* 27 (7), 1693-700

33 Silver, L.L. (2006) Does the cell wall of bacteria remain a viable source of targets for novel antibiotics? *Biochem Pharmacol* 71, 996-1005

34 Nosal, F. et al. (1998) Site-directed mutagenesis and chemical modification of the two cysteine residues of the UDP-N-acetylmuramoyl:L-alanine ligase of *Escherichia coli*. *FEBS Lett* 426 (3), 309-313

35 Hesse, L. et al. (2003) Functional and biochemical analysis of *Chlamydia trachomatis* MurC, an enzyme displaying UDP-N-acetylmuramate:amino acid ligase activity. *J Bacteriol* 185 (22), 6507-6512

36 Bertrand, J.A. et al. (1999) Determination of the MurD mechanism through crystallographic analysis of enzyme complexes. *J Mol Biol* 289 (3), 579-590

37 Bugg, T.D. and Walsh, C.T. (1992) Intracellular steps of bacterial cell wall peptidoglycan biosynthesis: enzymology, antibiotics, and antibiotic resistance. *Nat Prod Rep* 9 (3), 199-215

38 Mengin-Lecreulx, D. et al. (1999) Expression of the *Staphylococcus aureus* UDP-N-acetylmuramoyl-L-alanyl-D-glutamate:L-lysine ligase in *Escherichia coli* and effects on peptidoglycan biosynthesis and cell growth. *J Bacteriol* 181 (19), 5909-5914

39 Holtje, J.V. (1998) Growth of the stress-bearing and shape-maintaining murein sacculus of *Escherichia coli*. *Microbiol Mol Biol Rev* 62 (1), 181-203

40 Boniface, A. et al. (2006) The MurE synthetase from *Thermotoga maritima* is endowed with an unusual D-lysine-adding activity. *J Biol Chem* 281 (23), 15680-15686

41 Born, T.L. and Blanchard, J.S. (1999) Structure/function studies on enzymes in the diaminopimelate pathway of bacterial cell wall biosynthesis. *Curr Opin Chem Biol* 3 (5), 607-613

42 Gardete, S. et al. (2004) Role of *murE* in the expression of beta-lactam antibiotic resistance in *Staphylococcus aureus*. *J Bacteriol* 186 (6), 1705-1713

43 Ma, C. and Redfield, R.J. (2000) Point mutations in a peptidoglycan biosynthesis gene cause competence induction in *Haemophilus influenzae*. *J Bacteriol* 182 (12), 3323-3330

44 Walsh, C.T. (1989) Enzymes in the D-alanine branch of bacterial cell wall peptidoglycan assembly. *J Biol Chem* 264 (5), 2393-2396

45 Sobral, R.G. et al. (2006) Role of *murF* in cell wall biosynthesis: isolation and characterization of a *murF* conditional mutant of *Staphylococcus aureus*. *J Bacteriol* 188 (7), 2543-2553

46 Eberhardt, C. et al. (2003) Probing the catalytic activity of a cell division-specific transpeptidase in vivo with beta-lactams. *J Bacteriol* 185 (13), 3726-3734

47 Sheng, Y. et al. (2000) Structural and functional similarities in the ADP-forming amide bond ligase superfamily: implications for a substrate-induced conformational change in folylpolyglutamate synthetase. *J Mol Biol* 302 (2), 427-440

48 Ziegler, K. et al. (1998) Molecular characterization of cyanophycin synthetase, the enzyme catalyzing the biosynthesis of the cyanobacterial reserve material multi-L-arginyl-poly-L-aspartate (cyanophycin). *Eur J Biochem* 254 (1), 154-159

49 Bouhss, A. et al. (2002) MurC and MurD synthetases of peptidoglycan biosynthesis: borohydride trapping of acyl-phosphate intermediates. *Methods Enzymol* 354, 189-196

50 Bertrand, J.A. et al. (1997) Crystal structure of UDP-N-acetylmuramoyl-L-alanine:D-glutamate ligase from *Escherichia coli*. *EMBO J* 16 (12), 3416-3425

51 Bertrand, J.A. et al. (2000) "Open" structures of MurD: domain movements and structural similarities with folylpolyglutamate synthetase. *J Mol Biol* 301 (5), 1257-1266

52 Katz, A.H. and Caufield, C.E. (2003) Structure-based design approaches to cell wall biosynthesis inhibitors. *Curr Pharm Des* 9 (11), 857-866

53 Green, D.W. (2002) The bacterial cell wall as a source of antibacterial targets. *Expert Opin Ther Targets* 6 (1), 1-19

54 Mizyed, S. et al. (2005) UDP-N-acetylmuramic acid (UDP-MurNAc) is a potent inhibitor of MurA (enolpyruvyl-UDP-GlcNAc synthase). *Biochemistry* 44 (10), 4011-4017

55 Doublet, P. et al. (1994) The glutamate racemase activity from *Escherichia coli* is regulated by peptidoglycan precursor UDP-N-acetylmuramoyl-L-alanine. *Biochemistry* 33 (17), 5285-5290

56 Miller, D.J., Hammond, S.M., Anderluzzi, D., Bugg, T.D.H. (1998) Aminoalkylphosphinate inhibitors of D-Ala-D-Ala adding enzyme. *J Chem Soc Perkin Trans* 1, 131-142

57 Hancock, R.E. and Farmer, S.W. (1993) Mechanism of uptake of deglucoteicoplanin amide derivatives across outer membranes of *Escherichia coli* and *Pseudomonas aeruginosa*. *Antimicrob Agents Chemother* 37 (3), 453-456

58 Chene, P. (2003) The ATPases: a new family for a family-based drug design approach. *Expert Opin Ther Targets* 7 (3), 453-461

59 Chene, P. (2002) ATPases as drug targets: learning from their structure. *Nat Rev Drug Discov* 1 (9), 665-673

60 Nikaido, H. (2003) Molecular basis of bacterial outer membrane permeability revisited. *Microbiol Mol Biol Rev* 67 (4), 593-656

61 Yacoby, I. et al. (2006) Targeting antibacterial agents by using drug-carrying filamentous bacteriophages. *Antimicrob Agents Chemother* 50 (6), 2087-2097

Figure legends

Figure 1. Schematic representation of the cytoplasmic steps of cell wall biosynthesis carried out by the ATP-dependent Mur ligases and formation of the cell wall peptide moiety. MurC first catalyzes addition of L-Ala to the nucleotide substrate UDP-MurNAc. MurD then adds D-Glu to UDP-MurNAc-Ala, MurE ligates the meso-A2pm residue (in Gram-negative bacteria and bacilli) to yield the UDP-MurNAc-tripeptide and finally MurF catalyzes the addition of the terminal dipeptide D-Ala-D-Ala, yielding the UDP-MurNAc-pentapeptide. (In Gram-positive bacteria, MurE ligase typically adds L-Lys to the UDP-MurNAc-Ala-Glu substrate.)

Figure 2. (A) Catalytic reaction mechanism of the ATP-dependent amide-forming Mur ligase enzymes and (B) the general structure of a phosphorylated phosphinate inhibitor.

Figure 3. Tridimensional structures of the amide ligases MurC, MurD, MurE and MurF. (A) structure of MurC resolved to 1.7 Å [28]; domain 1 is yellow, domain 2 is red, domain 3 is green, UDP-MurNac-Ala product is blue and nonhydrolyzable ATP analogue AMPPNP is dark blue; (B) structure of MurD resolved to 1.7 Å [36]; domain 1 is yellow, domain 2 is red, domain 3 is green, UDP-MurNac-Ala is blue, and D-Glu is dark blue; (C) structure of MurE resolved to 2 Å [20]; domain 1 is yellow, domain 2 is red, domain 3 is green, UDP-MurNac-Ala-Glu is blue, and meso-A2pm is dark blue; (D) structure of MurF resolved to 2.3 Å [27]; domain 1 is yellow, domain 2 is red, and domain 3 is green. The image was created using INSIGHTII version 2000.1 (Accelrys) on a Silicon Graphics Fuel workstation. Crystal structure co-ordinates were retrieved from the Protein Data Bank (http://www.rcsb.org/pdb/): MurC, 1P3D; MurD, 2UAG; MurE, 1E8C; MurF, 1GG4.

Figure 1.

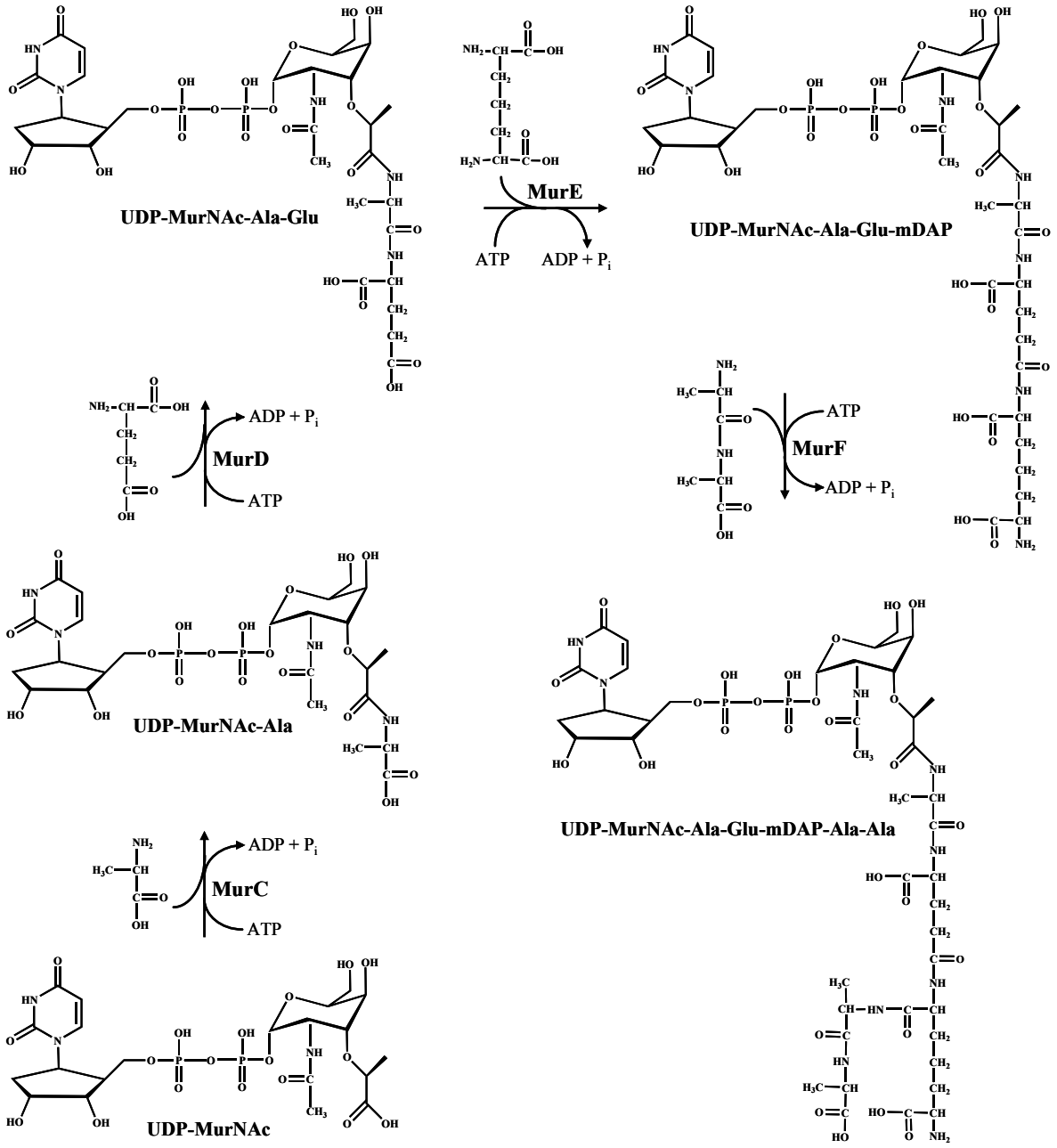
UDP-MurNAc-Ala-Glu
MurE
ATP
ADP + P$_i$
UDP-MurNAc-Ala-Glu-mDAP
ADP + P$_i$
MurD
ATP
ATP
MurF
ADP + P$_i$
UDP-MurNAc-Ala
UDP-MurNAc-Ala-Glu-mDAP-Ala-Ala
ADP + P$_i$
MurC
ATP
UDP-MurNAc

Figure 2.

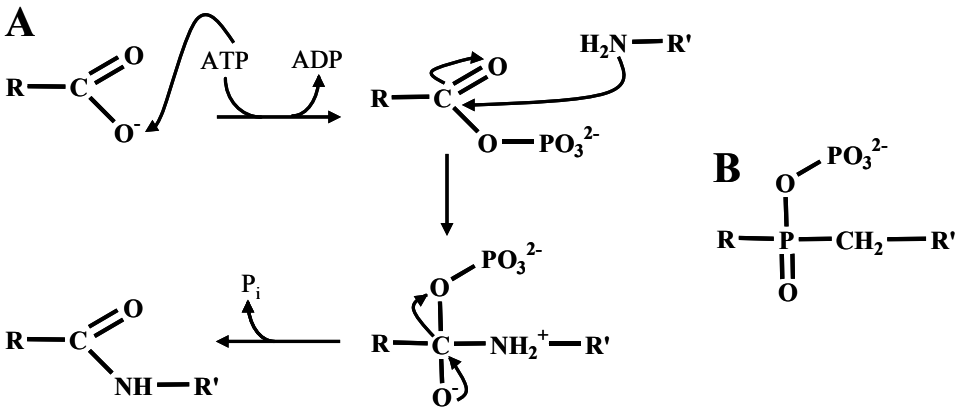

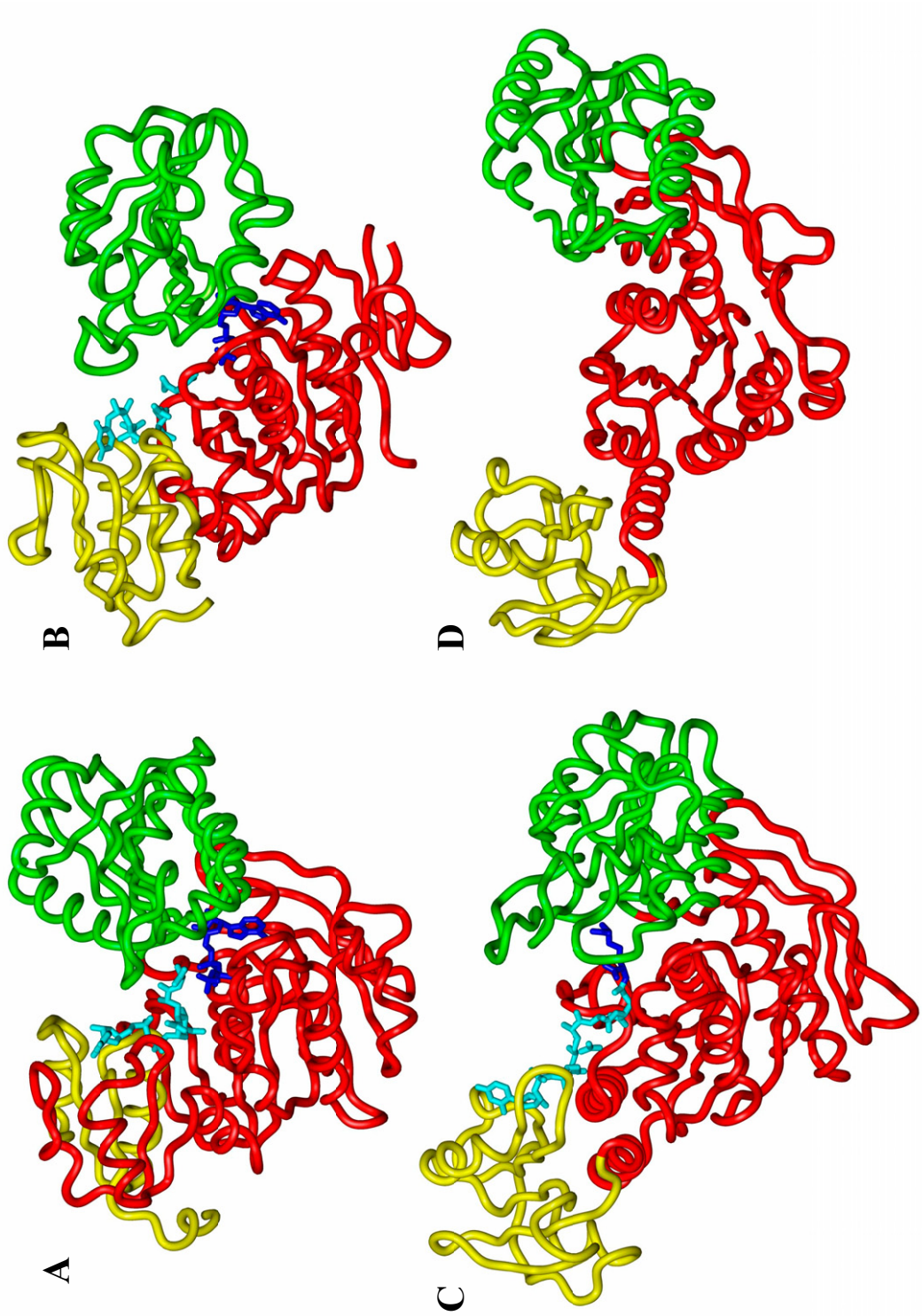

Figure 3.

Chapitre 5 - Selection of peptide inhibitors against the *Pseudomonas aeruginosa* MurD cell wall enzyme

Résumé

Sélection de peptides inhibiteurs contre l'enzyme MurD de *Pseudomonas aeruginosa* essentielle à la biosynthèse de la paroi bactérienne

Le pathogène opportuniste *P. aeruginosa* est hautement résistant aux antibiotiques et représente la principale cause de décès chez les patients atteints de fibrose kystique. Afin de développer de nouveaux agents antibactériens, l'amide ligase MurD de *P. aeruginosa* essentielle à la biosynthèse de la paroi bactérienne a été ciblée. La protéine MurD purifiée a été utilisée afin de cribler des banques de peptides C-7-C et 12 mers par présentation phagique. Une approche de biocriblage compétitif a été employée avec les substrats spécifiques de MurD; soit le D-glutamate et l'ATP. Suite au biocriblage, l'ADN phagique a été séquencé et 60 fusions peptidiques ont été identifiées. Les séquences correspondantes en acides aminés ont ensuite été alignées puis les deux consensus peptidiques sélectionnés contre MurD ont été synthétisés. Le substrat nucléotidique UDP-N-acetylmuramyl-L-alanine a été synthétisé, purifié et utilisé afin de développer un essai spectrophotométrique dosant l'activité enzymatique de MurD. Cet essai a permis d'évaluer le potentiel inhibiteur des peptides synthétisés. Le peptide C-7-C MurDp1 inhibe spécifiquement l'activité ATPase de MurD avec une CI_{50} estimée à 4 μM et la conformation en boucle de MurDp1 s'avère importante pour l'inhibition. Le peptide linéaire MurDp2 comprenant 12 résidus présente quant à lui une CI_{50} de 15 mM. Un motif d'acide aminé conservé a été identifié entre le peptide MurDp2 et la protéine bactérienne glycéraldehyde 3-phosphate déshydrogénase. Cela indique que MurDp2 se lie à un site d'intéraction protéine-protéine à la surface de MurD. Finalement, cette étude démontre que des peptides inhibiteurs efficaces ainsi que des domaines d'intéraction protéine-protéine peuvent être identifiés à l'aide d'une approche ciblée de présentation phagique.

Contribution des auteurs

Cet article scientifique publié dans la revue «Peptides» en mars 2006 a été réalisé par sept personnes. J'ai tout d'abord préparé l'enzyme MurD puis j'ai effectué le criblage peptidique par présentation phagique avec l'aide de la stagiaire Lydia Boudreault. J'ai ensuite analysé les résultats de séquences obtenus contre MurD. Adrian Lloyd a synthétisé, purifié et analysé le substrat nucléotidique de MurD qui n'est pas disponible commercialement. À ce moment, Adrian Lloyd était étudiant au doctorat sous la direction du Dr Timothy D. H. Bugg qui a supervisé cette étape du projet. Par la suite, la chimiste Mélanie Beaumont et le Dr François Sanschagrin ont mis au point un essai spectrophotométrique quantifiant l'activité ATPase de MurD afin d'analyser le potentiel inhibiteur des peptides synthétisés. Mélanie Beaumont a ensuite déterminé la CI_{50} pour chacun des peptides en utilisant l'essai spectrophotométrique et le substrat nucléotidique de MurD. J'ai finalement analysé les résultats obtenus, j'ai préparé les figures et les tableaux puis j'ai rédigé presque entièrement le manuscrit. Ainsi, la section du manuscrit concernant la synthèse du substrat nucléotidique a été écrite par Adrian Lloyd. J'ai également préparé la figure correspondante en collaboration avec Adrian Lloyd et le Dr Timothy D. H. Bugg. Finalement, le Dr Roger C. Levesque est à l'origine de l'idée de départ et de la conceptualisation du projet de recherche. Ce projet consiste à cibler les protéines bactériennes essentielles à la biosynthèse de la paroi bactérienne afin de développer une classe innovatrice d'agents antimicrobiens. Le Dr Levesque a également orienté le projet et révisé le manuscrit pour en augmenter la fluidité et la valeur scientifique.

Selection of peptide inhibitors against the *Pseudomonas aeruginosa* MurD cell wall enzyme

Catherine Paradis-Bleau[a], Mélanie Beaumont[a], Lydia Boudreault[a], Adrian Lloyd[b], François Sanschagrin[a], Timothy D. H. Bugg[b] and Roger C. Levesque[a, *]

[a] *Centre de recherche sur la fonction, la structure et l'ingénierie des protéines, Faculté de médecine, pavillon Charles-Eugène Marchand, Département de Biologie Médicale, Faculté de Médecine, Université Laval, Sainte-Foy, Québec, Canada, G1K 7P4*
[b] *Department of chemistry, University of Warwick, Coventry, United Kingdom, CV4 7AL*

[*] Corresponding author.
Tel: (1) (418) 656-3070; Fax: (1) (418) 656-7176.
E-mail address: rclevesq@rsvs.ulaval.ca

Available E-mail address of authors:
Catherine Paradis-Bleau: cparadis@rsvs.ulaval.ca
Lydia Boudreault: lydia.boudreault.1@ulaval.ca
Adrian Lloyd: ALloyd@bio.warwick.ac.uk
François Sanschagrin: fsanscha@rsvs.ulaval.ca
Timothy D.H. Bugg: T.D.Bugg@warwick.ac.uk
Roger C. Levesque: rclevesq@rsvs.ulaval.ca

Keywords: *Pseudomonas aeruginosa*; MurD; UDP-N-acetylmuramyl-L-alanine:D-glutamate ligase; Phage display; Inhibitory peptides.

Abstract

The purified *Pseudomonas aeruginosa* cell wall biosynthesis MurD amide ligase enzyme was used to screen C-7-C and 12 mers peptides from phage display libraries using competitive biopanning approaches with the specific substrates D-glutamate and ATP. From the 60 phage-encoded peptides identified, DNA was sequenced, deduced amino acid sequences aligned and two peptides were synthesized from consensus sequences identified. The UDP-*N*-acetylmuramyl-L-alanine MurD substrate was synthesized, purified and used to develop a spectrophotometric assay. One peptide synthesized was found to specifically inhibit ATPase activity of MurD. The IC_{50} value was estimated at 4 μM for the C-7-C MurDp1 peptide. The loop conformation of MurDp1 was shown to be important for the inhibition of the UDP-*N*-acetylmuramyl-L-alanine:D-glutamate MurD ligase. The linear 12 mers MurD2 peptide has an IC_{50} value of 15 mM. A conserved amino acid motif was found between MurDp2 and the bacterial glyceraldehyde 3-phosphate dehydrogenase indicating that MurDp2 binds at a protein–protein interacting site. The approach proposed and results obtained suggest that efficient peptide inhibitors as well as protein–protein interaction domains can be identified by phage display.

1. Introduction

The worldwide spread of antibiotic resistance among emerging and re-emerging bacterial pathogens promotes the development of structurally new antibacterials with novel modes of action against judiciously chosen targets [19]. The bacterial cell wall biosynthesis pathway represents an attractive antibacterial target source since it encodes essential enzymes whose inhibition gives a lethal phenotype. The enzymes are also highly conserved in bacterial species, absent in eukaryotic cells and sufficiently expressed during the infection of the host to constitute excellent antibacterial targets [28]. The MurA to MurF enzymes catalyze the synthesis of the bacterial cytoplasmic cell wall precursor UDP-*N*-acetylmuramyl pentapeptide. The second step in the biosynthesis pathway involves the transfer of the cytoplasmic precursor across the membrane by a lipophilic carrier and the addition of an *N*-acetylglucosamine molecule via enzymatic actions of the membrane translocases MraY and MurG. The final peptidoglycan precursor forms a branched structure with the growing cell

wall polymer by the transglycosylation and transpeptidation actions of periplasmic penicillin-binding proteins [12]. The cell wall layer, composed of alternating units of UDP-*N*-acetylglucosamine and UDP-*N*-acetylmuramic acid cross linked via short peptide chains, confers the bacterial cell shape and rigidity enabling the cell to survive variations in osmotic pressures [35].

Many clinically useful antibiotics interfere with the late cell wall biosynthesis steps but few antibacterial agents inhibit the enzymes involved in the early cytoplasmic steps of the pathway [12]. Among the cell wall biosynthesis enzymes, we selected the MurD UDP-*N*-acetylmuramyl-L-alanine:D-glutamate ligase as a specific target. This protein catalyzes the formation of an amide bond between a D-Glu residue and the nucleotide precursor UDP-*N*-acetylmuramyl-L-alanine (UDP-MurNac-Ala) with the concomitant hydrolysis of ATP into ADP and inorganic phosphate. The MurD enzyme active site is highly conserved among bacterial species [34] and its ATPase activity can be exploited to evaluate the inhibitory potential of lead peptide compounds. As a model system we are using the MurD enzyme from *Pseudomonas aeruginosa*, an opportunistic pathogen highly resistant to most classes of antibiotics and one of the most important opportunistic pathogen of chronic nosocomial infections [16,27].

To identify peptide inhibitors of MurD, we used a phage display approach coupled to a competitive biopanning assay using the enzyme substrates. We reasoned that amide ligases such as MurD interact and ligate small peptides and that peptide inhibitors could potentially be identified by phage display. This powerful tool allows the selection of short peptide ligands interacting with the targeted protein among a large pool of 10^9 random peptide permutations fused to the phage M13 pIII minor coat protein [6]. In addition, phage display screening of amide ligases would preferentially select phage encoded peptides which would bind to functional sites such as substrate binding sites, protein–protein interaction sites or allosteric regulatory sites [18]. This approach has been useful for the detection of various enzyme inhibitors [4,18] including the cell division proteins FtsZ and FtsA [25,26] as well as the cell wall biosynthesis MurC amide ligase enzyme [10]. To our knowledge, this is the first report of specific peptide inhibitors of MurD in the micromolar range.

2. Materials and methods

2.1. Purification of biologically active MurD enzyme

The MurD enzyme was overexpressed and purified as previously described [11]. All reagents used were purchased from Sigma–Aldrich (Oakville, Ont., Canada) unless otherwise indicated. All trace of phosphate in the MurD conservation buffer was removed by dialysis into 2 l of buffer B (20 mM Tris–HCl, pH 7.5, 2 mM DTT, 10 mM $MgCl_2$, 150 mM NaCl and 500 μM ATP). Extensive dialysis was repeated four times at room temperature. Purified MurD protein was visualized on SDS-PAGE and the protein concentration was determined using the Bradford method (BioRad, Mississauga, Ont., Canada). Enzymatic activity of MurD was confirmed using a thin layer chromatography (TLC) assay with P^{32}-labeled ATP as substrate. The MurD ATPase assay was done using 1 μM of purified MurD in reaction buffer B (50 mM BisTris propane, pH 8, 2.5 mM $MgCl_2$ and 2.5 mM DTT) using 1 μl of ATP^{32} 10 μCi/μl (Perkin-Elmer, Woodbridge, Ont., Canada), 20 μM of UDP-MurNac-Ala and 5 mM of D-Glu as substrates in a final volume of 20 μl. The mixture was incubated 1 h at 37 °C and 2 μl was deposited on a TLC along with negative controls without the enzyme or without UDP-MurNac-Ala. Hydrolysis of the ATP radioactive substrate was measured by autoradiography using a Phosphorimager (Fuji, Stanford, CA, US).

2.2. Affinity selection of phage displayed peptides against MurD

Phage display screenings were performed using the PH.D.-12 and PH.D.-C-7-C phage libraries containing 10^9 peptides fused to the phage M13 pIII minor coat protein (New England Biolabs, Mississauga, Ont., Canada) as described [10,26]. The screening specificity and stringency were optimized by increasing the Tween concentration during washes and by decreasing the time of contact between the phages and the targeted MurD protein used during the three rounds of biopanning. Competitive biopanning was done using D-Glu and ATP as the MurD substrates. Phage titers used as input are given in Table 1. Phage encoding peptides were eluted in the third round of biopanning using 100 μl of

0.2 M glycine–HCl (pH 2.2) [10] as well as by 100 µl of 1 mM ATP and 100 µl of 1 mM D-Glu during 30 min.

2.3. Peptide synthesis

Peptides encoding the C-7-C mers consensus amino acid sequence CIPSHTPRC and the 12 mers consensus sequence HLPTSSLFDTTH were synthesized as MurDp1 and MurDp2, respectively. Peptide synthesis was performed on an ABI 433A Peptide Synthesizer using FastMoc chemistry [10]. The peptides were purified on a Vydak 22 mm × 250 mm C18 reverse-phase HPLC column using 0.1% trifluoroacetic acid/acetonitrile gradient at 10 ml/min. Peptide purity was analyzed by HPLC (>90%) and molecular mass confirmed (1012.41 Da for C-7-C and 1355.73 Da for the 12 mers) by MALDI-TOF. Both peptides were solubilized in buffer A (200 mM Tris–HCl, pH 8) to a final concentration of 100 mM and the pH was adjusted to 7.

2.4. Synthesis of uridine 5'-diphosphoryl N-acetylmuramyl-L-alanine

Synthesis of UDP-MurNac-Ala was performed essentially as described [29] except that the steps involved in the synthesis of UDP-MurNac-Ala from UDP-GlcNac were carried out in a single reaction using the combined activities of *P. aeruginosa* MurA, MurB and MurC enzymes. The UDP-MurNac-Ala product from this incubation was purified from the reaction mixture by firstly removal of the Mur enzymes by ultrafiltration. UDP-MurNac-Ala was then purified from the ultrafiltrate by anion exchange chromatography at room temperature on DEAE sephacel, pre-equilibrated in 10 mM ammonium acetate, pH 7.5, where UDP-MurNac-Ala was eluted on a 10–800 mM ammonium acetate (pH 7.5) gradient.

UDP-MurNac-Ala was identified enzymically, using a pyruvate kinase/lactate dehydrogenase coupled assay for MurD and D-glutamate-dependent ADP generation. Fractions thus identified to contain UDP-MurNac-Ala were freeze dried from water three times to remove the ammonium acetate. Purity of the UDP-MurNac-Ala was assessed by analytical anion exchange by FPLC on MonoQ™ using a 0–0.5 M gradient of ammonium acetate which indicated that the product was 99.5% pure. Negative ion electrospray mass

spectrometric characterization gave an observed *m*/*z* of 749.13 Da identical to the expected *m*/*z* value for UDP-MurNac-Ala. The synthesized product was stored frozen in water at 21.2 mM.

2.5. Spectrophotometric coupled enzymatic assay

Quantitative analysis of the inorganic phosphate released from the MurD ATPase enzyme was done using the spectrophotometric coupled enzymatic assay with the *Enz*Check® Phosphate Assay Kit (Molecular Probes, Invitrogen, Burlington, Ont., Canada). The standard enzymatic reaction was performed as described by the manufacturer in a 100 µl reaction as depicted in Fig. 1. The purine nucleoside phosphorylase (PNP) enzyme was added with the substrate 2-amino-6-mercapto-7-methylpurine riboside (MESG) along with 400 nM of purified MurD, 300 µM of ATP, 20 µM of UDP-MurNac-Ala and 100 µM of D-Glu in a final volume of 100 µl. The optical density was continuously monitored at 360 nm for a period of 30 min at room temperature with a Cary spectrophotometer (Varian, Mississauga, Ont., Canada). The MurD enzymatic kinetics were determined from the linear curve portion using the least-squares calculation as previously described [30]. A positive control using the phosphate standard solution (*Enz*Check® Phosphate Assay Kit) was performed along with negative controls without the enzyme or without UDP-MurNac-Ala.

2.6. Evaluation of the MurD inhibitory potential of the synthesized consensus peptides

Inhibition of the MurD ATPase activity by consensus peptides was determined using various concentrations of peptides with the MurD coupled enzymatic assay (see Section 2.5). Enzymatic velocity for MurD was determined with each peptide concentration, compared to the reference enzymatic rate without peptide and used to calculate the percentage of inhibition values. The percentages of MurD inhibition values were used to determine the peptide concentrations required to inhibit 50% of the ATPase activity of MurD (IC_{50}) [25]. As controls, the effect of inhibitory concentrations of each peptide, established at 5 mM for MurDp1 and 15 mM for MurDp2, was analyzed on the coupled enzymatic assay. Their phosphate content was determined using the *Enz*Check® Phosphate Assay Kit. The inhibition capacities of both peptides were evaluated using the PNP enzyme

system with the phosphate standard solution. Interaction of peptides with proteins was evaluated using bovine serum albumin (BSA) at 10,000 times the MurD enzyme concentration. The effect of the reducing agent dithiothreitol (DTT) was analyzed on the inhibitory capacities of both peptides by determination of IC_{50} values with 10 mM of DTT.

2.7. Bioinformatics analysis

The peptide consensus sequences identified from the phage display screening were analyzed for homologs in the UniProt database using the software programs of the Wisconsin Package, Genetics Computer Group software (GCG, Version 10.2, Accelrys, Madison, WI). The BLAST, FASTA and SSearch programs from the GCG software and the fasts34 program from the FASTA software package were used to identify protein homologs with the consensus peptide sequences in the UniProt protein sequence database. For database searching, the flanked Cys residues of the C-7-C consensus peptide were removed from the amino acid sequence. The most relevant protein homologs were characterized using the Conserved Domain Architecture Retrieval Tool (CDART) from NCBI [14] as well as the BLAST program. As a control, a randomly chosen seven amino acid sequence from the known ϕKZ *P. aeruginosa* phage endolysin protein encoded by the ORF144 [21] was submitted to the fasts34 program.

3. Results

3.1. Purification of biologically active MurD enzyme

The purified *P. aeruginosa* MurD protein was visualized as a single 51 kDa band on SDS-PAGE (data not shown). The MurD ATPase assay showed that 1 μM of the MurD enzyme completely hydrolyzed the P^{32}-labeled ATP substrate giving a single inorganic phosphate spot on TLC (data not shown); the negative controls gave no ATP hydrolysis and confirmed that the purified MurD enzyme was biologically active.

3.2. Affinity selection of MurD binding peptides

As depicted in Table 1, each round of biopanning eluted a lower phage titer for each library used from approximately 10^{10}–10^{11} down to 3×10^{6} plaque forming units (PFUs). The first and second rounds of biopanning permitted an enrichment of the phage population visualized by the higher percentage values of phage recovered. We noted an increase in the percentage of elution after two rounds suggesting that specific phages had been identified. In contrast, the third round of biopanning gave lower phage recovery for each library and each elution strategy (Table 1). DNA sequencing of 10 randomly selected phages for each elution condition after the third round of biopanning identified a variety of peptide sequences containing consensus motifs (Fig. 2). Analysis of the frequency of peptide sequences gave a different consensus sequence for each library (Fig. 2). The 12 mers consensus peptide defined as HLPTSSLFDTTH presented a Ser–Ser–Leu–Phe predominantly conserved motif. The C-7-C consensus sequence CIPSHTPRC was more frequent than the 12 mers consensus and we noted that the Pro and Arg residues were particularly conserved (Fig. 2). Both consensus sequences were mostly recovered from the D-Glu and Gly elution steps. Even if the C-7-C mers consensus sequence was more frequent than the 12 mers, the overall sequence diversity was similar from both libraries (Fig. 2). For each phage display library, the different elution conditions used permitted the selection of different peptide sequences. Among the C-7-C library, the Gly and ATP elutions recovered the CYSAPVSAC peptide sequence (indicated by the superscript letter ‘a’ in Fig. 2). The 12 mers NPHWSSLYAPRN (marked by superscript letter ‘b’ in Fig. 2) was recovered twice in the Gly elution step and once in the ATP elution step. This peptide sequence contains the Ser–Ser–Leu motif predominantly conserved in the 12 mers consensus followed by a Tyr instead of a Phe residue that belongs to the same family of hydrophobic aromatic amino acids. The FAKNSNSRILDQ sequence (indicated by the superscript letter ‘c’ in Fig. 2) was also found in the Gly and ATP elution steps at round three.

3.3. Inhibition of MurD ATPase activity using consensus peptides

Peptides were synthesized from consensus sequences (see Section 2.3) to evaluate their inhibitory potential against the essential MurD enzyme. The C-7-C mers MurDp1 gave a decrease of MurD ATPase activity with a significant IC_{50} value of 4 μM (Fig. 3a). The 12 mers MurDp2 inhibited MurD with an IC_{50} value of 15 mM indicating a weak inhibition (Fig. 4). Both peptides showed a correlation between an increase in concentration versus an increase in inhibition values. This effect was more pronounced for MurDp2 as shown in Fig. 4. The reducing effect of DTT significantly altered the inhibitory potential of MurDp1. The DTT-exposed MurDp1 peptide showed a 100 times higher IC_{50} value of 400 μM (Fig. 3b). The three inhibition curves displayed a sigmoidal dose–response trend having variable slopes as shown in Fig. 3 and Fig. 4. DDT did not affect the IC_{50} values of the 12 mers MurDp2 peptide. Both peptides gave similar IC_{50} values in the presence of BSA. MurDp1 and MurDp2 peptides included in control reactions did not compete in the PNP coupled enzymatic assay (see Section 2.6 and Fig. 1) used to quantify the release of inorganic phosphate by MurD (data not shown). MurDp1 and MurDp2 peptides specifically inhibited MurD but MurDp2 was not considered as an inhibitor.

3.4. Bioinformatics analysis

To find additional information about the consensus peptides identified as interacting with MurD, we searched for homologs in the protein database. As a preliminary test, we used a 7 mers peptide encoded in the ϕKZ endolysin sequence; the fasts34 program identified the homolog of the seven amino acids in the UniProt database available (see Section 2.7). A perfect match was obtained with the ϕKZ phage endolysin identified as the most relevant protein homolog. The BLAST, FASTA and SSearch programs did not find any protein homologs with the ϕKZ 7 mers peptide. Analysis of MurDp1 and MurDp2 peptide sequences with the fasts34 program against the UniProt database identified a variety of protein homologs. The most relevant MurDp1 homolog was a hypothetical protein from *Azotobacter vinelandii* (UniProt accession number Q4ITH0). Human enterovirus and echovirus capsid proteins contained short peptide homologs with MurDp1 (Fig. 5A). Similar peptide homologs were found with two hypothetical proteins from

Corynebacterium diphtheriae and *Nocardia farcinica* (UniProt accession numbers Q6NFN2 and Q5Z0V8, respectively). Among bacterial protein homologs identified with fasts34, CDART analysis identified an aminopeptidase domain suggesting a potential role in amino acid metabolism. The MurDp1 alignment depicted in Fig. 5A was also obtained with the *Bacillus stearothermophilus* dehydroramnose epimerase protein implicated in bacterial surface glycosylation and with *Ralstonia metallidurans* and *Saccharomyces cerevisiae* DSBA oxydoreductase proteins. The fasts34 analysis of the 12 mers consensus sequence HLPTSSLFDTTH gave an alignment with proteins from *Pseudomonas* species. Each of the *P. aeruginosa*, *P. syringae*, *P. putida* and *P. fluorescens* protein homologous with MurDp2 was identified as cytoplasmic glyceraldehyde 3-phosphate dehydrogenase (GADPH) enzyme. GADPH from various other bacterial species such as *Legionella pneumophila* and *Anaeromyxobacter dehalogenans* were also recognized as MurDp2 homologs. All GADPH proteins showed the same eight amino acids overlapping sequence (Fig. 5B) defined as the best fasts34 MurDp2 homolog. We noted that the most conserved residues of the 12 mers consensus sequence were homologous with the GADPH protein (see Section 3.2 and Fig. 5B). The second most relevant MurDp2 homolog was the *Mycoplasma hyopneumoniae* glucokinase protein with eight similar amino acids found at the N-terminus of MurDp2 (data not shown). A CDART analysis predicted an *N*-acetylglucosamine kinase motif.

4. Discussion

To select for phage-encoded peptides that specifically interact with the MurD cell wall biosynthesis enzyme, three rounds of phage display were performed. Increasing the stringency of washes during the second round contributed to the selection of higher affinity binding phages; this is shown by obtaining only a fraction of phage PFUs when compared to the PFUs of the first round (Table 1). We noted that the second round of biopanning gave a higher percentage of phage eluted than the first round for each library as for MurC [10]. This indicated an enrichment of the phage population interacting with the targeted protein. The competitive biopanning of MurC gave a higher phage recovery titer after the third round of biopanning when compared with MurD [10]. Limiting the time of contact

between the phage peptides and MurD could explain the lower percentages of phages obtained in the third round (Table 1). Indeed, the time of contact between the phage peptides and MurD represents a more important factor for phage specificity than the stringency of washes. One can argue that only very specific phages could bind tightly to the targeted MurD protein in a short time. When the time of contact between phage peptides and MurD was restricted to 10 min instead of 60 min, this allowed a stringent selection of phage specificity for MurD. We cannot exclude the possibility that phages with the highest peptide affinity for MurD are difficult to elute. Phages encoding peptides with very high binding properties may not be recovered when using a gentle 5 min Gly elution step critical to preserve phage particle integrity [15]. If we assume that the two phage libraries used contained more phages having high affinity with MurD than with MurC, this could explain a lower percentage of phages obtained during the elution steps with MurD [10]. It should be noted that several other factors affect phage recovery such as phage infection and replication efficiency, protein translocation and folding bias as well as pIII coat stability [5].

As different elution conditions gave various peptides but consensus sequences (Fig. 2), we demonstrate here the importance of attempting different elution conditions. Indeed, the phage display screenings performed on the MurD, MurC, FtsZ and FtsA proteins using similar experimental conditions did not identify any redundant sequences [10,25,26]. Hence, we used a competitive biopanning with ATP and D-Glu at concentrations based upon their kinetic constants. The K_m for MurD is 57 μM for ATP and 64 μM for D-Glu [3]. We hypothesize that both consensus sequences predominantly interact with the D-Glu binding site of the MurD protein since the D-Glu and Gly elution steps mostly recovered those sequences (Fig. 2). The *E. coli* MurD protein crystal structure showed that the enzyme contains three distinct domains. The binding site for each substrate was localized in one particular domain; UDP-MurNac-Ala mainly interacts with the N-terminal domain, ATP binds principally to the central portion of MurD and D-Glu interacts at the C-terminus. The ATP molecule binds first to the MurD protein to enhance a conformational change that brings the C-terminal domain toward the N-terminal and central domains [2]. We entertain the possibility that ATP elution during biopanning could lead to a MurD conformational change displacing the peptides bound to the D-Glu interacting site.

The most conserved amino acid residues of the MurDp1 peptide sequence (see Section 3.2) could be essential for MurD binding and inhibition. The loop conformation of MurDp1 was shown to be important for the strong inhibition of MurD ATPase activity (see Section 3.3). MurDp1 is the best inhibitor identified by our phage display strategy with an IC_{50} value in the micromolar range [10,25,26]. The precise inhibition mechanism of MurDp1 must undergo further characterization as recent enzyme kinetics analysis did not reveal a general trend in the mechanism of peptide inhibition [18].

Peptide inhibitors containing short amino acid sequences are difficult to compare with amino acid motifs. We show here that the fasts34 software may represent an approach for finding short peptide homologs. The identification of aminopeptidase and surface glycosylation enzyme motifs with MurDp1 could indicate a relationship with peptidoglycan metabolism [20]. Identification of the DSBA amino acid sequence is of interest since this oxydoreductase is involved in disulfide bond formation in the bacterial periplasmic space [7]. The 12 mers MurDp2 homology to bacterial GADPH enzymes suggested that the MurDp2 peptide could interact with MurD at a GADPH binding site and have no significant effect on the active site. The surface-located GAPDH has been found in various bacterial and yeast pathogens and defined as a virulence factor [9,22,24]. There were no data supporting translocation of GADPH through the bacterial membrane and its association with the cell wall. Thus, MurD could bind the cytoplasmic GAPDH to the peptidoglycan [9]. Indeed, MurDp2 could potentially constitute an efficient MurD–GAPDH protein–protein interaction inhibitor that may block GAPDH integration into the bacterial cell wall.

4.1. Conclusion

This is the first report describing peptide inhibitors of MurD. Previously, a computer-based molecular design has been used to produce new macrocyclic systems targeted against MurD [17]. The novel metathesis-based cyclization gave good inhibition when assayed against MurD. Recently, Pulvinones have been synthesized as inhibitors of MurA–MurD enzymes with IC_{50} values of 1–10 μg/ml [1]. The design, synthesis and structure–activity relationships of new phosphinate inhibitors tested against MurD enzyme from *E. coli* gave

two compounds with IC_{50} values near 100 μM [33]. As an alternative approach to these small molecules, this work represents an example of using phage display for selecting peptides not only as potent enzyme inhibitors with an IC_{50} value at 4 μM, but also in identifying potential protein–protein interaction sites. A second phase in developing peptide inhibitors would be to enhance antimicrobial activity by using peptidomimetics [23]. Inhibitory peptides are notorious for not being able to cross bacterial membranes. To evade this problem, peptides may be conjugated to a bacterial transport molecule. To circumvent bacterial resistance [32], peptide vectors capable of transport into cells in the form of covalent conjugates may be more appropriate [13]. Peptide inhibitors described here are lead compounds whose amino acids could be modified to mimic antimicrobial peptides. Indeed, the activity of antimicrobial peptides is thought to be determined by helicity and hydrophobicity rather than by their specific amino acid sequences [8,31]. Finally, ribosome display could be exploited to optimize their antibacterial properties [4].

Acknowledgements

We thank Le Service de Séquence de Peptides de l'Est du Québec and Le Service d'analyse et de Synthèse d'acides Nucléiques de l'Université Laval as well as Jérome Laroche for bioinformatic advices. This work was funded by the Canadian Bacterial Diseases Network via the Canadian Centers of Excellence, a FCAR infrastructure team grant to R.C. Levesque and a CRSNG studentship to Catherine Paradis-Bleau.

References

[1] Antane S, Caufield CE, Hu W, Keeney D, Labthavikul P, Morris K, et al. Pulvinones as bacterial cell wall biosynthesis inhibitors. Bioorg Med Chem Lett 2006;16:176-80.

[2] Bertrand JA, Fanchon E, Martin L, Chantalat L, Auger G, Blanot D, et al. "Open" structures of MurD: domain movements and structural similarities with folylpolyglutamate synthetase. J Mol Biol 2000;301:1257-66.

[3] Bouhss A, Dementin S, Parquet C, Mengin-Lecreulx D, Bertrand JA, Le Beller D, et al. Role of the ortholog and paralog amino acid invariants in the active site of the UDP-MurNAc-L-alanine:D-glutamate ligase (MurD). Biochemistry 1999;38:12240-7.

[4] Burns KL, May SW. Separation methods applicable to the evaluation of enzyme-inhibitor and enzyme-substrate interactions. J Chromatogr B Analyt Technol Biomed Life Sci 2003;797:175-90.

[5] Carettoni D, Gomez-Puertas P, Yim L, Mingorance J, Massidda O, Vicente M, et al. Phage-display and correlated mutations identify an essential region of subdomain 1C involved in homodimerization of *Escherichia coli* FtsA. Proteins 2003;50:192-206.

[6] Christensen DJ, Gottlin EB, Benson RE, Hamilton PT. Phage display for target-based antibacterial drug discovery. Drug Discov Today 2001;6:721-7.

[7] Collet JF, Bardwell JC. Oxidative protein folding in bacteria. Mol Microbiol 2002;44:1-8.

[8] Dathe M, Wieprecht T. Structural features of helical antimicrobial peptides: their potential to modulate activity on model membranes and biological cells. Biochim Biophys Acta 1999;1462:71-87.

[9] Delgado ML, Gil ML, Gozalbo D. Starvation and temperature upshift cause an increase in the enzymatically active cell wall-associated glyceraldehyde-3-phosphate dehydrogenase protein in yeast. FEMS Yeast Res 2003;4:297-303.

[10] El Zoeiby A, Sanschagrin F, Darveau A, Brisson JR, Levesque RC. Identification of novel inhibitors of *Pseudomonas aeruginosa* MurC enzyme derived from phage-displayed peptide libraries. J Antimicrob Chemother 2003;51:531-43.

[11] El Zoeiby A, Sanschagrin F, Havugimana PC, Garnier A, Levesque RC. In vitro reconstruction of the biosynthetic pathway of peptidoglycan cytoplasmic precursor in *Pseudomonas aeruginosa*. FEMS Microbiol Lett 2001;201:229-35.

[12] El Zoeiby A, Sanschagrin F, Levesque RC. Structure and function of the Mur enzymes: development of novel inhibitors. Mol Microbiol 2003;47:1-12.

[13] Fischer PM, Krausz E, Lane DP. Cellular delivery of impermeable effector molecules in the form of conjugates with peptides capable of mediating membrane translocation. Bioconjug Chem 2001;12:825-41.

[14] Geer LY, Domrachev M, Lipman DJ, Bryant SH. CDART: protein homology by domain architecture. Genome Res 2002;12:1619-23.

[15] Hoess RH. Protein design and phage display. Chem Rev 2001;101:3205-18.

[16] Hoiby N. Understanding bacterial biofilms in patients with cystic fibrosis: current and innovative approaches to potential therapies. J Cyst Fibros 2002;1:249-54.

[17] Horton JR, Bostock JM, Chopra I, Hesse L, Phillips SE, Adams DJ, et al. Macrocyclic inhibitors of the bacterial cell wall biosynthesis enzyme MurD. Bioorg Med Chem Lett 2003;13:1557-60.

[18] Hyde-DeRuyscher R, Paige LA, Christensen DJ, Hyde-DeRuyscher N, Lim A, Fredericks ZL, et al. Detection of small-molecule enzyme inhibitors with peptides isolated from phage-displayed combinatorial peptide libraries. Chem Biol 2000;7:17-25.

[19] Levy SB, Marshall B. Antibacterial resistance worldwide: causes, challenges and responses. Nat Med 2004;10:S122-9.

[20] Ma Y, Stern RJ, Scherman MS, Vissa VD, Yan W, Jones VC, et al. Drug targeting *Mycobacterium tuberculosis* cell wall synthesis: genetics of dTDP-rhamnose synthetic enzymes and development of a microtiter plate-based screen for inhibitors of conversion of dTDP-glucose to dTDP-rhamnose. Antimicrob Agents Chemother 2001;45:1407-16.

[21] Mesyanzhinov VV, Robben J, Grymonprez B, Kostyuchenko VA, Bourkaltseva MV, Sykilinda NN, et al. The genome of bacteriophage phiKZ of *Pseudomonas aeruginosa*. J Mol Biol 2002;317:1-19.
[22] Modun B, Morrissey J, Williams P. The staphylococcal transferrin receptor: a glycolytic enzyme with novel functions. Trends Microbiol 2000;8:231-7.
[23] Nefzi A, Dooley C, Ostresh JM. Houghten RA. Combinatorial chemistry: from peptides and peptidomimetics to small organic and heterocyclic compounds. Bioorg Med Chem Lett 1998;8:2273-8.
[24] Pancholi V, Chhatwal GS. Housekeeping enzymes as virulence factors for pathogens. Int J Med Microbiol 2003;293:391-401.
[25] Paradis-Bleau C, Sanschagrin F, Levesque RC. Identification of *Pseudomonas aeruginosa* FtsZ peptide inhibitors as a tool for development of novel antimicrobials. J Antimicrob Chemother 2004;54:278-80.
[26] Paradis-Bleau C, Sanschagrin F, Levesque RC. Peptide inhibitors of the essential cell division protein FtsA. Protein Eng Des Sel 2005;18:85-91.
[27] Pierce GE. *Pseudomonas aeruginosa*, *Candida albicans*, and device-related nosocomial infections: implications, trends, and potential approaches for control. J Ind Microbiol Biotechnol 2005;32:309-18.
[28] Projan SJ. New (and not so new) antibacterial targets - from where and when will the novel drugs come? Curr Opin Pharmacol 2002;2:513-22.
[29] Reddy SG, Waddell ST, Kuo D,W, Wong KK, Pompliano DL. Preparative enzymatic synthesis and characterization of the cytoplasmic intermediates of murein biosynthesis. J Am Chem Soc 1999;121:1175-8.
[30] Savoie A, Sanschagrin F, Palzkill T, Voyer N, Levesque RC. Structure-function analysis of alpha-helix H4 using PSE-4 as a model enzyme representative of class A beta-lactamases. Protein Eng 2000;13:267-74.
[31] Shai Y, Oren Z. From "carpet" mechanism to de-novo designed diastereomeric cell-selective antimicrobial peptides. Peptides 2001;22:1629-41.
[32] Silver, LL. Novel inhibitors of bacterial cell wall synthesis. Curr Opin Microbiol 2003;6:431-8.
[33] Strancar K, Blanot D, Gobec S. Design, synthesis and structure-activity relationships of new phosphinate inhibitors of MurD. Bioorg Med Chem Lett 2006;16:343-8.
[34] Walsh AW, Falk PJ, Thanassi J, Discotto L, Pucci MJ, Ho HT. Comparison of the D-glutamate-adding enzymes from selected gram-positive and gram-negative bacteria. J Bacteriol 1999;181:5395-401.
[35] Young KD. Bacterial shape. Mol Microbiol 2003;49:571-80.

Figure Captions

Figure 1. Spectrophotometric MurD enzymatic coupled assay used to evaluate the inhibitory potential of synthesized peptides obtained from consensus sequences. The UDP-*N*-acetylmuramyl-l-Ala-d-Glu (UDP-MurNac-Ala-Glu) MurD amide ligase catalyzed the

addition of a d-Glu amino acid residue to the UDP-*N*-acetylmuramyl-l-Ala (UDP-MurNac-Ala) and the consequent release of inorganic phosphate from ATP. In the presence of inorganic phosphate, the substrate 2-amino-6-mercapto-7-methylpurine riboside (MESG) was converted by the purine nucleoside phosphorylase (PNP) to ribose 1-phosphate and 2-amino-6-mercapto-7-methylpurine and could be detected at 360 nm.

Figure 2. Peptide sequences obtained from the two phage display libraries obtained by sequencing of selected phages eluted after the third round of biopanning against MurD. Acidic amino acids (D and E) are in green, polar amino acids (Q and N) are in light green, basic amino acids (K, R and H) are in blue, hydrophobic amino acids (I, L, M and V) are in rose, hydrophobic aromatic amino acids (F, Y and W) are in red, small amino acids (A, S, C and T) are in pink, G (smallest amino acid) is in orange and P (leading to turn formation) is in black (classified according to the Venn diagram for defining the relationships between amino acids). Consensus sequences are boxed in black and the superscript letters 'a', 'b' and 'c' indicate peptide sequences recovered by both the Gly and ATP elution steps during biopanning. (For interpretation of the references to color in this figure legend, the reader is referred to the web version of the article.)

Figure 3. IC_{50} determination for the MurDp1 C-7-C mers peptide inhibitor of MurD ATPase activity (a) without and (b) with the reducing agent DTT. Percentage of inhibition was measured as a function of the concentration of the peptide inhibitor.

Figure 4. IC_{50} determination for the MurDp2 12 mers peptide inhibitor of MurD ATPase activity.

Figure 5. Alignment of homologous regions between the: (A) MurDp1 C-7-C mers consensus peptide and the human echovirus 30 capsid amino acid sequence and (B) MurDp2 12 mers consensus peptide and the *P. aeruginosa* glyceraldehyde 3-phosphate dehydrogenase (GADPH) amino acid sequence identified by the fasts34 program. The double dots refer to an identical amino acid residue in both sequences and a single dot refers to a residue from the same amino acid group.

Table I

Phage titers obtained after three rounds of biopanning using MurD and the C-7-C mers and 12 mers phage peptide libraries.

	C-7-C mers library			12 mers library		
	Phage input	Eluted phages	Elution (%)	Phage input	Eluted phages	Elution (%)
Round 1						
Gly-HCL	$2x10^{11}$	$3x10^{6}$	$1.5x10^{-3}$	$4x10^{10}$	$3x10^{6}$	$7.5x10^{-3}$
Round 2						
Gly-HCL	$1x10^{10}$	$1x10^{6}$	$1x10^{-2}$	$1.7x10^{11}$	$6.3x10^{7}$	$3.7x10^{-2}$
Round 3						
Gly-HCL	$1x10^{11}$	$3x10^{4}$	$3x10^{-5}$	$2x10^{12}$	$1.5x10^{4}$	$7.5x10^{-7}$
ATP		$4x10^{4}$	$4x10^{-5}$		$1x10^{4}$	$5x10^{-7}$
D-Glu		$2x10^{4}$	$2x10^{-5}$		$7.5x10^{3}$	$3.8x10^{-7}$

Figure 1.

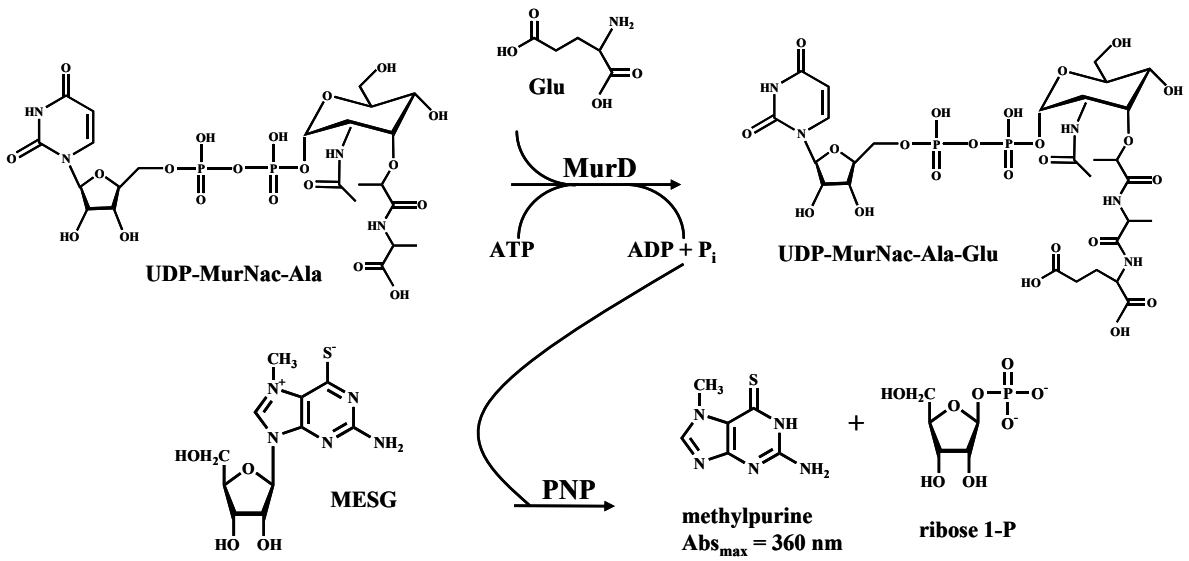
UDP-MurNac-Ala
Glu
MurD
ATP
ADP + P$_i$
UDP-MurNac-Ala-Glu
MESG
PNP
methylpurine
Abs$_{max}$ = 360 nm
ribose 1-P

Figure 2.

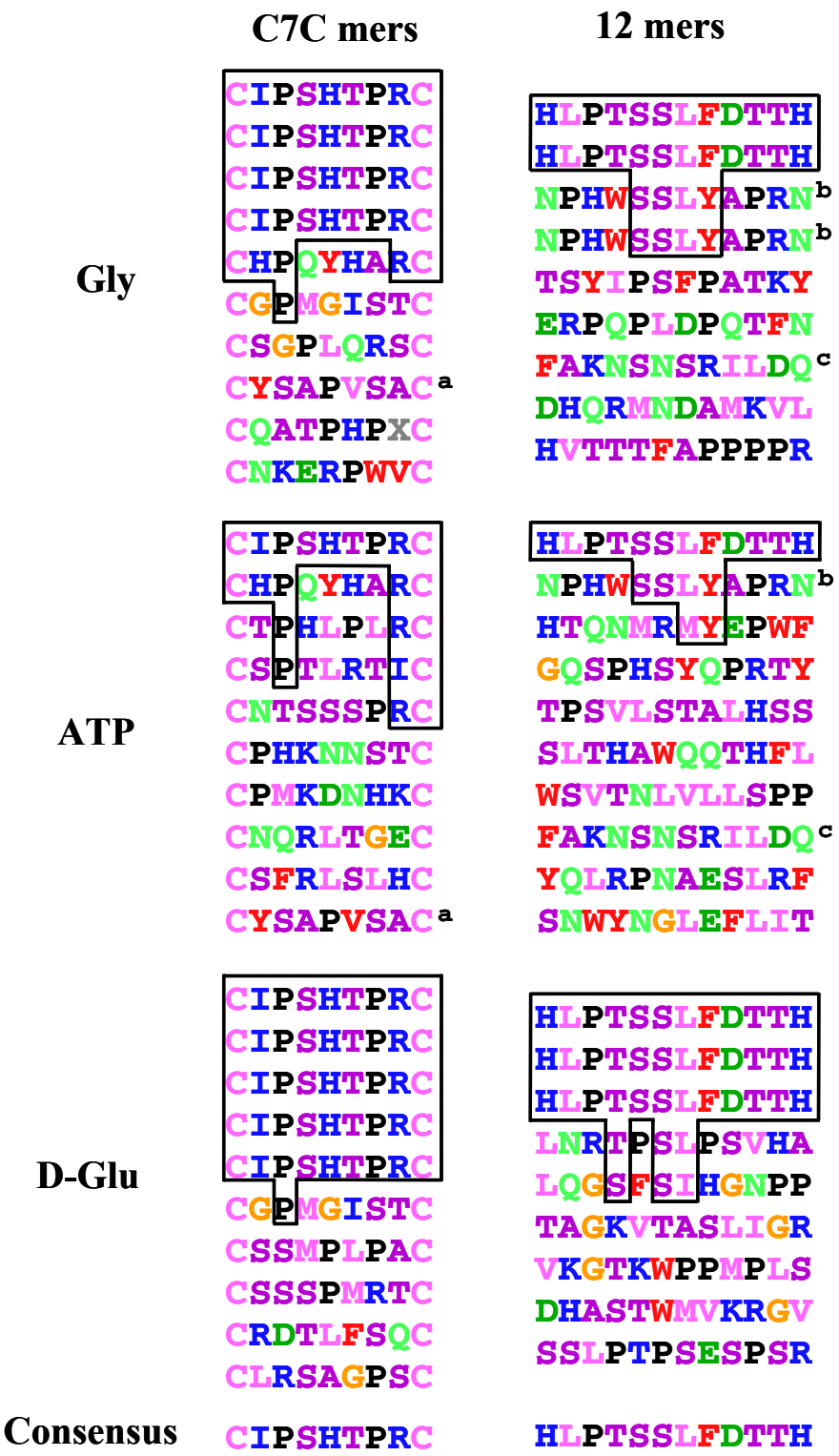
C7C mers
12 mers
Gly
CIPSHTPRC
CIPSHTPRC
CIPSHTPRC
CIPSHTPRC
CHPQYHARC
CGPMGISTC
CSGPLQRSC
CYSAPVSAC a
CQATPHPXC
CNKERPWVC
HLPTSSLFDTTH
HLPTSSLFDTTH
NPHWSSLYAPRN b
NPHWSSLYAPRN b
TSYIPSFPATKY
ERPQPLDPQTFN
FAKNSNSRILDQ c
DHQRMNDAMKVL
HVTTTFAPPPPR
ATP
CIPSHTPRC
CHPQYHARC
CTPHLPLRC
CSPTLRTIC
CNTSSSPRC
CPHKNNSTC
CPMKDNHKC
CNQRLTGEC
CSFRLSLHC
CYSAPVSAC a
HLPTSSLFDTTH
NPHWSSLYAPRN b
HTQNMRMYEPWF
GQSPHSYQPRTY
TPSVLSTALHSS
SLTHAWQQTHFL
WSVTNLVLLSPP
FAKNSNSRILDQ c
YQLRPNAESLRF
SNWYNGLEFLIT
D-Glu
CIPSHTPRC
CIPSHTPRC
CIPSHTPRC
CIPSHTPRC
CIPSHTPRC
CGPMGISTC
CSSMPLPAC
CSSSPMRTC
CRDTLFSQC
CLRSAGPSC
HLPTSSLFDTTH
HLPTSSLFDTTH
HLPTSSLFDTTH
LNRTPSLPSVHA
LQGSFSIHGNPP
TAGKVTASLIGR
VKGTKWPPMPLS
DHASTWMVKRGV
SSLPTPSESPSR
Consensus
CIPSHTPRC
HLPTSSLFDTTH

Figure 3.

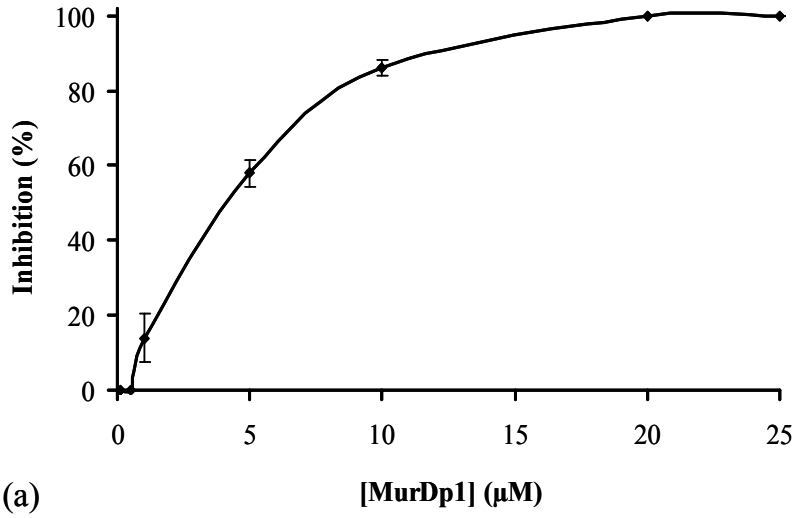
100
80
60
40
20
0
Inhibition (%)
0
5
10
15
20
25
[MurDp1] (µM)

(a)

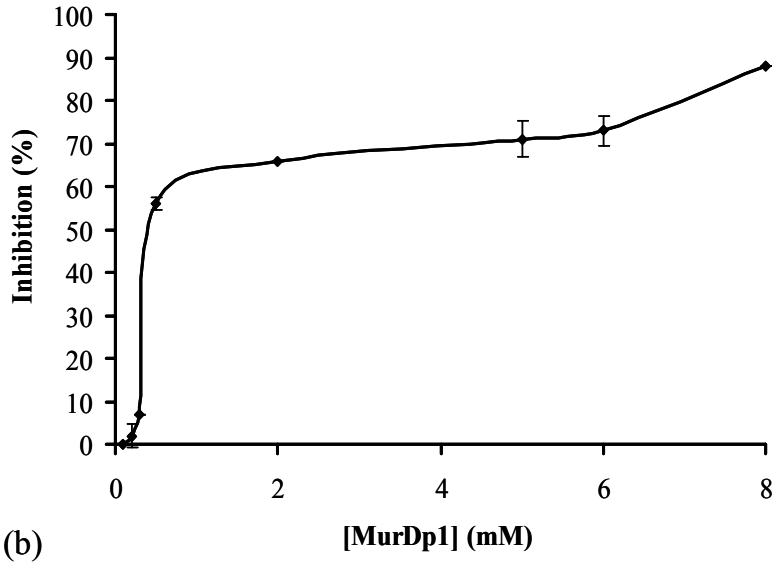
100
90
80
70
60
50
40
30
20
10
0
Inhibition (%)
0
2
4
6
8
[MurDp1] (mM)

(b)

Figure 4.

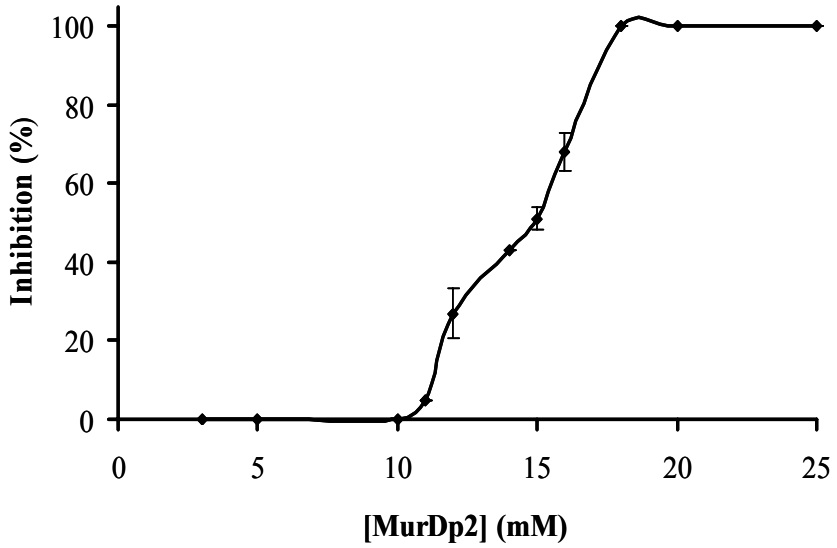

Figure 5.

(A)

```
MurDp1                                RPTHSPI
                                      : :::::.
human echovirus 30 capsid protein  284 RSTHSPL 290
```

(B)

```
MurDp2                             HLPTSSLFDTTH
                                   : : ::.::   :
P. aeruginosa GAPDH             288 HDPRSSIFDANH 299
```

Chapitre 6 - *Pseudomonas aeruginosa* MurE amide ligase: enzyme kinetics, specific interacting peptide sequences and inhibitory activity of a peptide targeting cell wall biosynthesis

Résumé

L'amide ligase MurE de *Pseudomonas aeruginosa*: analyse de la cinétique enzymatique, sélection de séquences peptidiques spécifiques interagissant avec la protéine et caractérisation de l'activité inhibitrice d'un peptide inhibiteur prometteur ciblant la biosynthèse de la paroi bactérienne

La dissémination des mécanismes de résistance aux antibiotiques parmi les pathogènes bactériens représente une problématique extrêmement préoccupante. Afin d'identifier une nouvelle classe d'inhibiteurs contre la biosynthèse de la paroi bactérienne, l'enzyme MurE de *P. aeruginosa* a été sélectionnée en tant que cible innovatrice. Cette enzyme essentielle catalyse la formation d'un lien amide entre l'acide meso-diaminopimélique (meso-A2pm) et le précurseur nucléotidique UDP-N-acetylmuramyle-L-alanyle-D-glutamate (UDP-MurNac-Ala-Glu) en hydrolysant de l'ATP en ADP et en phosphate inorganique. Le substrat nucléotidique de MurE a été synthétisé puis l'activité enzymatique de la protéine purifiée a été caractérisée. MurE a ensuite été utilisée pour cribler une banque contenant 10^9 peptides différents par présentation phagique. Les phages adhérés ont été élués avec de la glycine à pH acide et de façon compétitive avec l'ATP et le meso-A2pm. Le consensus peptidique prédominant a ensuite été synthétisé. Le peptide MurEp1 inhibe spécifiquement l'activité enzymatique de MurE avec une CI_{50} de 500 µM, un K_i de 160 µM contre le meso-A2pm et un K_i de 77 µM contre le UDP-MurNac-Ala-Glu. L'inhibition de MurE par MurEp1 est dépendante du temps de préincubation et elle est annulée par l'ajout du meso-A2pm ou du UDP-MurNac-Ala-Glu lors de la période de preincubation. Les résultats indiquent que le peptide MurEp1 est un inhibiteur de type mixte qui bloque la réaction enzymatique de MurE en inhibant la formation du lien amide entre le meso-A2pm et l'UDP-MurNac-Ala-Glu. Ainsi, cette étude a identifié le premier peptide inhibiteur de MurE dont le mode d'action innovateur permet d'envisager le développement de nouveaux antimicrobiens par peptidomimétisme.

Contribution des auteurs

Cinq auteurs signent la réalisation de cet article scientifique rédigé en vue d'une publication dans la revue scientifique «Proteins». En tant que première auteure, j'ai tout d'abord préparé l'enzyme MurE et j'ai effectué le criblage peptidique par présentation phagique. Adrian Lloyd a synthétisé, purifié et analysé le substrat nucléotidique de MurE qui n'est pas disponible commercialement. À ce moment, Adrian Lloyd était étudiant au doctorat sous la direction du Dr Timothy D. H. Bugg qui a supervisé cette étape du projet. J'ai ensuite mis au point un essai spectrophotométrique afin de quantifier et de caractériser l'activité enzymatique de MurE. À l'aide de cet essai, j'ai analysé le potentiel inhibiteur et le mode d'action du consensus peptidique sélectionné contre MurE lors du criblage par présentation phagique. J'ai finalement interprété les résultats, j'ai préparé les figures et les tableaux puis j'ai rédigé presque entièrement le manuscrit. La section décrivant la synthèse du substrat nucléotidique a été écrite par Adrian Lloyd et la figure correspondante a été préparée en collaboration avec Adrian Lloyd et le Dr Timothy D. H. Bugg. En ce qui concerne le Dr François Sanschagrin, il m'a apportée un support technique et scientifique au cours de cette étude. Finalement, le Dr Roger C. Levesque est à l'origine de l'idée de départ et de la conceptualisation du projet de recherche. Il a donc orienté le projet puis il a révisé le manuscrit pour en augmenter la fluidité et la valeur scientifique.

Pseudomonas aeruginosa MurE amide ligase: enzyme kinetics, specific interacting peptide sequences and inhibitory activity of a peptide targeting cell wall biosynthesis

Catherine Paradis-Bleau[1], Adrian Lloyd[2], François Sanschagrin[1], Tom Clarke[2], Ann Blewett[2] , Timothy D. H. Bugg[2], Roger C. Levesque[1*]

[1] *Département de Biologie Médicale, Université Laval, Québec, Québec, Canada, G1K 7P4*

[2] *Department of chemistry, University of Warwick, Coventry, United Kingdom, CV4 7AL*

[*] Corresponding author. Roger C. Levesque, Centre de recherche sur la fonction, la structure et l'ingénierie des protéines, pavillon Charles-Eugène Marchand, Université Laval, Québec, Québec, Canada, G1K 7P4, Tel: (1) (418) 656-3070; Fax: (1) (418) 656-7176; e-mail: rclevesq@rsvs.ulaval.ca.

Short title: kinetics of a novel MurE peptide inhibitor

Keywords: UDP-N-acetylmuramoyl-L-alanyl-D-glutamate:meso-diaminopimelate ligase, meso-diaminopimelic adding enzyme, phage display, peptide inhibitor, time-dependent mixed inhibitor

Abstract

The cell-wall-synthesizing enzyme MurE of *Pseudomonas aeruginosa* was studied, using the substrates uridine 5'-diphosphoryl N-acetylmuramoyl-L-alanyl-D-glutamate (UDP-MurNAc-Ala-Glu), meso-diaminopimelic acid (meso-A2pm) and ATP and a peptide inhibitor identified by phage display competitive biopanning. Biopanning was done with the specific substrates meso-A2pm and ATP using the M13 phage library encoding ~ 2.7 x 10^9 random peptide permutations. A consensus peptide thus identified among 30 phage-encoded peptides that interacted with MurE was synthesized as a potential inhibitor of MurE. Called MurEp1, this dodecamer was found to inhibit MurE ATPase activity specifically, with an IC_{50} value of 500 μM. The inhibition was shown to be time-dependent and reversed by the addition of meso-A2pm or UDP-MurNAc-Ala-Glu. MurEp1 acted as a mixed inhibitor against both substrates, with K_i values of 160 and 80 μM, respectively. MurEp1 thus interferes with the proximity of meso-A2pm and UDP-MurNAc-Ala-Glu necessary for amide bond formation between the substrates. The phage display approach has identified the first promising peptide inhibitor having a novel mode of action against the essential and unexploited MurE enzyme as a first step for future development of antibacterial agents targeting cell wall biosynthesis.

Introduction

The bacterial cell wall biosynthesis pathway constitutes one of the best targets for the design of new antibacterial agents needed to face the growing problem of antibiotic resistance among bacterial pathogens.[1,2] The enzymes involved in this pathway are essential for bacterial survival and pathogenesis leading to a lethal phenotype when inhibited, expressed during infection of the host, easily accessible for genetic manipulation, highly conserved among bacteria, and have no eukaryote counterpart.[3,4] Although many known antibiotics interfere with enzymes involved in the latter steps of the pathway, few target the enzymes that catalyze the cytoplasmic step. The unavailability of suitable intermediates has severely hampered kinetic and inhibitory studies of these enzymes.[4,5]

The cytoplasmic enzymes MurA through MurF achieve the first step of the pathway by catalyzing the synthesis of the precursor UDP-*N*-acetylmuramyl pentapeptide. We have

selected the highly specific MurE enzyme as the most suitable target. MurE is part of the sequence of four ATP-dependent amide ligases (MurC, MurD, MurE and MurF) that perform the stepwise addition of five amino acids (L-Ala, D-Glu, a di-amino acid, and D-Ala-D-Ala) to form the peptide moiety of the cell wall cytoplasmic precursor.[6] The non-ribosomal peptide bond formation involves a carboxyl activation of the nucleotide substrate to an acylphosphate intermediate by ATP followed by nucleophilic attack by the amino group of the condensing amino acids and elimination of the phosphate group.[4,6-12,13]

MurE is the only member of the Mur ligases for which amino acid substrate specificity differs among bacterial species. Typically, Gram-negative bacteria and bacilli contain a meso-diaminopimelic acid (meso-A2pm) residue at the third position of the cell wall peptide moiety, whereas Gram-positive bacteria contain L-lysine at this position.[14,15] MurE enzymes discriminate efficiently between substrates to catalyze the addition of either meso-A2pm or L-Lys to the nucleotide precursor UDP-N-acetylmuramoyl-L-alanyl-D-glutamate (UDP-MurNAc-Ala-Glu).[16,17] As a model system, we studied MurE or UDP-N-acetylmuramoyl-L-alanyl-D-glutamate:meso-diaminopimelate ligase from the Gram-negative bacterium *Pseudomonas aeruginosa*. This opportunistic pathogen is highly resistant to most classes of antibiotics and represents a major cause of chronic nosocomial infections.[18,19]

The addition of the meso-A2pm residue at the third position of the cell wall peptide moiety allows the formation of peptide side-chain cross-linkages and thus plays a key role in establishing the integrity of the shape-maintaining cell wall.[15,20] The latter steps of the biosynthesis involve essential transpeptidation reactions that form bonds between the meso-A2pm residue of one peptide moiety and a D-Ala or a meso-A2pm residue of an adjacent peptide side chain.[21] The meso-A2pm-meso-A2pm cross-bridge provides flexibility that enables bacteria to adapt the cross-linkage to different growth conditions and adverse environments.[20]

Phage display is a powerful tool for the selection of short peptide ligands that interact with proteins of interest among a large pool of random peptide permutations fused to the phage M13 pIII minor coat protein.[22,23] This approach has been useful for the identification of various peptide inhibitors of enzymes [24,25] including the Mur ligases MurC and MurD [26,27]. To study the kinetics of MurE amide ligase of *P. aeruginosa*, we

synthesized the UDP-MurNAc-Ala-Glu substrate and then used a phage display competitive biopanning approach with substrates meso-A2pm and ATP to identify a specific consensus peptide sequence potentially active against MurE.

Materials and methods

Purification of biologically active MurE enzyme

The MurE protein from *P. aeruginosa* was overexpressed, purified and sequenced as previously described.[30] All reagents were purchased from Sigma Aldrich (Oakville, Ontario, Canada) unless otherwise indicated. The phosphate present in the MurE conservation buffer was removed by dialyzing 3 ml three times against 3 l of buffer A (25 mM Bis-Tris Propane pH 8, 1 mM β-mercaptoethanol, 2.5 mM $MgCl_2$) at 4°C. Purified MurE protein was visualized on SDS-PAGE using SYPRO® Orange staining (Bio-Rad, Mississauga, Ontario, Canada) and the protein concentration was determined using the Bradford method (BioRad, Mississauga, Ontario, Canada) with bovine serum albumin as standard. Glycerol was added to the phosphate-free MurE solution to a concentration of 10% and the solution was aliquoted and kept at -20°C. The biological activity of MurE was assayed by *in vitro* reconstruction of the biosynthetic pathway of peptidoglycan cytoplasmic precursor in the presence of purified MurA, MurB, MurC, MurD and MurF as described previously.[30]

Synthesis and purification of UDP-MurNAc-Ala-Glu

Synthesis of UDP-MurNAc-Ala-Glu was performed according to a method described previously [31] except that the steps involved in the synthesis from UDP-GlcNAc were carried out in a single reaction using the combined activities of *P. aeruginosa* MurA, MurB, MurC and MurD enzymes. The Mur enzymes were removed by ultrafiltration and UDP-MurNAc-Ala-Glu was purified by loading the ultrafiltrate into a column packed with DEAE Sephacel pre-equilibrated in 10 mM ammonium acetate at pH 7.5 and eluting at room temperature with a 10-800 mM ammonium acetate (pH 7.5) gradient. A pyruvate kinase/lactate dehydrogenase coupled assay for meso-A2pm-dependent ADP generation by MurE was used to identify fractions containing the cell wall intermediate. Positive fractions

were freeze-dried three times to remove ammonium acetate. UDP-MurNAc-Ala-Glu purity was assessed by analytical anion exchange fast protein liquid chromatography on MonoQ^{TM} using a 0-0.5 M ammonium acetate gradient. Structure of the purified UDP-MurNAc-Ala-Glu was confirmed using negative ion electrospray mass spectrometry and the synthesized product was stored as frozen aqueous solution at 4.34 mM.

Kinetic characterization of MurE activity

The ATPase activity of the *P. aeruginosa* MurE protein was assessed by a spectrophotometric assay that quantifies released inorganic phosphate using the Lanzetta reagent.[32] The reaction was performed in 100 µl of reaction buffer B (50 mM Bis-Tris Propane pH 8.0, 1 mM dithiothreitol, 5 mM $MgCl_2$) containing purified MurE (40 nM, from a fresh aliquot for each assay), ATP (1 mM), UDP-MurNAc-Ala-Glu (200 µM) and meso-A2pm (10 mM). The MurE enzyme was allowed to react for 15 min at room temperature before the addition of 800 µl of the Lanzetta reagent. The mixture was incubated for 5 min to allow proper color development, 100 µl of a 34% (w/v) sodium citrate solution was added and the optical density was immediately measured at 660 nm with a Cary spectrophotometer (Varian, Mississauga, Ontario, Canada).[32] The amount of inorganic phosphate was determined by comparison to the linear portion of a phosphate standard curve with a minimum R^2 value of 0.99. The phosphate content of each component in the reaction was determined and subtracted from the total phosphate. Negative controls were performed without enzyme or substrate and assays were done in triplicate. Saturation curves were obtained individually for each substrate using fixed and optimal concentrations of the remaining substrates. The following parameters were determined for MurE with respect to each substrate: the maximal specific activity, the catalytic constant (k_{cat}), the Michaelis-Menten constant (K_m) and the enzyme efficiency (k_{cat}/K_m). Kinetic parameters were determined by nonlinear regression analysis by means of a square matrix of enzyme velocities based on the Michaelis-Menten equations using the Enzyme Kinetics Module version 1 of SigmaPlot version 8.

Affinity selection of phage displayed peptides against MurE

Phage display screening was performed using the PH.D.-12 M13 phage library containing ~ 2.7 x 10^9 peptide permutations (New England Biolabs, Mississauga, Ontario, Canada) as described previously.[26,28] The screening specificity and stringency were optimized by increasing the Tween concentration during washing and by decreasing the time of contact between the phages and the targeted MurE protein during the three rounds of biopanning. Phage titers used as input are given in Table III. Phages with encoded peptides were eluted at the third round of biopanning by 100 µl of 0.2 M glycine-HCl (pH 2.2) [26] as well as by 100 µl of 1 mM meso-A2pm and 100 µl of 1 mM ATP for 30 min. The DNA of ten phages was sequenced for each elution condition with a -96 gIII primer (New England Biolabs).[28] The deduced peptide sequences were aligned and consensus amino acids identified.

Peptide synthesis

The dodecamer peptide encoded by the strongest consensus sequence selected by the phage display screening (NHNMHRTTQWPL) was synthesized and purified as described previously.[26] Called MurEp1, its purity (>95%) was analyzed by HPLC and its molecular mass (1534.74 Daltons) was confirmed by MALDI-TOF. The peptide was dissolved in buffer C (200 mM Tris-HCl pH 8) at a concentration of 100 mM and the pH was adjusted to 7.0.

Bioinformatic analysis

The peptide consensus sequence was characterized using different algorithms of the ExPasy proteomics server such as the Compute pI/Mw and ProtParam tools [33] as well as the PSIpred and SSpro secondary structure prediction tools. [34,35,36] The consensus sequence was also analyzed for homologues in the UniProt database using the fasts34 program identified as the most efficient tool to determine protein homologues of small peptide sequences.[27,37]

Evaluation of MurEp1 as an inhibitor of MurE ATPase activity

Inhibition of MurE ATPase activity by MurEp1 was observed at room temperature in reaction buffer B using the spectrometry-based method described above. Substrates were

added after pre-incubation of the enzyme with the inhibitor. A test was done with 750 µM of MurEp1 for 0, 10, 30, 60 and 120 min of pre-incubation to observe possible time-dependence of inhibition. Tests were also done in which one substrate was added for pre-incubation with or without 750 µM MurEp1 and the remaining substrates were added after 30 min. MurE specific activity was determined in the presence of 75, 150 and 600 µM MurEp1 with pre-incubation periods of 10 and 30 min and compared to the reference activity without inhibitor. These data were used to estimate the inhibitor concentration required to reduce MurE activity by 50% (IC_{50}). The MurEp1 inhibitory constant (K_i) was determined separately for meso-A2pm and UDP-MurNAc-Ala-Glu using reaction velocity data obtained with the three inhibitor concentrations (with a 30 min pre-incubation) and either five concentrations of meso-A2pm (0.075, 0.25, 0.75, 3 and 10 mM) or five concentrations of UDP-MurNAc-Ala-Glu (12.5, 25, 50, 100 and 200 µM) each with fixed optimal concentrations of the other substrates. All experiments were done in triplicate. Kinetic data were fitted to the appropriate model equations using the Enzyme Kinetics Module of SigmaPlot. Steady-state inhibition kinetic parameters were determined by nonlinear regression analysis using the least squares method as a quality control to ensure accurate dataset fitting and to generate error estimates. The type of inhibition was identified with the Lineweaver-Burk plot and K_i values were determined using the Dixon plot regardless of the inhibition type, based on the following equation:

$$v = V_{max}*((1+\beta*I/(\alpha*K_i))/(1+I/(\alpha*K_i)))/(1+K_m/S)*(1+I/K_i)/(1+I/(\alpha*K_i)))$$

where v is MurE reaction velocity, V_{max} is the maximum initial velocity for the uninhibited MurE reaction, I is the inhibitor concentration, K_m is the Michaelis constant for the uninhibited MurE reaction, K_i is the competitive inhibition constant, α is the K_m factor change when MurEp1 is bound to the enzyme-substrate complex (ES) and β is the K_d factor change when MurEp1 is bound to ES (K_p being the rate constant associated specifically with enzyme-substrate complex dissociation to enzyme and product).[38,39] The expected K_m values for the inhibited MurE reactions were calculated from an increases of the uninhibited K_m value by a factor of 1 + [MurEp1]/K_i for meso-A2pm and 1 + [MurEp1])/3K_i for MurNAc-Ala-Glu.[38,39] As controls, non-specific peptides issued from phage display were tested at different concentrations for inhibition of MurE activity.[40]

Results

Purification of biologically active MurE amide ligase

The purified MurE protein was visualized as a single 55 kDa band on SDS-PAGE (not shown). Sequencing of the first 15 N-terminal residues confirmed its identity as MurE from *P. aeruginosa* (100% identical to the published sequence minus the initial methionine). Its biological activity was confirmed by reconstruction of the cell wall precursor UDP-N-acetylmuramyl pentapeptide in the presence of MurA, MurB, MurC, MurD and MurF proteins.[30] The phosphate content of the extensively dialyzed MurE solution was below the lower detection limit for the Lanzetta reagent.

Synthesis and purification of the UDP-MurNAc-Ala-Glu substrate

Analysis by anionic exchange indicated that the UDP-MurNAc-Ala-Glu synthesized using the *P. aeruginosa* MurA, MurB, MurC and MurD enzymes was 99.5 % pure [Fig. 1(A)]. Characterization of the purified product by mass spectrometry identified four different species with observed m/z identical to the expected m/z values (Table I). Results obtained confirmed the UDP-MurNAc-Ala-Glu structure as presented in Figure 1(B).

MurE amide ligase activity

Negative controls done without MurE or in the absence of any one of the substrates gave no phosphate release from ATP (data not shown). The best conditions for the MurE assay were 15 min of reaction at room temperature in buffer B. Addition of NaCl did not improve MurE activity (data not shown). As depicted in Figure 2(A), the optimal concentration of ATP was 1 mM while a concentration of 2 mM decreased MurE specific activity. The maximal specific activity (2.7 ± 0.4 μmol/min/mg) was reached at 10 mM meso-A2pm [Fig. 2(B)]. The optimal concentration of UDP-MurNAc-Ala-Glu was 200 μM and concentrations of 300 μM or greater decreased enzyme activity [Fig. 2(C)]. Based on K_m values, the affinity of MurE for UDP-MurNAc-Ala-Glu was about 4.5 times higher than for meso-A2pm and about 7.5 times higher than for ATP (Table II). The k_{cat} values indicated that each MurE active site hydrolyzed about 145 ATP molecules per min to ADP and inorganic phosphate and thus proceeded with about 145 amide ligase reactions between

meso-A2pm and UDP-MurNAc-Ala-Glu according to the demonstrated stoichiometric relationship.[16] The enzyme efficiency, as estimated by the k_{cat}/K_m ratio, indicated that MurE was more efficient with respect to UDP-MurNAc-Ala-Glu. Overall, the kinetic parameters were measured with reasonable precision, since the standard deviations were generally less than 30% of the values reported in Table II.

Selection of specific MurE binding peptides

As shown in Table III, each round of biopanning eluted a lower phage titer from approximately 10^{11} down to 10^5 plaque forming units (PFUs). Each round of biopanning also yielded a lower phage recovery in comparison to the previous round. This effect was more pronounced for the third round, indicating the strongest selection of specific MurE-interacting peptide sequences at this step. Each elution strategy gave similar phage recovery yields, indicating that the competitive elutions using specific MurE substrates were as potent as the well-known glycine-HCl elution.

Sequencing of ten phages selected for each of the three eluting buffers identified a variety of peptide sequences containing consensus motifs (Fig. 3). Analysis of peptide sequence frequencies gave the clear consensus sequence NHNMHRTTQWPL. This sequence was mostly recovered by the meso-A2pm competitive elution and weakly recovered by the glycine-HCl elution. The ATP competitive elution yielded several peptide sequences presenting conserved residues of the consensus sequence. Indeed, the "MHR" motif of the consensus sequence was particularly conserved among the MurE-selected sequences. Many sequences presented this precise motif or a variation of this motif with two basic residues next to a hydrophobic residue. The consensus sequence had a large proportion of polar and basic amino acids (Fig. 3). In addition to the consensus sequence, the sequences indicated by the superscripts a, b, c and d in Figure 3 were recovered more than once. The glycine-HCl elution also recovered a sequence that differed from sequence c by one residue, three sequences with an "EGRP" motif, four sequences starting with a lysine residue and three sequences with two proline residues followed by a "TRS" motif. The ATP competitive elution recovered a greater diversity of sequences than the other elution conditions. The different elution conditions were thus helpful in selecting different peptide sequences.

Bioinformatic analysis

The MurE-binding consensus peptide sequence was analyzed using different algorithms of the ExPasy server and by searching for protein homologues with fasts34. The theoretical isoelectric pH was established at 9.8, indicating that the peptide is positively charged at neutral pH. The consensus sequence does not contain any negatively charged residue and contains one positively charged residue. The ProtParam tool emphasized the high proportion of NHT residues in the consensus sequence and estimated the half-life of the peptide at more than 10 hours in *Escherichia coli* and at 1.4 hours in mammalian reticulocytes *in vitro*. The secondary structure prediction tools predicted a random coil structure with acceptable confidence. The fasts34 program did not identify any protein homologue having an E value < 5 in the UniProt database.

Kinetics of MurE ATPase activity inhibition by MurEp1

Since the specific activity of MurE decreased after 60 min of pre-incubation in the absence of inhibitor (data not shown), this effect was factored into the calculation of MurE ATPase percent residual activity following pre-incubation with MurEp1. As shown in Figure 4(A), the residual activity of MurE decreased in exponential fashion with increasing pre-incubation time in the presence of 750 μM MurEp1, indicating that this inhibition was time-dependent. IC_{50} values for MurEp1 determined with pre-incubation periods of 10 and 30 min were 800 and 500 μM respectively (Table IV). The response of MurE specific activity to 30 min pre-incubation with MurEp1 as a function of inhibitor concentration tended towards inverse linear dose-response character with varying slope [Fig. 4(B)]. To confirm the specificity of the MurEp1 inhibition, nonspecific peptides issued from phage display were analyzed for inhibition of the MurE ATPase activity; no inhibition was observed (data not shown).

The presence of meso-A2pm or UDP-MurNAc-Ala-Glu during 30 min pre-incubations completely restored MurE activity whereas adding ATP did not lessen inhibition by MurEp1 (data not shown). MurE reaction velocity was identical with or without UDP-MurNAc-Ala-Glu in the pre-incubation step but was slightly reduced in the presence of ATP or meso-A2pm. This effect was considered when determining the inhibitory capacity of MurEp1 (data not shown). Since meso-A2pm and UDP-MurNAc-

Ala-Glu both spared MurE from MurEp1 inhibition, K_i values for MurEp1 were evaluated separately for these substrates. The slopes and x-intercepts of fitted lines from both Lineweaver-Burk plots varied as a function of MurEp1 concentration, revealing a catalytic component in the inhibition (Fig. 5). The plot for meso-A2pm showed varied y-intercepts for the different MurEp1 concentrations, indicating a specific component in the inhibition [Fig. 5(A)]. The UDP-MurNAc-Ala-Glu plot did not present such y-intercept variation, the common intersection point between the fitted lines standing closer to the ordinate axis [Fig. 5(B)]. This point occurred to the left of the ordinate axis and above the abscissa, indicating that MurEp1 causes a reversible mixed type of inhibition sharing properties of competitive and non-competitive inhibitors against both meso-A2pm and UDP-MurNAc-Ala-Glu (Fig. 5). This inhibition type represented the model that statistically gave the best fit to the experimental data according to the Runs Test (data not shown), with R^2 values of 0.96 and 0.94, Akaike values of -230 and -195 and standard deviation of the residuals of 0.14 and 0.18 for meso-A2pm and UDP-MurNAc-Ala-Glu respectively. Dixon plots established the competitive K_i values at 160 ± 45 μM for the meso-A2pm substrate and at 80 ± 25 μM for UDP-MurNAc-Ala-Glu (Table IV). Even if MurEp1 behaved as a time-dependent inhibitor, the tight binding inhibition model was excluded since the MurE concentration was not approximately equal to or higher than the apparent K_i values. The α parameter required to calculate the K_i values indicated that MurEp1 binding to MurE-meso-A2pm decreased MurE affinity for meso-A2pm by a factor of 3 whereas MurEp1 binding to the complex MurE-UDP-MurNAc-Ala-Glu decreased the MurE affinity for UDP-MurNAc-Ala-Glu by a factor of 6 (Table IV). The β parameter was much higher for meso-A2pm then for UDP-MurNAc-Ala-Glu (Table IV). This indicated that the rate constant of ES complex dissociation to enzyme and product decreased slightly when MurEp1 bound to the complex in the case of meso-A2pm and to a greater extent in the case of UDP-MurNAc-Ala-Glu.

The V_{max} values for MurE decreased as a function of MurEp1 concentration with respect to meso-A2pm. Indeed, V_{max} at 600 μM MurEp1 was half its value for the uninhibited reaction. This effect was not observed for UDP-MurNAc-Ala-Glu (Table IV). The K_m values for meso-A2pm increased as the MurEp1 concentration increased, by a factor of 1 + [MurEp1]/K_i, as normally observed for competitive inhibitors. Expected

values of K_m in Table IV were calculated according to this factor. Observed K_m values for meso-A2pm were nearly identical to the expected values, with the exception of the lower K_m at 600 μM MurEp1. K_m values for UDP-MurNAc-Ala-Glu also increased as a function of MurEp1 concentration, but the effect was less pronounced. In this case, the factor 1 + [MurEp1]/K_i was less accurate than 1 + [MurEp1])/3K_i in predicting K_m value. Overall, the kinetic parameters were measured with reasonable precision, since the standard deviations were generally smaller than 30% of the reported values. Relative to the values, the standard deviations were generally greater for UDP-MurNAc-Ala-Glu.

Discussion

Due to the lack of commercially available pathway intermediates suitable for kinetic and inhibitory studies of MurE amide ligase, we began by synthesizing its UDP-MurNAc-Ala-Glu substrate (Fig. 1, Table I). Biologically active MurE from *P. aeruginosa* was then purified in order to allow spectrophotometric monitoring of inorganic phosphate release and hence quantification of MurE ATPase activity. The ATPase activity of MurE has been shown to be absolutely dependent on the di-amino acid and UDP-MurNAc-Ala-Glu substrates.[16] The vast majority of kinetic studies of MurE have measured activity as addition of a radioactive di-amino acid substrate to UDP-MurNAc-Ala-Glu, with quantification of radioactive UDP-MurNAc-tripeptide following separation by reverse-phase HPLC, HPLC cation exchange chromatography, high-voltage electrophoresis or thin layer chromatography.[15-17,41-45] These methods are time, cost and labor intensive compared to our simple, rapid and sensitive spectrophotometric assay, which does not require any radioactive isotope. Only one MurE ATPase assay has been previously reported, based on the ADP and NAD coupled reaction with pyruvate kinase and lactate dehydrogenase.[46] Our assay measures ATP hydrolysis directly rather than through an NAD-dependent additional enzymatic reaction, thus offering better screening capacities to analyze specific MurE inhibitors. Furthermore, our assay could be easily adapted to high throughput selection (HTS) screening in microtiter plates.

The *P. aeruginosa* MurE enzyme had greater specific activity at room temperature than its *E. coli* counterpart.[41] A high concentration of ATP was detrimental to MurE

activity [Fig. 2(A)] as has been observed for the *Staphylococcus aureus* MurE enzyme.[16] This inhibition may be caused by ATP-induced acidification of the reaction medium. MurE is highly sensitive to assay pH, 8.5 being optimal and enzyme activity ceasing below 7.[16,47,48] A UDP-MurNAc-dipeptide concentration above 300 μM caused strong substrate inhibition of MurE activity [Fig. 2(C)], as has been observed for MurE from *Thermotoga maritima*, *S. aureus* and *Bacillus cereus*.[16,47,48] Similar inhibition by the nucleotide cell wall precursor has been noted for other Mur ligases, such as MurF and for other cell wall biosynthesis enzymes such as MurA.[12,49] Unlike with the MurF enzyme,[12] adding NaCl did not suppress substrate inhibition for MurE. Substrate inhibition such as this is likely involved in regulation of the cell wall synthesis rate in order to allow cells to respond to different growth and environmental conditions. The optimal substrate concentrations and K_m values obtained for *P. aeruginosa* MurE were similar to those obtained for other MurE proteins. The K_m values obtained for UDP-MurNAc-Ala-Glu and meso-A2pm (Table II) were respectively nearly identical and higher than reported for the *E. coli* enzyme: 36 μM for meso-A2pm and 35 μM for UDP-MurNAc-Ala-Glu [42]; 36 μM for meso-A2pm and 76 μM for UDP-MurNAc-Ala-Glu [50]; 55 μM for UDP-MurNAc-Ala-Glu [51]; 40 μM and 11 μM for meso-A2pm [17 52]. K_m values of *P. aeruginosa* MurE for ATP and meso-A2pm were close to those obtained for the *B. cereus* meso-A2pm-adding enzyme: 130 μM, 320 μM and 340 μM for meso-A2pm, UDP-MurNAc-Ala-Glu and ATP, respectively.[47] The *T. maritima* MurE enzyme showed higher K_m values; 3.6 mM for ATP, 0.45 mM for UDP-MurNAc-Ala-Glu, 2.8 mM for L-Lysine and 4.8 mM for *meso*-A2pm.[48] The maximal *P. aeruginosa* MurE velocity of 2.7 μmol/min/mg was close to a published value of 3.31 μmol/min/mg for this species[46], higher than for its *E. coli* counterpart [17,42] (1.8 and 32 nmol/min) and lower than for its *T. maritima* counterpart [48] (55 μmol/min/mg). As for MurE of *T. maritima*, *P. aeruginosa* MurE was more efficient with respect to UDP-MurNAc-Ala-Glu than the two other substrates.[48] Finally, the K_m values we measured allowed us to focus the phage display method using competitive biopanning by adjusting ATP and meso-A2pm concentrations accordingly.

Limiting the time of contact between the phage peptides and MurE during the third round of phage display biopanning represented a much more stringent selection factor for MurE phage specificity than increasing the wash stringency during the second round. This

was indicated by the lower percentages of phages obtained in the third round (Table III). This selection pattern has been observed in phage display screening of the amide ligase MurD.[27] In contrast, screening of MurC amide ligase using the same phage display approach gave higher phage recovery titers for the second and third rounds, suggesting an enrichment of the phage population.[26] Earlier selection of specific MurC interacting phage-encoded peptides during the phage display screening than in the cases of MurE and MurD could explain this enrichment.[26,27] It should also be noted that several other factors affect phage recovery, such as phage infection and replication efficiency, protein translocation and folding bias as well as pIII coat stability.[53] As for the MurD amide ligase, the consensus peptide sequence was selected mostly by amino acid substrate competitive elution and Gly elution.[27] This validated the use of different elution conditions giving various peptides but with consensus amino acids (Fig. 3).

The synthesized MurEp1 peptide encoding the strongest consensus sequence represented a potent and specific time-dependent inhibitor of the essential ATPase activity of MurE (Fig. 4). We suggest that the most conserved residues of the MurEp1 sequence would likely be essential for MurE binding and inhibition. The K_i values determined for MurEp1 with meso-A2pm and UDP-MurNAc-Ala-Glu (Table IV) indicate that MurEp1 is a reversible inhibitor sharing properties of competitive and non-competitive inhibitors. MurEp1 acted as a competitive inhibitor since the inhibition was reversed by addition of meso-A2pm or UDP-MurNAc-Ala-Glu during pre-incubation, giving very similar y-intercepts for all MurEp1 concentrations on the Lineweaver-Burk plot in the case of UDP-MurNAc-Ala-Glu [Fig. 5(B)]. The slopes increased with MurEp1 concentration for both substrates, indicating an increase in inhibitor binding strength, MurE reaction velocity decreased as the MurEp1 concentration increased (Fig. 4(B) and Fig. 5) and the K_m increased by a factor of 1+[MurEp1]/K_i for meso-A2pm and 1+ [MurEp1])/3K_i for MurNAc-Ala-Glu (Table IV).[38,39] Like a non-competitive inhibitor that interferes with the enzymatic reaction without directly competing for the substrate binding site, MurEp1 inhibits MurE at high or low substrate concentrations, the V_{max} of MurE decreasing as a function of the MurEp1 concentration and the y-intercept of Lineweaver-Burk plot varying in the case of meso-A2pm (Fig. 5(A) and Table IV). MurEp1 binding to ES particularly thus decreased MurE affinity for UDP-MurNAc-Ala-Glu and slowed the rate of ES

dissociation to enzyme and product.[38,39] Overall, the kinetic data indicate that MurEp1 acts more as a competitive inhibitor in the case of meso-A2pm, closely matching the factor 1+[MurEp1]/K_i. In contrast, MurEp1 acts more like a non-competitive inhibitor of UDP-MurNAc-Ala-Glu; substrate binding to MurE occurred but with reduced affinity, slowing the conversion of bound substrate to product.[38,39]

Crystal structure of the *E. coli* MurE has revealed that the enzyme has a three-domain topology. The binding site for each substrate is localized in one particular domain. UDP-MurNAc-Ala-Glu binds in the N-terminal domain (domain 1), ATP binds principally to the central portion of MurE (domain 2) and meso-A2pm interacts with the C-terminus in domain 3.[54] For ligation to occur between UDP-MurNAc-Ala-Glu and meso-A2pm, MurE must bring together and correctly orient both substrates for acyl-phosphate intermediate formation after the binding of ATP and then orient meso-A2pm for nucleophilic attack and stabilize the tetrahedral intermediate, thereby lowering the activation barrier and accelerating catalysis.[54] The tridimensional structure of MurE thus excludes the possibility of MurEp1 binding at the juxtaposition of both meso-A2pm and UDP-MurNAc-Ala-Glu binding sites. Furthermore, MurEp1 is not likely close enough to the shape and size of the UDP-MurNAc-Ala-Glu to compete for its binding site on the enzyme surface.

Since MurEp1 was originally selected by competitive elution with the meso-A2pm substrate, MurEp1 and meso-A2pm likely target the same binding site at the C-terminal domain of MurE.[54] Phage display, kinetics and structural data thus corroborate that MurEp1 exerts its inhibitory action by obstructing the meso-A2pm binding site, thus interfering with meso-A2pm binding. This MurEp1 binding was not strictly competitive since it also inhibited participation of bound UDP-MurNAc-Ala-Glu substrate in the MurE reaction. This MurEp1 effect is perhaps achieved by inhibition of the structural change required to bring together and correctly orient meso-A2pm and UDP-MurNAc-Ala-Glu or by preventing interaction between the two substrates after the structural change. In either case, MurEp1 interferes with the substrate proximity required for proper amide bond formation and consequently reduces the MurE reaction rate. The co-crystallization of the MurEp1-MurE complex will help to investigate how MurEp1 is involved in the overall structural changes in MurE.

MurEp1 is likely a specific inhibitor of MurE even though the Mur ligase enzymes belong to a well-defined class of closely functionally related proteins.[7] Each amide ligase displays high specificity for its respective substrates with no cross-activity.[6] Indeed, phage display screenings performed on MurC, MurD and MurE amide ligases of *P. aeruginosa* using similar experimental conditions did not identify redundant sequences.[26,28] We suggest that MurEp1 could be a potent inhibitor of both Gram-negative and Gram-positive bacteria, since the MurE enzyme active sites are conserved among bacterial species.[54] As mammals lack the A2pm pathway, it will be of interest to evaluate the inhibitory potential of MurEp1 on enzymes implicated in this pathway such as DapF, LysA and A2pm dehydrogenase as well as transpeptidases.[45]

Few MurE inhibitors have been reported to date and none show antibacterial activity.[4] The most potent lead compound is phosphinate, which interferes with the tetrahedral intermediate of MurE and inhibits the MurE reaction with an IC_{50} value of 1.1 μM.[43] Two analogous species close to the natural UDP-MurNAc-Ala-Glu substrate have also been found to have a significant inhibitory effect on MurE at 1 mM.[51] Several analogs of meso-A2pm have been tested as competitive inhibitors of MurE.[4] The LD diastereoisomers of N-alpha-propionyl-dipeptides display moderate inhibitory effects [55]; (2*S*,3*R*,6*S*)-3-Fluoro-A2pm and N-Hydroxy-A2pm respectively have shown IC_{50} values of 2.3 and 0.56 mM with an expected K_i value of 0.4 mM for N-Hydroxy-A2pm [45] while a monophosphonomonocarboxy analog had an IC_{50} value around 10 mM [44]. MurEp1 did not present any structural homology with these reported meso-A2pm analogs and has a superior inhibitory capacity.

In this work, we demonstrated how a strategic biopanning approach may lead to the identification of specific interacting peptide sequences and how a clear consensus peptide sequence can significantly and specifically inhibit MurE ATPase activity. Indeed, we identified the first peptide inhibitor having novel mode of action against the essential and unexploited MurE enzyme. Characterization of *P. aeruginosa* MurE kinetics would also provide valuable insight for future development and rational design of a new generation of specific bacterial cell wall antibacterials. Furthermore, targeting MurE may lead to perturbation in the regulation of antibiotic resistance and competence mechanisms. MurE has recently been shown to influence methicillin resistance in *Staphylococcus aureus* by

regulating the expression of two penicillin binding proteins [56,57] and to influence DNA uptake in *Haemophilus influenzae* by causing induction of the normal competence pathway via a previously unsuspected signal [3].

Acknowledgements

We thank Le Service de séquence de peptides de l'Est du Québec and Le Service d'analyse et de synthèse d'acides nucléiques de l'Université Laval. This work was funded by The Canadian Bacterial Diseases Network via the Canadian Centers of Excellence, a FCAR infrastructure team grant to R. C. Levesque and a FRSQ studentship to Catherine Paradis-Bleau.

References

1. Projan SJ. New (and not so new) antibacterial targets - from where and when will the novel drugs come? Curr Opin Pharmacol 2002;2(5):513-522.
2. Levy SB, Marshall B. Antibacterial resistance worldwide: causes, challenges and responses. Nat Med 2004;10(12 Suppl):S122-129.
3. Ma C, Redfield RJ. Point mutations in a peptidoglycan biosynthesis gene cause competence induction in *Haemophilus influenzae*. J Bacteriol 2000;182(12):3323-3330.
4. El Zoeiby A, Sanschagrin F, Levesque RC. Structure and function of the Mur enzymes: development of novel inhibitors. Mol Microbiol 2003;47(1):1-12.
5. Bugg TD, Walsh CT. Intracellular steps of bacterial cell wall peptidoglycan biosynthesis: enzymology, antibiotics, and antibiotic resistance. Nat Prod Rep 1992;9(3):199-215.
6. Bouhss A, Mengin-Lecreulx D, Blanot D, van Heijenoort J, Parquet C. Invariant amino acids in the Mur peptide synthetases of bacterial peptidoglycan synthesis and their modification by site-directed mutagenesis in the UDP-MurNAc:L-alanine ligase from *Escherichia coli*. Biochemistry 1997;36(39):11556-11563.
7. Eveland SS, Pompliano DL, Anderson MS. Conditionally lethal *Escherichia coli* murein mutants contain point defects that map to regions conserved among murein and folyl poly-gamma-glutamate ligases: identification of a ligase superfamily. Biochemistry 1997;36(20):6223-6229.
8. Liger D, Masson A, Blanot D, van Heijenoort J, Parquet C. Study of the overproduced uridine-diphosphate-N-acetylmuramate:L-alanine ligase from *Escherichia coli*. Microb Drug Resist 1996;2(1):25-27.
9. Falk PJ, Ervin KM, Volk KS, Ho HT. Biochemical evidence for the formation of a covalent acyl-phosphate linkage between UDP-N-acetylmuramate and ATP in the *Escherichia coli* UDP-N-acetylmuramate:L-alanine ligase-catalyzed reaction. Biochemistry 1996;35(5):1417-1422.

10. Tanner ME, Vaganay S, van Heijenoort J, Blanot D. Phosphinate inhibitors of the D-glutamic acid-adding enzyme of peptidoglycan biosynthesis. J Org Chem 1996;61(5):1756-1760.
11. Vaganay S, Tanner ME, van Heijenoort J, Blanot D. Study of the reaction mechanism of the D-glutamic acid-adding enzyme from *Escherichia coli*. Microb Drug Resist 1996;2(1):51-54.
12. Anderson MS, Eveland SS, Onishi HR, Pompliano DL. Kinetic mechanism of the *Escherichia coli* UDPMurNAc-tripeptide D-alanyl-D-alanine-adding enzyme: use of a glutathione S-transferase fusion. Biochemistry 1996;35(50):16264-16269.
13. Bertrand JA, Auger G, Martin L, Fanchon E, Blanot D, Le Beller D, van Heijenoort J, Dideberg O. Determination of the MurD mechanism through crystallographic analysis of enzyme complexes. J Mol Biol 1999;289(3):579-590.
14. Schleifer KH, Kandler O. Peptidoglycan types of bacterial cell walls and their taxonomic implications. Bacteriol Rev 1972;36(4):407-477.
15. Mengin-Lecreulx D, Falla T, Blanot D, van Heijenoort J, Adams DJ, Chopra I. Expression of the *Staphylococcus aureus* UDP-N-acetylmuramoyl-L-alanyl-D-glutamate:L-lysine ligase in *Escherichia coli* and effects on peptidoglycan biosynthesis and cell growth. J Bacteriol 1999;181(19):5909-5914.
16. Ito E, Strominger JL. Enzymatic synthesis of the peptide in bacterial uridine nucleotides. III. Purification and properties of L-lysin-adding enzyme. J Biol Chem 1964;239:210-214.
17. Mengin-Lecreulx D, Blanot D, van Heijenoort J. Replacement of diaminopimelic acid by cystathionine or lanthionine in the peptidoglycan of *Escherichia coli*. J Bacteriol 1994;176(14):4321-4327.
18. Pierce GE. *Pseudomonas aeruginosa*, *Candida albicans*, and device-related nosocomial infections: implications, trends, and potential approaches for control. J Ind Microbiol Biotechnol 2005;32(7):309-318.
19. Hoiby N. Understanding bacterial biofilms in patients with cystic fibrosis: current and innovative approaches to potential therapies. J Cyst Fibros 2002;1(4):249-254.
20. Glauner B, Holtje JV, Schwarz U. The composition of the murein of *Escherichia coli*. J Biol Chem 1988;263(21):10088-10095.
21. Holtje JV. Growth of the stress-bearing and shape-maintaining murein sacculus of *Escherichia coli*. Microbiol Mol Biol Rev 1998;62(1):181-203.
22. Christensen DJ, Gottlin EB, Benson RE, Hamilton PT. Phage display for target-based antibacterial drug discovery. Drug Discov Today 2001;6(14):721-727.
23. Sidhu SS. Phage display in pharmaceutical biotechnology. Curr Opin Biotechnol 2000;11(6):610-616.
24. Burns KL, May SW. Separation methods applicable to the evaluation of enzyme-inhibitor and enzyme-substrate interactions. J Chromatogr B Analyt Technol Biomed Life Sci 2003;797(1-2):175-190.
25. Hyde-DeRuyscher R, Paige LA, Christensen DJ, Hyde-DeRuyscher N, Lim A, Fredericks ZL, Kranz J, Gallant P, Zhang J, Rocklage SM, Fowlkes DM, Wendler PA, Hamilton PT. Detection of small-molecule enzyme inhibitors with peptides isolated from phage-displayed combinatorial peptide libraries. Chem Biol 2000;7(1):17-25.
26. El Zoeiby A, Sanschagrin F, Darveau A, Brisson JR, Levesque RC. Identification of novel inhibitors of *Pseudomonas aeruginosa* MurC enzyme derived from phage-displayed peptide libraries. J Antimicrob Chemother 2003;51(3):531-543.

27. Paradis-Bleau C, Beaumont M, Boudreault L, Lloyd A, Sanschagrin F, Bugg TD, Levesque RC. Selection of peptide inhibitors against the *Pseudomonas aeruginosa* MurD cell wall enzyme. Peptides 2006;27(7):1693-1700.
28. Paradis-Bleau C, Sanschagrin F, Levesque RC. Peptide inhibitors of the essential cell division protein FtsA. Protein Eng Des Sel 2005;18(2):85-91.
29. Paradis-Bleau C, Sanschagrin F, Levesque RC. Identification of *Pseudomonas aeruginosa* FtsZ peptide inhibitors as a tool for development of novel antimicrobials. J Antimicrob Chemother 2004;54(1):278-280.
30. El Zoeiby A, Sanschagrin F, Havugimana PC, Garnier A, Levesque RC. *In vitro* reconstruction of the biosynthetic pathway of peptidoglycan cytoplasmic precursor in *Pseudomonas aeruginosa*. FEMS Microbiol Lett 2001;201(2):229-235.
31. Reddy SG, Waddell ST, Kuo DW, Wong KK, Pompliano DL. Preparative enzymatic synthesis and characterization of the cytoplasmic intermediates of murein biosynthesis. J Am Chem Soc 1999;121:1175-1178.
32. Lanzetta PA, Alvarez LJ, Reinach PS, Candia OA. An improved assay for nanomole amounts of inorganic phosphate. Anal Biochem 1979;100(1):95-97.
33. Walker JM. The proteomics protocols handbook. Totowa, N.J.: Humana Press; 2005. 988 p.; pp.571-607.
34. Jones DT. Protein secondary structure prediction based on position-specific scoring matrices. J Mol Biol 1999;292(2):195-202.
35. Bryson K, McGuffin LJ, Marsden RL, Ward JJ, Sodhi JS, Jones DT. Protein structure prediction servers at University College London. Nucleic Acids Res 2005;33(Web Server issue):W36-38.
36. Pollastri G, Przybylski D, Rost B, Baldi P. Improving the prediction of protein secondary structure in three and eight classes using recurrent neural networks and profiles. Proteins 2002;47(2):228-235.
37. Mackey AJ, Haystead TA, Pearson WR. Getting more from less: algorithms for rapid protein identification with multiple short peptide sequences. Mol Cell Proteomics 2002;1(2):139-147.
38. Cornish-Bowden A. Fundamentals of enzyme kinetics. London; Boston: Butterworths; 1979. XIII, 230 p.
39. Segal IH. Enzyme kinetics - behavior and analysis of rapid equilibrium and steady-state enzyme systems: John Wiley and Sons, Inc.; 1993. 992 p.
40. Sanschagrin F, Levesque RC. A specific peptide inhibitor of the class B metallo-beta-lactamase L-1 from *Stenotrophomonas maltophilia* identified using phage display. J Antimicrob Chemother 2005;55(2):252-255.
41. Lugtenberg EJ. Studies on *Escherichia coli* enzymes involved in the synthesis of uridine diphosphate-N-acetyl-muramyl-pentapeptide. J Bacteriol 1972;110(1):26-34.
42. Mengin-Lecreulx D, Flouret B, van Heijenoort J. Cytoplasmic steps of peptidoglycan synthesis in *Escherichia coli*. J Bacteriol 1982;151(3):1109-1117.
43. Zeng B, Wong KK, Pompliano DL, Reddy S, Tanner ME. A phosphinate inhibitor of the meso-diaminopimelic acid-adding enzyme (MurE) of peptidoglycan biosynthesis. J Org Chem 1998;63(26):10081-10085.
44. van Assche I, Soroka M, Haemers A, Hooper M, Blanot B, van Heijenoort J. Synthesis and antibacterial evaluation of phosphonic acid analogues of diaminopimelic acid. Eur J Med Chem 1991;26(5):505-515.

45. Auger G, van Heijenoort J, Vederas JC, Blanot D. Effect of analogues of diaminopimelic acid on the meso-diaminopimelate-adding enzyme from *Escherichia coli*. FEBS Lett 1996;391(1-2):171-174.
46. Azzolina BA, Yuan X, Anderson MS, El-Sherbeini M. The cell wall and cell division gene cluster in the Mra operon of *Pseudomonas aeruginosa*: cloning, production, and purification of active enzymes. Protein Expr Purif 2001;21(3):393-400.
47. Mizuno Y, Ito E. Purification and properties of uridine diphosphate N-acetylmuramyl-L-alanyl-D-glutamate:meso-2,6-diaminopimelate ligase. J Biol Chem 1968;243(10):2665-2672.
48. Boniface A, Bouhss A, Mengin-Lecreulx D, Blanot D. The MurE synthetase from *Thermotoga maritima* is endowed with an unusual D-lysine-adding activity. J Biol Chem 2006;281(23):15680-15686.
49. Eschenburg S, Priestman MA, Abdul-Latif FA, Delachaume C, Fassy F, Schonbrunn E. A novel inhibitor that suspends the induced fit mechanism of UDP-N-acetylglucosamine enolpyruvyl transferase (MurA). J Biol Chem 2005;280(14):14070-14075.
50. Michaud C, Mengin-Lecreulx D, van Heijenoort J, Blanot D. Over-production, purification and properties of the uridine-diphosphate-N-acetylmuramoyl-L-alanyl-D-glutamate: meso-2,6-diaminopimelate ligase from *Escherichia coli*. Eur J Biochem 1990;194(3):853-861.
51. Abo-Ghalia M, Michaud C, Blanot D, van Heijenoort J. Specificity of the uridine-diphosphate-N-acetylmuramyl-L-alanyl-D-glutamate: meso-2,6-diaminopimelate synthetase from *Escherichia coli*. Eur J Biochem 1985;153(1):81-87.
52. Mengin-Lecreulx D, Michaud C, Richaud C, Blanot D, van Heijenoort J. Incorporation of LL-diaminopimelic acid into peptidoglycan of *Escherichia coli* mutants lacking diaminopimelate epimerase encoded by *dapF*. J Bacteriol 1988;170(5):2031-2039.
53. Carettoni D, Gomez-Puertas P, Yim L, Mingorance J, Massidda O, Vicente M, Valencia A, Domenici E, Anderluzzi D. Phage-display and correlated mutations identify an essential region of subdomain 1C involved in homodimerization of *Escherichia coli* FtsA. Proteins 2003;50(2):192-206.
54. Gordon E, Flouret B, Chantalat L, van Heijenoort J, Mengin-Lecreulx D, Dideberg O. Crystal structure of UDP-N-acetylmuramoyl-L-alanyl-D-glutamate: meso-diaminopimelate ligase from *Escherichia coli*. J Biol Chem 2001;276(14):10999-11006.
55. Abo-Ghalia M, Flegel M, Blanot D, Van Heijenoort J. Synthesis of inhibitors of the meso-diaminopimelate-adding enzyme from *Escherichia coli*. Int J Pept Protein Res 1988;32(3):208-222.
56. Ludovice AM, Wu SW, de Lencastre H. Molecular cloning and DNA sequencing of the *Staphylococcus aureus* UDP-N-acetylmuramyl tripeptide synthetase (*murE*) gene, essential for the optimal expression of methicillin resistance. Microb Drug Resist 1998;4(2):85-90.
57. Gardete S, Ludovice AM, Sobral RG, Filipe SR, de Lencastre H, Tomasz A. Role of *murE* in the expression of beta-lactam antibiotic resistance in *Staphylococcus aureus*. J Bacteriol 2004;186(6):1705-1713.

Table I. ES-TOF mass spectrometric analysis of purified UDP-MurNAc-Ala-Glu.

Species	Expected m/z	Observed m/z
$m^{-1}/1$	878.18	878.20
$m^{-2}/2$	438.58	438.59
$(m+Na^{+})^{-2}/2$	449.58	449.58
$m^{-3}/3$	292.06	292.06

Table II. Kinetic parameters associated with MurE amide ligase activities

Parameter	Value
Specific ATP hydrolysis activity (μmol/min/mg)	2.6 ± 0.3
k_{cat} ATP (molecules min^{-1})	140 ± 25
K_m ATP (μM)	225 ± 90
k_{cat}/K_m ATP ($min^{-1}\mu M^{-1}$)	0.6 ± 0.2
Specific meso-A2pm-linked activity (μmol/min/mg)	2.6 ± 0.05
k_{cat} meso-A2pm (molecules min^{-1})	140 ± 20
K_m meso-A2pm (μM)	140 ± 15
k_{cat}/K_m meso-A2pm ($min^{-1}\mu M^{-1}$)	1 ± 0.2
Specific UDP-MurNAc-Ala-Glu-linked activity (μmol/min/mg)	2.9 ± 0.1
k_{cat} UDP-MurNAc-Ala-Glu (molecules min^{-1})	155 ± 25
K_m UDP-MurNAc-Ala-Glu (μM)	30 ± 5
k_{cat}/K_m meso-A2pm ($min^{-1}\mu M^{-1}$)	5 ± 1

Table III. Phage biopanning using MurE and the dodecamer phage peptide library

	Phage input	Eluted phages	% elution
Round 1			
Gly-HCl	4×10^{10}	1×10^{6}	2.5×10^{-3}
Round 2			
Gly-HCl	1×10^{11}	1.5×10^{6}	1.5×10^{-3}
Round 3			
Gly-HCl	2×10^{13}	8.7×10^{4}	4.4×10^{-7}
ATP		6.3×10^{4}	3.2×10^{-7}
Meso-A2pm		5.3×10^{4}	2.7×10^{-7}

Table IV. Kinetics of *P. aeruginosa* MurE inhibition by MurEp1.

Kinetic parameter	Value	Expected K_m value
IC_{50} for 10 min pre-incubation	800 ± 25 μM	
IC_{50} for 30 min pre-incubation	500 ± 15 μM	
α meso-A2pm	3 ± 1	
β meso-A2pm	0.8 ± 0.1	
K_i meso-A2pm	160 ± 45 μM	
V_{max} meso-A2pm with [MurEp1] at	nmol/min	
0 μM	0.56 ± 0.1	
75 μM	0.52 ± 0.1	
150 μM	0.51 ± 0.15	
600 μM	0.32 ± 0.15	
K_m meso-A2pm with [MurEp1] at	μM	
0 μM	140 ± 15	140 ± 15
75 μM	215 ± 25	205 ± 60
150 μM	275 ± 30	270 ± 80
600 μM	365 ± 70	665 ± 185
α UDP-MurNAc-Ala-Glu	6 ± 3	
β UDP-MurNAc-Ala-Glu	6.5 ± 0.3 (10^{-9})	
K_i UDP-MurNAc-Ala-Glu	80 ± 25 μM	
V_{max} UDP-MurNAc-Ala-Glu with [MurEp1] at	nmol/min	
0 μM	0.62 ± 0.25	
75 μM	0.60 ± 0.4	
150 μM	0.52 ± 0.3	
600 μM	0.56 ± 0.8	
K_m UDP-MurNAc-Ala-Glu with [MurEp1] at	μM	
0 μM	30 ± 5	30 ± 5
75 μM	45 ± 8	40 ± 10
150 μM	50 ± 8	50 ± 15
600 μM	90 ± 30	105 ± 35

Kinetic parameters α and β (K_m and K_p factor changes when MurEp1 is bound to ES) are shown with the corresponding competitive K_i values with respect to meso-A2pm and UDP-MurNAc-Ala-Glu. The expected K_m values were calculated from increases in the K_m value of the inhibited reaction by a factor of 1 + [MurEp1]/K_i for meso-A2pm and 1 + [MurEp1]/3K_i for UDP-MurNAc-Ala-Glu.

Figure Legends

Figure 1. (A) Chromatograph of anionic exchange performed with an ammonium acetate gradient, confirming the purity of synthesized UDP-MurNAc-Ala-Glu. (B) Chemical structure of purified UDP-MurNAc-Ala-Glu as confirmed by mass spectrometry.

Figure 2. Saturation profiles for (A) ATP, (B) meso-A2pm and (C) UDP-MurNAc-Ala-Glu in the MurE reaction. Note substrate inhibition by the ATP and UDP-MurNAc-Ala-Glu.

Figure 3. Peptide sequences obtained from the 12-mer phage display library obtained by sequencing of selected phages eluted after the third round of biopanning against MurE. Acidic amino acids (D, E) are turquoise, polar amino acids (Q, N) are light green, basic amino acids (K, R, H) are blue, hydrophobic amino acids (I, L, M, V) are pink, hydrophobic aromatic amino acids (F, Y, W) are red, small amino acids (A, S, C, T) are magenta, glycine (G) is in orange, and proline (P, introducing a bend into the chain) is in black (classified according to the Venn diagram for defining the relationships between amino acids). Consensus sequences and related conserved motifs are boxed in black and the superscript letters indicate peptide sequences recovered more than once.

Figure 4. (A) Inhibition of the ATPase activity of MurE by 750 μM MurEp1 at various pre-incubation times, revealing the time-dependent inhibition of MurE by MurEp1. (B) IC_{50} determination for MurEp1 for MurE ATPase activity with a 30 min pre-incubation.

Figure 5. Lineweaver–Burk plots for MurE ATPase activity inhibited by MurEp1 for (A) meso-A2pm and (B) the UDP-MurNAc-Ala-Glu. Inverted triangles: hydrolysis without MurEp1; hop triangles: 75 μM MurEp1; squares: 150 μM MurEp1 and circles: 600 μM MurEp1. The common intersection points between fitted lines indicate the mixed type of inhibition for both plots.

Figure 1.

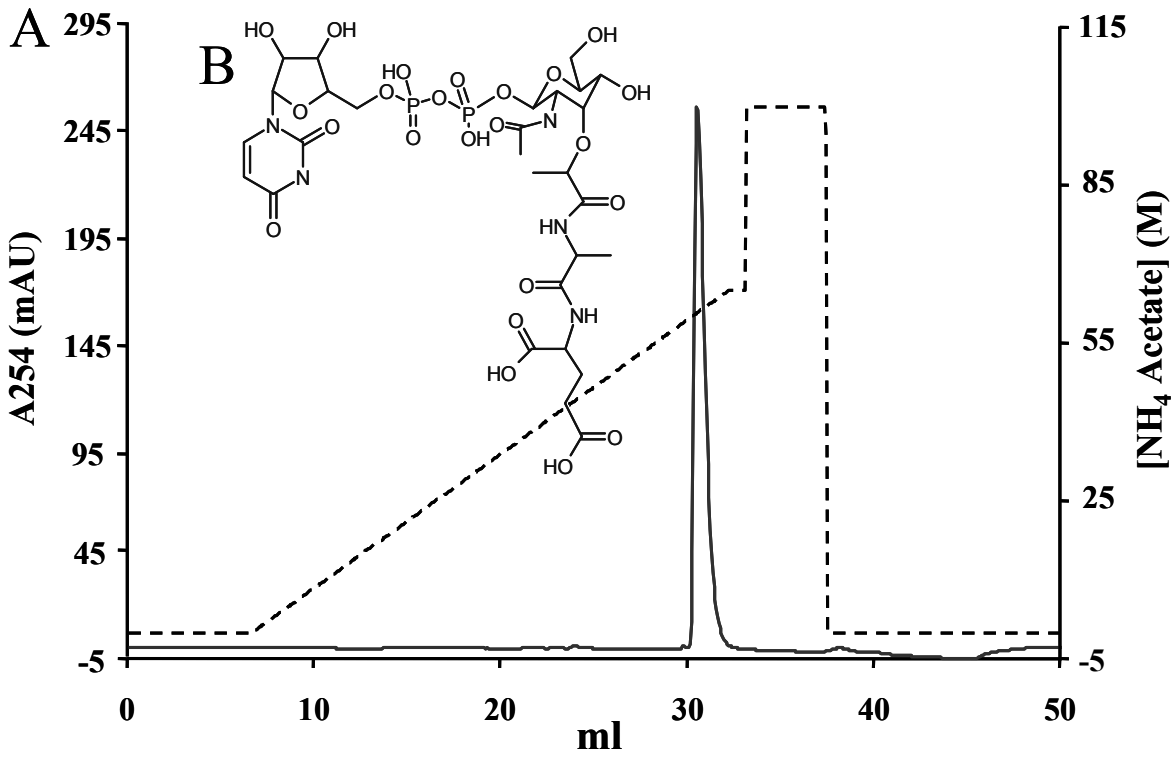
A
B
295
245
195
145
95
45
-5
A254 (mAU)
115
85
55
25
-5
[NH4 Acetate] (M)
0
10
20
30
40
50
ml

Figure 2.

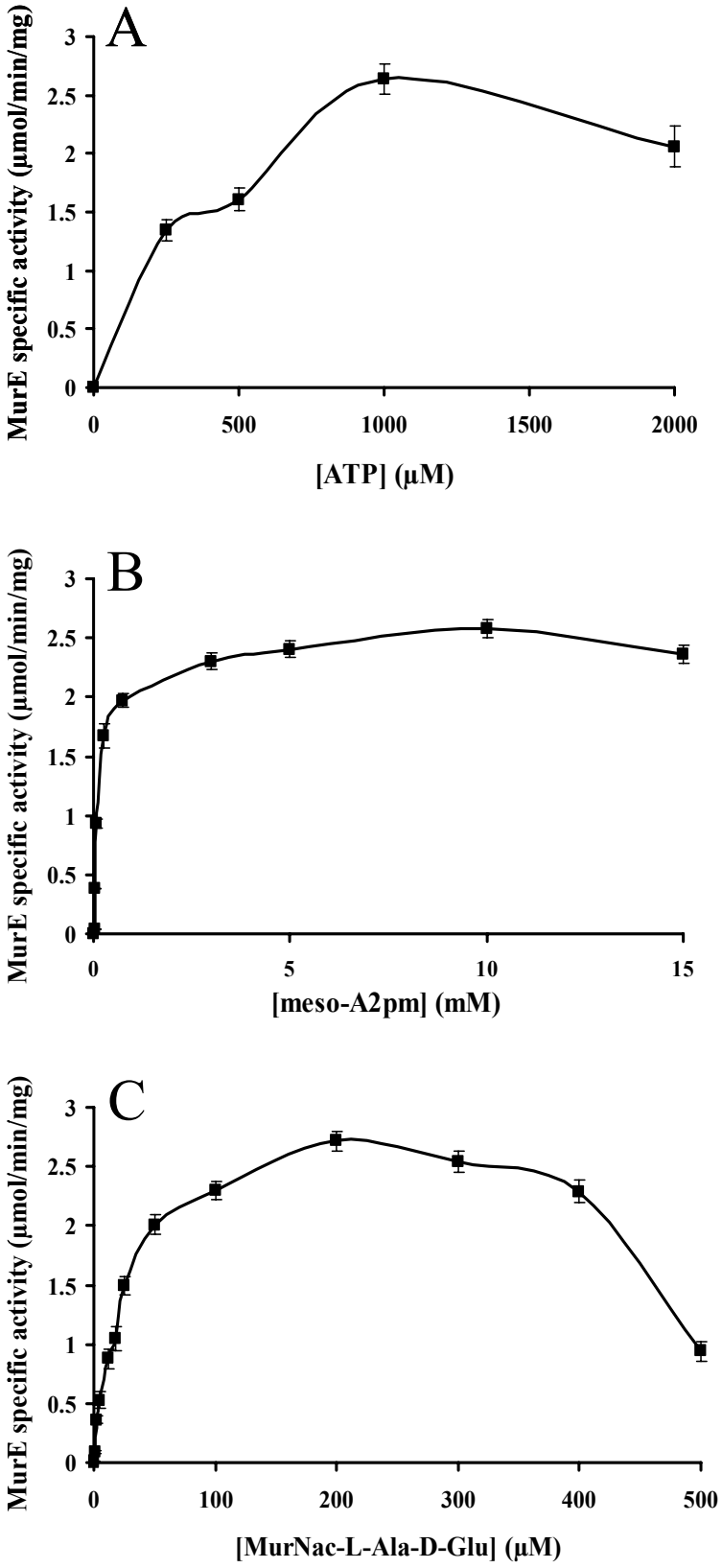
A
MurE specific activity (µmol/min/mg)
3
2.5
2
1.5
1
0.5
0
0
500
1000
1500
2000
[ATP] (µM)
B
MurE specific activity (µmol/min/mg)
3
2.5
2
1.5
1
0.5
0
0
5
10
15
[meso-A2pm] (mM)
C
MurE specific activity (µmol/min/mg)
3
2.5
2
1.5
1
0.5
0
0
100
200
300
400
500
[MurNac-L-Ala-D-Glu] (µM)

Figure 3.

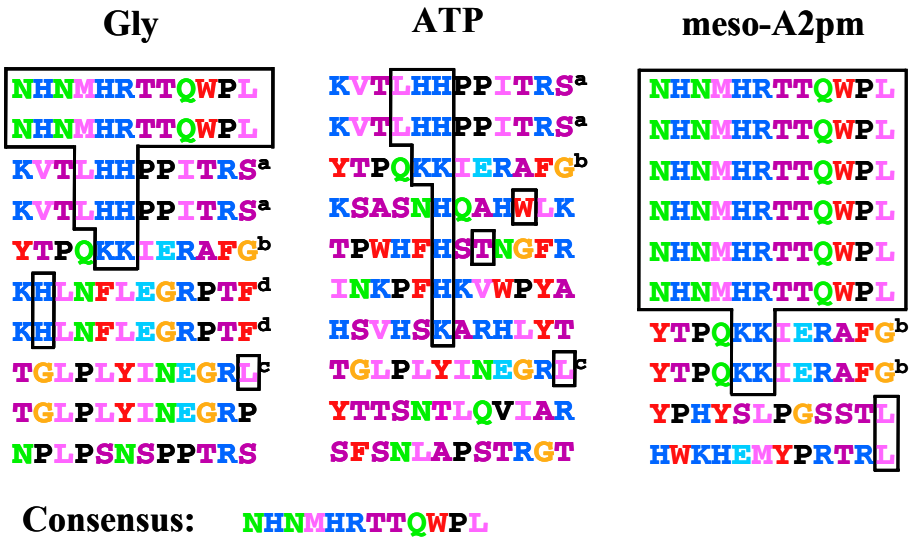
Gly
ATP
meso-A2pm
NHNMHRTTQWPL
NHNMHRTTQWPL
KVTLHHPPITRS[a]
KVTLHHPPITRS[a]
YTPQKKIERAFG[b]
KHLNFLEGRPTF[d]
KHLNFLEGRPTF[d]
TGLPLYINEGRL[c]
TGLPLYINEGRP
NPLPSNSPPTRS
KVTLHHPPITRS[a]
KVTLHHPPITRS[a]
YTPQKKIERAFG[b]
KSASNHQAHWLK
TPWHFHSTNGFR
INKPFHKVWPYA
HSVHSKARHLYT
TGLPLYINEGRL[c]
YTTSNTLQVIAR
SFSNLAPSTRGT
NHNMHRTTQWPL
NHNMHRTTQWPL
NHNMHRTTQWPL
NHNMHRTTQWPL
NHNMHRTTQWPL
NHNMHRTTQWPL
YTPQKKIERAFG[b]
YTPQKKIERAFG[b]
YPHYSLPGSSTL
HWKHEMYPRTRL
Consensus: NHNMHRTTQWPL

Figure 4.

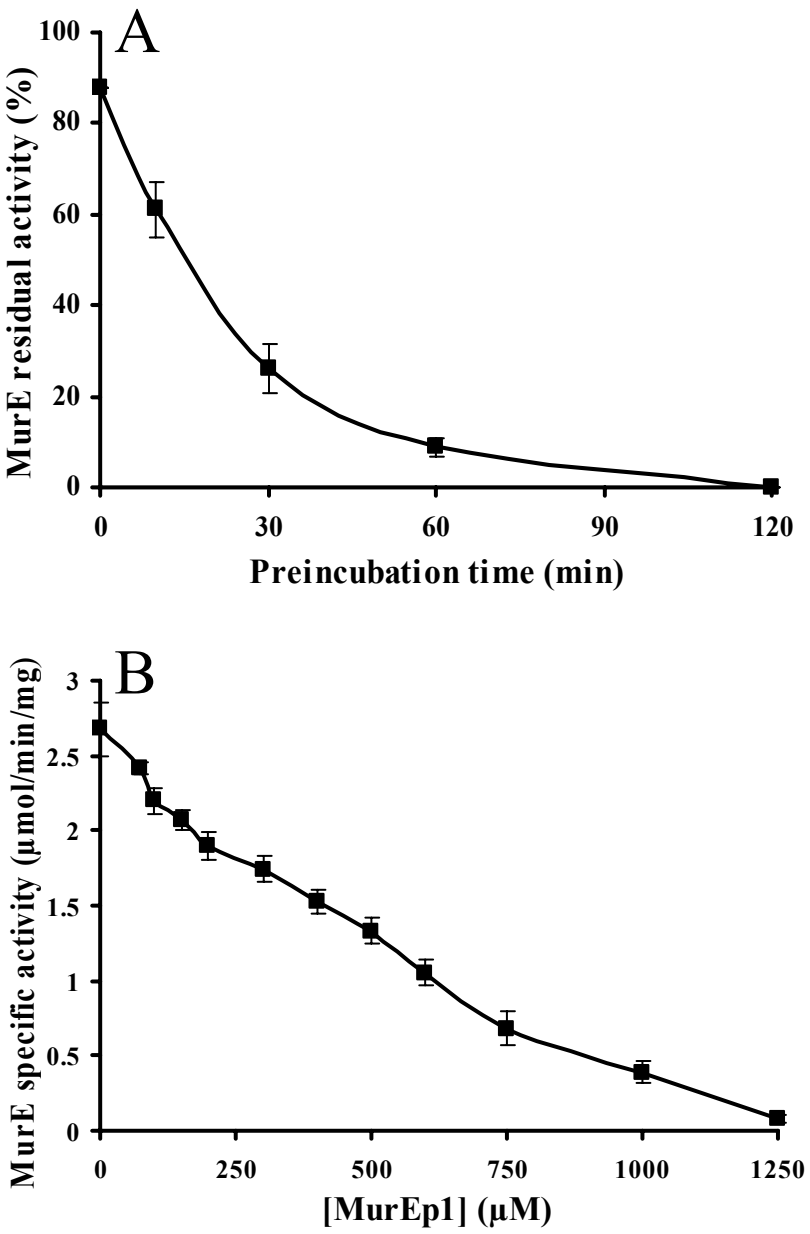
A
MurE residual activity (%)
100
80
60
40
20
0
0
30
60
90
120
Preincubation time (min)
B
MurE specific activity (µmol/min/mg)
3
2.5
2
1.5
1
0.5
0
0
250
500
750
1000
1250
[MurEp1] (µM)

Figure 5.

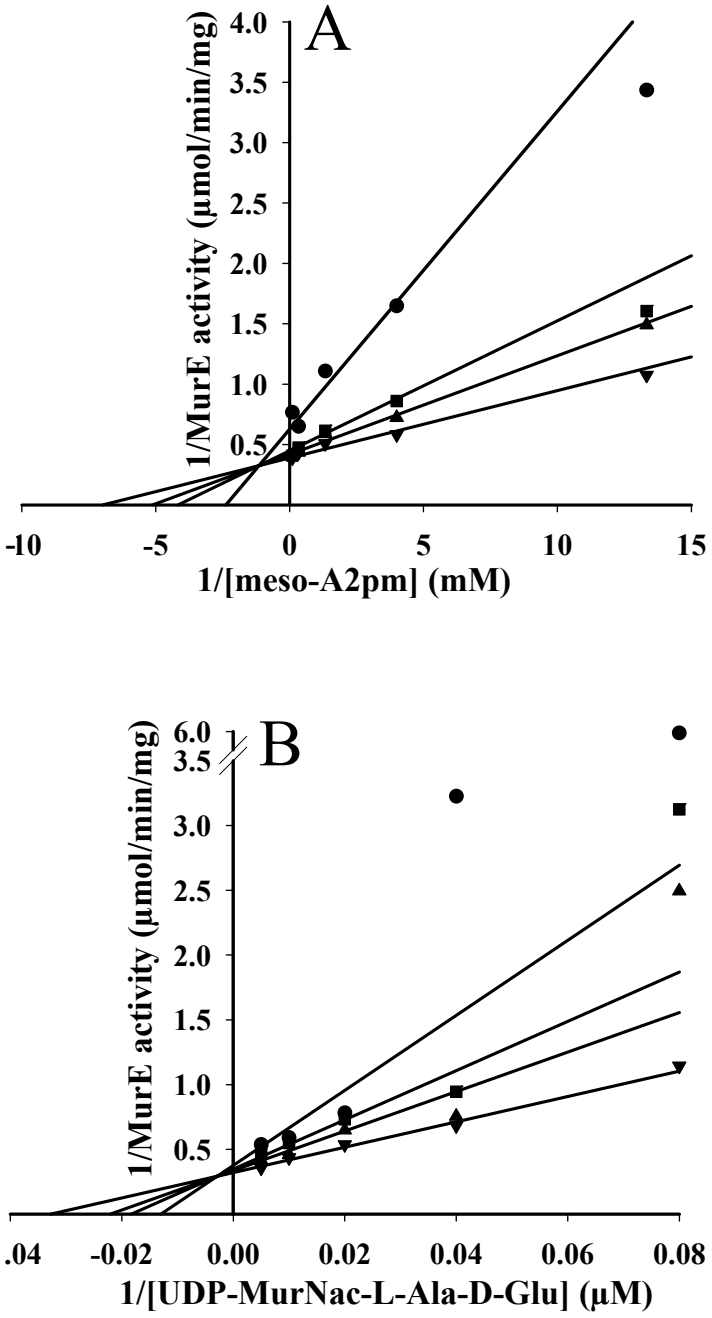
A
1/MurE activity (µmol/min/mg)
4.0
3.5
3.0
2.5
2.0
1.5
1.0
0.5
-10
-5
0
5
10
15
1/[meso-A2pm] (mM)
B
1/MurE activity (µmol/min/mg)
6.0
3.5
3.0
2.5
2.0
1.5
1.0
0.5
.04
-0.02
0.00
0.02
0.04
0.06
0.08
1/[UDP-MurNac-L-Ala-D-Glu] (µM)

Chapitre 7 - Phage display-derived inhibitor of the MurF cell wall enzyme as a lead compound for the development of novel antimicrobial agents

Résumé

Sélection d'un inhibiteur par présentation phagique contre l'enzyme MurF essentielle à la biosynthèse de la paroi bactérienne en vue du développement de nouveaux agents antibactériens

L'augmentation et la propagation des mécanismes de résistance parmi les pathogènes bactériens engendrent un besoin impératif de nouveaux agents antibactériens. Cette étude se concentre sur l'enzyme MurF essentielle à la biosynthèse de la paroi bactérienne en tant que cible thérapeutique. MurF catalyse la formation d'un lien amide entre le D-Alanine-D-Alanine (D-Ala-D-Ala) et le précurseur nucléotidique UDP-N-acetylmuramyle-L-alanyle-D-glutamyle-meso-diaminopimélate (UDP-MurNac-Ala-Glu-meso-A2pm) en hydrolysant de l'ATP en ADP et phosphate inorganique. La protéine MurF biologiquement active a été utilisée pour cribler une banque de peptides par présentation phagique. Les phages adhérés ont été élués avec de la glycine à pH acide et de façon compétitive avec l'ATP et le D-Ala-D-Ala. Un consensus peptidique prédominant a été identifié et synthétisé en tant que MurFp1. Le substrat nucléotidique a été synthétisé puis un essai spectrophotométrique a été mis au point afin de caractériser l'activité enzymatique de MurF et d'analyser le potentiel inhibiteur de MurFp1. Ce peptide inhibe spécifiquement MurF avec une CI_{50} de 250 μM et un K_i de 420 μM contre le D-Ala-D-Ala lorsque MurF est préincubée avec l'UDP-MurNac-Ala-Glu-meso-A2pm. L'inhibition de MurF par MurFp1 est dépendante du temps et elle augmente de façon importante lorsque le UDP-MurNac-Ala-Glu-meso-A2pm ou l'ATP est ajouté lors de la période de preincubation. Par contre, l'ajout du D-Ala-D-Ala pendant la preincubation annule le pouvoir inhibiteur de MurFp1. Les résultats obtenus indiquent que MurFp1 exploite un changement conformationnel provoqué par la liaison de l'UDP-MurNAc-Ala-Glu-meso-A2pm ou de l'ATP afin d'inhiber l'utilisation du D-Ala-D-Ala par MurF. Ainsi, cette étude présente le premier inhibiteur peptidique de MurF en vue du développement d'une nouvelle classe d'agents antibactériens.

Contribution des auteurs

Cet article complétant la deuxième section du corps de ma thèse est signé par cinq auteurs. En tant que première auteure, j'ai effectué l'ensemble des expériences décrites à l'exception de la synthèse du substrat nucléotidique de MurF réalisée par l'équipe de Adrian Lloyd et du Dr Timothy D. H. Bugg. J'ai également interprété les résultats, j'ai préparé les figures et tableaux puis et j'ai rédigé presque entièrement le manuscrit en vue d'une publication dans la revue scientifique «Journal of Antibacterial Chemotherapy». La section décrivant la synthèse du substrat nucléotidique a été écrite par Adrian Lloyd et la figure correspondante a été préparée en collaboration avec Adrian Lloyd et le Dr Timothy D. H. Bugg. En ce qui concerne le Dr François Sanschagrin, il m'a apportée un support technique et scientifique au cours de ce projet de recherche. Finalement, le Dr Roger C. Levesque est à l'origine de l'idée de départ et de la conceptualisation de cette étude. Il a donc orienté le projet puis il a révisé le manuscrit pour en augmenter la fluidité et la valeur scientifique.

Phage display-derived inhibitor of the MurF cell wall enzyme as a lead compound for the development of novel antimicrobial agents

Catherine Paradis-Bleau[1], Adrian Lloyd[2], François Sanschagrin[1], Tom Clarke[2], Ann Blewett[2] , Timothy D. H. Bugg[2] and Roger C. Levesque[1*]

[1] *Département de Biologie Médicale, Université Laval, Québec, Québec, Canada, G1K 7P4*

[2] *Department of chemistry, University of Warwick, Coventry, United Kingdom, CV4 7AL*

[*] Corresponding author. Roger C. Levesque, Centre de recherche sur la fonction, la structure et l'ingénierie des protéines, pavillon Charles-Eugène Marchand, Université Laval, Québec, Québec, Canada, G1K 7P4, Tel: (1) (418) 656-3070; Fax: (1) (418) 656-7176; e-mail: rclevesq@rsvs.ulaval.ca.

Abstract

Objective: To develop antibacterial agents having novel modes of action against bacterial cell wall biosynthesis, we targeted the essential MurF enzyme of the antibiotic resistant pathogen *Pseudomonas aeruginosa*.

Methods: Purified *P. aeruginosa* MurF enzyme was used to screen a phage-display 12-mer library using competitive biopanning with the specific substrates D-Ala-D-Ala and ATP. The MurF substrate uridine 5'-diphosphoryl N-acetylmuramoyl-L-alanyl-D-glutamyl-meso-diaminopimelic acid (UDP-MurNAc-Ala-Glu-meso-A2pm) was synthesized, purified and used to quantify MurF kinetics and MurF inhibition using a sensitive spectrophotometric assay.

Results: A peptide we called MurFp1 was synthesized, based on the strongest biopanning consensus sequence. MurFp1 acted as a weak, time-dependent inhibitor of MurF ATPase activity but was a specific and potent inhibitor when MurF was pre-incubated with UDP-MurNAc-Ala-Glu-meso-A2pm or ATP. Adding the substrate D-Ala-D-Ala during the pre-incubation nullified inhibition. The IC_{50} value of MurFp1was evaluated at 250 μM and the K_i was established at 420 μM with respect to the mixed type of inhibition against D-Ala-D-Ala.

Conclusion: MurFp1 exerts its inhibitory action by interfering with the utilization of D-Ala-D-Ala by the MurF amide ligase reaction. We propose that MurFp1 exploits UDP-MurNAc-Ala-Glu-meso-A2pm-induced or ATP-induced structural changes for better interaction with the enzyme. To our knowledge, we present the first peptide inhibitor of MurF, an enzyme that should be exploited as a target for future antimicrobial drug development via peptide mimesis.

Keywords: UDP-N-acetylmuramoyl-L-alanyl-D-glutamyl-meso-diaminopimelyl:D-alanine-D-alanine amide ligase, D-alanine-D-alanine adding enzyme; MurF enzyme kinetics, peptide inhibitor, peptidoglycan

Introduction

The antibiotic revolution of the twentieth century has been overwhelmed by the astonishing ability of microorganisms to develop resistance. The worldwide spread of resistance to all clinically useful antibiotics among emerging bacterial pathogens represents one of the most critical current public health problems, increasing morbidity, mortality and health care costs.[1] In order to address this alarming situation, high priority has been given to the development of antibacterial agents with novel structures and modes of action directed against judiciously chosen hitherto unexploited physiological targets.

The bacterial cell wall biosynthetic machinery represents a pool of attractive antibacterial targets. This pathway encodes essential and highly conserved enzymes, the inhibition of which leads to lethal phenotypic expression due to impairment of cell wall biosynthesis and cell division. The essential bacterial cell wall enzymes have no eukaryotic counterparts and are sufficiently expressed during the infection of the host to constitute excellent antibacterial targets.[2] The first portion of the pathway is catalyzed by a series of enzymes, MurA through MurF, which synthesize the cytoplasmic cell wall precursor UDP-*N*-acetylmuramyl-pentapeptide. Membrane translocases MraY and MurG then add *N*-acetylglucosamine to *N*-acetylmuramyl-pentapeptide and transfer the precursor across the cytoplasmic membrane. The periplasmic precursor forms a branched structure with the growing cell wall polymer by the transglycosylation and transpeptidation actions of periplasmic penicillin-binding proteins (PBPs).[3] The cell wall polymer layer, composed of alternating units of *N*-acetylglucosamine and *N*-acetylmuramic acid cross-linked via short peptide chains, maintains cell shape and integrity, enabling the bacterium to survive variations in osmotic pressure. This network also provides rigidity, flexibility and strength, all necessary for cell growth and division. Indeed, bacterial cells with defective cell wall synthesis eventually burst and die.[4]

Interfering with cell wall synthesis has been one of the most effective antibacterial strategies and many clinically useful naturally occurring antibiotics target this pathway. The β-lactams, the glycopeptides and bacitracin all interfere with cell wall cross-linking or assembly.[3, 5, 6] D-cycloserine interferes with the formation of the dipeptide D-Alanine-D-Alanine (D-Ala-D-Ala), targeting the enzymes alanine racemase and D-Ala:D-Ala ligase.[5,7]

However, no antibacterial agents target the Mur enzymes involved in the cytoplasmic portion of the pathway, except for fosfomycin, a MurA inhibitor in limited clinical use.[3, 8] This under-exploitation may be explained in part by the lack of commercially available substrates for studying these enzymes, with the exception of the substrate of MurA.[3, 9]

We selected MurF as a specific cytoplasmic target for inhibiting cell wall biosynthesis. MurF is one of the four ATP-dependent amide ligases (MurC, MurD, MurE and MurF) that perform the non-ribosomal stepwise addition of the five amino acids that form the peptide moiety of the cell wall precursor.[10] MurF catalyzes the formation of the peptide bond between D-Ala-D-Ala and the nucleotide precursor UDP-*N*-acetylmuramoyl-L-alanyl-D-glutamyl-meso-diaminopimelic acid (UDP-MurNAc-Ala-Glu-meso-A2pm) with the concomitant hydrolysis of ATP to ADP and inorganic phosphate, yielding UDP-*N*-acetylmuramoyl-L-alanyl-D-glutamyl-meso-diaminopimelyl-D-alanyl-D-alanine.[11] MurF is at a crucial junction in cell wall biosynthesis, mobilizing the cytoplasmic building block UDP-*N*-acetylmuramyl-pentapeptide for the next steps of the pathway. While the roles of MurC, MurD and MurE may be substituted in a single step by the muropeptide ligase Mpl which is involved in the cell wall recycling process,[12] MurF remains the sole D-Ala-D-Ala adding enzyme. The study of various *murF* mutants has demonstrated the essentiality of this enzymatic function.[13, 14] Indeed, the step catalyzed by MurF is both essential and non-redundant, its active site amino acid sequence is highly conserved among bacterial species and both Gram-positive and Gram-negative bacteria have only a single copy of the *murF* gene.[15] Furthermore, strict limitation to D-amino acid substrates[9] makes MurF an especially attractive target for the development of selective and broad-spectrum antibacterial agents, since these amino acids are metabolized only in prokaryotes, presumably to make the cell wall resistant to hydrolysis by proteases.[5] D-Ala-D-Ala is the central molecule in the cell wall cross-linking assembly. The transpeptidation reaction between two glycan strands is energized by the hydrolysis of the D-Ala-D-Ala bond and PBPs cleave the D-Ala-D-Ala of a donor pentapeptide precursor, with concomitant release of the terminal D-Ala and formation of the covalent cross-linkage with a meso-A2pm residue in an acceptor peptide moiety.[16] D-Ala-D-Ala residues also have an important role in bacterial cell wall recognition and the action of PBPs, β-lactams and glycopeptides.[17, 18,14]

Since MurF acts on a dipeptide to form peptide bonds of a highly distinctive type, we investigated the possibility of inhibiting this enzyme with amino acid or peptide derivatives and chose to identify such inhibitors by phage display screening using a competitive approach with the substrates D-Ala-D-Ala and ATP. Phage display allows the identification, among a pool of 10^9 random permutations, of peptide ligands having high binding affinities for a targeted protein.[19] The peptides are expressed or "displayed" on the surface of a phage coat and bind to functional sites such as substrate binding sites, protein-protein interaction sites or allosteric regulatory sites.[20] Phage display biopanning has proven useful for the selection of various enzyme inhibitors including the amide ligases MurC and MurD and has become a valuable tool for antibacterial drug discovery.[21, 22] The results we present herein constitute, to the best of our knowledge, the first report of a specific peptide inhibitor of MurF which we identified using a phage-display library. We focused this effort on the Gram-negative bacterium *Pseudomonas aeruginosa*, an ubiquitous opportunistic pathogen responsible for a wide variety of chronic nosocomial infections in patients with burns or neutropenia and one of the most difficult microorganisms to combat, due to resistance to most antibiotics in clinical use.[23] This bacterium also represents the major cause of chronic lung infection and death in cystic fibrosis patients.[24]

2. Materials and methods

MurF enzyme preparation

The MurF protein was over-expressed, purified and sequenced as previously described.[25] All reagents were from Sigma Aldrich (Oakville, Ontario, Canada) unless otherwise indicated. Phosphate in the MurF preservation buffer was removed by dialyzing 5 ml against 3 L of buffer A (25 mM Bis-Tris Propane pH 8.0, 1 mM β-mercaptoethanol, 2.5 mM $MgCl_2$) three times at 4°C. Purified MurF protein was visualized on SDS-PAGE using a SYPRO® Orange staining (Bio-Rad Inc., Mississauga, Ontario, Canada) and the protein concentration was determined by the Bradford method (BioRad Inc., Mississauga, Ontario, Canada) using bovine serum albumin as standard. The phosphate-free MurF protein was divided into aliquots and preserved at -20°C with glycerol a final concentration of 10%.

Affinity selection of phage displayed peptides against MurF

Phage display screening was performed with the PH.D.-12 phage library (New England Biolabs, Mississauga, Ontario, Canada) containing ~ 2.7 x 10^9 random dodecamer peptide sequences. Peptide permutations are fused to the minor coat protein pIII of phage M13 via the flexible linker Gly-Gly-Gly-Ser. Three rounds of biopanning were performed with increasing specificity and stringency obtained by increasing the Tween concentration during washes and by decreasing the time of contact between the phage-encoded peptides and the targeted MurF protein as previously described.[21, 26] Phages encoding selected peptides were eluted at the end of the third round of biopanning using 100 µl of 0.2 M glycine-HCl (pH 2.2)[21] as well as by 100 µl of 1 mM ATP and 100 µl of 1 mM D-Ala-D-Ala for 30 min. The DNA of ten phages was prepared and sequenced with a -96 gIII primer (New England Biolabs) for each elution condition.[26] The peptides thus selected were aligned in order to identify the consensus amino acid sequence of the inhibitory peptide candidate.

Bioinformatic analysis

The consensus peptide sequence was characterized using different bioinformatic analysis algorithms of the ExPasy server including the Compute pI/Mw and ProtParam tools [27] as well as the PSIpred and SSpro secondary structure prediction tools.[28] The consensus sequence was analyzed for similar patterns in the UniProt protein sequence database using the fasts34 program from the FASTA software package, previously identified as the most efficient tool for identifying proteins with similarities to small peptide sequences.[22, 29]

Peptide synthesis

The consensus dodecamer peptide (TMGFTAPRFPHY) identified by phage display biopanning was synthesized on an ABI 433A Peptide Synthesizer using FastMoc chemistry[21] and purified on a Vydak 22 X 250 mm C18 reverse-phase HPLC column using a 0.1% trifluoroacetic acid/acetonitrile gradient at 10 ml/min. Peptide purity (> 95%) was analyzed by HPLC and molecular mass (1424.68 daltons) was confirmed by MALDI-TOF

mass spectroscopy. Named MurFp1, the peptide was dissolved in buffer B (200 mM Tris-HCl pH 8.0) at a final concentration of 100 mM and the pH was adjusted to 7.0.

Synthesis and purification of UDP-MurNAc-Ala-Glu-meso-A2pm

Synthesis of the UDP-MurNAc-Ala-Glu-meso-A2pm substrate was performed as previously described[30] except that the reactions starting from UDP-*N*-acetylglucosamine were carried out in a single mixture using the combined activities of *P. aeruginosa* enzymes MurA, MurB, MurC, MurD and MurE. The product was purified from the reaction mixture by first removing the Mur enzymes by ultrafiltration and then purifying the ultrafiltrate by anion exchange chromatography at room temperature on DEAE-Sephacel pre-equilibrated in 10 mM ammonium acetate at pH 7.5, using a 10-800 mM ammonium acetate (pH 7.5) gradient for elution. UDP-MurNAc-Ala-Glu-meso-A2pm was identified by a pyruvate kinase/lactate dehydrogenase coupled assay for D-Ala-D-Ala-dependent ADP generation by MurF. Fractions thus found to contain UDP-MurNAc-Ala-Glu-meso-A2pm were freeze-dried from water three times to remove the ammonium acetate. UDP-MurNAc-Ala-Glu-meso-A2pm purity was assessed by FPLC analytical anion exchange on MonoQ^{TM} using a 0-0.5 M ammonium acetate gradient. The structure of the purified UDP-MurNAc-Ala-Glu-meso-A2pm was characterized using negative ion electrospray mass spectrometry and the synthesized product was stored frozen in water at 6.23 mM.

Characterization of MurF ATPase activity by spectrophotometric assay

The ATPase activity of *P. aeruginosa* MurF was quantified by a colorimetric assay that measures the release of nanomoles of inorganic phosphate using the Lanzetta reagent.[31] The reaction mixture (100 µl), held at room temperature, contained purified MurF (40 nM) from a fresh aliquot, ATP (1 mM), UDP-MurNAc-Ala-Glu-meso-A2pm (100 µM) and D-Ala-D-Ala (5 mM) in buffer C (100 mM Tris-HCl pH 8.6, 40 mM KCl, 500 mM NaCl, 1 mg/ml bovine serum albumin and 10 mM $MgCl_2$).[11] Reaction time was 15 min before adding 800 µl of the Lanzetta reagent. After an additional 5 min for colour development, 100 µl of 34% (w/v) sodium citrate was added to stop the reaction.[31] The optical density at 660 nm was

immediately measured with a Cary spectrophotometer (Varian, Mississauga, Ontario, Canada). The amount of inorganic phosphate released by the MurF amide ligase was determined by comparison to the linear portion of a phosphate standard curve with a minimum R^2 value of 0.99. The phosphate content of each component in the reaction was subtracted from the total phosphate measured and negative controls were done without enzyme or substrate. Analyses of MurF activity were done in triplicate. Different concentrations of each substrate and NaCl were tested in order to determine optimal conditions for the study of the activity of the inhibitor.

Maximal specific activity, the catalytic constant (k_{cat}) or number of substrate molecules hydrolyzed per active site per min, the Michaelis-Menten constant (K_m) or concentration of substrate giving half the maximal velocity and the enzyme efficiency (k_{cat}/K_m) were determined for MurF with respect to D-Ala-D-Ala. Kinetic parameters were determined by nonlinear regression analysis with a square matrix of enzyme velocities following the Michaelis-Menten equations using the Enzyme Kinetics Module version 1 of SigmaPlot version 8.

Kinetics of MurF inhibition by MurFp1

The inhibition of MurF ATPase activity by MurFp1 at different concentrations was measured by the spectrophotometric assay and the concentration required to produce 50% inhibition (IC_{50}) was noted. The substrates were added after 30 min of pre-incubation of the enzyme and inhibitor. Tests were also done in which UDP-MurNAc-Ala-Glu-A2pm was added for pre-incubation with the enzyme and inhibitor and the remaining substrates were added after 30 min. Pre-incubations for 0, 5, 10, 30 and 60 min with 2 mM MurFp1 were also tested. The reaction was carried out at room temperature in buffer C. The specific activity of MurF for each substrate at each MurFp1 concentration was expressed relative to the corresponding velocity in the absence of the inhibitor. To identify potential interactions between MurFp1 and the MurF substrates, each substrate was added separately at a fixed concentration with or without 2 mM MurFp1 and the two remaining substrates were added after 30 min of pre-incubation. The MurFp1 inhibitory constant (K_i) was determined for D-Ala-D-Ala using reaction velocity data obtained with a 30 min pre-incubation of MurF,

UDP-MurNAc-Ala-Glu-A2pm and inhibitor. MurFp1 concentrations tested were 0, 75, 150, 300 and 600 μM with D-Ala-D-Ala concentrations of 50, 100, 250, 500 and 1000 μM and fixed optimal concentrations of the remaining substrates.

Kinetic data were fitted to the appropriate model equations using the Sigmaplot Enzyme Kinetics Module. Steady-state inhibition kinetic parameters were determined by nonlinear regression analysis using the least squares method as a reference to ensure accurate dataset fitting and to generate error estimates for each individual observation. The Michaelis-Menten plot of MurF initial velocity as a function of substrate concentration was used to determine the apparent kinetic parameters V_{max} and K_m with respect to D-Ala-D-Ala using equation 1:

$$v = V_{max} * [S]/(K_m + [S]) \quad (1)$$

where v is MurF initial velocity, V_{max} is the maximum initial velocity and [S] is the concentration of D-Ala-D-Ala.[32, 33] The type of inhibition was identified using the Lineweaver-Burk plots of reciprocal initial velocity to reciprocal substrate concentration for the various inhibitor concentrations. Competitive K_i value was determined using the Dixon graphic re-plotting of reciprocal initial velocity versus MurFp1 concentration for each substrate concentration, which provides the inhibition components regardless of the inhibition type according to equation 2:

$$v = V_{max}*((1+\beta*I/(\alpha*K_i))/(1+I/(\alpha*K_i)))/(1+K_m/S)*(1+I/K_i)/(1+I/(\alpha*K_i))) \quad (2)$$

where V_{max} is the maximum initial velocity for the uninhibited MurF reaction, I is MurFp1, K_m is the Michaelis constant for the uninhibited MurF reaction, K_i is the competitive inhibition constant (dissociation constant of complex MurF-MurFp1), α is the K_m factor change when MurFp1 is bound to the MurF-D-Ala-D-Ala complex (ES) and β is the K_p factor (the rate constant when the enzyme-substrate complex breaks down to enzyme and product) change when MurFp1 is bound to ES.[32, 33] The non-competitive K_i was calculated using equation 3:

$$v = V_{max}/((1+K_m/S)*(1+I/K_i)/(1+I*\beta/K_i)) \quad (3)$$

The inhibition of MurF by non-specific peptides identified by phage display and known to inhibit a β-lactamase was tested for comparison purposes with and without the UDP-MurNAc-Ala-Glu-A2pm in the pre-incubation step.[34]

Results

Purification of biologically active MurF enzyme

The purified MurF protein was visualized as a single 52 kDa band on SDS-PAGE (data not shown). N-terminal sequencing of the first 15 amino acid residues confirmed its identity as *P. aeruginosa* MurF ligase (100% identical to the published sequence, including the initial Met). MurF biological activity was confirmed by mass spectrometric identification of the cytoplasmic cell wall precursor UDP-N-acetylmuramyl pentapeptide synthesized *in vitro* in the presence of the purified enzymes MurA, MurB, MurC, MurD and MurE.[25] Quantification of inorganic phosphate using the Lanzetta reagent did not reveal any trace of phosphate in the extensively dialyzed MurF protein solution.

Affinity selection of MurF binding peptides

As shown in Table I, each of the three rounds of biopanning selected only a fraction of the phage input, which decreased from approximately 10^{11} down to 10^{7} plaque forming units (PFUs). Phage recoveries were between 0.02% and 0.000065%. The third round gave a lower phage recovery compared to the two previous rounds, indicating a strong selection of specific MurF-interacting peptide sequences at this step. Each elution strategy employed at the end of the third round gave similar phage recovery yields. The competitive elution conditions using specific MurF substrates were as effective as the well-known glycine-HCl elution strategy.

The different elution conditions allowed the selection of different peptide sequences with specific motifs (Fig. 1). Analysis of peptide sequence frequencies and conserved motifs identified the consensus sequence TMGFTAPRFPHY from the 12-mer library. This consensus sequence, which we called MurFp1, was predominant in elution by glycine-HCl but less so in competitive elutions with ATP or D-Ala-D-Ala. The consensus sequence was rich in hydrophobic aromatic residues, P residues and basic residues but contained no acidic or polar residues. The N-terminal T residue and the basic R residue of the consensus peptide were particularly conserved, especially in the ATP and D-Ala-D-Ala elution groups. Two hydrophobic aromatic residues or two P residues often occurred close to each

other in the selected peptide sequences as they do in the consensus sequence. P residues occurred mostly near a hydrophobic aromatic residue or a basic residue, as in the consensus sequence (Fig. 1). Apart from the consensus sequences found in more than one elution group, the sequence VSANRHLGGNLP was recovered once by both the ATP and D-Ala-D-Ala elutions (Fig. 1). Elution with glycine-HCl gave two sequences with a "SRL" motif, which was absent in the other elution groups. Among the ATP elution group, two sequences presented a "YST" motif also absent in the other elution groups. The vast majority of the sequences eluted with D-Ala-D-Ala presented hydrophobic residues near small residues. Indeed, the D-Ala-D-Ala elution group contained more small amino acids than the other groups. Overall, the competitive elutions yielded more sequence diversity than the glycine-HCl elution.

Bioinformatic analysis

Analysis by the various algorithms of the ExPasy server established the theoretical pI of MurFp1 at 8.44, indicating that it would be positively charged at physiological pH. Indeed, MurFp1 includes a single amino acid (R) that would bear this positive charge and no amino acid bearing a counter-balancing negative charge. The ProtParam tool estimated the half-life of the peptide at more than 10 hours in *Escherichia coli in vivo* and at 7.2 hours in mammalian reticulocytes *in vitro*. The secondary structure prediction tools indicated with relative certainty a random coil structure. The fasts34 program did not identify any relevant protein in the UniProt database having similarities to MurFp1.

Synthesis and purification of UDP-MurNAc-Ala-Glu-meso-A2pm

Analysis of UDP-MurNAc-Ala-Glu-meso-A2pm synthesized by the *P. aeruginosa* enzymes MurA, MurB, MurC, MurD and MurE by FPLC anionic exchange indicated a purity of 95% (Fig. 2A). Characterization of the purified product by mass spectrometry identified four species of UDP-MurNAc-Ala-Glu-meso-A2pm with observed m/z identical to the expected values (Table II). The mass spectra confirmed the UDP-MurNAc-Ala-Glu-meso-A2pm structure presented in Figure 2B.

Characterization of the MurF ATPase activity

The ATP and UDP-MurNAc-Ala-Glu-meso-A2pm preparations contained traces of phosphate subtracted from the total phosphate content of the enzyme reaction mixture (values not shown). The controls performed without the MurF enzyme or without any one of the substrates did not yield any phosphate from ATP (data not shown), indicating that the reaction mixture was devoid of contaminating ATPase activities that might interfere with the assay. The optimal ATP concentration was 1 mM, and MurF reached noticeable activity with 100 μM of the UDP-MurNAc-Ala-Glu-meso-A2pm substrate (data not shown). Steady state kinetic analysis indicated that MurF obeyed Michaelis–Menten kinetics, reaching a maximal specific activity of 4.4 ± 0.4 μmole/min/mg at 5 mM D-Ala-D-Ala with a K_m of 115 ± 10 μM (Table III). Addition of NaCl to the reaction buffer improved MurF activity by a factor of 1.75 (data not shown). The enzyme was very sensitive to buffer pH, with maximal activity at pH 8.6. The k_{cat} value indicated that each MurF active site performed about 100 ligations of D-Ala-D-Ala to UDP-MurNAc-Ala-Glu-meso-A2pm, and hydrolyzed about 100 ATP molecules per min, releasing the same amount of ADP and inorganic phosphate in accordance with the known stoichiometric relationship.[35] The level of certainty for the measured kinetic parameters may be considered high, as the standard deviations were always smaller than 20% of the corresponding data (Table III).

Inhibitory kinetics of MurFp1

Uninhibited MurF ATPase activity decreased after 60 min of pre-incubation (data not shown). This effect was incorporated into the calculation of enzyme inhibition in the presence of MurFp1. Inhibition increased as a function of pre-incubation time in the presence of MurFp1, following an overall linear relationship and indicating that MurFp1 behaved as a weak time-dependent inhibitor. At a concentration of 2 mM, 50% inhibition was obtained following a pre-incubation period of 30 min (Fig. 3A).

Adding ATP or UDP-MurNAc-Ala-Glu-meso-A2pm during the pre-incubation step unexpectedly increased the inhibitory action of MurFp1, an effect less pronounced for ATP (data not shown). MurF reaction velocity in the absence of inhibitor was similar with or

without ATP or UDP-MurNAc-Ala-Glu-meso-A2pm in the pre-incubation step. The IC_{50} value for MurFp1 determined with pre-incubation period of 30 min with MurF and UDP-MurNAc-Ala-Glu-A2pm was 250 μM. The inhibition curve displayed a linear dose-response trend having variable slopes (Figure 4B). MurFp1 inhibited MurF ten times more efficiently when UDP-MurNAc-Ala-Glu-A2pm was added to the pre-incubation step (Fig. 3B and Table IV).

The presence of D-Ala-D-Ala during the pre-incubation step completely nullified the inhibition of MurF by MurFp1, restoring enzyme activity fully (data not shown). MurF reaction velocity was nearly identical in the presence or absence of D-Ala-D-Ala in the pre-incubation step. The Michaelis-Menten plot allowed the determination of the apparent kinetic parameters V_{max} and K_m for each MurFp1 concentration used to determine the K_i value (Fig. 4A and Table IV). MurF V_{max} decreased significantly as a function of MurFp1 concentration with respect to D-Ala-D-Ala. At 600 μM MurFp1, V_{max} was three times lower than for the uninhibited reaction (Table IV) while K_m values remained almost the same irrespective of MurFp1 concentration. The slopes and the y-intercept of the fitted lines of the Lineweaver-Burk plot varied with MurFp1 concentration, indicating a catalytic and a specific component in the inhibition (Fig. 4B). The common intersection point between the fitted lines shifted between extremes: left to the ordinate and down to the abscissa (Fig. 4B). This observation revealed that MurFp1 caused a reversible mixed type of inhibition sharing properties of competitive and non-competitive inhibitors against D-Ala-D-Ala. This inhibition type represented the most appropriate model, based on statistical convergence to the experimental data according to the Runs Test (data not shown), giving the highest R^2 value (0.97), the lowest Akaike value (-275) and the lowest standard deviation of the residuals (0.15). The non-competitive type of inhibition was the second best model, giving statistical values close to the mixed model (data not shown). The Dixon plot established the competitive K_i values at 420 ± 100 μM for the mixed type of inhibition against D-Ala-D-Ala, while the non-competitive K_i was evaluated at 370 ± 55 μM. The α parameter required to calculate the K_i value for the mixed type of inhibition indicated that MurFp1 binding to ES did not significantly change MurF affinity for D-Ala-D-Ala. The β parameter was nearly identical for both the mixed and non-competitive types of inhibition,

indicating that the rate constant of ES breaking down to enzyme and product dropped when MurFp1 was bound to ES (Table IV).

A non-specific peptide identified by phage display and pre-incubated for 30 min with MurF with or without UDP-MurNAc-Ala-Glu-A2pm did not inhibit MurF ATPase activity, confirming the specificity of MurF inhibition by MurFp1 (data not shown). The reactions were carried out in the presence of excess bovine serum albumin compared to the MurF concentration, suggesting that MurFp1 did not interact non-specifically with proteins. Overall, kinetic parameters had standard deviations no larger than 30% of the corresponding data.

Discussion

Since MurF has yet to be exploited as a target for antibacterial agents, there has been no opportunity for resistance to such agents to evolve. This makes MurF an excellent choice of target for the development of novel agents for combating bacterial infections. Using phage display competitive biopanning with ATP and D-Ala-D-Ala at concentrations in excess of their affinity constants, we have identified the first peptide inhibitor of MurF.

K_m values of 220 μM [36] and 164 μM [11] for ATP have been reported for *E. coli* MurF. The K_m value determined in our study for D-Ala-D-Ala with *P. aeruginosa* MurF, 115 ± 10 μM, is in the same range as values published previously for this enzyme (220 μM,[37] 208 μM,[11] 100 μM,[38] 60 μM[36]) and for its *E. coli* (54 μM[17]), *Bacillus* (300 μM[39]) and *Streptococcus faecaeli*s (160 μM [40]) equivalents. These values are roughly equal to the concentration of the D-Ala-D-Ala intracellular pool in *E. coli,* established at 200 μM.[11, 41]

Biopanning third-round contact time between the phage peptides and MurF was a much more stringent selection factor than second-round washing for MurF phage specificity (data not shown). This selection pattern was also observed for phage display screening of the amide ligase MurD.[22] In contrast, higher phage recovery titers in the second and third rounds, indicating enrichment of the phage population, were obtained during screening of MurC.[21] This is likely due to specific MurC-interacting phage-encoded peptide selection occurring earlier in the phage display screening in comparison to the selection of MurF and MurD interacting peptides. Indeed, stronger consensus sequences

were obtained against MurC than against MurD or MurF.[21, 22] Intrinsic factors such as phage infection and replication efficiency, protein translocation and folding bias as well as pIII coat stability also affect phage recovery.[42] It should also be noted that phage display screenings of *P. aeruginosa* proteins MurD, MurC, FtsZ and FtsA done under similar conditions did not identify any redundant sequences.[21, 26, 43]

The ATPase activity of MurF has been shown to depend absolutely on the presence of both D-Ala-D-Ala and UDP-MurNAc-Ala-Glu-A2pm.[35] The vast majority of the published kinetic studies of MurF bypassed the need for UDP-MurNAc-Ala-Glu-A2pm by measuring enzyme activity in terms of radioactive D-Ala-D-Ala incorporated into the cell wall precursor.[13, 38-40, 41 MurNAc, 44-46] A recent study described the generation of a mixture of UDP-MurNAc-Ala-Glu-Lys and UDP-MurNAc-Ala-D-Glu-A2pm using the Mpl enzyme.[15] These methods are time, cost and effort intensive compared to our quantification of MurF ATPase activity by a simple, rapid, sensitive and reliable assay using the Lanzetta reagent. MurF has also been assayed for ATPase activity by means of an ADP-coupled enzymatic method using pyruvate kinase and lactate dehydrogenase [11, 17, 35, 37, 47, 48] and by monitoring the release of radio-labelled inorganic phosphate from ATP.[49] Our assay does not involve any enzyme intermediate or radioactive isotope, makes screening potential MurF inhibitors easier and faster and could be well adapted to high throughput selection (HTS) screening in microtiter plates.

The optimal substrate concentrations for the *P. aeruginosa* MurF enzyme were nearly identical to those obtained for its *E. coli* counterpart under the same experimental conditions.[36] As for *E. coli* MurF, addition of NaCl increased the activity of *P. aeruginosa* MurF, probably by suppressing substrate inhibition by UDP-MurNAc-Ala-Glu-A2pm.[11] MurF was also very sensitive to the reaction buffer pH, as previously demonstrated.[35, 39] The maximal specific activity of *P. aeruginosa* MurF (4.4 μmole/min/mg) was similar to the published value of 3.41 μmole/min/mg.[48] The *P. aeruginosa* MurF enzyme appeared to be less efficient than its *E. coli* counterpart, for which maximal activities of 15.7 μmol/min/mg,[11] 11.2 μmol/min/mg[47] and 16 μmol/min/mg[37] have been reported. However, *E. coli* MurF has also been reported to have maximal activities as low as 1.270 μmol/min/mg,[44] 1.4 μmol/min/mg[35] and 0.13 μmol/min/mg[45] whereas *Streptococcus*

faecalis MurF has been found to have a specific activity of 0.83 μmoles/min/mg[40]. The k_{cat} value of the *P. aeruginosa* MurF enzyme (100 ± 15 min^{-1}) was smaller than for its *E. coli* counterpart, for which values of 1160 min^{-1},[11] 780 min^{-1} [37] and 1080 min^{-1} [17] have been measured. The k_{cat}/K_m value for D-Ala-D-Ala (0.85 ± 0.15 $min^{-1}\mu M^{-1}$) was also lower than for *E. coli* MurF (5.6 $min^{-1}\mu M^{-1}$ [11] and 19.8 $min^{-1}\mu M^{-1}$ [17])

It has been shown previously that the binding order for substrates to Mur ligases begins with ATP, followed by the nucleotide substrate and ending with the amino acid.[11,10] It has been further shown that the nucleotide substrate binds efficiently to MurD without ATP inducing conformational changes in the C-terminal and N-terminal domains.[50] To explain how MurFp1 could be a much stronger inhibitor following pre-incubation of MurF with its substrate UDP-MurNAc-Ala-Glu-meso-A2pm, we hypothesize that binding of the nucleotide to MurF induces a structural change that optimizes binding of MurFp1. *E. coli* MurF crystal structure suggests that UDP-MurNAc-Ala-Glu-meso-A2pm interacts mainly with the N-terminal domain, ATP binds principally to the central domain and D-Ala-D-Ala interacts at the C-terminus.[51] The N-terminal domain binds the uracyl ring of UDP but does not present the typical nucleotide-binding fold. Indeed, part of the central domain extends out towards the N-terminal domain to bind the pyrophosphate portion of the nucleotide.[51] This suggests a conformational change upon UDP-MurNAc-Ala-Glu-meso-A2pm binding and could explain why ATP binding to the central domain also increased inhibition by MurFp1. The open conformation of MurF is expected to undergo significant conformational change, bringing the domains into close proximity for forming a functional enzyme-substrate complex.[51] Binding of ATP may enhance such a conformational change in the case of MurD while the details of MurF substrate interactions remain unclear.[50, 51] To our knowledge, we have presented the first compound having Mur ligase inhibitory action that is enhanced by pre-incubation with the nucleotide substrate. However, appropriately substituted phosphinate inhibitors of ATP-dependent amide-forming enzymes depend on their phosphorylation via the ATP substrate. These ATP-dependent phosphinate analogues exhibit a transition-state time-dependent inhibition closely mimicking the tetrahedral intermediate involved in Mur ligase reactions.[3] It will therefore be of primary interest to

determine if the time dependent MurFp1 inhibitor is phosphorylated and subsequently acts as tetrahedral intermediate inhibitor.

Based on classical interpretation[32, 33] of our kinetic and statistical data, MurFp1 is a reversible mixed inhibitor sharing properties of competitive and non-competitive inhibitors. MurFp1 acted as a competitive inhibitor as the inhibition was reversed by addition of D-Ala-D-Ala during pre-incubation and the slopes of fitted lines from the Lineweaver-Burk plot increased as a function of MurFp1 concentration, revealing an increase in inhibitor binding strength (Fig. 4B).[32, 33] Like a non-competitive inhibitor that interferes with the enzymatic reaction without directly competing for the substrate binding site, MurFp1 inhibits MurF at high or low substrate concentrations, the V_{max} of MurF decreasing as a function of MurFp1 concentration and the y-intercept of the Lineweaver-Burk plot varying as a function of MurFp1 (Fig. 4 and Table IV). MurFp1 appears not to alter MurF affinity for the dipeptide but rather inhibit breakdown of the enzyme substrate complex to enzyme and product. Indeed, MurFp1 acted more like a non-competitive inhibitor than a competitive inhibitor of D-Ala-D-Ala. MurFp1 must thus bind elsewhere than at the D-Ala-D-Ala binding site, which remains available for the substrate. Furthermore, phage display and kinetic data indicated that D-Ala-D-Ala binding released MurFp1 from the MurF surface. It should be noted that Gly-HCl elution yielded more consensus sequences than D-Ala-D-Ala competitive elution, which did not efficiently elute MurFp1 (Fig. 1). We speculate that competitive elution during biopanning could lead to conformational changes that displace peptides bound to the MurF surface. MurFp1 could exert inhibition by inducing conformational change, sequestering D-Ala-D-Ala or interfering with MurF structural changes necessary for substrate proximity and amide bond formation. It will be of primary interest to investigate the exact binding site of MurFp1 and whether it induces structural changes by co-crystallization of the MurF-MurFp1 complex with each individual substrate. This will also yield valuable information for further directed optimization by medicinal chemistry.

Few MurF inhibitors have been reported and none have been shown to have antibacterial activity. The non-hydrolyzable ATP analogue AMP-PCP has been found to be a potent competitive inhibitor of MurF ATPase activity, with a K_{is} value of 33.6 μM, but

may not be a specific inhibitor.[11] The only phosphinate inhibitors of MurF, the aminoalkylphosphinate compounds, act as time-independent inhibitors competing with D-Ala-D-Ala and having K_i values between 200 and 700 μM.[36] Some dipeptide analogues have been shown to be competitive inhibitors of MurF with low affinity,[9] presenting moderate inhibition at 1 mM.[40] These analogues also acted as substrates and were incorporated into the cell wall.[40,17] A thiazolylaminopyrimidine series of MurF inhibitors have been identified having IC_{50} values as low as 2.5 μM.[15] Identification of a novel class of inhibitors has led to several potent compounds with IC_{50} values between 22 and 70 nM for MurF of *Streptococcus pneumoniae*.[49] Co-crystal structures of these inhibitors have indicated the path to the discovery of more efficient low-nanomolar inhibitors.[52] Their binding overlaps with the uridine–ribose binding site and captures MurF in a topologically compact state in which the C-terminal domain has undergone a large conformational change.[53] These observations support our hypothesis that conformational changes induced by UDP-MurNAc-Ala-Glu-meso-A2pm increase the inhibitory efficiency of MurFp1.

MurFp1 likely represents a specific inhibitor of MurF, as each of the Mur ligases displays a high specificity for its respective substrates with no cross-activity.[10, 47] MurFp1 is likely also a broad-spectrum inhibitor, as MurF is a key enzyme present in all medically relevant bacteria, with an active site highly conserved among bacterial species.[15] As mammals lack the D-Ala-D-Ala pathway, the inhibitory potential of compounds like MurFp1 against alanine racemase and D-Ala:D-Ala ligase should also be examined.[5] MurF has been shown to affect the level of *β*-lactam antibiotic resistance in methicillin-resistant *Staphylococcus aureus*, to influence the control of cell division, to affect the transcription of PBPs[14] and to play a key role in the glycopeptide resistance mechanism.[17, 18] Indeed, targeting MurF may lead to perturbation in cell division and in antibiotic resistance, allowing acute inhibition of the essential PBP reactions. The likelihood of antibiotic resistance would be much lower if a potent MurF inhibitor was used as part of an antibacterial cocktail comprising fosfomycin to inhibit MurA and D-cycloserine to interfere with the formation of D-Ala-D-Ala, as mutations conferring resistance would need to occur in many genes. Vancomycin or teicoplanin derivatives can also be used respectively on Gram-positive and Gram-negative bacteria to increase permeability and produce synergistic

effects.[54] Such effects will thus be amplified since D-Ala:D-Ala ligases are highly sensitive to feed-back inhibition by D-Ala-D-Ala, which could accumulate under these conditions.[36] This may allow decreases in D-cycloserine and glycopeptide doses and their associated toxic side effects.

We have identified the first peptide inhibitor having a novel mode of action against the essential and unexploited bacterial cell wall ligase MurF. Furthermore, characterization of *P. aeruginosa* MurF kinetics should provide valuable insight into the rational design of a new generation of specific bacterial-cell-wall-directed antibacterial agents. To enhance the pharmacological properties of MurFp1, its sequence will be the object of peptidomimetism.[55] Inhibitory peptides are notorious for not being able to cross bacterial membranes. To avoid this problem, peptides may be conjugated to a bacterial transport molecule essential for virulence.[56] To thwart bacterial resistance, peptide vectors capable of transport into cells in the form of covalent conjugates may be suitable.[57] MurFp1 could likely be modified to mimic antimicrobial peptides as their activity is thought to be determined by helicity and hydrophobicity rather than by their specific amino acid sequences.[58, 59] Finally, ribosome display could be exploited to optimize the antibacterial properties. [60]

Acknowledgements

We thank Le Service de séquence de peptides de l'Est du Québec and Le Service d'analyse et de synthèse d'acides nucléiques de l'Université Laval as well as Jérome Laroche for bioinformatic advice. This work was funded by The Canadian Bacterial Diseases Network via the Canadian Centers of Excellence, a FCAR infrastructure team grant to R. C. Levesque and a FRSQ studentship to Catherine Paradis-Bleau.

Transparency declarations

None to declare

References

1. Levy, S. B. & Marshall, B. (2004). Antibacterial resistance worldwide: causes, challenges and responses. *Nat Med* **10,** S122-129.
2. Projan, S. J. (2002). New (and not so new) antibacterial targets - from where and when will the novel drugs come? *Curr Opin Pharmacol* **2,** 513-522.
3. El Zoeiby, A., Sanschagrin, F. & Levesque, R. C. (2003). Structure and function of the Mur enzymes: development of novel inhibitors. *Mol Microbiol* **47,** 1-12.
4. Young, K. D. (2003). Bacterial shape. *Mol Microbiol* **49,** 571-580.
5. Walsh, C. T. (1989). Enzymes in the D-alanine branch of bacterial cell wall peptidoglycan assembly. *J Biol Chem* **264,** 2393-2396.
6. Silver, L. L. (2003). Novel inhibitors of bacterial cell wall synthesis. *Curr Opin Microbiol* **6,** 431-438.
7. Neuhaus, F. C. & Lynch, J. L. (1964). The enzymatic synthesis of D-alanyl-D-alanine. 3. On the inhibition of D-alanyl-D-alanine synthetase by the antibiotic D-cycloserine. *Biochemistry* **3,** 471-480.
8. Christensen, B. G., Leanza, W. J., Beattie, T. R., Patchett, A. A., Arison, B. H., Ormond, R. E.*, et al.* (1969). Phosphonomycin: structure and synthesis. *Science* **166,** 123-125.
9. Bugg, T. D. & Walsh, C. T. (1992). Intracellular steps of bacterial cell wall peptidoglycan biosynthesis: enzymology, antibiotics, and antibiotic resistance. *Nat Prod Rep* **9,** 199-215.
10. Bouhss, A., Mengin-Lecreulx, D., Blanot, D., van Heijenoort, J. & Parquet, C. (1997). Invariant amino acids in the Mur peptide synthetases of bacterial peptidoglycan synthesis and their modification by site-directed mutagenesis in the UDP-MurNAc:L-alanine ligase from *Escherichia coli*. *Biochemistry* **36,** 11556-11563.
11. Anderson, M. S., Eveland, S. S., Onishi, H. R. & Pompliano, D. L. (1996). Kinetic mechanism of the *Escherichia coli* UDPMurNAc-tripeptide D-alanyl-D-alanine-adding enzyme: use of a glutathione S-transferase fusion. *Biochemistry* **35,** 16264-16269.
12. Mengin-Lecreulx, D., van Heijenoort, J. & Park, J. T. (1996). Identification of the *mpl* gene encoding UDP-N-acetylmuramate: L-alanyl-gamma-D-glutamyl-meso-diaminopimelate ligase in *Escherichia coli* and its role in recycling of cell wall peptidoglycan. *J Bacteriol* **178,** 5347-5352.
13. Lugtenberg, E. J. & v Schijndel-van Dam, A. (1972). Temperature-sensitive mutants of *Escherichia coli* K-12 with low activities of the L-alanine adding enzyme and the D-alanyl-D-alanine adding enzyme. *J Bacteriol* **110,** 35-40.
14. Sobral, R. G., Ludovice, A. M., de Lencastre, H. & Tomasz, A. (2006). Role of *murF* in cell wall biosynthesis: isolation and characterization of a *murF* conditional mutant of *Staphylococcus aureus*. *J Bacteriol* **188,** 2543-2553.
15. Baum, E. Z., Crespo-Carbone, S. M., Abbanat, D., Foleno, B., Maden, A., Goldschmidt, R.*, et al.* (2006). Utility of muropeptide ligase for identification of inhibitors of the cell wall biosynthesis enzyme MurF. *Antimicrob Agents Chemother* **50,** 230-236.
16. Holtje, J. V. (1998). Growth of the stress-bearing and shape-maintaining murein sacculus of *Escherichia coli*. *Microbiol Mol Biol Rev* **62,** 181-203.

17. Bugg, T. D., Wright, G. D., Dutka-Malen, S., Arthur, M., Courvalin, P. & Walsh, C. T. (1991). Molecular basis for vancomycin resistance in *Enterococcus faecium* BM4147: biosynthesis of a depsipeptide peptidoglycan precursor by vancomycin resistance proteins VanH and VanA. *Biochemistry* **30,** 10408-10415.
18. Reynolds, P. E. (1989). Structure, biochemistry and mechanism of action of glycopeptide antibiotics. *Eur J Clin Microbiol Infect Dis* **8,** 943-950.
19. Pierce, G. E. (2005). *Pseudomonas aeruginosa*, *Candida albican*s, and device-related nosocomial infections: implications, trends, and potential approaches for control. *J Ind Microbiol Biotechnol* **32,** 309-318.
20. Davies, J. C. (2002). *Pseudomonas aeruginosa* in cystic fibrosis: pathogenesis and persistence. *Paediatr Respir Rev* **3,** 128-134.
21. Christensen, D. J., Gottlin, E. B., Benson, R. E. & Hamilton, P. T. (2001). Phage display for target-based antibacterial drug discovery. *Drug Discov Today* **6,** 721-727.
22. Hyde-DeRuyscher, R., Paige, L. A., Christensen, D. J., Hyde-DeRuyscher, N., Lim, A., Fredericks, Z. L.*, et al.* (2000). Detection of small-molecule enzyme inhibitors with peptides isolated from phage-displayed combinatorial peptide libraries. *Chem Biol* **7,** 17-25.
23. El Zoeiby, A., Sanschagrin, F., Darveau, A., Brisson, J. R. & Levesque, R. C. (2003). Identification of novel inhibitors of *Pseudomonas aeruginosa* MurC enzyme derived from phage-displayed peptide libraries. *J Antimicrob Chemother* **51,** 531-543.
24. Paradis-Bleau, C., Beaumont, M., Boudreault, L., Lloyd, A., Sanschagrin, F., Bugg, T. D.*, et al.* (2006). Selection of peptide inhibitors against the *Pseudomonas aeruginosa* MurD cell wall enzyme. *Peptides* **27**, 1693-1700.
25. El Zoeiby, A., Sanschagrin, F., Havugimana, P. C., Garnier, A. & Levesque, R. C. (2001). *In vitro* reconstruction of the biosynthetic pathway of peptidoglycan cytoplasmic precursor in *Pseudomonas aeruginosa*. *FEMS Microbiol Lett* **201,** 229-235.
26. Paradis-Bleau, C., Sanschagrin, F. & Levesque, R. C. (2005). Peptide inhibitors of the essential cell division protein FtsA. *Protein Eng Des Sel* **18,** 85-91.
27. Walker, J. M. (2005). *The proteomics protocols handbook*. Humana Press, Totowa, N.J.
28. Jones, D. T. (1999). Protein secondary structure prediction based on position-specific scoring matrices. *J Mol Biol* **292,** 195-202.
29. Mackey, A. J., Haystead, T. A. & Pearson, W. R. (2002). Getting more from less: algorithms for rapid protein identification with multiple short peptide sequences. *Mol Cell Proteomics* **1,** 139-147.
30. Reddy, S. G., Waddell, S.T., Kuo, D, W., Wong, K. K. and Pompliano, D.L (1999). Preparative enzymatic synthesis and characterization of the cytoplasmic intermediates of murein biosynthesis. *Journal of the American Chemical Society* **121,** 1175-1178.
31. Lanzetta, P. A., Alvarez, L. J., Reinach, P. S. & Candia, O. A. (1979). An improved assay for nanomole amounts of inorganic phosphate. *Anal Biochem* **100,** 95-97.
32. Cornish-Bowden, A. (1979). *Fundamentals of enzyme kinetics*. Butterworths, London ; Boston.
33. Segal, I. H. (1993). *Enzyme kinetics - behavior and analysis of rapid equilibrium and steady-state enzyme systems*. John Wiley and Sons, Inc.

34. Sanschagrin, F. & Levesque, R. C. (2005). A specific peptide inhibitor of the class B metallo-beta-lactamase L-1 from *Stenotrophomonas maltophilia* identified using phage display. *J Antimicrob Chemother* **55,** 252-255.
35. Comb, D. G. (1962). The enzymatic addition of D-alanyl-D-alanine to a uridine nucleotide-peptide. *J Biol Chem* **237,** 1601-1604.
36. Miller, D. J., Hammond, S.M., Anderluzzi, D., Bugg, T.D.H. (1998). Aminoalkylphosphinate inhibitors of D-Ala-D-Ala adding enzyme. *J Chem Soc Perkin Trans* **1,** 131-142.
37. Duncan, K., van Heijenoort, J. & Walsh, C. T. (1990). Purification and characterization of the D-alanyl-D-alanine-adding enzyme from *Escherichia coli*. *Biochemistry* **29,** 2379-2386.
38. Michaud, C., Blanot, D., Flouret, B. & Van Heijenoort, J. (1987). Partial purification and specificity studies of the D-glutamate-adding and D-alanyl-D-alanine-adding enzymes from *Escherichia coli* K12. *Eur J Biochem* **166,** 631-637.
39. Egan, A., Lawrence, P. & Strominger, J. L. (1973). Enzymatic synthesis of the peptide in bacterial ridine nucleotides. V. Co ++ -dependent reversal of peptide bond formation. *J Biol Chem* **248,** 3122-3130.
40. Neuhaus, F. C. & Struve, W. G. (1965). Enzymatic synthesis of analogs of the cell-wall precursor. I. Kinetics and specificity of uridine diphospho-N-acetylmuramyl-L-alanyl-D-glutamyl-L-lysine:D-alanyl-D-alanine ligase (adenosine diphosphate) from *Streptococcus faecalis* R. *Biochemistry* **4,** 120-131.
41. Mengin-Lecreulx, D., Flouret, B. & van Heijenoort, J. (1982). Cytoplasmic steps of peptidoglycan synthesis in *Escherichia coli*. *J Bacteriol* **151,** 1109-1117.
42. Carettoni, D., Gomez-Puertas, P., Yim, L., Mingorance, J., Massidda, O., Vicente, M., *et al.* (2003). Phage-display and correlated mutations identify an essential region of subdomain 1C involved in homodimerization of *Escherichia coli* FtsA. *Proteins* **50,** 192-206.
43. Paradis-Bleau, C., Sanschagrin, F. & Levesque, R. C. (2004). Identification of *Pseudomonas aeruginosa* FtsZ peptide inhibitors as a tool for development of novel antimicrobials. *J Antimicrob Chemother* **54,** 278-280.
44. Dementin, S., Bouhss, A., Auger, G., Parquet, C., Mengin-Lecreulx, D., Dideberg, O., *et al.* (2001). Evidence of a functional requirement for a carbamoylated lysine residue in MurD, MurE and MurF synthetases as established by chemical rescue experiments. *Eur J Biochem* **268,** 5800-5807.
45. Mengin-Lecreulx, D., Blanot, D. & van Heijenoort, J. (1994). Replacement of diaminopimelic acid by cystathionine or lanthionine in the peptidoglycan of *Escherichia coli*. *J Bacteriol* **176,** 4321-4327.
46. Lugtenberg, E. J. (1972). Studies on *Escherichia coli* enzymes involved in the synthesis of uridine diphosphate-N-acetyl-muramyl-pentapeptide. *J Bacteriol* **110,** 26-34.
47. Eveland, S. S., Pompliano, D. L. & Anderson, M. S. (1997). Conditionally lethal *Escherichia coli* murein mutants contain point defects that map to regions conserved among murein and folyl poly-gamma-glutamate ligases: identification of a ligase superfamily. *Biochemistry* **36,** 6223-6229.
48. Azzolina, B. A., Yuan, X., Anderson, M. S. & El-Sherbeini, M. (2001). The cell wall and cell division gene cluster in the Mra operon of *Pseudomonas aeruginosa*: cloning, production, and purification of active enzymes. *Protein Expr Purif* **21,** 393-400.

49. Gu, Y. G., Florjancic, A. S., Clark, R. F., Zhang, T., Cooper, C. S., Anderson, D. D.*, et al.* (2004). Structure-activity relationships of novel potent MurF inhibitors. *Bioorg Med Chem Lett* **14,** 267-270.
50. Bertrand, J. A., Fanchon, E., Martin, L., Chantalat, L., Auger, G., Blanot, D.*, et al.* (2000). "Open" structures of MurD: domain movements and structural similarities with folylpolyglutamate synthetase. *J Mol Biol* **301,** 1257-1266.
51. Yan, Y., Munshi, S., Leiting, B., Anderson, M. S., Chrzas, J. & Chen, Z. (2000). Crystal structure of *Escherichia coli* UDPMurNAc-tripeptide D-alanyl-D-alanine-adding enzyme (MurF) at 2.3 A resolution. *J Mol Biol* **304,** 435-445.
52. Stamper, G. F., Longenecker, K. L., Fry, E. H., Jakob, C. G., Florjancic, A. S., Gu, Y. G.*, et al.* (2006). Structure-based optimization of MurF inhibitors. *Chem Biol Drug Des* **67,** 58-65.
53. Longenecker, K. L., Stamper, G. F., Hajduk, P. J., Fry, E. H., Jakob, C. G., Harlan, J. E.*, et al.* (2005). Structure of MurF from *Streptococcus pneumoniae* co-crystallized with a small molecule inhibitor exhibits interdomain closure. *Protein Sci* **14,** 3039-3047.
54. Hancock, R. E. & Farmer, S. W. (1993). Mechanism of uptake of deglucoteicoplanin amide derivatives across outer membranes of *Escherichia coli* and *Pseudomonas aeruginosa*. *Antimicrob Agents Chemother* **37,** 453-456.
55. Nefzi, A., Dooley, C., Ostresh, J. M. & Houghten, R. A. (1998). Combinatorial chemistry: from peptides and peptidomimetics to small organic and heterocyclic compounds. *Bioorg Med Chem Lett* **8,** 2273-2278.
56. Silver, L. L. (2006). Does the cell wall of bacteria remain a viable source of targets for novel antibiotics? *Biochem Pharmacol* **71,** 996-1005.
57. Fischer, P. M., Krausz, E. & Lane, D. P. (2001). Cellular delivery of impermeable effector molecules in the form of conjugates with peptides capable of mediating membrane translocation. *Bioconjug Chem* **12,** 825-841.
58. Dathe, M. & Wieprecht, T. (1999). Structural features of helical antimicrobial peptides: their potential to modulate activity on model membranes and biological cells. *Biochim Biophys Acta* **1462,** 71-87.
59. Shai, Y. & Oren, Z. (2001). From "carpet" mechanism to de-novo designed diastereomeric cell-selective antimicrobial peptides. *Peptides* **22,** 1629-1641.
60. Rothe, A., Hosse, R. J. & Power, B. E. (2006). Ribosome display for improved biotherapeutic molecules. *Expert Opin Biol Ther* **6,** 177-187.

Table I - Phage titers obtained after each round of biopanning using MurF and the phage-encoded 12-mer peptide library.

	Phage input	Eluted phages	Elution (%)
Round 1			
Gly-HCl	4×10^{10}	8.2×10^{6}	2×10^{-2}
Round 2			
Gly-HCl	1.5×10^{11}	4.1×10^{7}	2.7×10^{-2}
Round 3			
Gly-HCl	2×10^{13}	1.1×10^{7}	5.5×10^{-5}
ATP		1.3×10^{7}	6.5×10^{-5}
D-Ala-D-Ala		5.6×10^{6}	2.8×10^{-5}

Table II. Electrospray-TOF mass spectrometric analysis of purified UDP-MurNac-Ala-Glu-meso-A2pm.

Species	Expected m/z	Observed m/z
$m^{-2}/2$	524.63	524.60
$(m+Na^{+})^{-2}/2$	535.62	535.61
$(m+2Na^{+})^{-2}/2$	546.61	546.58
$m^{-3}/3$	349.42	349.41

Table III. Kinetic parameters of the *P. aeruginosa* enzyme MurF with respect to the substrate D-Ala-D-Ala

Kinetic parameters	MurF
Specific activity (μmol/min/mg)	4.4 ± 0.1
k_{cat} (min^{-1})	100 ± 15
K_m (μM)	115 ± 10
k_{cat}/K_m ($min^{-1}\mu M^{-1}$)	0.85 ± 0.15

Table IV. Kinetics of MurF inhibition by MurFp1 following 30 min pre-incubation with the inhibitor and the substrate UDP-MurNAc-Ala-Glu-meso-A2pm. Mixed α is the K_m factor change when MurFp1 is bound to the enzyme-substrate complex and mixed β is the K_p factor change when MurFp1 is bound to the enzyme-substrate complex. Mixed competitive and non-competitive data are with respect to D-Ala-D-Ala.

Parameter	Value
IC_{50} (μM)	250 ± 10
IC_{50} without UDP-MurNAc-Ala-Glu-meso-A2pm (μM)	2000 ± 180
Mixed α	0.85 ± 0.25
Mixed β	$8.5 \times 10^{-10} \pm 0.6 \times 10^{-10}$
Mixed competitive K_i (μM)	420 ± 100
Non-competitive β	$8 \times 10^{-10} \pm 0.7 \times 10^{-10}$
Non-competitive K_i (μM)	370 ± 55
V_{max} (nmol/min)	0.61 ± 0.01
at 75 μM MurFp1	0.49 ± 0.01
at 150 μM MurFp1	0.4 ± 0.01
at 300 μM MurFp1	0.36 ± 0.02
at 600 μM MurFp1	0.22 ± 0.01
K_m (μM)	115 ± 10
at 75 μM MurFp1	100 ± 10
at 150 μM MurFp1	85 ± 5
at 300 μM MurFp1	140 ± 30
at 600 μM MurFp1	115 ± 25

Figure Legends

Figure 1. Peptides from the phage display 12-mer library obtained by sequencing phages eluted after the third round of biopanning against MurF. Acidic amino acids (D, E) are in turquoise blue, polar amino acids (Q, N) are in light green, basic amino acids (K, R, H) are in blue, hydrophobic amino acids (I, L, M, V) are in pink, hydrophobic aromatic amino acids (F, Y, W) are in red, small amino acids (A, S, C, T) are in magenta, G is in orange, and P is in black (classified according to the Venn diagram for defining the relationships between amino acids). Consensus sequences and related conserved motifs are boxed in black and the superscript letters indicate peptide sequences recovered more than once.

Figure 2. (A**)** Chromatograph of the anionic exchange chromatography performed with an ammonium acetate gradient confirming the purity of synthesized UDP-MurNAc-Ala-Glu-A2pm. (B) Chemical structure of purified UDP-MurNAc-Ala-Glu-A2pm as confirmed by mass spectrometry analysis.

Figure 3. (A) Inhibition of MurF ATPase activity by MurFp1 as a function of pre-incubation time in the presence of 2 mM inhibitor. (B**)** IC_{50} determination for the inhibition of MurF ATPase activity following 30 min of pre-incubation in the presence of inhibitor and the substrate UDP-MurNAc-Ala-Glu-A2pm.

Figure 4. (A) Michaelis-Menten and (B) Lineweaver–Burk plots for MurF ATPase activity with respect to D-Ala-D-Ala showing inhibition by MurFp1 at 0 μM (circles), 75 μM (squares), 150 μM (right-side-up triangles), 300 μM (inverted triangles) and 600 μM (diamonds).

Figure 1.

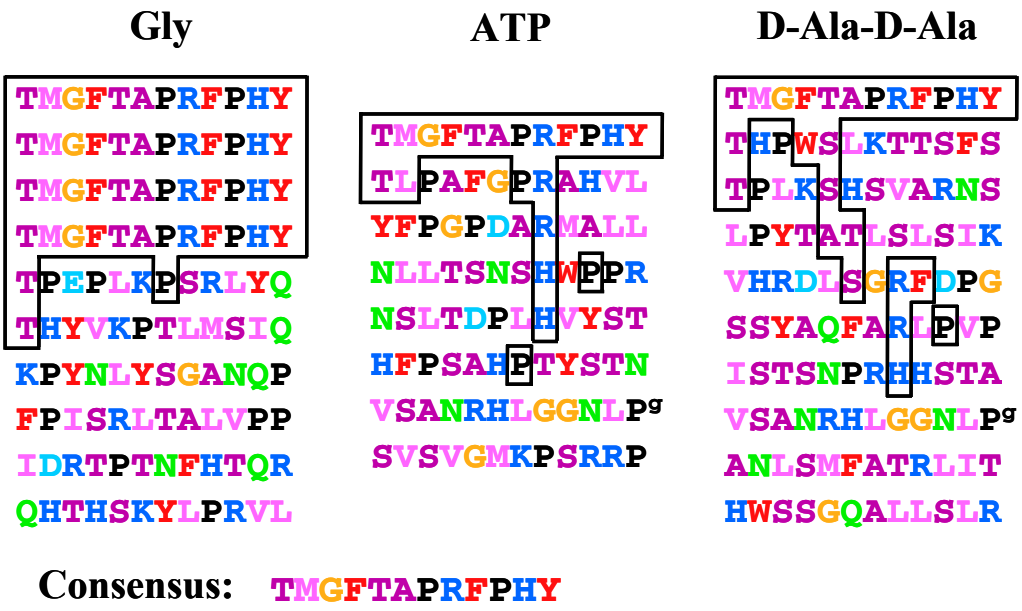
Gly
ATP
D-Ala-D-Ala
TMGFTAPRFPHY
TMGFTAPRFPHY
TMGFTAPRFPHY
TMGFTAPRFPHY
TPEPLKPSRLYQ
THYVKPTLMSIQ
KPYNLYSGANQP
FPISRLTALVPP
IDRTPTNFHTQR
QHTHSKYLPRVL
TMGFTAPRFPHY
TLPAFGPRAHVL
YFPGPDARMALL
NLLTSNSHWPPR
NSLTDPLHVYST
HFPSAHPTYSTN
VSANRHLGGNLPg
SVSVGMKPSRRP
TMGFTAPRFPHY
THPWSLKTTSFS
TPLKSHSVARNS
LPYTATLSLSIK
VHRDLSGRFDPG
SSYAQFARLPVP
ISTSNPRHHSTA
VSANRHLGGNLPg
ANLSMFATRLIT
HWSSGQALLSLR
Consensus: TMGFTAPRFPHY

Figure 2.

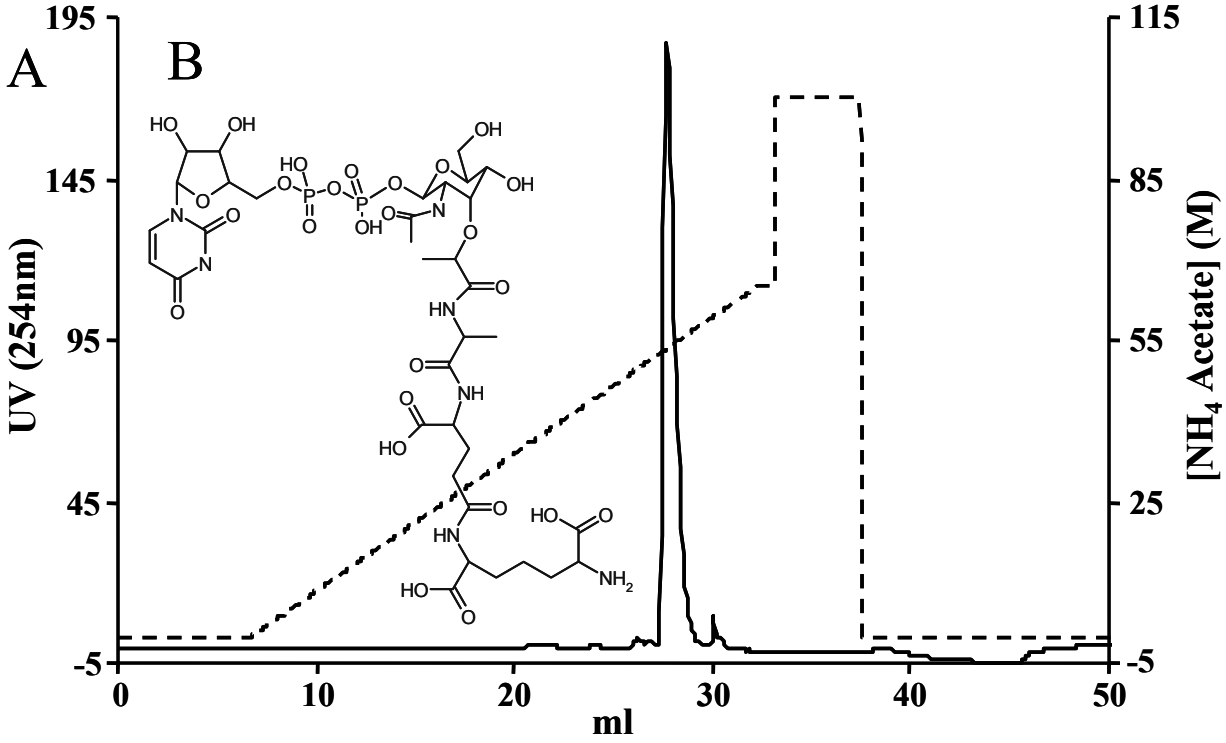
A
B
195
145
95
45
-5
UV (254nm)
115
85
55
25
-5
[NH4 Acetate] (M)
0
10
20
30
40
50
ml

Figure 3.

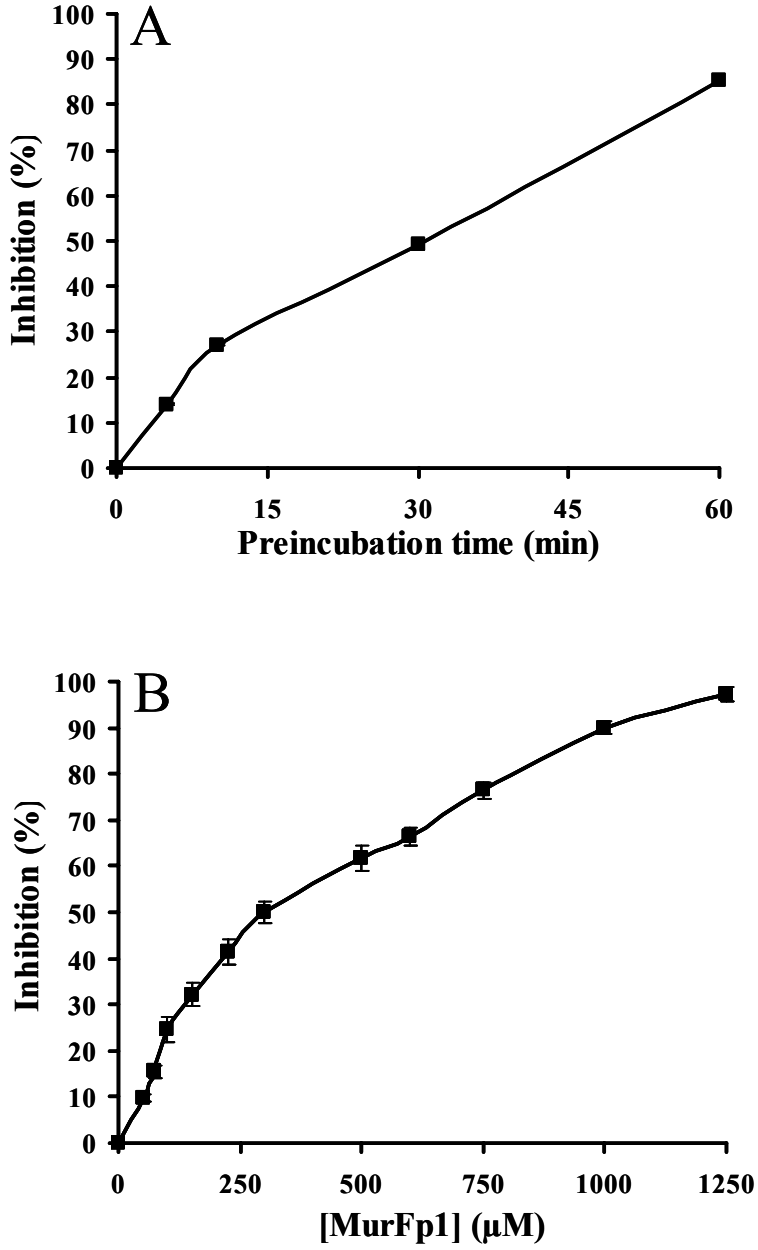
A
Inhibition (%)
100
90
80
70
60
50
40
30
20
10
0
0
15
30
45
60
Preincubation time (min)
B
Inhibition (%)
100
90
80
70
60
50
40
30
20
10
0
0
250
500
750
1000
1250
[MurFp1] (µM)

Figure 4.

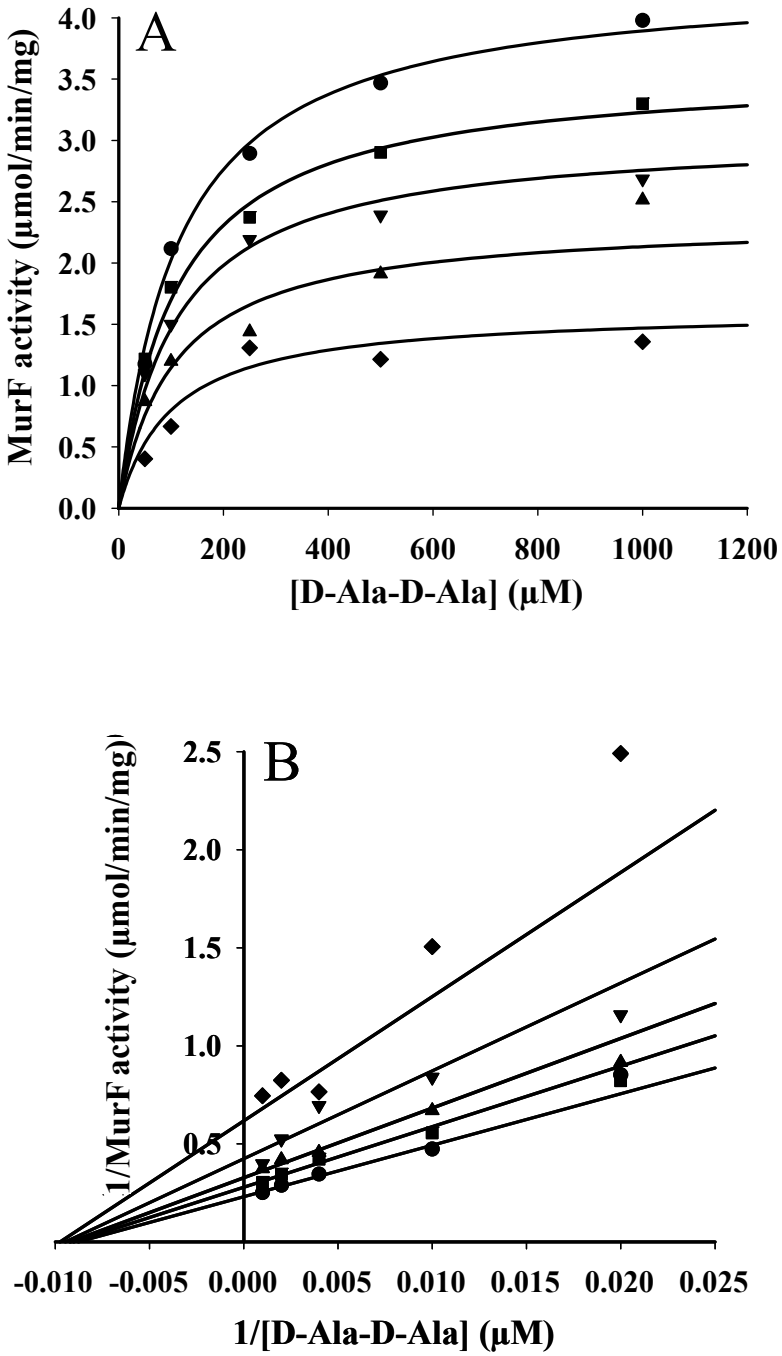
A
MurF activity (µmol/min/mg)
4.0
3.5
3.0
2.5
2.0
1.5
1.0
0.5
0.0
0
200
400
600
800
1000
1200
[D-Ala-D-Ala] (µM)
B
1/MurF activity (µmol/min/mg)
2.5
2.0
1.5
1.0
0.5
-0.010
-0.005
0.000
0.005
0.010
0.015
0.020
0.025
1/[D-Ala-D-Ala] (µM)

Section IV - Les endolysines de bactériophages en tant que nouveaux agents antibactériens ciblant l'intégrité de la paroi bactérienne

Cette dernière section du corps de ma thèse englobe deux articles rédigés en anglais en vue d'une publication au sein de revues scientifiques anglophones. Le premier manuscrit fait office d'introduction en décrivant le mode d'action et la biologie des endolysines de bactériophages en tant qu'agents antibactériens efficaces ciblant l'intégrité de la paroi bactérienne. Ces enzymes d'origine phagique dégradent rapidement et spécifiquement la paroi bactérienne et de multiples avenues peuvent être envisagées afin d'exploiter leur potentiel antibactérien de façon sécuritaire et efficace. Par la suite, un article scientifique soumis à la revue «FEMS Microbiology Letters» reporte une étude réalisée sur l'endolysine du bactériophage ϕKZ infectant *P. aeruginosa*. Cet article décrit la capacité de l'endolysine du bactériophage ϕKZ à hydrolyser la paroi bactérienne des espèces bactériennes à Gram-négatif et à outrepasser les membranes bactériennes. Ainsi, cette endolysine représente un bon exemple du pouvoir antibactérien des endolysines de bactériophages.

Chapitre 8 - Phage endolysin enzymes as antibacterial agents targeting cell wall integrity

Résumé

Les endolysines de bactériophages en tant qu'agents antibactériens efficaces ciblant l'intégrité de la paroi bactérienne

Dans la perspective d'un développement incessant et d'une propagation continuelle des mécanismes de résistance aux antibiotiques parmi les pathogènes bactériens en émergence à travers le monde, les endolysines de bactériophages captivent la communauté scientifique. En effet, la nature renferme une source extraordinairement diversifiée et évoluée d'enzymes lytiques d'origine phagique qui attendent leur approbation en tant que thérapies antibactériennes. Ces enzymes représentent de puissants agents antibactériens qui dégradent rapidement et spécifiquement la paroi recouvrant les cellules bactériennes. Cette paroi maintient la forme des bactéries et leur permet de croître, de se diviser et de survivre aux variations de pressions osmotique. Ainsi, la destruction de la paroi bactérienne par les endolysines entraîne inévitablement la mort bactérienne. Cet article de revue décrit les différents mécanismes catalytiques, les propriétés structurales et la spécificité des endolysines de bactériophages. L'article expose ensuite le potentiel fort intéressant des endolysines en tant qu'agents antibactériens contre les pathogènes bactériens à Gram-positif et à Gram-négatif. Les avantages de thérapies antibactériennes basées sur les endolysines sont également rapportés en comparaison avec les thérapies classiques. Finalement, de multiples avenues sont proposées afin d'exploiter le potentiel des endolysines de façon sécuritaire et efficace pour contrôler la problématique de résistance aux antibiotiques.

Contribution des auteurs

En tant que première auteure de cet article, j'ai réalisé une revue approfondie et détaillée de la littérature scientifique sur le mode d'action et la biologie des endolysines de bactériophages. J'ai porté une attention particulière au pouvoir antibactérien de ces enzymes et aux avenues possibles afin d'exploiter ce potentiel de façon sécuritaire et efficace pour développer de nouveaux traitements antibactériens. J'ai sélectionné les articles scientifiques les plus pertinents afin de rédiger une revue scientifique concise et ciblée puis j'ai préparé la première figure du manuscrit. La deuxième figure illustrant les structures tridimensionnelles des endolysines des bactériophages T4, T7 et λ a été préparée par le Dr François Sanschagrin. J'ai finalement rédigé intégralement le manuscrit en vue d'une soumission à la revue «Molecular Microbiology» puis j'ai émis mon opinion scientifique sur l'avenir des endolysines en tant que traitement thérapeutique en Occident. Le Dr Roger C. Levesque m'a guidée dans la conception de l'article, il m'a aidée à conserver un esprit de synthèse puis il a révisé le manuscrit afin d'en augmenter la fluidité et la qualité de la langue anglaise.

Phage endolysin enzymes as antibacterial agents targeting cell wall integrity

Catherine Paradis-Bleau and Roger C. Levesque

Département de Biologie Médicale, Faculté de Médecine, Université Laval, Québec, Québec, Canada, G1K 7P4

Keywords: phage lysis mechanisms, phage endolysins, cell wall integrity, cell wall degrading enzymes, antibacterial activity

Running title: Antibacterial potential of phage endolysin enzymes

Address correspondence to: Roger C. Levesque, Département de Biologie Médicale, Pavillon Charles-Eugène Marchand, Université Laval, Québec, Québec, Canada, G1K 7P4, Tel: (1) 418 656-3070; Fax: (1) 418 656-7176; E-Mail: rclevesq@rsvs.ulaval.ca

Abstract

Given the relentless worldwide increase in the frequency of antibiotic resistance among long-established bacterial pathogens and now among emerging pathogens as well, phage endolysin enzymes are captivating the scientific community as attractive alternative antibacterial agents for targeting the integrity of the essential cell wall. Indeed, the extraordinary evolutionary patterns and diversity of the existing pool of phage-encoded cell-wall-degrading enzymes represent vast commercial potential, pending regulatory approval of an endolysin-based therapy. In this review, we highlight the catalytic mechanisms, structural features and specificity of phage endolysin enzymes as well as their promising potential as antibacterial agents for the safe and effective control of clinically significant Gram-positive and Gram-negative pathogens. Finally, we propose pragmatic strategies for successful development and the optimization of endolysin-based novel therapies to face the impending antibiotic resistance crisis.

Introduction

Antibiotic resistance has spread to every clinically useful antibacterial agent and all bacterial pathogens and now represents one of the most serious human health hazards worldwide (Levy and Marshall, 2004). The development of effective new approaches to antibacterial therapy constitutes an urgent task to defend human wellbeing against continually emerging resistant pathogens. As an alternative to conventional time-consuming pharmaceutical drug research, the scientific community has begun to clear a path that may lead to gainful exploitation of the naturally occurring antibacterial strategies in continuous development among the bacteriophages.

These bacteria-specific viruses have had billions of years to develop efficient mechanisms that enable them to continue to infect and lyse their hosts. Indeed, phages evolve at astonishing rates that chemists tinkering with new generations of antibiotics can never hope to replicate (Thiel, 2004). In order to promote host cell lysis and the subsequent release of phage progeny, lytic bacteriophages must disrupt bacterial cell wall integrity. Phages having small, single-stranded genomes encode a single lytic protein that specifically inhibits cell wall biosynthesis. In contrast, phages having double-stranded genomes

typically use a holin-endolysin mechanism. Cell-wall-degrading endolysin usually lacks a secretory signal sequence and is restricted to the bacterial cytoplasm until holin renders the internal membrane permeable at an optimal programmed time, thus enabling endolysin to access the targeted periplasmic cell wall layer (Young *et al.*, 2000). Endolysins constitute an evolved pool of muralytic enzymes that efficiently target and hydrolyze the essential cell wall layer, thereby leading to bacterial cell lysis. These enzymes represent a promising avenue for exploiting the evolutionary power of phage antibacterial capability without the inconveniences of whole biological particles such as the possibility of gene transfer by transduction.

It has long been known that the essential cell wall layer of bacteria is a strong physical barrier composed of a sugar backbone of alternating units of *N*-acetylglucosamine and *N*-acetylmuramic acid cross-linked via short peptide chains. This structure confers the shape of the bacterial cell and enables it to survive variations in osmotic pressures as well as providing rigidity, flexibility and strength for cell integrity, growth and division. Indeed, bacterial cells with defective cell wall eventually burst and die (Young, 2003). The remarkable cell wall layer structure represents one of the best antibacterial targets, since it is essential, accessible and highly conserved among almost all clinically relevant bacterial pathogens and has no eukaryotic counterpart.

The aim of this review is to focus on the catalytic mechanisms, structural features and specificity of phage-encoded cell-wall-degrading enzymes and to discuss their use as antibacterial agents that function by targeting cell wall integrity. We report the recent advances made towards understanding phage endolysin enzymes and the characterization of endolysins of special interest as the basis of a novel therapy against Gram-positive and Gram-negative pathogens.

Structure and function of the different types of phage endolysin enzymes

The vast majority of phage endolysins display a cooperative modular organization in which the N-terminal domains perform the catalytic activity while the C-terminal domains direct enzyme binding to specific cell-wall-associated substrates (Loessner, 2005). The catalytic

domains recognize and cleave specific biochemical bonds of the cell wall layer, thus providing four different enzymatic activities, as depicted in Figure 1.

Muramidases cleave the *N*-acetylmuramyl-β-1,4-*N*-acetylglucosamine bonds and typically proceed via general acid/base hydrolysis, the glutamate catalyst acting as a proton donor to the glycosidic oxygen of *N*-acetylmuramic acid to cleave the bond and produce an oxocarbonium ion intermediate. The negatively charged aspartate residue then acts as a nucleophile/base to stabilize the intermediate and allow the nucleophilic water molecule to diffuse into the active site and attack the C1-carbon of the oxocarbonium ion (Hermoso *et al.*, 2003; Leung *et al.*, 2001). Phage T4 lysozyme is a globular protein consisting of two domains connected by a long α-helix and between which the active-site cleft is formed, as shown in Figure 2 (McHaourab *et al.*, 1997). In contrast to typical retaining muramidases, T4 lysozyme is an inverting glycosidase performing a single-displacement reaction with inversion of the oxocarbonium C1-carbon configuration (Kuroki *et al.*, 1999). Lytic transglycosylases break the same glycosidic bond as muramidases, but further catalyze the intramolecular transfer of the *O*-muramyl residue to the C6 hydroxyl group of muramic acid, yielding 1,6-anhydromuramyl disaccharides. Such endolysins harbor a single glutamate catalyst and the absence of the aspartate residue coincides with tighter binding of the sugar substrate to the active site. This more stable interaction prevents the water molecule from attacking the oxocarbonium ion and allows transglycosylation. The tridimensional structure of the lytic transglycosylase from phage λ has been determined for its complex with a saccharide substrate (Fig. 2). The active site is a deep elongated cleft located between the lower and upper domains and contains the conserved glutamate catalyst. The enzyme interacts with four *N*-acetylglucosamine units from one hexasaccharide and two units from another hexasaccharide, resulting in all active site subsites being filled (Leung *et al.*, 2001).

N-acetylmuramoyl-L-alanine amidases such as phage T7 endolysin hydrolyze the bond between *N*-acetylmuramic acid and the primary L-alanine of the peptide cross-bridge (Vasala *et al.*, 1995). The few known endopeptidase endolysins hydrolyze the bond between L-alanine and D-glutamate of the cell wall cross-bridge or peptide bond of host specific interpeptide cross-bridges (Loessner, 2005). These enzymes share the same general

catalytic mechanism and act principally as metallo-aminopeptidases or cysteine-dependent amidohydrolases. In the first case, a positively charged residue interacts with the substrate carbonyl, a water molecule then initiates a nucleophilic attack typically promoted by the Zn^{2+} associated cation and a negatively charged residue, the intermediate is resolved and a hydrogen is given to the leaving amino group (Cheng *et al.*, 1994). The cysteine, histidine-dependent amidohydrolase/peptidase (CHAP) domain is present in a large number of amidase and peptidase endolysins. These enzymes utilize the thiol group of the cysteine catalyst in a nucleophilic attack on the carbon of the carbonyl group implicated in the targeted peptide bond (Bateman and Rawlings, 2003; Rigden *et al.*, 2003). Phage T7 amidase behaves as a metallo-aminopeptidase and folds into an α/β-sheet structure that has a prominent cleft with the Zn^{2+} ion bound directly to three amino acids and, through a water molecule, to a fourth (Cheng *et al.*, 1994). To our knowledge, no CHAP-containing endolysin has yet been crystallized, but the CHAP domain is predicted to belong to the α + β structural class and the position of the conserved residues is consistent with a distant relationship to the papain-like cysteine proteinase fold (Rigden *et al.*, 2003).

Specificity of phage endolysins for bacterial cell walls

It is noted with interest that most endolysins are fairly specific for bacterial species (Matsuzaki *et al.*, 2005). Few known endolysins display a broad-spectrum activity while most are genus-specific or even species-specific (Loessner, 2005). The unconserved C-terminal cell-wall-binding domain seems to be necessary and sufficient to direct endolysins selectively to their substrates and to confer the exclusive recognition specificity. Furthermore, these domains recognize their ligands and bind to them in non-covalent associations with affinities of the same magnitude as for antibody-antigen association (Loessner *et al.*, 2002). Indeed, the cell-wall-binding domains provide the enzyme–substrate proximity necessary for the catalytic activity of the N-terminal domains and the resulting lytic activities of endolysins. Furthermore, the catalytic domains of some endolysins require activation through binding of key C-terminal domains to the specific cell wall ligands in order to function effectively (Loessner, 2005; Low *et al.*, 2005).

Since the cell wall bonds cleaved by endolysins are ubiquitous among both Gram-positive and Gram-negative bacteria, the C-terminal domains must recognize specific cell-wall-associated ligands at the surface of susceptible bacteria. Indeed, endolysins exploit the physiological surface variations occurring among bacterial species. The cell wall layer of Gram-positive bacteria is much thicker and more branched than in Gram-negative bacteria, which are covered by an external membrane. It is well known that Gram-positive cell walls typically contain teichoic acids, lipoteichoic acids and glycolipids while the envelopes of Gram-negative bacteria include lipopolysaccharides. The composition, structure and conformation of these cell-wall-associated components vary significantly among bacterial species and therefore could constitute the specific target of endolysins. Some C-terminal domains have been shown in effect to recognize in a specific manner unique structural motifs such as cell wall carbohydrates and aminoalcohol choline moieties of teichoic acid at the surface of Gram-positive bacteria (Fischetti, 2005; Loessner *et al.*, 2002).

Antibacterial activity of endolysins against Gram-positive pathogens

Endolysins have been employed for various *in vitro* and *in vivo* purposes, in food science, biotechnology, industrial microbiology, microbial diagnostics and for treatment of plant and animal experimental infections (Loessner, 2005). It has thus been confirmed that endolysins exert their lethal effects by forming holes in the cell wall layer, resulting in extrusion of the cytoplasmic membrane and ultimately hypotonic lysis. Adding small quantities of endolysin to a medium containing Gram-positive bacteria produces total lysis of susceptible cells within seconds of contact (Delisle *et al.*, 2006; Donovan *et al.*, 2006a; Fischetti, 2005; Loessner, 2005; O'Flaherty *et al.*, 2005; Schuch *et al.*, 2002; Yoong *et al.*, 2004). This impressive effect has been observed for a wide variety of Gram-positive pathogens including *Clostridium perfringens*, *Listeria monocytogenes, Actinomyces naeslundii*, *Streptococcus pyogenes*, *Streptococcus agalactiae*, *Streptococcus dysgalactiae*, penicillin-resistant *Streptococcus pneumoniae*, methicillin-resistant *Staphylococcus aureus*, vancomycin-resistant *Enterococcus faecalis* and *Enterococcus faecium* and vegetative cells and germinating spores of *Bacillus anthracis* (Delisle *et al.*, 2006; Donovan *et al.*, 2006a; Fischetti, 2005; Loessner, 2005; O'Flaherty *et al.*, 2005; Schuch *et al.*, 2002; Yoong *et al.*, 2004).

It has also been demonstrated that small amounts of endolysins provide safe and effective control of various Gram-positive pathogens (notably *S. pneumoniae*, *S. pyogenes*, *S. agalactiae* and *B. anthracis*) on mucosal surfaces and in blood in various animal models (Fischetti, 2005; Yoong *et al.*, 2006). For example, a single dose of 2.5 ng of PlyC endolysin administered to the oral cavity of mice provides protection against group A streptococci colonization (Nelson *et al.*, 2001). A single nasal and pharyngeal treatment with the Pal endolysin cures mice colonized with *S. pneumoniae* and prevents subsequent re-colonization (Loeffler *et al.*, 2001). Furthermore, administration of 2 mg of Cpl-1 endolysin 10 h after intravenous *S. pneumoniae* challenge reduced bloodstream titers from $\log_{10}$ 4.7 colony forming units (CFU) ml^{-1} to undetectable levels within 15 min and led to 100% survival of bacteremic mice (Loeffler *et al.*, 2003).

Therapeutic potential of endolysins against Gram-negative pathogens

Endolysins are effective against Gram-positive bacteria because the cell wall is accessible from the outside even when covered by capsular material (Loeffler *et al.*, 2001; Schuch *et al.*, 2002). In contrast, access to the Gram-negative bacterial cell wall is prevented by the presence of an LPS-containing outer membrane. When this membrane is disrupted by permeabilizing agents, cells immediately become vulnerable to external muralytic enzymes (Loessner, 2005). The first evidence of the therapeutic potential of endolysins against Gram-negative pathogens came from a study by Morita and collaborators (2001a,b) in which a *Bacillus amyloliquefaciens* phage endolysin was shown to induce lysis of *E. coli* from inside the cells without production of the cognate holin. It is noted with interest that this endolysin shows strong exogenous antibacterial activity against Gram-negative bacterial pathogens such as *Pseudomonas aeruginosa*, one of the most difficult organisms to treat because of high antibiotic resistance due in part to low outer membrane permeability. Indeed, the viable cell density of an overnight culture of *P. aeruginosa* decreased by two and three log cycles from $\log_{10}$ 9 CFU ml^{-1} after a 10-minute treatment with endolysin at concentrations of 40 μg ml^{-1} and 200 μg ml^{-1}; respectively (Morita *et al.*, 2001a).

The N-terminal domain of the *B. amyloliquefaciens* phage endolysin has a relatively high degree of homology with the T4 lysozyme and the conserved glutamate and threonine catalytic residues have been proven to be essential for the enzymatic and antibacterial activities but not for the permeabilization capacity. The C-terminal cell-wall-binding domain shows high affinity with *P. aeruginosa* exogenously and is responsible for the enhancement of outer membrane permeability. Embedded in the C-terminal region are two homologous helical structures rich in positively charged residues surrounded by hydrophobic residues. The C-terminal domain may thus interact with polyanionic LPS to displace in competitive fashion the divalent cations that bridge and partly neutralize the LPS, thereby causing disruption of the outer membrane. The hydrophobic region of this endolysin may therefore penetrate the membrane, permitting the N-terminal catalytic domain to reach the periplasmic cell wall layer and cause bacterial lysis. Indeed, the normally rod-shaped *P. aeruginosa* cells appeared minicell-like and ghost-like after external exposure to the endolysin and ruptured spontaneously. This *Bacillus* phage endolysin may pave the way to the control of gram-negative pathogens (Morita *et al.*, 2001b; Orito *et al.*, 2004).

Validity of an endolysin-based therapy

The recent detailed characterization of endolysin catalytic mechanisms, cell wall binding properties, structural features and antibacterial capacities opens the door to potent endolysin-based therapies to treat and prevent infections by clinically relevant human and animal pathogens via a novel mode of action. The highly evolved endolysin enzymes are among the most powerful antimicrobial agents known and represent a huge pool of unexploited candidates able to eradicate or reduce bacterial pathogens to a level with which the host immune system can cope (Cheng *et al.*, 2005; Jado *et al.*, 2003; Loessner, 2005).

Phage-encoded muralytic enzymes offer many advantages over antibiotics. First of all, endolysins are refractory to resistance development (Donovan *et al.*, 2006a). To optimize phage aptness, endolysins appear to have evolved to target essential bacterial moieties not amenable to mutational change. Moreover, endolysins can eliminate specific disease-causing bacteria without disturbing beneficial normal microbiota (Fischetti, 2005;

Takac and Blasi, 2005). Entenza et al. (2005) recently demonstrated that the Cpl-1 endolysin is more effective than vancomycin for treating bacteria protected by physical barriers. In fact, endolysins can reach and kill pathogens colonizing mucosal surfaces, in blood or deep foci, capabilities that were previously unavailable (Entenza *et al.*, 2005; Fischetti, 2005; Takac and Blasi, 2005). In contrast with most antibiotics, endolysins can destroy cell walls of nongrowing bacteria with great efficiency, which would both shorten the therapy and decrease the risk of re-infection (Matsuzaki *et al.*, 2005; Pritchard *et al.*, 2004). Furthermore, many endolysins are potent at low pH, giving them a great advantage over antibiotics in situations where acidic conditions prevail, such as in the human vaginal tract, in biofilms or pus (Cheng *et al.*, 2005; Loeffler *et al.*, 2003). Since endolysins retain their catalytic activity under various conditions, are remarkably heat stable and are easy to produce and purify, these enzymes would be amenable to therapeutic applications at pennies per dose (Fischetti, 2005; Yoong *et al.*, 2006). Finally, a great diversity of endolysins can be found in nature against nearly all pathogenic bacteria and it has been shown recently that phage-associated muralytic enzymes used to weaken the cell wall at the site of phage DNA entry also represent effective antimicrobial agents (Takac and Blasi, 2005).

An endolysin-based therapy should be safe for eukaryotic cells as the cell wall bonds targeted and hydrolyzed by endolysins are present only in bacteria. As proteins typically stimulate an immune response, one concern with the use of endolysins is the potential development of neutralizing antibodies. Somehow, antibodies produced against endolysins do not neutralize their catalytic activities and immunized mice remain as sensitive as naive mice to endolysin treatment. No adverse effects have been observed in mice or on cultured mammalian cells, suggesting that endolysins could be used safely and repeatedly to control pathogens (Cheng *et al.*, 2005; Donovan *et al.*, 2006a; Fischetti, 2005; Jado *et al.*, 2003; Yoong *et al.*, 2006). Another concern is the potential *in vivo* release of cell wall fragments, LPS (endotoxin), teichoic and lipoteichoic acids by rapid endolysin-mediated lysis of Gram-negative and Gram-positive bacterial cells. These constituents temporarily boost the host innate immunity against infections and yield an inflammatory response that may cause undesirable effects such as circulatory toxic shock, particularly in patients with high bacterial loads due to sepsis, meningitis or other complications. This

outcome is not expected to be more severe than for cell-wall active antibiotics such as β-lactams, since endolysins would cause lysis of specific primary pathogens only. Treatment protocols may still have to be organized to reduce pro-inflammatory adverse effects in particularly susceptible cases. This may include pre-treatment with a bacterial protein synthesis inhibitor, use of the lipoteichoic acid biosynthesis inhibitor daptomycin, endotoxin-neutralizing compounds, anti-inflammatory drugs and pro-inflammatory agonists, protein C to cope with the formation of multiple thrombi generated during septic shock, anti-apoptosis agents to prevent lymphatic organ necrosis and even hemofiltration to remove circulating bacterial cell wall components, pro-inflammatory mediators and cytotoxic agents (Ginsburg, 2002; Nau and Eiffert, 2005).

Development and optimization of endolysin-based therapies

To optimize antibacterial therapies, physicians could choose among phage-encoded enzymes that display multiple cell wall hydrolytic capacities, such as phage ϕ11 endolysin, which contains amidase and endopeptidase activities, PlyGBS and B30 endolysins, which display endopeptidase and muramidase activities, and Ply187 endolysin, which contains three different catalytic domains (Cheng *et al.*, 2005; Navarre *et al.*, 1999; Pritchard *et al.*, 2004). In fact, the remarkable synergistic effect of different types of endolysins suggests that the presence of different cell-wall-cleaving sites on one enzyme enhances its ability to lyse bacterial cells (Pritchard *et al.*, 2004).

To obtain the desired enzymatic activities and pathogen specificities, chimeric endolysins can be designed by reorganization and swapping of the independently active catalytic and cell wall binding domains (Fischetti, 2005). The CHAP domain is of special interest since it is often found in association with other catalytic modules and can direct the enzyme to its target substrate in the absence of the C-terminal domain (Bateman and Rawlings, 2003; Donovan *et al.*, 2006a; Donovan *et al.*, 2006b). Another catalytic domain is of interest because it can protect endolysins against potential development of resistance due to cell wall acetylation. Although cell wall biosynthesis leads to a fully *N*-acetylated glycan backbone, many bacteria can perform *N*-acetylglucosamine deacetylation or O-acetylation at the C6 hydroxyl of muramyl residues. The resulting lack of *N*-acetyl

substitutions or the presence of O-acetyl groups blocks the catalytic action of muramidases and lytic transglycosylases (Ginsburg, 2002; Vollmer and Tomasz, 2000). N-acetyl groups engage in strong interactions with the glutamate and aspartate catalysts of the majority of muramidases except for enzymes of the GH-25 family such as the Cpl-1 endolysin, which display different structural features and are indifferent to deacetylation. Indeed, designing endolysins with CHAP and GH-25 muramidase domains would allow useful therapeutic applications. Furthermore, a proper endolysin organization with suitable linker and interactions between modules can optimize enzyme activity since the C-terminal domain helps to orient the substrate within the catalytic cavity (Hermoso *et al.*, 2003). A recent report by Nelson and collaborators (2006) illustrates the importance of proper modular organization for effective endolysin function. PlyC is the most potent endolysin studied to date and only nanogram quantities are required to cause a multi-log drop of target bacteria within minutes, in contrast with micrograms or milligrams for most endolysins. This high activity seems to be linked to the unusual multimeric structure of the PlyC holo-enzyme, composed of eight subunits of PlyCB forming a cell-wall-binding domain for each PlyCA subunit containing a CHAP amidase function (Nelson *et al.*, 2006).

Invasive Gram-negative pathogens cause about one third of all bacterial infections. Effective therapies could be developed based on the described *Bacillus* phage endolysin. The cell outer membrane can also be perturbed via displacement of LPS by specific polycationic compounds such as polymyxins, cationic peptides and aminoglycosides (Nau and Eiffert, 2005). Permeabilizing agents such as these can be used synergistically with endolysins or permeabilization moieties could be complexed to highly active endolysins from Gram-positive phages in order to kill Gram-negative pathogens. Endolysins may thus be equipped with a surface-exposed hydrophobic carrier that mediates outer membrane interaction and insertion to enable access to the periplasmic cell wall layer (Ibrahim *et al.*, 2002). Membrane-penetrating moieties can be added either by fatty acylation of lysine residues through catalyzed ester exchange or by genetic fusion of hydrophobic peptides or amphiphilic polyprolines to endolysin C-termini without unfavorable interference (Ibrahim *et al.*, 2002; Ito *et al.*, 1997). Finally, the host inflammatory environment may help endolysins gain access to the cell wall layer since peroxides, defensins, cationic elastases

and the complement system can induce the formation of holes in the outer membrane (Ginsburg, 2002).

In a more practical way, therapies can be performed with highly specific endolysins when the identity of the disease-causing bacteria is known or with endolysins having broad lytic spectra when the pathogen cannot be identified due to a lack of rapid and precise diagnostic tools. Furthermore, endolysins may be used effectively as diagnostic agents (Schuch *et al.*, 2002). Another attractive application is to exploit naturally occurring or designed endolysin enzymes specific for the treatment of serious infections caused by multiple unrelated pathogens (Cheng *et al.*, 2005; Donovan *et al.*, 2006a; Yoong *et al.*, 2004). Finally, endolysins may be administered topically or intravenously using multiple doses or a constant infusion to preserve pharmacological concentrations and eliminate the organisms completely (Fischetti, 2005). As internalized bacteria may be able to repopulate the infection site several hours or days after treatment, endolysins could be produced by unsusceptible recombinant bacteria that may reach the intracellular pathogens (Nelson *et al.*, 2001; Zimmer *et al.*, 2002).

Concluding remarks

Over the past few years, there has been growing interest in developing lytic enzymes from bacteriophages as a novel therapeutic approach to deal with the menace represented by the worldwide emergence of antibiotic resistant bacterial pathogens. In the improbable event of resistance occurring against a particular endolysin, the producer phage could be exploited to evolve a new and improved enzyme. A second generation of endolysins could also be developed through random mutagenesis or directed evolution, which may improve activity and stability of enzymes (Cheng *et al.*, 2005). The next obstacle to overcome will be acceptance of the effectiveness and safety of the endolysin-based therapy in western nations. The success of such promising therapies will likely depend to a large degree on judicious negotiation of intellectual property rights and patents associated with phage-encoded cell-wall-degrading enzymes.

References

Bateman, A., and Rawlings, N.D. (2003) The CHAP domain: a large family of amidases including GSP amidase and peptidoglycan hydrolases. *Trends Biochem Sci* 28: 234-237.

Cheng, Q., Nelson, D., Zhu, S., and Fischetti, V.A. (2005) Removal of group B streptococci colonizing the vagina and oropharynx of mice with a bacteriophage lytic enzyme. *Antimicrob Agents Chemother* 49: 111-117.

Cheng, X., Zhang, X., Pflugrath, J.W., and Studier, F.W. (1994) The structure of bacteriophage T7 lysozyme, a zinc amidase and an inhibitor of T7 RNA polymerase. *Proc Natl Acad Sci U S A* 91: 4034-4038.

Delisle, A.L., Barcak, G.J., and Guo, M. (2006) Isolation and expression of the lysis genes of *Actinomyces naeslundii* phage Av-1. *Appl Environ Microbiol* 72: 1110-1117.

Donovan, D.M., Dong, S., Garrett, W., Rousseau, G.M., Moineau, S., and Pritchard, D.G. (2006a) Peptidoglycan hydrolase fusions maintain their parental specificities. *Appl Environ Microbiol* 72: 2988-2996.

Donovan, D.M., Foster-Frey, J., Dong, S., Rousseau, G.M., Moineau, S., and Pritchard, D.G. (2006b) The cell lysis activity of the *Streptococcus agalactiae* bacteriophage B30 endolysin relies on the cysteine, histidine-dependent amidohydrolase/peptidase domain. *Appl Environ Microbiol* 72: 5108-5112.

Entenza, J.M., Loeffler, J.M., Grandgirard, D., Fischetti, V.A., and Moreillon, P. (2005) Therapeutic effects of bacteriophage Cpl-1 lysin against *Streptococcus pneumoniae* endocarditis in rats. *Antimicrob Agents Chemother* 49: 4789-4792.

Fischetti, V.A. (2005) Bacteriophage lytic enzymes: novel anti-infectives. *Trends Microbiol* 13: 491-496.

Ginsburg, I. (2002) The role of bacteriolysis in the pathophysiology of inflammation, infection and post-infectious sequelae. *Apmis* 110: 753-770.

Hermoso, J.A., Monterroso, B., Albert, A., Galan, B., Ahrazem, O., Garcia, P., Martinez-Ripoll, M., Garcia, J.L., and Menendez, M. (2003) Structural basis for selective recognition of pneumococcal cell wall by modular endolysin from phage Cp-1. *Structure* 11: 1239-1249.

Ibrahim, H.R., Aoki, T., and Pellegrini, A. (2002) Strategies for new antimicrobial proteins and peptides: lysozyme and aprotinin as model molecules. *Curr Pharm Des* 8: 671-693.

Ito, Y., Kwon, O.H., Ueda, M., Tanaka, A., and Imanishi, Y. (1997) Bactericidal activity of human lysozymes carrying various lengths of polyproline chain at the C-terminus. *FEBS Lett* 415: 285-288.

Jado, I., Lopez, R., Garcia, E., Fenoll, A., Casal, J., and Garcia, P. (2003) Phage lytic enzymes as therapy for antibiotic-resistant *Streptococcus pneumoniae* infection in a murine sepsis model. *J Antimicrob Chemother* 52: 967-973.

Kuroki, R., Weaver, L.H., and Matthews, B.W. (1999) Structural basis of the conversion of T4 lysozyme into a transglycosidase by reengineering the active site. *Proc Natl Acad Sci U S A* 96: 8949-8954.

Leung, A.K., Duewel, H.S., Honek, J.F., and Berghuis, A.M. (2001) Crystal structure of the lytic transglycosylase from bacteriophage lambda in complex with hexa-N-acetylchitohexaose. *Biochemistry* 40: 5665-5673.

Levy, S.B., and Marshall, B. (2004) Antibacterial resistance worldwide: causes, challenges and responses. *Nat Med* 10: S122-129.

Loeffler, J.M., Nelson, D., and Fischetti, V.A. (2001) Rapid killing of *Streptococcus pneumoniae* with a bacteriophage cell wall hydrolase. *Science* 294: 2170-2172.

Loeffler, J.M., Djurkovic, S., and Fischetti, V.A. (2003) Phage lytic enzyme Cpl-1 as a novel antimicrobial for pneumococcal bacteremia. *Infect Immun* 71: 6199-6204.

Loessner, M.J., Kramer, K., Ebel, F., and Scherer, S. (2002) C-terminal domains of *Listeria monocytogenes* bacteriophage murein hydrolases determine specific recognition and high-affinity binding to bacterial cell wall carbohydrates. *Mol Microbiol* 44: 335-349.

Loessner, M.J. (2005) Bacteriophage endolysins--current state of research and applications. *Curr Opin Microbiol* 8: 480-487.

Low, L.Y., Yang, C., Perego, M., Osterman, A., and Liddington, R.C. (2005) Structure and lytic activity of a *Bacillus anthracis* prophage endolysin. *J Biol Chem* 280: 35433-35439.

Matsuzaki, S., Rashel, M., Uchiyama, J., Sakurai, S., Ujihara, T., Kuroda, M., Ikeuchi, M., Tani, T., Fujieda, M., Wakiguchi, H., and Imai, S. (2005) Bacteriophage therapy: a revitalized therapy against bacterial infectious diseases. *J Infect Chemother* 11: 211-219.

McHaourab, H.S., Oh, K.J., Fang, C.J., and Hubbell, W.L. (1997) Conformation of T4 lysozyme in solution. Hinge-bending motion and the substrate-induced conformational transition studied by site-directed spin labeling. *Biochemistry* 36: 307-316.

Mengin-Lecreulx, D., Falla, T., Blanot, D., van Heijenoort, J., Adams, D.J., and Chopra, I. (1999) Expression of the *Staphylococcus aureus* UDP-N-acetylmuramoyl-L-alanyl-D-glutamate:L-lysine ligase in *Escherichia coli* and effects on peptidoglycan biosynthesis and cell growth. *J Bacteriol* 181: 5909-5914.

Morita, M., Tanji, Y., Mizoguchi, K., Soejima, A., Orito, Y., and Unno, H. (2001a) Antibacterial activity of *Bacillus amyloliquefaciens* phage endolysin without holin conjugation. *J Biosci Bioeng* 91: 469-473.

Morita, M., Tanji, Y., Orito, Y., Mizoguchi, K., Soejima, A., and Unno, H. (2001b) Functional analysis of antibacterial activity of *Bacillus amyloliquefaciens* phage endolysin against Gram-negative bacteria. *FEBS Lett* 500: 56-59.

Nau, R., and Eiffert, H. (2005) Minimizing the release of proinflammatory and toxic bacterial products within the host: a promising approach to improve outcome in life-threatening infections. *FEMS Immunol Med Microbiol* 44: 1-16.

Navarre, W.W., Ton-That, H., Faull, K.F., and Schneewind, O. (1999) Multiple enzymatic activities of the murein hydrolase from staphylococcal phage phi11. Identification of a D-alanyl-glycine endopeptidase activity. *J Biol Chem* 274: 15847-15856.

Nelson, D., Loomis, L., and Fischetti, V.A. (2001) Prevention and elimination of upper respiratory colonization of mice by group A streptococci by using a bacteriophage lytic enzyme. *Proc Natl Acad Sci U S A* 98: 4107-4112.

Nelson, D., Schuch, R., Chahales, P., Zhu, S., and Fischetti, V.A. (2006) PlyC: a multimeric bacteriophage lysin. *Proc Natl Acad Sci U S A* 103: 10765-10770.

O'Flaherty, S., Coffey, A., Meaney, W., Fitzgerald, G.F., and Ross, R.P. (2005) The recombinant phage lysin LysK has a broad spectrum of lytic activity against

clinically relevant staphylococci, including methicillin-resistant *Staphylococcus aureus*. *J Bacteriol* 187: 7161-7164.

Orito, Y., Morita, M., Hori, K., Unno, H., and Tanji, Y. (2004) *Bacillus amyloliquefaciens* phage endolysin can enhance permeability of *Pseudomonas aeruginosa* outer membrane and induce cell lysis. *Appl Microbiol Biotechnol* 65: 105-109.

Pritchard, D.G., Dong, S., Baker, J.R., and Engler, J.A. (2004) The bifunctional peptidoglycan lysin of *Streptococcus agalactiae* bacteriophage B30. *Microbiology* 150: 2079-2087.

Rigden, D.J., Jedrzejas, M.J., and Galperin, M.Y. (2003) Amidase domains from bacterial and phage autolysins define a family of gamma-D,L-glutamate-specific amidohydrolases. *Trends Biochem Sci* 28: 230-234.

Schuch, R., Nelson, D., and Fischetti, V.A. (2002) A bacteriolytic agent that detects and kills *Bacillus anthracis*. *Nature* 418: 884-889.

Takac, M., and Blasi, U. (2005) Phage P68 virion-associated protein 17 displays activity against clinical isolates of *Staphylococcus aureus*. *Antimicrob Agents Chemother* 49: 2934-2940.

Thiel, K. (2004) Old dogma, new tricks--21st Century phage therapy. *Nat Biotechnol* 22: 31-36.

van Heijenoort, J. (2001) Recent advances in the formation of the bacterial peptidoglycan monomer unit. *Nat Prod Rep* 18: 503-519.

Vasala, A., Valkkila, M., Caldentey, J., and Alatossava, T. (1995) Genetic and biochemical characterization of the *Lactobacillus delbrueckii* subsp. *lactis* bacteriophage LL-H lysin. *Appl Environ Microbiol* 61: 4004-4011.

Vollmer, W., and Tomasz, A. (2000) The *pgdA* gene encodes for a peptidoglycan N-acetylglucosamine deacetylase in *Streptococcus pneumoniae*. *J Biol Chem* 275: 20496-20501.

Yoong, P., Schuch, R., Nelson, D., and Fischetti, V.A. (2004) Identification of a broadly active phage lytic enzyme with lethal activity against antibiotic-resistant *Enterococcus faecalis* and *Enterococcus faecium*. *J Bacteriol* 186: 4808-4812.

Yoong, P., Schuch, R., Nelson, D., and Fischetti, V.A. (2006) PlyPH, a bacteriolytic enzyme with a broad pH range of activity and lytic action against *Bacillus anthracis*. *J Bacteriol* 188: 2711-2714.

Young, I., Wang, I., and Roof, W.D. (2000) Phages will out: strategies of host cell lysis. *Trends Microbiol* 8: 120-128.

Young, K.D. (2003) Bacterial shape. *Mol Microbiol* 49: 571-580.

Zimmer, M., Vukov, N., Scherer, S., and Loessner, M.J. (2002) The murein hydrolase of the bacteriophage phi3626 dual lysis system is active against all tested *Clostridium perfringens* strains. *Appl Environ Microbiol* 68: 5311-5317.

Figure legends

Figure 1. Schematic representation of the different cleavage sites of endolysins on the cell wall structure of Gram-positive bacteria. The sole typical difference between the Gram-positive and Gram-negative cell wall structure is the nature of the third residue of the peptide cross-bridge. Gram-negative bacteria and bacilli usually contain a meso-diaminopimelic acid whereas Gram-positive bacteria contain an L-lysine residue at this position. (Mengin-Lecreulx *et al.*, 1999)

Figure 2. Tridimensional structures of the coliphage (A) T4, (B) λ and (C) T7 endolysins. The image was created using INSIGHTII version 2000.1 (Accelrys) on a Silicon Graphics Fuel workstation.

Figure 1.

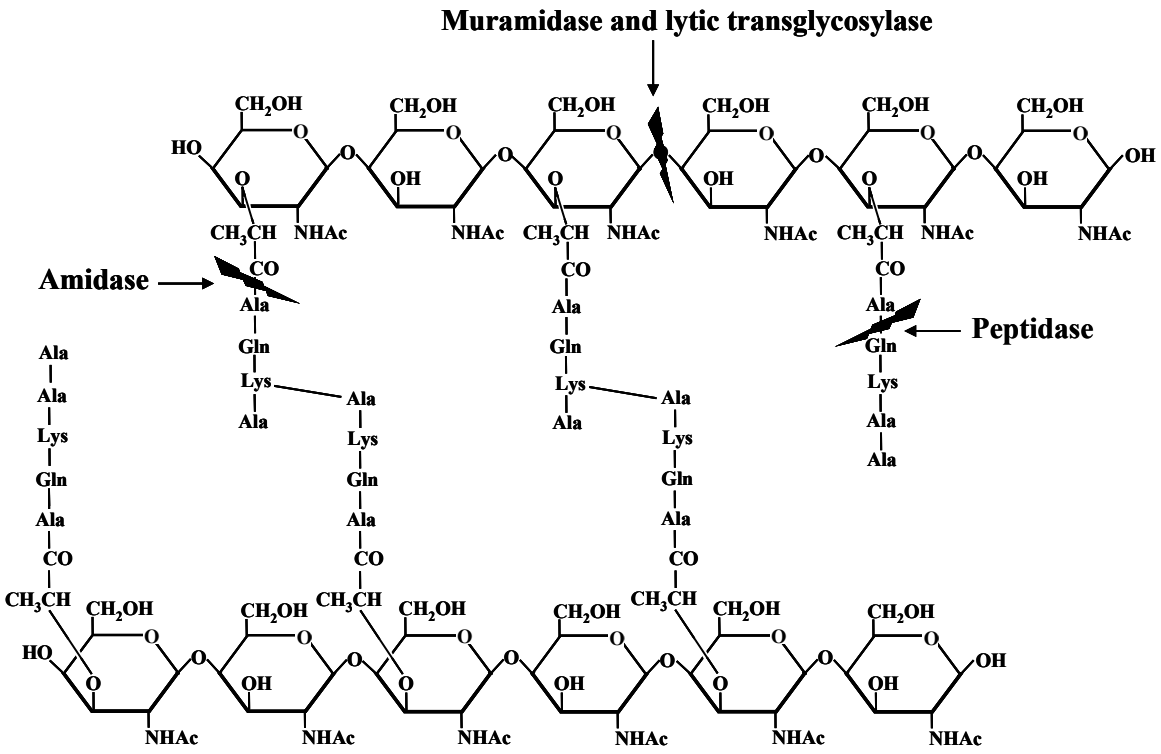
Muramidase and lytic transglycosylase
Amidase
Peptidase

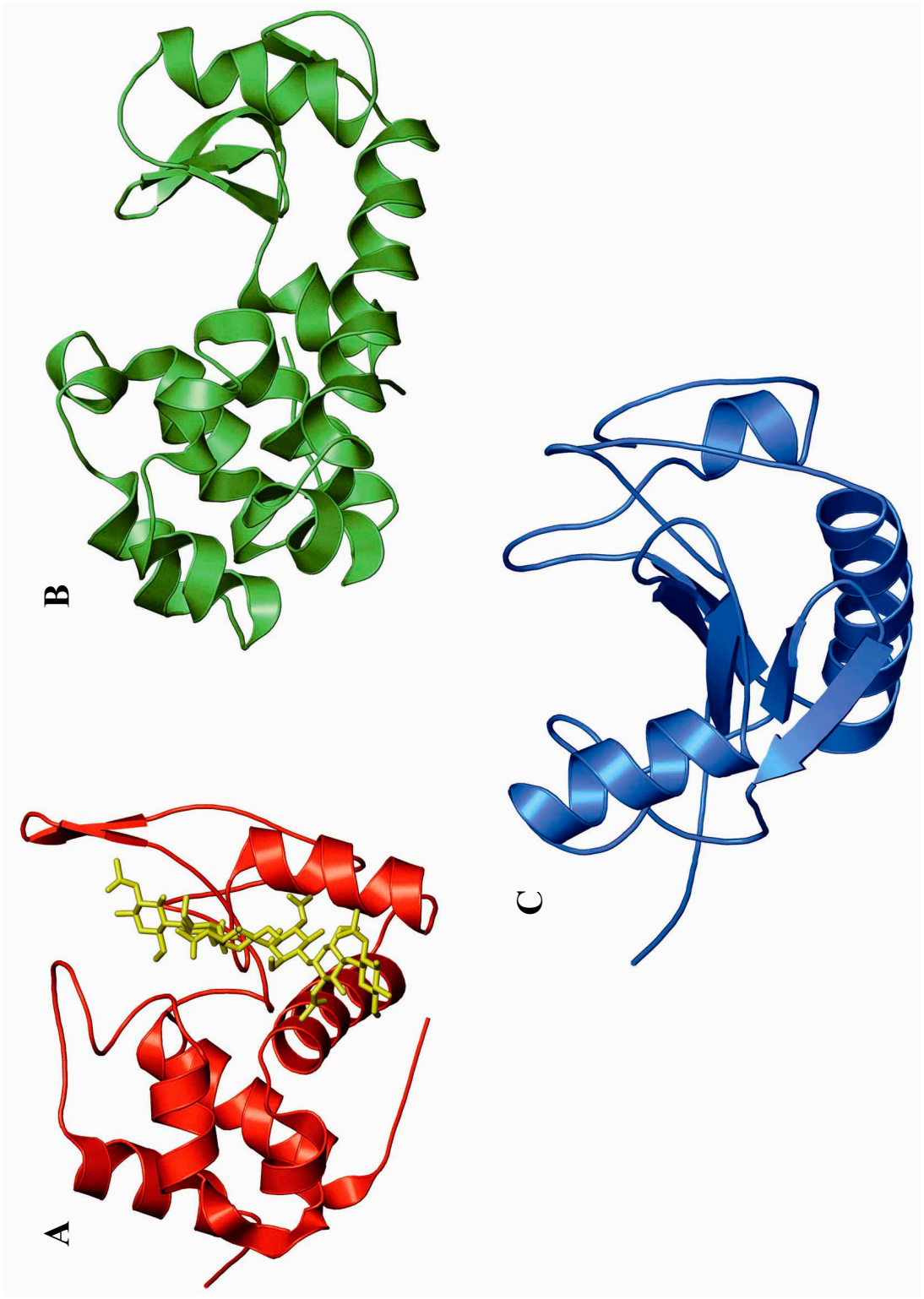

Figure 2.

Chapitre 9 - Peptidoglycan lytic activity of the *Pseudomonas aeruginosa* phage ϕKZ gp144 lytic transglycosylase

Résumé

Caractérisation du mécanisme d'hydrolyse du peptidoglycane par la transglycosylase lytique gp144 du phage ϕKZ de *Pseudomonas aeruginosa*

Les endolysines de bactériophages suscitent un vif intérêt de la part de la communauté scientifique en cette ère où le pouvoir évolutif des bactéries prend progressivement le dessus sur la capacité de l'être humain à développer de nouveaux antibiotiques. Dans cette étude, l'endolysine du bactériophage ϕKZ infectant *P. aeruginosa* est caractérisée en tant que nouvel agent antibactérien ciblant les espèces bactériennes à Gram-négatif. L'endolysine gp144 du phage ϕKZ a tout d'abord été clonée et exprimée dans des cellules recombinantes de *E. coli*. L'expression de gp144 a entraîné la lyse cellulaire de *E. coli* et la protéine a été purifiée directement à partir du surnageant de culture et des cellules bactériennes. L'endolysine purifiée démontre une activité antibactérienne contre le pathogène opportuniste *P. aeruginosa* et dégrade le peptidoglycane purifié des bactéries à Gram-négatif. Des analyses en spectrométrie de masse ont permis d'identifier le site de clivage du peptidoglycane et ont confirmé l'activité transglycosylase lytique de l'enzyme gp144. L'expression de gp144 en présence d'azide de sodium et dans un mutant *E. coli* $secA_{ts}$ a démontré que la translocation de l'endolysine est indépendante du système de sécrétion protéique bactérien Sec. Des analyses de dichroïsme circulaire indiquent que gp144 contient 61 % d'hélice α. En présence de dimyristoylphosphatidylglycérol (DMPG), un lipide anionique typique des membranes bactériennes, la protéine gp144 perd 72 % de sa conformation en hélice α. L'endolysine gp144 entraîne également une relâche immédiate de calcéine fluorescente lorsqu'elle interagit avec des vésicules membranaires synthétiques composées de DMPG contenant de la calcéine. Les résultats obtenus indiquent que la transglycosylase lytique gp144 interagit de façon spécifique avec les membranes bactériennes afin de les désorganiser et d'accéder à la paroi bactérienne. Ainsi, l'endolysine gp144 possède un potentiel antibactérien fort intéressant contre les espèces bactériennes à Gram-négatif.

Contribution des auteurs

Huit auteurs signent la réalisation de cet article scientifique récemment publié par la revue scientifique «FEMS Microbiology Letters». Ainsi, cette étude n'aurait pu être menée à bien sans l'aide précieuse des nombreuses collaborations. En tant que première auteure, j'ai tout d'abord participé à la conceptualisation et à l'orientation du projet de recherche avec le support du Dr Roger C. Levesque. Par la suite, j'ai effectué la majorité des expériences décrites. Ainsi, j'ai cloné le gène codant pour l'endolysine gp144 à partir du bactériophage ϕKZ. J'ai également exprimé et purifié la protéine en grande quantité puis j'ai procédé aux essais d'hydrolyse du peptidoglycane. Par la suite, j'ai mis au point l'immunodétection de l'endolysine avec des anticorps polyclonaux. J'ai alors réalisé les expériences d'expression de l'endolysine en présence de l'inhibiteur azide de sodium et dans un mutant *E. coli* $SecA_{ts}$. Les essais de dichroïsme circulaire et de fluorescence ont été réalisés en collaboration avec Isabelle Cloutier et la Dre Michèle Auger. J'ai participé aux expériences de dichroïsme circulaire avec Isabelle Cloutier. Cette étudiante au doctorat a préparé par elle même les vésicules lipidiques employées au cours de cette étude puis elle a réalisé les essais de fluorescence sous la supervision de la Dre Michèle Auger. Les analyses par spectrométrie de masse ont été effectuées en collaboration avec Lise Lemieux et le Dr Alain Garnier. La mise au point de l'analyse des muropeptides par spectrométrie de masse et les déconvolutions ont été exécutées par Lise Lemieux sous la direction du Dr Alain Garnier. J'ai ensuite interprété les données de déconvolution afin d'identifier les muropeptides correspondants aux masses moléculaires obtenues. Quant au Dr Jérôme Laroche, il s'est chargé des analyses bioinformatiques effectuées sur l'imposant génome du bactériophage ϕKZ. Le Dr François Sanschagrin m'a apportée un support technique et scientifique tout au long de ce projet de recherche. J'ai finalement assemblé et analysé les résultats afin de préparer les figures et tableaux puis et j'ai rédigé le manuscrit. Les figures de dichroïsme circulaire et de fluorescence ont été préparées par Isabelle Cloutier. Enfin, ce projet n'aurait vu le jour sans l'aide incontestable du Dr Levesque qui m'a fournit un support constant et un environnement de travail propice à la réussite. Il a également révisé le manuscrit pour en augmenter la fluidité et la valeur scientifique.

Peptidoglycan lytic activity of the *Pseudomonas aeruginosa* phage ϕKZ gp144 lytic transglycosylase

Catherine Paradis-Bleau[1], Isabelle Cloutier[2], Lise Lemieux[3], François Sanschagrin[1], Jérôme Laroche[4], Michèle Auger[2], Alain Garnier[3] and Roger C. Levesque[1]

Département de Biologie Médicale[1], Faculté de Médecine[1], Faculté des Sciences et Génie[2, 3], Département de Chimie[2], Département de Génie Chimique[3], Centre de Bioinformatique[4], Université Laval, Sainte-Foy, Québec, Canada, G1K 7P4

Keywords: *Pseudomonas aeruginosa*, phage ϕKZ, endolysin, phage lysis, peptidoglycan, lytic transglycosylase

Correspondence: Dr. Roger C. Levesque, Département de Biologie Médicale, Pavillon Charles-Eugène Marchand, Université Laval, Sainte-Foy, Québec, Canada, G1K 7P4, Tel: (1) 418 656-3070; Fax: (1) 418 656-7176; E-Mail: rclevesq@rsvs.ulaval.ca

Abstract

The *gp144* endolysin gene from the *Pseudomonas aeruginosa* phage ϕKZ was cloned and studies of gp144 expression into *Escherichia coli* showed host cell lysis. The gp144 protein was purified directly from the culture supernatant and from the bacterial cell pellet and showed *in vitro* antibacterial lytic activity against *P. aeruginosa* bacteria and degraded purified peptidoglycan of Gram-negative bacteria. MS analysis identified the gp144 peptidoglycan cleavage site and confirmed a lytic transglycosylase enzyme. Studies of gp144 expression in the presence of sodium azide (NaN_3), an inhibitor of the protein export machinery, and into an *E. coli* MM52 $secA_{ts}$ mutant at permissive and restrictive temperatures showed that gp144 was secreted independently of the Sec system. The solution conformation of purified gp144 analyzed by circular dichroism spectroscopy was 61% in α-helical content, and showed a 72% decrease when interacting with dimyristoylphosphatidylglycerol (DMPG), one of the major components of bacterial membranes and less than 10% with dimyristoylphosphatidylcholine (DMPC) found in eukaryotic membranes. Membrane vesicles of DMPG anionic lipids containing calcein indicated that gp144 caused a rapid release of fluorescent calcein when interacting with synthetic membranes. These results indicated that gp144 from ϕKZ is a lytic transglycosylase capable of interacting with and disorganizing bacterial membranes and has potential as an antipseudomonal in phage therapy.

Introduction

To promote bacterial host cell lysis and release of phage progeny, double-stranded DNA phages typically use a holin–endolysin mechanism. Endolysin is restricted to the cytoplasm until the holin destabilizes the internal membrane, permitting hydrolysis of peptidoglycan and cell lysis (Young *et al.*, 2000; Wang *et al.*, 2000; Fischetti, 2005).

Phage ϕKZ infects *Pseudomonas aeruginosa*, a Gram-negative opportunistic pathogen causing nosocomial infections difficult to treat because of antibiotic resistance (Davies, 2002; Hancock & Brinkman, 2002). The Myoviridae ϕKZ contains the largest

sequenced double-stranded DNA phage genome with 306 ORFs (Mesyanzhinov *et al.*, 2002).

During the course of this work, Mesyanzhinov and colleagues described some of the properties of gp144 (Miroshnikov *et al.*, 2006). Recombinant gp144 purified from *Escherichia coli* effectively degraded chloroform-treated *P. aeruginosa* cells. The gp144 protein was found in solution in stoichometric monomer: dimer and trimer equilibrium. In this study, we extend these observations and have developed a method for expression, purification and analysis of a biologically active recombinant gp144. We also demonstrate that gp144 is a lytic transglycosylase, and that the enzyme goes through conformational changes when interacting with dimyristoylphosphatidylglycerol (DMPG) calcein vesicles reflecting the net anionic nature of bacterial membranes, which only have 15–30% phosphatidylcholine.

Materials and methods

Bioinformatics

The ϕKZ 280.3 Kb sequence was analyzed for ORFs using software programs of the University of Wisconsin Package (GCG, version 10.2, Madison, WI). The sequence was split into 312 overlapping fragments and compared with sequences of the viral, bacterial and phage divisions of GenBank using TBLASTX (Benson *et al.*, 2005). Similar search was done with BLASTX against the 1137 reported holins. ϕKZ ORFs were compared with the PFAM-A database using hmmpfam HMMER (Eddy, 1998). The results were analyzed using a developed PYTHON program (van Rossum & de Boer, 1991). Retrieval from databases and sequence splitting were performed with EMBOSS (Rice *et al.*, 2000). Gp144 was analyzed for Sec, signal-arrest-release sequence (SAR) and TAT signal sequences and characterized using BLAST, CDART and EXPASY algorithms (Berks *et al.*, 2000; Geer *et al.*, 2002; Xu *et al.*, 2004).

Cloning of ϕKZ ORF 144

Phage amplification was performed using phage PhiKZ DNA genomic DNA (Sambrook *et al.*, 1989). DNA was purified with the Lambda Maxi Kit (Qiagen, Mississauga, Ontario, Canada). PCR was used to obtain ORF144 encoding gp144 fused with a C-terminal His-tag using genomic DNA (300 ng), the primers 5'-GTAGAGGTTATCATATGAAAGTATTA-3' and 5'-TGCTACCTCGAGTTTTCT-3', 5 mM $MgCl_2$ and 2.5 U of Hot start TAQ polymerase (Qiagen) at touchdown temperatures of 40–30°C. The amplified product was purified, digested with NdeI and Xho1 and ligated into corresponding sites of pET24a (Novagen, Madison, WI). Plasmid pMON2266 was electroporated into *E. coli recA*$^-$ ElectroMAX™ DH10B™ and sequenced using the T7 primers (Novagen).

Overexpression and purification of gp144

Plasmid pMON2266 was transformed into *E. coli* BL21 (λDE3) using $CaCl_2$ (Sambrook *et al.*, 1989). Isopropyl-β-D-thiogalactopyranoside (IPTG) at 1 mM was added to a tryptic soy broth culture (kanamycin 50 μg mL^{-1}) at an $OD_{600\,nm}$ of 0.8 and incubated for 6 h at 37°C under agitation. The supernatant from a 1-L culture was treated with DNAse and concentrated to 200 mL using a stirred ultrafiltration cell and a filter with a 10 kDa cut-off. Expressing cells were resuspended in sonication buffer [50 mM Tris-HCl pH 8.6, 1 mM ethylenediaminetetraaectic acid (EDTA)], sonicated 30 s mL^{-1} before addition of protease inhibitors. Fractions were analyzed by sodium dodecyl sulfate polyacrylamide gel electrophoresis (SDS-PAGE). Gp144 was purified from the supernatant and the cell pellet by affinity chromatography using a HisTrap™ HP nickel column (Amersham Biosciences, Baie d'Urfé, Québec, Canada). Final purification was performed by gel filtration (Superdex 75 10/300 column, LMW gel filtration Calibration Kit, Amersham Biosciences). Fractions containing gp144 were concentrated, maintained at −80°C in 50 mM Tris-HCl pH 7.4, 25 mM $MgCl_2$ and 10 mM NaCl and N-terminal sequencing was performed (Paradis-Bleau *et al.*, 2005).

Peptidoglycan degrading assay

Peptidoglycan from *P. aeruginosa* PAO1, *E. coli* ATCC 25922, *Staphylococcus aureus* ATCC 25923 and *Bacillus cereus* ATCC 27877 was prepared from 50-mL cultures of Gram-positive bacteria and 500 mL for Gram-negatives (Moak & Molineux, 2004). Peptidoglycan was sonicated, diluted in water to an $OD_{600\,nm}$ of 1, monitored for 250 min with and without purified gp144 at various concentrations and performed in triplicate.

Identification of the gp144 peptidoglycan cleavage site by LCMS

The molecular mass of the gp144 peptidoglycan degradation products was determined using an Agilent 1100 LCMS. A 200 µg aliquot of peptidoglycan was incubated with 250 µM of purified gp144 at 37°C in 100 µL. Peptidoglycan hydrolysis was stopped by adding 10% trifluoroacetic acid (TFA) and TFA-soluble muropeptides were collected (Navarre *et al.*, 1999). Dried muropeptides were resuspended in 70 µL of mobile phase A (H_2O, 0.1% formic acid, 0.025% TFA) and 10 µL was injected into a ZORBAX 300 SB-C18 reversed-phase column protected by a Zorbax 300 SB-C18 analytical guard-column (Agilent Technologies, Montreal, Québec, Canada). Separation of muropeptides was performed at a flow rate of 200 µL min^{-1}. A gradient of mobile phase B (acetonitrile, 0.1% formic acid, 0.025% TFA) was used from 1% increasing 1.36% min^{-1}. The eluted muropeptides were identified at 214 nm at 4°C and the column was at 40°C. The molecular mass of muropeptides was determined with an Agilent 1100 MSD ESI mass spectrometer using the positive electrospray ionization mode, in full scan from 50 to 2950 *m/z* with a step of 0.1 and a cycle time of 2.25 s.

Expression of gp144 in *E. coli* with sodium azide (NaN_3)

Gp144 was expressed at an $OD_{600\,nm}$ of 0.3, 0.6, 0.7, 0.8 and 0.9 with and without 1 mM NaN_3. *Escherichia coli* BL21-induced and noninduced cultures for gp144 were monitored. CFUs were determined in triplicate at time points 0, 3, 6, 9, 12 and 25 h after induction at an $OD_{600\,nm}$ of 0.8. Cell pellets and supernatants from 0, 1, 2, 3, 4, 6, 8, 10 and 12 h were analyzed by SDS-PAGE. Western blots of gp144 supernatants were performed using rabbit polyclonal anti-gp144 antibodies (Harlow & Lane, 1988). Immunodetection was performed

with the ECL Advance Western Blotting Detection Kit using the rabbit anti-gp144 serum 1 : 50 000 and the ECL anti-rabbit peroxidase-linked antibody 1 : 15 000 (Amersham). *Escherichia coli* XL1-blue was lysogenized using the λDE3 Lysogenization Kit (Novagen) and transformed with pMON2266. Expression of gp144 was determined at $OD_{600\,nm}$ values of 0.6, 0.7 and 0.8 and was monitored with and without NaN_3.

Expression of gp144 in an *E. coli* $secA_{ts}$ mutant

Escherichia coli MM52 (pMON2266) was grown at 30°C for SecA expression and at the nonpermissive (42°C) temperature with induction of gp144 at an $OD_{600\,nm}$ of 0.05 to 0.7 (Oliver & Beckwith, 1981). Cell extracts and supernatants were analyzed by SDS-PAGE and gp144 in the supernatants was confirmed by Western blot. As control, cultures containing 0.4% maltose to induce the SecA-translocated maltose-binding protein (MBP) were used. At the time of induction (after 4 h at a permissive or nonpermissive temperature), 30 mL of each culture was treated with lysozyme-EDTA (Oliver & Beckwith, 1981). Spheroplasts were resuspended in 200 µL of sonication buffer and sonicated for 30 s. $OD_{600\,nm}$ values were used to standardize periplasmic and cytoplasmic proteins analyzed by SDS-PAGE. The MBP content was evaluated by Western blot using the anti-MBP monoclonal antibody conjugated to HRP 1 : 500 (New England Biolabs, Mississauga, Ontario, Canada) and the Immobilon™ Western Chemiluminescent HRP Substrate detection assay (Millipore, Nepean, Ontario, Canada).

Circular dichroism

Fifteen scans were collected from 190 to 250 nm using a 1-nm wavelength increment on a Jasco J-710 spectropolarimeter with a 2-mm path length cell. Spectra were obtained by comparisons with the base line of a CD buffer (2.5 mM Tris-HCl pH 7.4, 1.25 mM $MgCl_2$, 0.5 mM NaCl). Ellipticity was measured at 225 nm. Spectra were collected using 30 µM of gp144 and with concentrations of 1–25 mM of dithiothreithol (DTT). For interactions with synthetic membranes, 166 µM of gp144 was used with zwitterionic dimyristoylphosphatidylcholine (DMPC) or anionic DMPG lipid vesicles. The data were analyzed using the CDESTIMA software to predict the percentage of α-helix content.

Gp144 permeabilization assays of calcein-containing vesicles

For calcein release assays, vesicles were prepared by dispersing 5 mg of DMPC or DMPG dried lipids into 250 μL of phosphate buffer (50 mM pH 7.4). After five cycles of freeze in liquid nitrogen, thaw at 37°C and mixing, the dispersions were extruded 11 times using a polycarbonate 0.1 μm filter. The stability of calcein-containing vesicles was confirmed by monitoring the calcein release for each preparation.

DMPC and DMPG calcein vesicles and gp144 permeabilization assays were performed as described (Biron *et al.*, 2004) with the following modifications: 20 mg of DMPC or DMPG was directly dispersed in 1 mL of internal buffer and five cycles of freeze at −180°C, thaw at 37°C and mixing were performed before sonication. A final concentration of 4 μM of gp144 was added to 3 mL of external buffer at room temperature to yield a 100 : 1 lipid $gp^{-1}144$ ratio.

Results

Bioinformatic analysis for an endolysin-holin system in the ϕKZ genome sequence

Bioinformatic analysis of the 280 334 bps sequence of ϕKZ and the 306 ORFs identified ORF144 as a putative peptidoglycan-degrading enzyme. We noted 52% amino acid identity between the catalytic domain of gp144 and the C-terminus of gp181, a ϕKZ tail fiber protein. The deduced amino acid sequence of the ϕKZ endolysin (gp144) indicated a putative cytoplasmic protein of 28.8 kDa with a pI value of 9.1 having no transmembrane domains, and secondary structures containing 51–54% of α-helix, 1–3% of β-sheet and 44–46% of loop. CDART identified a putative peptidoglycan-binding domain composed of three α-helices at the N-terminus and a lytic transglycosylase catalytic domain at the C-terminus. Exhaustive bioinformatic analysis did not identify a typical holin sequence.

Expression and purification of gp144 into *E. coli*

Analysis of the gp144 expression into *E. coli* was studied using bacterial growth curves. The gp144-expressing culture contained 1.8×10^7 CFUs mL^{-1} after 5 h in comparison with 4.4×10^9 CFUs mL^{-1} for the noninduced culture (data not shown). Significant differences

between induced and non induced cultures for expression of gp144 were *c*. 3 logs in CFUs after 9 h. The *E. coli* colonies containing cells expressing gp144 appeared irregular, rough and smaller than nonexpressing colonies on Tryptic Soy Agar plates.

Analysis by SDS-PAGE indicated that the 30.1 kDa band (28.8 kDa plus a C-terminus fusion of LDLEHHHHHH) identified as gp144 was released directly into the culture supernatant extracellular media (300 mg L^{-1}) and was also present in the cell pellet as soluble (100 mg L^{-1}) and insoluble fractions (data not shown). Based upon SDS-PAGE analysis (1 μg $lane^{-1}$) and SYPRO® Orange staining, gp144 was purified to >99% homogeneity and N-terminal sequencing of the 15 first amino acids confirmed gp144 identity. As previously reported, purification by gel filtration gave two major peaks corresponding to the monomer (30.1 kDa) and dimer (60.2 kDa) forms of gp144 (data not shown; Miroshnikov *et al.*, 2006). The dimer form was predominant in the culture supernatant, whereas the monomer was predominant in the cytoplasm of the cell pellet fraction (data not shown). SDS-PAGE analysis showed that purified gp144 was present as monomers, dimers and trimers that were resistant to boiling and to 1% SDS; nondenaturing PAGE showed gp144 oligomers of high molecular mass (data not shown). The monomer form was found to dimerize rapidly after 24 h at 4°C, whereas DTT-treated gp144 gave only monomers.

Peptidoglycan-degrading activities

Addition of purified gp144 to purified peptidoglycan from four bacterial species caused a rapid $OD_{600\ nm}$ decrease of peptidoglycan from Gram-negative bacteria in a dose-dependent fashion. As presented in Fig. 1a, 100 μM of gp144 hydrolyzed *P. aeruginosa* peptidoglycan in 2 min and in *c*. 25 min for *E. coli*. In contrast, an apparent lag of more than 60 min was observed for peptidoglycan of *B. cereus* and *S. aureus* and significant hydrolysis was detected only after 120 min. These results indicated that gp144 caused specific hydrolysis of peptidoglycan from Gram-negative bacteria.

Identification of gp144 cleavage site in peptidoglycan

The HPLC chromatogram of peptidoglycan from *P. aeruginosa* hydrolyzed by gp144 gave major peptidoglycan degradation products, and the results are summarized in Table 1. The first peak identified contained gp144 amino acid autodegradation products with molecular masses of 119.11 and 370.23 Da because the same elution products were obtained for gp144 only (data not shown). By using the peak surface area, we selected seven major elution products as shown in Fig. 1b. The main peptidoglycan degradation product GlcNac-anhydroMurNac–Ala–iGln–mDAP–Ala–mDAP–iGln–Ala–Ala was defined as the parent ion as all muropeptides identified by MS converged to this compound (Table 1, Fig. 1b). The unique cell wall-degrading enzyme that could lead to this activity is a lytic transglycosylase. This enzyme cleaves the β(1,4)-glycosidic bond between *N*-acetylmuramic acid and *N*-acetylglucosamine and adds a new glycosidic bond within the C6 hydroxyl group of the same muramic acid residue. The lytic transglycosylase reaction gave distinctive (1,6)-anhydro *N*-acetylmuramic muropeptides frequently recovered in the gp144 digestion pattern, and the identified compounds are indicated in bold in Table 1. The molecular masses obtained from gp144 hydrolysis did not correspond to the size of degradation products for other types of peptidoglycan degrading enzymes such as *N*-acetylglucosaminidase, amidase or peptidase.

Expression of gp144 in the presence of an inhibitor of the protein export machinery

As *in silico* bioinformatics analysis for Sec, SAR and TAT signal sequences using BLAST, CDART and EXPASY algorithms was negative for gp144 and as the cytoplasmic gp144 was secreted directly into the culture supernatant, we evaluated whether typical bacterial secretion systems could still potentially be involved. It is well known that bacterial cell cultures treated with NaN_3 show inhibition of azide-sensitive components of one of the major bacterial protein export machineries such as Sec (Fortin *et al.*, 1990). To evaluate the role of the Sec system in gp144 translocation, growth rates of *E. coli* were measured in liquid media induced for the expression of gp144 with or without 1 mM NaN_3. As depicted in Fig. 2a, the results obtained showed that NaN_3 did not affect gp144 hydrolytic activity. We noted a difference of 3 logs in CFUs from *E. coli* cultures expressing gp144 containing

NaN_3. SDS-PAGE analysis at selected time-points of the cell culture supernatants and cell pellets treated or not with NaN_3 (Fig. 2b) showed that the concentration of gp144 with NaN_3 was similar to the control without NaN_3 after 1 h of expression (Fig. 2b, upper panels, left and right). Specific anti-gp144 immunodetection revealed gp144 in culture supernatants apparent after 1 h and up to 12 h after induction. Gp144 was also found in cultures grown with NaN_3 and could be detected from 1 h up to 12 h (Fig 2b, lower panels, left and right). These data indicate that gp144 transport does not depend on the typical bacterial transport machinery.

Expression of gp144 in *E. coli* $secA_{ts}$ defective mutant

To confirm the NaN_3 data, we studied expression of the gp144 lytic transglycosylase into an *E. coli* $secA_{ts}$ defective mutant. As a control, we first tested the SecA-dependent MBP translocation at both the permissive and restrictive temperatures. Immunodetection of the SecA-translocated MBP at the time of induction indicated that the 43.4 kDa protein accumulated in the periplasm at 30°C, while only a trace of MBP was detected in the periplasm at 42°C, confirming the $SecA_{ts}$ phenotype (data not shown). To confirm gp144 activity at the restrictive temperature, we analyzed expression of gp144 in *E. coli* BL21 and *E. coli* XL1-blue grown at 30°C and at 42°C. Growth curve analysis demonstrated that gp144 was functional at both temperatures because $OD_{600\,nm}$ values declined from 0.85 to 0.4, confirming gp144 activity and thermostability at 42°C (data not shown).

As shown in Fig. 3a, induction of gp144 at 30°C caused cell lysis and reduced CFUs at *c*. 0.5 $\log_{10}$ when compared with the noninduced control but not as significantly as at 37°C. This indicated less nonspecific cell lysis caused by the release of gp144 at lower temperature. At the nonpermissive temperature (42°C), *E. coli* cells showed a delay in growth for 6.5 h until the exponential phase was reached (Fig. 3a). Induction of gp144 caused cell lysis at 42°C and gave growth curves similar to gp144 at normal temperature (37°C). Gp144 was found in the cell pellet (Fig. 3b, upper left panel) after 1 h of expression at 30°C, accumulated until 4 h and decreased after 10 h. Gp144 was constantly present after induction at 42°C from 1 h up to 12 h, but at a much lower concentration (Fig. 3b, upper right panel). Specific anti-gp144 immunodetection confirmed that gp144 was released in

the culture supernatant after 4 h of expression at 30°C, indicating a tight control of expression (Fig. 3b, lower left panel). In contrast, gp144 was found in the culture supernatant 1 h and up to 12 h after expression at 42°C (Fig. 3b, lower right panel), indicating that SecA was not necessary for secretion.

Analysis of gp144 by circular dichroism and interaction with lipid vesicles

Analysis of purified gp144 by circular dichroism showed a content of 61±5% in the α-helix structure stable up to 50°C. To evaluate whether gp144 could interact directly with bacterial membranes and be liberated into the extracellular media, we used a biophysical approach with DMPG-containing vesicles. As shown in Fig. 4, gp144 was added to preparations of anionic DMPG vesicles and subsequent analysis of the CD spectra gave a decrease of 72±3% in α-helical content. In contrast, a small increase of gp144 α-helical content was observed with zwitterionic DMPC vesicles, a compound mimicking eukaryotic membranes. These studies indicated that gp144 was capable of interacting directly with anionic membranes. This indicated the potential of gp144 to interact with bacterial membranes that would facilitate its liberation.

To extend these experiments, we decided to incubate gp144 with calcein-containing DMPG vesicles and measure indirectly the permeabilization of these artificial membranes by gp144 by measuring the fluorescence of calcein. As shown in Fig. 5, addition of gp144 to DMPG vesicles caused a rapid calcein release, reaching 55% after 50 s and reaching a plateau at 90%. Control experiments showed that calcein-containing vesicles were stable, that bovine serum albumin (BSA) did not enhance calcein release and that Triton released 100% of the fluorescent calcein. In contrast, gp144 did not release fluorescent calcein from DMPC vesicles (Fig. 5). These data would indicate that gp144 interacted with, disorganized and augmented the permeability of these artificial membranes.

Discussion

Phage lysis proteins are exciting prospects as antibacterial agents (Fischetti, 2005). Overexpression of the ϕKZ gp144 endolysin into *E. coli* retained peptidoglycan lytic

activity against Gram-negative bacteria. Gp144 was released into culture supernatants after IPTG induction and lysed neighboring cells.

Gp144 peptidoglycan-degrading activity indicated a predominant activity against Gram-negative bacteria, and LCMS analysis of gp144 hydrolytic products identified a lytic transglycosylase. We noted a weak hydrolytic activity against the peptidoglycan of Gram-positive bacteria that O-acetylate their peptidoglycan, a modification that totally precludes the function of lytic transglycosylases because the O-acetylation occurs at the C-6 hydroxyl of muramyl residues, the same group involved in the formation of the 1,6-anhydromuramyl product of lytic transglycosylase activity (Ginsburg, 2002). The O-acetyl groups on the tested peptidoglycan may have been lost during its purification (a strong possibility, given the liability of the acetate ester linkage), which could explain residual activity against *S. aureus* and *B. cereus*. An apparent lag exists in hydrolysis of peptidoglycans from Gram-positive bacteria, which could reflect the prior need for spontaneous de-esterification of acetyl groups (if still present on the substrates) and the poor recognition of the peptidoglycan-binding domain of gp144 of Gram-positive bacteria.

The vast majority of secreted proteins use the Sec or Tat pathways requiring specific N-terminal signal sequences (Berks *et al.*, 2000). Gp144 does not possess typical Sec or Tat secretion motifs. We assessed whether gp144 exploits the Sec pathway via a nontypical signal as for phage P1 endolysin (Sao-Jose *et al.*, 2000). Inactivation of SecA blocked translocation and lytic activities of phages P1 and fOg44 endolysins (Sao-Jose *et al.*, 2000; Xu *et al.*, 2004). Gp144 activity and cell lysis was evident in a $SecA_{ts}$ mutant at a non permissive temperature. We also studied the effect of NaN_3 on gp144 expression and transport; NaN_3 did not affect cell lysis by gp144, suggesting a bypass of typical secretion pathways (Fortin *et al.*, 1990). However, expression of gp144 from a multicopy plasmid and subsequent cell lysis could be caused by levels of expression toxic to the host cell where gp144 is liberated and lytic transglycosylase activity may lyse neighboring cells.

LytA autolysin and Eji phage endolysin activation depends upon dimerization (Diaz *et al.*, 1989; Saiz *et al.*, 2002). Gp144 has a secondary structure similar to the Eji endolysin (Saiz *et al.*, 2002). Recently, a SAR mediated export and control of phage P1 endolysin was identified (Xu *et al.*, 2004). Lyz of P1 caused host lysis without a holin. Instead, export was

mediated by an N-terminal transmembrane domain and required host *sec* function. Exported Lyz of identical SDS-PAGE mobility was found in both the membrane and periplasmic compartments, indicating that periplasmic Lyz was not generated by the proteolytic cleavage of the membrane-associated form. The N-terminal domain of Lyz is both necessary and sufficient not only for export to the membrane but also for release into the periplasm. The unusual N-terminal domain, rich in residues weakly hydrophobic, functions as an SAR sequence, acting as a normal signal-arrest domain to direct the endolysin to the periplasm in membrane-tethered form and then allows its release in the periplasm.

Disulfide isomerization after membrane release of its SAR domain also activates the P1 lysozyme (Xu *et al.*, 2005). Crystal structures confirmed the alternative disulfide linkages in the two forms of Lyz and revealed dramatic conformational differences in the catalytic domain. Thus, the exported P1 endolysin is kept inactive by three levels of control-topological, conformational and covalent-until its release from the membrane is triggered by the P1 holin.

Examination of the protein sequences of related bacteriophage endolysins suggests that the presence of an N-terminal SAR sequence is not unique to Lyz. Analysis of the gp144 N-terminal region revealed a weakly positive charged region, followed by a hydrophobic α-helical region. This region may serve as a leader sequence and define a unique translocation process. Experiments are in progress to engineer a truncated derivative and confirm the function of this region as a secretion signal peptide for gp144.

Acknowledgements

We thank Dr Sylvain Moineau and Denise Tremblay from the Banque de phages Félix d'Hérelle, Université Laval, Québec, Canada, for providing ϕKZ. This work was funded by the CREFSIP, by an FQRNT Infrastructure Team grant to R.C. Levesque and by an FRSQ studentship to Catherine Paradis-Bleau.

References

Benson DA, Karsch-Mizrachi I, Lipman DJ, Ostell J & Wheeler DL (2005) GenBank. *Nucleic Acids Res* 33: (Database issue): D34–D38.

Berks BC, Sargent F & Palmer T (2000) The Tat protein export pathway. *Mol Microbiol* 35: 260–274.

Biron E, Otis F, Meillon JC, Robitaille M, Lamothe J, Van Hove P, Cormier ME & Voyer N (2004) Design, synthesis, and characterization of peptide nanostructures having ion channel activity. *Bioorg Med Chem* 12: 1279–1290.

Davies JC (2002) *Pseudomonas aeruginosa* in cystic fibrosis: pathogenesis and persistence. *Paediatr Respir Rev* 3: 128–134.

Diaz E, Garcia E, Ascaso C, Mendez E, Lopez R & Garcia JL (1989) Subcellular localization of the major pneumococcal autolysin: a peculiar mechanism of secretion in *Escherichia coli*. *J Biol Chem* 264: 1238–1244.

Eddy SR (1998) Profile hidden markov models. *Bioinformatics* 14: 755–763.

Fischetti VA (2005) Bacteriophage lytic enzymes: novel antiinfectives. *Trends Microbiol* 13: 491–496.

Fortin Y, Phoenix P & Drapeau GR (1990) Mutations conferring resistance to azide in *Escherichia coli* occur primarily in the secA gene. *J Bacteriol* 172: 6607–6610.

Geer LY, Domrachev M, Lipman DJ & Bryant SH (2002) CDART: protein homology by domain architecture. *Genome Res* 12: 1619–1623.

Ginsburg I (2002) The role of bacteriolysis in the pathophysiology of inflammation, infection and post-infectious sequelae. *Apmis* 110: 753–770.

Hancock RE & Brinkman FS (2002) Function of pseudomonas porins in uptake and efflux. *Annu Rev Microbiol* 56: 17–38.

Harlow E & Lane D (1988) *Antibodies: A Laboratory Manual*, Cold Spring Harbor Laboratory, Cold Spring Harbor, NY.

Mesyanzhinov VV, Robben J, Grymonprez B, Kostyuchenko VA, Bourkaltseva MV, Sykilinda NN, Krylov VN & Volckaert G (2002) The genome of bacteriophage phiKZ of *Pseudomonas aeruginosa*. *J Mol Biol* 317: 1–19.

Miroshnikov KA, Faizullina NM, Sykilinda NN & Mesyanzhinov VV (2006) Properties of the endolytic transglycosylase encoded by gene 144 of *Pseudomonas aeruginosa* bacteriophages phiKZ. *Biochemistry (Moscow)* 71: 300–305.

MoakM&Molineux IJ (2004) Peptidoglycan hydrolytic activities associated with bacteriophage virions. *Mol Microbiol* 51: 1169–1183.

Navarre WW, Ton-That H, Faull KF & Schneewind O (1999) Multiple enzymatic activities of the murein hydrolase from staphylococcal phage ϕ11. Identification of a D-alanyl-glycine endopeptidase activity. *J Biol Chem* 274: 15847–15856.

Oliver DB & Beckwith J (1981) *E. coli* mutant pleiotropically defective in the export of secreted proteins. *Cell* 25: 765–772.

Paradis-Bleau C, Sanschagrin F & Levesque RC (2005) Peptide inhibitors of the essential cell division protein FtsA. *Protein Eng Des Sel* 18: 85–91.

Rice P, Longden I & Bleasby A (2000) EMBOSS: the European molecular biology open software suite. *Trends Genet* 16: 276–277.

Saiz JL, Lopez-Zumel C, Monterroso B, Varea J, Arrondo JL, Iloro I, Garcia JL, Laynez J & Menendez M (2002) Characterization of Ejl, the cell-wall amidase coded by the pneumococcal bacteriophage Ej-1. *Protein Sci* 11: 1788–1799.

Sambrook J, Fritsch EF & Maniatis T (1989) *Molecular Cloning: A Laboratory Manual*, Cold Spring Harbor Laboratory, Cold Spring Harbor, NY.

Sao-Jose C, Parreira R, Vieira G & Santos MA (2000) The N-terminal region of the *Oenococcus oeni* bacteriophage fOg44 lysin behaves as a bona fide signal peptide in *Escherichia coli* and as a cis-inhibitory element, preventing lytic activity on oenococcal cells. *J Bacteriol* 182: 5823–5831.

van Rossum G & de Boer J (1991) Interactively testing remote servers using the python programming language: CWI Quarterly. 4: 283–303.

Wang IN, Smith DL & Young R (2000) Holins: the protein clocks of bacteriophage infections. *Annu Rev Microbiol* 54: 799–825.

Xu M, Struck DK, Deaton J,Wang IN & Young R (2004) A signal-arrest-release sequence mediates export and control of the phage P1 endolysin. *Proc Natl Acad Sci* USA 101: 6415–6420.

Xu M, Arulandu A, Struck DK, Swanson S, Sacchettini JC & Young R (2005) Disulfide isomerization after membrane release of its SAR domain activates P1 lysosyme. *Science* 307:113–117.

Young I, Wang I & Roof WD (2000) Phages will out: strategies of host cell lysis. *Trends Microbiol* 8: 120–128.

Figure Legends

Figure 1. Gp144 peptidoglycan-degrading activity. (a) Spectrophotometric curves showing hydrolysis of purified peptidoglycan from *Escherichia coli*, *Pseudomonas aeruginosa*, *Staphylococcus aureus* and *Bacillus subtilis* by gp144 visualized as a decrease of $OD_{600\ nm}$ absorption. (b) Determination of the gp144 peptidoglycan cleavage site by LCMS. HPLC chromatogram of the gp144-digested peptidoglycan products from *P. aeruginosa*. (c) Schematic representation of the LCMS parent ion characteristics of lytic transglycosylase.

Figure 2. Expression of gp144 in *Escherichia coli* with NaN_3. (a) Bacterial growth curves of *E. coli* BL21 cultures noninduced (□) and induced for gp144-expression (■) without NaN_3; noninduced (Δ) and induced for gp144-expression (▲) with NaN_3 added at the time of induction with IPTG. (b) Time-course expression of gp144 with and without NaN_3; SDS-PAGE showing gp144 in the cell pellet and from the culture supernatants by specific detection in Western Blots using an anti-gp144 polyclonal antibody. Total cell protein

content was prepared by adding 50µL of SDS-PAGE sample buffer and boiling for 5 min. CFUs were determined to standardize the cell numbers used and for estimation of the protein concentration. Fifteen microliters of culture supernatant was analyzed directly into gels.

Figure 3. Expression of gp144 in an *Escherichia coli* $secA_{ts}$ mutant. (a) *E. coli* MM52 growth curves showing noninduced (□) and induced (■) cultures at a permissive temperature (30 °C) and noninduced (Δ) and induced (▲) cultures at a nonpermissive temperature (42 °C) using a $SecA_{ts}$ phenotype. An overnight *E. coli* MM52 (λDE3) culture incubated at 30 °C, supplemented with 50µgmL^{-1} kanamycin, was used to inoculate two 500mL Tryptic Soy Broth cultures. Cultures were adjusted to $OD_{600\ nm}$ of 0.015 and 0.15 and incubated for 1 h at 30 °C. The 0.15 $OD_{600\ nm}$ starting culture was switched to 42 °C for 4 h while the 0.015 $OD_{600\ nm}$ starting culture remained at 30 °C. Expression of gp144 was induced with 1mM of IPTG 4 h after the temperature shift at an $OD_{600\ nm}$ of 0.5. (b) Time-course expression of gp144 at permissive and nonpermissive temperatures; SDS-PAGE showing gp144 in the cell pellets and from culture supernatants. Specific detection of gp144 in culture supernatants was performed by Western Blots using an antigp144 polyclonal antibody.

Figure 4. Structural changes of gp144 interacting with anionic lipids. Circular dichroism spectra showing gp144 secondary structure alone and with DMPC or DMPG small unilamellar lipid vesicles. 50µL of each vesicle preparation was combined to 166µM of gp144 to obtain a 100 : 1 lipid gp 144^{-1} ratio before collection of the CD spectra at room temperature.

Figure 5. Permeabilization and release of fluorescence from DMPG calcein-containing vesicles. Vesicles were prepared (as described in materials and methods) and were analyzed by spectrophotometry. Spectrophotometric curves indicate specific release of fluorescent calcein from anionic DMPG vesicles when interacting with the gp144 lytic transglycosylase.

Table I. Molecular mass of the gp144-digested *P. aeruginosa* cell peptidoglycan obtained by LCMS and corresponding muropeptide structures

mz^{-1} observed	MH^+ predicted	Proposed structure
Peak 1		
119.11	N.D.	gp144 degradation product
370.23	N.D.	gp144 degradation product
Peak 2		
629.33	**629.5**	***anhydroMurNac–Ala–iGln–mDAP (-OH)**
415.2	415.46	mDAP–Ala-mDAP (-H_2O)
186.1	186.2	Ala-iGln (-CH_2-OH)
424.15	424.43	Ala-iGln-mDAP (+OH)
Peak 3		
347.17	**347.19**	***anhydroMurNac–Ala (+H)**
187.09	187.2	Ala-iGln (-CH-OH)
Peak 4		
560.26	560.6	*iGln-mDAP–Ala-mDAP (-H)
390.24	390.43	Ala-iGln-mDAP (+H)
Peak 5		
509.27	508.96	half mass
1018.47	**1017.92**	***anhydroMurNac–Ala–iGln–mDAP–Ala–mDAP–iGln**
Peak 6		
557.3	556.59	Ala–iGln–mDAP–Ala–Ala (+2H+Na)
786.36	**786.65**	**anhydroMurNac–Ala–iGln– mDAP–Ala–Ala (-2H)**
1114.47	**1114.84**	***GlcNac-O-anhydroMurNac–Ala–iGln– mDAP–Ala– mDAP (-H+Na)**
Peak 7		
672.33	671.74	iGln–mDAP-Ala-mDAP-iGln (-H_2O)
694.31	**695.41**	**GlcNac-anhydroMurNac-Ala-iGln (+H_2O)**
887.5	**887.78**	**anhydroMurNac–Ala–iGln– mDAP–Ala– mDAP (-2H)**
1344.55	**1345.15**	****GlcNac-anhydroMurNac–Ala–iGln–mDAP–Ala–mDAP–iGln–Ala–Ala (-H_2O)**

The major cell wall degradation products considered for each peak is indicated by an asterisk, the parent ion is identified by two

asterisks and the lytic transglycosylase characteristics (1,6)-anhydro *N*-acetylmuramic muropeptides are in bold. N.D., not defined.

Figure 1.

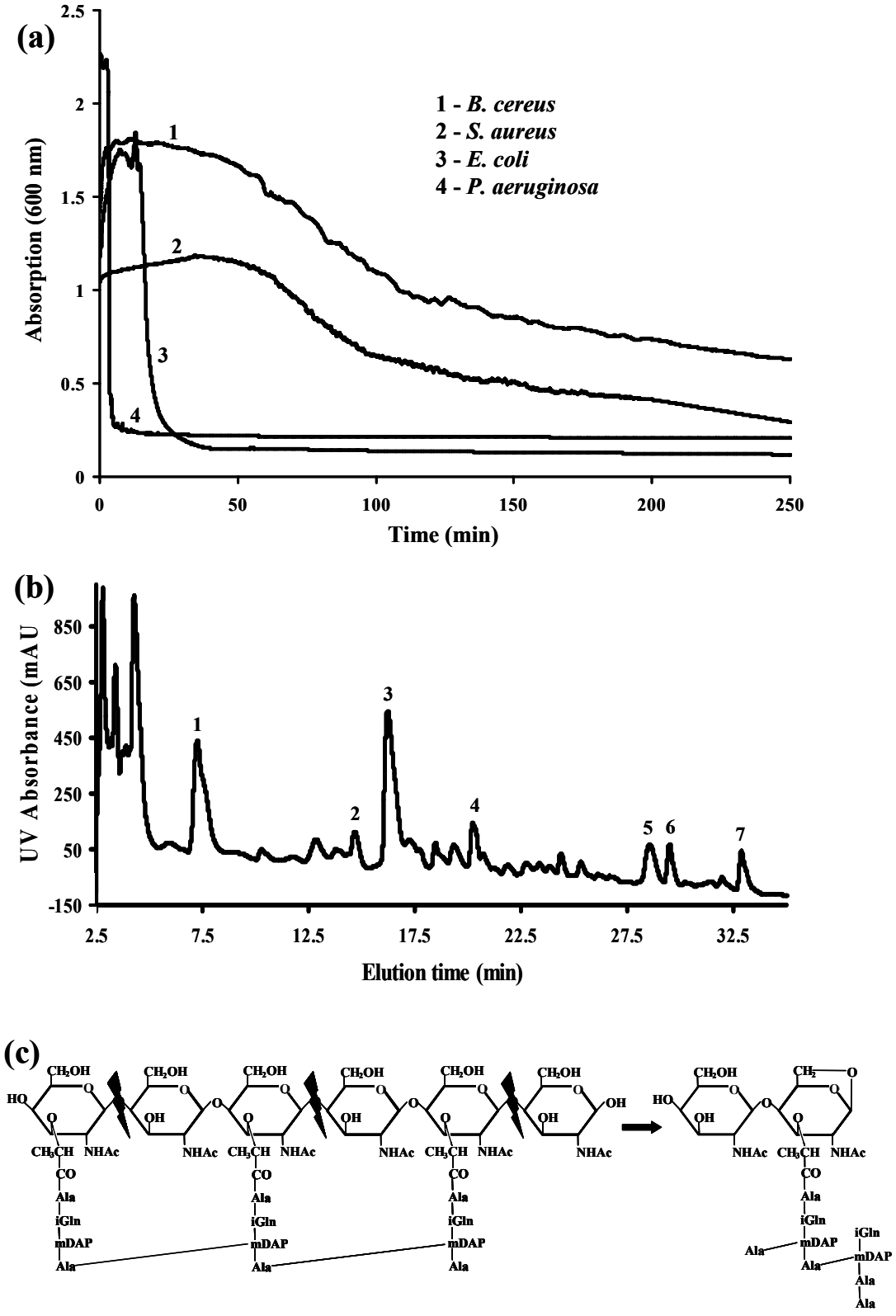
(a)
Absorption (600 nm)
Time (min)
1 - B. cereus
2 - S. aureus
3 - E. coli
4 - P. aeruginosa
(b)
UV Absorbance (mAU
Elution time (min)
(c)
CH2OH
HO
O
OH
NHAc
CH3CH
CO
Ala
iGln
mDAP
Ala

Figure 2.

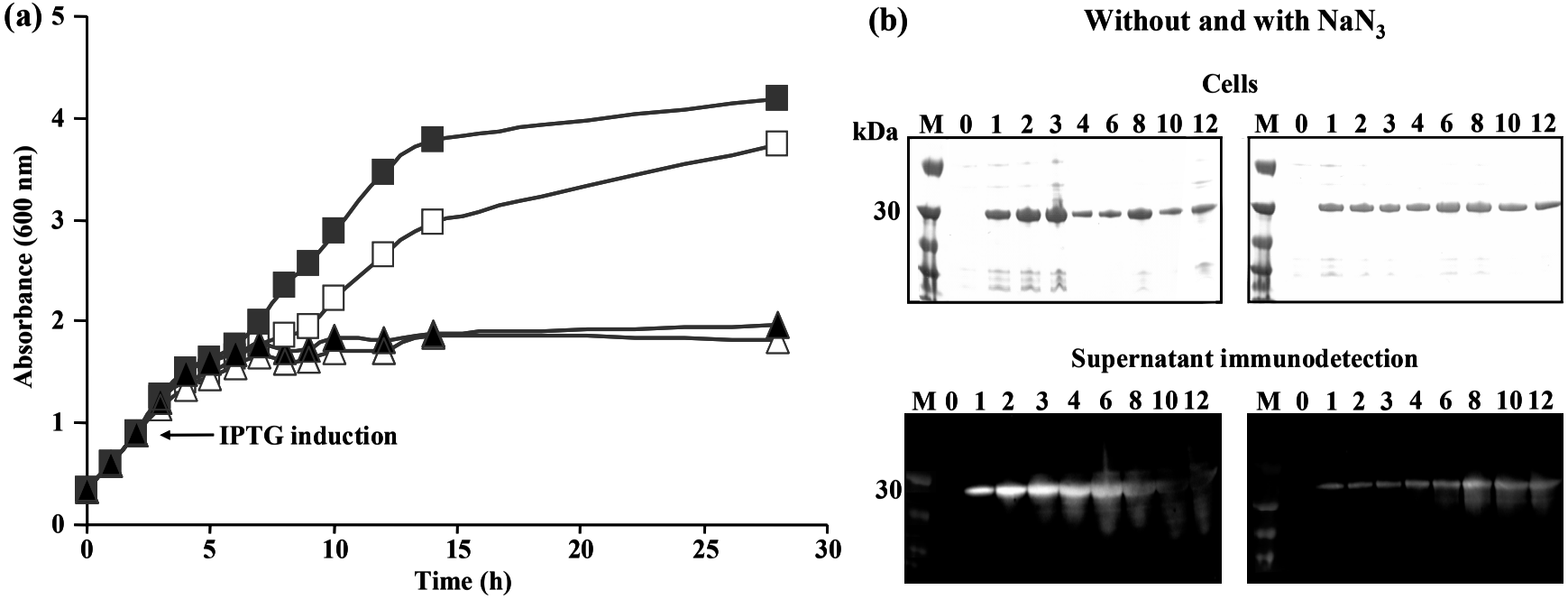
(a)
Absorbance (600 nm)
Time (h)
IPTG induction
(b)
Without and with NaN3
Cells
kDa
M 0 1 2 3 4 6 8 10 12
30
Supernatant immunodetection

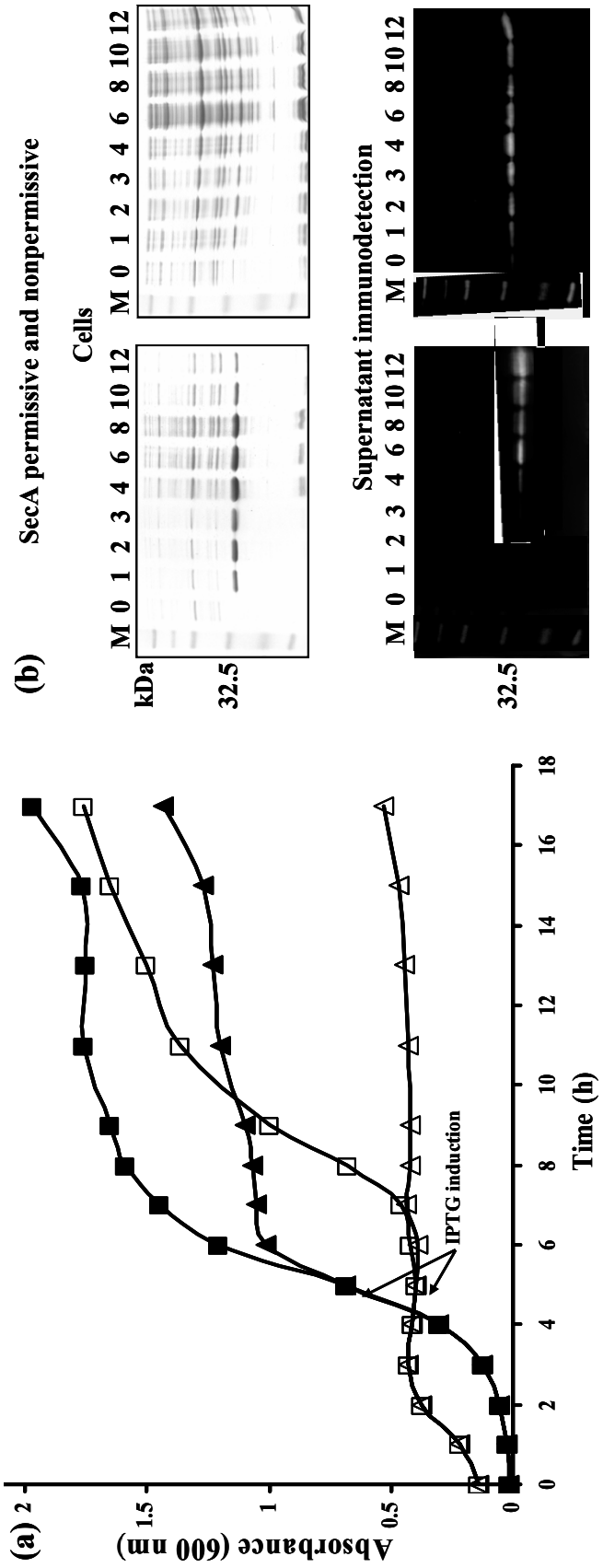
(a)
Absorbance (600 nm)
2
1.5
1
0.5
0
0
2
4
6
8
10
12
14
16
18
Time (h)
IPTG induction
(b)
SecA permissive and nonpermissive
Cells
kDa
M 0 1 2 3 4 6 8 10 12
32.5
Supernatant immunodetection
M 0 1 2 3 4 6 8 10 12
32.5

Figure 3.

Figure 4.

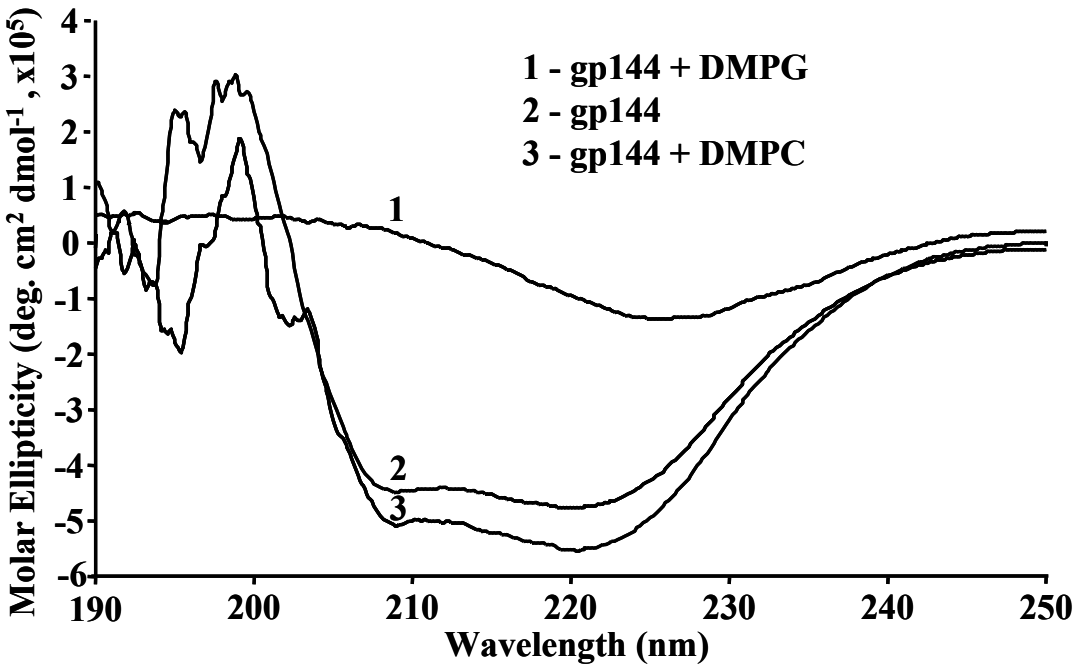
1 - gp144 + DMPG
2 - gp144
3 - gp144 + DMPC
Molar Ellipticity (deg. cm2 dmol-1, x10^5)
Wavelength (nm)
1
2
3
4
3
2
1
0
-1
-2
-3
-4
-5
-6
190
200
210
220
230
240
250

Figure 5.

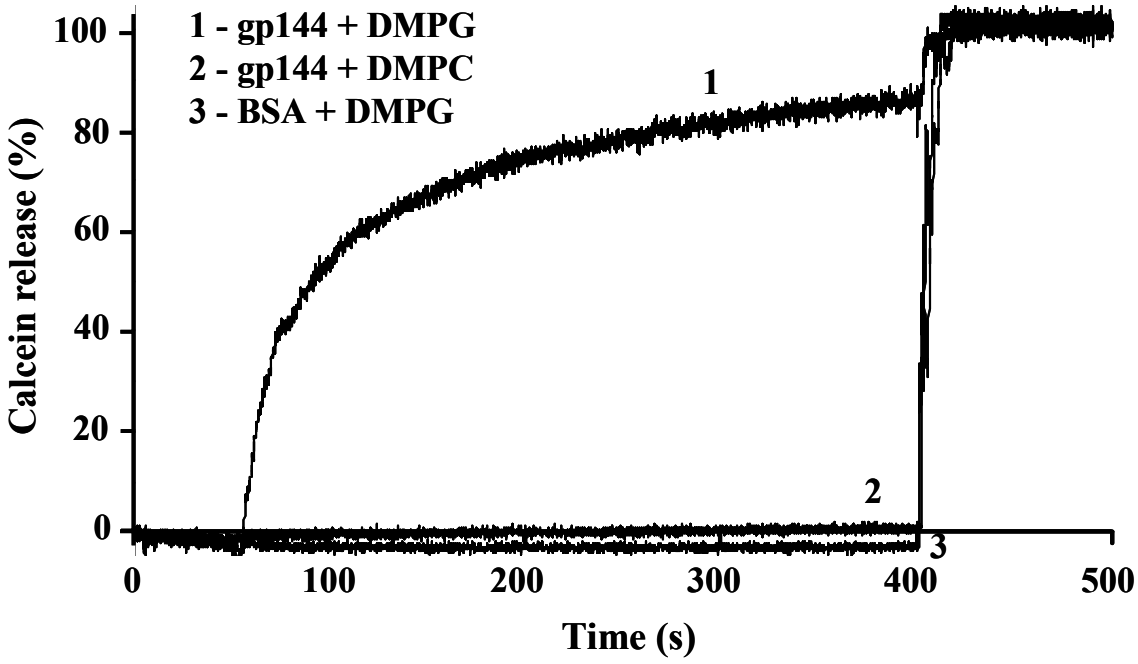
1 - gp144 + DMPG
2 - gp144 + DMPC
3 - BSA + DMPG
Calcein release (%)
Time (s)
0
20
40
60
80
100
0
100
200
300
400
500
1
2
3

Section V - Conclusion et discussion

La recrudescence des infections bactériennes combinée au développement et à la propagation des mécanismes de résistance aux antibiotiques représente une des problématiques les plus préoccupantes en santé publique (Cohen 2000; Normark and Normark 2002). En effet, la diminution de l'efficacité des traitements antibactériens met en danger la vie des personnes infectées. Ainsi, le besoin de nouvelles classes d'agents antibactériens se fait de plus en plus pressant. Les méthodes traditionnelles telles que le criblage d'antibiotiques naturels et la modification des agents antibactériens utilisés en médecine humaine ne proposent pas d'alternative durable. En fait, ces méthodes mènent inévitablement à l'identification de molécules appartenant aux classes de composés chimiques déjà sur le marché. Ainsi, ces molécules sélectionneront rapidement des mécanismes de résistance bactériens adaptés et le succès sera de trop courte durée (Desnottes 1996; Chan, Macarron et al. 2002). Le blocage des mécanismes de résistance bactériens apparaît extrêmement ardu alors que la solution se trouve plutôt du côté de la chimie combinatoire et de l'identification de nouvelles cibles antibactériennes (Hamilton-Miller 2004).

Dans le but de développer de nouvelles classes d'agents antibactériens, cette thèse de doctorat rapporte l'exploitation de la machinerie de division cellulaire, de la biosynthèse et de l'intégrité de la paroi bactérienne en tant que cibles thérapeutiques. Les cibles spécifiques abordées au cours de ce projet de recherche sont les protéines de division cellulaire FtsZ et FtsA, les amides ligases essentielles à la biosynthèse de la paroi ainsi que le peptidoglycane bactérien. Toutes ces cibles rencontrent la majorité des critères caractérisant la cible antibactérienne idéale. Ainsi, les cibles sélectionnées sont à l'origine d'une fonction biologique essentielle pour la viabilité bactérienne et l'inhibition ou la dégradation de ces cibles entraîne un phénotype létal. Les cibles à l'objet de cette étude sont génétiquement et structuralement conservées parmi les pathogènes bactériens puis elles sont exprimées en quantité suffisante lors de l'infection. De plus, aucun antibiotique utilisé en médecine humaine ne s'attaque spécifiquement à ces cibles. Ainsi, les bactéries ne devraient pas avoir développé de mécanismes de résistance envers les classes potentielles d'inhibiteurs ciblant ces constituants bactériens. Les Mur ligases et le peptidoglycane ne possèdent pas de contrepartie eucaryote mais les protéines de division cellulaire FtsZ et FtsA sont respectivement homologues à la tubuline et à l'actine

eucaryote. Cependant, l'article de revue sur la division cellulaire présenté au premier chapitre du corps de cette thèse démontre que cela ne constitue pas un inconvénient majeur. En effet, les différences structurales et fonctionnelles entre FtsZ et la tubuline et entre FtsA et l'actine peuvent être exploitées afin de développer des agents antibactériens sécuritaires et spécifiques à la cible bactérienne.

Le peptidoglycane est exposé à la surface des espèces bactériennes à Gram-positif mais son accès est restreint par la membrane externe des espèces bactériennes à Gram-négatif. Cette thèse relate plusieurs approches possibles afin de déstabiliser la membrane externe et de permettre l'accès à la paroi bactérienne constituée de peptidoglycane. De plus, l'endolysine du bactériophage ϕKZ démontre une activité muralytique très efficace contre les bactéries à Gram-négatif. Cette enzyme possède la capacité d'interagir et de déstabiliser de façon spécifique les membranes bactériennes anioniques sans interférer avec les membranes eucaryotes neutres. Cette endolysine représente ainsi un candidat fort intéressant afin de cibler le peptidoglycane des pathogènes bactériens à Gram-négatif. En ce qui concerne les pathogènes à Gram-positif, les endolysines des bactériophages correspondants dégradent leur paroi d'une façon efficace et spécifique. Tel que relaté par la revue de littérature présentée au huitième chapitre de cette thèse, le pouvoir antibactérien des endolysines de bactériophages n'est plus à démontrer. Cependant, la communauté scientifique hésite encore à approuver l'usage de ces agents antibactériens en médecine humaine. Cette thèse propose différentes avenues possibles afin d'optimiser ces enzymes pour mettre au point des stratégies antibactériennes sécuritaires et efficaces basées sur les endolysines.

Contrairement au peptidoglycane, les cibles antibactériennes FtsZ, FtsA, MurC, MurD, MurE et MurF constituent des enzymes cytoplasmiques et leur accessibilité représente la principale barrière au développement de nouvelles classes d'agents antibactériens. Cette thèse de doctorat propose de nombreuses solutions au problème d'accessibilité. D'ailleurs, la stratégie ingénieuse de synthèse organique en parallèle employée au cours de ce projet de recherche a mis au jour des inhibiteurs de FtsZ avec des propriétés antibactériennes prometteuses. Cela démontre que la barrière de l'accessibilité des cibles antibactériennes cytoplasmiques peut être franchit de façon adéquate. Les enzymes FtsZ, FtsA, MurC, MurD, MurE et MurF représentent d'excellentes cibles

thérapeutiques et il serait désolant d'abandonner les recherches sous prétexte de leur localisation cytoplasmique. En fait, de nombreux agents antibactériens reconnus en médecine humaine possèdent des cibles cytoplasmiques tel que les aminoglycosides, la tétracycline, le chloramphénicol, les macrolides, la rifampicine, les quinolones, les sulfamides et le triméthoprime (Franklin and Snow 1989; Axelsen 2002; Walsh 2003).

Cette thèse de doctorat présente donc l'identification et la caractérisation d'inhibiteurs prometteurs contre les cibles antibactériennes sélectionnées. La chimie combinatoire, la présentation phagique et le pouvoir antibactérien naturel des endolysines ont été exploités afin de mettre au jour des molécules inhibitrices de structure et de mode d'action inusités. Par conséquent, l'objectif de base de ce projet de recherche a été atteint et cette thèse de doctorat contribue de façon significative à l'avancée de la science. En effet, les cibles thérapeutiques à l'étude ont été caractérisées et des inhibiteurs efficaces et spécifiques ont été identifiés. Ainsi, cette thèse relate l'identification des premiers inhibiteurs de FtsA et des premiers inhibiteurs peptidiques de MurD, MurE et MurF. Le développement de nouvelles classes d'agents antibactériens représente un défi de taille et constitue un processus laborieux de longue haleine. Les résultats de ce projet de recherche de doctorat représentent donc une première étape et beaucoup reste à faire afin d'optimiser les inhibiteurs présentés.

Bibliographie

Acar, J. and P. Courvalin. (1998). "La fin de l'âge d'or des antibiotiques." La Recherche **314**: 50-2.

Axelsen, P. H. (2002). Essentials of antimicrobial pharmacology : a guide to fundamentals for practice. Totowa, NJ, Humana Press.

Bloom, B. R. and C. J. Murray (1992). "Tuberculosis: commentary on a reemergent killer." Science **257**(5073): 1055-64.

Breithaupt, H. (1999). "The new antibiotics." Nat Biotechnol **17**(12): 1165-9.

Brown, E. D. and G. D. Wright (2005). "New targets and screening approaches in antimicrobial drug discovery." Chem Rev **105**(2): 759-74.

Chan, P. F., R. Macarron, et al. (2002). "Novel antibacterials: a genomics approach to drug discovery." Curr Drug Targets Infect Disord **2**(4): 291-308.

Christensen, D. J., E. B. Gottlin, et al. (2001). "Phage display for target-based antibacterial drug discovery." Drug Discov Today **6**(14): 721-27.

Cohen, M. L. (2000). "Changing patterns of infectious disease." Nature **406**(6797): 762-7.

Cunha, B. A. (2001). "Effective antibiotic-resistance control strategies." Lancet **357**(9265): 1307-8.

Davies, J. C. (2002). "*Pseudomonas aeruginosa* in cystic fibrosis: pathogenesis and persistence." Paediatr Respir Rev **3**(2): 128-34.

Desnottes, J. F. (1996). "New targets and strategies for the development of antibacterial agents." Trends Biotechnol **14**(4): 134-40.

Fauci, A. S. (2001). "Infectious diseases: considerations for the 21st century." Clin Infect Dis **32**(5): 675-85.

Franklin, T. J. and G. A. Snow (1989). Biochemistry of antimicrobial action. London ; New York, Chapman and Hall.

Goldberg, J. B. and G. B. Pier (2000). "The role of the CFTR in susceptibility to *Pseudomonas aeruginosa* infections in cystic fibrosis." Trends Microbiol **8**(11): 514-20.

Hamilton-Miller, J. M. (2004). "Antibiotic resistance from two perspectives: man and microbe." Int J Antimicrob Agents **23**(3): 209-12.

Hancock, R. E. and F. S. Brinkman (2002). "Function of pseudomonas porins in uptake and efflux." Annu Rev Microbiol **56**: 17-38.

Harbarth, S. and M. H. Samore (2005). "Antimicrobial resistance determinants and future control." Emerg Infect Dis **11**(6): 794-801.

Haselbeck, R., D. Wall, et al. (2002). "Comprehensive essential gene identification as a platform for novel anti-infective drug discovery." Curr Pharm Des **8**(13): 1155-72.

Hoess, R. H. (2001). "Protein design and phage display." Chem Rev **101**(10): 3205-18.

Hughes, D. (2003). "Microbial genetics: exploiting genomics, genetics and chemistry to combat antibiotic resistance." Nat Rev Genet **4**(6): 432-41.

Kaplan, J. E., K. Sepkowitz, et al. (2001). "Opportunistic infections in persons with HIV or other immunocompromising conditions." Emerg Infect Dis **7**(3 Suppl): 541.

Kay, B. K., J. Kasanov, et al. (2001). "Screening phage-displayed combinatorial peptide libraries." Methods **24**(3): 240-6.

Levy, S. B. and B. Marshall (2004). "Antibacterial resistance worldwide: causes, challenges and responses." Nat Med **10**(12 Suppl): S122-9.

May, T. B., D. Shinabarger, et al. (1991). "Alginate synthesis by *Pseudomonas aeruginosa*: a key pathogenic factor in chronic pulmonary infections of cystic fibrosis patients." Clin Microbiol Rev **4**(2): 191-206.

McDermott, P. F., R. D. Walker, et al. (2003). "Antimicrobials: modes of action and mechanisms of resistance." Int J Toxicol **22**(2): 135-43.

Meyer, A. L. (2005). "Prospects and challenges of developing new agents for tough Gram-negatives." Curr Opin Pharmacol **5**(5): 490-4.

Miesel, L., J. Greene, et al. (2003). "Genetic strategies for antibacterial drug discovery." Nat Rev Genet **4**(6): 442-56.

Normark, B. H. and S. Normark (2002). "Evolution and spread of antibiotic resistance." J Intern Med **252**(2): 91-106.

Peczuh, M. W. and A. D. Hamilton (2000). "Peptide and protein recognition by designed molecules." Chem Rev **100**(7): 2479-94.

Prentice, T., Ed. (2000). Rapport sur la santé dans le monde. Genève, Organisation mondiale de la santé.

Projan, S. J. (2002). "New (and not so new) antibacterial targets - from where and when will the novel drugs come?" Curr Opin Pharmacol **2**(5): 513-22.

Rice, L. B. (2006). "Antimicrobial resistance in gram-positive bacteria." Am J Infect Control **34**(5 Suppl): S11-9.

Salyers, A. A. and D. D. Whitt (2002). Bacterial pathogenesis : a molecular approach. Washington, D.C., ASM Press.

Sidhu, S. S. (2000). "Phage display in pharmaceutical biotechnology." Curr Opin Biotechnol **11**(6): 610-6.

Stover, C. K., X. Q. Pham, et al. (2000). "Complete genome sequence of *Pseudomonas aeruginosa* PA01, an opportunistic pathogen." Nature **406**(6799): 959-64.

Tenover, F. C. (2006). "Mechanisms of antimicrobial resistance in bacteria." Am J Infect Control **34**(5 Suppl): S3-S10.

Walsh, C. (2003). Antibiotics : actions, origins, resistance. Washington, D.C., ASM Press.

Annexe A - Identification of *Pseudomonas aeruginosa* FtsZ peptide inhibitors as a tool for development of novel antimicrobials

Publication d'un article scientifique sur l'identification de peptides inhibiteurs de l'enzyme FtsZ par présentation phagique. Cet article a été publié en anglais dans la revue scientifique «Journal of Antibacterial Chemotherapy» en mai 2004 suite à mes travaux de maîtrise portant sur le développement d'inhibiteurs de la division cellulaire bactérienne.

Résumé

Identification d'inhibiteurs peptidiques contre la protéine de division cellulaire FtsZ de *Pseudomonas aeruginosa* en tant qu'outil pour le développement de nouveaux agents antibactériens

L'ère révolutionnaire des antibiotiques est aujourd'hui dépassée par la capacité évolutive des microorganismes à développer des mécanismes de résistance. Dans le but d'identifier de nouveaux agents antimicrobiens, nous utilisons la machinerie de division cellulaire bactérienne en tant que cible. Nous étudions plus particulièrement la protéine essentielle FtsZ de *P. aeruginosa*. FtsZ est la protéine de division cellulaire la plus importante et la plus conservée. Le gène *ftsZ* a tout d'abord été cloné et la protéine a été purifiée par chromatographie d'affinité. Le séquençage en N-terminal a confirmé l'identité de FtsZ et un essai de chromatographie sur couche mince a confirmé l'activité GTPase de FtsZ. L'enzyme purifiée a été utilisée pour identifier des peptides inhibiteurs avec la technique de présentation phagique. Les phages possédant une affinité spécifique pour FtsZ ont été élués selon quatre conditions spécifiques; la glycine à pH acide, le GTP, un analogue non-hydrolysable du GTP et avec FtsA. Nous avons identifié trois consensus peptidiques contre FtsZ. Ces trois consensus peptidiques ont été synthétisés et testés sur l'activité GTPase de FtsZ. Les deux peptides C7C inhibent l'activité enzymatique de FtsZ avec des valeurs de CI_{50} de 0.45 mM et 1.2 mM alors que le peptide 12 mers démontre une CI_{50} de 5 mM. Ainsi, la technique de présentation phagique a permis la découverte de peptides inhibiteurs prometteurs et le peptidomimétisme devrait permettre le développement d'une nouvelle classe d'agents antimicrobiens.

Contribution des auteurs

Trois auteurs signent la réalisation de cet article scientifique. En tant que première auteure, j'ai réalisé l'ensemble des expériences décrites, j'ai analysé les résultats et j'ai rédigé le manuscrit. Dr François Sanschagrin m'a guidée et supportée quotidiennement au laboratoire. Sa logique scientifique et ses vastes connaissances se reflètent tout au long du manuscrit. Le Dr Roger C. Levesque est à l'origine de l'idée de départ et de la conceptualisation du projet de recherche à la base de cet article. Ce projet consiste à cibler les protéines bactériennes essentielles à la division cellulaire afin de développer une classe innovatrice d'agents antibactériens. Le Dr Levesque a judicieusement sélectionné la méthodologie et cela m'a permis de mener à bien le projet. De plus, il a contribué à la réalisation du projet en élaborant un échéancier scientifique réalisable, en orientant le projet semaine après semaine et en me fournissant un environnement de travail propice à la réussite.

Identification of *Pseudomonas aeruginosa* FtsZ peptide inhibitors as a tool for development of novel antimicrobials

Catherine Paradis-Bleau[1], François Sanschagrin[1] and Roger C. Levesque[1*]

[1]*Centre de recherche sur la fonction, structure et ingénierie des protéines, Faculté de médecine, pavillon Charles-Eugène-Marchand, Université Laval, Sainte-Foy, Québec, Canada G1K 7P4*

Keywords: bacterial cell division, phage display, FtsA

*Corresponding author. Tel: (1) 418-656-3070; Fax: (1) 418-656-7176; E-mail: rclevesq@rsvs.ulaval.ca

Sir,

The alarming increase and spread of antibiotic resistance among bacterial pathogens is one of the most serious public health problems of the last decade.[1] This critical situation necessitates the design of novel classes of antibacterial agents having new mechanisms of action against novel targets. We selected the essential and highly conserved FtsZ protein from the cell division machinery of *Pseudomonas aeruginosa* as the most attractive target. FtsZ is at the top of hierarchic recruitment in the divisosome, its polymerization into the Z-ring coupled with GTPase activity and interactions with FtsA allow the physical separation of daughter cells.[2]

To identify specific inhibitors, we used the phage-display technique for the selection of short peptide ligands having high binding affinities to FtsZ among a large pool of random peptide permutations.[3]

The *P. aeruginosa* FtsZ and FtsA proteins fused with a His-tag at their C terminus were expressed in *Escherichia coli* under the control of the T7 promoter and purified to homogeneity on an affinity nickel column (Novagen) and by the renaturation of purified inclusion bodies for FtsA (Protein Refolding Kit, Novagen, Madison, USA). N-terminal sequencing confirmed the identity of both proteins. The GTPase activity of FtsZ and the ATPase activity of FtsA were measured using a thin layer chromatography (TLC) assay with ^{32}P-labelled nucleotides (Perkin-Elmer) as substrates. A UV cross-link specific nucleotide binding assay confirmed that FtsZ binds preferentially GTP and that FtsA binds preferentially ATP.

Purified FtsZ was used to screen for GTPase peptide inhibitors by phage-display using the PH.D.-12 and PH.D.-C-7-C phage libraries (New England Biolabs) containing ~ 2.7 x 10^9 12-mer and ~3.7 x 10^9 C-7-C-mer random peptide sequences, respectively. The specificity of the three rounds of biopanning was raised by increasing the stringency of the washes and by decreasing the time of contact between the phage encoding peptide fusions and FtsZ. Phages encoding peptides having specific affinity with FtsZ were eluted by non-specific disruption using glycine and by competitive elutions using nucleotide substrate GTP, non-hydrolysable substrate analogue 5'-guanylylimidodiphosphate and FtsA. This unique biopanning identified two C-7-C mers and one 12-mer consensus peptide sequences

against FtsZ, reported here as FtsZp1 (CSYEKRPMC), FtsZp2 (CLTKSYTSC) and FtsZp3 (GAVTYSRISGQY).

These three peptides were synthesized and their inhibitory capacities of the GTPase activity of FtsZ were evaluated by calculating the percentage of residual enzyme activity. Various concentrations of peptide buffered solutions were pre-incubated with 12 μM of FtsZ in reaction buffer (50 mM Bis-Tris propane pH 7.4, 10 mM $MgCl_2$) for 20 min at room temperature. [^{32}P]GTP was added and mixtures were immediately incubated for 1 h at 37°C. The enzyme reaction was visualized using 2 μL of each reaction sample separated by TLC along with positive (FtsZ alone) and negative (without FtsZ) controls. The percentage of hydrolysis of radioactive substrate was measured by autoradiography. The values of 50% inhibitory concentration (IC_{50}s) for peptides were obtained by plotting the percentage of residual enzymic activity as a function of increasing peptide concentrations (Figure 1).

When compared to BSA protein in a competitive assay and to random peptides, the three consensus peptides were able to specifically inhibit the FtsZ GTPase activity. The C-7-C-mers FtsZp1 and FtsZp2 gave an IC_{50} of 0.45 mM and 1.2 mM whereas the 12-mer gave an IC_{50} of 5 mM (Figure 1). The three-dimensional crystal structure of FtsZ showed a compact and globular protein.[4] We hypothesized that the C-7-C-mer peptides would have more affinity for FtsZ than the 12-mers. The reducing agent dithiothreitol (DTT) had no effect on the inhibitory capacity of the 12-mer peptide FtsZp3. In contrast, DTT reduced significantly the inhibitory potential of the two C-7-C peptides. These results indicated that the disulphide bond formed by the two cysteines of the C-7-C peptides and the subsequent loop conformation were important for their inhibitory potential.

Cell division proteins have rarely been used as target proteins and the sole small molecule viriditoxin that inhibits FtsZ was discovered during the course of this work.[5]

This study allowed the identification of three peptides inhibiting the GTPase activity of the essential cell division protein FtsZ. In perspective, it will be useful to determine their inhibitory constant (K_i) values and to analyse their inhibitory capacities on other GTPases so as to define their specificity. In order to obtain promising lead compounds, inhibitory peptides will undergo chemical modifications and their sequences will constitute the core for the synthesis of libraries of peptidomimetic molecules.[6]

Acknowledgements

We thank Le Service de séquence de peptides de l'Est du Québec and Le Service d'analyse et de synthèse d'acides nucléiques de l'Université Laval. This work was funded by The Canadian Bacterial Diseases Network via the Canadian Centers of Excellence and a FCAR infrastructure team grant to R. C. Levesque and a CRSNG studentship to C. Paradis-Bleau.

References

1. Normark, B. H. & Normark, S. (2002). Evolution and spread of antibiotic resistance. *Journal of Internal Medicine* **252**, 91–106.

2. Lutkenhaus, J. & Addinall, S. G. (1997). Bacterial cell division and the Z ring. *Annual Review of Biochemistry* **66**, 93–116.

3. Christensen, D. J., Gottlin, E. B., Benson, R. E. et al. (2001). Phage display for target-based antibacterial drug discovery. *Drug Discovery Today* **6**, 721–7.

4. Lowe, J. & Amos, L. A. (1998). Crystal structure of the bacterial cell-division protein FtsZ. *Nature* **391**, 203–6.

5. Wang, J., Galgoci, A., Kodali, S. et al. (2003). Discovery of a small molecule that inhibits cell division by blocking FtsZ, a novel therapeutic target of antibiotics. *Journal of Biological Chemistry* **278**, 44424–8.

6. Nefzi, A., Dooley, C., Ostresh, J. M. et al. (1998). Combinatorial chemistry: from peptides and peptidomimetics to small organic and heterocyclic compounds. *Bioorganic and Medicinal Chemistry Letters* **8**, 2273–8.

Figure legend

Figure 1. IC_{50} determinations for the phage-display-derived peptide inhibitors of FtsZ GTPase. The residual enzymic activity was measured as a function of the concentration of the C-7-C peptides (a) FtsZp1, (b) FtsZp2 and (c) the 12-mer FtsZp3. The peptide sequences are given in the text.

Figure 1

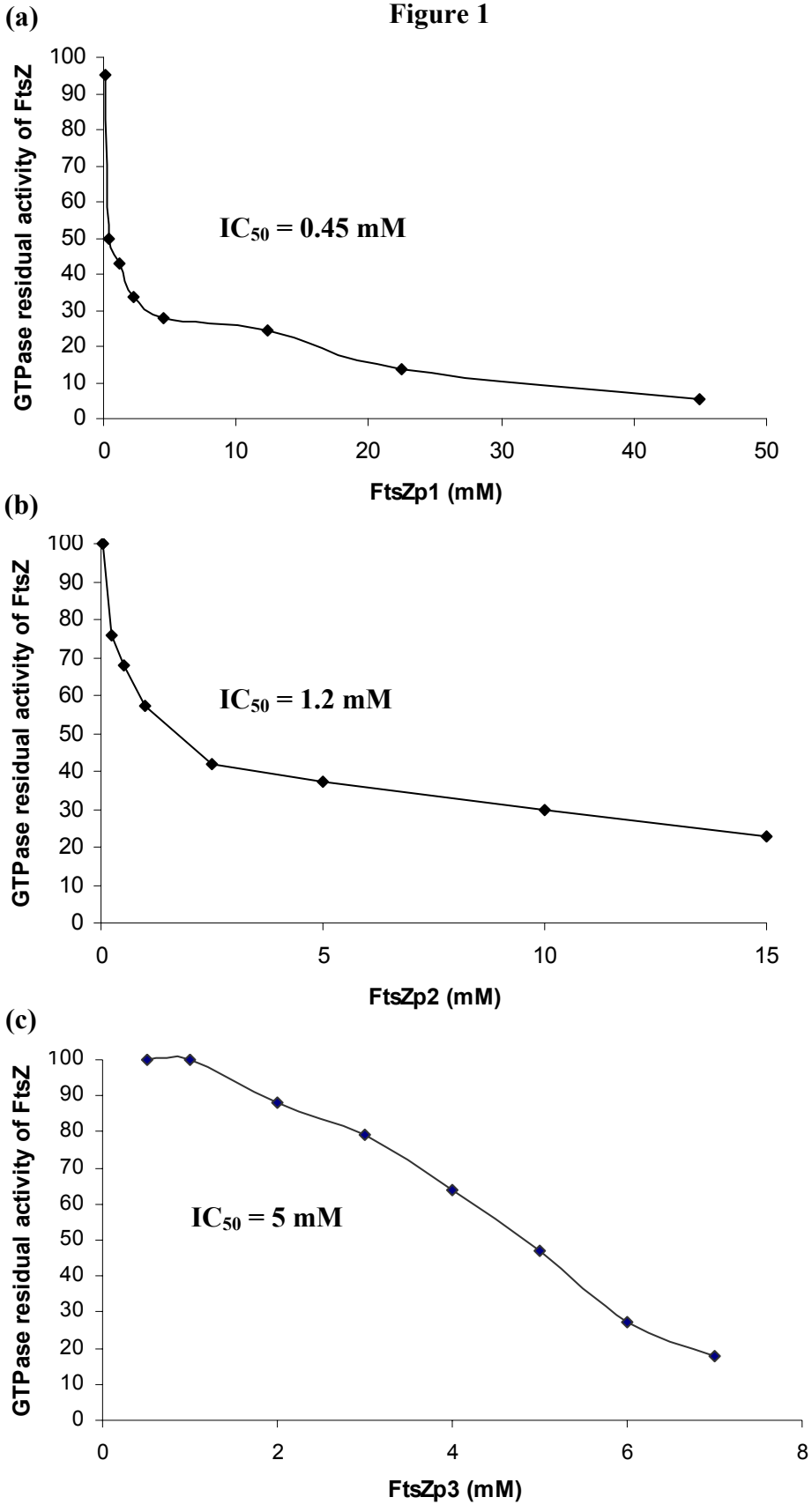
(a)
GTPase residual activity of FtsZ
IC50 = 0.45 mM
FtsZp1 (mM)
(b)
GTPase residual activity of FtsZ
IC50 = 1.2 mM
FtsZp2 (mM)
(c)
GTPase residual activity of FtsZ
IC50 = 5 mM
FtsZp3 (mM)

Annexe B - Bifunctional Activities of the phiKZ Bacteriophage Endolysin

Présentation orale en tant qu'étudiante chercheure invitée lors du "105th Annual Meeting of the American Society for Microbiology", Atlanta, Georgia, USA; le 7 juin 2005. Le résumé de cette conférence a été publié dans le American Society for Microbiology 105th General Meeting Abstracts session 076 no. M-013. Le sujet de cette présentation orale a également fait office d'une présentation par affiche lors de ce même congrès.

Présentation orale :

Paradis-Bleau C.

Bifunctional Activities of the phiKZ Bacteriophage Endolysin.

Résumé publié et presentation par affiche:

Paradis-Bleau C., Cloutier I., Lemieux L., Sanschagrin F., Auger F., Garnier A. and Levesque R.C.

Bifunctional Activities of the phiKZ Bacteriophage Endolysin.

Background: Double stranded DNA phages use the holin-endolysin mechanism to promote the host cell lysis and the consequent release of progeny phages. The peptidoglycan degrading endolysin is restricted to the bacterial cytoplasm until the holin destabilises the internal membrane to optimise the timing of the lysis with the phage cycle. Since no holin gene or homologue was detected in the *P. aeruginosa* phage ϕKZ 280 Kb genome, we hypothesized that the ϕKZ endolysin encoded by the ORF144 may represent a bifunctional lysis protein having an holin and endolysin function. **Methods:** The endolysin gene was cloned into the pET24b vector and the 29.6 Kda overexpressed protein was purified by FPLC on a nickel affinity chromatography and gel filtration columns. The ϕKZ endolysin peptidoglycan hydrolytic activity was determined in a spectrophotometric assay

using purified murein from *P. aeruginosa, E. coli, S. aureus and B. subtilis*. The peptidoglycan cleavage site was identified by analysis of the degradation products with LCMS. To evaluate endolysin membrane interactions, we analyse the conformational change of the enzyme by circular dichroism. **Results:** Overexpression of the ϕKZ endolysin lead to a loss of viability of *E. coli* expressing cells and permitted the purification of 200 mg/L of active enzyme. Studies using purified enzyme showed that the monomeric endolysin oligomerises in multimeric forms. The spectrophotometric assay confirmed that the ϕKZ endolysin hydrolysed the murein of both Gram-negative and Gram-positive bacterias. LCMS analysis identified the enzyme cleavage site at the L-alanine–N-acetylmuramyl; the ϕKZ endolysin is thus an amidase. Circular dichroism experiments showed that the endolysin secondary conformation is significantly destabilised by anionic lipid formed membranes in comparison with zwitterionic lipids. **Conclusion:** We conclude that the ϕKZ endolysin has an holin activity along with an amidase hydrolytic function. Our model suggested that the enzyme oligomerises and interacts with anionic lipids that mimic bacterial membranes in an holin-like structure promoting the amidase peptidoglycan hydrolysis.

Annexe C - Caractérisation de l'endolysine du bactériophage ϕKZ: un nouvel agent antibactérien pour la thérapie phagique

Présentation orale en tant qu'étudiante chercheure invitée lors de la 7ième Journée annuelle de la Recherche de la Faculté de médecine de l'Université Laval, Québec, Québec, Canada; le 25 mai 2005. Le résumé de cette conférence a été publié dans le Programme de la 7ième Journée annuelle de la Recherche de la Faculté de médecine de l'Université Laval à la page 53.

Présentation orale :

Paradis-Bleau, C.

Caractérisation de l'endolysine du bactériophage ϕKZ: un nouvel agent antibactérien pour la thérapie phagique.

Résumé publié :

Paradis-Bleau C., Cloutier I., Lemieux L., Sanschagrin F., Auger F., Garnier A. et Levesque R.C.

Caractérisation de l'endolysine du bactériophage ϕKZ: un nouvel agent antibactérien pour la thérapie phagique.

OBJECTIFS: Afin d'identifier de nouveaux antibactériens, nous exploitons les bactériophages représentant une source hautement évoluée de protéines lytiques. Les phages à ADNdb causent la lyse bactérienne à l'aide d'une holine qui déstabilise la membrane interne et d'une endolysine hydrolysant le peptidoglycane. Nous avons caractérisé l'endolysine du phage ϕKZ de *Pseudomonas aeruginosa* entraînant la lyse sans holine. MÉTHODES: L'endolysine a été purifiée suite à sa surexpression dans *E. coli* puis

son activité hydrolytique a été démontrée par spectrophotométrie et LCMS avec du peptidoglycane bactérien purifié. L'interaction de l'endolysine avec les membranes a été caractérisée par dichroïsme circulaire et par fluorescence avec des vésicules de calcéine. RÉSULTATS: L'expression de l'endolysine entraîne une perte de viabilité des cellules bactériennes qui relargent la protéine dans le surnageant. La visualisation de la protéine purifiée démontre qu'elle oligomérise en formant des ponts disulfures. Les résultats confirment que l'endolysine hydrolyse le peptidoglycane des bactéries à Gram-négatif et à Gram-positif en coupant le lien entre les sucres acide N-acetylmuramique et N-acétylglucosamine telle une transglycosidase lytique. Le dichroïsme circulaire et les essais en fluorescence indiquent la déstabilisation des membranes bactériennes. CONCLUSION: Notre modèle suggère que l'endolysine oligomerise afin de déstabiliser les membranes bactériennes et d'accéder au peptidoglycane en permettant l'hydrolyse et la lyse bactérienne. Cette enzyme bifonctionnelle holine-endolysine s'avère intéressante en tant que potentiel agent antibactérien.

Annexe D - *Pseudomonas* ϕKZ Phage Endolysin: a Novel Tool for Phage Therapy

Présentation orale en tant qu'étudiante chercheure invitée au 5ième Symposium Annuel du CREFSIP (Centre de Recherche sur la Structure et la Fonction des Protéines) à l'Université Laval, Québec, Québec, Canada; le 20 mai 2005. Le résumé de cette conférence a été publié dans le Programme du 5ième Symposium Annuel du CREFSIP à la page xii.

Présentation orale :

Paradis-Bleau C.

***Pseudomonas* ϕKZ Phage Endolysin: a Novel Tool for Phage Therapy.**

Résumé publié :

Paradis-Bleau C., Cloutier I., Lemieux L., Sanschagrin F., Auger F., Garnier A. et Levesque R.C.

Caractérisation du mécanisme lytique bifonctionnel de l'endolysine du bactériophage ϕKZ en tant que nouvel agent antibactérien.

La thérapie par les phages regagne l'intérêt de la communauté scientifique en cette ère de dissémination des mécanismes de résistance aux antibiotiques parmi les pathogènes bactériens en émergence. Les phages à ADN double brin (db) ou ARNdb terminent habituellement leur cycle réplicatif en entraînant la lyse bactérienne à l'aide de deux protéines; une holine et une endolysine permettant le relargage des virions infectieux. La régulation temporelle de la lyse est assurée par la holine qui s'accumule au niveau de la membrane bactérienne interne tandis que l'endolysine muralytique demeure confinée au cytoplasme. Au moment opportun, les molécules de holine oligomérisent afin de perméabiliser la membrane interne et de libérer l'endolysine cytoplasmique. Cette protéine de type lysosyme dégrade alors le peptidoglycane dont la résultante est la lyse bactérienne. Cependant, le bactériophage ϕKZ de *Pseudomonas aeruginosa* possédant un génome à

ADNdb de 280 334 pbs entièrement séquencé n'encode pas de holine. L'hypothèse proposée suggère que l'endolysine du phage ϕKZ représente la première protéine de lyse bifonctionnelle ayant une activité intrinsèque holine- endolysine. Le gène de l'endolysine a d'abord été amplifié par PCR et cloné en fusion avec une étiquette histidine dans un vecteur d'expression pET. Selon des conditions d'expression optimales chez *Escherichia coli*, l'endolysine a été purifiée par chromatographie d'affinité au nickel et tamissage moléculaire. L'activité muralytique a été quantifiée par un essai spectrophotométrique en utilisant du peptidoglycane bactérien purifié de *P. aeruginosa, E. coli, Staphylococcus aureus* et *Bacillus subtilis* comme substrat. Le site de clivage de l'endolysine a été identifié en analysant les produits de dégradation du peptidoglycane hydrolysé purifiés par spectrométrie de masse. L'implication du système de sécrétion bactérien Sec a été étudiée à l'aide d'un mutant *E. coli* SecA thermosensible à 42°C et des essais d'inhibition de la sécrétion d'endolysine à l'azide de sodium. L'interaction de l'endolysine avec les membranes synthétiques reconstituées a été caractérisée par le dichroïsme circulaire et par la fluorescence en construisant des vésicules de calcéine. L'expression de l'endolysine entraîne une perte de viabilité des cellules bactériennes qui relargent la protéine dans le surnageant en permettant la purification de 200 mg/L d'endolysine active. L'identité de la protéine a été confirmée par séquençage en N-terminal et la visualisation de la protéine purifiée démontre qu'elle oligomérise en formant spontanément des ponts disulfures en absence d'agent réducteur. Les résultats confirment que l'endolysine hydrolyse le peptidoglycane des bactéries à Gram-négatif et à Gram-positif en coupant le lien entre les sucres acide N-acetylmuramique et N-acétylglucosamine telle une transglycosidase lytique. Les essais d'inhibition à l'azide de sodium et l'expression de l'endolysine dans le mutant SecA démontrent que l'endolysine n'emprunte pas le système de sécrétion Sec afin d'accéder au peptidoglycane. Le dichroïsme circulaire et les essais en fluorescence indiquent la déstabilisation des membranes bactériennes. Nous concluons que l'endolysine du phage ϕKZ agit comme une holine en oligomerisant et en déstabilisant les membranes bactériennes afin d'accéder au peptidoglycane en permettant l'hydrolyse et la lyse bactérienne. Cette enzyme bifonctionnelle holine-endolysine s'avère intéressante en tant que potentiel agent antibactérien en thérapie par les phages.

Annexe E - Peptides inhibiteurs des enzymes MurE et MurF essentielles à la biosynthèse de la paroi bactérienne

Présentation par affiche lors du 6ième Symposium Annuel du CREFSIP à l'Université Laval, Québec, Québec, Canada; le 25 mai 2006. Le résumé de cette présentation a été publié dans Programme du 6ième Symposium Annuel du CREFSIP page 35, affiche no. 18

Paradis-Bleau C., Lloyd A., Sanschagrin F., Bugg. T.D.H. et Levesque R.C.

Peptides inhibiteurs des enzymes MurE et MurF essentielles à la biosynthèse de la paroi bactérienne.

La dissémination des mécanismes de résistance aux antibiotiques parmi les pathogènes bactériens en émergence représente une des problématiques les plus préoccupantes en santé publique. L'objectif de notre projet vise à identifier des agents antibactériens innovateurs contre la biosynthèse de la paroi bactérienne constituée de peptidoglycane. Nous avons sélectionné les enzymes MurE et MurF essentielles à la biosynthèse du peptidoglycane en tant que cibles antibactériennes. L'enzyme MurE catalyse la formation d'un lien amide entre l'acide meso-diaminopimélique (meso-A2pm) et le précurseur de peptidoglycane UDP-N-acetylmuramyle-L-alanyle-D-glutamate (UDP-MurNac-Ala-Glu). Par la suite, l'enzyme MurF catalyse la formation d'un lien amide entre le D-Alanine-D-Alanine (D-Ala-D-Ala) et le produit de la réaction de MurE: l'UDP-N-acetylmuramyle-L-alanyle-D-glutamyle-meso-diaminopimélate (UDP-MurNac-Ala-Glu-meso-A2pm). Les amides ligases MurE et MurF hydrolysent de l'ATP en ADP et phosphate inorganique au cours de leur réaction enzymatique.

Nous avons cloné, surexprimé et purifié les enzymes MurE et Mur F du pathogène *Pseudomonas aeruginosa*. Cette bactérie à Gram négatif est hautement résistante à la majorité des classes d'antibiotiques et elle représente l'une des principales causes

d'infections nosocomiales chroniques. Les protéines MurE et MurF biologiquement actives ont été utilisées pour cribler des banques contenant 10^9 peptides différents par présentation phagique (phage display). La spécificité du criblage a été maximisée en effectuant 3 rondes de biocriblage et en optimisant le contact peptide-enzyme via les paramètres de temps et de lavage. Les phages adhérés ont été élués avec de la glycine à pH acide et de façon compétitive avec l'ATP et le meso-A2pm ou le D-Ala-D-Ala. Pour chaque protéine ciblée, le consensus peptidique prédominant a été synthétisé et son potentiel inhibiteur a été évalué sur l'activité enzymatique de MurE et MurF. Le peptide MurEp1 inhibe l'activité de MurE avec une CI_{50} de 500 µM, un K_i de 160 µM contre le meso-A2pm et un K_i de 77 µM contre le UDP-MurNac-Ala-Glu. Les résultats indiquent que le peptide MurEp1 bloque la réaction enzymatique de MurE en inhibant la formation du lien amide entre le meso-A2pm et l'UDP-MurNac-Ala-Glu. Le peptide consensus MurFp1 inhibe l'activité de MurF avec une CI_{50} de 250 µM et un K_i de 600 µM contre le D-Ala-D-Ala lorsque la protéine MurF est préincubée avec son substrat UDP-MurNac-Ala-Glu-meso-A2pm. Ce peptide inhibe la liaison du substrat D-Ala-D-Ala au site actif de MurF. L'inhibition des enzymes MurE et MurF est d'un intérêt majeur car elle mène à un phénotype létal permettant d'envisager la production de nouveaux antimicrobiens par peptidomimétisme.

Annexe F - Functional genomics of the *Pseudomonas aeruginosa* ϕKZ and PP7 phage lysis proteins: development of phage therapy and cell wall inhibitors

Présentation par affiche lors du Pseudomonas 10th International Meeting, Marseilles, France; du 28 au 31 août 2005. Le résumé de cette présentation a été publié dans le Pseudomonas 10th International Meeting Congress Abstract Book page 52 no.P6.

Paradis-Bleau C., Paquet-Bouchard C., Cloutier I., Trépanier J., Sanschagrin F., Lemieux L., Garnier A., Auger M. and Levesque R.C.

Functional genomics of the *Pseudomonas aeruginosa* ϕKZ and PP7 phage lysis proteins: development of phage therapy and cell wall inhibitors.

In the perspective to identify new antimicrobial agents targeting the integrity or biosynthesis of the peptidoglycan (PG) layer, we are studying lysis proteins of *P. aeruginosa* phages ϕKZ and PP7. To promote host cell disruption, dsDNA phages normally use a holin to destabilise the internal membrane along with a PG degrading endolysin. Phages with SS nucleic acid genomes inhibit cell wall biosynthesis via a single lysis protein. The dsDNA ϕKZ phage genome encodes an endolysin that was cloned into pET24b, overexpressed and purified by FPLC, demonstrating oligomeric forms. PG hydrolysis from both Gram-negative and Gram-positive bacteria was measured by spectrophotometry. LCMS analysis with purified PG identified a lytic transglycosidase. Circular dichroism and calcein vesicles showed that the endolysin destabilised anionic lipid formed membranes. Thus, we propose that the ϕKZ endolysin has bifunctional holin and PG hydrolytic activities. The ssRNA PP7 phage lysis protein of 6.3 kDa was obtained using RT-PCR. Cloning, expression and growth studies confirmed rapid cell lysis. We hypothesize, as for ϕX174 and Qβ inhibiting MurA and MraY, that PP7 lysis protein inhibits an essential enzyme in the PG biosynthesis pathway. Using an *in vitro* model of PG

precursor biosynthesis with purified MurA to MurF enzymes, the PP7 phage lysis protein will be used to identify its target. The A2 lysis protein from ssRNA coliphage Qβ inhibiting MurA and the E protein of ϕX174 inhibiting MraY will be used in a complementation assay for gene dosage of MurA and MraY. To find other potential targets, we are studying the ssRNA AP205 *Acinetobacter* phage lysis protein. A synthetic gene encoding the 5 kDa protein was constructed *in vitro* using overlapping oligonucleotides in a streamlined gene assembly by PCR. Cell lysis, similar to the PP7 lysis protein, was apparent after approximately 30 min. Analysis of phage lysis proteins will contribute to the phage therapy and to the development of new antibiotics against *P. aeruginosa* infections.

Annexe G - Identification of peptide inhibitors of bacterial cell wall biosynthesis

Présentation par affiche lors du congrès scientifique PEGS: The Protein Engineering Summit Event Guide Phage Display for Engineering Protein, Cambridge. Massachusetts USA; du 16 au 17 mai 2005. (Therapeutics Conference, affiche no. 222)

Paradis-Bleau C., Sanschagrin F. and Levesque R.C.

Identification of peptide inhibitors of bacterial cell wall biosynthesis.

Short Proposal:

With the objective of developing new antimicrobial agents, we exploited the phage display technology to identify peptide inhibitors of the MurD, E and F enzymes essential for the synthesis of the peptidoglycan precursor. Purified proteins were used to screen C-7-C and 12 mer libraries using 3 rounds of selective biopanning. We identified a promising peptide that inhibit the essential ATPase activity of MurD with an IC_{50} value of <10 μM.

Annexe H - Identification of inhibitor peptides of the FtsA protein essential for bacterial cell division

Présentation par affiche lors du congrès scientifique PEGS: The Protein Engineering Summit Event Guide Phage Display for Engineering Protein, Cambridge. Massachusetts USA; du 16 au 17 mai 2005. (Therapeutics Conference, affiche no. 223)

Paradis-Bleau C., Sanschagrin F. and Levesque R.C.

Identification of inhibitor peptides of the FtsA protein essential for bacterial cell division.

Short Proposal:

In the perspective of identifying new antimicrobial agents using novel strategies, we target the essential and highly conserved FtsA protein from the bacterial cell division machinery. Selective phage display biopanning identified two consensus peptide sequences and affinity ELISA identified peptides having high affinity for the target FtsA. Five synthesized peptides showed specific inhibition of the essential ATPase activity of FtsA and one peptide gave an IC_{50} value of 0.7 mM.

Annexe I - Functional genomics of the ϕKZ endolysin and phage PP7 small lysis protein for development of phage therapy and cell wall inhibitors

Présentation par affiche lors du 15th Annual Meeting of the Canadian Bacterial Diseases Networks Centre of Excellence, Banff, Alberta, Canada; du 13 au 16 février 2005. Le résumé de cette présentation a été publié dans le CBDN/CMCI AGM Poster Abstracts Book no. 38.

Paradis-Bleau C., Cloutier I., Lemieux L., Sanschagrin F., Auger F., Garnier A. and Levesque R.C.

Functional genomics of the ϕKZ endolysin and phage PP7 small lysis protein for development of phage therapy and cell wall inhibitors.

Small SS nucleic acid genomes have a single gene required for lysis and inhibit cell wall biosynthesis. The lysis E protein of phage ϕX174 is a specific inhibitor of the MraY. As a spin-off of our CBDN funded project studying cell wall inhibitors, we focus efforts on phage lysis proteins. We present data on lysis proteins of phages ΦX174, PP7 and phage PhiKZ. The ϕX174 E lysis protein of 91 aa and the PP7 of 56 aa were obtained from total RNA using RT-PCR and cloned into pET24b. *E. coli* cells were grown for 6 h, cell lysis was apparent after 30 min of induction and showed a rapid decrease in optical density. Large amounts of pure biologically active E and PP7 will permit the development of HTS assay for MurA to MurF, MraY and MurG. The ϕKZ endolysin gene was cloned into pET24b and the 29.6 KDa overexpressed protein was purified. ϕKZ hydrolytic activity was determined in a spectrophotometric assay using purified murein and the peptidoglycan cleavage site was identified by LCMS. To evaluate endolysin membrane interactions, we analysed the conformational change of the enzyme by circular dichroism. Overexpression

of the ϕKZ endolysin lead to a loss of viability of *E. coli* expressing cells and permitted the purification of 200 mg/L of active enzyme. Studies using purified enzyme showed that the monomeric endolysin oligomerises in multimeric forms. The spectrophotometric assay confirmed that the ϕKZ endolysin hydrolysed the murein of both Gram-negative and Gram-positive bacterias. LCMS analysis identified the enzyme cleavage site at the L-alanine – N-acetylmuramyl; the ϕKZ endolysin is thus an amidase. Circular dichroism experiments showed that the endolysin secondary conformation is significantly destabilised by anionic lipid formed membranes in comparison with zwitterionic lipids. Thus, ϕKZ endolysin has an holin activity along with an amidase hydrolytic function. Our model suggested that the enzyme oligomerises and interacts with anionic lipids that mimic bacterial membranes in an holin-like structure promoting the amidase peptidoglycan hydrolysis.

Annexe J - Identification of *Pseudomonas aeruginosa* FtsZ and FtsA peptide inhibitors as a potential novel class of antimicrobials

Présentation par affiche lors du Pseudomonas 2003 International Meeting, Québec, Québec, Canada; du 6 au 10 septembre 2003. Le résumé de cette présentation a été publié dans le Pseudomonas 2003 International Meeting Abstract Book page 158 abstract no. 158.

Paradis-Bleau C., Robitaille M., Sanschagrin F. and Levesque R.C.

Identification of *Pseudomonas aeruginosa* FtsZ and FtsA peptide inhibitors as a potential novel class of antimicrobials.

The revolutionary era of antibiotics has been overwhelmed by the evolutionary capacity of microorganisms to develop resistance. The acute resistance of the opportunistic pathogen *Pseudomonas aeruginosa* lowers the treatment efficiency of infected cystic fibrosis patients and immuno-compromised individuals. In the perspective of identify new antimicrobial agents, we are using the bacterial cell division machinery of *P. aeruginosa* as a new target. We exploited the sequenced genome of *P. aeruginosa* to study FtsZ and FtsA, two essential and highly conserved proteins. As a first step, *ftsZ* and *ftsA* were cloned and fused with a his tag at the C-terminus. Overexpressed FtsZ was purified by a single nickel affinity chromatography step. Overexpression of FtsA led to the accumulation of the protein in inclusion bodies. We developed a protocol permitting the purification of inclusion bodies and refolding of biologically active FtsA. N-terminal sequencing confirmed the identity of both proteins and a TLC assay confirms the enzymatic activity of each enzyme. A UV cross-linking showed that FtsZ binds preferentially GTP and that FtsA binds preferentially ATP among the 4 nucleotides used as substrates. Purified enzymes were used to screen for GTPase and ATPase peptide inhibitors with the phage display technique using 12-mer and the C7C-mer phage libraries containing 10^9 different peptide fusions. Specifically bounded

phages from each library were eluted with 4 different conditions; acidic glycine, substrate, non-hydrolysable substrate analogue and with FtsA against FtsZ and vice-versa. We identified 3 consensus peptide sequences against FtsZ and two against FtsA. The specificity of the interaction between chosen peptide against FtsZ or FtsA was analysed by ELISA and revealed the best binding peptides. The 3 FtsZ consensus peptides have been synthesized and were tested on the GTPase activity of FtsZ. The C7C-mer peptides showed inhibition of FtsZ GTPase activity with an IC_{50} value of 0.45 mM and 1.2 mM hence the 12-mer peptide showed IC_{50} value of 5 mM. The phage display technique was helpful in the discovery of new promising peptides for the development of new antimicrobial agents. Analysis technique coupled to in vivo whole bacteria cell monitoring is a promising approach for the identification of new antimicrobial agents via peptidomimetism and high throughput screening.

Annexe K - Molecular genomics and biochemical characterization of the FtsA and FtsZ cell division proteins from *P. aeruginosa*

Présentation par affiche lors du 53rd Annual Meeting of the Canadian Society of Microbiologists, Laval, Québec, Canada; le 26 mai 2003. Le résumé de cette présentation a été publié dans le CSM abstract book ID: F4.

Paradis-Bleau C., Sanschagrin F. and Levesque R.C.

Molecular genomics and biochemical characterization of the FtsA and FtsZ cell division proteins from *P. aeruginosa*.

The revolutionary era of antibiotics has been surpassed by the evolutionary capacity of microorganisms to develop resistance. The acute resistance of the opportunistic pathogen *Pseudomonas aeruginosa* to most classes of antibiotics is a good example. With the objective of developing new classes of antimicrobial agents, we must have a better understanding of essential prokaryotic mechanisms such as bacterial cell division. We studied FtsA and FtsZ, two essential and highly conserved proteins in bacteria. FtsA and FtsZ from *P. aeruginosa* were cloned in the pET30a overexpression vector and fused with a his tag at the C terminus. Overexpression of FtsA in *E. coli* BL21-(λDE3) led to the accumulation of the protein in inclusion bodies. To overcome this frequent problem, we developed a protocol permitting the isolation, refolding and production of a biologically active FtsA. We obtained 5 mg of 99% pure FtsA with a concentration of 0.5 mg/mL and N-terminal sequencing confirmed the identity of the protein. Overexpression of FtsZ permitted the accumulation of soluble proteins in the cytoplasm of *E. coli* BL21-(λDE3) and FtsZ was purified on a nickel affinity chromatography. We obtained 20 mg of 99% pure FtsZ with a concentration of 13.5 mg/mL with an identity confirmed by N-terminal sequencing. A UV cross-linking assay was used to study the FtsA binding of ATP and

showed that FtsZ binds preferentially GTP among the 4 nucleotides used as substrates. We characterized the specificity of enzymatic activity of each enzyme through a TLC assay. Hydrolysis of nucleotide substrates was measured using P^{32}-labelled nucleotides. We noted that FtsA hydrolyses predominantly ATP and weakly GTP, CTP and TTP. It was also noted that FtsZ hydrolyses predominantly GTP and weakly ATP, CTP and TTP. This information could be useful for the development of screening assays for analysis new inhibitors of prokaryotic cell division.

Annexe L - Molecular studies of *Pseudomonas aeruginosa* FtsA and FtsZ interactions and screening for ATPase peptide inhibitors of FtsA by phage display

Présentation par affiche lors du 53rd Annual Meeting of the Canadian Society of Microbiologists, Laval, Québec, Canada; le 26 mai 2003. Le résumé de cette présentation a été publié dans le CSM abstract book ID: F5.

Paradis-Bleau C., Sanschagrin F. and Levesque R.C.

Molecular studies of *Pseudomonas aeruginosa* FtsA and FtsZ interactions and screening for ATPase peptide inhibitors of FtsA by phage display.

The complete 6.3 Mpb genome sequence and the resistance of the opportunistic pathogen *Pseudomonas aeruginosa* to most classes of antibiotics represent a genomics tool for identification of novel targets for new antibacterials. With the prospect of finding new inhibitors of prokaryotic cell division, we screened for ATPase peptide inhibitors of FtsA and studied the interaction of two essential proteins: FtsA and FtsZ. As a first step, purified FtsA from *P. aeruginosa* was used to carry out each of the 3 rounds of phage display with the C-7-C and the 12-mers libraries containing 10^9 different peptides. The specificity of the 3 rounds of biopanning was raised by increasing the stringency of the wash and by decreasing the time of contact between the peptide and the protein. A competitive elution was done with 1 mM ATP and 5'-adenylylimidodiphosphate (a non-hydrolysable analogue of ATP). Peptides were isolated as phages and DNA of 20 phages per screening were sequenced. We identified many peptide sequences witch could be ATPase peptide inhibitors of FtsA. A competitive elution with FtsZ gave us 2 consensus peptide sequences. These promising peptides were synthesised as they could also be inhibitors of the FtsA-FtsZ interaction. To characterize the effect of these peptides, we developed a new protein-protein interaction assay. FtsA was coated in a microplate well and biotinylated FtsZ was

added. HRP-streptavidine and its substrate ABTS were used to quantify the FtsA-FtsZ interaction. This interaction is essential for the constriction of the Z-ring and is sensitive to this specific alteration witch can be quantified *in vitro*. Analysis technique coupled to *in vivo* whole bacteria cell monitoring is a promising approach for the identification of new antimicrobial agents via high throughput screening *in vivo*.

Annexe M - Identification of peptide inhibitors of the *Pseudomonas aeruginosa* FtsZ GTPase activity using phage display

Présentation par affiche lors du 53rd Annual Meeting of the Canadian Society of Microbiologists, Laval, Québec, Canada; le 26 mai 2003. Le résumé de cette présentation a été publié dans le CSM abstract book ID: F7.

Paradis-Bleau C., Boudreault L., Zoeiby A., Sanschagrin F. and Levesque R.C. Identification of peptide inhibitors of the *Pseudomonas aeruginosa* FtsZ GTPase activity using phage display.

The opportunistic pathogen *Pseudomonas aeruginosa* frequently infects cystic fibrosis patients and immuno-compromised individuals. The acute resistance of *P. aeruginosa* to most classes of antibiotics lowers the efficacy of treatment. We are using the bacterial cell division machinery as a tool to identify new antimicrobial agents. The essential and highly conserved protein FtsZ from *P. aeruginosa* was used to screen for GTPase peptide inhibitors with the phage display technique. We used a C-7-C and a 12-mer libraries containing 10^9 different peptide fusions. The specificity of the screening was done by 3 rounds of biopanning and each round specificity was raised by increasing the stringency of the wash and by decreasing the time of contact between the phage and FtsZ. A competitive elution was done with 1 mM GTP and 5'-guanylylimidodiphosphate (a non-hydrolysable analogue of GTP). Peptides were isolated as phages and DNA of 20 phages per screening were sequenced. We identified 3 interesting consensus peptides witch could be GTPase peptide inhibitors of FtsZ. The specificity of the interaction between each peptide and FtsZ was analysed by ELISA. FtsZ was coated in a microplate well and the phage clone containing the corresponding peptide fusion was added. Biotinylated anti-fd rabbit polyclonal antibodies, HRP-streptavidine and its substrate ABTS were used to estimate

protein-protein interaction. The 3 promising peptides have been synthesized and were tested on the GTPase activity of FtsZ. The inhibition of FtsZ represents a crucial target because the constriction of the Z-ring is the most important step in prokaryotic cell division. The phage display technique was helpful in the discovery of new promising peptides for the development of new antimicrobial agents.

Annexe N - Identification de peptides inhibiteurs des protéines bactériennes FtsA et FtsZ contrôlant la division cellulaire

Présentation par affiche lors de la 5ième Journée de la Recherche de la Faculté de médecine, Université Laval, Québec, Québec, Canada; le 8 mai 2003.

Paradis-Bleau C., Boudreault L., El Zoeiby A., Sanschagrin F., et Levesque, R.C.

Identification de peptides inhibiteurs des protéines bactériennes FtsA et FtsZ contrôlant la division cellulaire.

Objectifs : Le pathogène opportuniste *Pseudomonas aeruginosa* hautement résistant aux antibiotiques infecte 90 % des patients atteints de fibrose kystique. Afin d'identifier de nouveaux antimicrobiens, nous exploitons la machinerie de division cellulaire procaryote en tant que cible. **Méthodes:** FtsA et FtsZ, deux enzymes essentielles hautement conservées, ont été surexprimées dans *E. coli* puis purifiées. L'activité ATPase de FtsA et GTPase de FtsZ ont été démontrées par TLC puis leur identité a été confirmée par séquençage. Nous avons criblé les banques de bactériophages C-7-C et 12-mers contenant chacune 10^9 fusions peptidiques différentes avec les enzymes actives. Les phages adhérés aux protéines ont été élués avec de la glycine à pH acide puis de façon compétitive avec le substrat de l'enzyme, un analogue non hydrolysable du substrat ainsi qu'avec FtsZ pour FtsA et vice-versa. L'ADN a été extrait des phages et les peptides ont été identifiés. La spécificité de l'interaction entre les peptides et FtsA ou FtsZ a été analysée par ELISA. **Résultats :** Nous avons identifié trois consensus peptidiques contre FtsZ ainsi que plusieurs séquences peptidiques contre FtsA. De plus, l'élution compétitive FtsA-FtsZ a mené à l'identification d'un fort consensus peptidique. La spécificité de l'interaction entre chacun des peptides mentionnés et FtsA ou FtsZ a été analysée. **Conclusion :** Les peptides synthétisés pourraient inhiber l'activité ATPase, GTPase et l'interaction cruciale entre FtsA et FtsZ. L'inhibition de ces enzymes est d'un intérêt majeur car elle mène à un phénotype létal permettant d'envisager la production de nouveaux antimicrobiens.

Annexe O - Sélection de peptides inhibiteurs de la fonction GTPase de l'enzyme FtsZ essentielle à la division cellulaire procaryote

Présentation par affiche lors du 2ième Symposium Annuel du CREFSIP, Université Laval, Québec, Québec, Canada; le 2 mai 2003. Le résumé de cette présentation a été publié dans le Programme page 14, affiche no. 2.

Paradis-Bleau C., Boudreault L., Sanschagrin F., et Levesque, R.C.

Sélection de peptides inhibiteurs de la fonction GTPase de l'enzyme FtsZ essentielle à la division cellulaire procaryote.

Le pathogène opportuniste *Pseudomonas aeruginosa* hautement résistant aux antibiotiques infecte 90 % des patients atteints de fibrose kystique ainsi que les personnes immunodéprimées. Afin d'identifier de nouveaux antimicrobiens, nous exploitons la machinerie de division cellulaire procaryote en tant que cible. Tout d'abord, le gène *ftsZ* de *P. aeruginosa* a été cloné dans le vecteur de surexpression pET30a et fusionné avec une étiquette histidine en C-terminal. L'enzyme essentielle et hautement conservée FtsZ a été surexprimée dans *E. coli* BL21 (λDE3) puis purifiée à plus de 99% par chromatographie d'affinité au nickel. L'activité GTPase de FtsZ a été démontrée par TLC puis son identité a été confirmée par séquençage en N-terminal. Nous avons criblé les banques de bactériophages C-7-C et 12-mers avec l'enzyme active. Ces banques contiennent 10^9 peptides différents fusionnés à la protéine mineur pIII de la capside du phage M13. La spécificité de la technique de présentation phagique a été maximisée et effectuant 3 rondes de biocriblage au cours desquelles la rigueur des lavages a été augmentée puis le temps de contact des phages avec FtsZ a été diminué. Les phages adhérés ont été élués avec de la glycine à pH acide puis de façon compétitive avec le GTP, un analogue non hydrolysable du substrat (5'-guanylylimidodiphosphate) et avec la protéine FtsA qui stabilise l'anneau

FtsZ. Ces phages ont été purifiés et l'ADN phagique a été extrait et séquencé. La bioinformatique nous a permis d'identifier trois consensus peptidiques prometteurs contre FtsZ soit deux peptides C7C FtsZp1 et FtsZp2 ainsi qu'un 12 mers FtsZp3. La spécificité de l'interaction entre chacun de ces peptides et FtsZ a été analysée par ELISA. Les peptides synthétisés inhibent l'activité GTPase de FtsZ avec une CI_{50} de 1,5mM pour les deux peptides C7C et de 5mM pour FtsZp3. Le DTT, un agent réducteur, diminue l'inhibition par FtsZp2 et indique que la conformation du peptide C7C avec son pont disulfure apporte beaucoup à son activité inhibitrice. L'inhibition de FtsZ est d'un intérêt majeur car elle mène à un phénotype létal permettant d'envisager la production de nouveaux antimicrobiens.

Annexe P - Strategy for screening and identification of inhibitor peptides of the bacterial divisosome and peptidoglycan synthesis

Présentation par affiche lors du 13th CBDN Annual Meeting of the Canadian Bacterial Diseases Networks Centre of Excellence, Calgary, Alberta, Canada; le 25 avril 2003. Le résumé de cette présentation a été publié dans le CBDN/CMCI AGM 2003 Poster Abstracts Book page 20.

Paradis-Bleau C., El Zoeiby A., Beaumont M., Boudreault L., Sanschagrin F., Loyd A. and Levesque R.C.

Strategy for screening and identification of inhibitor peptides of the bacterial divisosome and peptidoglycan synthesis.

With the objective of developing new classes of antimicrobial agents and inhibitors, we exploited the phage display technology against essential bacterial divisosome proteins. The FtsZ-FtsA protein complex is responsible for septation of daughter cells; while the MurD, E and F enzymes are essential for the synthesis of the peptidoglycan precursor. *Pseudomonas aeruginosa* genes encoding FtsZ, FtsA, MurD, MurE and MurF were cloned into pET expression vectors with His-tag fusions and proteins were expressed in *E. coli* BL21 (λDE3) and purified. Enzyme purity was estimated at >99% homogeneity and their identities were confirmed by N-terminal sequencing. The ATPase activity of FtsZ and MurD along with the GTPase activity of FtsZ was confirmed by thin layer chromatography and by development of an HTS microtiter plate coupled enzyme assay. We used FtsZ, FtsA, MurD, MurE and MurF purified proteins to screen C-7-C and 12-mers libraries containing 10^9 peptides fused to the phage M13 pIII minor coat protein. Screening was done using 3 rounds of biopanning with stringent washes; competitive elution was done using specific substrates synthesized *in vitro*, analogues and with FtsA known to bind FtsZ.

Phages were selected from each biopanning step and DNA encoding peptides sequenced. Bioinformatics analysis identified consensus peptide sequences for the 5 enzymes studied. A collection of peptides were synthesized, purified and used to determine specific inhibition of ATPase and GTPase activity. Peptide/protein interactions were analysed by ELISA. The peptides FtsZp1 and FtsZp2 showed inhibition of FtsZ GTPase activity with an IC_{50} value of 450 μM and of 1 mM for FtsZp3. Studies done with MurD identified a peptide with an IC_{50} of <10 μM. Peptides identified will be used for HTS screening of a combinatorial library of peptidomimetic molecules.

Annexe Q - Combinatorial Enzymatic Assay for the HTS screening of a new class of small molecule inhibitor of bacterial cell division

Présentation par affiche lors du 13th CBDN Annual Meeting of the Canadian Bacterial Diseases Networks Centre of Excellence, Calgary, Alberta, Canada; le 25 avril 2003. Le résumé de cette présentation a été publié dans le CBDN/CMCI AGM 2003 Poster Abstracts Book page 21.

Paradis-Bleau C., Beaumont M., Sanschagrin F. and Levesque R.C.

Combinatorial Enzymatic Assay for the HTS screening of a new class of small molecule inhibitor of bacterial cell division.

As a model system for designing inhibitors of prokaryotic cell division, we studied the essential and highly conserved FtsZ divisome protein from *P. aeruginosa* against a collection of substrate analogues synthesized by combinatorial chemistry. The *ftsZ* gene cloned into pET30a was expressed; conditions were optimized with a yield of 20 mg/L of FtsZ and purified with more than 99% homogeneity. A series of assays was used to study and identify FtsZ preferred substrate and specificity. Substrate specificity and hydrolysis was used as a tool to measure FtsZ activity and develop an enzyme assay where the decrease in absorbance was confirmed to proportionally follow FtsZ activity. The enzyme assay was optimized for specificity and for several parameters including substrate, reaction buffer and additives. A high throughput assay was thus developed and optimized. For a preliminary analysis in combinatorial chemistry and HTS screening of FtsZ, we synthesized a family of small molecule substrate analogues. HTS screening identified 10 compounds inhibiting FtsZ activity and with IC_{50} values between 450 µM and 2.8 mM. Antibacterial activity was tested against *E. coli* and *S. aureus* whole cells and 2 compounds inhibited *S. aureus* growth. The HTS assay developed for future screening of compound libraries and for the screening of families of analogues synthesized from lead compounds identified is the first step in identification of a bacterial cell division inhibitor.

Annexe R - Une nouvelle avenue pour traiter les infections bactériennes:la thérapie par les bactériophages

Texte de vulgarisation publié dans la revue *Cahiers du Lab-oratoire*, pages 77-82 en 2006. Le sujet de cette présentation orale a également fait office d'une présentation par affiche lors de l'évènement de vulgarisation Lab-oratoire public édition 2005, Québec, Québec, Canada; les 19 et 20 octobre 2005.

Texte de vulgarisation publié:
Paradis-Bleau C. et Paquet-Bouchard C.
Une nouvelle avenue pour traiter les infections bactériennes:la thérapie par les bactériophages.

Présentation par affiche:
Paradis-Bleau C. et Paquet-Bouchard, C., Sanschagrin, F. et Levesque, R.C. La thérapie par les bactériophages: la solution aux infections bactériennes?

L'augmentation de la résistance aux antibiotiques et des infections bactériennes représente une problématique préoccupante en santé publique. Afin de développer une thérapie antibactérienne alternative aux antibiotiques, notre recherche s'intéresse aux bactériophages: de petits virus s'attaquant seulement aux bactéries. L'objectif de ce projet est de comprendre le mode d'action des armes antibactériennes produites par les bactériophages nommés ϕKZ, PP7 et AP205. Ces bactériophages causent la mort bactérienne en détruisant la paroi bactérienne qui se compare à un mur entourant et protégeant les bactéries. La paroi est essentielle à la survie bactérienne car les bactéries meurent si leur paroi est détruite ou défectueuse. Les résultats démontrent que les bactériophages étudiés utilisent des stratégies différentes pour tuer les bactéries en attaquant leur paroi. En conclusion, les armes antibactériennes des bactériophages ϕKZ, PP7 et AP205 permettront de combattre les bactéries telles que *Pseudomonas aeruginosa* qui cause de multiples infections intraitables et mortelles.